Journal of Immunology Research

Immune System and Chronic Diseases 2020

Lead Guest Editor: Margarete D. Bagatini
Guest Editors: Fabiano Carvalho, Charles Elias Asmann, and Cristina R. Reschke

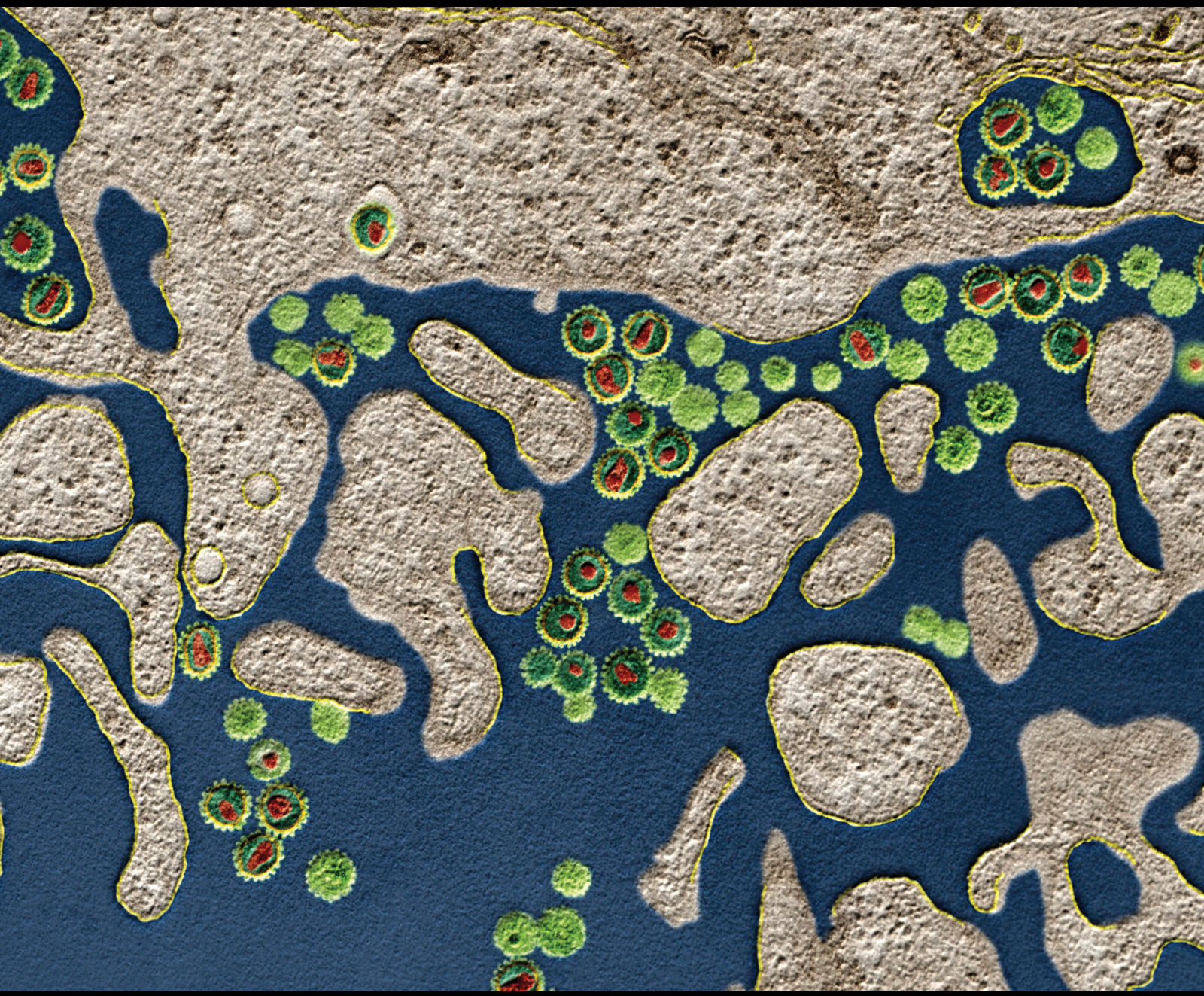

Immune System and Chronic Diseases 2020

Journal of Immunology Research

Immune System and Chronic Diseases 2020

Lead Guest Editor: Margarete D. Bagatini
Guest Editors: Fabiano Carvalho, Charles Elias Asmann, and Cristina R. Reschke

Contents

Contents

Hindawi
Journal of Immunology Research
Volume 2021, Article ID 2695490, 10 pages
https://doi.org/10.1155/2021/2695490

Research Article

Aluminum-Induced Alterations in Purinergic System Parameters of BV-2 Brain Microglial Cells

Charles Elias Assmann,[1] **Vitor Bastianello Mostardeiro**,[1] **Grazielle Castagna Cezimbra Weis**,[2] **Karine Paula Reichert**,[1] **Audrei de Oliveira Alves**,[3] **Vanessa Valéria Miron**,[1] **Margarete Dulce Bagatini**,[4] **Taís Vidal Palma**,[1] **Cinthia Melazzo de Andrade**,[1] **Micheli Mainardi Pillat**,[5] **Fabiano Barbosa Carvalho**,[6] **Cristina Ruedell Reschke**,[7,8] **Ivana Beatrice Mânica da Cruz**,[3,9] **Maria Rosa Chitolina Schetinger**,[1] **and Vera Maria Melchiors Morsch**[1]

[1]*Postgraduate Program in Biological Sciences, Toxicological Biochemistry, Department of Biochemistry and Molecular Biology, Federal University of Santa Maria, Santa Maria, RS, Brazil*
[2]*Postgraduate Program in Food Science and Technology, Department of Food Science and Technology, Federal University of Santa Maria, Santa Maria, RS, Brazil*
[3]*Postgraduate Program in Pharmacology, Department of Physiology and Pharmacology, Federal University of Santa Maria, Santa Maria, RS, Brazil*
[4]*Postgraduate Program in Biomedical Sciences, Federal University of Fronteira Sul, Chapecó, SC, Brazil*
[5]*Department of Microbiology and Parasitology, Federal University of Santa Maria, Santa Maria, RS, Brazil*
[6]*Federal University of Health Sciences of Porto Alegre, Porto Alegre, RS, Brazil*
[7]*School of Pharmacy and Biomolecular Sciences, Royal College of Surgeons in Ireland, Dublin, Ireland*
[8]*FutureNeuro Research Centre, Dublin, Ireland*
[9]*Postgraduate Program in Gerontology, Federal University of Santa Maria, Santa Maria, RS, Brazil*

Correspondence should be addressed to Charles Elias Assmann; charles.ufsm@gmail.com
and Vera Maria Melchiors Morsch; veramorsch@gmail.com

Received 21 April 2020; Revised 6 August 2020; Accepted 19 September 2020; Published 19 January 2021

Academic Editor: Peirong Jiao

Aluminum (Al) is ubiquitously present in the environment and known to be a neurotoxin for humans. The trivalent free Al anion (Al^{3+}) can cross the blood-brain barrier (BBB), accumulate in the brain, and elicit harmful effects to the central nervous system (CNS) cells. Thus, evidence has suggested that Al increases the risk of developing neurodegenerative diseases, particularly Alzheimer's disease (AD). Purinergic signaling has been shown to play a role in several neurological conditions as it can modulate the functioning of several cell types, such as microglial cells, the main resident immune cells of the CNS. However, Al effects on microglial cells and the role of the purinergic system remain elusive. Based on this background, this study is aimed at assessing the modulation of Al on purinergic system parameters of microglial cells. An *in vitro* study was performed using brain microglial cells exposed to Al chloride ($AlCl_3$) and lipopolysaccharide (LPS) for 96 h. The uptake of Al, metabolism of nucleotides (ATP, ADP, and AMP) and nucleoside (adenosine), and the gene expression and protein density of purinoceptors were investigated. The results showed that both Al and LPS increased the breakdown of adenosine, whereas they decreased nucleotide hydrolysis. Furthermore, the findings revealed that both Al and LPS triggered an increase in gene expression and protein density of P2X7R and A2AR receptors, whereas reduced the A1R receptor expression and density. Taken together, the results showed that Al and LPS altered the setup of the purinergic system of microglial cells. Thus, this study provides new insights into the involvement of the purinergic system in the mechanisms underlying Al toxicity in microglial cells.

1. Introduction

The prevalence of chronic neurodegenerative disorders, such as Alzheimer's disease (AD), is growing considerably with the rise of global life expectancy. The gradual decline of motor and/or cognitive capacities associated with these morbidities is of major concern; however, the underlying mechanisms are still not fully understood [1, 2]. Evidence has pointed out that some environmental factors, such as aluminum (Al), could be an etiological cause and associated with a higher risk of developing AD [3, 4]. Al is a lightweight metal ubiquitously found in the environment, resulting in a nearly unavoidable contact of humans to this element [5]. Human exposure to this metal can occur by several routes, including drinking water, foods, occupational exposure, and vaccines, among others [5, 6].

Its highly toxic form, the trivalent free Al ion (Al^{3+}), can cross the blood-brain barrier (BBB), alter membrane function, and accumulate in the human brain throughout life [6–9]. Literature data have indicated that Al is a neurotoxic metal that may lead to alterations associated with neurodegeneration and brain aging, among others, characteristics also found in AD [3, 9–11]. Moreover, recent evidence using a model of neural progenitor cells (NPCs) have suggested that Al^{3+} may also affect neurogenesis [12] and purinergic signaling [13].

The purinergic signaling system includes a cascade of extracellular nucleotides- and nucleoside-catalyzing enzymes that participate in the metabolism of ATP (adenosine triphosphate) to ADP (adenosine diphosphate) and/or AMP (adenosine monophosphate) (NTPDase/CD39, nucleoside triphosphate diphosphohydrolase), followed by the conversion of AMP to adenosine ($5'$-NT/CD73, $5'$-nucleotidase) and of adenosine to inosine (ADA, adenosine deaminase) [14–17]. Moreover, ATP and adenosine can operate as signaling molecules through their binding to specific purinergic receptors. P1 adenosine receptors (A1, A2A, A2B, and A3), which are all G protein-coupled receptors, are selective to adenosine. Purine nucleotides, such as ATP and ADP, and pyrimidine nucleotides, such as UTP (uridine triphosphate) and UDP (uridine diphosphate), act on P2 receptors, which are subdivided into P2X ionotropic receptors (P2X1-7) and P2Y receptors (P2Y1/2/4/6/11/12/13/14) which are coupled to G proteins [18–20].

Purinergic signaling may operate in a wide range of biological functions including neurotransmission and neuroinflammation and also in disease conditions [21–23]. Particularly in the central nervous system (CNS), this signaling pathway may also orchestrate immune cell responses, including microglial activation and the release of inflammatory cytokines, among others [22, 24]. Microglia comprise the main cells of the neuroimmune system acting in the clearance of noxious stimuli and limiting tissue damage [25, 26] and exhibit fundamentally all the repertoire of components of the purinergic system [22, 24].

However, mechanisms of Al toxicity in the brain related to the purinergic system, especially on microglial cells, remain elusive and it is essential to understand the role of this metal in the neuroinflammatory responses and neurodegenerative conditions. In this sense, this study is aimed at primarily investigating whether the exposure to Al (in the $AlCl_3$ form) could alter some purinergic system parameters using an *in vitro* model of microglial cells.

2. Materials and Methods

2.1. Chemicals and Reagents. This investigation used chemicals and reagents of analytical grade obtained from Sigma-Aldrich Inc. (St. Louis, MO, USA) and Merck KGaA (Darmstadt, Germany). All other reagents otherwise not stated were of chemical purity. Materials used in cell culture procedures were acquired from Kasvi (São José dos Pinhais, PR, Brazil), Corning Inc. (Corning, NY, USA), and Vitrocell Embriolife (Campinas, SP, Brazil). Western blot and molecular biology reagents were purchased from Bio-Rad Laboratories (Hercules, CA, USA), Merck KGaA, and Sigma-Aldrich Inc. All measurement analyses were carried out using a SpectraMax® i3 Multimode Plate Reader (Molecular Devices, Sunnyvale, CA, USA). The fluorescent images were captured using an Olympus Fluorescent Microscope (Fluoview FV101, Olympus, Tokyo, Japan).

2.2. Al. For this research, Al^{3+} in the chloride form ($AlCl_3$; molecular weight 133.34 g mol^{-1}; 99% purity) was purchased from Sigma-Aldrich Inc. All laboratory materials (flasks, plates, tips, tubes, etc.) and glassware were immersed in a 10% HNO_3/ethanol (v/v) solution for 48 h and then washed with Milli-Q® ultrapure water to avoid external contamination by the metal. All solutions were prepared using decontaminated materials and Milli-Q® ultrapure water. All laboratory and cell culture protocols were performed in a clean workbench to avoid contamination by external Al sources.

2.3. Experimental Design of Cell Culture Protocols and Exposure to Toxicants. This *in vitro* study used the mouse brain BV-2 microglial cell line, purchased from the Rio de Janeiro Cell Bank (BCRJ, Rio de Janeiro, RJ, Brazil). The cells were cultured using *Roswell Park Memorial Institute* (RPMI) 1640 medium (4500 mg/L glucose, 1500 mg/L sodium bicarbonate, 2 mM L-glutamine, and 1 mM sodium pyruvate), added with fetal bovine serum (FBS) to a final concentration of 10% and supplemented with 1% penicillin/streptomycin (10.000 U/mL; 10 mg/mL). The cells were grown in standard conditions by using a humidified and controlled atmosphere of 5% carbon dioxide (CO_2) at 37°C.

The cells were treated with an increasing concentration-effect curve of the trivalent free Al ion (Al^{3+}) in the form of Al chloride ($AlCl_3$), consisting of 1, 5, 10, 50, 100, 500, and 1000 μM of $AlCl_3$, based on a previous work [27]. The control group (C) consisted of cells that received only the culture medium. Lipopolysaccharide (LPS) at the concentration of 1 μg/mL was used as a positive inflammatory control since it has been suggested that this agent causes neuroinflammatory states [28, 29]. For culture protocols, cells were grown in 6-well plates at the concentration of 1×10^5 cells/mL for 96 h to investigate the subchronic effects of Al and LPS exposure.

2.4. Al Staining. Lumogallion (Santa Cruz Biotechnology, Inc., Dallas, TX, USA) is a reagent that can be used for the detection of Al in both tissues and cells. In brief, for this assay, cells were initially prepared on poly-lysine-coated slides and then incubated in the dark at 37°C for 24 h with Lumogallion (100 μM). Then, slides were washed with ultrapure water, air-dried, and fixed in paraformaldehyde (PFA, 4%) at room temperature for 15 min and washed again. DAPI (4′,6-diamidino-2-phenylindole) reagent (0.3 mg/mL, Sigma-Aldrich Inc.) was used to stain cell nuclei. Labeling with DAPI was performed protected from light during 5 min at room temperature, and subsequently, the staining solution was removed, cells were washed, and coverslips were placed on slides, following similar procedures described before [30, 31]. Finally, images were taken using an Olympus Fluorescent Microscope.

2.5. Purinergic System Enzyme Activities

2.5.1. NTPDase and 5′-NT Activities. The release of inorganic phosphate was employed to determine the enzymatic activities of NTPDase [32] and 5′-NT [33], similarly to guidelines published before. Briefly, cells were initially suspended in saline (NaCl, 0.9%), and 20 μL of samples was added to the reaction mixture of each enzyme and preincubated at 37°C for 10 min. The enzymatic reaction was initiated by adding the specific substrates for each enzyme: ATP and ADP for NTPDase and AMP for 5′-NT.

The reactions were stopped by the addition of trichloroacetic acid (TCA, 10%), and the released inorganic phosphate due to ATP, ADP, and AMP hydrolysis was determined by using malachite green as the colorimetric reagent. A standard curve was prepared with KH_2PO_4, and absorbance was read at 630 nm. Controls were performed to correct for nonenzymatic hydrolysis. Enzyme-specific activities were reported as nmol of Pi released per min per mg of protein.

2.5.2. ADA Activity. ADA activity was performed based on the measurement of ammonia produced when this enzyme acts in the excess of adenosine, following a previously published method [34]. In brief, 50 μL of cell suspension reacted with 21 mmol/L of adenosine (pH 6.5) at 37°C for 60 min. After the incubation period, the reaction was stopped by the addition of 167.8 mM sodium nitroprusside, 106.2 mM phenol, and a sodium hypochlorite solution. The amount of ammonia produced was quantified at 620 nm, and the results were expressed as U Ado (adenosine) per mg of protein.

2.6. Purinergic System Receptors

2.6.1. Gene Expression. The gene expression modulation of the purinergic receptors P2X7R (*P2rx7*), A2AR (*Adora2a*), and A1R (*Adora1*) was carried out by real-time quantitative polymerase chain reaction (RT-qPCR) analysis, based on a previous report [35]. Briefly, RNA was initially obtained from samples with TRIzol™ reagent (Invitrogen™), quantified spectrophotometrically, and reversely transcribed into cDNA with the iScript™ cDNA synthesis kit (Bio-Rad Laboratories), by the addition to each sample of 1 μL of iScript reverse transcriptase and 4 μL of the iScript Mix. Steps of the reaction were as follows: 25°C for 5 min, 42°C for 30 min, 85°C for 5 min, and a final step of 5°C for 60 min, performed using a thermal cycler equipment.

The RT-qPCR reaction was performed using 19 μL of a mix containing the iTaq Universal SYBR Green Supermix (Bio-Rad Laboratories) and 1 μL of the cDNA sample. The parameters used were a holding step of 3 min at 95°C, followed by a cycling step of 40 cycles at 95°C for 10 s, 60°C for 30 s, and last a melting step with a melting curve of 65°C to 95°C with an increase of 0.5°C for 5 s. The relative expression of each gene was represented as the fold expression compared to the control group and calculated by using the comparative $^{\Delta\Delta}$CT value. The β-actin (*Actb*) gene was used as the internal control to normalize gene expression. The forward and reverse sequences of oligos (5′-3′) used for each gene were as follows: β-actin (F): CCGTAAAGA CCTCTATGCCAAC; β-actin (R): AGGAGCCAGAGCAG TAATCT; P2X7R (F): CTTTGCTTTGGTGAGCGATAAG; P2X7R (R): CACCTCTGCTATGCCTTTGA; A1R (F): GGCCATAAAGTCCTTGGGAAT; A1R (R): CAGGAA GTTCAGGGCAAGAA; A2AR (F): TCACGTCTCAGGAT TGAGTTTAG; A2AR (R): CCCGAAGGAAAGGCAGTAG.

2.6.2. Protein Density. Protein density by Western blot analysis of the P2X7R, A2AR, and A1R receptors was performed based on a prior work [36]. In brief, cells were initially homogenized in ice-cold radioimmunoprecipitation assay (RIPA) buffer added with 1 mM phosphatase and protease inhibitors and centrifuged at 12,000 rpm at 4°C for 10 min. Subsequently, samples were separated using sodium dodecyl sulfate-polyacrylamide gel electrophoresis (SDS-PAGE) and transferred to Immun-Blot® PVDF membranes (Bio-Rad Laboratories). After blocking, membranes were incubated overnight at 4°C with the primary antibodies: P2X7R (dilution 1 : 500), A2AR (dilution 1 : 800), and A1R (dilution 1 : 500), all obtained from Santa Cruz Biotechnology, Inc. After this step, membranes were washed with Tris-buffered saline (pH 7.6) with 0.1% Tween 20 (TBST) and further incubated with anti-rabbit or anti-mouse secondary antibodies (dilution 1 : 10.000, Santa Cruz Biotechnology, Inc.) at room temperature for 90 min. The membranes were washed again, incubated with an enhanced chemifluorescent substrate (Immobilon® Forte Western HRP Substrate, Merck KGaA), and analyzed with a ChemiDoc Imaging System (Bio-Rad Laboratories). As a control for protein concentration, membranes were reprobed and tested for β-actin immunoreactivity (dilution 1 : 1000, Santa Cruz Biotechnology, Inc.).

2.7. Protein Determination. The protein in samples was determined using the Coomassie Blue reagent following the method previously described and using serum albumin as standard [37]. The protein of samples (mg/mL) was adjusted according to each assay.

2.8. Statistical Analysis. The results were compared by one-way analysis of variance (ANOVA) followed by Tukey's *post hoc* test and presented as the mean ± SD. The GraphPad Prism software version 6 (GraphPad Software, Inc.; La Jolla, CA, USA) was used to perform statistical analysis. The results

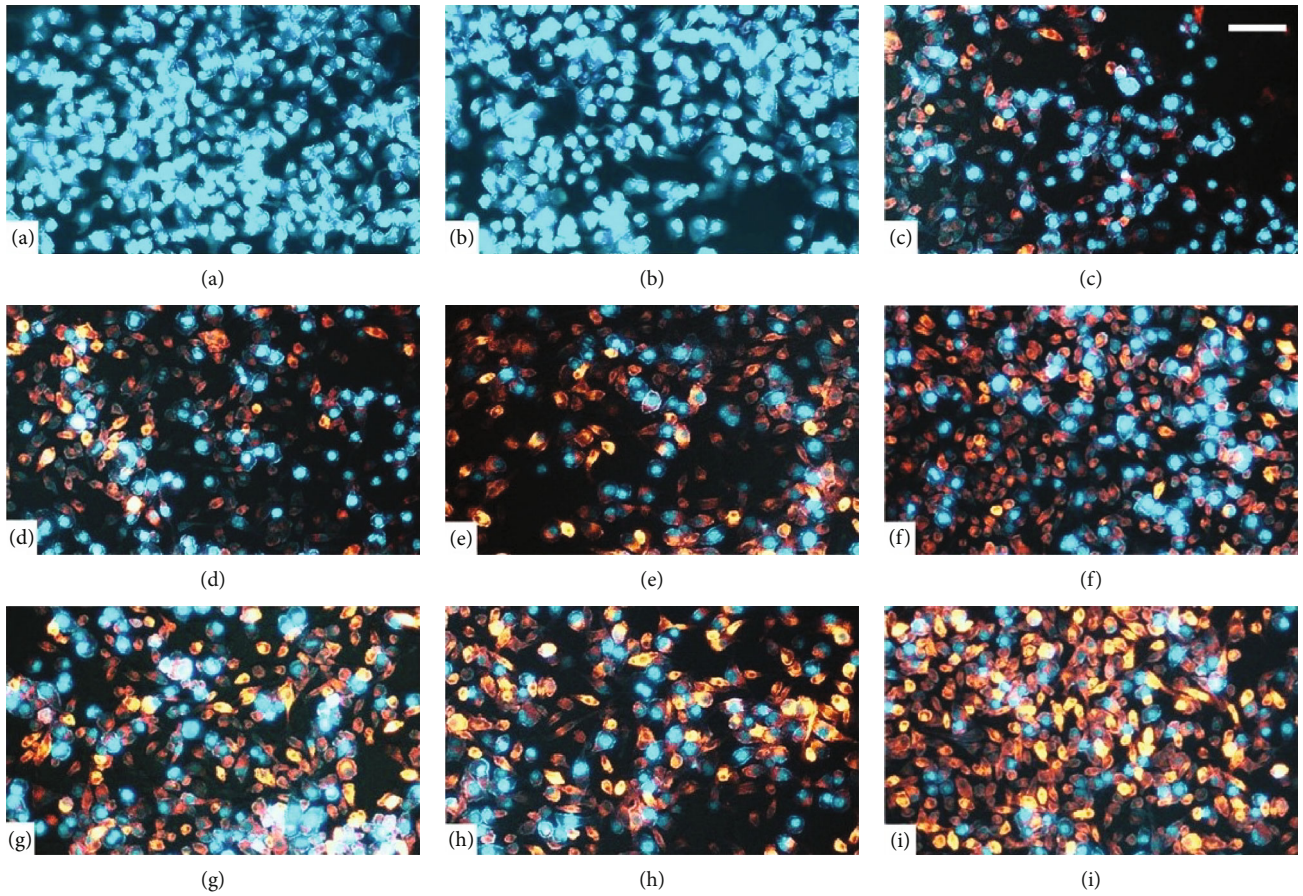

Figure 1: Representative fluorescence microscopy of microglial cells stained with DAPI (blue, cell nuclei) and Lumogallion probe (orange) to track uptake of Al: (a) control; (b) lipopolysaccharide (LPS, 1 μg/mL); (c) $AlCl_3$ (1 μM); (d) $AlCl_3$ (5 μM); (e) $AlCl_3$ (10 μM); (f) $AlCl_3$ (50 μM); (g) $AlCl_3$ (100 μM); (h) $AlCl_3$ (500 μM); (i) $AlCl_3$ (1000 μM). Magnification = 200x. Scale bar = 20 μm. $n = 3$.

were considered statistically significant when $p < 0.05$. All experiments were carried out in triplicate.

3. Results

3.1. Al Can Be Tracked by Lumogallion Fluorescent Probe in BV-2 Microglial Cells. To track the possible uptake of Al by cells, we used Lumogallion staining and demonstrative images are shown in Figure 1. Control cells (Figure 1(a)) and cells cultured with LPS (Figure 1(b)), both in the absence of Al, only showed blue fluorescence produced by DAPI, which is used to indicate cell nuclei. In this case, when images taken with DAPI and Lumogallion reagent were overlaid, only blue fluorescence was emitted. However, cells cultured in the presence of $AlCl_3$ at the concentrations of 1-1000 μM (Figure 1(c)–1(i)) showed an orange labeling representative of Lumogallion staining, and overlaid images also revealed a blue fluorescence related to DAPI nuclei staining. Thus, the free Al ion can be internalized by microglial cells as suggested by the orange concentration-dependent intensity tracked by Lumogallion staining.

3.2. Al and LPS Alter the Activity of Purinergic System Ectoenzymes. To verify if Al and LPS could modulate the activity of purinergic system ectoenzymes, the breakdown of nucleotides and nucleoside was evaluated in microglial cells and the results are shown in Figure 2. NTPDase activity was assessed by ATP and ADP hydrolysis (Figures 2(a) and 2(b)). LPS was shown to significantly reduce the hydrolysis of ATP and ADP when compared to control cells. Moreover, the $AlCl_3$ concentrations of 500 and 1000 μM also reduced ATP hydrolysis, and $AlCl_3$ at 1000 μM also decreased ADP hydrolysis when compared to control cells. The activity of 5′-NT was assessed by AMP hydrolysis (Figure 2(c)), and results revealed that LPS and $AlCl_3$ at 500 and 1000 μM decreased AMP hydrolysis when compared to control cells. Following the ectoenzyme cascade, ADA activity (Figure 2(d)) was measured by the deamination of adenosine and findings revealed that LPS and $AlCl_3$ at the concentrations of 500 and 1000 μM augmented nucleoside breakdown compared to control cells.

3.3. Al and LPS Modulate the Expression and Density of Purinoceptors. Since Al and LPS modulated ectoenzyme activities, we also investigated whether these compounds could alter the expression and density of purinergic receptors. Figure 3 shows the results from the analysis by RT-qPCR performed to assess the modulation of the P2X7R,

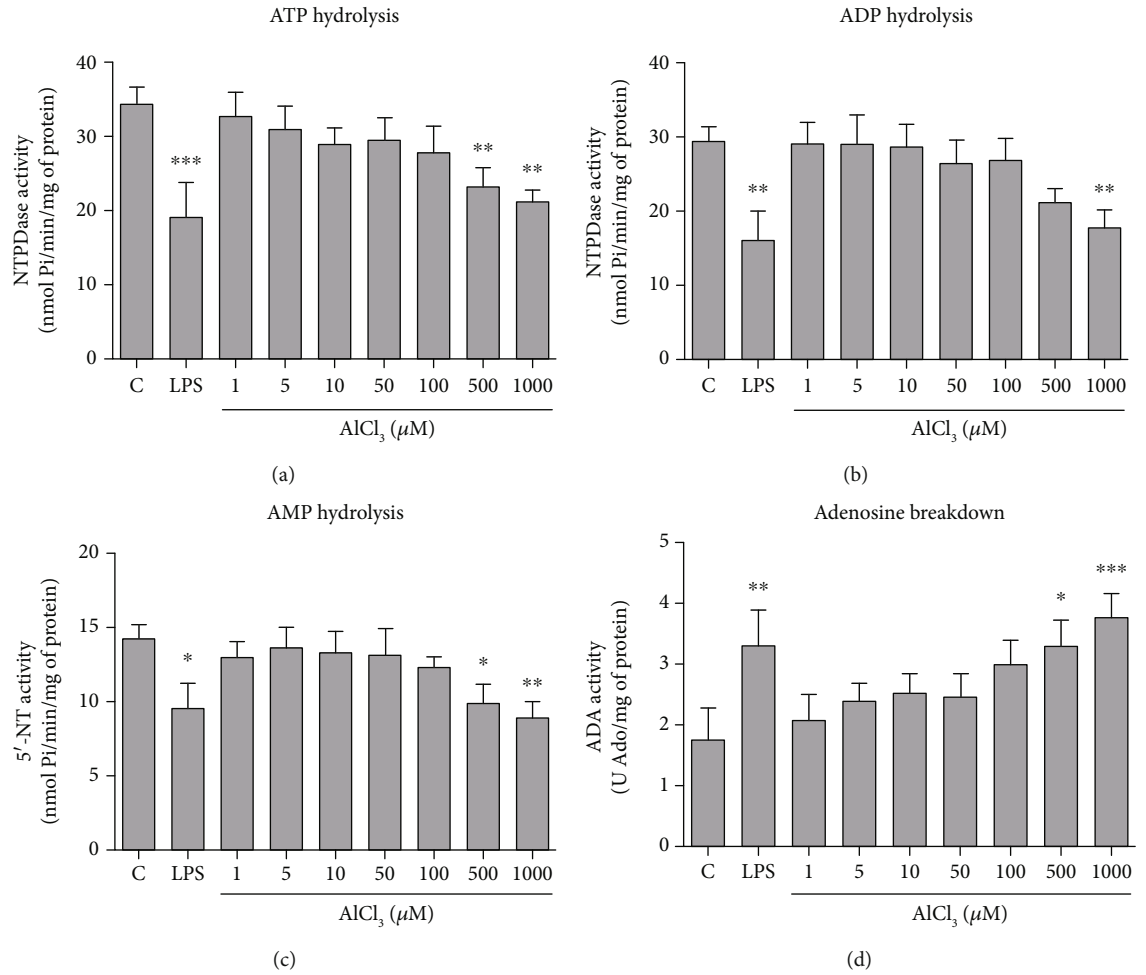

FIGURE 2: Purinergic enzyme activities of microglial cells treated with LPS (1 μg/mL) and increasing concentrations of $AlCl_3$ (1–1000 μM) for 96 h. NTPDase activity using (a) ATP and (b) ADP as substrates, (c) 5′-NT activity using AMP as substrate, (d) ADA activity using adenosine as substrate. C = control group; LPS = lipopolysaccharide. Values are expressed as mean ± SD ($n = 3$). *Statistical significance in comparison to the control group. $^*p < 0.05$, $^{**}p < 0.01$, and $^{***}p < 0.001$. One-way ANOVA followed by Tukey's *post hoc* test.

A2AR, and A1R purinoceptor gene expression. Results showed that both LPS and Al significantly upregulated the expression of the P2X7R and A2AR purinoceptors whereas they downregulated the expression of the A1R purinoceptor when compared to the control group. Complementary to RT-qPCR findings, Western blot analysis also showed that LPS and Al were capable of modulating the protein levels of purinoceptors by significantly upregulating the density of the P2X7R and A2AR receptors and downregulating the density of the A1R receptor compared to the control group (Figure 4).

4. Discussion

Literature data have underlined the involvement of the purinergic system in the inflammatory responses and microglia behavior within the CNS [22, 24]. However, the impact of Al on the modulation of the purinergic system in microglial cells is poorly understood. In the current study, we showed that Al, and also LPS, disturbed some purinergic system parameters of BV-2 cells, evidenced by the changes in ectoenzymes activities and expression/density of purinoceptors.

Since Al^{3+}, the neurotoxic and biologically reactive Al free ion, can pass the BBB and deposit in the brain tissue [6–9], microglial cells are within the reach of this element. Therefore, the possible uptake of Al was tracked qualitatively using Lumogallion fluorescent probe. This chemical has been proposed to generate an orange fluorescence signal when binding to the soluble Al^{3+} free ion [13, 31], as indicated in Figure 1(c)–1(i), leading to the suggestion that Al can be internalized by these immune cells.

Based on this assumption, it is relevant to comprehend the possible mechanisms related to the toxicity of the different stimuli used here in microglial cells. It is also noteworthy to comment that, although there are shortcomings of employing *in vitro* cellular models, the cell line used here has been proposed as a valuable substitute platform for *in vivo* microglia [38], suggesting these immune cells as a potential tool to investigate the effects triggered by the exposure to toxic agents.

Insults and noxious stimuli that alter CNS homeostasis, such as Al and LPS, may trigger the outpour of key purinergic

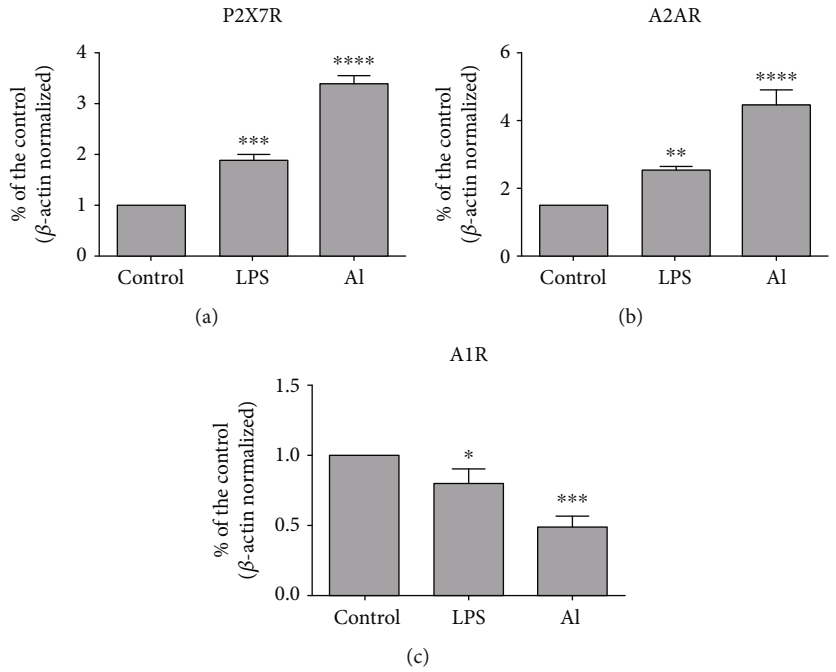

Figure 3: Gene expression of purinoceptors by RT-qPCR analysis of microglial cells treated with LPS (1 μg/mL) and $AlCl_3$ (1000 μM) for 96 h. Al = aluminum; LPS = lipopolysaccharide. Values are expressed as mean ± SD ($n = 3$) of the relative concentration compared to the control group. *Statistical significance in comparison to the control group. $^{*}p < 0.05$, $^{**}p < 0.01$, $^{***}p < 0.001$, and $^{****}p < 0.001$. One-way ANOVA followed by Tukey's *post hoc* test.

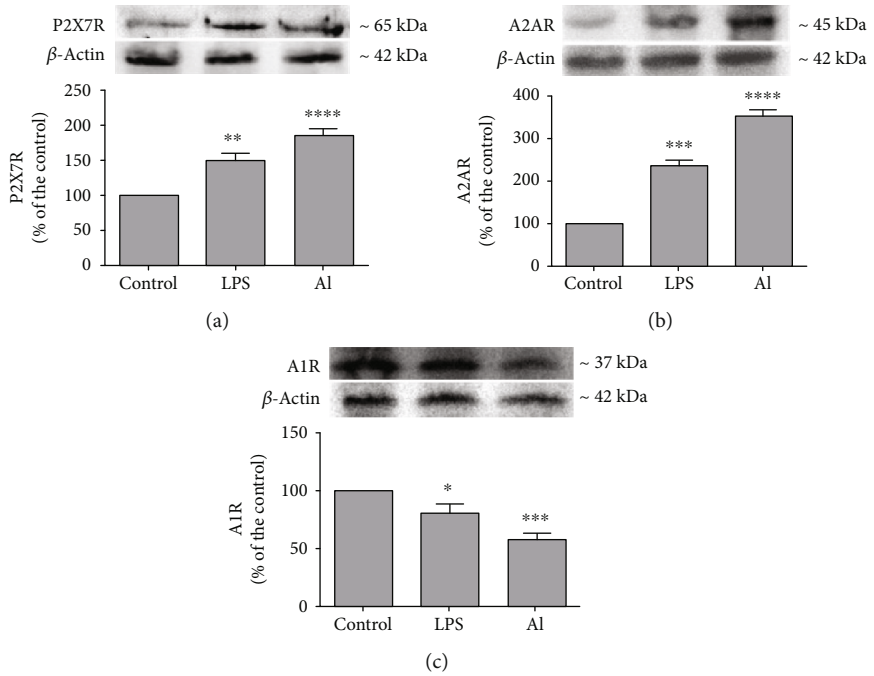

Figure 4: Protein density of purinoceptors by Western blot analysis of microglial cells treated with LPS (1 μg/mL) and $AlCl_3$ (1000 μM) for 96 h. Al = aluminum; LPS = lipopolysaccharide. Values are expressed as mean ± SD ($n = 3$). *Statistical significance in comparison to the control group. $^{*}p < 0.05$, $^{**}p < 0.01$, $^{***}p < 0.001$, and $^{****}p < 0.001$. One-way ANOVA followed by Tukey's *post hoc* test.

messengers from microglial cells [24]. Changes in the levels of extracellular molecules, such as ATP and its breakdown products, are sensed by membrane-bound enzymes of the purinergic pathway, including NTPDase, 5′-NT, and ADA [14–17]. In this way, the possible changes in the activity of these key enzymes were further investigated. Similar to our findings, a previous investigation using blood lymphocytes of rats [39] also reported that LPS may affect the metabolism

of nucleotides and nucleoside, reducing ATP hydrolysis and increasing adenosine breakdown. Moreover, ATP and AMP hydrolysis as well as NTPDase1 and 5′-NT expression have been shown diminished in a model of M1 macrophages (challenged with LPS) [40].

Concerning the effects observed for Al on enzyme activities, these could reflect the capacity of Al^{3+} to substitute metal ions and/or its interaction with nucleotides. The Al free ion may be able to displace native ions, such as Mg^{2+}, at protein binding sites, thus being able to affect their biological functions [9, 41–43]. For instance, NTPDase is a metalloenzyme that requires Ca^{2+} or Mg^{2+} ions for its optimal activity and may have its functioning altered in the lack of these ions [15]. Moreover, the ability of Al^{3+} to interact with molecules, such as ATP [43], could reduce the availability of this nucleotide and interfere with the activity of membrane-bound enzymes of the purinergic pathway [13].

A coordinated upregulation of 5′-NT and purinoceptor expression, particularly A2AR expression, has been suggested by previous reports such as in hippocampal astrocytes of human patients with mesial temporal lobe epilepsy (MTLE) [44], in a rat model of Parkinson's disease [45], and in a rat model of AD [46]. However, although our results regarding the A2AR receptor are in agreement with these previous reports, the decrease in 5′-NT activity was also indicated when neurospheres were treated with Al^{3+} [13].

Also, an increase in ADA enzyme activity for cells treated with Al and LPS was found here. Adenosine, the main ATP breakdown product binds to P1 type of receptors, including A1R and A2AR subtypes of receptors, and together with ATP presents central neuromodulatory and immunomodulatory functions in the brain [19, 22, 47, 48]. Thus, the alterations evoked by LPS and Al regarding purinergic parameters could also influence immune/microglial responses in the brain, but these effects are issues to be addressed in more detail by further studies.

As microglial cells are recognized to express essentially all types of purinergic system proteins [22, 24], the effect of Al and LPS exposure on the modulation of purinoceptors could also be a relevant mechanism underlying the toxicity of these agents in neuroimmune cells. P2X7R receptors are ATP-gated ionotropic channels indicated to present a major role in neurodegeneration and neuroinflammation [49]. The increased expression of P2X7R receptors has also been suggested in microglial cells of Aβ-injected rat brains and human brains of AD patients [50], in microglia of a model using LPS administration [51], in immature rat brains exposed to lead (Pb) [52], and in the hippocampus of mouse pups also exposed to Pb [53]. In this sense, P2X7R receptors and downstream signaling pathways triggered by their activation may have a central contribution in the toxic mechanisms triggered by Al and LPS and offer the possibility for future exploration.

Adenosine signaling is also of particular relevance in the brain [47, 48]. For instance, an increased expression of the A2AR receptor has also been indicated for other brain insult models, for example, perinatal brain injury [54] and in LPS-treated microglial cells [55]. In our study, the expression/-density of the A1R receptor were found decreased whereas A2AR receptor expression/density were increased. These findings are of significance considering that A1R receptors (inhibitory) have been mainly associated with neuroprotection whereas the A2AR receptors (facilitatory) to neurodegeneration and neuroinflammation. Moreover, the antagonism of A2AR receptors may also provide neuroprotection in several disease conditions [47, 48, 56–58]. However, inhibition of both adenosine receptors, A1R and A2AR, has also been suggested to afford neuroprotection against $AlCl_3$ exposure in neuroblastoma cells [59]. Therefore, these outcomes and the findings of our study highlight that adenosine receptors are also candidates for further investigation.

Taken together, our findings suggested that microglial cells can uptake the Al^{3+} free ion, displayed by the orange fluorescence labeling tracked by Lumogallion reagent. The activities of ectoenzymes showed a decrease/increase in the metabolism of nucleotides/nucleoside, respectively, when cells were exposed to both stimuli. Moreover, Al and LPS upregulated the expression/density of purinoceptors generally associated with neurotoxicity and neuroinflammation and downregulated the expression/density of purinoceptors related to neuroprotection. In this sense, our current findings provide a possible link between Al and also LPS toxic effects and purinergic system alterations in microglial cells and support future studies to clarify these issues.

5. Conclusions

In summary, to the best of our knowledge, our results report some first indication on the possible involvement of the purinergic system in the mechanisms of Al toxicity in brain microglial cells. This agent evoked alterations in the setup of the purinergic system suggesting that this signaling pathway may be further investigated as a pivotal factor to understand the effects triggered by toxic compounds in the CNS.

Abbreviations

5′-NT:	5′-Nucleotidase
A1R:	Adenosine A1 receptor
A2AR:	Adenosine A2A receptor
AD:	Alzheimer's disease
ADA:	Adenosine deaminase
Ado:	Adenosine
ADP:	Adenosine diphosphate
Al:	Aluminum
Al^{3+}:	Al trivalent ion
$AlCl_3$:	Aluminum chloride
AMP:	Adenosine monophosphate
ANOVA:	Analysis of variance
ATP:	Adenosine triphosphate
BBB:	Blood-brain barrier
CNS:	Central nervous system
DAPI:	4′,6-Diamidino-2-phenylindole
FBS:	Fetal bovine serum
LPS:	Lipopolysaccharide
NPCs:	Neural progenitor cells

NTPDase: Nucleoside triphosphate diphosphohydrolase
P1: Adenosine receptors
P2: ATP/ADP receptors
PFA: Paraformaldehyde
RT-qPCR: Real-time quantitative polymerase chain reaction
RIPA: Radioimmunoprecipitation assay
TBST: Tris-buffered saline with Tween
UDP: Uridine diphosphate
UTP: Uridine triphosphate

Data Availability

The data used to support the findings of this study are available from the corresponding author, upon reasonable request.

Additional Points

Highlights. Aluminum (Al) and lipopolysaccharide (LPS) modulated purinergic system parameters of BV-2 brain microglial cells. Al and LPS altered the metabolism of nucleotides (ATP, ADP, and AMP) and nucleoside (adenosine). Al and LPS upregulated the expression/density of purinoceptors associated with neurodegeneration and neuroinflammation. Al and LPS downregulated the expression/density of purinoceptors associated with neuroprotection.

Disclosure

The funding agencies had no role in the study design, in the collection, analysis, and interpretation of the data, in the writing of the manuscript, and in the decision for publication.

Conflicts of Interest

The authors declare that there are no conflicts of interest.

Acknowledgments

The authors are grateful for the funding provided by Conselho Nacional de Desenvolvimento Científico e Tecnológico (CNPq), Fundação de Amparo à Pesquisa do Estado do Rio Grande do Sul (FAPERGS), and Coordenação de Aperfeiçoamento de Pessoal de Nível Superior (CAPES/PROEX fellowship grant, process number 88882.182154/2018-01). CAPES/PrInt process number 88881.310287/2018-01 is also acknowledged.

References

[1] M. Prince, R. Bryce, E. Albanese, A. Wimo, W. Ribeiro, and C. P. Ferri, "The global prevalence of dementia: a systematic review and metaanalysis," *Alzheimer's & Dementia*, vol. 9, no. 1, pp. 63–75, 2013.

[2] L. Gan, M. R. Cookson, L. Petrucelli, and A. R. La Spada, "Converging pathways in neurodegeneration, from genetics to mechanisms," *Nature Neuroscience*, vol. 21, no. 10, pp. 1300–1309, 2018.

[3] Z. Wang, X. Wei, J. Yang et al., "Chronic exposure to aluminum and risk of Alzheimer's disease: a meta-analysis," *Neuroscience Letters*, vol. 610, pp. 200–206, 2016.

[4] C. Exley, "Aluminum should now be considered a primary etiological factor in Alzheimer's disease," *Journal of Alzheimer's Disease Reports*, vol. 1, no. 1, pp. 23–25, 2017.

[5] C. Exley, "Human exposure to aluminium," *Environmental Science: Processes and Impacts*, vol. 15, no. 10, pp. 1807–1816, 2013.

[6] A. Becaria, A. Campbell, and S. C. Bondy, "Aluminum as a toxicant," *Toxicology and Industrial Health*, vol. 18, no. 7, pp. 309–320, 2002.

[7] W. A. Banks and A. J. Kastin, "Aluminum-induced neurotoxicity: alterations in membrane function at the blood-brain barrier," *Neuroscience & Biobehavioral Reviews*, vol. 13, no. 1, pp. 47–53, 1989.

[8] D. Julka, R. K. Vasishta, and K. D. Gill, "Distribution of aluminum in different brain regions and body organs of rat," *Biological Trace Element Research*, vol. 52, no. 2, pp. 181–192, 1996.

[9] C. Exley, "What is the risk of aluminium as a neurotoxin?," *Expert Review of Neurotherapeutics*, vol. 14, no. 6, pp. 589–591, 2014.

[10] S. C. Bondy, "Prolonged exposure to low levels of aluminum leads to changes associated with brain aging and neurodegeneration," *Toxicology*, vol. 315, pp. 1–7, 2014.

[11] S. C. Bondy, "Low levels of aluminum can lead to behavioral and morphological changes associated with Alzheimer's disease and age-related neurodegeneration," *Neurotoxicology*, vol. 52, pp. 222–229, 2016.

[12] K. P. Reichert, M. R. C. Schetinger, M. M. Pillat et al., "Aluminum affects neural phenotype determination of embryonic neural progenitor cells," *Archives of Toxicology*, vol. 93, no. 9, pp. 2515–2524, 2019.

[13] K. P. Reichert, M. M. Pillat, M. R. C. Schetinger et al., "Aluminum-induced alterations of purinergic signalling in embryonic neural progenitor cells," *Chemosphere*, vol. 251, p. 126642, 2020.

[14] H. Zimmermann, "Ectonucleotidases in the nervous system," *Novartis Foundation Symposium*, vol. 276, pp. 113–128, 2006.

[15] M. R. C. Schetinger, V. M. Morsch, C. D. Bonan, and A. T. S. Wyse, "NTPDase and 5′-nucleotidase activities in physiological and disease conditions: new perspectives for human health," *BioFactors*, vol. 31, no. 2, pp. 77–98, 2007.

[16] G. G. Yegutkin, "Nucleotide- and nucleoside-converting ectoenzymes: important modulators of purinergic signalling cascade," *Biochimica et Biophysica Acta-Molecular Cell Research*, vol. 1783, no. 5, pp. 673–694, 2008.

[17] H. Zimmermann, M. Zebisch, and N. Sträter, "Cellular function and molecular structure of ecto-nucleotidases," *Purinergic Signalling*, vol. 8, no. 3, pp. 437–502, 2012.

[18] B. B. Fredholm, A. P. IJzerman, K. A. Jacobson, K. N. Klotz, and J. Linden, "International Union of Pharmacology. XXV. Nomenclature and classification of adenosine receptors," *Pharmacological Reviews*, vol. 53, no. 4, pp. 527–552, 2001.

[19] G. Burnstock, B. B. Fredholm, and A. Verkhratsky, "Adenosine and ATP receptors in the brain," *Current Topics in Medicinal Chemistry*, vol. 11, no. 8, pp. 973–1011, 2011.

[20] G. Burnstock, "Purine and purinergic receptors," *Brain and Neuroscience Advances*, vol. 2, 2018.

[21] G. Burnstock, "Purinergic signalling and disorders of the central nervous system," *Nature Reviews Drug Discovery*, vol. 7, no. 7, pp. 575–590, 2008.

[22] E. Beamer, F. Gölöncsér, G. Horváth et al., "Purinergic mechanisms in neuroinflammation: an update from molecules to behavior," *Neuropharmacology*, vol. 104, pp. 94–104, 2016.

[23] G. Burnstock, "Purinergic signalling and neurological diseases: an update," *CNS & Neurological Disorders Drug Targets*, vol. 16, no. 3, pp. 257–265, 2017.

[24] S. Calovi, P. Mut-Arbona, and B. Sperlágh, "Microglia and the purinergic signaling system," *Neuroscience*, vol. 405, pp. 137–147, 2019.

[25] V. H. Perry, J. A. R. Nicoll, and C. Holmes, "Microglia in neurodegenerative disease," *Nature Reviews Neurology*, vol. 6, no. 4, pp. 193–201, 2010.

[26] S. Hickman, S. Izzy, P. Sen, L. Morsett, and J. El Khoury, "Microglia in neurodegeneration," *Nature Neuroscience*, vol. 21, no. 10, pp. 1359–1369, 2018.

[27] T. Toimela and H. Tähti, "Mitochondrial viability and apoptosis induced by aluminum, mercuric mercury and methylmercury in cell lines of neural origin," *Archives of Toxicology*, vol. 78, no. 10, pp. 565–574, 2004.

[28] L. Qin, X. Wu, M. L. Block et al., "Systemic LPS causes chronic neuroinflammation and progressive neurodegeneration," *Glia*, vol. 55, no. 5, pp. 453–462, 2007.

[29] A. D. Bachstetter, B. Xing, L. de Almeida, E. R. Dimayuga, D. M. Watterson, and L. J. Van Eldik, "Microglial p38α MAPK is a key regulator of proinflammatory cytokine up-regulation induced by toll-like receptor (TLR) ligands or beta-amyloid (Aβ)," *Journal of Neuroinflammation*, vol. 8, p. 79, 2011.

[30] M. Mold, H. Eriksson, P. Siesjö, A. Darabi, E. Shardlow, and C. Exley, "Unequivocal identification of intracellular aluminium adjuvant in a monocytic THP-1 cellline," *Scientific Reports*, vol. 4, p. 6287, 2014.

[31] M. Mold, M. Kumar, A. Mirza, E. Shardlow, and C. Exley, "Intracellular tracing of amyloid vaccines through direct fluorescent labelling," *Scientific Reports*, vol. 8, no. 1, p. 2437, 2018.

[32] M. R. Schetinger, N. M. Porto, M. B. Moretto et al., "New benzodiazepines alter acetylcholinesterase and ATPDase activites," *Neurochemical Research*, vol. 25, pp. 949–955, 2000.

[33] D. Heymann, M. Reddington, and G. W. Kreutzberg, "Subcellular localization of 5′-nucleotidase in rat brain," *Journal of Neurochemistry*, vol. 43, no. 4, pp. 971–978, 1984.

[34] G. Giusti and B. Galanti, "Colorimetric method," in *Methods of Enzymatic Analysis*, H. U. Bergmeyer, Ed., pp. 315–323, Verlag Chemie, Berlin, Weinheim, Germany, 3rd edition, 1984.

[35] C. E. Assmann, F. C. Cadoná, B. S. R. Bonadiman, E. B. Dornelles, G. Trevisan, and I. B. M. da Cruz, "Tea tree oil presents *in vitro* antitumor activity on breast cancer cells without cytotoxic effects on fibroblasts and on peripheral blood mononuclear cells," *Biomedicine & Pharmacotherapy*, vol. 103, pp. 1253–1261, 2018.

[36] N. Rebola, P. C. Pinheiro, C. R. Oliveira, J. O. Malva, and R. A. Cunha, "Subcellular localization of adenosine A (1) receptors in nerve terminals and synapses of the rat hippocampus," *Brain Research*, vol. 987, no. 1, pp. 49–58, 2003.

[37] M. M. Bradford, "A rapid and sensitive method for the quantitation of microgram quantities of protein utilizing the principle of protein-dye binding," *Analytical Biochemistry*, vol. 72, no. 1-2, pp. 248–254, 1976.

[38] A. Henn, S. Lund, M. Hedtjärn, A. Schrattenholz, P. Pörzgen, and M. Leist, "The suitability of BV2 cells as alternative model system for primary microglia cultures or for animal experiments examining brain inflammation," *ALTEX*, vol. 26, no. 2, pp. 83–94, 2009.

[39] V. V. Miron, N. B. Bottari, C. E. Assmann et al., "Physical exercise prevents alterations in purinergic system and oxidative status in lipopolysaccharide-induced sepsis in rats," *Journal of Cellular Biochemistry*, vol. 120, no. 3, pp. 3232–3242, 2018.

[40] R. F. Zanin, E. Braganhol, L. S. Bergamin et al., "Differential macrophage activation alters the expression profile of NTPDase and ecto-5′-nucleotidase," *PLoS One*, vol. 7, no. 2, article e31205, 2012.

[41] T. Kiss, K. Gajda-Schrantz, and P. F. Zatta, "The role of aluminum in neurotoxic and neurodegenerative processes," *In: Neurodegenerative Diseases and Metal Ions*, vol. 1, pp. 371–393, 2006.

[42] E. Rezabal, J. M. Mercero, X. Lopez, and J. M. Ugalde, "Protein side chains facilitate Mg/Al exchange in model protein binding sites," *ChemPhysChem*, vol. 8, no. 14, pp. 2119–2124, 2007.

[43] P. Cardiano, C. Foti, F. Giacobello, O. Giuffrè, and S. Sammartano, "Study of Al^{3+} interaction with AMP, ADP and ATP in aqueous solution," *Biophysical Chemistry*, vol. 234, pp. 42–50, 2018.

[44] A. R. Barros-Barbosa, F. Ferreirinha, Â. Oliveira et al., "Adenosine A2A receptor and ecto-5′-nucleotidase/CD73 are upregulated in hippocampal astrocytes of human patients with mesial temporal lobe epilepsy (MTLE)," *Purinergic Signalling*, vol. 12, no. 4, pp. 719–734, 2016.

[45] M. Carmo, F. Q. Gonçalves, P. M. Canas et al., "Enhanced ATP release and CD73-mediated adenosine formation sustain adenosine A2A receptor over-activation in a rat model of Parkinson's disease," *British Journal of Pharmacology*, vol. 176, no. 18, pp. 3666–3680, 2019.

[46] F. Q. Gonçalves, J. P. Lopes, H. B. Silva et al., "Synaptic and memory dysfunction in a β-amyloid model of early Alzheimer's disease depends on increased formation of ATP-derived extracellular adenosine," *Neurobiology of Disease*, vol. 132, article 104570, 2019.

[47] R. A. Cunha, "Neuroprotection by adenosine in the brain: from A1 receptor activation to A2A receptor blockade," *Purinergic Signalling*, vol. 1, no. 2, pp. 111–134, 2005.

[48] R. A. Cunha, "How does adenosine control neuronal dysfunction and neurodegeneration?," *Journal of Neurochemistry*, vol. 139, no. 6, pp. 1019–1055, 2016.

[49] S. D. Skaper, P. Debetto, and P. Giusti, "The P2X7 purinergic receptor: from physiology to neurological disorders," *FASEB Journal*, vol. 24, no. 2, pp. 337–345, 2009.

[50] J. G. McLarnon, J. K. Ryu, D. G. Walker, and H. B. Choi, "Upregulated expression of purinergic P2X(7) receptor in Alzheimer disease and amyloid-beta peptide-treated microglia and in peptide-injected rat hippocampus," *Journal of Neuropathology and Experimental Neurology*, vol. 65, no. 11, pp. 1090–1097, 2006.

[51] H. B. Choi, J. K. Ryu, S. U. Kim, and J. G. McLarnon, "Modulation of the purinergic P2X7 receptor attenuates lipopolysaccharide-mediated microglial activation and neuronal damage in inflamed brain," *Journal of Neuroscience*, vol. 27, no. 18, pp. 4957–4968, 2007.

[52] I. Baranowska-Bosiacka, B. Dąbrowska-Bouta, and L. Strużyńska, "Regional changes in purines and selected

purinergic receptors in immature rat brain exposed to lead," *Toxicology*, vol. 279, no. 1-3, pp. 100–107, 2011.

[53] N. Li, P. Zhang, M. Qiao, J. Shao, H. Li, and W. Xie, "The effects of early life lead exposure on the expression of P2X7 receptor and synaptophysin in the hippocampus of mouse pups," *Journal of Trace Elements in Medicine and Biology*, vol. 30, pp. 124–128, 2015.

[54] M. Colella, M. Zinni, J. Pansiot et al., "Modulation of microglial activation by adenosine A2a receptor in animal models of perinatal brain injury," *Frontiers in Neurology*, vol. 9, p. 605, 2018.

[55] A. G. Orr, A. L. Orr, X.-J. Li, R. E. Gross, and S. F. Traynelis, "Adenosine A2A receptor mediates microglial process retraction," *Nature Neuroscience*, vol. 12, no. 7, pp. 872–878, 2009.

[56] N. Rebola, A. P. Simões, P. M. Canas et al., "Adenosine A2A receptors control neuroinflammation and consequent hippocampal neuronal dysfunction," *Journal of Neurochemistry*, vol. 117, no. 1, pp. 100–111, 2011.

[57] J. Stockwell, E. Jakova, and F. S. Cayabyab, "Adenosine A1 and A2A receptors in the brain: current research and their role in neurodegeneration," *Molecules*, vol. 22, no. 4, p. 676, 2017.

[58] R. Franco and G. Navarro, "Adenosine A2A receptor antagonists in neurodegenerative diseases: huge potential and huge challenges," *Frontiers in Psychiatry*, vol. 9, p. 68, 2018.

[59] S. Giunta, V. Andriolo, and A. Castorina, "Dual blockade of the A1 and A2A adenosine receptor prevents amyloid beta toxicity in neuroblastoma cells exposed to aluminum chloride," *The International Journal of Biochemistry & Cell Biology*, vol. 54, pp. 122–136, 2014.

Hindawi
Journal of Immunology Research
Volume 2021, Article ID 4678087, 18 pages
https://doi.org/10.1155/2021/4678087

Research Article

Yangxue Jiedu Fang Ameliorates Psoriasis by Regulating Vascular Regression via Survivin/PI3K/Akt Pathway

Hongpeng Lv,[1,2] Xin Liu,[1,3] Weiwen Chen,[1,2] Shiju Xiao,[1,4] Yunrun Ji,[1] Xuyang Han,[1,3] Yafan Li,[1,2] Xiaoxu Wang,[1,4] Guangzhong Zhang,[1] and Ping Li[1,3]

[1]*Beijing Hospital of Traditional Chinese Medicine, Capital Medical University, Beijing 100010, China*
[2]*Beijing University of Chinese Medicine, Beijing 100029, China*
[3]*Beijing Institute of Traditional Chinese Medicine, Beijing 100010, China*
[4]*Graduate School, Capital Medical University, Beijing 100069, China*

Correspondence should be addressed to Guangzhong Zhang; guangzhzh@163.com and Ping Li; liping61871@sina.com

Received 24 April 2020; Accepted 18 December 2020; Published 18 January 2021

Academic Editor: Cristina R. Reschke

Background. Psoriasis (PA) is a chronic autoimmune disease of the skin that adversely affects patients' quality of life. Yangxue Jiedu Fang (YXJD) has been used for decades to treat psoriasis in China. However, its antipsoriatic mechanisms are still poorly understood. In this study, we explored the effects of YXJD on angiogenesis and apoptosis of microvessels in PA, the underlying mechanisms in HUVEC cells transfected by Survivin overexpression plasmid and in a mouse model of imiquimod-induced psoriasis and the relationship between VEGF (vascular endothelial growth factor) and Survivin. *Methods*. A BALB/c mouse model of imiquimod- (IMQ-) induced PA was established, and the mice were treated with YXJD. Cell viability was assessed by CCK8 assay. Apoptosis was detected by annexin V–FITC/PI double-staining and caspase-3 assays. The PI3K/Akt/β-catenin pathway was analyzed by western blotting, ELISA, and immunochemical analysis. *Results*. YXJD ameliorated symptoms and psoriasis area and severity index (PASI) scores and also reduced the number of microvessels, as determined by the microvessel density (MVD). The expression of apoptotic protein Survivin in endothelial cells, autophagy-related proteins p62, and angiogenic proteins VEGF was inhibited by YXJD, and the repressed expression of LC3II/I increased by YXJD. The proteins related to the PI3K/Akt pathway and β-catenin expression and the nuclear entry of β-catenin were reduced in IMQ-induced PA mice treated with YXJD. In HUVEC cells transfected by Survivin overexpression plasmid, we observed YXJD regulated the expression of Survivin, LC3II/I, and p62, VEGF, and PI3K/Akt pathway-relative proteins and the nuclear entry of β-catenin. *Conclusions*. YXJD inhibited the expression of Survivin via PI3K/Akt pathway to adjust apoptosis, autophagy, and angiogenesis of microvessels and thus improve the vascular sustainability in psoriasis. YXJD may represent a new direction of drug research and development for immunomodulatory therapy for psoriasis.

1. Introduction

Psoriasis (PA) is a chronic, autoimmune skin disease that is recognized as a major global health problem by the World Health Organization, and it affects 2-4% of the population [1]. PA is characterized by hyperkeratosis, an increased number of microvessels, tortuous morphology, and the infiltration of lymphocytes around the superficial blood vessels of the dermis [2]. Apoptosis/autophagy and angiogenesis in microvessels of the dermis of normal skin are balance. In psoriatic lesions, the disorder in vascular regression, which is the result of microvessels apoptosis, autophagy, and angiogenesis, results in red plaques on the skin.

Our previous study shows several specific plasma miRNA-targeted pathways associated with psoriasis, such as the VEGF, PI3K/Akt, and WNT signaling pathways, which are regulating angiogenesis in psoriasis [3]. We also found the amelioration in angiogenesis restricted the occurrence, persistence, and recurrence of psoriasis. Yangxue Jiedu Fang (YXJD), a Chinese traditional formula used in the clinic to treat PA in China, was previously evaluated by double-blind randomized controlled clinical trials, and its total

effective rate was found to be 67.09% [4]. Our previous experimental studies showed that YXJD can reduce the expression of VEGF, VEGFR, and related mRNAs via the ERK/NF-κB pathway and inhibit the proliferation and migration of HDMECs, which plays a therapeutic role in the pathology of angiogenesis in psoriasis [5]. The active ingredients of YXJD can inhibit angiogenesis. The total flavonoids of purified methanol extracts of *Spatholobi caulis* (one of the herbs in YXJD) (PSC) present proangiogenic activity both in zebrafish and HUVECs [6]. Tanshinone IIA (the main active ingredient of *Salvia miltiorrhiza*, which is one of the herbs in YXJD) effectively inhibits the secretion of VEGF and bFGF in HUVECs and a mouse colon tumor model and can suppress proliferation, tube formation, and metastasis in vitro [7].

Overexpressing Survivin tumor cells induce the synthesis and secretion of VEGF as well as microvascular hyperplasia [8]. Survivin is currently the strongest known inhibitor of apoptosis. It can inhibit apoptosis by inhibiting the signaling pathway regulated by the caspase family of apoptotic proteins [9]. The expressions of Survivin, VEGF, and Akt in keratinocytes of psoriatic lesions in humans were significantly upregulated, and the expression of Survivin and Akt gradually elevated with the increase of PASI score. Survivin increased β-catenin-Tcf/Lef transcription through the PI3K/Akt pathway and promoted the generation of VEGF, thereby promoting tumor microvessel formation induced by the secretion of VEGF [10], which we call Survivin/PI3K/AKT pathway. However, it is still unclear whether Survivin can interfere with the PI3K/Akt pathway leading to the occurrence and development of psoriasis. Other research shows the herbs in YXJD can also promote apoptosis. *Spatholobi caulis* tannin (SCT) can mediate related circRNAs to inhibit proliferation and promote apoptosis in HeLa cells, as determined by techniques such as bioinformatics analysis of relevant genes [11]. Tanshinone IIA can also inhibit the activity of the PI3K/AKT pathway and the expression of VEGFR, GSK-3β, and apoptosis-related proteins such as Bax, Bcl-2, and caspase-3 in vitro [12–14].

In this study, we investigated the effects of YXJD on apoptosis/autophagy and angiogenesis in vivo and vitro and its underlying mechanisms via the Survivin/PI3K/AKT pathway. Mouse model was established by imiquimod (IMQ) and in cell experiment HUVEC cells transfected with Survivin overexpression plasmid.

2. Materials and Methods

2.1. Animal. Twenty-four specific pathogen-free (SPF) male BALB/c mice (19 to 21 g, 8 week-old) were purchased from the Beijing WTLH Experimental Animal Technology Co., Ltd., (China) (certification No. SCXK (Beijing) 2012-0001). Mice were housed in the SPF conditions with a relative humidity of 60% and at a temperature of 25°C and had free access to food and water. All animal experiments were performed in accordance with the National Institutes of Health Guidelines on Laboratory Research and approved by the Animal Care Committee of Capital Medical University, Beijing, China (approval number: 2019060201).

2.2. Preparation of Herb Extract. The preparation of YXJD contains 10 kinds of traditional Chinese herbal medicine, which are *Salvia miltiorrhiza Bge* (15 g; Beijing Xinglin Pharmaceutical Co. Ltd., Beijing, China), *Angelica Sinensis* (15 g; Beijing Xinglin Pharmaceutical Co. Ltd., Beijing, China), *Rehmannia glutinosa Libosch* (15 g; Beijing Xinglin Pharmaceutical Co. Ltd., Beijing, China), *Ophiopogon japonicus* (10 g; Beijing Xinglin Pharmaceutical Co. Ltd., Beijing, China), Scrophularia ningpoensis Hemsl (15 g; Beijing Xinglin Pharmaceutical Co. Ltd., Beijing, China), *Spatholobi Caulis* (15 g; Beijing Xinglin Pharmaceutical Co. Ltd., Beijing, China), *Smilax glabra Roxb*. (15 g; Beijing Xinglin Pharmaceutical Co. Ltd., Beijing, China), *Paris polyphylla* (9 g; Beijing Xinglin Pharmaceutical Co. Ltd., Beijing, China), *Wrightia laevis* (15 g; Beijing Xinglin Pharmaceutical Co. Ltd., Beijing, China), seed of Asiatic plantain (15 g; Beijing Xinglin Pharmaceutical Co. Ltd., Beijing, China). The herbs were decocted with pure water boiled for 1.5 h (1500 mL). Filtered water extract was concentrated to 513 mg/mL under reduced pressure and then reconstituted in distilled water to achieve the required dose for all subsequent experiments.

2.3. Fingerprint Analysis of YXJD through Ultraperformance Liquid Chromatography-Tandem Mass Spectrometry (UPLC-MS/MS). UPLC-MS/MS was used to analyze the chemical composition and the stability of YXJD. Chromatographic analysis was performed (Agilent Technologies, USA) on a XS205 Triple Quadrupole Mass Spectrometer (Mettler Toledo Technologies, USA). The analytes of YXJD were separated on a ACQUITY UPLC BEH C18 column (2.1 mm × 5 mm, 1.8 μm) with a mobile phase consisting of acetonitrile (A) and 0.1% aqueous solution of formic acid (B); the following gradient program was used: 2% A–27% A at 0–8.5 min, 27% A–100% A at 8.5–10 min, 100% A–2% A at 10–13 min. The injection volume was 5 μL, the flow rate is 0.4 mL/min, and the column temperature was 45°C.

2.4. Preparation of Psoriasis Mice Models and Drug Administration. The mice were randomly separated into the following four groups (six mice per group) including the control group, psoriasis model group, YXJD group (10 mL/kg), and cyclosporin group (80 mg/kg). Psoriasis model, a model of IMQ-induced psoriasis, was established by administering a daily topical dose of 62.5 mg of a cream preparation containing 5% IMQ (Mingxinlidi Laboratory, China) on the hair-free back of the mice, in which the area size is 3 cm × 4 cm [13]. Mice in the control group were smeared with the same dose of Vaseline (Baotou Kunlun Petrochemical Co., Ltd.) once a day continuously for 6 days and was orally administered daily with 10 mL/kg saline twice a day. Except for the control group, the other three groups were all established the psoriasis model by applying IMQ continuously for 6 days. The psoriasis model group was given saline (10 mL/kg) intragastrically until the detection time point. The YXJD group was orally administered with YXJD twice per day (10 mL/kg); the cyclosporin group was applied cyclosporine A capsule (Solarbio) one time every 3 days on the day of the first cream application. After six days, mice were sacrificed by cervical dislocation under sodium pentobarbital

anesthesia, and skin lesions and serum samples were collected. The corresponding skin lesions were cut off in each group, some of them were fixed in 10% formaldehyde solution to prepare paraffin sections, and the other parts were placed in the refrigerator at-80°C.

2.5. Evaluation of Lesion Symptoms. Psoriasis Area Severity Index (PASI) as a modified scoring system for monitoring the severity was used in the study. Erythema, scaling, and thickening were scored independently on a scale from 0 to 4: 0, none; 1, slight; 2, moderate; 3, marked; 4, very marked. The level of erythema was scored using a scoring table with red taints. The cumulative score (erythema plus scaling plus thickening) served as a measure of the severity of inflammation (scale 0–12). At the days indicated, the ear thickness of the right ear was measured in duplicate using a micrometer (Mitutoyo).

2.6. MVD. Skin samples from the back lesions of mice were collected in 4% paraformaldehyde and embedded in paraffin. Sections (4 μm) were added anti-Rabbit CD31 and goat anti-rabbit secondary antibodies and then observed the number of microvessels under a microscope (Olympus, Japan).

2.7. Cell Culture. The HUVEC and HaCaT cell lines were obtained from the Cell Culture Unit of Shanghai Science Academy (Shanghai, China). The cells were incubated with MEM (Gibco, USA)—containing 10% FBS (Hyclone, USA) at 37°C.

2.8. Western Blotting and Elisa. Skin samples were lysed, and the proteins were resolved in 10% SDS-PAGE. The membrane fraction was incubated with mouse-antitotal or phosphorylated Akt, GSK3-β, β-catenin, VEGF and Survivin antibodies, and rabbit-anti-β-actin antibody (Santa Cruz, CA), then IRDye 700DX- or 800DX-conjugated secondary antibodies (Rockland Inc., Gilbertsville, PA). Supernatant levels of total VEGF and Survivin were measured via enzyme-linked immunosorbent assay (ELISA) according to the manuals of VEGF and Survivin Elisa Assay kits (Nanjing Jiancheng Bioengineering Institute, Nanjing, China).

2.9. Immunochemical Staining and Immunofluorescence Staining. Skin samples from the dorsal lesions of mice were collected in 10% formalin and embedded in paraffin. Sections (5 μm) were stained with hematoxylin and eosin (HE) and anti-Rabbit CD31, 4′,6-diamidino-2-phenylindole(DAPI), involucrin, and β-catenin, VEGF, and Survivin antibodies (Abcam, USA) diluted 1 : 100, and staining was assessed using light and fluorescence microscopes (Olympus, Japan).

2.10. Real-Time Polymerase Chain Reaction (RT-PCR). Total RNA was extracted from skin lesions using TRIzol (Invitrogen, USA) and purified using a NucleoSpin RNA Clean-up Kit (Macherey-Nagel, Germany). Complementary DNA was generated using an Affinity Script Multiple Temperature cDNA Synthesis Kit (Agilent Technologies, USA) and specific primers (Homo VEGF: forward: 5'-ATCCAATCGAGACCCTGGTG -3', reverse: 5'-ATCTCTCCTATGTGCTGGCC -3';Homo GAPDH: forward: 5'- TCAAGAAGGTGGTGAAGCAGG -3', reverse: 5'- TCAAAGGTGGAGGAGTGGGT -3'.), and the relative expression levels of genes were determined with an ABI 7500 Fast Real-Time PCR System using a real-time PCR master mix (Roche, USA). The actin gene was used as a reference to normalize the data.

2.11. Flow Cytometric Quantification of Apoptosis. HUVEC cells were harvested to assess apoptosis. After two washes with PBS at 1500 rpm for 5 min, the cells were resuspended in 500 μL of Binding Buffer and mix 5 Annexin V-FITC (KeyGen Biotech, Nanjing) with 5 μl PI (KeyGen Biotech, Nanjing) at room temperature for 5-15 min to light avoidance reaction (control group: normal cells without Annexin V-FITC and PI). Finally, the samples were analyzed using a FACSCalibur flow cytometer (Beckman, USA).

2.12. Cell Viability Assays. Cell viability was assessed using the Cell Counting Kit-8 (CCK8) assay (Beyotime C0037, USA). 10 μL CCK8 was added to each well and incubated at 37°C for 4 h. The absorbance value of each well was detected by a microplate reader (Thermo Multiskan MK3, USA).

2.13. Statistical Analysis. The results were analyzed using SPSS for Windows version 21.0 (SPSS, Chicago, IL, USA) and expressed as mean ± standard deviation (SD). Between-group comparisons were performed using one-way ANOVA and analyzed by LSD t-test (when equal variances are assumed), and $P < 0.05$ indicated statistical significance.

3. Results

3.1. YXJD Fingerprint. The components of 10 groups of YXJD consisting of different batches of herbs were analyzed by UPLC-MS/MS. Figure 1(a) shows the total ion chromatograms of the 5 groups of standard samples; Figure 1(b) shows the total ion chromatograms of YXJD which displayed a high degree of similarity. As shown in Figure 1(c), 25 peaks in the total ion chromatograms of YXJD were assigned as common peaks, and the relative standard deviations of the relative retention time (RRT) of these 25 common peaks were lower than 1.0%, indicating that the RRTs of the 25 components are comparatively stable.

3.2. YXJD Ameliorated PASI Scores in a Mouse Model of PA. On the 5th day after the establishment of the psoriasis-like model, the psoriasis group exhibited inflamed thickened patches covered with silvery scales (Figure 2(a)). PASI scores were determined to evaluate the therapeutic effect of YXJD. The PASI score of the model group increased compared with the control group (Figure 2(b)) ($P < 0.01$). The PASI scores of the YXJD group and cyclosporin-A group were significantly lower than the score of the model group, demonstrating YXJD had a therapeutic effect on PASI scores in the PA mouse model, and its effect was equal to cyclosporin-A, which has a curative effect.

3.3. YXJD Improved Histomorphology in a Mouse Model of PA. HE staining was conducted to evaluate the effect of YXJD on histopathological changes in the lesion. The HE results (Figure 2(c)) show that the epidermal layer in the model

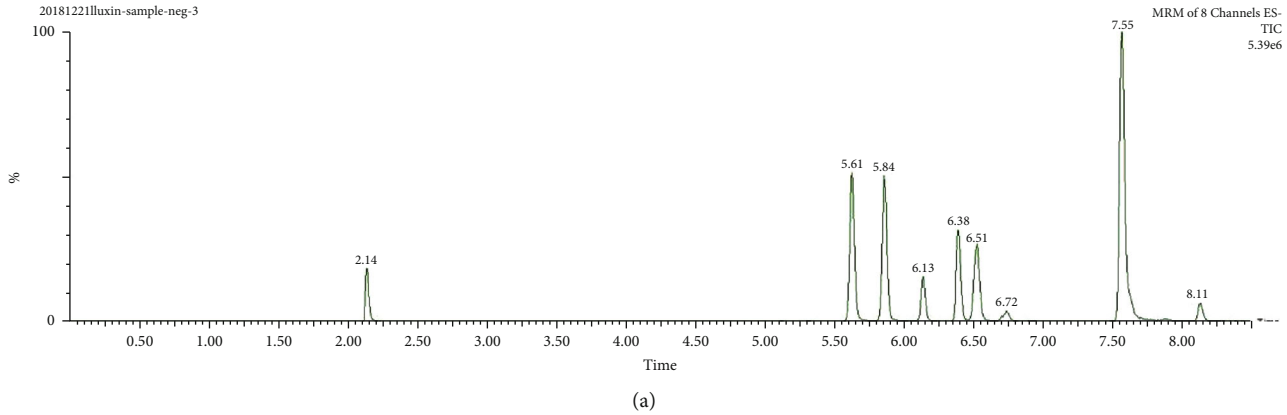

(a)

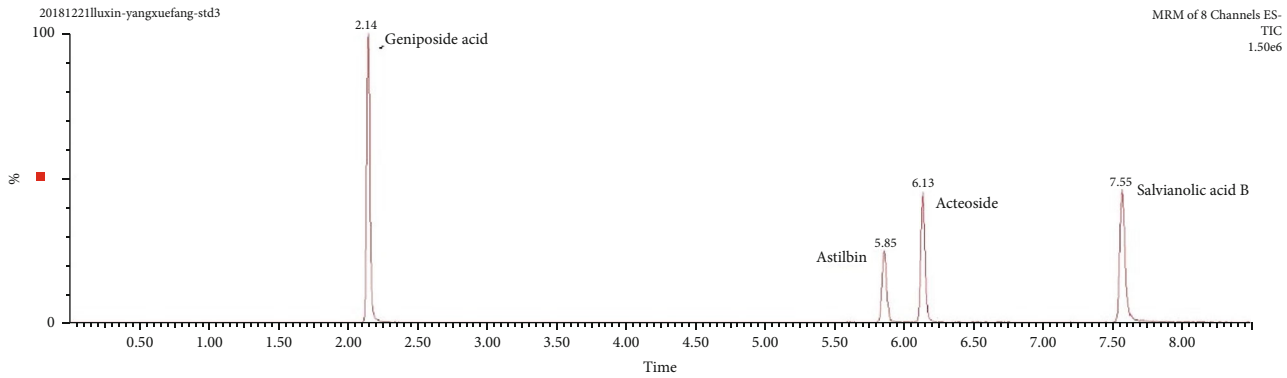

(b)

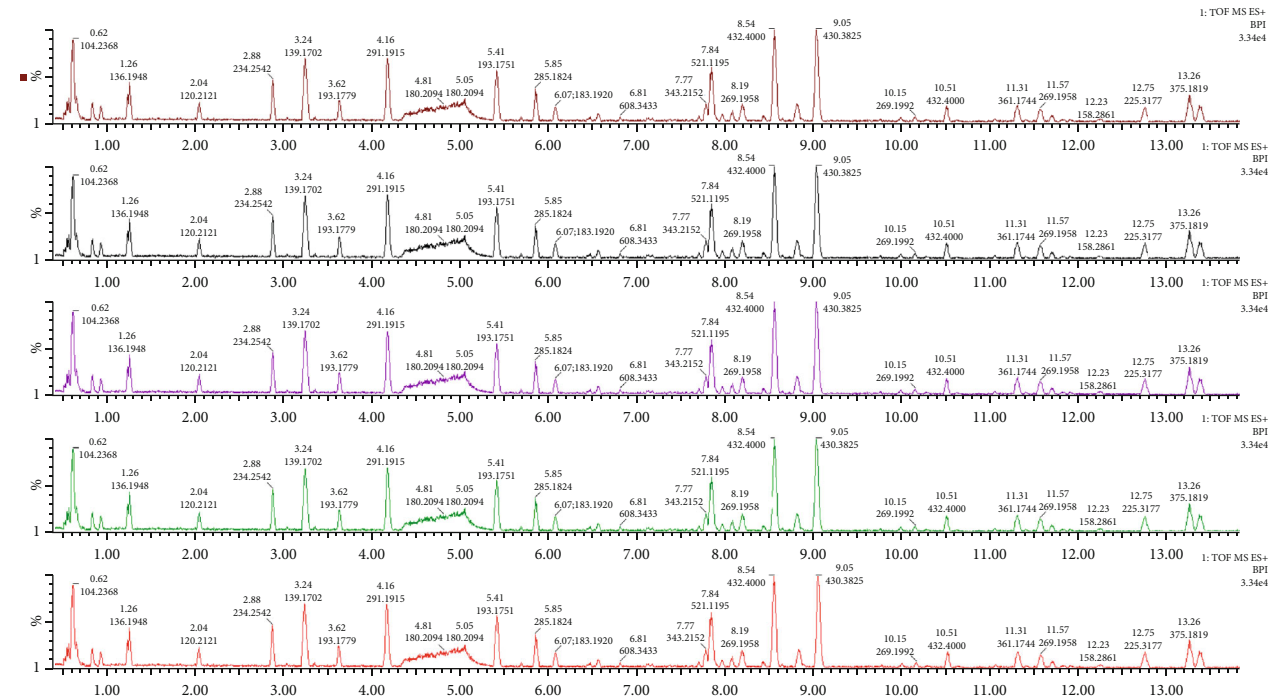

(c)

Figure 1: Continued.

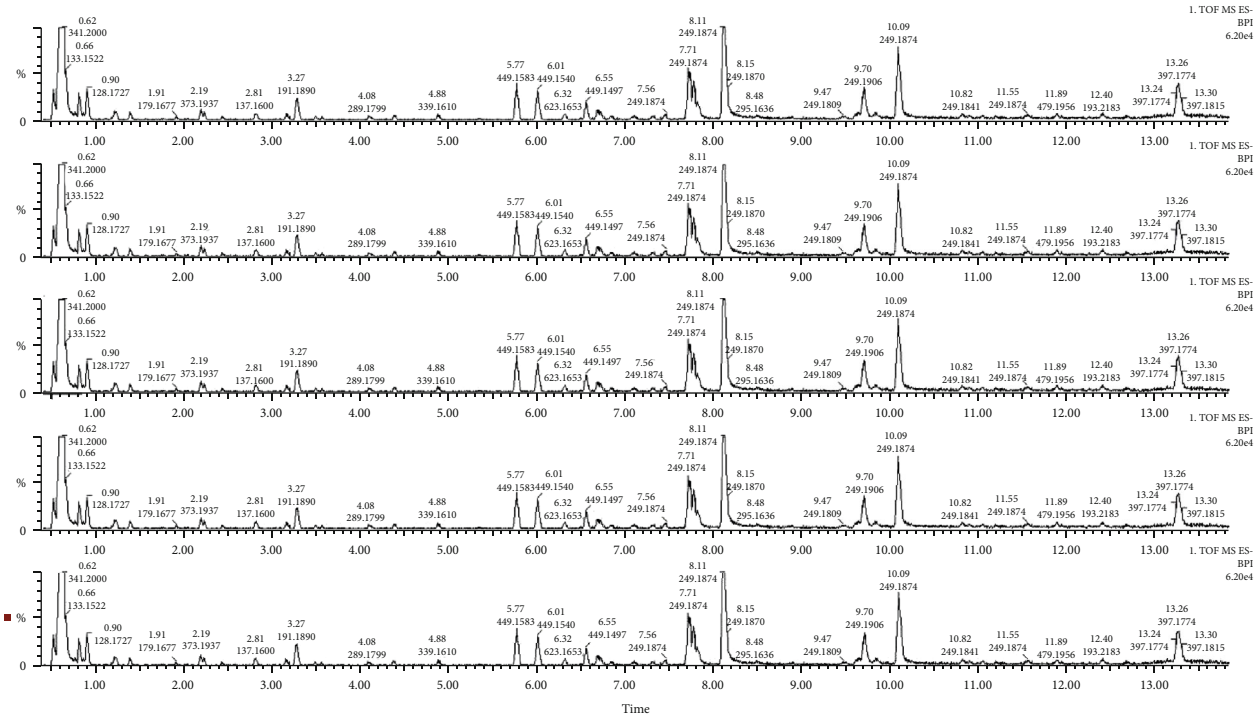

(d)

Figure 1: Total ion chromatograms of YXJD. Five groups of YXJD consisting of different batches were diluted to 0.06 g/mL and precipitated with an equal amount of methanol. The supernatants were obtained by centrifugation (10000 rpm) for 40 min and analyzed by UPLC-MS/MS using a mobile phase consisting of acetonitrile and 0.1% formic acid aqueous solution with a gradient program. The external standard one-point method was used to calculate the sample content based on the following formula: control sample injection quantity/sample peak area = sample injection quantity/sample peak area (a, b). Total ion flow in ESI positive mode. Counts (%) versus acquisition time (min) (c). Total ion flow in ESI anion mode. Counts (%) versus acquisition time (min) (d).

group was obviously thicker and with incomplete keratinization. In the upper dermis, inflammatory cells infiltrated around capillaries, and the number of tortuous capillaries increased. The histological manifestations were psoriatic lesions in both the epidermis and dermis. However, YXJD and cyclosporin significantly reduced the thickness of the lesions in the IMQ-induced PA model.

3.4. YXJD Inhibited Microvessel Density (MVD) in a Mouse Model of PA. The number of microvessels was evaluated by measuring the microvessel density (MVD). The MVD in the lesions of the model group was increased compared with that in the control group, but the MVD was decreased distinctly in the groups treated with YXJD and cyclosporin. It showed that YXJD can reduce the number of microvessels, which might be a therapeutic mechanism for the treatment of psoriasis (Figure 2(e)).

3.5. YXJD Reduced the Levels of Survivin in a Mouse Model of PA. Survivin can affect the apoptosis of microvessels. The level of Survivin was increased in the psoriasis-like model mice (Figures 3(a) and 3(b)), and Survivin was mainly localized to the endothelial cells in the dermis (Figure 3(c)). YXJD inhibited the excessive expression of Survivin and had the same effect as that of cyclosporin.

3.6. The PI3K/Akt Pathway Mediated the Inhibitory Effects of YXJD in a Mouse Model of Psoriasis. PI3K/Akt signaling interferes with important activities such as the apoptosis and proliferation of cells. Compared with those in the control group, the levels of Akt and GSK3-β phosphorylation and nonphosphorylated β-catenin were increased, as detected by Western blotting in the model group. The expression of the abovementioned proteins was decreased in the lesions of psoriasis-like mice treated with YXJD. YXJD and cyclosporin did not change the levels of Akt or GSK3-β phosphorylation, but cyclosporin had a stronger effect than YXJD in decreasing the expression of β-catenin (Figures 4(a)–4(d)). Immunochemical staining and immunofluorescence analysis of the nuclear entry of β-catenin in lesions showed that the number of endothelial cells in microvessels (CD31-labelled) increased in the lesions of IMQ-induced PA model mice; β-catenin was mainly observed in epidermal keratinocytes and endothelial cells in microvessels in the dermis (Figure 4(e)), but in YXJD-treated mice, the nuclear entry of β-catenin was reduced. These results suggest that YXJD might inhibit cell activity through a molecular mechanism involving the inhibition or interruption of the PI3K/Akt pathway to ameliorate the symptoms of PA model mice.

3.7. YXJD Reduced the Levels of VEGF in a Mouse Model of PA. VEGF can affect the angiogenesis of microvessels. The

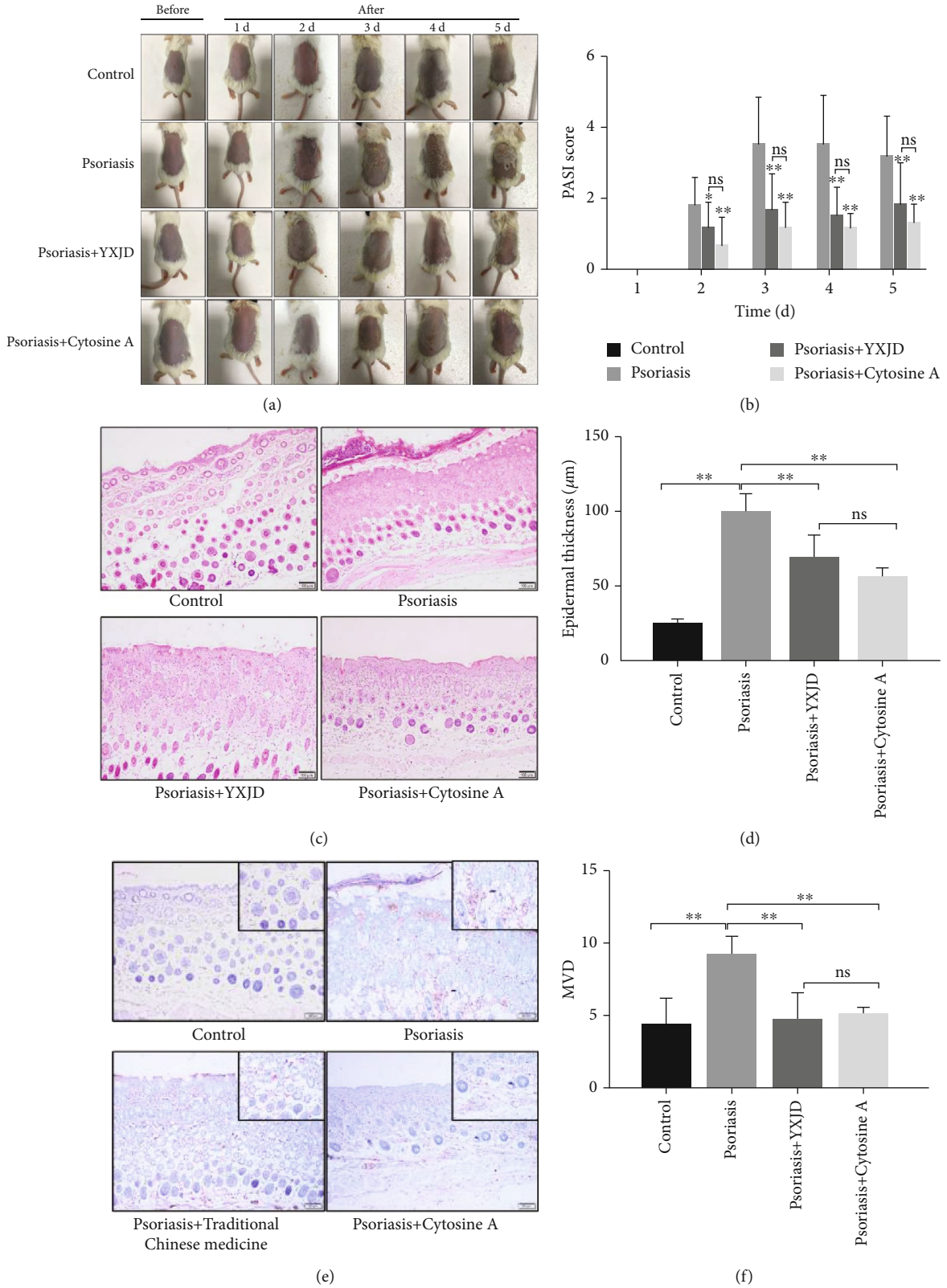

Figure 2: PASI scores, histomorphology, and MVD of the different groups. The effect of YXJD on IMQ-induced psoriasis-like lesions in mice (a). The PASI scores of the mice were evaluated from the 2nd day to the 5th day after model construction, and the PASI scores of each group were compared (b). The lesion samples were stained with hematoxylin and eosin (HE) (c), and the thickness was determined for each group (d). The microvessel density (MVD) of the four groups (e) was detected by immunocytochemistry. Bar = 100 μm. $^*P < 0.05$ vs. the model mice. The difference in MVD among the 4 groups showed that MVD in the group treated with YXJD was reduced (f).

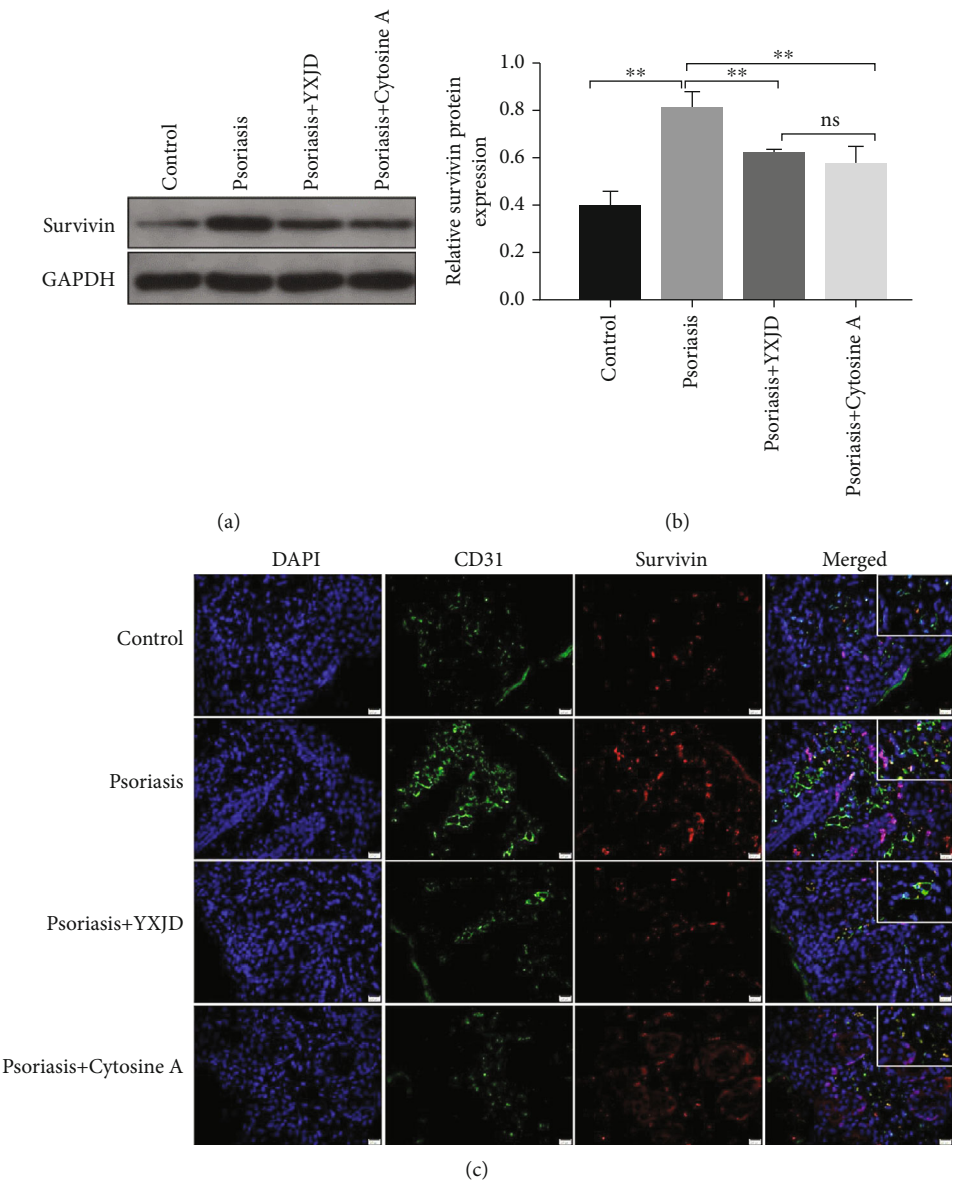

Figure 3: Protein levels and localization of Survivin, as detected by Western blot and immunochemical staining and immunofluorescence analysis. Survivin expression was evaluated by Western blotting (a). The expression of Survivin was increased in the model groups compared with the control groups, and YXJD inhibited the expression of Survivin in the lesions of IMQ-induced PA mice (b). Survivin protein expression in the mice was measured by immunochemical staining and immunofluorescence analysis (c). Double immunofluorescence staining for CD31 (green) and Survivin (red) in a representative skin sample from the 4 groups are shown. Nuclei were counterstained with DAPI (blue).

expression of VEGF in the model group was increased significantly compared with that in the control group (Figures 5(a) and 5(b).), and we observed the expression of VEGF in keratinocyte and endothelial cells in the psoriasis-like model mice (Figure 5(c)). YXJD inhibited the excessive expression of VEGF in the corneum as well as corium of the lesion.

3.8. YXJD Ameliorates the Suppression of Autophagy in a Mouse Model of PA. Autophagy-associated proteins, LC3II, LC3I, and p62 proteins, can show the occurrence of autophagy. The expression of LC3II/I protein in the model group was decreased compared with that in the control group (Figures 6(a) and 6(b)), while the expression of p62 protein, on the contrary, was significantly increased in the model group compared with the control group ($P < 0.05$) (Figures 6(a) and 6(c)). The downregulation of LC3II/I protein and upregulation of p62 protein demonstrate that the autophagy in psoriatic mice is significantly decreased. While the level of LC3II/I protein increased and p62 protein decreased in mouse model treated by YXJD and YXJD inhibited the excessive suppression of autophagy in PA lesions and had the same effect as that of cyclosporin, which suggests a decreased autophagic potential for YXJD.

3.9. The Effect of YXJD on HUVEC Cells Induced by Survivin and Its Molecular Mechanism. Survivin overexpression can

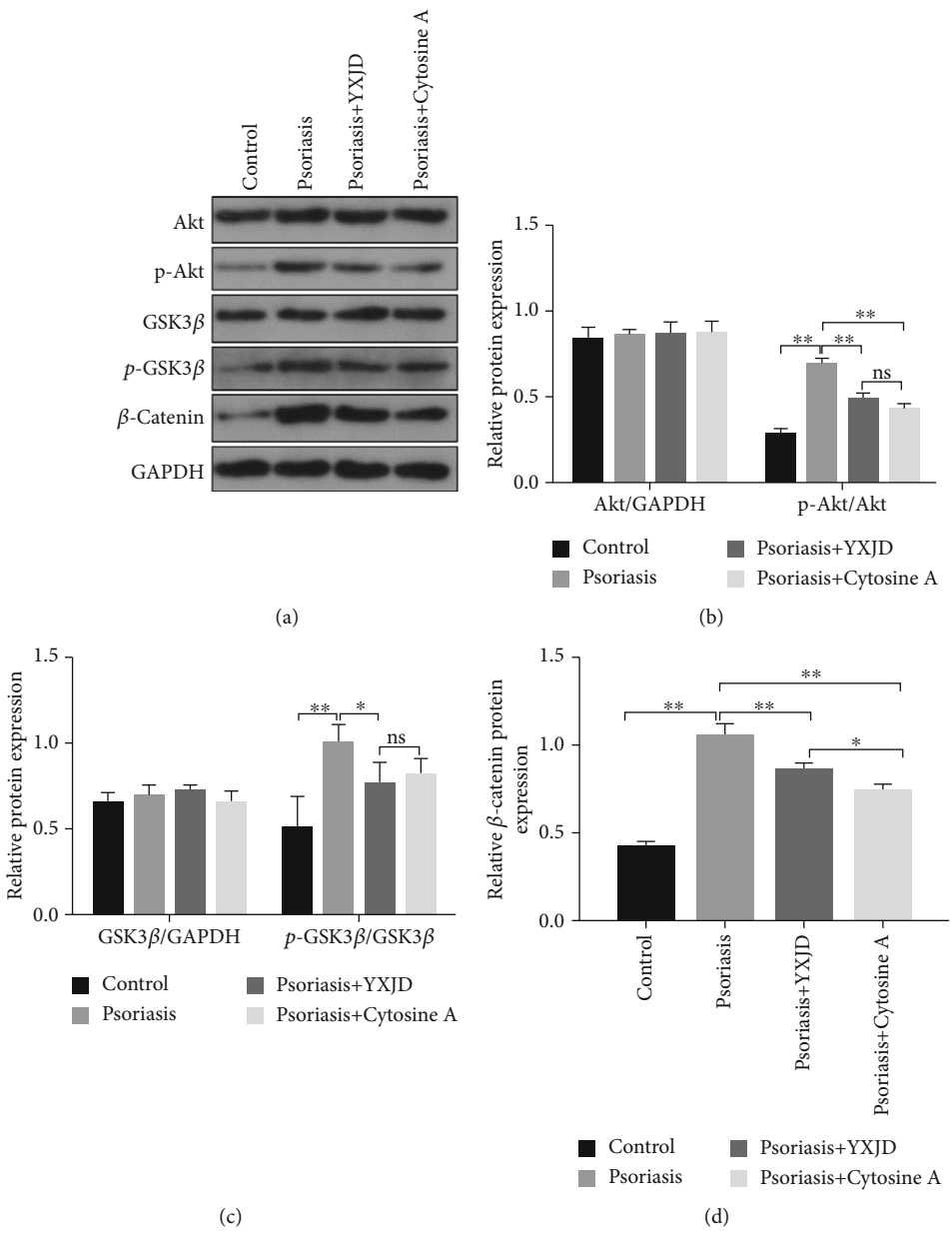

Figure 4: Continued.

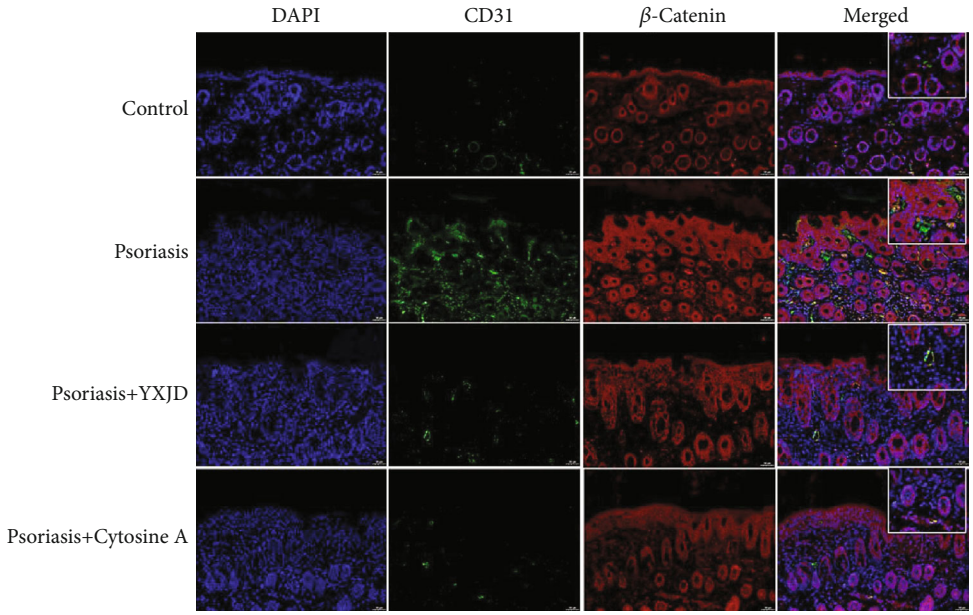

(e)

Figure 4: Protein levels of p-Akt, Akt, p-GSK3-β, GSK3-β, and β-catenin and the nuclear entry of β-catenin, as detected by Western blot, immunochemical staining, and immunofluorescence analysis YXJD inhibited the activation of the PI3K/Akt pathway. The levels of p-Akt, Akt, p-GSK3-β, GSK3-β, and β-catenin were reduced in YXJD-treated mice, as assessed by Western blotting (a–d). The nuclear entry of β-catenin (e) was decreased in the YXJD group mice compared with the model mice. Double immunofluorescence staining for CD31 (green) for vessels and β-catenin (red) in a representative skin sample from the 4 groups is shown. Nuclei were counterstained with DAPI (blue).

significantly increase cell viability, and different concentrations of YXJD can inhibit HUVEC cell viability, which is dose-dependent. After the preliminary experiment, we screened out the appropriate concentration of YXJD (1 mg/mL and 4 mg/mL) (the supplementary materials for details). In HUVEC cells transfected by Survivin overexpression plasmid (Survivin OE), we observed that the cell viability increased compared with the HUVEC cells transfected by normal control plasmid (NC), and when different concentrations of YXJD (0, 1, and 4 mg/mL) intervened into Survivin OE, we found YXJD could inhabit the cell viability (Figure 7(a)). The apoptosis level of Survivin OE with 4 mg/mL YXJD treatment group was significantly higher than Survivin OE with 1 mg/mL treatment group (Figures 7(b) and 7(c)).

Compared with the NC group, the migration ability of HUVEC cells rose after Survivin overexpression plasmid transfection, and YXJD could inhibit the increase of HUVEC cell migration caused by Survivin overexpression, and the inhibitory effect of a high concentration of YXJD on HUVEC cells migration was prominent ($P < 0.01$) (Figures 7(d) and 7(e)). In the Survivin OE group, the ability of HUVEC cells was increased as well as the meshes number and length of the master segment length (Figures 7(f)–7(h)). The tube formation ability of HUVEC cells decreased, and the lumen length became shorter induced by high concentrations of YXJD. Therefore, transfection of Survivin overexpression plasmid can increase the tube-forming ability of HUVEC cells, while YXJD inhibited the tube formation ability of HUVEC cells to a certain extent, and the inhibition of HUVEC cells migration induced by a high concentration of YXJD was enhanced. After Survivin overexpression plasmid transfection, the proportion of Survivin OE group in G0/G1 phase was evidently lower than that in the NC group, while that in S phase was opposite. The proportion of Survivin OE group treated with different concentrations of YXJD in G0/G1 phase was relatively increased and in S phase was decreased (Figures 7(i)–7(j)).

3.10. YXJD Inhibited the Expression of Survivin and the Decrease of Autophagy, PI3K/Akt Pathway Relative Proteins, and VEGF in HUVEC Cell Transfected Survivin Overexpression Plasmid. To observe the effect of YXJD on the expression of Survivin and the decrease of autophagy, PI3K/Akt pathway relative proteins, and VEGF, we detected the proteins by ELISA, Western blot, and qRT-PCR. The result indicated that the expression of Survivin, p62, PI3K/Akt pathway relative proteins, and VEGF relative expressions increased and LC3II/I decreased in the Survivin OE group. YXJD can inhibit the expression of Survivin and VEGF in a dose-dependent manner (Figures 8(a)–8(c)). For the expression of PI3K/Akt pathway relative proteins, the result showed that the expression of Akt and GSK3β protein in each group has no significant change in all groups, while in the Survivin OE group, the total protein content of p-Akt, p-GSK3β, β-catenin, and the entry of β-catenin into the nucleus promoted, on the contrary, Caspase3 shearing decreased. After being treated by YXJD, the phosphorylation level of Akt and GSK-3β and the content of β-catenin decreased and the shearing of Caspase3 increased, all of the

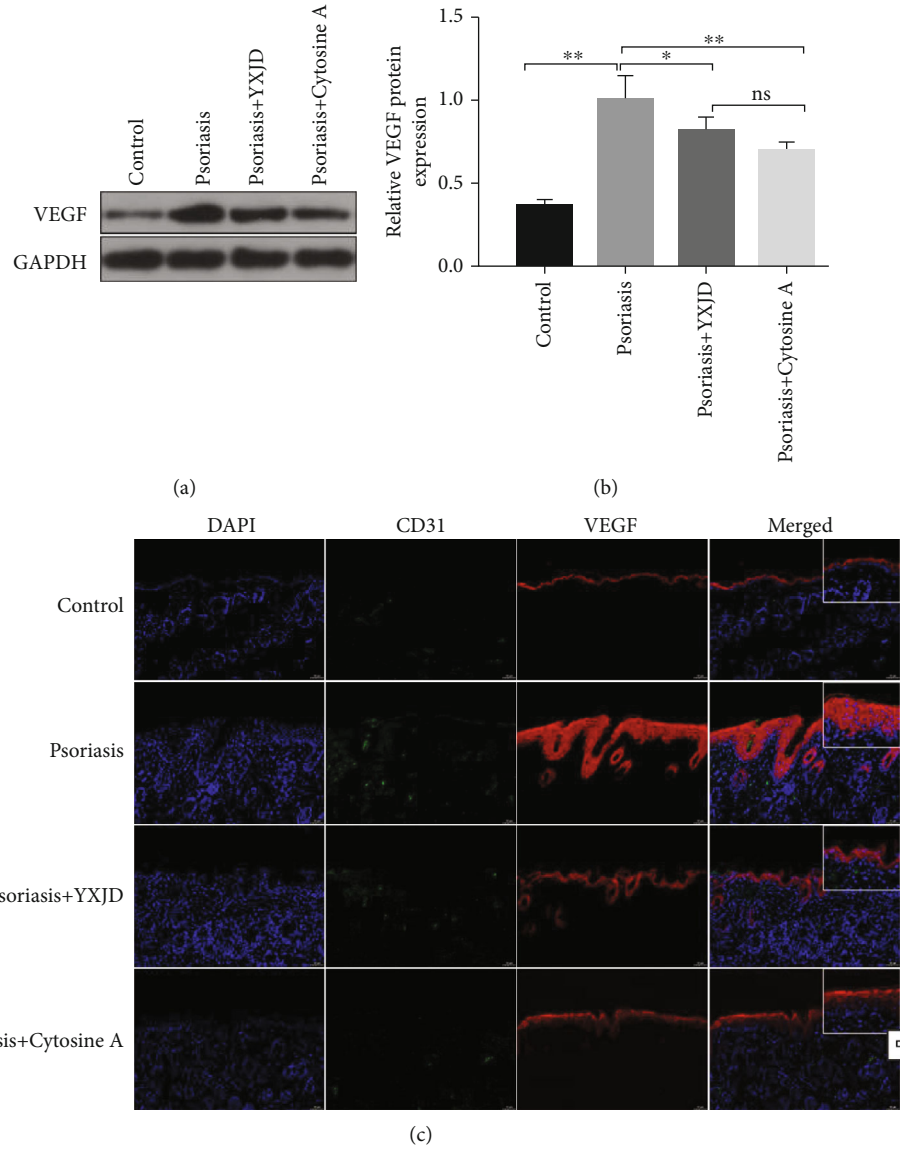

Figure 5: Protein levels and localization of VEGF, as detected by Western blot and immunochemical staining and immunofluorescence analysis VEGF expression, were evaluated by Western blotting (a). The expression of VEGF increased in the model groups compared with the control groups, and YXJD inhibited the expression of VEGF in the lesions of IMQ-induced PA mice (b). VEGF protein expression in the mice was measured by immunochemical staining and immunofluorescence analysis (d). Double immunofluorescence staining for CD31 (green), VEGF, and Survivin (red) in a representative skin sample from the 4 groups is shown. Nuclei were counterstained with DAPI (blue).

groups in a dose-dependent manner (Figure 8(e)). The expression of LC3II/I protein decreased, while the level of p62 increased in the Survivin OE group. YXJD could increase the content of LC3II/I and reduce the content of p62, which demonstrated YXJD could inhibit the downregulation of autophagy in HUVEC cells caused by the overexpression of Survivin (Figure 8(d)).

4. Discussion

Survivin is a member of the inhibitor family of apoptosis protein discovered by Ambrosini et al. in 1997 [15] and is currently the strongest protein that inhibits apoptosis. It participates in the inhibition of apoptosis by inhibiting the signaling pathway and regulating the apoptosis protein of the Caspase family, while interfering different cell cycles to participate in the mitotic activity of cells. The apoptosis of microvessels plays an important role in the occurrence and development of psoriasis. Abnormal apoptosis leads to a relative increase in the number of microvessels. In the terminal stage of psoriasis, stilled microvessels are related to the apoptosis inhibition of vascular endothelial cells. The process of apoptosis in psoriasis is regulated by several factors, such as the Bcl-2 family of proteins, the inhibitor of apoptosis (IAP) family of proteins, and the caspase family of proteins. Koch et al. [16] first discovered that the expression of Survivin is significantly increased in the lesions of psoriasis. Survivin can participate in the processes of angiogenesis and

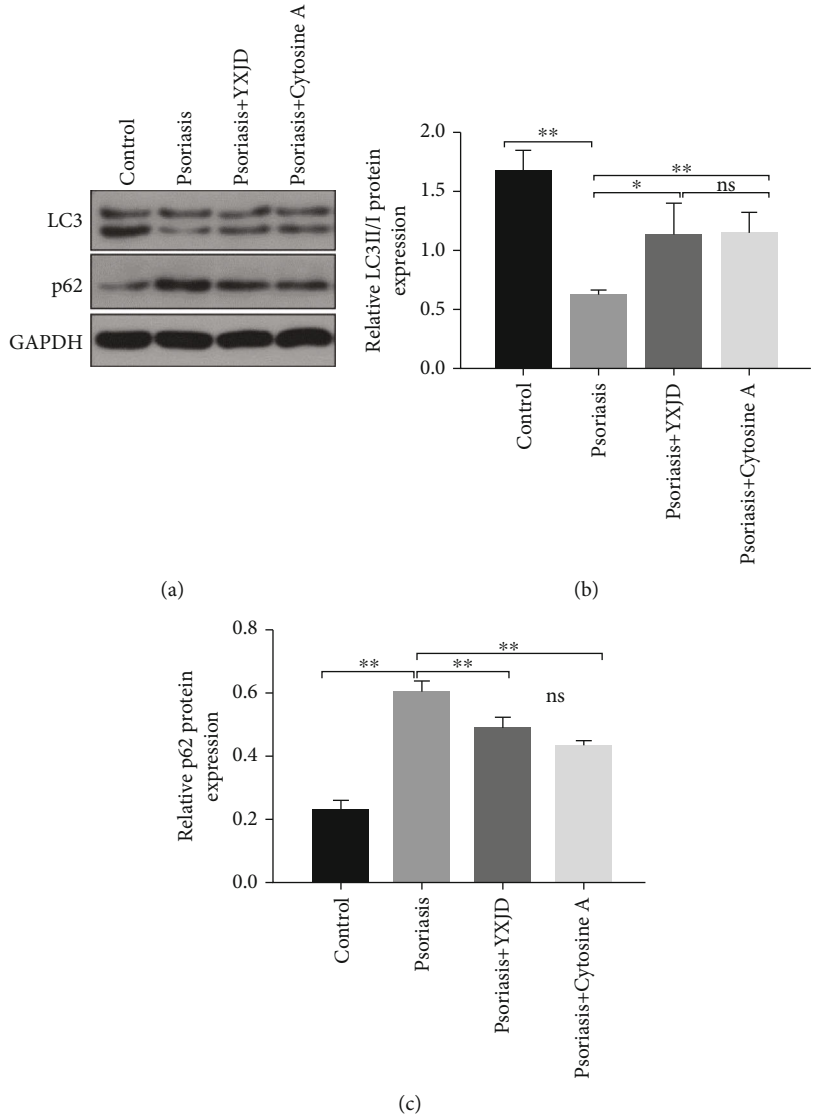

Figure 6: Protein levels of LC3II/I and p62, as detected by Western blot. LC3II/I and p62 expression were evaluated by Western blotting (a–c).

apoptosis. When Survivin acts on subdermal microvascular endothelial cells, normal physiological apoptotic activity in microvessels in the downstream apoptotic pathway can be suppressed by regulating the expression of apoptotic proteins such as caspase-3 and Bcl-2, and the relative number of microvessels increases, which is an important pathological cause of psoriasis, leading to erythema. Survivin mRNA and protein expression were significantly higher in lesions than in nonlesional skin in psoriasis patients [17]. Survivin mRNA expression was positive in the peripheral blood of patients with psoriasis but not in normal patients [18]. In the psoriasis-like mice, we observed increased Survivin staining for CD31 in representative psoriasis-like lesions, which suggests that YXJD can inhibit angiogenesis under pathological conditions. In vitro, we used HUVEC cells transfected with Survivin overexpressed plasmid as psoriasis cell model and found YXJD reduced the activity of HUVEC cells in a dose-dependent manner as well as the secretion of VEGF. Therefore, YXJD ameliorates the overexpression of Survivin in psoriasis.

Autophagy plays a crucial role in cell growth development and occurrence of diseases, which is a highly conservative protein degradation pathway from eukaryotic cells to humans and is essential for removing protein amounts and misfolded proteins in healthy cells. More and more evidences show that autophagy plays a vital role in cell survival, aging, and homeostasis, which is associated with many diseases, including psoriasis, cancer, inflammatory disease, infectious diseases, and metabolic diseases [19–22]. Immune functions, such as intracellular bacterial clearance, inflammatory factor secretion, and lymphocyte development, are impacted by autophagy-related proteins. Autophagy runs through the pathogenesis of psoriasis and is an important target for the treatment of psoriasis. Autophagy runs through the pathogenesis of psoriasis and is an important target for the treatment of psoriasis. The infiltration of T lymphocytes is an

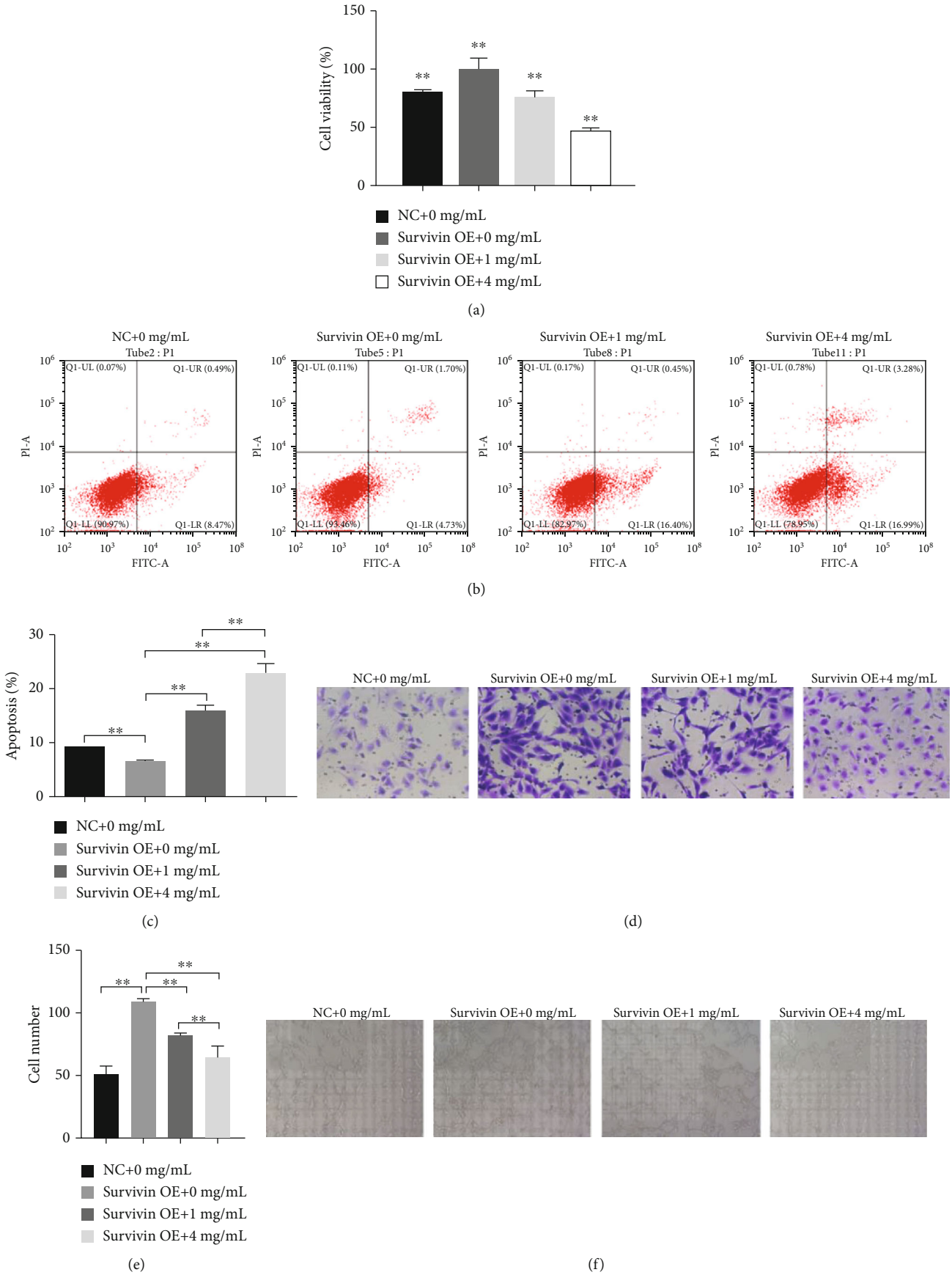

Figure 7: Continued.

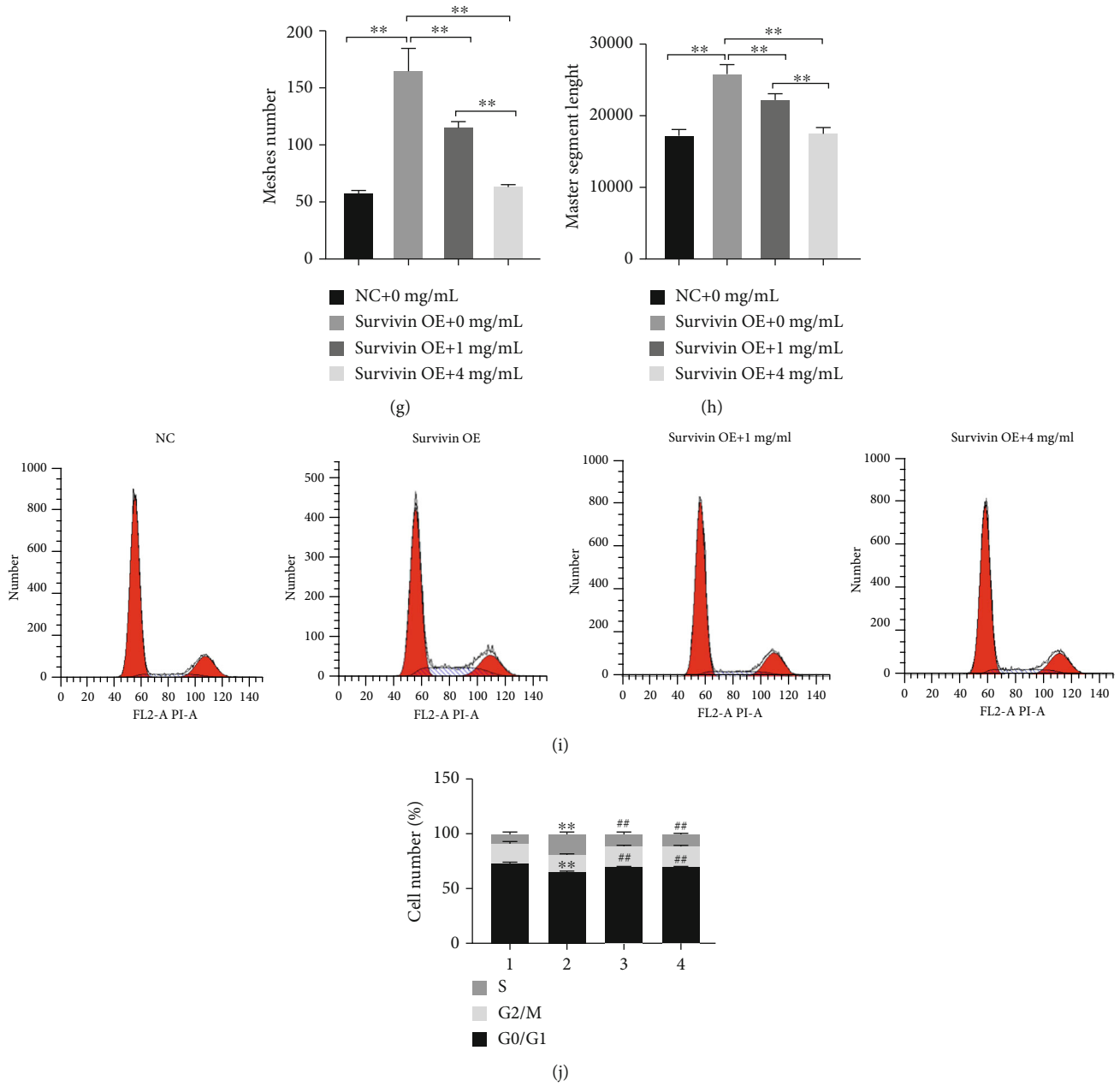

Figure 7: The effect of YXJD on HUVEC cells induced by Survivin and its molecular mechanism HUVEC cells transfected with Survivin overexpressed plasmid were treated with different concentrations of YXJD (0, 1, and 4 mg/mL) for 24 h by CKK-8 detection (a). The induction of apoptosis was determined by annexin V–FITC/PI staining assay (b, c). Transwell: the effect of different concentrations of YXJD (0, 1, and 4 mg/mL) on the migration ability of HUVEC cells transfected with Survivin overexpression plasmid (d). Statistical chart: ordinate: number of cells (e). Tube formation detection was used to detect the effects of different concentrations of YXJD on the angiogenic ability of HUVEC cells transfected with Survivin overexpression plasmid (f). Meshes number (g) and master segments length (h). Statistical chart: ordinate: number of lumen/length of lumen. Magnification: 100× (f–h). Flow cytometry cell detected cycle distribution of HUVEC cells transfected with Survivin overexpression plasmid with different concentrations of YXJD (i). Statistical chart: ordinate: cell number (j).

important pathogenesis that mediates psoriasis. IL-17 produced by T-helper (Th) 17 cells plays a key role in the occurrence of autoimmunity and allergies [23], and its level is elevated in psoriasis [24]. mTOR also plays a critical role in regulating autophagy [25]. IL-17A stimulates keratinocytes to activate the PI3K/AKT/mTOR signal and inhibits autophagy by suppressing the formation of autophagosomes simultaneously [26]. Excessive proliferation of keratinocytes is another important pathological manifestation of psoriasis [27], and it is also the key to the treatment of psoriasis. In human keratinocyte, the expression of p62 which is the autophagy negatively regulated protein is essential to prevent excessive inflammation and induce cathelicidin. TLR2/6 or TLR4 in keratinocytes activates the expression of p62 by

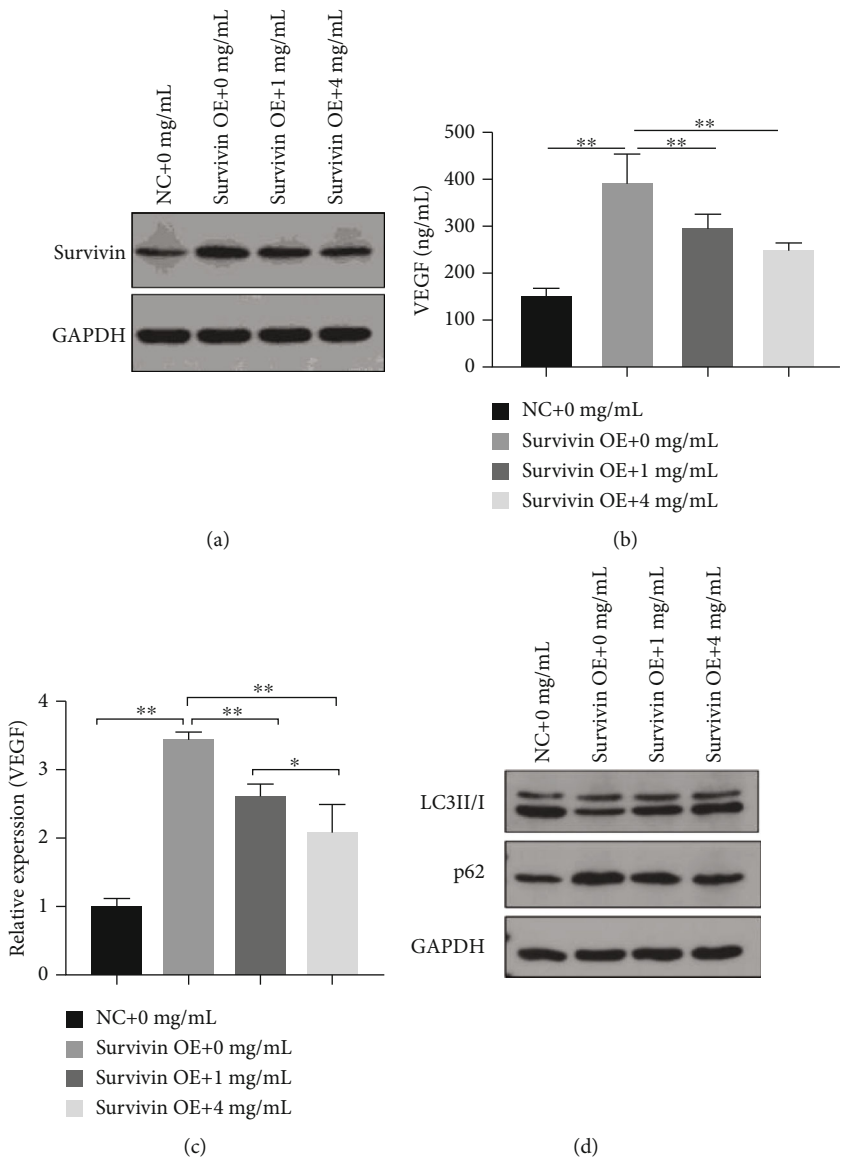

Figure 8: Continued.

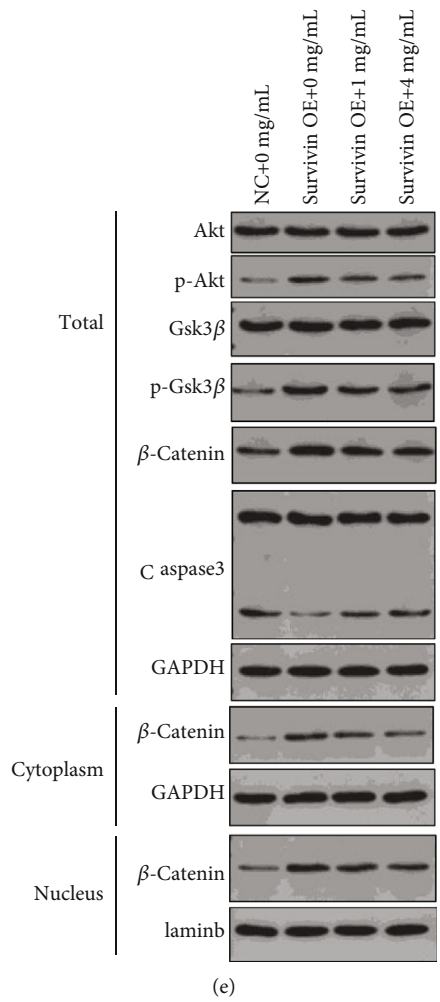

Figure 8: Western blot: the effect of different concentrations of YXJD on the expression of Survivin (a), LC3II/I, and p62 (d) in HUVEC cells transfected with Survivin overexpression plasmid, and the expression of PI3K/Akt- β catenin pathway and Caspase3 (e). ELISA: the effect of different concentrations of YXJD (0, 1, and 4 mg/mL, for 72 h) on the secretion of VEGF in HUVEC cells transfected by Survivin overexpression plasmid (b). qRT-PCR: the effect of different concentrations of YXJD on the synthesis of VEGF in HUVEC cells transfected by Survivin overexpression plasmid (c). GAPDH was used as the internal reference for cytoplasmic protein content and total protein content; Laminb as the internal reference for nuclear protein content; total stands for total protein; cytoplasm for cytoplasmic protein; nucleus for nuclear protein.

inducing NADPH oxidase 2 and 4 and generating reactive oxygen species [28]. We found autophagy is repressed in psoriasis-like mice, which is in line with Pallavi's research. At present, there are few studies on autophagy of microvessels in psoriasis. Our results show that autophagy is inhibited in HUVEC cells transfected by Survivin overexpression plasmid, and YXJD can improve the disorder. However, the occurrence of autophagy is intricate that various factors can affect it. In the future, we will do more in-depth studies on how YXJD can interfere with autophagy in microvessels of psoriasis.

The relationship between autophagy and apoptosis is intricate. Bcl family proteins inhibit the occurrence of autophagy after binding to Beclin1 [29]. In reverse, the occurrence of autophagy also inhibits apoptosis. After the inoculation of Peste des petits ruminants virus (PPRV) in goat endometrial epithelial cells (EECS), cell autophagy is activated and apoptosis is suppressed, and after knocking out autophagy-related genes Beclin-1 and ATG7, apoptosis occurred [30]. The research [31] observing repressive LC3 and Beclin1 levels in the lesions of imiquimod-induced and IL-33 intraperitoneal injection psoriasis model mice that demonstrated the autophagy and apoptosis is suppressed, which, the results of autophagy, is consistent with our experimental results. The relationship between autophagy and apoptosis is complex and in most diseases, autophagy, and apoptosis trade-off. In our study, we found that the expression of the inhibitory apoptosis protein Survivin rose in psoriatic mouse model lesions, which indicated that apoptosis was suppressed; while the expression of LC3II/I was decreased and p62 protein was active in psoriatic mouse model lesions and Survivin overexpressing HUVEC cells, which manifested the autophagy was inhibited. Our experimental results observed that both autophagy and apoptosis in the lesions of psoriasis model mice reduced, which is pivotal in vascular regression in psoriasis. Besides, YXJDD

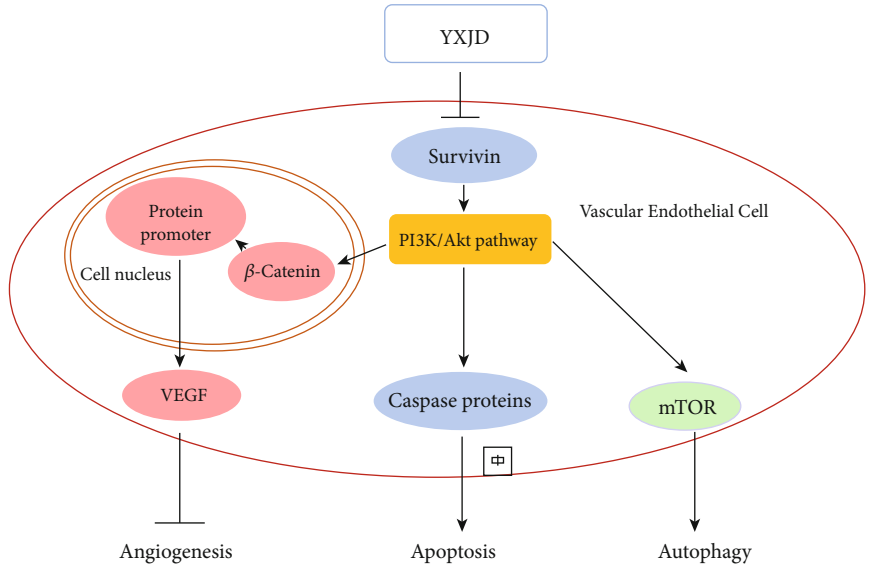

Figure 9: YXJD regulated vascular regression via Survivin/PI3K/Akt pathway in morbigenous signal propagation.

can alleviate the suppression of autophagy in psoriasis lesions. Studies on the relationship between apoptosis and autophagy in psoriasis remain limited, which desiderates more research to verify.

The PI3K/Akt pathway interferes with cell apoptosis, proliferation, and other important activities. The PI3K family is related to the regulation of cell activities. Akt plays an important role in maintaining the physiological function of cells such as apoptosis, proliferation, membrane transportation, and secretion. Increasing the expression of p-GSK3-β results in the inactivation of GSK3-β, which leads to the accumulation and activation of β-catenin [32]. β-Catenin enters the nucleus to promote the DNA transcription of proteins important for cell proliferation and migration, such as Survivin. β-catenin can not only regulate the production of VEGFR-2 but can also regulate the level of VEGF and relative mRNA expression [33, 34]. We found that the level of VEGF and the PI3K/AKT pathway-related proteins activated after HUVEC cells transfected with Survivin overexpression plasmid, The results demonstrate Survivin overexpression can stimulate the secretion of VEGF via PI3K/AKT pathway. PI3K activates AKT and then activates tuberous sclerosis complex 1/2(TSC1/TSC2) and phosphorylates TSC2, which suppressed the TSC1/TSC2 complex and enables mTOR activation [35–37]. In psoriasis lesions of IQM-induced mice and HUVEC cells transfected with Survivin overexpression plasmid, we observed the activation of PI3K/AKT pathway, and YXJD could alleviate such morbigenous signal propagation (Figure 9).

In our study, Survivin regulated the VEGF via PI3K/Akt pathway, which exacerbated vascular regression in psoriasis. VEGF is a proangiogenic factor that plays an important role in angiogenesis [38]. The earliest pathological process of psoriasis is the angiogenesis of microvessels in the dermal papilla [9]. Angiogenesis occurs throughout psoriasis. In the early period of psoriasis, the capillaries of the dermal papilla exhibit abnormal expansion. Excessive dilatation and increased permeability of the venous branches of the capillary plexuses of the dermal papilla result in a large amount of inflammation and chemokine exudation. The process of angiogenesis in psoriasis is regulated by several factors, such as VEGF, MMPs, and TGF-β. VEGF is the most important mediator of angiogenesis under physiological and pathological conditions. It can increase microvessel permeability, promote endothelial cell division and proliferation to lead to angiogenesis, and has a tendency towards inflammatory cells and endothelial cells, which are the main causes of vascular changes. VEGF is synthesized in keratinocytes and endothelial cells in the skin. Clinical studies have confirmed that the level of VEGF in the skin lesions of patients with psoriasis is significantly higher than that in the nonlesion areas and normal skin, and that the level of VEGF is related to the severity of the disease [39] and is also significantly increased in the serum [40]. In our study, we found that the level of VEGF was increased, and YXJD inhibited the excessive expression of VEGF as well as the secretion of VEGF and related proteins expression in HUVEC cells transfected by Survivin overexpression and IMQ-induced psoriasis-like mouse model, which inferred YXJD can ameliorate the abnormal neovascularization in psoriasis (Figure 9.).

5. Conclusion

In conclusion, we demonstrate YXJD alleviates IMQ-induced psoriasis-like pathological changes in microvessels by inhibiting the expression of Survivin in endothelial cells via Survivin/PI3K/Akt pathway, which are related to apoptosis, autophagy, and angiogenesis of microvessels in psoriasis. Our study provides good evidence for the targeted treatment of psoriasis with TCM, and we expect to study more on the effect of effective component in YXJD in the future.

Data Availability

The data used to support the findings of this study are available from the corresponding author upon request.

Conflicts of Interest

The authors declare no financial or commercial conflict of interest.

Authors' Contributions

Hongpeng Lv and Xin Liu contributed to the work equally and should be regarded as co-first authors.

Acknowledgments

This work was supported by the National Natural Science Foundation of China (Nos. 81673974, 81974572, and 82004121) and the Beijing Natural Science Foundation (7172097).

Supplementary Materials

Figure 1: running gum chart: PCR product recovery gel (a). Double enzyme digestion to recover the running rubber (b). PCR identification running map (c). Sequencing analysis (d). Western Blot: the effect of Survivin overexpression plasmid transfection on the expression of Survivin in HUVEC cell (e). Figure 2: CCK-8 was used to detect the effect of different concentrations of YXJD on HUVEC cell activity. Data statistics were analyzed by two-way ANOVA analysis of variance. Error bars indicate SD, ** indicates $P < 0.01$ vs. 0 mg/mL group at the same test time. Figure 3: the effect of different concentrations of YXJDD (0, 0.01, 0.05, 0.2, 1, 5, and 20 mg/mL) on cell viability of HUVEC cells transfected with control plasmid (a) and Survivin overexpression plasmid (b) for 24 h, 48 h, and 72 h by CCK8. Figure 4: HUVEC cells transfected with Survivin overexpressed plasmid were treated with 0.25, 0.5, or 1 mg/ml YXJDD for 24 h. The induction of apoptosis was determined by annexin V–FITC/PI staining assay (a). The apoptosis rate of HUVEC cells (b). The same drug concentration at the same time. *(Supplementary Materials)*

References

[1] I. M. Michalek, B. Loring, S. M. John, and World Health Organization, *Global Report on Psoriasis*, 2016.

[2] G. K. Perera, P. Di Meglio, and F. O. Nestle, "Psoriasis," *Annual Review of Pathology*, vol. 7, no. 1, pp. 385–422, 2012.

[3] S. Xiao, X. Liu, X. Wang et al., "Plasma microRNA expression profiles in psoriasis," *Journal of Immunology Research*, vol. 2020, 12 pages, 2020.

[4] W. Chen, D. Zhou, and P. Wang, "Multi-center clinical study of traditional Chinese medicine diagnosis and treatment for psoriasis," *Journal of Traditional Chinese Medicine*, vol. 53, no. 18, pp. 1557–1561, 2012.

[5] X. Liu, P. Li, and L. Zhang, "Effects of Yangxue Jiedu decoction and its separated formula containing serum on ERK/NF-κB pathway of phorbol ester induced in vascular endothelial cells," *Journal of Traditional Chinese Medicine*, vol. 59, no. 16, pp. 1410–1415, 2018.

[6] Z. Y. Zhou, L. Y. Huan, W. R. Zhao, N. Tang, Y. Jin, and J. Y. Tang, "_Spatholobi Caulis_ extracts promote angiogenesis in HUVECs in vitro and in zebrafish embryos in vivo via up-regulation of VEGFRs," *Journal of Ethnopharmacology*, vol. 200, pp. 74–83, 2017.

[7] H. Sui, J. Zhao, L. Zhou et al., "Tanshinone IIA inhibits β-catenin/VEGF-mediated angiogenesis by targeting TGF-β1 in normoxic and HIF-1α in hypoxic microenvironments in human colorectal cancer," *Cancer Letters*, vol. 403, pp. 86–97, 2017.

[8] C. Sanhueza, S. Wehinger, J. Castillo Bennett, M. Valenzuela, G. I. Owen, and A. F. G. Quest, "The twisted survivin connection to angiogenesis," *Molecular Cancer*, vol. 14, no. 1, p. 198, 2015.

[9] D. C. Altieri, "Survivin, cancer networks and pathway-directed drug discovery," *Nature Reviews. Cancer*, vol. 8, no. 1, pp. 61–70, 2008.

[10] J. G. Fernández, D. A. Rodríguez, M. Valenzuela et al., "Survivin expression promotes VEGF-induced tumor angiogenesis via PI3K/Akt enhanced β-catenin/Tcf-Lef dependent transcription," *Molecular Cancer*, vol. 13, no. 1, p. 209, 2014.

[11] N. Wang, J. Wang, X. Meng, T. Li, S. Wang, and Y. Bao, "The pharmacological effects of Spatholobi Caulis tannin in cervical cancer and its precise therapeutic effect on related circRNA," *Molecular Therapy-Oncolytics*, vol. 14, pp. 121–129, 2019.

[12] X. Z. Liao, Y. Gao, S. Huang et al., "Tanshinone IIA combined with cisplatin synergistically inhibits non-small-cell lung cancer in vitro and in vivo via down-regulating the phosphatidylinositol 3-kinase/Akt signalling pathway," *Phytotherapy Research*, vol. 33, no. 9, pp. 2298–2309, 2019.

[13] Y. Zhang, Y. Geng, J. He et al., "Tanshinone IIA induces apoptosis and autophagy in acute monocytic leukemia via downregulation of PI3K/Akt pathway," *American Journal of Translational Research*, vol. 11, no. 5, pp. 2995–3006, 2019.

[14] C. C. Su, "Tanshinone IIA can inhibit MiaPaCa-2 human pancreatic cancer cells by dual blockade of the Ras/Raf/MEK/ERK and PI3K/AKT/mTOR pathways," *Oncology Reports*, vol. 40, no. 5, pp. 3102–3111, 2018.

[15] G. Ambrosini, C. Adida, and D. C. Altieri, "A novel anti-apoptosis gene, _survivin_, expressed in cancer and lymphoma," *Nature Medicine*, vol. 3, no. 8, pp. 917–921, 1997.

[16] C. A. Koch, A. O. Vortmeyer, R. Diallo et al., "Survivin: a novel neuroendocrine marker for pheochromocytoma," *European Journal of Endocrinology*, vol. 146, no. 3, pp. 381–388, 2002.

[17] T. Markham, C. Mathews, S. Rogers et al., "Downregulation of the inhibitor of apoptosis protein Survivin in keratinocytes and endothelial cells in psoriasis skin following infliximab therapy," *The British Journal of Dermatology*, vol. 155, no. 6, pp. 1191–1196, 2006.

[18] H. Liu, S. Gou, and R. Gao, "Expression of Survivin in peripheral blood mononuclear cells of patients with psoriasis vulgaris," *Chinese Remedies & Clinics*, vol. 9, no. 5, pp. 394–396, 2009.

[19] B. Levine and G. Kroemer, "Autophagy in the pathogenesis of disease," *Cell*, vol. 132, no. 1, pp. 27–42, 2008.

[20] B. Levine, N. Mizushima, and H. W. Virgin, "Autophagy in immunity and inflammation," *Nature*, vol. 469, no. 7330, pp. 323–335, 2011.

[21] A. Doria, M. Gatto, and L. Punzi, "Autophagy in human health and disease," *New England Journal of Medicine*, vol. 368, no. 19, p. 1845, 2013.

[22] D. J. Wu and I. E. Adamopoulos, "Autophagy and autoimmunity," *Clinical Immunology*, vol. 176, pp. 55–62, 2017.

[23] E. Bettelli, M. Oukka, and V. K. Kuchroo, "T_H-17 cells in the circle of immunity and autoimmunity," *Nature Immunology*, vol. 8, no. 4, pp. 345–350, 2007.

[24] S. Kagami, H. L. Rizzo, J. J. Lee, Y. Koguchi, and A. Blauvelt, "Circulating Th17, Th22, and Th1 cells are increased in psoriasis," *The Journal of Investigative Dermatology*, vol. 130, no. 5, pp. 1373–1383, 2010.

[25] H. Zou, L.-X. Wang, M. Wang et al., "MTOR-mediated autophagy is involved in the protective effect of ketamine on allergic airway inflammation," *Journal of Immunology Research*, vol. 2019, Article ID 5879714, 2019.

[26] V. Pallavi and S. Neeru, "PI3K/AKT/mTOR activation and autophagy inhibition plays a key role in increased cholesterol during IL-17A mediated inflammatory response in psoriasis," *Biochimica et Biophysica Acta - Molecular Basis of Disease*, vol. 11864, pp. 1795–1803, 2018.

[27] L. Bianchi, G. Nini, M. G. Farrace, and M. Piacentini, "Abnormal Bcl-2 and "tissue" transglutaminase expression in psoriatic skin," *The Journal of Investigative Dermatology*, vol. 103, no. 6, pp. 829–833, 1994.

[28] H. M. Lee, D. M. Shin, J. M. Yuk et al., "Autophagy negatively regulates keratinocyte inflammatory responses via scaffolding protein p62/SQSTM1," *Journal of Immunology*, vol. 186, no. 2, pp. 1248–1258, 2011.

[29] M. C. Maiuri, G. le Toumelin, A. Criollo et al., "Functional and physical interaction between Bcl-XL and a BH3-like domain in Beclin-1," *The EMBO Journal*, vol. 26, no. 10, pp. 2527–2539, 2007.

[30] B. Yang, Q. Xue, X. Qi et al., "Autophagy enhances the replication of Peste des petits ruminants virus and inhibits caspase-dependent apoptosis in vitro," *Virulence*, vol. 9, no. 1, pp. 1176–1194, 2018.

[31] Y. Duan, Y. Dong, H. Hu et al., "IL-33 contributes to disease severity in psoriasis-like models of mouse," *Cytokine*, vol. 119, pp. 159–167, 2019.

[32] R. Pai, D. Dunlap, J. Qing, I. Mohtashemi, K. Hotzel, and D. M. French, "Inhibition of fibroblast growth factor 19 reduces tumor growth by modulating -catenin signaling," *Cancer Research*, vol. 68, no. 13, pp. 5086–5095, 2008.

[33] T. Ishikawa, Y. Tamai, A. M. Zorn et al., "Mouse Wnt receptor gene Fzd5 is essential for yolk sac and placental angiogenesis," *Development*, vol. 128, no. 1, pp. 25–33, 2001.

[34] S. Monkley, S. Delaney, D. Pennisi, J. H. Christiansen, and B. J. Wainwright, "Targeted disruption of the Wnt2 gene results in placentation defects," *Development*, vol. 122, no. 11, pp. 3343–3353, 1996.

[35] B. D. Manning and L. C. Cantley, "Rheb fills a GAP between TSC and TOR," *Trends in Biochemical Sciences*, vol. 28, no. 11, pp. 573–576, 2003.

[36] K. D. Courtney, R. B. Corcoran, and J. A. Engelman, "The PI3K pathway as drug target in human cancer," *Journal of Clinical Oncology*, vol. 28, no. 6, pp. 1075–1083, 2010.

[37] E. A. Beierle, A. Nagaram, W. Dai, M. Iyengar, and M. K. Chen, "VEGF-mediated survivin expression in neuroblastoma cells," *The Journal of Surgical Research*, vol. 127, no. 1, pp. 21–28, 2005.

[38] N. Ferrara and R. S. Kerbel, "Angiogenesis as a therapeutic target," *Nature*, vol. 438, no. 7070, pp. 967–974, 2005.

[39] M. Canavese, F. Altruda, T. Ruzicka, and J. Schauber, "Vascular endothelial growth factor (VEGF) in the pathogenesis of psoriasis–a possible target for novel therapies?," *Journal of Dermatological Science*, vol. 58, no. 3, pp. 171–176, 2010.

[40] A. Henno, S. Blacher, C. Lambert et al., "Altered expression of angiogenesis and lymphangiogenesis markers in the uninvolved skin of plaque-type psoriasis," *The British Journal of Dermatology*, vol. 160, no. 3, pp. 581–590, 2009.

Hindawi
Journal of Immunology Research
Volume 2020, Article ID 6261814, 10 pages
https://doi.org/10.1155/2020/6261814

Research Article

Gastrospheres as a Model of Gastric Cancer Stem Cells Skew Th17/Treg Balance toward Antitumor Th17 Cells

Alaleh Rezalotfi,[1,2] **Ghasem Solgi**,[1,3] **and Marzieh Ebrahimi**[2]

[1]*Department of Immunology, School of Medicine, Hamadan University of Medical Sciences, Hamadan, Iran*
[2]*Department of Stem Cells and Developmental Biology, Cell Science Research Center, Royan Institute for Stem Cell Biology and Technology, ACECR, Tehran, Iran*
[3]*Psoriasis Research Center, Hamadan University of Medical Sciences, Hamadan, Iran*

Correspondence should be addressed to Ghasem Solgi; gh.solgi@umsha.ac.ir and Marzieh Ebrahimi; marzieh.ebrahimi@gmail.com

Received 5 June 2020; Revised 5 December 2020; Accepted 14 December 2020; Published 24 December 2020

Academic Editor: Margarete D. Bagatini

Background. Gastrosphere, an enriched cellular population with stem-like properties believed to be responsible for an escape from immune-mediated destruction. Th17 and Treg cells play a major role in gastric cancer; however, their interaction with gastrospheres remained elusive. *Method*. Peripheral blood mononuclear cells were isolated from healthy donors and were cultured with conditioned media of MKN-45 (parental) cells as well as gastrospheres' conditioned media in the context of mixed lymphocyte reaction and in the presence of anti-CD3/CD28 beads. The proliferation was evaluated using CFSE staining; the percentages of $CD4^+CD25^+FoxP3^+$ Treg and $CD4^+IL\text{-}17^+$ Th17 cells and IFN-γ+cells and the production of IL-17, TGF-β, and IL-10 were assessed by flow cytometry and ELISA, respectively. Finally, the cytotoxic potential of induced immune cells was measured by examining the secretion of lactate dehydrogenase from target cells. *Results*. The results revealed a decreased expansion of PBMCs postexposure to gastrospheres' conditioned medium which was concomitant with an increased percentage of Th17 and an enhanced Th17 to Treg ratio. The conditioned media of gastrospheres enhanced the secretion of IL-10 and IL-17 and decreased TGF-β. Interestingly, immune cells induced by gastrospheres showed significant cytotoxicity in terms of producing IFN-γ and death induction in target cells. All these changes were related to the upregulation of IL-6, IL-10, and IL-22 in gastrospheres compared to parental cells. *Conclusion*. Our study showed that the condition media of gastrospheres can potentially induce Th17 with increasing in their cytotoxic effect. Based on our knowledge, the present study is the first study that emphasizes the role of gastrospheres in the induction of antitumor Th17 cells. However, it should be confirmed with complementary studies *in vivo*.

1. Introduction

Gastric cancer stem cells (CSCs) are considered as the key player for the initiation and development of tumors which give rise to nontumorigenic and invasive tumor cells. They are responsible for metastasis and immune escape [1] and can be isolated and enriched by different mechanisms including stem cell surface markers, intracellular enzyme activity, the concentration of reactive oxygen species, the identification of side population cells, resistance to cytotoxic compounds or hypoxia, invasiveness/adhesion, immunoselection, and sphere formation in nonadherent conditions [2]. Gastrosphere is an *in vitro* tridimensional (3D) culture model of gastric CSCs with stemness properties [3].

In general, CSCs employ several mechanisms to evade the immune system such as impairment of antigen presentation to prevent cytotoxic T cell activation, downregulation of CD80 and upregulation of PDL-1 to induce T cell anergy, and induction of immunosuppressive M2 macrophages by the production of CSF, TGF-β, and MIC-1 in which in turn inhibits the induction of proinflammatory antitumor M1 macrophages. Furthermore, M2 macrophages impair the activation and proliferation of T cells through IL-10 and

TGF-β secretion. They recruit and expand immune suppressive Treg cells to the tumor microenvironment [4].

In addition to Treg cells as a wholly immunosuppressive population, changes in Treg and Th17 paradigm have recently been taken into consideration in cancers [5, 6]. Recent studies suggest that both Th17 cells and FoxP3$^+$ T cells are able to regulate antitumor responses negatively or positively depending on the microenvironment and type of cancer which have a remarkable effect on the number and function of these cells [7]. According to the previous data, the accumulation of Th17 and Treg cells in the gastric tumor microenvironment is associated with the clinical stage and leads to an imbalanced Th17/Treg in patients with advanced gastric cancer [8–10]. These studies demonstrated the distribution of Th17 cells in relation to Treg in peripheral blood, tumor-draining lymph nodes, and tumor tissues of patients with gastric cancer compared to healthy individuals [10, 11]. IL-6 and TGF-β induce Th17 differentiation either in normal condition [12, 13] or in gastric cancer that it leads to an imbalanced Th17/Treg.

Activation of gastric CSCs could be one of the candidates for the imbalanced Th17/Treg in advanced gastric cancer due to their secretions. More recently, it was shown that the presence of IL-17 in the tumor microenvironment of advanced gastric cancer is correlated with stemness upregulation [14] and transforms gastric CSCs into active ones [15]. This other point of view implies a reciprocal relationship between Th17 and gastric CSC activation. Due to the lack of enough data regarding the effect of gastric CSCs on the Th17/Treg paradigm, the present study was designed to further explore the relationship between CSCs and Th/Treg balance and their subsequences in tumor immunity in vitro. For this purpose, we investigated the frequency and the balance of Th17 and Treg cells in peripheral blood mononuclear cells postexposure to conditioned media derived from human gastric cancer cells and their enriched gastrospheres as a model for gastric CSCs.

2. Material and Methods

2.1. Parental Cell Culture and Sphere Formation. The human gastric cancer cell line (MKN-45) from a 62-year-old woman with poorly differentiated gastric adenocarcinoma (NCBI code: C615) was provided by the National Center for Genetic Resources of Iran. MKN-45 cells were cultured in Roswell Park Memorial Institute (RPMI) medium-1640 (Gibco, USA) supplemented with 10% fetal bovine serum (FBS, Gibco, USA), 100 U/ml penicillin, and streptomycin (Thermo Fisher, USA) as an adherent monolayer culture and were trypsinized to a single cell preparation.

In the following, sphere formation was performed to enrich cancer stem cells from parental cells [3, 16]. Briefly, sphere bodies were obtained by seeding MKN-45 cells at a density of 10^5 cells/ml in serum-free RPMI supplemented with B27 2% (50X, Gibco, USA), 20 ng/ml of basic fibroblast growth factor (bFGF, Royan Biotech, Iran), and epidermal growth factor (EGF, Royan Biotech, Iran) in T-25 nonadhesive poly(2-hydroxyethyl methacrylate) (poly-HEMA, Sigma, USA) coated flasks. B27, bFGF, and EGF were refreshed every 48 hours. Sphere formation was examined using an inverted microscope at ×10 and ×20 magnifications. The gastrospheres were formed after 4-5 days and then were dissociated enzymatically with trypsin (Gibco, USA) into single cells and moved to other flasks to obtain secondary passage.

2.2. Conditioned Media Preparation. Appropriate density (about 70%) of monolayer cell culture and also the enriched gastric CSCs in passage two were dissociated in single cells and seeded in a concentration of 3×10^4 cells/well in two separate poly-HEMA coated and uncoated 96-well plates for obtaining parental cells and gastric CSCs' conditioned media, respectively, in serum-free RPMI with a volume of 200 μl at 37°C and 5% CO2. The conditioned media were collected and centrifuged at 400xg after 24 hours and were then filtered by 0.2 μm filter to remove debris and transferred to 1.5 μl microtubes for storage at -80°C. Parental cells and gastric CSCs were also collected in RNase-free tubes and stored at -80°C.

2.3. Peripheral Blood Mononuclear cell (PBMC) Preparation and General Expansion. PBMCs were isolated from two healthy volunteers using Hydroxyethyl Starch (HES 6%) (GRIFOLS, Spain) to remove red blood cells, followed by buffy coat isolation using Lymphodex (Inno-Train, Germany) density gradient centrifugation. Mixed lymphocyte reaction)MLR(was performed to obtain an appropriate ratio of PBMCs to secreting parental cells/gastric CSCs as follows. To inhibit the proliferation of the group that plays the role of a stimulator, a population of PBMCs was treated with mitomycin C at a final concentration of 10 μg/ml within 60-90 minutes. Mitomycin C acts via the inhibition of DNA and RNA synthesis, rendering the lymphocytes unable to proliferate or activate. The PBMCs were washed three times with 5 ml complete medium to neutralize and remove mitomycin C traces and prepared as the stimulator. The responder and stimulator populations were cultured in the presence of parental cells and gastric CSCs' conditioned media at ratios 1 : 1, 1 : 5, and 1 : 10 with prepared parental and CSC conditioned media for 5 days. One, 5, and 10 correspond to PBMCs of the responder to the number of parental cells and CSCs whose conditioned media has been collected. A group with a fresh medium was considered as the control group.

To stimulate T cell expansion through the first and second signal activation, PBMCs isolated from healthy individuals and were stimulated by anti-CD3/CD28 microbeads (Dynabeads Human T-Activator, Gibco, USA) based on the company's instructions in the presence of conditioned media of parental cells and gastric CSCs in a ratio of 1 : 5 for 5 days. A group with a fresh medium was also considered as a control group. IL-2 (Royan Biotech, Iran) was used for T cell proliferation in 30 IU/ml concentration.

To evaluate the PBMCs' proliferation in the study groups, responder populations were prestained with CFSE (carboxyfluorescein succinimidyl ester, Invitrogen, USA) in each group, according to the company's instructions, and analyzed using a flow cytometer (BD FACSAria, USA) at the first and last days of culture.

2.4. Immunophenotyping. PBMCs were resuspended at a density of $1 - 1.5 \times 10^5/100\,\mu l$ in phosphate-buffered saline (PBS) and were incubated with surface antigen markers APC-labeled anti-CD4 (BD, USA) and FITC-labeled anti-CD25 (AbD Serotec, UK) for 30 minutes at 4°C in the dark. To fix the surface markers and increase the permeability of the membrane, Cytofix/Cytoperm™ solution (BD, USA) was applied as per manufacturer's instruction and placed at 4°C. After 20 minutes, PBMCs were washed twice using a Perm/Wash™ (1X) (BD, USA) solution. Cells in each group were incubated with the intracellular antibodies PE-labeled anti-FoxP3 (Biolegend, USA) and PE-labeled anti-IL-17 (Invitrogen, USA) in the dark for 60-45 minutes and then washed increase using Perm/Wash™ (1X) to analyze by flow cytometer.

2.5. Enzyme-Linked Immunosorbent Assay. To measure the concentrations of IL-17a, IL-10, and TGF-β in PBMC's supernatant, an enzyme-linked immunosorbent assay (ELISA) was performed using commercially available kits for cytokine detection (R&D systems for human IL-17a, IL-10, and TGF-β, USA). The preparation of all reagents, the working standards, and protocol were followed according to the manufacturer's instructions. The absorbance was read using an ELISA reader (BIO-RAD, UK) at 450 nm and 570 nm dual filters. The detection ranges for IL-17a and TGF-β were 31.2-2,000 pg/ml, and for IL-10 were 7.8-500 pg/ml. All the samples were thawed only once.

2.6. LDH Release Assay. MKN-45 cells were plated at a density of 3×10^4 cells per well in 96-well culture plates and incubated for 24 h as target cells. PBMCs postculture of parental cells and gastrospheres' conditioned media were collected and then added to each well in the ratio of 1 : 3 (3 corresponds to PBMCs to target MKN-45 cells) and incubated at 37°C for a further 72 h. One group consisted of MKN-45 cells in the absence of PBMCs, and one group consisted of MKN-45 cells containing 20% Triton were considered as negative and positive control, respectively. A colorimetric assay was applied according to the LDH assay kit (Pars azmoon, Iran), and then, the content of LDH released from the cells to the culture medium was calculated according to the recipe kit.

2.7. RNA Extraction and qRT-PCR. Parental MKN-45 cells and their derived gastrosphere in passage two were collected and stored at -80°C until RNA extraction. Total RNA was isolated using Trizol reagent (Qiagen, USA). The quality of RNA samples was assessed by agarose gel electrophoresis and a spectrophotometer (Biowave II, UK). A total of 2 μg of RNA was reverse transcribed with a cDNA synthesis kit (Takara) according to the manufacturer's instructions. Transcript levels were determined using the SYBR Green master mix (Takara, Japan). Primer sequences for quantitative real-time polymerase chain reaction (qRT–PCR) are listed in Table 1. Expression of genes involved in the differentiation of Th17 and Treg was normalized to the *GAPDH* housekeeping gene. Relative quantification of gene expression was calculated using the $\Delta\Delta$Ct method.

Table 1: Primer sequences used for quantitative real-time polymerase chain reaction.

Primer name	Primer sequence
IL-17	F: 5′ AACCGATCCACCTCACCTTG 3′
	R: 5′ CCCACGGACACCAGTATCTT 3′
IL-6	F: 5′ A G G A G A C T T G C C T G G T G A AA 3′
	R: 5′ C A G GGG T G G T T A T T G C A T C T 3′
IL-8	F: 5′ T A G C A AAA T T G A G G C C A A G G 3′
	R: 5′ A G C A G A C T A G GG T T G C C A G A 3′
IL-10	F: AAG CTG AGA ACC AAG ACC CA
	R: AAG GCA TTC TTC ACC TGC TC
IL-22	F: TGTGAGCTCTTTCCTTATGG
	R: TGCGGTTGGTGATATAGGGC
IL-23	F: GCAGATTCCAAGCCTCAGTC
	R: CCTTGAGCTGCTGCCTTTAG
STAT3	F: 5′ GAAGAATCCAACAACGGCAG 3′
	R: 5′ TCACAATCAGGGAAGCATCAC 3′
TNF-α	F: 5′ CCTCTCTCTAATCAGCCCTCTG 3′
	R: 5′ GAGGACCTGGGAGTAGATGAG 3′
IFN-γ	F: 5′ GGTTCTCTTGGCTGTTACTG 3′
	R: 5′ TCTTTTGGATGCTCTGGTCA 3′
TGF-β	F: 5′ AACCCACAACGAAATCTATGAC 3′
	R: 5′ TAACTTGAGCCTCAGCAGAC 3′

IL-17: interleukin 17; IL-8: interleukin 8; IL-6: interleukin 6; IL-10: interleukin 10; IL-22: interleukin 22; IL-23: interleukin 23; STAT3: signal transducer and activator of transcription 3; TNF-α: tumor necrosis factor alpha; IFN-γ: interferon gamma; TGF-β: transforming growth factor beta.

2.8. Statistical Analysis. Statistical analyses were carried out using the GraphPad Prism 6.01 statistical software. Data were presented as mean ± SD for 3 replicates. Significant differences among mean values were evaluated by two-way ANOVA for T cells' colony size, proliferation index, and qRT-PCR, one-way ANOVA for phenotyping and LDH assays, and the Student *t*-test for comparison of Th17 to Treg ratio between groups. $P < 0.05$ was considered as statistically significant.

3. Results

3.1. Gastrospheres Inhibit PBMC Expansion. Our previous studies determined the stem-like properties of gastrospheres [3]. Therefore, in the present study, we used gastrospheres (Figure 1(a)) as a model of gastric CSCs in comparison to their parental cells. To evaluate the effect of gastric-CSCs on the immune cells on peripheral blood, the conditioned media of gastrospheres and parental cells were used. Our results depicted that the secretion of gastrospheres caused a reduction in colony size ($P = 0.0001$, Supplementary Fig 1, Figures 1(a) and 1(b)) and cell proliferation index ($P = 0.7$, Figures 1(c)–1(e)) of PBMSCs at all different ratios. Moreover,

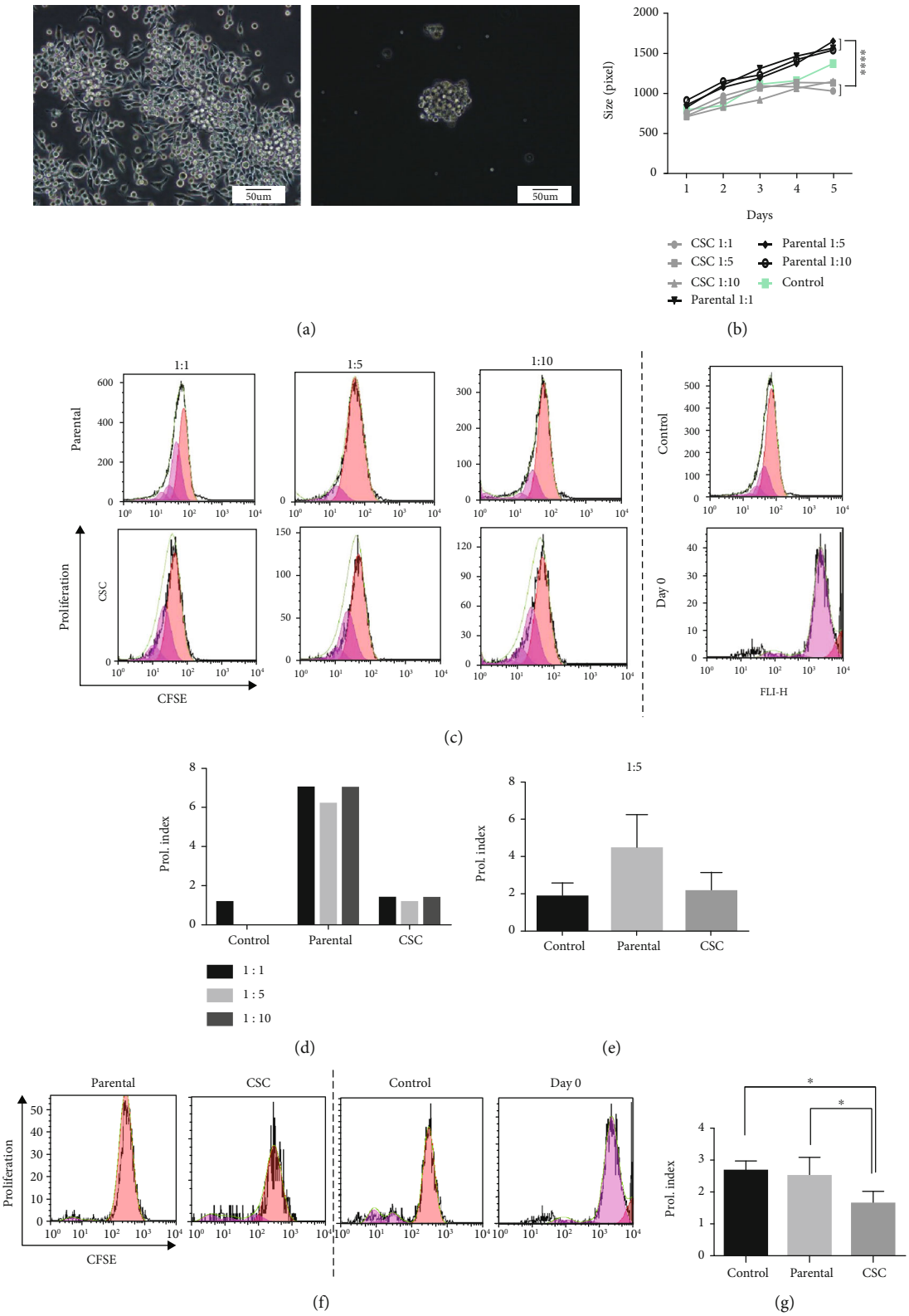

Figure 1: Gastrospheres' conditioned medium limits PBMC proliferation. (a) Monolayer culture of MKN-45 gastric cancer cell line and its derived-loose grape-like shape gastrospheres. (b) Colony size of PBMCs in exposure to MKN-45 parental cells or gastrosphere-derived conditioned media in MLR. (c, d) PBMCs' proliferation in exposure to parental or gastrospheres' conditioned media in MLR ($n = 1$). (e) PBMCs' proliferation in exposure to parental or gastrospheres' conditioned media in MLR at ratio 1 : 5. (f, g) PBMCs' proliferation in exposure to parental or gastrospheres' conditioned media in the presence of anti-CD3/CD28 microbeads at ratio 1 5. CSC: gastrospheres. Data are mean ± SD of three independent experiments. $^*P < 0.05$.

CFSE proliferation assay revealed a reduction in stimulated PBMCs with anti-CD3/CD28 microbeads posttreatment of gastrospheres' conditioned media at the ratio of 1 : 5 ($P = 0.04$, Figures 1(f) and 1(g)). All these changes may be related to the promotion of cell differentiation in PBMSCs posttreatment with gastric CSCs secretome.

3.2. Gastrospheres Have a Distinct Effect on Th17 and Treg Differentiation. To understand how gastric CSCs affect Th17 and Treg cell differentiation, the conditioned media of gastrospheres and parental cells were added to the culture media of MLR or in the setting of T cell proliferation with anti-CD3/CD28 microbeads. Our data revealed that gastrospheres' secretions not only increased the levels of Th17 ($P = 0.9$) but also enhanced the ratio of Th17 to Treg cells in the MLR (Figures 2(a)–2(d)) and even when T cells cultivated in the presence of anti-CD3 and CD28 microbeads ($P = 0.0008$, Figure 3(b)). However, the parental cell secretions just promoted the level of Treg cells ($P = 0.5$) in the MLR setting (Figure 2(a)) and even in PBMCs which were stimulated by anti-CD3 and CD28 microbeads (Figure 3(a)). Importantly, the ratio of Th17 to Treg and the concentrations of IL-17 and IL-10 in the presence of gastrospheres' conditioned medium were higher than of the parental cells' conditioned medium (Figures 3(c) and 3(d)). In contrast, TGF-β level which is the most important cytokine produced by Treg cells was notably higher in the supernatant of PBMCs treated with parental cells' conditioned medium ($P = 0.0024$, Figure 3(d)).

3.3. Mediators Expressed by Gastrospheres Are Involved in Th17/Treg Balance. To further understand that how gastric CSCs could affect Th17/Treg balance, we evaluated the expression of IL-17, IL-6, IL-8, IL-10, IL-22, IL-23, TNF-α, TGF-β, IFN-γ, and STAT3 that believed to be important in changing the Th17/Treg balance using qRT-PCR in parental and gastrospheres. Our results revealed a significant increase in the expression of IL-6 ($P = 0.0007$) which is crucial in changing the balance towards Th17, as well as IL-10 ($P = 0.0009$) and IL-22 ($P = 0.0478$) in gastrospheres compared to parental cells (Figure 4).

3.4. Gastrospheres Induced Cytotoxic Immune Populations. To assess the function of gastric CSC-induced immune cells, we investigated the production of IFN-γ in PBMCs posttreatment with conditioned media of gastrospheres and parental cells. Interestingly, we observed an increase in the level of IFN-γ following treatment with gastrospheres' secretion ($P = 0.009$, Figure 5(a)). To further understand the function of induced immune cells by the conditioned media of gastrospheres and parental cells, we also examined the cytotoxicity of induced immune cells as effector cells in direct culture with MKN-45 gastric cancer cell line as target cells. The toxicity was assessed by the target cell release rate of LDH. LDH is a cytoplasmic enzyme retained by viable cells with intact plasma membranes but released from necrotic cells with damaged membranes. Our results showed a high concentration of LDH in the supernatant derived from the interaction of gastrosphere-induced immune cells and target cells ($P = 0.02$, Figure 5(b)). These data suggested that gastrosphere-induced immune cells had an antitumor effect by killing MKN-45 cells. We further examined the possible existence of mature dendritic cells in experimental groups. Our results showed that gastrosphere-derived conditioned medium induced mature dendritic cells expressing CD11c and CD80 markers among PBMCs, while similar results were not observed in PBMCs treated with parental cells' conditioned medium (data not shown).

4. Discussion

CSCs are responsible for the tumor genesis, metastasis, and recurrence of cancers. Identifying these cells in different cancers and introducing their distinctive features in comparison with other tumor cells, especially their effect on the immune system, can be promising targets in therapies. The tumor microenvironment can invoke and induce Th17 and Treg cells and change the Th17/Treg balance in advanced and metastatic gastric cancer [10]. Nevertheless, how the cells among the tumor mass are responsible for the induction and disturbing the balance between Th17 and Treg yet to be determined. In this study, we intended to answer the question that whether there is a difference in inducing a change in the balance of Th17/Treg due to the factors secreted by gastric parental cells and gastric CSCs. For this purpose, gastrospheres were used as a model due to stemness properties, which we proved in our previous study [3].

Our results showed that the conditioned medium of gastrospheres decreased the proliferation of PBMCs, even if the PBMCS stimulated with anti-CD3/CD28 microbeads as a strong stimulator of T cell expansion. This suggested that the secretome of gastrospheres can inhibit immune cell expansion. Although there is no evidence on decreasing T cell expansion by gastric CSCs, it has been reported that tumor cells, directly and/or indirectly, limit $CD4^+$ and $CD8^+$ T cell expansion, function, and memory formation in many cancers including gastric cancer [17, 18]. Conversely, the conditioned medium of parental cells increased the proliferation of PBMCs. Accumulating data have shown an increased frequency of T cells peripherally and locally by different mechanisms in several cancers [19–21]. A possible mechanism for the increase of lymphocyte proliferation index could be the recognition of antigens by lymphocytes especially by T cells or the presence of soluble factors that induce an increase in lymphocyte proliferation in parental cell secretome.

Currently, Treg cells are known to be the main subset of immune cells that increased during cancer progression. Several types of tumor cells can also recruit Treg cells into the tumor site by their secretions [22]. Our results indicated that the conditioned medium of gastrospheres derived from gastric cancer cells can increase Th17 frequency. We also observed that gastrospheres skewed Th17/Treg balance toward Th17 differentiation through their secretion. Despite insufficient data on disturbance of Th17/Treg balance in cancers, previous reports determined the induction of Th17 producing IL-10 cells in vivo, in vitro, and in gastric cancer patients [10, 23]. Moreover, many studies also have reported

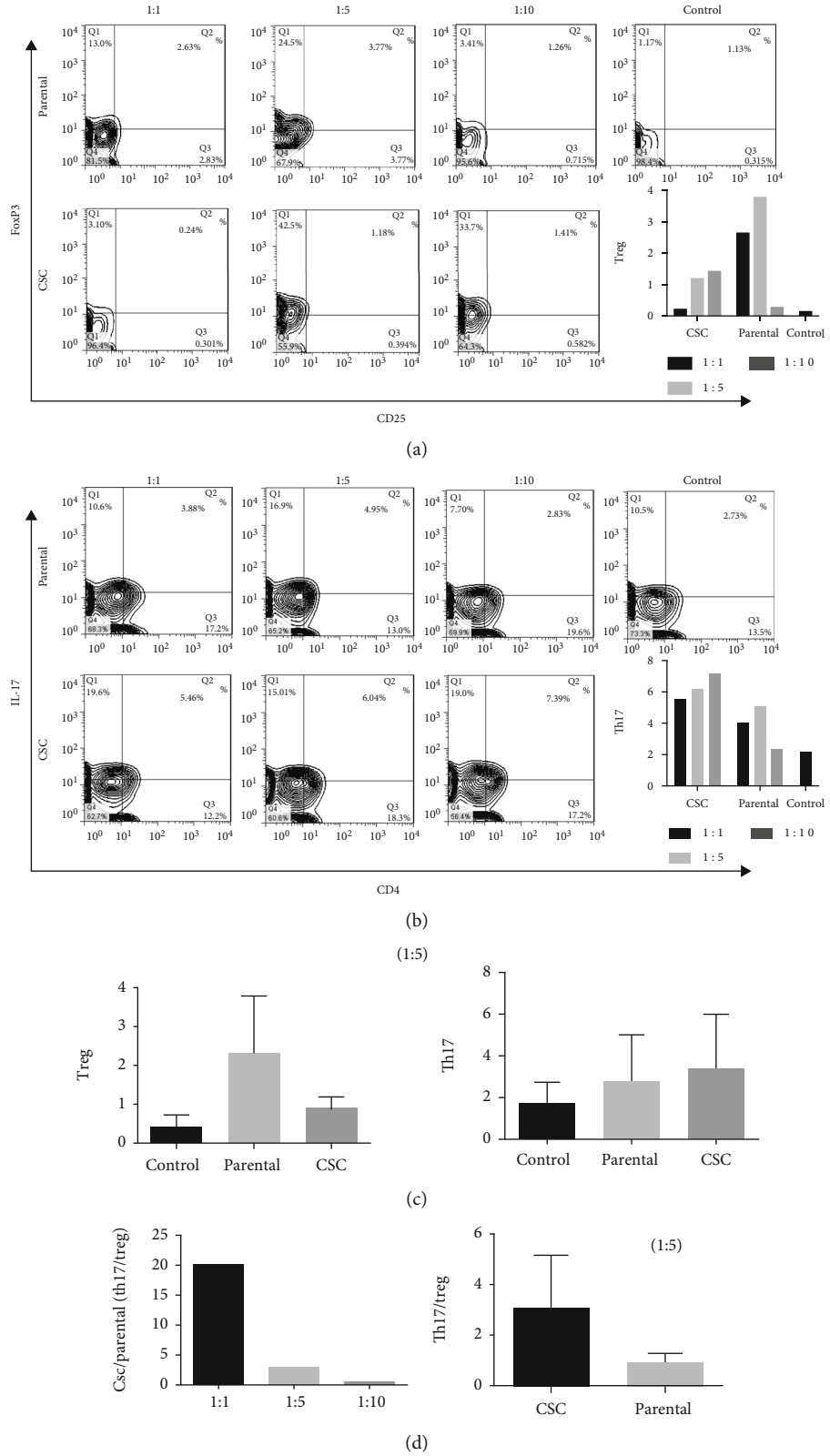

Figure 2: Differentiation of Th17 and Treg in exposure to parental cells and gastrosphere-derived condition media in MLR. (a, c) $CD4^+CD25^+FoxP3^+$ Treg cell differentiation after exposure to gastrospheres or parental-derived condition media. (b, c) $CD4^+IL\text{-}17^+$ Th17 cell differentiation after exposure to gastrospheres or parental-derived condition media. (d) The ratio of Th17 to Treg after exposure to gastrospheres or parental-derived condition media. CSC: gastrospheres. Data are mean ± SD of three independent experiments.

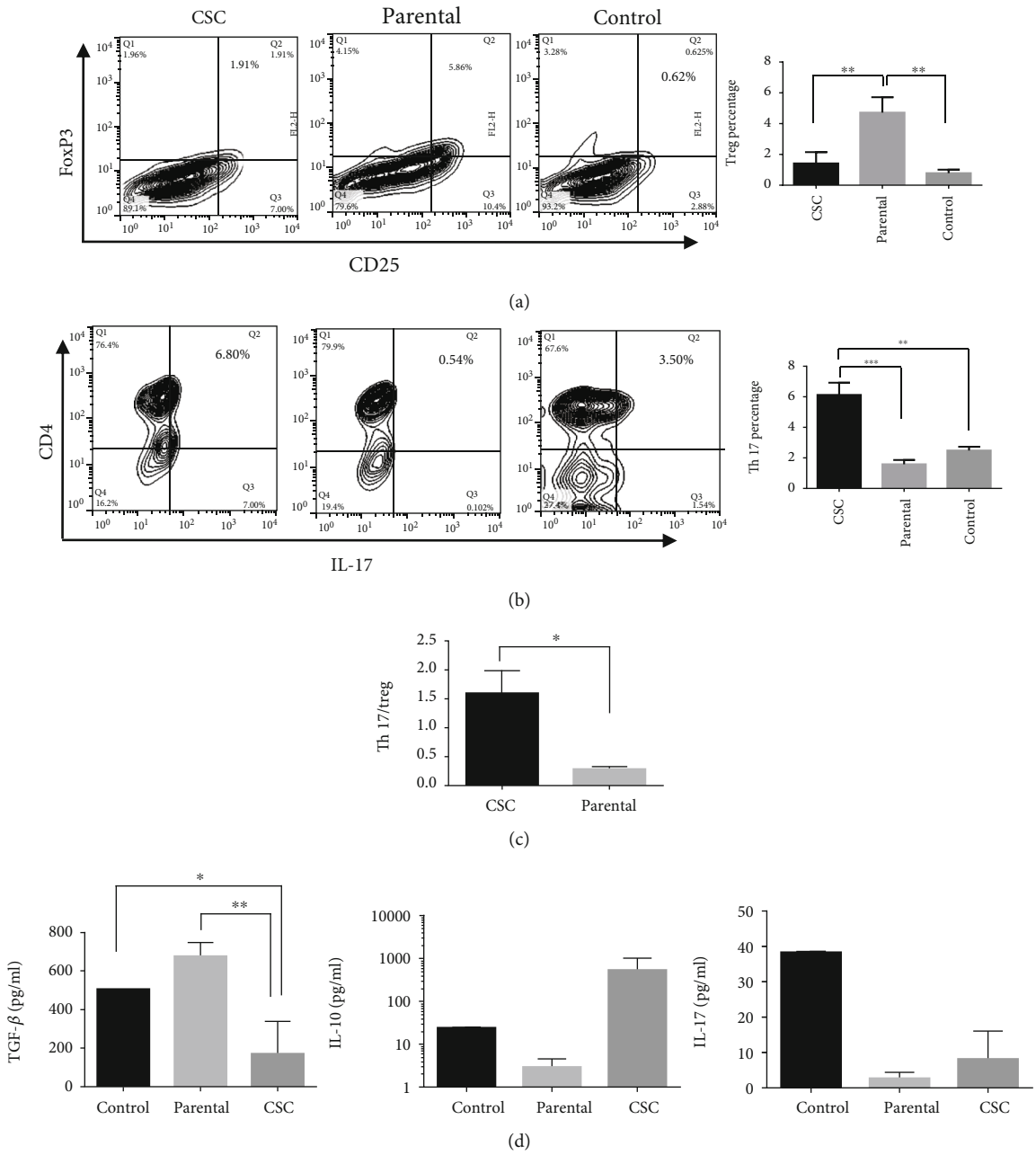

Figure 3: Differentiation of Th17 and Treg after exposure to gastrospheres and parental-derived condition media in the presence of anti-CD3/CD28 microbeads. (a) $CD4^+CD25^+FoxP3^+$ Treg cell differentiation after exposure to gastrospheres or parental cell-derived condition media. (b) $CD4^+IL\text{-}17^+$ Th17 cell differentiation after exposure to gastrospheres or parental cell-derived conditioned media. (c) Th17 to Treg ratio after exposure to gastrospheres or parental cell-derived conditioned media. (d) Concentrations of IL-17, TGF-β, and IL-10 cytokines measured by ELISA in supernatants of PBMCs after being exposed to gastrospheres or parental cells' conditioned media. CSC: gastrospheres. Data are mean ± SD of three independent experiments. $^*P < 0.05$, $^{**}P < 0.01$, and $^{***}P < 0.001$.

the increase of Treg cells within the tumor microenvironment of gastric cancer patients [10, 24]. It seems that the accumulation of Th17 and Treg cells in the tumor microenvironment following disease progression leads to an imbalance in Th17/Treg cells in cancers including advanced gastric cancer [10, 25, 26]. Previous studies have reported a concomitant increase in Th17 cells and the metastasis of gastric cancer [25, 27]. Another recent study showed a decreased number of Th17 cells despite an increase in the number of Treg cells accompanied by an increased expression of the immunosuppressive axis of PD-1/PD-L1 in patients who underwent gastric cancer resection. In this study, silencing PD-1 has been shown to alter the Th17/Treg toward Th17 cells [28].

Soluble mediators and cell to cell communications are two main factors enabling CSCs to induce th17 differentiation [29]. Moreover, CSCs seem to have an important role in changing the balance of Th17 and Treg cells in advanced

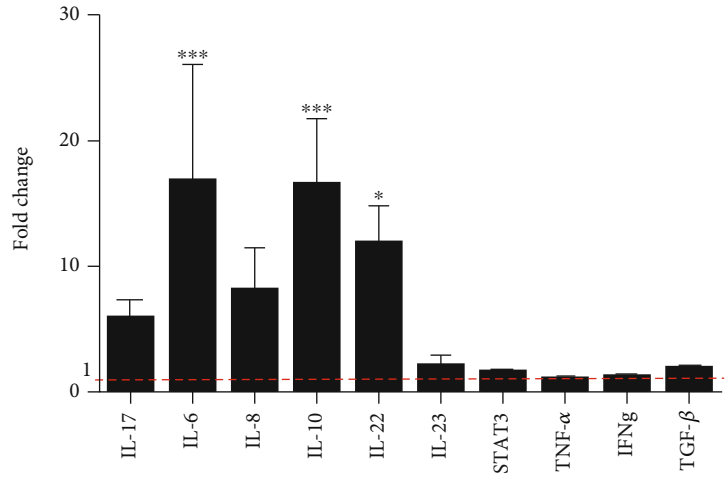

Figure 4: Gene expression of IL-17, IL-6, IL-8, IL-10, IL-22, IL-23, STAT3, TNF-α, and TGF-β in gastrospheres compare to parental cells. Data are mean ± SD of four independent experiments. $^{*}P < 0.05$, $^{**}P < 0.01$, and $^{***}P < 0.001$.

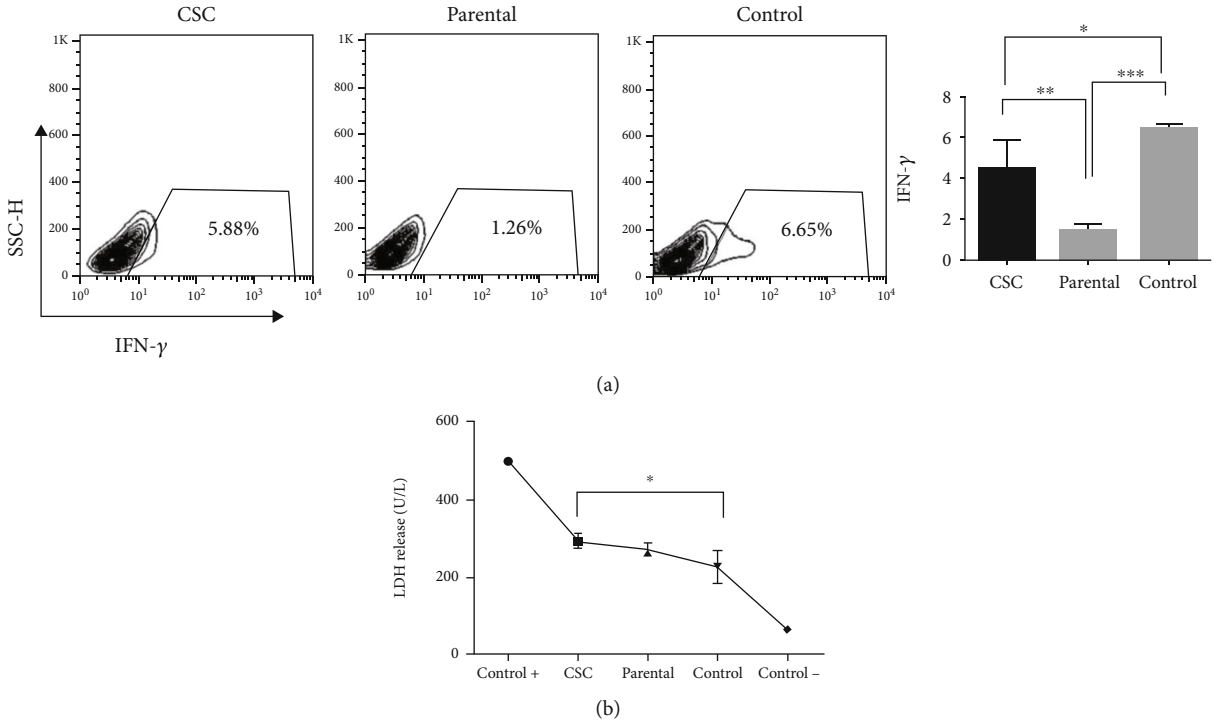

Figure 5: Cytotoxicity of T cells after exposure to gastrospheres and parental cell-derived conditioned media. (a) IFN-γ levels in PBMCs after exposure to gastrospheres or parental cell-derived conditioned media. (b) LDH release of MKN-45 cells (target) in culture with gastrospheres or parental conditioned media induced lymphocytes (effector). CSC: gastrospheres. Data are mean ± SD of three independent experiments. $^{*}P < 0.05$, $^{**}P < 0.01$, and $^{***}P < 0.001$.

gastric cancer. Our findings suggest that the expression of IL-6 by gastrospheres as a game-changer in the expression of FoxP3 or RORγ contributes to the differentiation of Th17 and changing the balance of Th17/Treg. IL-6 is an important mediator which secretes from cancer cells in high concentrations and highly promotes tumorigenesis and protects the cancer cells from therapy-induced DNA damage, oxidative stress, and apoptosis by inducing several pathways [30]. Besides, it prevents apoptosis and skews naïve $CD4^{+}$ T cells towards proinflammatory Th17 by inhibiting TGF-β-driven expression of Foxp3 [12, 31, 32]. Similar to our results, higher production of IL-6 has been reported in CSCs of head and neck squamous cell carcinoma [33]. Moreover, there is evidence that secretion of IL-10 from cancer stem cells reduces the proliferation of T cells and promotes tumor progression [34, 35]. Furthermore, increased level of intratumoral and circulating IL-22 have been found in gastric cancer patients and are associated with cell survival, migration, proliferation,

and angiogenesis [36]. Accordingly, higher expression of IL-6, IL-10, and IL-22 by gastric CSCs, along with the immunoregulatory effects, be primarily is in favor of gastric CSCs themselves and may contribute to maintaining stemness and self-renewal of CSC cells by an autocrine effect [37].

Interestingly, in the present study, we presented data that gastric CSCs' conditioned medium can induce cytotoxicity in PBMCs through increasing of IFN-γ producing cells and induction of necrosis in cancer cells. It seems that IL-17^+/IFN-γ^+ cells exert a strong antitumor effect *in vitro* and *in vivo* [38]. Antitumor activity of a new population of IL-17^+/IFN-γ^+ CD8 T cells (known as Tc17 cells) has also been reported in some cancers, and interestingly, noncytotoxic Tc17 cells can become cytotoxic in the presence of IL-12. These studies show that the polarity and functions of the IL-17^+ subset depend on the cytokine profile in the tumor microenvironment [39].

In conclusion, our findings suggest that gastrospheres as a model of gastric CSCs affect immune cells differently than the cancer cells. They secret different factors that (1) potentially affect the plasticity and the balance between Th17 and Treg cells, (2) possibly induce IFN-γ-producing T cells with antitumor properties, and (3) help to maintain self-renewal properties in gastrospheres. However, this data should be confirmed by other experiments.

Data Availability

(1) The data (original) used to support the findings of this study are included within the article. (2) The data (original) used to support the findings of this study are included within the supplementary file.

Conflicts of Interest

The authors declare that they have no conflict of interests.

Acknowledgments

This project has been conducted by grants from Hamadan University of Medical Sciences and Royan Institute for Stem Cell Biology and Technology and also by an external grant from Cancer Research Center of Cancer Institute of Iran (Sohrabi cancer charity, Grant No: 37381-202-01-97). The authors thank Hajar Rajaee for her kind support.

Supplementary Materials

Supplementary Figure 1: T cell colonies under treatment of parental and gastrospheres' conditioned media in ratios of 1 : 1, 1 : 5, and 1 : 10 in MLR. CSC: gastrospheres; CM: conditioned medium. *(Supplementary Materials)*

References

[1] E. Batlle and H. Clevers, "Cancer stem cells revisited," *Nature Medicine*, vol. 23, no. 10, pp. 1124–1134, 2017.

[2] J. J. Duan, W. Qiu, S. L. Xu et al., "Strategies for isolating and enriching cancer stem cells: well begun is half done," *Stem Cells and Development*, vol. 22, no. 16, pp. 2221–2239, 2013.

[3] M. Hajimoradi, Z. M. Hassan, M. Ebrahimi et al., "STAT3 is overactivated in gastric cancer stem-like cells," *Cell Journal*, vol. 17, no. 4, pp. 617–628, 2016.

[4] M. Sultan, K. M. Coyle, D. Vidovic, M. L. Thomas, S. Gujar, and P. Marcato, "Hide-and-seek: the interplay between cancer stem cells and the immune system," *Carcinogenesis*, vol. 38, no. 2, pp. 107–118, 2017.

[5] N. Obermajer and M. H. Dahlke, "(Compl)Ex-Th17-Treg cell inter-relationship," *Oncoimmunology*, vol. 5, no. 1, p. e1040217, 2015.

[6] S. Downs-Canner, S. Berkey, G. M. Delgoffe et al., "Suppressive IL-17A+Foxp3+ and ex-Th17 IL-17AnegFoxp3+ Treg cells are a source of tumour-associated Treg cells," *Nature Communications*, vol. 8, no. 1, 2017.

[7] K. C. Regulatory, "Regulatory T-Cells and Th17 Cells in Tumor Microenvironment," *Cancer Immunology*, pp. 91–106, 2020.

[8] B. Zhang, G. Rong, H. Wei et al., "The prevalence of Th17 cells in patients with gastric cancer," *Biochemical and Biophysical Research Communications*, vol. 374, no. 3, pp. 533–537, 2008.

[9] T. Iida, M. Iwahashi, M. Katsuda et al., "Tumor-infiltrating CD4+ Th17 cells produce IL-17 in tumor microenvironment and promote tumor progression in human gastric cancer," *Oncology Reports*, vol. 25, no. 5, pp. 1271–1277, 2011.

[10] Q. Li, Q. Li, J. Chen et al., "Prevalence of Th17 and Treg cells in gastric cancer patients and its correlation with clinical parameters," *Oncology Reports*, vol. 30, no. 3, pp. 1215–1222, 2013.

[11] X. Meng, S. Zhu, Q. Dong, S. Zhang, J. Ma, and C. Zhou, "Expression of Th17/Treg related molecules in gastric cancer tissues," *The Turkish Journal of Gastroenterology*, vol. 29, no. 1, pp. 45–51, 2018.

[12] A. Kimura and T. Kishimoto, "IL-6: regulator of Treg/Th17 balance," *European Journal of Immunology*, vol. 40, no. 7, pp. 1830–1835, 2010.

[13] S. Omenetti and T. T. Pizarro, "The Treg/Th17 axis: a dynamic balance regulated by the gut microbiome," *Frontiers in Immunology*, vol. 6, 2015.

[14] Q. Bie, C. Sun, A. Gong et al., "Non-tumor tissue derived interleukin-17B activates IL-17RB/AKT/β-catenin pathway to enhance the stemness of gastric cancer," *Scientific Reports*, vol. 6, no. 1, 2016.

[15] Y. X. Jiang, S. W. Yang, P. A. Li et al., "The promotion of the transformation of quiescent gastric cancer stem cells by IL-17 and the underlying mechanisms," *Oncogene*, vol. 36, no. 9, pp. 1256–1264, 2017.

[16] M. Bakhshi, J. Asadi, M. Ebrahimi, A.-V. Moradi, and M. Hajimoradi, "Increased expression of mi R-146a, mi R-10b, and mi R-21 in cancer stem-like gastro-spheres," *Journal of Cellular Biochemistry*, vol. 120, no. 10, pp. 16589–16599, 2019.

[17] Y. Tian, S. B. Mollo, L. E. Harrington, and A. J. Zajac, "IL-10 regulates memory T cell development and the balance between Th1 and follicular Th cell responses during an acute viral infection," *Journal of Immunology*, vol. 197, no. 4, pp. 1308–1321, 2016.

[18] S. Lee, M. Loecher, and R. Iyer, "Immunomodulation in hepatocellular cancer," *Journal of Gastrointestinal Oncology*, vol. 9, no. 1, pp. 208–219, 2018.

[19] M. Beyer and J. L. Schultze, "Regulatory T cells in cancer," *Blood*, vol. 108, no. 3, pp. 804–811, 2006.

[20] A. M. Wolf, D. Wolf, M. Steurer, G. Gastl, E. Gunsilius, and B. Grubeck-Loebenstein, "Increase of regulatory T cells in the peripheral blood of cancer patients," *Clinical Cancer Research*, vol. 9, 2003.

[21] K. Kono, H. Kawaida, A. Takahashi et al., "CD4(+)CD25high regulatory T cells increase with tumor stage in patients with gastric and esophageal cancers," *Cancer Immunology, Immunotherapy*, vol. 55, no. 9, pp. 1064–1071, 2006.

[22] C. Li, P. Jiang, S. Wei, X. Xu, and J. Wang, "Regulatory T cells in tumor microenvironment: new mechanisms, potential therapeutic strategies and future prospects," *Molecular Cancer*, vol. 19, no. 1, pp. 1–23, 2020.

[23] K.-K. Chang, L.-B. Liu, L.-P. Jin et al., "IL-27 triggers IL-10 production in Th17 cells via a c-Maf/RORγt/Blimp-1 signal to promote the progression of endometriosis," *Cell Death & Disease*, vol. 8, no. 3, p. e2666, 2017.

[24] X.-L. Yuan, L. Chen, T.-T. Zhang, Y.-H. Ma, Y.-L. Zhou, Y. Zhao et al., "Gastric cancer cells induce human CD4+Foxp 3+ regulatory T cells through the production of TGF-β1," *World Journal of Gastroenterology*, vol. 17, no. 15, pp. 2019–2027, 2011.

[25] Y. Yamada, H. Saito, and M. Ikeguchi, "Prevalence and clinical relevance of Th17 cells in patients with gastric cancer," *The Journal of Surgical Research*, vol. 178, no. 2, pp. 685–691, 2012.

[26] E. A. Marshall, K. W. Ng, S. H. Y. Kung et al., "Emerging roles of T helper 17 and regulatory T cells in lung cancer progression and metastasis," *Molecular Cancer*, vol. 15, no. 1, p. 67, 2016.

[27] Z. Su, Y. Sun, H. Zhu et al., "Th17 cell expansion in gastric cancer may contribute to cancer development and metastasis," *Immunologic Research*, vol. 58, no. 1, pp. 118–124, 2014.

[28] X. Zheng, L. Dong, K. Wang et al., "MiR-21 participates in the PD-1/PD-L1 pathway-mediated imbalance of Th17/Treg cells in patients after gastric cancer resection," *Annals of Surgical Oncology*, vol. 26, no. 3, pp. 884–893, 2019.

[29] A. Shahid and M. Bharadwaj, "The connection between the Th17 cell related cytokines and cancer stem cells in cancer: novel therapeutic targets," *Immunology Letters*, vol. 213, pp. 9–20, 2019.

[30] N. Kumari, B. S. Dwarakanath, A. Das, and A. N. Bhatt, "Role of interleukin-6 in cancer progression and therapeutic resistance," *Tumor Biology*, vol. 37, no. 9, pp. 11553–11572, 2016.

[31] L. Wang, A. K. Miyahira, D. L. Simons et al., "IL6 signaling in peripheral blood T cells predicts clinical outcome in breast cancer," *Cancer Research*, vol. 77, no. 5, pp. 1119–1126, 2017.

[32] T. Korn, M. Mitsdoerffer, A. L. Croxford et al., "IL-6 controls Th17 immunity in vivo by inhibiting the conversion of conventional T cells into Foxp 3+ regulatory T cells," *Proceedings of the National Academy of Sciences of the United States of America*, vol. 105, no. 47, pp. 18460–18465, 2008.

[33] K. Chikamatsu, G. Takahashi, K. Sakakura, S. Ferrone, and K. Masuyama, "Immunoregulatory properties of CD44+ cancer stem-like cells in squamous cell carcinoma of the head and neck," *Head & Neck*, vol. 33, no. 2, pp. 208–215, 2011.

[34] Y. Chen, W. Tan, and C. Wang, "Tumor-associated macrophage-derived cytokines enhance cancer stem-like characteristics through epithelial–mesenchymal transition," *Onco-targets and Therapy*, vol. 11, pp. 3817–3826, 2018.

[35] P. M. Aponte and A. Caicedo, "Stemness in cancer: stem cells, cancer stem cells, and their microenvironment," *Stem Cells International*, vol. 2017, 17 pages, 2017.

[36] A. Markota, S. Endres, and S. Kobold, "Targeting interleukin-22 for cancer therapy," *Human Vaccines & Immunotherapeutics*, vol. 14, no. 8, pp. 2012–2015, 2018.

[37] H. Korkaya, S. Liu, and M. S. Wicha, "Regulation of cancer stem cells by cytokine networks: attacking cancer's inflammatory roots," *Clinical Cancer Research*, vol. 17, no. 19, pp. 6125–6129, 2011.

[38] A. Rezalotfi, E. Ahmadian, H. Aazami, G. Solgi, and M. Ebrahimi, "Gastric cancer stem cells effect on Th17/Treg balance; a bench to beside perspective," *Frontiers in Oncology*, vol. 9, 2019.

[39] P. Parajuli, "Role of IL-17 in glioma progression," *Journal of Spine & Neurosurgery*, vol. 11, p. 3817, 2013.

Hindawi
Journal of Immunology Research
Volume 2020, Article ID 7638365, 12 pages
https://doi.org/10.1155/2020/7638365

Review Article

The Potential Role of Regulatory B Cells in Idiopathic Membranous Nephropathy

Zhaocheng Dong,[1,2] **Zhiyuan Liu**,[3] **Haoran Dai**,[4] **Wenbin Liu**,[1] **Zhendong Feng**,[5] **Qihan Zhao**,[2,6] **Yu Gao**,[2,6] **Fei Liu**,[1,2] **Na Zhang**,[2,6] **Xuan Dong**,[2,6] **Xiaoshan Zhou**,[1,2] **Jieli Du**,[1,2] **Guangrui Huang**,[1] **Xuefei Tian**,[7] **and Baoli Liu**[2]

[1]*Beijing University of Chinese Medicine, No. 11, North Third Ring Road, Chaoyang District, Beijing 100029, China*
[2]*Beijing Hospital of Traditional Chinese Medicine Affiliated to Capital Medical University, No. 23 Meishuguanhou Street, Dongcheng District, Beijing 100010, China*
[3]*Shandong First Medical University, No. 619 Changcheng Road, Tai'an City, Shandong 271016, China*
[4]*Shunyi Branch, Beijing Traditional Chinese Medicine Hospital, Station East 5, Shunyi District, Beijing 101300, China*
[5]*Beijing Chinese Medicine Hospital Pinggu Hospital, No. 6, Pingxiang Road, Pinggu District, Beijing 101200, China*
[6]*Capital Medical University, No. 10, Xitoutiao, You'anmenwai, Fengtai District, Beijing 100069, China*
[7]*Department of Internal Medicine, Yale University School of Medicine, New Haven, Connecticut, USA*

Correspondence should be addressed to Baoli Liu; liubaoli@bjzhongyi.com

Received 22 June 2020; Revised 22 November 2020; Accepted 10 December 2020; Published 22 December 2020

Academic Editor: Charles Elias Asmann

Regulatory B cells (Breg) are widely regarded as immunomodulatory cells which play an immunosuppressive role. Breg inhibits pathological autoimmune response by secreting interleukin-10 (IL-10), transforming growth factor-β (TGF-β), and adenosine and through other ways to prevent T cells and other immune cells from expanding. Recent studies have shown that different inflammatory environments induce different types of Breg cells, and these different Breg cells have different functions. For example, Br1 cells can secrete IgG4 to block autoantigens. Idiopathic membranous nephropathy (IMN) is an autoimmune disease in which the humoral immune response is dominant and the cellular immune response is impaired. However, only a handful of studies have been done on the role of Bregs in this regard. In this review, we provide a brief overview of the types and functions of Breg found in human body, as well as the abnormal pathological and immunological phenomena in IMN, and propose the hypothesis that Breg is activated in IMN patients and the proportion of Br1 can be increased. Our review aims at highlighting the correlation between Breg and IMN and proposes potential mechanisms, which can provide a new direction for the discovery of the pathogenesis of IMN, thus providing a new strategy for the prevention and early treatment of IMN.

1. Introduction

The human immune system has the ability to distinguish self and nonself. Under normal circumstances, the immune system only produces an immune response to nonautoantigens, while it has no response to the autoantibodies or only produces a weak response; that is, the immune system is in an immune tolerance state to its own tissue components [1, 2]. In the state of immune tolerance, there are certain amounts of autoantibodies against autoantigens or autoreactive T cells and autoreactive B cells, thus producing an autoimmune response. This response is physiological, and its main function is to clear the aging in vivo apoptotic or aberrant autocells [3–5]. However, when the autoimmune tolerance state is broken, the immune system produces a pathological immune response to the autoantigen, resulting in the damage or dysfunction of its own tissues and cells, thus forming an autoimmune disease [6, 7]. The characteristics of autoimmune diseases compared with other diseases is that the patients can be detected with autoreactive T and B cells

which can cause immune damage to the components of their own tissues [8, 9]. B cells play a crucial role in autoimmune diseases in particular.

B cells are professional antigen-presenting cells (APCs) and can differentiate into plasma cells capable of producing autoantibodies [8, 10, 11]. B cells are both the beginning of autoimmune diseases and the effect of most autoimmune diseases. Breg, as one of the members of B cells, plays a vital role in immune regulation, exerting a myriad of influences on the occurrence and development of autoimmune diseases, such as type I diabetes, lupus erythematosus, and rheumatoid arthritis [11–15].

IMN belongs to autoimmune nephropathy and is one of the common pathological types of nephrotic syndrome [16]. The increase in the incidence of this disease and the discovery of autoantigens such as phospholipase A2 receptor (PLA2R) attracted the attention of many researchers [17]. Although few basic studies have been published on IMN and its immunological mechanisms, the efficacy of rituximab has encouraged researchers to focus on B-cell studies [18, 19]. At the same time, the oligoinflammatory nature of IMN makes it different from other autoimmune nephropathies, which indicates the important role of immune regulation in the pathogenesis of this disease [11]. Therefore, we reviewed the role of B cells in autoimmune diseases and attempted to hypothesize the relationship between Bregs and IMN.

2. Overview of Breg

2.1. A Brief History of Breg. The activation of the immune system is compulsory. However, if the occurrence of autoimmune reactions such as autoimmunity against autoantigens, immunity against allogeneic fetus, hypersensitivity against allergens, and immune response against normal intestinal flora is not effectively suppressed, it will lead to serious autoimmune diseases [20–22]. Therefore, the weakening of the immune response is more important. Besides being able to recognize antigens such as APC, B cells can be differentiated into plasma cells to secrete antibodies and provide immune protection for the human body [11]. It is important to understand how B cells properly control the immune response under normal conditions and suppress a wrong or excessive immune response to avoid damage to the body. This part of the function of controlling the uncontrolled immune response belongs to immune regulation, and the B cells responsible for immune regulation become Bregs [23].

The discovery of Bregs is almost parallel to that of regulatory T cells (Tregs), but less importance was given to Breg. As early as 1974, Neta and Salvin discovered a B cell in the spleen of guinea pigs that specifically inhibits delayed hypersensitivity [24]. In 1996, Janeway et al. found that B-cell-deficient mice were allergic to myelin oligodendrocyte protein (MOG) and were unable to prevent the occurrence of experimental autoimmune encephalomyelitis (EAE) that worsened the autoimmune response [25]. These studies have shown that there is the presence of a type of B cell involved in immune regulation. In 2002, Fillatreau et al. found that these B cells secrete IL-10 [26]. In 2006, the concept of Breg was formally proposed by Mizoguchi and Bhan [27]. Since then, there have been numerous studies on Breg, mostly in mice; however, the existence of Breg in humans remains a mystery. In 2010, Blair et al. found the presence of Breg in lupus patients [28]. In 2011, Iwata et al. found the presence of Breg in human peripheral blood performing the same function as B10 cells in mice [29]. B10 cells are a subtype of mouse Breg. The phenotype of this cell is $CD5^{+}CD1d^{hi}$, while in humans this phenotype is $CD24^{hi}CD27^{+}$, which suggests that Breg phenotypes in humans are not universal in relation to those derived from animal studies. Thus, the academic world began a new era of exploration of Breg species and their functions in the human body.

2.2. Types and Functions of Breg. Breg production differs from Tregs, i.e., it can be differentiated from B cells at different stages and show the functions of B cells at different stages (Figure 1) [23]. This also leads to a wide variety of Breg phenotypes. Different phenotypes of human Bregs are known in Table 1. Different types of Bregs play different functions and regulate different autoimmune responses to different immune cells.

2.2.1. The Role of IL-10 in Breg Function. Breg plays an immunosuppressive role in most people mainly by secreting IL-10 (Figure 2) [28–34]. It can also suppress the function of different kinds of immune cells. In terms of T cells, Breg inhibited the production of interferon-γ (IFN-γ) and IL-17 and other proinflammatory cytokines by Th1 and Th17 through IL-10, and inhibited the differentiation of initial T cells into Th1 and Th17 [35–38]. IL-10 can also directly inhibit the activity of cytotoxic T lymphocytes (CTL) and ultimately inhibit cellular immunity [39, 40]. In addition, in the IL-10 environment, Breg expressing B7 can induce the differentiation of Treg and Tr1 and thus promote the occurrence of immune regulation; however, not all Breg can do this [41]. Therefore, Breg plays a key role in immune regulation through the dynamic diversification interaction between secreted IL-10 and T cells. In addition to T cells, Breg can inhibit the expression of major histocompatibility complex II (MHC II) on the surface of dendritic cells by secreting IL-10, thereby inhibiting antigen presentation [42–44]. In addition, IL-10 can also inhibit the activity of monocytes and natural killer cells (NK cells), thereby inhibiting the innate immune response [45–47]. It is worth noting that IL-10 promotes the proliferation of B cells, which may lead to the possibility that Breg can play an accessory role in regulating adaptive immunity in the continuation of humoral immune response [46].

2.2.2. In Addition to IL-10 in Breg Function. In addition to the secretion of IL-10, Breg can achieve immunomodulatory effects through other means. Tim-1 B cells, as a type of Breg, can secrete not only IL-10 but also TGF-β to play an immunomodulation role [31]. TGF-β can inhibit the proliferation and differentiation of various immune cells and the production of cytokines, especially regulating the differentiation of Th17 and Treg cells [31, 48, 49]. It also promotes the proliferation of fibroblasts, osteoblasts, and Schwann cells to help

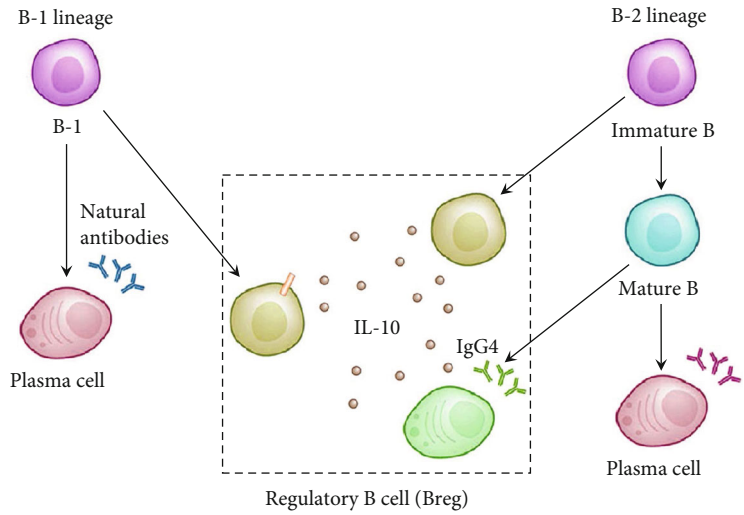

Figure 1: The source of Breg. Different from Treg, Breg has more extensive sources. It does not matter whether they are B1 cells or B2 cells, or if they are immature B cells or mature B cells, under certain conditions of stimulation, Breg with immunomodulation function can be differentiated. At present, the main mechanism by which Breg plays the immune regulatory function in the human body is the secretion of IL-10.

Table 1: Breg found in human peripheral blood.

Name	Breg cell phenotype	Method of stimulation in vitro	Mechanism of suppression	References
B10	$CD24^{hi}CD27^{+}$	$CD40L^{+}$CpG, LPS	IL-10	29
Immature B cell	$CD24^{hi}CD38^{hi}CD27^{-}$	CD40L, CpG^{+}pDC	IL-10, PD-L1, CD80/CD86	28
GrB^{+} B cell	$CD38^{+}CD1d^{hi}IgM^{+}CD147^{+}$	$IL\text{-}21^{+}$ anti-BCR	IL-10, GrB, IDO	30
Tim-1 B cell	$Tim\text{-}1^{+}$	—	IL-10, TGF-β	31
—	$CD39^{+}CD73^{+}$	$CD40L^{+}$IL-4	Adenosine	64
—	$IgD^{lo}CD38^{+}CD24^{lo}CD27^{-}$	—	CD62L	65
Plasmablasts	$CD24^{hi}CD27^{int}CD38^{+}$	$GpG^{+}IL\text{-}2^{+}IL\text{-}6^{+}IFN\alpha$	IL-10	32
Br1 cell	$CD25^{hi}CD71^{hi}$	CpG	IL-10, IgG4	33
B-1 cell	$CD27^{+}CD43^{+}CD11b^{+}$	—	IL-10, CD80/CD86	34

repair damaged tissues [50–53]. In addition, Th9 differentiation requires TGF-β and IL-4 induction, and some allergic inflammation is associated with Th9 overactivation [54, 55]. It is worth noting that Breg which can secrete IL-35 has not been found in the human body, and the specific mechanism needs to be explored [56, 57]. In addition to promoting Treg differentiation, immature B cells with immunomodulation can express programmed cell death protein ligand 1 (PD-L1), which can directly kill T cells [58]. Recent studies have shown that in terms of infection, Breg in human immunodeficiency virus (HIV) patients inhibited antigen presentation and the activity of $CD4^{+}$ T cells through interaction between IL-10 and PD-1/PD-L1, and it inhibited anti-HIV cytotoxic T lymphocytes at the same time [59]. In terms of tumor, PD-L1 is highly expressed in tumor invasive B cells in patients, which may assist the tumor to achieve immune escape [60]. At the same time, the presence of B cells with a high expression of PD-L1 in malignant B lymphoblastoma provides a theoretical basis for PD-1 inhibitor treatment of this disease [61, 62]. In addition to secreting IL-10, GrB^{+} B cells also play an immunosuppressive role by producing granzyme B (GrB) and indoleamine 2,3-dioxygenase (IDO) [30]. The phenotype of this cell is $CD38^{+}CD1d^{+}IgM^{+}$ $CD147^{+}$. GrB^{+} B cells can infiltrate tumors and inhibit the $CD4^{+}$ T cell response after being activated by IL-21 [63]. Breg with phenotype $CD39^{+}CD73^{+}$ can secrete adenosine, which affects the activity and proliferation of various immune cells, mainly neutrophils, monocytes, and T cells, and plays an immunomodulatory function [64]. In vitro, such cells can be activated in IL-4 by stimulating their CD40 [64]. Breg with $IgD^{lo}CD38^{+}CD24^{lo}CD27^{-}$ controls B7 expression through CD62L, thereby inhibiting dendritic cell maturation [65]. Br1 cells with phenotype $CD25^{hi}CD71^{hi}$ can directly secrete IgG4 to block autoantigens, and this antibody is currently considered to have a protective effect in patients with chronic allergy [33]. We can activate this type of cell by stimulating its TLR9 [33]. To sum up, Breg mainly inhibits innate immune response and cellular immune response in specific immunity, but it lacks corresponding means to regulate humoral immune response.

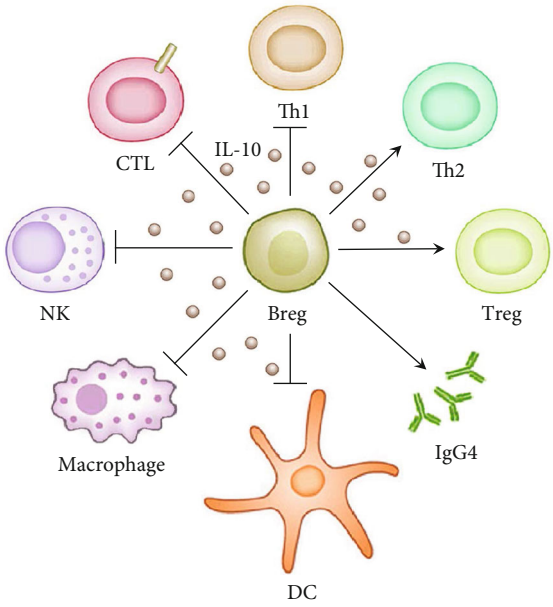

FIGURE 2: The function of Breg. Breg can promote Th2 cell differentiation and inhibit Th1 cell differentiation by secreting IL-10. In addition, its secretion of inhibitory cytokines such as IL-10, TGF-β, and adenosine can inhibit the activity of NK cells, monocytes, and CTL, and impair the antigen presentation function of dendritic cells. In addition, some Bregs can also promote the differentiation of Treg, enhance the immune regulation effect, and secrete IgG4 blocking autoantibodies to protect the body from hypersensitivity damage.

3. Abnormal Features of IMN

3.1. Abnormal Pathological Features of IMN. IMN is one of the common pathologic types of nephrotic syndrome. At an early stage, the glomerular subepithelial deposits can only be seen under a light microscope, and then the glomerular basement membrane is diffusely thickened [16]. At late stages, the mesangial matrix increases, capillary loops are compressed and occluded, and glomerulosclerosis occurs [66]. However, the glomerulus is usually free of cell proliferation and immune cell infiltration throughout the process [67]. In immunofluorescence examination, IgG was diffusely deposited in the glomerular capillary wall, but not in IgM [68]. Most patients are associated with C3 deposition [69]. In general, there are no deposits of multiple immunoglobulin and complement C1q, and they are not deposited in the area outside the glomerular capillary wall. With the detection of the anti-PLA2R antibody on serum and kidney sections, IgG deposited on the glomerular capillary wall of IMN patients is the most common IgG, followed by IgG1 [68].

It is not difficult to see that the pathological characteristics of IMN are very abnormal. Firstly, the antigen antibody complex was deposited only under the glomerular epithelial cells, and mesangial cell proliferation was rare, indicating that the immune complex was generated by an in situ immune complex [70, 71]. Recently, Liu et al. hypothesized that the autoantigen of IMN came from human lungs [72]. This statement broke the current research deadlock and was widely recognized by peers. Secondly, IgG4 is the dominant antibody in patients, indicating that the disease is at the end of the immune response [73–75]. The pathogenesis of IMN is necessarily different from that of IgG4-related diseases (IgG4-RD), because IMN does not have systemic multitissue IgG4$^+$ plasma cell infiltration like IgG4-RD, and the incidence of kidney disease is concentrated in the renal interstitium [76, 77]. Thirdly, although IgG and C3 deposition can be seen in the renal tissues of IMN patients, C1q deposition is rare, and there is no obvious abnormality in serum C1q and C3, indicating that there is no significant complement depletion in the patients [78, 79]. Also, the passive Heymann nephritis rat model has demonstrated that C5b-9 deposition is one of the factors leading to proteinuria, and the complement of IMN patients can be activated by the alternative pathway or the mannose-binding lectin pathway [79–82]. However, there are no reports on the effectiveness of the direct use of eculizumab in the treatment of this disease, which indicates that kidney damage in IMN patients is not mainly caused by the complement [83]. Many contradictory phenomena have obscured the pathogenesis of IMN. So let us see what happens to the immune cells and cytokines in this disease.

3.2. Abnormal Immunological Characteristics of IMN. As an autoimmune disease, the main autoantibodies of IMN are PLA2R, accounting for 70-80% [84–86]. PLA2R is a member of the C-type lectin superfamily, also known as the mannose receptor family [87–89]. It is a type I transmembrane protein that contains long extracellular segments, long transmembrane segments, and short intracellular segments [88]. It has been reported that PLA2R inhibits inflammatory response by binding to the PLA2 protein, and the increased expression of PLA2R is related to inflammatory stimulation and aging [72, 90, 91]. This also proves that IMN is more common among the elderly. The onset of this disease is related to environmental pollution or the history of respiratory tract infection during the adolescent period [92, 93]. At the gene level, Stanescu et al. found that the HLA-DQA1 allele on chromosome 6p21 was closely related to the pathogenesis of IMN after collecting the relevant data of 556 white IMN patients [94]. The single nucleotide polymorphism of PLA2R and HLA-DQA1 can be related to IMN susceptibility [94, 95]. Interestingly, about 7% of patients with this disease were seropositive for the anti-PLA2R antibody but negative for renal tissue PLA2R [96]. There are also many cases of recurrence of IMN after renal transplantation [97]. However, this protein is expressed in the lungs and kidneys [82, 98], and it is also found in neutrophils and alveolar macrophages [99–101]. The evidence raises the question of whether IMN's autoimmune response really originated in the kidney.

In terms of immune cells, there was no significant increase in the number of T and B cells in the patients [102, 103]. In terms of T cells, the most significant reduction was in CD8$^+$ T cells, while Th2 cells accounted for the largest proportion in CD4$^+$ T cells, and the number of Th1 and Treg cells decreased [103, 104]. In terms of cytokines, IL-4, IL-10, and IL-13 were significantly increased, while there was no significant change in IFN-γ and IL-12 [103, 105–107]. Ifuku et al.

compared the expression levels of renal cytokine mRNA with those of antineutrophil cytoplasmic autoantibody-associated crescentic glomerulonephritis (ANCAGN) and membrane proliferative glomerulonephritis (MPGN) in IMN patients and found that IL-6, IL-12, and IL-17 in IMN patients were significantly reduced compared with the other two groups, while IL-4, IL-5, TGF-β, and Foxp3 significantly increased compared with the other two groups [108]. Kawasaki et al. compared the serum cytokine levels of IMN children with lupus nephritis children, MPGN, Henoch-Schönlein purpura nephritis, and IgA nephritis, and found that serum IL-2, IL-6, IL-12, and IFN-γ were not significantly increased, while the contents of IL-4 were significantly increased [109]. All these cytokines with insufficient content have the effect of strengthening cellular immune response, while the increased cytokines have the effect of strengthening humoral immune response and inhibiting cellular immunity. From the perspective of source cells, IL-6 is mainly produced by mononuclear macrophages, endothelial cells, fibroblasts, and other cells [110–112]. IL-12 is mainly produced by dendritic cells, macrophages, and B cells [113, 114]. IFN-γ is mostly produced by NK cells and Th1 cells [115, 116]. Therefore, IMN is a disease dominated by humoral immune response, while the innate immune response and cellular immune response in specific immunity are weakened.

4. Role of Breg in IMN

4.1. Breg Activation Is Present in IMN. Professional APCs recognize their own antigens, activate T helper cells, and induce activation of cellular and humoral immunity. The antibodies produced in the first response of humoral immunity are mainly IgM, and IgG can be produced at a later period [117, 118]. Although cytokines produced by activation of humoral immune response, such as IL-4 and IL-10, can weaken cellular immune response [119, 120], cellular immune response of a large number of autoimmune diseases coexists with humoral immune response [121–124], indicating that cellular immunity will not be easily attenuated due to activation of humoral immunity. However, when the immunomodulatory cells intervene, the innate and specific immune responses are weakened, and the humoral immune response is the main stream. This is precisely because whether Treg or Breg play an immunomulatory role, they mainly rely on the secretion of IL-10, IL-35, and TGF-β to suppress cellular immunity, but lack the means to secrete IFN-γ to inhibit Th2 differentiation or block B cell-activating factor receptor (BAFF-R), B cell maturation antigen (BCMA), transmembrane activator, and CAML interactor (TACI), and other ways to inhibit B cell proliferation, thus inhibiting humoral immune response [125–129]. Therefore, for IMN, where humoral immune response is dominant, only active immune regulation can explain all kinds of abnormalities in IMN. The presence of tumor-related MN, and the pathological characteristics of the disease are very similar to those of IMN, is a strong evidence of active immune regulation [85, 130, 131]. Tumors are known to escape the body's immune system by escaping [132, 133]. Autoimmune diseases, however, are characterized by overactivation of the immune system. Therefore, if the cells play an immunomodulatory role, they can participate in and even lead to the occurrence of autoimmune diseases. In this environment, tumors can coexist with autoimmune diseases [134, 135].

Interestingly, however, the peripheral number of Treg and the blood IL-35 content of IMN patients were lower than those of normal people, indicating that Treg activity in IMN patients was insufficient [104, 136]. As mentioned above, Breg which can secrete IL-35 has not been found in humans. Therefore, Breg should be the main immune regulatory cells in IMN patients [56, 137]. Moreover, not all Bregs have the ability to activate Tregs. In addition, B cells themselves also belong to professional antigen-presenting cells [138, 139], although immune regulatory activation can lead to a decreased antigen presentation function of dendritic cells and macrophages, which are professional APCs [42–44]. Moreover, IMN patients contain more lipopolysaccharide (LPS) than normal people, which is enough to activate the resting B cells to perform an antigen presentation function [140, 141]. Meanwhile, B cells are mainly presented with soluble antigen, and the soluble PLA2R is present in the circulation of IMN patients [142, 143]. Hence, it is clear that under the activation of Breg, the autoimmune response can continue even if the antigen presentation ability of dendritic cells and macrophages is inhibited [42–44].

4.2. IgG4 Antibody Is Produced by Br1 Cells. Br1 cells were discovered in 2013 by van de Veen et al. in beekeepers, people who had been chronically exposed to allergens, and in patients receiving desensitization therapy [33]. This cell production requires toll-like receptor 9 (TLR9) to be activated. The main means of immune regulation is secretion of IL-10 and production of the IgG4 antibody. However, the incidence of IMN is also related to air pollution; that is, long-term exposure of patients to air with excessive PM2.5 content meets the condition of long-term exposure to allergens [93]. In addition, the single nucleotide polymorphism of TLR9 is related to the pathogenesis of IMN [144]. Happily, Cantarelli et al. have confirmed the presence of increased Breg cells in the periphery of IMN patients [145]. The proliferation of these cells confirmed Br1. It is safe to assume that the patient has a factor that activates TLR9 or something that activates Br1. And our next study is to prove our point, in order to better study the pathogenesis of IMN (Figure 3).

4.3. Time Point of Breg Activation. To answer the time point of Breg activation in IMN progression, we should first determine when the cellular immune response in IMN patients is weaker than the cellular immune response. If it is in the course of disease, why is there no trace of cell infiltration found in the kidneys of a large number of IMN patients [146]? Namely, $CD8^+$ T cell infiltration should be seen in the renal pathology of patients with early MN. If the PLA2R antigens were not from the kidney, IFN-γ concentrations or RNA levels in the peripheral blood should either be higher than at other time points or the proportion of $CD8^+$ T cells should be higher [103, 134].

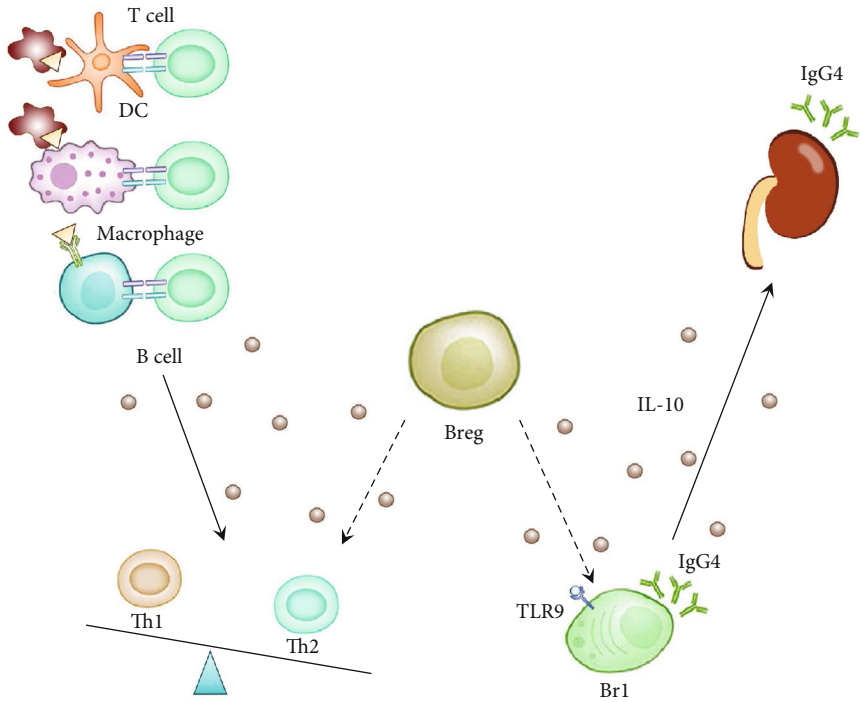

Figure 3: The role of Breg in IMN. Common autoantigens of IMN include PLA2R and THSD7A. Dendritic cells and macrophages phagocytose damaged cells or particles carrying this antigen, or B cells recognize the circulating soluble antigen. These professional APCs capture, process, and present their antigens to Th cells. Th cells reactivate B cells and induce differentiation. In an in vivo high-IL-10 environment, Br1 cells' TLR9 is also stimulated. This stimulates the secretion of IgG4 by Br1 cells. This happens even though IgG4 blocks autoantibodies, forming immune complexes beneath the glomerular epithelium, leading to IMN.

We do not deny the involvement of cellular immune response in IMN, but just why is this immune response so weak? However, in IMN patients, activation of the cellular immune response is inadequate at the onset of the disease. In other words, the level of IL-4 and IL-10 in IMN patients is already elevated before the onset of the disease, which can satisfy this phenomenon. This is because both of these cytokines are major cytokines that inhibit Th1 [36, 115, 147]. Among the cells that can secrete IL-4, basophils, NKT cells, and Th2 cells are common [148, 149]. Monocytes, mast cells, Th2 cells, Treg cells, and Breg cells are common among the cells that can secrete IL-10 [35, 36, 106, 150–153]. At present, there is no obvious correlation between mast cells and IMN [154]. Mononuclear cells showed no significant changes before and after treatment [106]. Treg cells showed low activity in IMN patients [104].

At the same time, no literature could prove the correlation between basophils and NKT cells and IMN. Therefore, Th2 and Breg levels were already elevated before the onset of the disease. To prove whether our opinion is valid, it only needs to prove that the IL-4 and IL-10 levels of patients before the diagnosis of IMN are higher than those of ordinary people, and the occurrence of hypoproteinemia and nephropathic proteinuria in most people is later than the increase of these two cytokines. However, the rise of Th2 did not cause all patients to suffer from allergic diseases such as asthma, precisely because a type of Breg can protect patients from hyperactive autoimmune response even when exposed to allergens [155, 156]. And this kind of Breg is the Br1 cell.

5. Conclusion

We made three significant conclusions. First, we concluded that there are phenotypes and functions of Breg in humans. Second, IMN has many characteristics that are different from other autoimmune diseases. Third, we reasoned that the number of Br1 cells in the activated state in IMN patients is increased.

At present, there are abundant articles about the role of Breg in autoimmune diseases. However, its role in membranous nephropathy is still unknown. This is because it is widely believed that immune-regulating cells in the body play a role in alleviating or even blocking autoimmune diseases and are unlikely to become pathogenic. In this review, we discuss the main functions of Breg and propose relevant hypotheses based on the abnormal pathological and immunological characteristics of IMN. An interesting finding was that Breg has a cell that can secrete IgG4, and IgG4 is the main pathogenic antibody of IMN. Therefore, we believe that IMN may have abnormal Breg function and is related to the activity of Br1 cells. In addition, renal pathology in IMN patients, even at an early stage, is characterized by rare IgM deposition or $CD8^+$ T cell infiltration. Therefore, we suspect that patients already have an autoimmune response at the beginning of IMN, and the number of Breg cells and Th2 cells in these patients is in a comparative advantage, which makes their autoimmune response mainly based on humoral immunity from the beginning. This is the central idea of our hypothesis.

Although Breg is only one type of B cell or immune regulatory cell, its role cannot be ignored. We hope to confirm these views through basic experiments and clinical trials, looking for the number of Breg and subtype abnormalities in the peripheral blood of IMN patients. When conditions permit, a case review is conducted in patients with IMN to investigate the changes of cytokines in their peripheral blood before and after the disease, so as to explore how these abnormal Breg proportions are activated. At the same time, in terms of treatment, we observed whether the efficacy of the drug was related to the change of Breg of the patient, and then developed a treatment method to prevent or inhibit the incidence of IMN and renal damage caused by IMN, so as to be beneficial to the clinical treatment of IMN patients. Finally, through the above series of studies, it is proved that Breg plays a crucial role in IMN, and some new Breg is even found to expand our understanding of Breg.

Conflicts of Interest

The authors declare that there is no conflict of interest regarding the publication of this paper.

Acknowledgments

This work was supported by grants from the National Key Research and Development Project (No. 2019YFC1709402), National Natural Science Foundation of China (Nos. 81673907 and 81973793 to L. B.), Natural Science Foundation of Beijing Municipality (No. 7182070 to L. B.), Capital's Funds for Health Improvement and Research (No. 2020-2-2234 to L. B.), and Beijing Municipal Administration of Hospitals Clinical Medicine Development of Special Funding Support.

References

[1] S. K. Devarapu, G. Lorenz, O. P. Kulkarni, H.-J. Anders, and S. R. Mulay, "Cellular and molecular mechanisms of autoimmunity and lupus nephritis," *International Review of Cell and Molecular Biology*, vol. 332, pp. 43–154, 2017.

[2] G. Papp, P. Boros, B. Nakken, P. Szodoray, and M. Zeher, "Regulatory immune cells and functions in autoimmunity and transplantation immunology," *Autoimmunity Reviews*, vol. 16, no. 5, pp. 435–444, 2017.

[3] G. Thorlacius-Ussing, J. F. Sørensen, H. H. Wandall, and A. E. Pedersen, "Auto-reactive T cells revised. Overestimation based on methodology?," *Journal of Immunological Methods*, vol. 420, pp. 56–59, 2015.

[4] J. Spetz, A. G. Presser, and K. A. Sarosiek, "T cells and regulated cell death: kill or be killed," *International Review of Cell and Molecular Biology*, vol. 342, pp. 27–71, 2019.

[5] C. Ding and J. Yan, "Regulation of autoreactive B cells: checkpoints and activation," *Archivum Immunologiae et Therapiae Experimentalis (Warsz)*, vol. 55, no. 2, pp. 83–89, 2007.

[6] J. Harbige, M. Eichmann, and M. Peakman, "New insights into non-conventional epitopes as T cell targets: the missing link for breaking immune tolerance in autoimmune disease?," *Journal of Autoimmunity*, vol. 84, pp. 12–20, 2017.

[7] K. S. Cashman, S. A. Jenks, M. C. Woodruff et al., "Understanding and measuring human B-cell tolerance and its breakdown in autoimmune disease," *Immunological Reviews*, vol. 292, no. 1, pp. 76–89, 2019.

[8] G. F. Salinas, F. Braza, S. Brouard, P.-P. Tak, and D. Baeten, "The role of B lymphocytes in the progression from autoimmunity to autoimmune disease," *Clinical Immunology*, vol. 146, no. 1, pp. 34–45, 2013.

[9] S. Tsai and P. Santamaria, "MHC class II polymorphisms, autoreactive T-cells, and autoimmunity," *Frontiers in Immunology*, vol. 4, p. 321, 2013.

[10] E. Mariño and S. T. Grey, "B cells as effectors and regulators of autoimmunity," *Autoimmunity*, vol. 45, no. 5, pp. 377–387, 2012.

[11] W. Hoffman, F. G. Lakkis, and G. Chalasani, "B cells, antibodies, and more," *Clinical Journal of the American Society of Nephrology*, vol. 11, no. 1, pp. 137–154, 2016.

[12] S. Bugatti, L. Bogliolo, C. Montecucco, and A. Manzo, "B cell autoimmunity and bone damage in rheumatoid arthritis," *Reumatismo*, vol. 68, no. 3, pp. 117–125, 2016.

[13] M. J. Smith, K. M. Simmons, and J. C. Cambier, "B cells in type 1 diabetes mellitus and diabetic kidney disease," *Nature Reviews. Nephrology*, vol. 13, no. 11, pp. 712–720, 2017.

[14] P. Mota, V. Reddy, and D. Isenberg, "Improving B-cell depletion in systemic lupus erythematosus and rheumatoid arthritis," *Expert Review of Clinical Immunology*, vol. 13, no. 7, pp. 667–676, 2017.

[15] K. Ma, W. Du, X. Wang et al., "Multiple functions of B cells in the pathogenesis of systemic lupus," *International Journal of Molecular Sciences*, vol. 20, no. 23, p. 6021, 2019.

[16] W. G. Couser, "Primary membranous nephropathy," *Clinical Journal of the American Society of Nephrology*, vol. 12, no. 6, pp. 983–997, 2017.

[17] A. Pozdzik, F. Touzani, I. Brochériou, and F. Corazza, "Molecular classification of membranous nephropathy," *Current Opinion in Nephrology and Hypertension*, vol. 28, no. 4, pp. 336–344, 2019.

[18] J. Zhang, L. Bian, F. Z. Ma, Y. Jia, and P. Lin, "Efficacy and safety of rituximab therapy for membranous nephropathy: a meta-analysis," *European Review for Medical and Pharmacological Sciences*, vol. 22, no. 22, pp. 8021–8029, 2018.

[19] W. Lu, S. Gong, J. Li, H. W. Luo, and Y. Wang, "Efficacy and safety of rituximab in the treatment of membranous nephropathy: a systematic review and meta-analysis," *Medicine*, vol. 99, no. 16, 2020.

[20] T. Skaaby, L. L. Husemoen, B. H. Thuesen, R. V. Fenger, and A. Linneberg, "Specific IgE positivity against inhalant allergens and development of autoimmune disease," *Autoimmunity*, vol. 48, no. 5, pp. 282–288, 2015.

[21] V. V. Borba, G. Zandman-Goddard, and Y. Shoenfeld, "Exacerbations of autoimmune diseases during pregnancy and postpartum," *Best Practice & Research. Clinical Endocrinology & Metabolism*, vol. 33, no. 6, p. 101321, 2019.

[22] J. T. Russell, L. F. W. Roesch, M. Ördberg et al., "Genetic risk for autoimmunity is associated with distinct changes in the human gut microbiome," *Nature Communications*, vol. 10, no. 1, p. 3621, 2019.

[23] E. C. Rosser and C. Mauri, "Regulatory B cells: origin, phenotype, and function," *Immunity*, vol. 42, pp. 607–612, 2015.

[24] R. Neta and S. B. Salvin, "Specific suppression of delayed hypersensitivity: the possible presence of a suppressor B cell

in the regulation of delayed hypersensitivity," *The Journal of Immunology*, vol. 113, pp. 1716–1725, 1974.

[25] S. D. Wolf, B. N. Dittel, F. Hardardottir, and C. A. Janeway Jr., "Experimental autoimmune encephalomyelitis induction in genetically B cell-deficient mice," *The Journal of Experimental Medicine*, vol. 184, no. 6, pp. 2271–2278, 1996.

[26] S. Fillatreau, C. H. Sweenie, M. J. McGeachy, D. Gray, and S. M. Anderton, "B cells regulate autoimmunity by provision of IL-10," *Nature Immunology*, vol. 3, no. 10, pp. 944–950, 2002.

[27] A. Mizoguchi and A. K. Bhan, "A case for regulatory B cells," *Journal of Immunology*, vol. 176, no. 2, pp. 705–710, 2006.

[28] P. A. Blair, L. Y. Noreña, F. Flores-Borja et al., "$CD19^{+-}$ $CD24^{hi}CD38^{hi}$ B cells exhibit regulatory capacity in healthy individuals but are functionally impaired in systemic lupus erythematosus patients," *Immunity*, vol. 32, no. 1, pp. 129–140, 2010.

[29] Y. Iwata, T. Matsushita, M. Horikawa et al., "Characterization of a rare IL-10-competent B-cell subset in humans that parallels mouse regulatory B10 cells," *Blood*, vol. 117, no. 2, pp. 530–541, 2011.

[30] S. Lindner, K. Dahlke, K. Sontheimer et al., "Interleukin 21-induced granzyme B-expressing B cells infiltrate tumors and regulate T cells," *Cancer research*, vol. 73, pp. 2468–2479, 2013.

[31] O. Aravena, A. Ferrier, M. Menon et al., "TIM-1 defines a human regulatory B cell population that is altered in frequency and function in systemic sclerosis patients," *Arthritis research & therapy*, vol. 19, no. 8, 2017.

[32] M. Matsumoto, A. Baba, T. Yokota et al., "Interleukin-10-producing plasmablasts exert regulatory function in autoimmune inflammation," *Immunity*, vol. 41, no. 6, pp. 1040–1051, 2014.

[33] W. van de Veen, B. Stanic, G. Yaman et al., "IgG_4 production is confined to human IL-10-producing regulatory B cells that suppress antigen-specific immune responses," *Journal of Allergy and Clinical Immunology*, vol. 131, no. 4, pp. 1204–1212, 2013.

[34] D. O. Griffin and T. L. Rothstein, "Human "orchestrator" CD11b(+) B1 cells spontaneously secrete interleukin-10 and regulate T-cell activity," *Molecular Medicine*, vol. 18, no. 6, pp. 1003–1008, 2012.

[35] S. Schülke, "Induction of Interleukin-10 producing dendritic cells as a tool to suppress allergen-specific T helper 2 responses," *Frontiers in Immunology*, vol. 9, p. 455, 2018.

[36] D. Fang and J. Zhu, "Molecular switches for regulating the differentiation of inflammatory and IL-10-producing anti-inflammatory T-helper cells," *Cellular and Molecular Life Sciences*, vol. 77, no. 2, pp. 289–303, 2020.

[37] B. Wu and Y. Wan, "Molecular control of pathogenic Th17 cells in autoimmune diseases," *International Immunopharmacology*, vol. 80, p. 106187, 2020.

[38] R. Stadhouders, E. Lubberts, and R. W. Hendriks, "A cellular and molecular view of T helper 17 cell plasticity in autoimmunity," *Journal of Autoimmunity*, vol. 87, pp. 1–15, 2018.

[39] M. Oft, "Immune regulation and cytotoxic T cell activation of IL-10 agonists—preclinical and clinical experience," *Seminars in Immunology*, vol. 44, p. 101325, 2019.

[40] H. Mollazadeh, A. F. G. Cicero, C. N. Blesso, M. Pirro, M. Majeed, and A. Sahebkar, "Immune modulation by curcumin: the role of interleukin-10," *Critical Reviews in Food Science and Nutrition*, vol. 59, pp. 89–101, 2017.

[41] C. Mauri and A. Bosma, "Immune regulatory function of B cells," *Annual Review of Immunology*, vol. 30, no. 1, pp. 221–241, 2012.

[42] C. Burrello, F. Garavaglia, F. M. Cribiù et al., "Therapeutic faecal microbiota transplantation controls intestinal inflammation through IL10 secretion by immune cells," *Nature Communications*, vol. 9, no. 1, 2018.

[43] C. Mauri and M. R. Ehrenstein, "The "short" history of regulatory B cells," *Trends in Immunology*, vol. 29, no. 1, pp. 34–40, 2008.

[44] R. Sabat, G. Grütz, K. Warszawska et al., "Biology of interleukin-10," *Cytokine & Growth Factor Reviews*, vol. 21, no. 5, pp. 331–344, 2010.

[45] K. N. Couper, D. G. Blount, and E. M. Riley, "IL-10: the master regulator of immunity to infection," *Journal of Immunology*, vol. 180, no. 9, pp. 5771–5777, 2008.

[46] G. Tian, J. L. Li, D. G. Wang, and D. Zhou, "Targeting IL-10 in auto-immune diseases," *Cell Biochemistry and Biophysics*, vol. 70, no. 1, pp. 37–49, 2014.

[47] G. M. Konjević, A. M. Vuletić, K. M. Mirjačić-Martinović, A. K. Larsen, and V. B. Jurišić, "The role of cytokines in the regulation of NK cells in the tumor environment," *Cytokine*, vol. 117, pp. 30–40, 2019.

[48] Y. Guo, X. Zhang, M. Qin, and X. Wang, "Changes in peripheral $CD19^{+}Foxp3^{+}$ and $CD19^{+}TGF\beta^{+}$ regulatory B cell populations in rheumatoid arthritis patients with interstitial lung disease," *Journal of Thoracic Disease*, vol. 7, no. 3, pp. 471–477, 2015.

[49] G. R. Lee, "The balance of Th17 versus Treg cells in autoimmunity," *International Journal of Molecular Sciences*, vol. 19, 2018.

[50] D. Sheppard, "Epithelial-mesenchymal interactions in fibrosis and repair. Transforming growth factor-β activation by epithelial cells and fibroblasts," *Annals of the American Thoracic Society*, vol. 12, pp. 21–23, 2015.

[51] I. Grafe, S. Alexander, J. R. Peterson et al., "TGF-β family signaling in mesenchymal differentiation," *Cold Spring Harbor Perspectives in Biology*, vol. 10, no. 5, 2018.

[52] P. Garg, M. M. Mazur, A. C. Buck, M. E. Wandtke, J. Liu, and N. A. Ebraheim, "Prospective review of mesenchymal stem cells differentiation into osteoblasts," *Orthopaedic Surgery*, vol. 9, no. 1, pp. 13–19, 2017.

[53] W. Sulaiman and D. H. Nguyen, "Transforming growth factor beta 1, a cytokine with regenerative functions," *Neural Regeneration Research*, vol. 11, no. 10, pp. 1549–1552, 2016.

[54] F. Meylan and J. Gomez-Rodriguez, "T cell receptor and costimulatory signals for Th9 generation," *Methods in Molecular Biology*, vol. 1585, pp. 59–71, 2017.

[55] P. Angkasekwinai, "Th9 cells in allergic disease," *Current Allergy and Asthma Reports*, vol. 19, no. 5, 2019.

[56] C. M. Wortel and S. Heidt, "Regulatory B cells: phenotype, function and role in transplantation," *Transplant Immunology*, vol. 41, pp. 1–9, 2017.

[57] R. Y. Alhabbab, E. Nova-Lamperti, O. Aravena et al., "Regulatory B cells: development, phenotypes, functions, and role in transplantation," *Immunological Reviews*, vol. 292, no. 1, pp. 164–179, 2019.

[58] Z. I. Komlósi, N. Kovács, W. van de Veen et al., "Human CD40 ligand-expressing type 3 innate lymphoid cells induce IL-10-producing immature transitional regulatory B cells," *The Journal of Allergy and Clinical Immunology*, vol. 142, no. 1, pp. 178–194.e11, 2018.

[59] B. Siewe, J. T. Stapleton, J. Martinson et al., "Regulatory B cell frequency correlates with markers of HIV disease progression and attenuates anti-HIV $CD8^+$ T cell function in vitro," *Journal of Leukocyte Biology*, vol. 93, no. 5, pp. 811–818, 2013.

[60] H. Guan, Y. Wan, J. Lan et al., "PD-L1 is a critical mediator of regulatory B cells and T cells in invasive breast cancer," *Scientific Reports*, vol. 6, no. 1, 2016.

[61] Y. Han, J. Wu, L. Bi et al., "Malignant B cells induce the conversion of $CD4^+CD25^-$ T cells to regulatory T cells in B-cell non-Hodgkin lymphoma," *PLoS One*, vol. 6, no. 12, 2011.

[62] X. Sun, T. Zhang, M. Li, L. Yin, and J. Xue, "Immunosuppressive B cells expressing PD-1/PD-L1 in solid tumors: a mini review," *QJM*, vol. 26, pp. 1–6, 2019.

[63] M. Arabpour, R. Rasolmali, A. R. Talei, F. Mehdipour, and A. Ghaderi, "Granzyme B production by activated B cells derived from breast cancer-draining lymph nodes," *Molecular Immunology*, vol. 114, pp. 172–178, 2019.

[64] Z. Saze, P. J. Schuler, C. S. Hong, D. Cheng, E. K. Jackson, and T. L. Whiteside, "Adenosine production by human B cells and B cell-mediated suppression of activated T cells," *Blood*, vol. 122, no. 1, pp. 9–18, 2013.

[65] A. Morva, S. Lemoine, A. Achour, J. O. Pers, P. Youinou, and C. Jamin, "Maturation and function of human dendritic cells are regulated by B lymphocytes," *Blood*, vol. 119, no. 1, p. 106, 2012.

[66] M. J. Stangou, S. Marinaki, E. Papachristou et al., "Histological grading in primary membranous nephropathy is essential for clinical management and predicts outcome of patients," *Histopathology*, vol. 75, no. 5, pp. 660–671, 2019.

[67] K. C. Keri, S. Blumenthal, V. Kulkarni, L. Beck, and T. Chongkrairatanakul, "Primary membranous nephropathy: comprehensive review and historical perspective," *Postgraduate Medical Journal*, vol. 95, no. 1119, pp. 23–31, 2019.

[68] B. Huang, Y. Zhang, L. Wang et al., "Phospholipase A2 receptor antibody IgG4 subclass improves sensitivity and specificity in the diagnosis of idiopathic membranous nephropathy," *Kidney & Blood Pressure Research*, vol. 44, no. 4, pp. 848–857, 2019.

[69] Y. Chen, L. Tang, Z. Feng et al., "Pathological predictors of renal outcomes in nephrotic idiopathic membranous nephropathy with decreased renal function," *Journal of Nephrology*, vol. 27, no. 3, pp. 307–316, 2014.

[70] C. Meyer-Schwesinger, S. Dehde, P. Klug et al., "Nephrotic syndrome and subepithelial deposits in a mouse model of immune-mediated anti-podocyte glomerulonephritis," *Journal of Immunology*, vol. 187, no. 6, pp. 3218–3229, 2011.

[71] C. Hanrotel-Saliou, I. Segalen, Y. Le Meur, P. Youinou, and Y. Renaudineau, "Glomerular antibodies in lupus nephritis," *Clinical Reviews in Allergy & Immunology*, vol. 40, no. 3, pp. 151–158, 2010.

[72] W. Liu, C. Gao, H. Dai et al., "Immunological pathogenesis of membranous nephropathy: focus on PLA2R1 and its role," *Frontiers in Immunology*, vol. 10, 2019.

[73] A. M. Davies and B. J. Sutton, "Human IgG4: a structural perspective," *Immunological Reviews*, vol. 268, no. 1, pp. 139–159, 2015.

[74] S. Crescioli, I. Correa, P. Karagiannis et al., "IgG4 characteristics and functions in cancer immunity," *Current Allergy and Asthma Reports*, vol. 16, p. 7, 2016.

[75] T. H. Scott-Taylor, S. C. Axinia, S. Amin, and R. Pettengell, "Immunoglobulin G: structure and functional implications of different subclass modifications in initiation and resolution of allergy," *Immunity, Inflammation and Disease*, vol. 6, pp. 13–33, 2017.

[76] R. Wang, D. He, L. Zhao et al., "Role of complement system in patients with biopsy-proven immunoglobulin G4-related kidney disease," *Human Pathology*, vol. 81, pp. 220–228, 2018.

[77] S. A. Muhsin, R. Masia, R. N. Smith et al., "Phospholipase A2 receptor-associated membranous nephropathy in a patient with IgG4-related disease: a case report," *Medicine*, vol. 98, no. 20, 2019.

[78] H. Ma, D. G. Sandor, and L. H. Beck, "The role of complement in membranous nephropathy," *Seminars in Nephrology*, vol. 33, no. 6, pp. 531–542, 2013.

[79] R. A. Sinico, N. Mezzina, B. Trezzi, G. M. Ghiggeri, and A. Radice, "Immunology of membranous nephropathy: from animal models to humans," *Clinical and Experimental Immunology*, vol. 183, no. 2, pp. 157–165, 2016.

[80] T. Takano, H. Elimam, and A. V. Cybulsky, "Complement-mediated cellular injury," *Seminars in Nephrology*, vol. 33, no. 6, pp. 586–601, 2013.

[81] W. Luo, O. Florina, J. H. Miner et al., "Alternative pathway is essential for glomerular complement activation and proteinuria in a mouse model of membranous nephropathy," *Frontiers in Immunology*, vol. 9, 2018.

[82] N. Hayashi, K. Okada, Y. Matsui et al., "Glomerular mannose-binding lectin deposition in intrinsic antigen-related membranous nephropathy," *Nephrology Dialysis Transplantation*, vol. 33, no. 5, pp. 832–840, 2018.

[83] K. Kaartinen, A. Safa, S. Kotha, G. Ratti, and S. Meri, "Complement dysregulation in glomerulonephritis," *Seminars in Immunology*, vol. 45, p. 101331, 2019.

[84] L. H. Beck, R. G. Bonegio, G. Lambeau et al., "M-type phospholipase A2 receptor as target antigen in idiopathic membranous nephropathy," *The New England Journal of Medicine*, vol. 361, no. 1, pp. 11–21, 2009.

[85] A. Radice, F. Pieruzzi, B. Trezzi et al., "Diagnostic specificity of autoantibodies to M-type phospholipase A2 receptor (PLA2R) in differentiating idiopathic membranous nephropathy (IMN) from secondary forms and other glomerular diseases," *Journal of Nephrology*, vol. 31, no. 2, pp. 271–278, 2018.

[86] H. Kaga, A. Komatsuda, S. Yamamoto et al., "Comparison of measurements of anti-PLA2R antibodies in Japanese patients with membranous nephropathy using in-house and commercial ELISA," *Clinical and Experimental Nephrology*, vol. 23, no. 4, pp. 465–473, 2019.

[87] N. D. Quach, J. N. Mock, N. E. Scholpa et al., "Role of the phospholipase A2 receptor in liposome drug delivery in prostate cancer cells," *Molecular Pharmaceutics*, vol. 11, no. 10, pp. 3443–3451, 2014.

[88] Y. Dong, L. Cao, H. Tang, X. Shi, and Y. He, "Structure of human M-type phospholipase A2 receptor revealed by cryo-electron microscopy," *Journal of Molecular Biology*, vol. 429, no. 24, pp. 3825–3835, 2017.

[89] S. Jaber, D. Goehrig, P. Bertolino et al., "Generation of a conditional transgenic mouse model expressing human

phospholipase A2 receptor 1," *Scientific Reports*, vol. 10, no. 1, 2020.

[90] A. Augert, C. Payré, Y. de Launoit, J. Gil, G. Lambeau, and D. Bernard, "The M-type receptor PLA2R regulates senescence through the p53 pathway," *EMBO Reports*, vol. 10, no. 3, pp. 271–277, 2009.

[91] A. Griveau, C. Wiel, B. Le Calvé et al., "Targeting the phospholipase A2 receptor ameliorates premature aging phenotypes," *Aging Cell*, vol. 17, no. 6, 2018.

[92] S. Bally, H. Debiec, D. Ponard et al., "Phospholipase A2 receptor-related membranous nephropathy and mannan-binding lectin deficiency," *Journal of the American Society of Nephrology*, vol. 27, pp. 3539–3544, 2016.

[93] X. Xu, G. Wang, N. Chen et al., "Long-term exposure to air pollution and increased risk of membranous nephropathy in China," *Journal of the American Society of Nephrology*, vol. 27, pp. 3739–3746, 2016.

[94] H. C. Stanescu, M. Arcos-Burgos, A. Medlar et al., "Risk HLA-DQA1 and PLA2R1 alleles in idiopathic membranous nephropathy," *The New England Journal of Medicine*, vol. 364, no. 7, pp. 616–626, 2011.

[95] K. Z. Latt, K. Honda, M. Thiri et al., "Identification of a two-SNP *PLA2R1* haplotype and *HLA-DRB1* alleles as primary risk associations in idiopathic membranous nephropathy," *Scientific Reports*, vol. 8, no. 1, 2018.

[96] H. Debiec and P. Ronco, "PLA2R autoantibodies and PLA2R glomerular deposits in membranous nephropathy," *The New England Journal of Medicine*, vol. 364, no. 7, pp. 689-690, 2011.

[97] J. Leon, M. J. Pérez-Sáez, I. Batal et al., "Membranous nephropathy posttransplantation: an update of the pathophysiology and management," *Transplantation*, vol. 103, no. 10, pp. 1990–2002, 2019.

[98] J. D. Nolin, H. L. Ogden, Y. Lai et al., "Identification of epithelial phospholipase A2 receptor 1 as a potential target in asthma," *American Journal of Respiratory Cell and Molecular Biology*, vol. 55, no. 6, pp. 825–836, 2016.

[99] C. C. Silliman, E. E. Moore, G. Zallen et al., "Presence of the M-type sPLA(2) receptor on neutrophils and its role in elastase release and adhesion," *American Journal of Physiology-Cell Physiology*, vol. 283, pp. 1102–1113, 2002.

[100] F. Granata, A. Petraroli, E. Boilard et al., "Activation of cytokine production by secreted phospholipase A2 in human lung macrophages expressing the M-type receptor," *The Journal of Immunology*, vol. 174, pp. 464–474, 2004.

[101] M. Menschikowski, U. Platzbecker, A. Hagelgans et al., "Aberrant methylation of the M-type phospholipase A2 receptor gene in leukemic cells," *BMC Cancer*, vol. 12, no. 1, 2012.

[102] B. Wang, K. Zuo, Y. Wu et al., "Correlation between B lymphocyte abnormality and disease activity in patients with idiopathic membranous nephropathy," *Journal of International Medical Research*, vol. 39, no. 1, pp. 86–95, 2011.

[103] A. Kuroki, M. Iyoda, T. Shibata, and T. Sugisaki, "Th2 cytokines increase and stimulate B cells to produce IgG4 in idiopathic membranous nephropathy," *Kidney International*, vol. 68, no. 1, pp. 302–310, 2005.

[104] M. Rosenzwajg, E. Languille, H. Debiec et al., "B- and T-cell subpopulations in patients with severe idiopathic membranous nephropathy may predict an early response to rituximab," *Kidney International*, vol. 92, no. 1, pp. 227–237, 2017.

[105] Z. Zhang, Y. Shi, K. Yang, R. Crew, H. Wang, and Y. Jiang, "Higher frequencies of circulating ICOS, IL-21 T follicular helper cells and plasma cells in patients with new-onset membranous nephropathy," *Autoimmunity*, vol. 50, no. 8, pp. 458–467, 2017.

[106] J. Hou, M. Zhang, Y. Ding et al., "Circulating $CD14^{+}CD163^{+-}$ $CD206^{+}$ M2 monocytes are increased in patients with early stage of idiopathic membranous nephropathy," *Mediators Inflamm*, vol. 2018, article 5270657, 10 pages, 2018.

[107] Z. Zhang, X. Liu, H. Wang et al., "Increased soluble ST2 and IL-4 serum levels are associated with disease severity in patients with membranous nephropathy," *Molecular Medicine Reports*, vol. 17, no. 2, pp. 2778–2786, 2018.

[108] M. Ifuku, K. Miyake, M. Watanebe et al., "Various roles of Th cytokine mRNA expression in different forms of glomerulonephritis," *American Journal of Nephrology*, vol. 38, no. 2, pp. 115–123, 2013.

[109] Y. Kawasaki, J. Suzuki, N. Sakai et al., "Evaluation of T helper-1/-2 balance on the basis of IgG subclasses and serum cytokines in children with glomerulonephritis," *American Journal of Kidney Diseases*, vol. 44, no. 1, pp. 42–49, 2004.

[110] C. Muangchan and J. E. Pope, "Interleukin 6 in systemic sclerosis and potential implications for targeted therapy," *The Journal of Rheumatology*, vol. 39, no. 6, pp. 1120–1124, 2012.

[111] W. G. McMaster, A. Kirabo, M. S. Madhur, and D. G. Harrison, "Inflammation, immunity, and hypertensive end-organ damage," *Circulation Research*, vol. 116, no. 6, pp. 1022–1033, 2015.

[112] S. Garbuzova-Davis, J. Ehrhart, P. R. Sanberg, and C. Borlongan, "Potential role of humoral IL-6 cytokine in mediating pro-inflammatory endothelial cell response in amyotrophic lateral sclerosis," *International Journal of Molecular Sciences*, vol. 19, no. 2, p. 423, 2018.

[113] L. Sun, C. He, L. Nair, J. Yeung, and C. E. Egwuagu, "Interleukin 12 (IL-12) family cytokines: role in immune pathogenesis and treatment of CNS autoimmune disease," *Cytokine*, vol. 75, no. 2, pp. 249–255, 2015.

[114] H. Zheng, Y. Ban, F. Wei, and X. Ma, "Regulation of interleukin-12 production in antigen-presenting cells," *Advances in Experimental Medicine and Biology*, vol. 941, pp. 117–138, 2016.

[115] A. Cope, G. Le Friec, J. Cardone, and C. Kemper, "The Th1 life cycle: molecular control of IFN-γ to IL-10 switching," *Trends in Immunology*, vol. 32, no. 6, pp. 278–286, 2011.

[116] Y. Guo, N. K. Patil, L. Luan, J. K. Bohannon, and E. R. Sherwood, "The biology of natural killer cells during sepsis," *Immunology*, vol. 153, no. 2, pp. 190–202, 2018.

[117] S. Kracker and A. Durandy, "Insights into the B cell specific process of immunoglobulin class switch recombination," *Immunology Letters*, vol. 138, no. 2, pp. 97–103, 2011.

[118] K. Yu and M. R. Lieber, "Current insights into the mechanism of mammalian immunoglobulin class switch recombination," *Critical Reviews in Biochemistry and Molecular Biology*, vol. 54, no. 4, pp. 333–351, 2019.

[119] I. C. Ho and S. C. Miaw, "Regulation of IL-4 expression in immunity and diseases," *Advances in Experimental Medicine and Biology*, vol. 941, pp. 31–77, 2016.

[120] M. Saraiva and A. O'Garra, "The regulation of IL-10 production by immune cells," *Nature Reviews Immunology*, vol. 10, no. 3, pp. 170–181, 2010.

[121] E. F. McKinney, P. A. Lyons, E. J. Carr et al., "A CD8+ T cell transcription signature predicts prognosis in autoimmune disease," *Nature Medicine*, vol. 16, no. 5, pp. 586–591, 2010.

[122] H. Carvalheiro, J. A. da Silva, and M. M. Souto-Carneiro, "Potential roles for $CD8^+$ T cells in rheumatoid arthritis," *Autoimmunity Reviews*, vol. 12, no. 3, pp. 401–409, 2013.

[123] A. Mak and N. Y. Kow, "The pathology of T cells in systemic lupus erythematosus," *Journal of Immunology Research*, vol. 2014, Article ID 419029, 8 pages, 2014.

[124] P. Wehr, H. Purvis, S. C. Law, and R. Thomas, "Dendritic cells, T cells and their interaction in rheumatoid arthritis," *Clinical and Experimental Immunology*, vol. 196, no. 1, pp. 12–27, 2019.

[125] P. Hillyer, N. Raviv, D. M. Gold et al., "Subtypes of type I IFN differentially enhance cytokine expression by suboptimally stimulated CD4(+) T cells," *European Journal of Immunology*, vol. 43, no. 12, pp. 3197–3208, 2013.

[126] F. B. Vincent, D. Saulep-Easton, W. A. Figgett, K. A. Fairfax, and F. Mackay, "The BAFF/APRIL system: emerging functions beyond B cell biology and autoimmunity," *Cytokine & Growth Factor Reviews*, vol. 24, no. 3, pp. 203–215, 2013.

[127] G. S. Dickinson, M. Akkoyunlu, R. J. Bram, and K. R. Alugupalli, "BAFF receptor and TACI in B-1b cell maintenance and antibacterial responses," *Annals of the New York Academy of Sciences*, vol. 1362, no. 1, pp. 57–67, 2015.

[128] C. M. Coquery and L. D. Erickson, "Regulatory roles of the tumor necrosis factor receptor BCMA," *Critical Reviews in Immunology*, vol. 32, no. 4, pp. 287–305, 2012.

[129] E. Sanchez, E. J. Tanenbaum, S. Patil et al., "The clinical significance of B-cell maturation antigen as a therapeutic target and biomarker," *Expert Review of Molecular Diagnostics*, vol. 18, no. 4, pp. 319–329, 2018.

[130] C. Murtas and G. M. Ghiggeri, "Membranous glomerulonephritis: histological and serological features to differentiate cancer-related and non-related forms," *Journal of Nephrology*, vol. 29, no. 4, pp. 469–478, 2016.

[131] D. Zhang, C. Zhang, F. Bian, W. Zhang, G. Jiang, and J. Zou, "Clinicopathological features in membranous nephropathy with cancer: a retrospective single-center study and literature review," *The International Journal of Biological Markers*, vol. 34, no. 4, pp. 406–413, 2019.

[132] P. Alessandro, M. Alessandra, D. Irene, and M. R. Zocchi, "Mechanisms of tumor escape from immune system: role of mesenchymal stromal cells," *Immunology Letters*, vol. 159, pp. 55–72, 2014.

[133] L. Yang and C. Xuetao, "Immunosuppressive cells in tumor immune escape and metastasis," *Journal of Molecular Medicine*, vol. 94, pp. 509–522, 2016.

[134] P. Kumar, P. Bhattacharya, and B. S. Prabhakar, "A comprehensive review on the role of co-signaling receptors and Treg homeostasis in autoimmunity and tumor immunity," *Journal of Autoimmunity*, vol. 95, pp. 77–99, 2018.

[135] N. Kumar, H. Chugh, R. Tomar, V. Tomar, V. K. Singh, and R. Chandra, "Exploring the interplay between autoimmunity and cancer to find the target therapeutic hotspots," *Artificial Cells, Nanomedicine, and Biotechnology*, vol. 46, no. 4, pp. 658–668, 2018.

[136] D. Roccatello, S. Sciascia, D. Di Simone et al., "New insights into immune mechanisms underlying response to rituximab in patients with membranous nephropathy: a prospective study and a review of the literature," *Autoimmunity Reviews*, vol. 15, no. 6, pp. 529–538, 2016.

[137] C. Mauri and M. Menon, "The expanding family of regulatory B cells," *International Immunology*, vol. 27, no. 10, pp. 479–486, 2015.

[138] A. S. Chong, "B cells as antigen-presenting cells in transplantation rejection and tolerance," *Cellular Immunology*, vol. 349, p. 104061, 2020.

[139] E. Kuokkanen, V. Šuštar, and P. K. Mattila, "Molecular control of B cell activation and immunological synapse formation," *Traffic*, vol. 16, no. 4, pp. 311–326, 2015.

[140] G. H. Wang, J. Lu, K. L. Ma et al., "The release of monocyte-derived tissue factor-positive microparticles contributes to a hypercoagulable state in idiopathic membranous nephropathy," *Journal of Atherosclerosis and Thrombosis*, vol. 26, no. 6, pp. 538–546, 2019.

[141] S. Cheng, H. Wang, and H. Zhou, "The role of TLR4 on B cell activation and anti-GPI antibody production in the antiphospholipid syndrome," *Journal of immunology research*, vol. 2016, Article ID 1719720, 2016.

[142] M. I. Yuseff, P. Pierobon, A. Reversat, and A. M. Lennon-Duménil, "How B cells capture, process and present antigens: a crucial role for cell polarity," *Nature Reviews Immunology*, vol. 13, no. 7, p. 475, 2013.

[143] A. E. van de Logt, M. Fresquet, J. F. Wetzels, and P. Brenchley, "The anti-PLA2R antibody in membranous nephropathy: what we know and what remains a decade after its discovery," *Kidney International*, vol. 96, no. 6, pp. 1292–1302, 2019.

[144] Y. T. Chen, C. C. Wei, K. L. Ng et al., "Toll-like receptor 9 SNPs are susceptible to the development and progression of membranous glomerulonephritis: 27 years follow-up in Taiwan," *Renal Failure*, vol. 35, no. 10, pp. 1370–1375, 2013.

[145] C. Cantarelli, M. Jarque, A. Angeletti et al., "A comprehensive phenotypic and functional immune analysis unravels circulating anti-phospholipase A2 receptor antibody secreting cells in membranous nephropathy patients," *Kidney International Reports*, vol. 5, no. 10, pp. 1764–1776, 2020.

[146] X. Chen, Y. Chen, K. Shi et al., "Comparison of prognostic, clinical, and renal histopathological characteristics of overlapping idiopathic membranous nephropathy and IgA nephropathy versus idiopathic membranous nephropathy," *Scientific Reports*, vol. 7, 2017.

[147] E. Şahin, S. A. Bafaqeeh, S. G. Güven et al., "Mechanism of action of allergen immunotherapy," *American Journal of Rhinology & Allergy*, vol. 30, 5_supplement, pp. S1–S3, 2016.

[148] A. Sahoo, S. Wali, and R. Nurieva, "T helper 2 and T follicular helper cells: regulation and function of interleukin-4," *Cytokine & Growth Factor Reviews*, vol. 30, pp. 29–37, 2016.

[149] C. Iwamura and T. Nakayama, "Role of NKT cells in allergic asthma," *Current Opinion in Immunology*, vol. 22, no. 6, pp. 807–813, 2010.

[150] D. Elieh Ali Komi and D. Ribatti, "Mast cell-mediated mechanistic pathways in organ transplantation," *European Journal of Pharmacology*, vol. 857, p. 172458, 2019.

[151] T. Boonpiyathad, P. Satitsuksanoa, M. Akdis, and C. A. Akdis, "Il-10 producing T and B cells in allergy," *Seminars in Immunology*, vol. 44, p. 101326, 2019.

[152] J. Geginat, M. Vasco, M. Gerosa et al., "IL-10 producing regulatory and helper T-cells in systemic lupus erythematosus," *Seminars in Immunology*, vol. 44, p. 101330, 2019.

[153] C. Cerqueira, B. Manfroi, and S. Fillatreau, "IL-10-producing regulatory B cells and plasmocytes: molecular mechanisms and disease relevance," *Seminars in Immunology*, vol. 44, p. 101323, 2019.

[154] M. Danilewicz and M. Wagrowska-Danilewicz, "Quantitative analysis of interstitial mast cells in lupus and non-lupus membranous glomerulopathy," *Polish Journal of Pathology*, vol. 52, pp. 211–217, 2001.

[155] W. van de Veen, B. Stanic, O. F. Wirz, K. Jansen, A. Globinska, and M. Akdis, "Role of regulatory B cells in immune tolerance to allergens and beyond," *The Journal of Allergy and Clinical Immunology*, vol. 138, pp. 654–665, 2016.

[156] W. van de Veen, "The role of regulatory B cells in allergen immunotherapy," *Current Opinion in Allergy and Clinical Immunology*, vol. 17, no. 6, pp. 447–452, 2017.

Hindawi
Journal of Immunology Research
Volume 2020, Article ID 8632048, 14 pages
https://doi.org/10.1155/2020/8632048

Review Article

Potential Therapeutic Role of Purinergic Receptors in Cardiovascular Disease Mediated by SARS-CoV-2

Fernanda dos Anjos[1], **Júlia Leão Batista Simões**[1], **Charles Elias Assmann**[2], **Fabiano Barbosa Carvalho**[3] and **Margarete Dulce Bagatini**[4]

[1]*Medical School, Federal University of Fronteira Sul, Chapecó, SC, Brazil*
[2]*Department of Biochemistry and Molecular Biology, Federal University of Santa Maria, Santa Maria, RS, Brazil*
[3]*Federal University of Health Sciences of Porto Alegre, Porto Alegre, RS, Brazil*
[4]*Graduate Program in Biomedical Sciences, Federal University of Fronteira Sul, Chapecó, SC, Brazil*

Correspondence should be addressed to Margarete Dulce Bagatini; margaretebagatini@yahoo.com.br

Received 24 July 2020; Revised 6 November 2020; Accepted 24 November 2020; Published 2 December 2020

Academic Editor: Ravirajsinh Jadeja

Novel coronavirus disease 2019 (COVID-19) causes pulmonary and cardiovascular disorders and has become a worldwide emergency. Myocardial injury can be caused by direct or indirect damage, particularly mediated by a cytokine storm, a disordered immune response that can cause myocarditis, abnormal coagulation, arrhythmia, acute coronary syndrome, and myocardial infarction. The present review focuses on the mechanisms of this viral infection, cardiac biomarkers, consequences, and the possible therapeutic role of purinergic and adenosinergic signalling systems. In particular, we focus on the interaction of the extracellular nucleotide adenosine triphosphate (ATP) with its receptors P2X1, P2X4, P2X7, P2Y1, and P2Y2 and of adenosine (Ado) with A2A and A3 receptors, as well as their roles in host immune responses. We suggest that receptors of purinergic signalling could be ideal candidates for pharmacological targeting to protect against myocardial injury caused by a cytokine storm in COVID-19, in order to reduce systemic inflammatory damage to cells and tissues, preventing the progression of the disease by modulating the immune response and improving patient quality of life.

1. Introduction

It took three months for a sudden outbreak of novel coronavirus disease 2019 (COVID-19) to become a pandemic by March 11, according to the World Health Organization (WHO) [1]. The new coronavirus causes severe damage to the respiratory tract (initially the upper and eventually the lower) sometimes resulting in acute respiratory syndrome. Studies showed that the COVID-19 pandemic emerged as a zoonosis, given the shared history of more than 40 patients in Wuhan, China, who were exposed at the Huanan Seafood Market [2]. By sequencing the entire viral RNA genome, it was revealed that this contamination may be due to human contact with certain types of bats, because SARS-CoV-2 (the causative agent of COVID-19) appears to be closely related to two coronaviruses responsible for acute respiratory syndrome, bat-SL-CoVZC45 and bat-SL-CoVZXC21 [3]. Researchers in Guangzhou, China, suggested that human contact with pangolins occurred, making these animals the likely biological source of the COVID-19 outbreak [4].

The inflammatory process mediated by SARS-CoV-2 is essential for the organism to effectively fight the invasion of the virus, because, after the initial recognition of the pathogens, immune cell recruitment then activates cascades in order to eliminate the pathogen and, finally, restore homeostasis to the injured tissue. Nevertheless, excessive and prolonged responses of cytokines and chemokines such as a cytokine storm (CS) can occur [5].

In particular, we wish to focus on immune responses involving the nucleotide adenosine triphosphate (ATP), an intracellular energy molecule released from various types of cells after damage, which accumulates at sites of tissue injury

and inflammation as well [1]. After release, it can activate receptors or be rapidly decomposed by ectonucleotidases [2]. Extracellular ATP in low concentrations opens cation channels and sometimes leads to cell proliferation, while at high concentrations, it is a proinflammatory danger signal [3] that upregulates P2X purinoceptors located on immune cells (neutrophils, eosinophils, monocytes, macrophages, mast cells, and lymphocytes) [1, 4]. The ATP that is released due to the action of SARS-CoV-2 is an important mediator of inflammation, promoting the proliferation of immune cells and T cell activation [4], possibly contributing to the exacerbation of the immunological response and damaging the myocardium.

In the purinergic system, adenosine, a product of ATP decomposition, has a primary immunosuppressive action by inhibiting the proliferation of T cells and the release of proinflammatory cytokines. This occurs via hydrolysis of ATP in the extracellular medium through the action of ectonucleotidases, NTPDase converting ATP to adenosine $5'$-diphosphate (ADP) and ADP to adenosine monophosphate (AMP). Consequently, ecto-$5'$-nucleotidase converts AMP to adenosine, which is ultimately degraded to inosine by the action of adenosine deaminase (ADA) [6]. This immune exacerbation leads to dysfunction of several organs, including the heart [5]. For these reasons, immunosuppressive substances that regulate inflammatory responses can increase the success rate of treatment and reduce the mortality rate in patients with COVID-19 [6].

2. COVID-19: The Current Pandemic Context

The first case of COVID-19 was reported in Wuhan, China, at the end of 2019. Within two months, it spread around the globe by virtue of its high level of contagion. Transmission can occur through direct contact or through respiratory droplets, as well as through contact with contaminated surfaces [7]. Most of the available case reports show mild to severe respiratory disease with fever, fatigue, cough, myalgia, and difficulty breathing [8]. The main sources of infection are patients with pneumonia infected by the new coronavirus; it is estimated that the infection has an average incubation period of 6.4 days and a basic reproduction number of 2.24–3.58 [3].

Coronaviruses are enveloped positive-chain RNA viruses belonging to the *Coronaviridae* family of the order *Nidovirales*. They are classified into four genera: *Alphacoronavirus*, *Betacoronavirus*, *Gammacoronavirus*, and *Deltacoronavirus* [2, 9]. Of these, only the gamma genus cannot infect mammals; however, due to their genetic organization, they are prone to mutations and possible host exchange because they have the largest genome among RNA viruses. The coronaviruses that have already been identified may just be "the tip of the iceberg," with potentially newer and more serious zoonotic events to be revealed, because SARS-CoV and MERS-CoV are betacoronaviruses, as is the new SARS-CoV-2. SARS-CoV infected 8,000 people with a mortality rate of approximately 10%; MERS-CoV infected 1,700 people, with a mortality rate of 36% [2].

According to the Chinese Center for Disease Control and Prevention, which recorded approximately 44,500 confirmed cases of COVID-19, 81% had mild illness (asymptomatic or mild pneumonia); 14% were severe, including dyspnoea, hypoxia, or pulmonary involvement; and 5% became critically ill, characterized by respiratory failure, shock, or involvement in other systems. The overall case mortality rate was 2.3% without registration of noncritical cases [10, 11]. Patients with metabolic diseases and comorbidities, especially cardiovascular ones, may face greater risks of progressing to severe conditions associated with worse prognoses [10, 12, 13].

3. COVID-19 Stages and Progression

Siddiqi and Mehra [14] proposed a 3-stage classification model, recognizing that COVID-19 illness exhibited three grades of increasing severity, corresponding to distinct clinical findings, responses to therapy, and clinical outcome [15], COVID-19: mild, moderate, and severe. The severe classification describes patients with difficulty in breathing, or a respiratory rate (RR) greater than 29 breaths per minute at rest, or average oxygen saturation less than 92%, or partial pressure of arterial oxygen in the blood (PaO_2/fraction of inspired oxygen concentration FiO_2) less than or equal to 300 mmHg. Critically ill patients are characterized by respiratory failure requiring mechanical ventilation, shock, or combined failure of other organs [7].

The third stage of infection, characterized by extrapulmonary systemic hyperinflammation with elevated inflammatory marks, appears to be less common in COVID-19 patients [14]; however, these symptoms must be studied because the mortality rate is much higher in patients in the third and most severe stage. With higher prevalence in hospitalized patients in intensive care, 7.2%, 8.7%, and 16.7% of acute cardiac injury, shock, and arrhythmia, respectively, were observed in a clinical cohort of patients with COVID-19 [16].

Upon entering the cell, the virus uses four mechanisms to circumvent the immune response. Initially, it inhibits interferon type 1 (IFN-1), known as the initial alarm, characterized by the rapid expression [17]. Then, the virus inhibits STAT-1 [18] phosphorylation to interfere with IFN-1 signalling; the third defensive mechanism is the exaggerated and prolonged production of IFN-1 by plasmacytoid dendritic cells (pDCs) to cause exhaustion so that the influx of inflammatory macrophages/monocytes and activated neutrophils occurs, resulting in pulmonary immunopathology such as acute respiratory distress syndrome (ARDS) [19]. Finally, there is a CS that further weakens the immune system through IFN-1-mediated T cell apoptosis [5, 20].

It was also reported that the duration of symptoms in the severe group was longer than that in the mild group. It was also reported that the duration of symptoms was longer and the incidence of comorbidities was greater in the severe group. CD4+ and CD8+ T lymphocytes are reduced in the severe group, suggesting that they act as an important defence against SARS-CoV-2. Critically ill patients have other common characteristics that demonstrate the

deterioration of the immune system, including atrophy of the spleen and lymph nodes, along with reduced lymphocytes in lymphoid organs, and much lower levels of lymphocytes, especially natural killer (NK) cells; the majority of infiltrated immune cells in lung lesions are monocytes and macrophages, with minimal lymphocyte infiltration [15].

According to reports, patients infected with SARS-CoV-2 may have symptoms similar to those of SARS 2002. In the first analysis, the initial symptoms were fever, dry cough, rhinorrhoea, headache, and fatigue, in addition to diarrhoea, odynophagia, anosmia, and ageusia. The scenario may worsen, although approximately 80% of patients have mild symptoms, with lymphopenia and interstitial pneumonia [21, 22]. When COVID-19 rapidly progresses, these immune and inflammatory responses are capable of creating a severe CS and releasing proinflammatory markers such as interleukin 2 (IL-2), interleukin 6 (IL-6), interleukin 7 (IL-7), interleukin 10 (IL-10), granulocyte colony-stimulating factor (G-CSF), gamma interferon-inducible protein 10 (IP-10), monocyte chemotactic protein-1 (MCP-1), macrophage inflammatory protein 1-alpha (MIP-1α), and tumour necrosis factor-alpha (TNF-α) [21, 23]. In this situation, an exaggerated immune system response and an excessive inflammatory response may cause multiple organ failure and ARDS and may possibly cause death [21, 22].

Burnstock (2017) claims that purinergic signalling plays a major role in both physiology and pathophysiology in the heart, brain, gut, and lung. However, in the pandemic context in which elderly patients are more susceptible to complications, it is necessary to consider the age-related changes of purine receptors and their relationship with the following: (a) diseases of the central nervous system such as epilepsy, brain injury, psychiatric disorders, and neuropathic pain; (b) cardiovascular diseases such as hypertension, atherosclerosis, thrombosis, and stroke; (c) diseases of the airways such as chronic obstructive pulmonary disease, airway infections, asthma, lung injury, pulmonary fibrosis, cystic fibrosis, lung tumours, and chronic cough; and (d) gut disorders such as ulcerative colitis, Crohn's disease, irritable bowel syndrome, diarrhoea, and constipation.

4. COVID-19 and Cardiovascular Disease

Cardiac manifestations of coronavirus infections may be understood as a combination of factors, and damage may be caused directly or indirectly by viral infection [24, 25]. A recent study reported that patients with previous SARS infections had cardiovascular consequences and myocardial injury [26, 27] with systolic and diastolic dysfunction followed by heart failure, arrhythmias, and death [13]. These findings suggest that the SARS coronavirus subfamily has the potential to infect and alter cardiac tissue, potentiating myocardial damage [26–28].

Lau et al. [29] reported palpitations in the form of tachycardia at rest or light effort in patients who were recovering from SARS. The possible causes include cardiac arrhythmia, anaemia, state of anxiety, impaired lung function, thyroid dysfunction, and autonomic dysfunction [29]. A meta-analysis suggested that patients with underlying cardiovascular diseases would be more likely to be infected with MERS-CoV [30], while other studies showed that, during periods of high influenza activity, there is a greater propensity for shock-treated ventricular arrhythmias, in the context of systemic, arterial, and severe myocardial inflammation [12, 31].

The primary diagnostic tests (Table 1) used to diagnose COVID-19 with cardiovascular involvement include N-terminal probrain natriuretic peptide (NT-proBNP). Higher levels are associated with high risk, worse prognoses, and intensive care unit (ICU) admission [23, 32, 33]. A high-sensitivity assay for troponin may be helpful for risk assessment in patients requiring ICU care and myocardial injury [23, 34]. Patients with higher levels of D-dimer may require ICU care [23, 35]. Procalcitonin (PCT) is used to assess the need for care in the ICU. Complete blood counts reveal leukopenia and lymphocytopenia [23, 32, 36] High levels of ferritin signal poor outcomes [23, 32, 36, 37]. High concentrations of IL-6 are associated with worse prognoses [32, 36, 38]. Cardiac computed tomography (CT) is used in uncertain cases with elevated troponins with or without obstructive coronary artery disease. In ECG, the most common changes include ST and PR segment elevation and T and Q waves. Echocardiography shows myocardial systolic dysfunction and demonstrates myocyte necrosis and mononuclear cell infiltration [23].

A cohort study of 416 patients associated cardiac injury with mortality in patients with COVID-19 at Renmin University Hospital in Wuhan, China. The average age was 64 years, and the majority were women. The most common symptoms were fever (80.3%), cough (34.6%), and shortness of breath (28.1%). Cardiac injury was present in 82 patients, and the associated comorbidities were hypertension ($p < 0.001$), elevated leukocyte counts (median: 9,400), and elevated levels of CRP (median: 10.2), PCT (median: 0.27), CK-MB (median: 3.2), myohaemoglobin (median: 128), hs-TnI (median: 0.19), NT-proBNP (median: 1,689), aspartate aminotransferase (AST, median: 40), and creatinine (median: 1.15). In addition, there was diffuse mottling and ground-glass opacities on radiographic findings (64.6%). Frequent complications in those with cardiac injury were ARDS (58.5%), acute kidney injury (8.5%), electrolyte disturbances (15.9%), hypoproteinaemia (13.4%), and coagulation disorders (7.3%). The mortality rate among patients with cardiac injury (51.2%) was much higher than that among those without cardiac injury (4.5%) [39].

There was a case report of a patient with pneumonia and cardiac symptoms who demonstrated elevated troponin I (Trop I) (11.37 g/L), myoglobin (Myo) (390.97 ng/mL), and NT-proBNP (22,600 pg/mL). The ECG showed sinus tachycardia; echocardiography revealed an enlarged left ventricle (61 mm), diffuse myocardial dyskinesia, low left ventricular ejection fraction (LVEF) (32%), and pulmonary hypertension (44 mmHg) [40].

Recent studies suggest that cardiac injury is due to the close relationship between the course of the disease and the cardiovascular system (see Figure 1). We focus on three main mechanisms resulting from COVID-19 responsible for myocardial injury: the angiotensin-converting enzyme II (ACE2), cytokine storm syndrome [13, 23, 41], and respiratory

Table 1: Cardiological findings related to disease severity and mortality.

Exam	Result	Association	Reference
NT-proBNP	High level	Heart failure	[28, 29]
Troponin (I or T)	High sensitivity	Myocardial injury	[28, 30]
D-dimer	Greater than 2.0 μg/mL	Thrombosis	[28, 31, 34]
Prothrombin time	Longer	Investigation of coagulopathies	[28, 34]
Fibrinogen	High level	Analysis of consumption coagulopathies	[28, 34]
Full blood count	Lymphocytes and platelet count	Anaemia, leucocytosis/leucopenia, lymphopenia, thrombocytopenia	[28]
Procalcitonin	High level	Inflammatory marker, evaluation of bacterial coinfection	[28, 32]
C-reactive protein	High level	Inflammatory marker	[28, 32]
IL-6	High level	Inflammatory marker	[28, 32, 33]
Ferritin	Increases	Infection/inflammatory response	[28, 33]
Lactate dehydrogenase (LDH)	High level	Tissue damage	[35, 36]
Cardiac computed tomography (CT)	Used in uncertain cases with elevated troponins	Cardiac injury	[19]
ECG	Changes include ST and PR segment elevation and T and Q waves	Cardiac injury	[19]
Echocardiography	—	Myocardial systolic dysfunction and demonstrates myocyte necrosis and mononuclear cell infiltration	[19]

dysfunction and hypoxemia due to COVID-19, resulting in damage to the myocardium [42].

4.1. Myocardial Injury and ACE2. To better understand the myocardial injury caused by ACE2, it is necessary to remember the pathophysiology of COVID-19. The ACE2 protein is the cellular receptor through which SARS-CoV-2 enters cells [39, 40]; it is a membrane protein necessary for viral binding and internalization, similar to SARS-CoV [43]. After binding, activation of viral peak glycoprotein occurs and the C-terminal segment of ACE2 is cleaved by proteases such as TMPRSS2 and FURIN that are expressed in lung tissue [13, 26, 43].

Hair cells and goblet cells are concentrated in the upper nasal region and have high levels of ACE2 and TMPRSS [44], a fact that facilitates the entry of viruses in host cells, because serine protease assists with cleavage and glycoproteic activation of the viral envelope [45]. When infected, the respiratory epithelial cells undergo ciliary damage and become vacuolated [46]. In this situation, there is the production of inflammatory mediators that promote nasal secretions, inflammation, and local swelling, as well as stimulate sneezing, obstruction of the airways, and increase of the temperature of the mucosa [47]. In this manner, SARS-CoV-2 inserts into type 2 pneumocytes, cardiomyocytes, and macrophages via ACE2 [23]. In response, there may be myocardial, endothelial, and microvascular damage and dysfunction, plaque instability, and myocardial infarction (MI) [46].

In the heart, ACE2 is also highly expressed, and in some states of overactivation such as atherosclerosis, hypertension, and congestive heart failure, the effects of angiotensin II are neutralized [48, 49]. When a hospitalized patient has an early assessment, cardiac damage and clotting are monitored continuously; parameters such as cTnI, NT-proBNP, and D-dimer are elevated; and cardiac injuries can be identified, increasing the chance of predicting possible complications in COVID-19 [23]. Therefore, comorbidities that promote changes in metabolism can trigger a series of biochemical events that lead to increased expression of the *ACE2* gene, causing these patients to have an exacerbation of infected cells and therefore more severe clinical manifestations [49].

There is no relationship between the use of ACE inhibitors or angiotensin receptor blockers (ARBs) and the adverse outcomes [23]. ACE2 is widely distributed in the heart, testicles, kidneys, and lungs, where it functions as an antagonist of the classic RAS system; it is able to protect against organ damage in cases of hypertension, diabetes, cardiovascular diseases, and severe lung injuries, including ARDS, which is associated with high mortality [50]. Thus, ACE2 participates in cardiovascular homeostasis and is a functional receptor and gateway for coronavirus, as well as coronavirus 2. In this context, there is a connection between SARS-CoV-2 and ACE2 in that the negative regulation of this receptor is closely associated with cardiac protection [51].

4.2. Myocardial Injury and Hypoxia. Hypoxemia caused by COVID-19 can result in serious damage to myocardial cells [42]. A recent review pointed out that the supposed basic pathophysiological interaction between haemoglobin and SARS-CoV-2 is made by ACE2, CD147, and CD26 receptors located on erythrocytes or blood precursor cells. After viral endocytosis, there is a link between the cell receptor and the spike proteins that bind to the porphyrin that attacks haemoglobin in its heme portion. This would result in

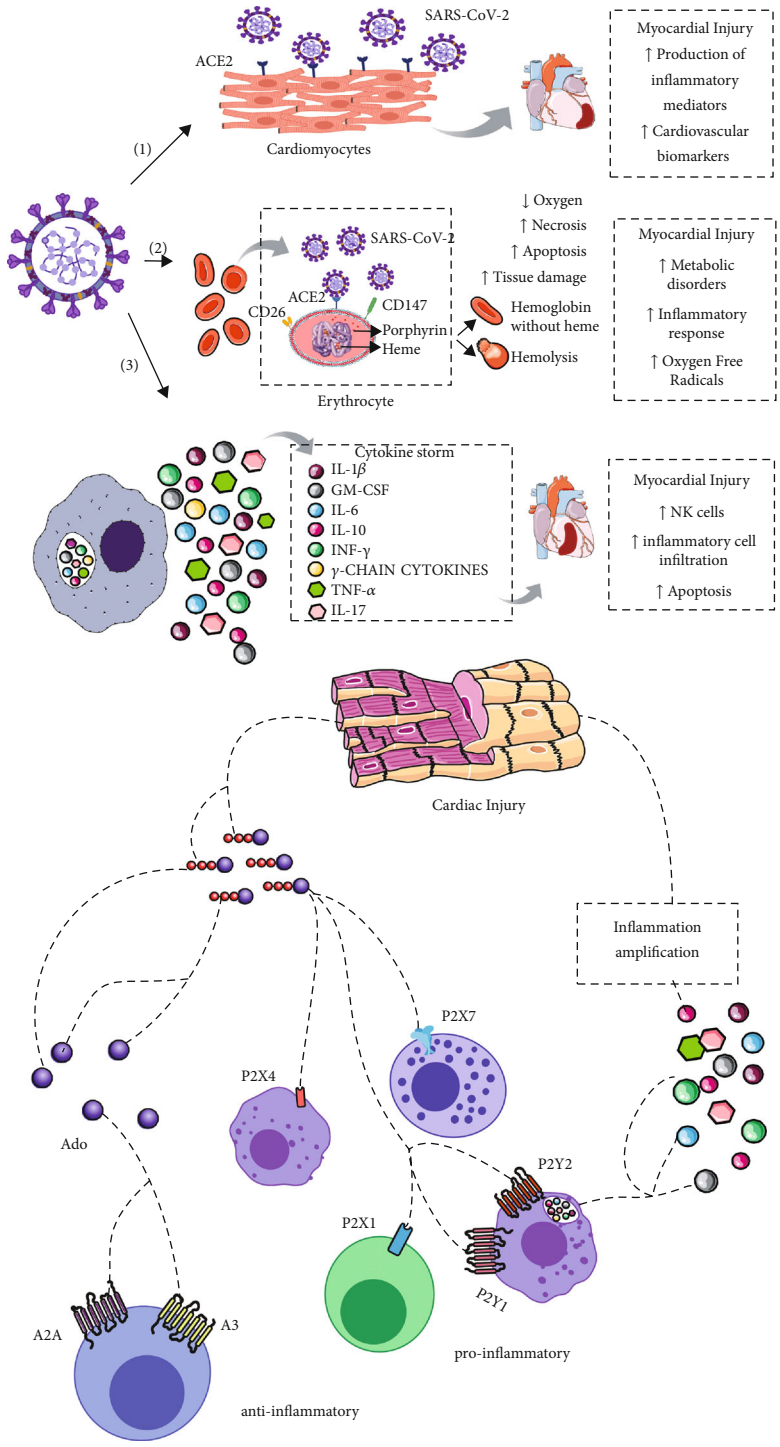

Figure 1: The cardiovascular system can be affected by COVID-19 and can cause myocardial injury. We focused on three mechanisms: (1) by the angiotensin-converting enzyme II (ACE2), (2) by the respiratory dysfunction and hypoxemia due to COVID-19, and (3) by the cytokine storm syndrome, which results in damage to the myocardium. Myocardial injury releases extracellular nucleotide adenosine triphosphate (ATP), a proinflammatory danger signal via the upregulation of P2 purinoceptors located on immune cells (neutrophils, eosinophils, monocytes, macrophages, mast cells, and lymphocytes). ATP released due to the action of SARS-CoV-2 is an important mediator of inflammation, promoting the proliferation of immune cells and T cell activation, possibly contributing to the exacerbation of immunological responses and myocardial damage.

haemolysis or the formation of dysfunctional haemoglobin without heme with impaired transport of oxygen and carbon dioxide [52]. Another marker of haemolysis is the increase of lactate dehydrogenase (LDH) levels [53] that differentiates between the severe and mild cases of COVID-19, in addition to a reduction in haemoglobin levels [54].

Tissue damage such as necrosis and apoptosis is associated with loss of oxygen that causes the degeneration of mitochondria, giving rise to anaerobic glycolysis instead of the Krebs cycle and oxidative phosphorylation [52]. Cytotoxic cell death was also found to be caused by excessive autophagy [42]. Several metabolic disorders, inflammatory processes, oxygen free radicals, and several signalling pathways act to damage the myocardium [53].

4.3. Myocardial Injury and Cytokine Storm. Another possible mechanism of myocardial damage is CS [13, 27]. Laboratory data from patients with severe COVID-19 identified a marked inflammatory process, or CS, which is common in viral infections [55]. This hypercytokinaemia is characterized by elevation of levels of inflammatory markers associated with cytopenia and hyperferritinaemia [56]. Many studies [7, 46, 51, 56–62] of CS confirmed that levels of IL-2, IL-7, IL-10, TNF-α, granulocyte colony-stimulating factor (G-CSF), IP-10, MCP-1, and macrophage inflammatory protein 1-alpha (MIP-1α) were significantly higher in patients admitted to the ICU for COVID-19, although other studies [7] demonstrated little difference between IL-4, IL-17, and TNF and significant differences in IL-6 and IL-10 levels, suggesting a systemic inflammatory process in critically ill patients.

According to Ye et al. [5], the rapid replication of the virus induces the delayed release of IFN-α/β, as well as the influx of pathogenic inflammatory mononuclear macrophages that, upon receiving signals of activation through IFN-α/β receptors on their surface, attract monocytes, CCL2, CCL7, and CCL12. When activated, mononucleated macrophages produce TNF, IL-6, IL-1β, and inducible nitric oxide synthase proinflammatory cytokines [63]. Accordingly, another factor that contributes to the failure of viral clearance is the action of other proinflammatory cytokines derived from IFN-α/β or mononuclear macrophages responsible for inducing apoptosis of T cells. IFN-α/β and IFN-γ directly induce damage to lung tissue through ligand Fas-FasL inflammatory cell infiltration and cause apoptosis of cells in the pulmonary epithelium, causing vascular leakage, alveolar oedema, and hypoxia [5]. In short, this condition is due to the failure of the action of NK cells and cytotoxic T lymphocytes to eliminate activated macrophages, a condition called haemophagocytic histiocytosis, responsible for immune hyperactivation leading to an exacerbation in the production of proinflammatory cytokines and consequent injury [64]. These findings suggest that CS is closely related to the severity of the disease [65].

Reports revealed that preexisting cardiovascular conditions are risk factors, given that among the 99 patients hospitalized for pneumonia associated with SARS-CoV-2, 40% have such conditions [66]. At Zhongnan Hospital of Wuhan University, 26% of the 138 hospitalized patients required intensive cardiological therapy, of which 16.7% manifested arrhythmias and 7.2% developed acute coronary syndrome (ACS) [16].

5. Cardiac Consequences due to SARS-CoV-2

5.1. Myocarditis, Acute Coronary Syndrome, and COVID-19. Myocarditis is a specific inflammatory disease of the heart characterized by myocardial injury; viral infection is one of the most common causes [67]. Viral myocarditis has pathological phases and begins with virus-mediated myocyte lysis that generates an innate immune response through the release of proinflammatory cytokines. Myocyte lysis releases proteins that can be presented by antigen-presenting cells due to the similarity of epitopes to antigens such as the myosin heavy chain. After the acute phase, the immune system activates the immune response acquired through cellular activation of B and T lymphocytes that activate the inflammatory cascade, attracting macrophages. This inflammatory disease can be aggravated by the CS described above, including IL-6, and is explained by direct tissue injury and cytotoxic T lymphocytes that cause necrosis, local or generalized inflammation of the myocardium, and ultimately ventricular dysfunction [68].

Cardiovascular magnetic resonance imaging is used for the diagnosis of acute myocarditis [69]; it detects typical signs of acute myocardial injury. Recent studies have reported the use of this test during SARS-CoV-2 infection [70]. Endomyocardial biopsy (EMB), long considered the gold standard diagnostic test, directly demonstrates myocyte necrosis and mononuclear cell infiltration [71]. Clinical diagnosis can be made through clinical symptoms such as chest pain, as well as elevation of troponin T (TnT) or troponin I (TnI). The diagnosis of myocarditis by the ECG electrocardiogram is limited; nevertheless, the most common changes include ST segment elevation, T and Q waves, PR depression [67], myocardial ischaemia [39], and arrhythmias including ventricular tachycardia and ventricular fibrillation [69].

ACS is one of the most dangerous types of coronary heart disease (CHD). Patients with acute viral myocarditis commonly present with chest pain, elevated troponin levels, wall motion abnormalities, and ST segment depression or elevated T waves due to the development of ACS [72].

5.2. Arrhythmia and COVID-19. Viral infections promote electrolyte imbalances, metabolic dysfunction, nonmyocardial inflammatory processes, and activation of the central nervous system, all of which are factors that predispose to cardiac arrhythmia [23]. According to Kang et al. [73], the first symptom of COVID-19 may be arrhythmia, being an indicator of cardiac impairment of recent onset and progression. This electrolyte imbalance reduces the connection between the RAAS system and the SARS-CoV-2 viruses by increasing the degree of hypocalcaemia [74]. Arrhythmia is also associated with myocarditis. The main clinical manifestations are atrial and ventricular fibrillation, ventricular tachycardia, and conduction block. In addition, there are cases in which some patients present with cardiovascular and respiratory symptoms. In patients who were not admitted to the ICU, the rate of arrhythmia was 7%; by contrast, 44% of those who manifested arrhythmias were admitted [23]. Troponin levels appear to be associated with a greater number of malignant arrhythmias seen by patients with increased Tn levels, with higher mortality rates than those with lower levels of Tn [73]. A recent study pointed out that constant monitoring is necessary by means of the ECG of patients who already have inherited or acquired arrhythmias,

and many protocols include medications that promote worsening of arrhythmogenic activity; for example, chloroquine and hydroxychloroquine can cause increased QT intervals [74].

5.3. Coagulopathy and COVID-19. Depending on the situation, SARS-CoV-2 activates or deactivates the complement system and induces vascular endothelial damage by increasing permeability and by the formation of inflammatory thrombi. In patients with COVID-19, thrombus formation must be activated by the fibrinolytic system which, when activated, releases fragments of fibrin degradation (D-dimers) in the circulation and overtraining of thrombin, a state of hypercoagulation in patients with infection [32, 38, 75]. Blood vessels are altered in two ways: type L, characterized by mild damage to the alveolar space, and type H, characterized by involvement of the alveolar space [38].

A recent study indicated four pathways responsible for the imbalance, contributing directly to the formation of thrombi. The first pathway involves a CS syndrome that causes the release of proinflammatory and hyperactive cytokines from the immune system such as IL-1β and IL-6 already mentioned in this study. This exacerbation of the active immune response is an extrinsic cascade of coagulation caused by stimulating tissue factor expression in cells of the immune system. In the second pathway, suppression of the fibrinolytic system occurs, or there is a reduction by the activity of the urokinase-type plasminogen activator or by increases in the inhibitor responsible for activating plasminogen. A third pathway involves the action of proinflammatory cytokines on plaques that cause them to activate and bind to the endothelium, causing damage. The fourth and final route involves direct damage caused by the inflammatory process and immune responses to endothelial damage with the contribution to the formation of thrombi [76].

Tang et al. [38] stated that hypoxia due to COVID-19 is possibly related to the formation of thrombi by increasing blood viscosity and by the signalling pathway dependent on the hypoxia-inducible transcription factor, because the dissection of lungs of critically ill patients revealed microthrombosis in small vessels [75]. In addition, there are a number of factors that increase the risk of thrombosis and pulmonary embolism, including obesity, advanced age, and immobilization in hospital beds [77]. Virchow's triad explains the increased risk of venous thromboembolic disease in critically ill patients admitted to the ICU, as there are venous stasis due to prolonged bed rest, prothrombotic changes due to the exacerbated action of the immune system, and endothelial injury. These patients are candidates for thromboprophylaxis, and the following parameters should be monitored: D-dimer, prothrombin time, platelet count, and fibrinogen, in order to control and improve prognoses [78].

5.4. Myocardial Infarction and COVID-19. Patients with comorbid cardiac impairments are likely to suffer complications caused by COVID-19 [7, 15, 21, 23, 38], especially acute events such as ischaemia due to the formation of clots developed as a result of systemic responses to viral invasion. According to Guzik et al. [23], the pathophysiology of CS that contributes to endothelial dysfunction and high expression levels of ECA2 in cardiac tissue may be localized microvascular inflammation that causes severe myocardial infarction. A study found that acute myocardial ischaemia was present in two of five patients who died from SARS and MERS, with MI type 2 being the most common subtype of virus infections [23].

6. Potential Therapeutic Manipulation of the Purinergic System

The purinergic system is characterized by the action of extracellular nucleotides and nucleosides that are degraded by the action of several ectonucleotidases [79]. The hydrolysis of ATP to adenosine (Ado) starts with the action of ectonucleotidases, NTPDase in adenosine 5′-diphosphate (ADP) and ADP in adenosine monophosphate (AMP). Consequently, ecto-5′-nucleotidase converts AMP to adenosine which is ultimately degraded to inosine by the action of adenosine deaminase (ADA) [6]. ATP is an intracellular energy molecule, but it can be released from various types of cells after damage. Thus, after release, it can activate receptors or be rapidly decomposed by ectonucleotidases [79].

Purinergic signalling receptors are classified into two main groups: P1 nucleoside receptor and P2 purinoceptor. The first group, P1 adenosine receptors, has four subtypes (A1, A2A, A2B, and A3). The second group, P2, can be classified into two subfamilies: P2X ionotropic nucleotide receptors, which are ligand-gated ion channels selective for cations with seven subtypes (P2X1-7), and P2Y metabotropic nucleotide receptors, which are G protein-coupled receptors with eight subtypes (P2Y1-2, P2Y4, P2Y6, and P2Y11-14) [76].

According to Tang et al. [75], in the immune system, purinergic components perform important regulatory functions, including mitogenesis and DNA synthesis in the cells of the thymus, macrophage activation and death, aggregation of neutrophils, secretory responses in basophils, chemotactic responses in eosinophils, and release of proinflammatory factors. The system also modulates proliferative responses in lymphocytes, release of histamine, and degranulation of mast cells and mediates intercellular Ca^{2+} waves in mast cells. Thus, the expression of receptors and ectonucleotidases in immune cells varies according to the amount of nucleotide and nucleoside available in the extracellular medium in normal conditions or in the context of certain diseases [79].

Immune system cells express receptors for adenosine. They have specific names, as follows: adenosine A1 receptor (ADORA1), adenosine A2A receptor (ADORA2a), adenosine A2B receptor (ADORA2b), and adenosine A3 receptor (ADORA3). The adenosine receptors ADORA2a and ADORA2b are associated with Gs protein inducing cAMP production while ADORA1 and ADORA3 with Gi protein which inhibits cAMP production [80].

Studies show anti-inflammatory functions of A2A signalling as stop signals of activation of different immune-inflammatory effector cells [81]. They are expressed in lymphocytes and neutrophils and are involved in the development of regulatory T cells (Treg) that express CD39 and

CD73 and thus negatively regulate the activation of T cells. A2A also inhibits macrophage adhesion, macrophage recruitment, and transition of M1 to M2 by proinflammatory cytokines acting as stop signals [81]. These receptors suppress inflammation in a delayed, negative feedback manner because of inhibition by cAMP of molecular intermediates of proinflammatory signalling pathways, thereby allowing for the "acquisition" of an immunosuppressive "OFF button" and creation of a time window for immunomodulation [82]. Furthermore, adenosine plays an important anti-inflammatory role through T cell regulation, proliferation, activation, and cell death [77]. A pioneering study of Ado receptors evaluated the effects of reducing pH from 7.4 to 6.8; the authors concluded that the A2A adenosine receptor mediated the dilation of the mesenteric arterial bed of the rats and that the response to activation of this receptor was potentiated by a reduction in pH that was similar to that observed in ischaemic conditions [83]. In addition, signalling by A3 inhibits neutrophil degranulation in neutrophil-mediated tissue injury, TNF-α and platelet activation, and factor-induced chemotaxis of human eosinophils [78].

Adenosinergic inhibition of synaptic potentials was significantly enhanced in hippocampal slices from aged rats, contributing to age-related decline in synaptic efficacy. A1 and A2A receptor binding was modified in the aged striatum, hippocampus, and cortex of the rats. Another change observed in these animals was reduced adenosine A1 receptor and Gα protein coupling in the ventricular myocardium during ageing [84]. These findings suggest that changes of purines should be considered relevant contributors to the more serious consequences of COVID-19 in elderly patients [85].

A recent study hypothesized that a process called viral sepsis is crucial to the disease mechanism of COVID-19, like that of severe influenza infection. The cytokine storm might play an important role in immunopathology in severe or critical cases resulting in uncontrolled inflammation [86]. There is interest in modulating A2A receptors to control sepsis. In vivo studies were provided, testing the prediction that the absence would lead to increased inflammation and increased tissue damage using mice deficient in the A2A receptor gene. Agonists did indeed prevent tissue damage models in the heart, kidney, lung, skin, vascular smooth muscle, and spinal cord [82].

From another point of view, despite the fact that ATP is an important intracellular molecule, it accumulates at sites of tissue injury and inflammation as well [87]. Extracellular ATP in low concentrations opens cation channels and sometimes leads to cell proliferation, while in high concentrations, it is a proinflammatory danger signal [88] that upregulates P2X purinoceptors located on immune cells (neutrophils, eosinophils, monocytes, macrophages, mast cells, and lymphocytes) [87, 89]. The ATP that is released due to the action of SARS-CoV-2 is an important mediator of inflammation, promoting the proliferation of immune cells and T cell activation [89], possibly contributing to the exacerbation of the immunological response and damaging the myocardium.

Regarding subtypes of ATP receptors (P2X1-7), ligand-gated ion channels [90] P2X1, P2X4, and P2X7 receptors play central roles in inflammation because they are expressed on T and B lymphocytes and NK cells [91]. Therefore, it is possible to infer a close relationship in the expression of these receptors in myocarditis, a consequence of myocardial injury during acquired immune responses [68].

The activation of T lymphocytes is favoured by the P2X1 receptor (P2X1R), which allows the entry of calcium and the activation of the transcription factor NFAT [92], while the P2X4 receptor (P2X4R) is associated with an early inflammatory mediator [91]. In addition, P2X4R is expressed at high levels of mRNA in immune cells and is the main receptor responsible for the entry of calcium into the cell. Another mechanism involves extracellular calcium levels dramatically reducing; channels are opened, allowing larger molecules to enter and favouring apoptosis [92]. In relation to pH, high ATP concentration in the lysosomes does not activate P2X4 at low concentration. The study showed that P2X4 is functioning as a Ca^{2+} channel after the fusion of late endosomes and lysosomes; P2X4 becomes activated by intralysosomal ATP only in its fully dissociated tetra-anionic form, when the pH increases to 7.4 [93]. P2X4R can act as an initial immune response, while the P2X7 receiver (P2X7R) amplifies inflammatory signals [91].

According to Antonioli et al., during infection, the surface expression of P2X4 receptors reduced and decreased ATP-evoked currents without altering total P2X4 receptor protein levels. Another point of the study was that inflammatory stimuli elicit rapid trafficking of P2X4 receptors to the macrophage cell surface, causing increased Ca^{2+} influx, thereby promoting their activity. After termination of macrophage activation, a feedback mechanism develops to curb P2X4 receptor trafficking to the cell membrane and function, probably aimed at facilitating the resolution of inflammation [94]. Another study showed that expression levels of P2X4 in myeloid cells were higher in males than in females, with potentially important consequences for several pathologies; eosinophils were by far the cell type expressing the highest level of P2X4 on the cell surface, suggesting that ATP-dependent activation could be important in the eosinophil biology in the context of COVID-19 [95].

P2X7R can be responsible for CS by releasing inflammatory cytokines and chemokines IL-1, IL-2, IL-6, IL-18, IL-1β, and IL-1α [91]. This suggests that P2X7R blockers may be beneficial for COVID-19 patients with exacerbated immune responses such as myocarditis, abnormal coagulation, arrhythmia, acute coronary syndrome, and myocardial infarction, as described above [38, 41, 65, 67, 73].

Extracellular ATP can increase immune responses, CS, and myocardial injury by the action of macrophages that express elevated levels of P2Y1R and P2Y2R and are important immune cells for production of inflammatory mediators such as TNF-α, IL-1β, and IL-6, as well as amplification of immune responses by NO [96]. The P2Y2R receptor has also been described as a regulator of mucus production on airway epithelia. ATP may reach concentrations capable of promoting P2Y2 receptor activation and promotes mucin secretion via complex Ca^{2+} and diacylglycerol- (DAG-) regulated mechanisms. Therefore, they believed that the P2Y2 receptor has promising perspectives as a therapeutic target to promote

the otherwise poor ASL volume production associated with the pathophysiology of inflammatory airway diseases [97].

Regarding therapeutic potential, ATP is also a viable candidate. A study showed that removing extracellular ATP in a model of LPS-induced systemic inflammation in mice through the action of the enzyme that degrades ATPase protected against mortality associated with a significant reduction of proinflammatory cytokines that induce cell death (TNF, IL-1, and anti-inflammatory cytokine IL-10) [98]. Another study showed that ATP hydrolysis to adenosine (an anti-inflammatory mediator) by ectonucleotidases CD39 and CD73 suppressed the production of proinflammatory cytokines [91] (see Figure 2).

6.1. Purinergic Signalling in Ischemia-Reperfusion and Hypoxia. In myocardial ischaemia, positive modulation of the P2Y2 subtype looks promising, because it was shown to be protective during ischaemia-reperfusion in mouse hearts; however, in another study, they were able to increase cell death during hypoxia while P2Y4 acted as protectors in cultured cardiomyocytes [9]. In addition, the ischaemia-reperfusion picture reduced gene expression and protein content of purinergic receptors of the P2Y2 subtype and increased gene expression and protein content of the P2X7 subtype. Thus, treatment with the agonist of the P2Y2 subtype 2-thio-UTP and with the antagonist of the P2X7 subtype Brilliant Blue improved myocardial function parameters, reduced cell death, and increased myocardial expression of antiapoptotic markers after ischaemia-reperfusion [99].

In hypoxic conditions, with hypoxia-induced factor 1-alpha being the main response factor, the production of extracellular CD73-derived adenosine (ecto-5′-nucleotidase/NT5E) is considered an important pathway in the attenuation of induced inflammation [81, 99, 100] and protection of several central bodies [101–103]. Once in these conditions, Ado activates protein kinase C and improves mitochondrial function, modulating mitochondrial-sensitive potassium channels [104], ratifying the notion proposed by Burnstock and Pelleg, in which nucleotides are contributors to the hypoxia, while Ado is generally protective [105].

ATP exerts varying effects on vascular tone, acting as a constrictor or dilator, depending on the situation, such that, in endothelial cells through P2 receptors, there is the release of relaxing factors derived from the endothelium that diffuse to the vascular smooth muscle, inducing vasodilation. However, in pathophysiological situations such as hypoxia and ischaemia, the main source of intraluminal ATP is likely to be endothelial cells in sufficient quantities for the activation of local P2R [106].

Released with norepinephrine as a cotransmitter by sympathetic nerves, ATP acts as a vasoconstrictor by binding with P2X receptors located in vascular smooth muscle, whereas P2Y receptors, located in the vascular endothelium, mediate vascular relaxation when linked to the locally produced nucleotide. However, in some vessels, the presence of P2Y in the smooth muscle can cause direct relaxation when it binds ATP released in a neural manner by the connection with purinergic or sensory nerves [106, 107]. Thus, P2 assumes the role of an attenuator of inflammation, vasodilating and protecting central organ [81, 100–103] but also inducing heart injury, while P1 acts as a cardioprotector [105].

Therefore, the role of P2 is uncertain, although P1 is active in protecting the heart. Thus, in the condition of hypoxia and ischaemia-reperfusion, Ado receptors are anti-inflammatory [108], as is the inhibition of P2 receptors, especially P2X7, because the expression of this subtype is increased in this situation, and they have therapeutic potential in critical infections with SARS-CoV-2 [91].

The importance of Ado A1 receptor ischaemic preconditioning in the heart should be considered in the context of COVID-19. Ado is involved in classic preconditioning and acts in particular through adenosine A1 and A3 receptors. A recent study demonstrated that remote ischaemic preconditioning activates adenosine A1 receptors during early reperfusion which induced Akt/endothelial nitric oxide (NO) synthase phosphorylation and improved mitochondrial function, thereby reducing the myocardial infarct size [109].

6.2. Purinergic Signalling in Heart Failure and Acute Coronary Syndrome. The development of heart failure causes structural cardiac damage to the point of leading to increased leukocyte infiltration, such that, in a situation of generalized inflammation, the purinergic system can act on the immune system through the action of CD73 acting in an anti-inflammatory way [110]. Studies provided evidence of the anti-inflammatory role of CD73 in T cells in the context of heart failure induced by transverse aortic constriction (TAC), probably related to antifibrotic activity and reduced production of proinflammatory cytokines by activating the A2A Ado receptor [110]. Ado therapy therefore has a cardioprotective role, however, with the signalling of A1R and A3R [111–114], while other studies used P2XR as a potent mediator [115]. However, the commitment of Ado action was associated with worsening CHF pathophysiology in another study [116].

In inflammatory conditions such as those associated with COVID-19, cell injury, and cardiac dysfunction with pulmonary lipopolysaccharide, A2AR deletion increased the inflammatory levels according to studies of interleukin levels, systemic inflammatory stress (haptoglobin and C-reactive protein), and myocardial injury by increased troponin I [117].

In the case of ACS, other investigators used P2Y12 inhibitors to reduce complications, including antithrombotic regimens that included apixaban, without aspirin, resulting in less bleeding and fewer hospitalizations without significant differences in the incidence of ischaemic events [117]. Similarly, ticagrelor was recognized as a new oral antagonist of the P2Y12 adenosine diphosphate receptor, with faster onset and with more significant platelet inhibition function in patients with ACS [118].

7. Conclusion

The main mechanisms of cardiovascular diseases caused by SARS-CoV-2 infection are related to host immune responses

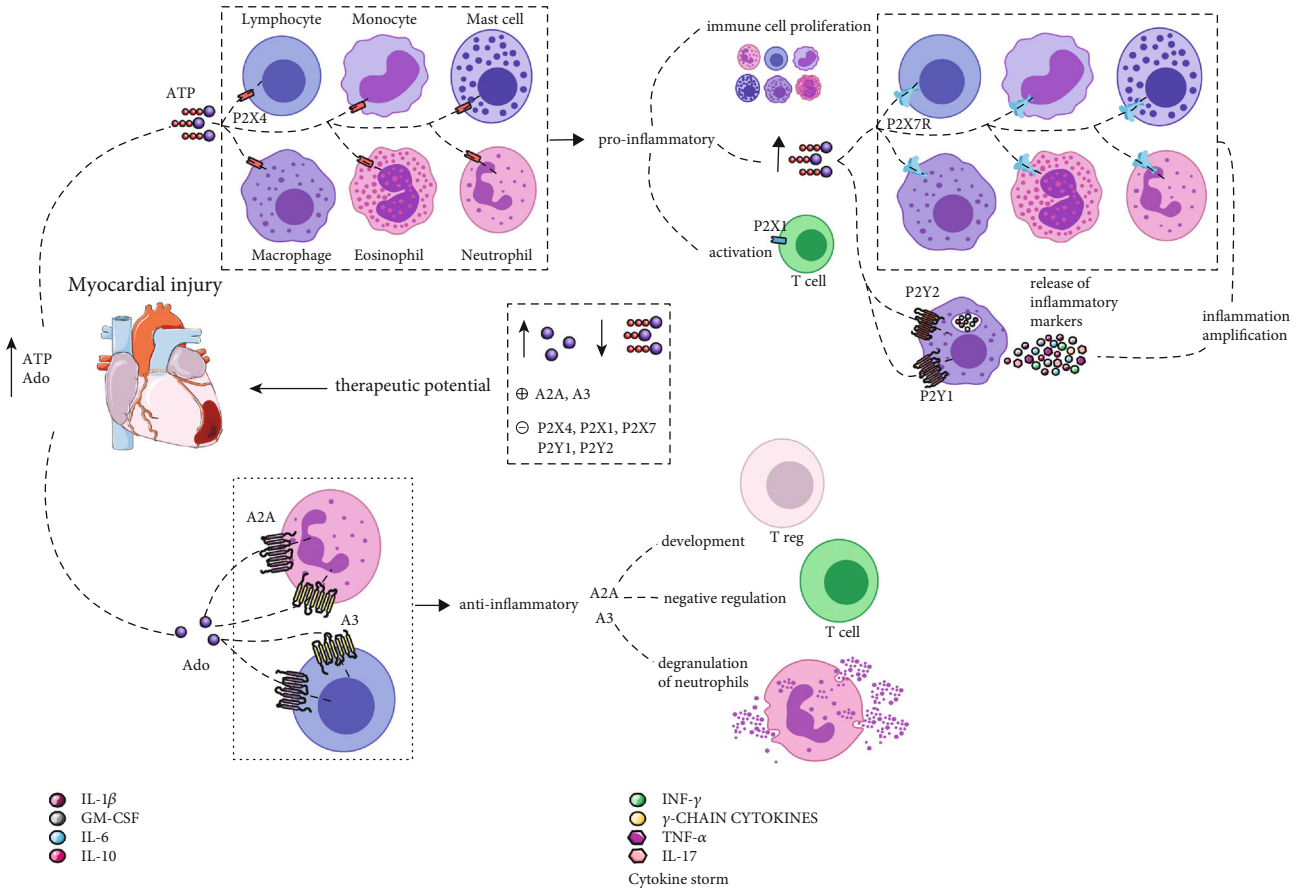

Figure 2: Myocardial injury increases levels of ATP and Ado such that different purinergic receptors are signalled. Initially, ATP signals P2X4 located on the membrane of immune cells such as mast cells, macrophages, and neutrophils. In response, there is the promotion of the inflammatory condition and the increase in ATP, promoting the proliferation of these immune cells, activating T cells by the P2X1 receptor, and signalling the P2X7 receptors of immune cells and the P2Y1 and P2Y2 in macrophages that trigger the release of inflammatory markers such as IL-1β, GM-CSF, IL-6, IL-10, INF-γ, γ-chain cytokines, TNF-α, and IL-17, amplifying inflammation. When increases in Ado, A2A and A3, are signalled, the first is responsible for the development of Tregs cells and for the negative regulation of T cells, while A3 is responsible for the degranulation of neutrophils. Thus, as a therapeutic potential for improving myocardial injury, deeper reductions in Ado and ATP occur, as well as positive modulation of A2A and A3 and negative modulation of P2X4, P2X1, P2X7, P2Y1, and P2Y2.

to viral invasion. Thus, the three mechanisms elucidated in this review result in myocardial damage, inflammatory processes, extensive release of proinflammatory cytokines and chemokines, and activation of immune cells. This exacerbation of the immune system generates CS that is responsible for increased levels of IL-2, IL-6, IL-7, IL-10, TNF-α, granulocyte colony-stimulating factor (G-CSF), IP-10, MCP-1, and macrophage inflammatory protein 1-alpha (MIP-1α), suggesting a systemic inflammatory process in critically ill patients.

COVID-19 infection has been associated with myocardial lesions in critical cases. Bearing in mind that the main damage pathways include exacerbations of inflammatory responses, the purinergic system has a high therapeutic potential in patients with cardiovascular diseases affected by COVID-19 in order to reduce the damage or prevent the progress of the disease by modulating immune responses. The development of anti-inflammatory therapies with P1R might reduce inflammatory levels in the heart, especially therapies targeting A2A, A1, and A3 in heart failure and heart dysfunction. In addition, the P2Y2 subtype should be studied in myocardial ischaemia, whereas, in cases of hypoxia and reperfusion-ischaemia, P2X7 inhibition appears effective.

Therefore, considering the immunomodulatory potential of the purinergic system, we believe that the blockade of P2X1R, P2X4R P2X7R, P2Y1R, and P2Y2R and upregulation of A2AR and A3R could be ideal mechanisms for pharmacological therapy of myocardial injury caused by CS in COVID-19. In addition, the suppression of extracellular ATP may be a strategy to inhibit purinergic signalling at P2 receptors, while increased Ado levels appear to reduce the immune response. These interventions may reduce systemic inflammatory damage to cells and tissues, preventing disease progression and modulating the immune response.

Conflicts of Interest

No conflict of interest is reported by the authors.

Authors' Contributions

Fernanda dos Anjos and Júlia Leão Batista Simões share the first authorship of the manuscript.

References

[1] "Coronavirus disease 2019," 2020, https://www.who.int/emergencies/diseases/novel-coronavirus-2019.

[2] C. Huang, Y. Wang, X. Li et al., "Clinical features of patients infected with 2019 novel coronavirus in Wuhan, China," *The Lancet*, vol. 395, no. 10223, pp. 497–506, 2020.

[3] C. C. Lai, T. P. Shih, W. C. Ko, H. J. Tang, and P. R. Hsueh, "Severe acute respiratory syndrome coronavirus 2 (SARS-CoV-2) and coronavirus disease-2019 (COVID-19): the epidemic and the challenges," *International Journal of Antimicrobial Agents*, vol. 55, no. 3, article 105924, 2020.

[4] P. Liu, W. Chen, and J. P. Chen, "Viral metagenomics revealed Sendai virus and coronavirus infection of Malayan pangolins (Manis javanica)," *Viruses*, vol. 11, no. 11, p. 979, 2019.

[5] Q. Ye, B. Wang, and J. Mao, "The pathogenesis and treatment of the 'cytokine storm' in COVID-19," *Journal of Infection*, vol. 80, no. 6, pp. 607–613, 2020.

[6] M. D. Bagatini, K. Bertolin, A. Bridi et al., "1α, 25-Dihydroxyvitamin D3 alters ectonucleotidase expression and activity in human cutaneous melanoma cells," *Journal of Cellular Biochemistry*, vol. 120, no. 6, pp. 9992–10000, 2019.

[7] S. Wan, Q. Yi, S. Fan et al., "Relationships among lymphocyte subsets, cytokines, and the pulmonary inflammation index in coronavirus (COVID-19) infected patients," *British Journal of Haematology*, vol. 189, no. 3, pp. 428–437, 2020.

[8] S. Tian, N. Hu, J. Lou et al., "Characteristics of COVID-19 infection in Beijing," *Journal of Infection*, vol. 80, no. 4, pp. 401–406, 2020.

[9] R. Charlet, B. Sendid, S. V. Kaveri, D. Poulain, J. Bayry, and S. Jawhara, "Intravenous immunoglobulin therapy eliminates Candida albicans and maintains intestinal homeostasis in a murine model of dextran sulfate sodium-induced colitis," *International Journal of Molecular Sciences*, vol. 20, no. 6, p. 1473, 2019.

[10] F. Zhou, T. Yu, R. Du et al., "Clinical course and risk factors for mortality of adult inpatients with COVID-19 in Wuhan, China: a retrospective cohort study," *The Lancet*, vol. 395, no. 10229, pp. 1054–1062, 2020.

[11] Z. Wu and J. M. McGoogan, "Characteristics of and important lessons from the coronavirus disease 2019 (COVID-19) outbreak in China," *JAMA*, vol. 323, no. 13, pp. 1239–1242, 2020.

[12] Z. Zheng, F. Peng, B. Xu et al., "Risk factors of critical & mortal COVID-19 cases: a systematic literature review and meta-analysis," *Journal of Infection*, vol. 81, no. 2, pp. e16–e25, 2020.

[13] A. Akhmerov and E. Marbán, "COVID-19 and the heart," *Circulation Research*, vol. 126, no. 10, pp. 1443–1455, 2020.

[14] H. K. Siddiqi and M. R. Mehra, "COVID-19 illness in native and immunosuppressed states: a clinical–therapeutic staging proposal," *The Journal of Heart and Lung Transplantation*, vol. 39, no. 5, pp. 405–407, 2020.

[15] W. Zhang, Y. Zhao, F. Zhang et al., "The use of anti-inflammatory drugs in the treatment of people with severe coronavirus disease 2019 (COVID-19): the perspectives of clinical immunologists from China," *Journal of Infection*, vol. 214, article 108393, 2020.

[16] D. Wang, B. Hu, C. Hu et al., "Clinical characteristics of 138 hospitalized patients with 2019 novel coronavirus-infected pneumonia in Wuhan, China," *JAMA*, vol. 323, no. 11, pp. 1061–1069, 2020.

[17] E. Kindler and V. Thiel, "SARS-CoV and IFN: too little, too late," *Cell Host & Microbe*, vol. 19, no. 2, pp. 139–141, 2016.

[18] E. De Wit, N. Van Doremalen, D. Falzarano, and V. J. Munster, "SARS and MERS: recent insights into emerging coronaviruses," *Nature Reviews Microbiology*, vol. 14, no. 8, pp. 523–534, 2016.

[19] E. Prompetchara, C. Ketloy, and T. Palaga, "Immune responses in COVID-19 and potential vaccines: lessons learned from SARS and MERS epidemic," *Asian Pacific Journal of Allergy and Immunology*, vol. 38, no. 1, pp. 1–9, 2020.

[20] R. Channappanavar, A. R. Fehr, R. Vijay et al., "Dysregulated type I interferon and inflammatory monocyte-macrophage responses cause lethal pneumonia in SARS-CoV-infected mice," *Cell Host & Microbe*, vol. 19, no. 2, pp. 181–193, 2016.

[21] G. di Mauro, C. Scavone, C. Rafaniello, F. Rossi, and A. Capuano, "SARS-CoV-2 infection: response of human immune system and possible implications for the rapid test and treatment," *International Immunopharmacology*, vol. 84, article 106519, 2020.

[22] Y. F. Tu, C. S. Chien, A. A. Yarmishyn et al., "A review of SARS-CoV-2 and the ongoing clinical trials," *International Journal of Molecular Sciences*, vol. 21, no. 7, article 2657, 2020.

[23] T. J. Guzik, S. A. Mohiddin, A. Dimarco et al., "COVID-19 and the cardiovascular system: implications for risk assessment, diagnosis, and treatment options," *Cardiovascular Research*, vol. 116, no. 10, pp. 1666–1687, 2020.

[24] A. N. Kochi, A. P. Tagliari, G. B. Forleo, G. M. Fassini, and C. Tondo, "Cardiac and arrhythmic complications in patients with COVID-19," *Journal of Cardiovascular Electrophysiology*, vol. 31, no. 5, pp. 1003–1008, 2020.

[25] T. Y. Xiong, S. Redwood, B. Prendergast, and M. Chen, "Coronaviruses and the cardiovascular system: acute and long-term implications," *European Heart Journal*, vol. 41, no. 19, pp. 1798–1800, 2020.

[26] S. Babapoor-Farrokhran, D. Gill, J. Walker, R. T. Rasekhi, B. Bozorgnia, and A. Amanullah, "Myocardial injury and COVID-19: possible mechanisms," *Life Sciences*, vol. 253, article 117723, 2020.

[27] Y. Y. Zheng, Y. T. Ma, J. Y. Zhang, and X. Xie, "COVID-19 and the cardiovascular system," *Nature Reviews Cardiology*, vol. 17, no. 5, pp. 259-260, 2020.

[28] F. Moccia, A. Gerbino, V. Lionetti et al., "COVID-19-associated cardiovascular morbidity in older adults: a position paper from the Italian Society of Cardiovascular Researches," *GeroScience*, vol. 42, no. 4, pp. 1021–1049, 2020.

[29] S.-T. Lau, W.-C. Yu, N.-S. Mok, P.-T. Tsui, W.-L. Tong, and S. W. C. Cheng, "Tachycardia amongst subjects recovering from severe acute respiratory syndrome (SARS)," *International Journal of Cardiology*, vol. 100, no. 1, pp. 167–169, 2005.

[30] A. Badawi and S. G. Ryoo, "Prevalence of comorbidities in the Middle East respiratory syndrome coronavirus (MERS-

CoV): a systematic review and meta-analysis," *International Journal of Infectious Diseases*, vol. 49, pp. 129–133, 2016.

[31] M. Madjid, A. T. Connolly, Y. Nabutovsky, P. Safavi-Naeini, M. Razavi, and C. C. Miller, "Effect of high influenza activity on risk of ventricular arrhythmias requiring therapy in patients with implantable cardiac defibrillators and cardiac resynchronization therapy defibrillators," *The American Journal of Cardiology*, vol. 124, no. 1, pp. 44–50, 2019.

[32] E. J. Favaloro and G. Lippi, "Recommendations for minimal laboratory testing panels in patients with COVID-19: potential for prognostic monitoring," *Seminars in Thrombosis and Hemostasis*, vol. 46, no. 3, pp. 379–382, 2020.

[33] T. Guo, Y. Fan, M. Chen et al., "Cardiovascular implications of fatal outcomes of patients with coronavirus disease 2019 (COVID-19)," *JAMA Cardiology*, vol. 5, no. 7, pp. 811–818, 2020.

[34] I. Ohtsuki and S. Morimoto, "Troponin," in *Encyclopedia of Biological Chemistry: Second Edition*, pp. 445–449, Elsevier Inc., 2013, June 2020, https://www.ncbi.nlm.nih.gov/books/NBK507805/.

[35] L. Zhang, X. Yan, Q. Fan et al., "D-dimer levels on admission to predict in-hospital mortality in patients with COVID-19," *Journal of Thrombosis and Haemostasis*, vol. 18, no. 6, pp. 1324–1329, 2020.

[36] F. Liu, L. Li, and M. Xu, "Prognostic value of interleukin-6, C-reactive protein, and procalcitonin in patients with COVID-19," *Journal of Clinical Virology*, vol. 127, article 104370, 2020.

[37] B. M. Henry, M. H. S. De Oliveira, S. Benoit, M. Plebani, and G. Lippi, "Hematologic, biochemical and immune biomarker abnormalities associated with severe illness and mortality in coronavirus disease 2019 (COVID-19): a meta-analysis," *Clinical Chemistry and Laboratory Medicine*, vol. 58, no. 7, pp. 1021–1028, 2020.

[38] N. Tang, D. Li, X. Wang, and Z. Sun, "Abnormal coagulation parameters are associated with poor prognosis in patients with novel coronavirus pneumonia," *Journal of Thrombosis and Haemostasis*, vol. 18, no. 4, pp. 844–847, 2020.

[39] S. Shi, M. Qin, B. Shen et al., "Association of cardiac injury with mortality in hospitalized patients with COVID-19 in Wuhan, China," *JAMA Cardiology*, vol. 5, no. 7, p. 802, 2020.

[40] J. H. Zeng, Y. X. Liu, J. Yuan et al., "First case of COVID-19 complicated with fulminant myocarditis: a case report and insights," *Infection*, vol. 48, no. 5, pp. 773–777, 2020.

[41] M. Bansal, "Cardiovascular disease and COVID-19," *Diabetes & Metabolic Syndrome: Clinical Research & Reviews*, vol. 14, no. 3, pp. 247–250, 2020.

[42] G. Fan, J. Yu, P. F. Asare et al., "Danshensu alleviates cardiac ischaemia/reperfusion injury by inhibiting autophagy and apoptosis via activation of mTOR signalling," *Journal of Cellular and Molecular Medicine*, vol. 20, no. 10, pp. 1908–1919, 2016.

[43] R. Lu, X. Zhao, J. Li et al., "Genomic characterisation and epidemiology of 2019 novel coronavirus: implications for virus origins and receptor binding," *The Lancet*, vol. 395, no. 10224, pp. 565–574, 2020.

[44] W. Sungnak, N. Huang, C. Bécavin et al., "SARS-CoV-2 entry factors are highly expressed in nasal epithelial cells together with innate immune genes," *Nature Medicine*, vol. 26, no. 5, pp. 681–687, 2020.

[45] A. Shulla, T. Heald-Sargent, G. Subramanya, J. Zhao, S. Perlman, and T. Gallagher, "A transmembrane serine protease is linked to the severe acute respiratory syndrome coronavirus receptor and activates virus entry," *Journal of Virology*, vol. 85, no. 2, pp. 873–882, 2011.

[46] S. Jawhara, "Could intravenous immunoglobulin collected from recovered coronavirus patients protect against COVID-19 and strengthen the immune system of new patients?," *International Journal of Molecular Sciences*, vol. 21, no. 7, article 2272, 2020.

[47] A. S. Monto, B. J. Cowling, and J. S. M. Peiris, "Coronaviruses," in *Viral Infections of Humans: Epidemiology and Control*, pp. 199–223, Springer US, 2014, June 2020, https://www.ncbi.nlm.nih.gov/books/NBK7782/.

[48] K. J. Clerkin, J. A. Fried, J. Raikhelkar et al., "COVID-19 and cardiovascular disease," *Circulation*, vol. 141, pp. 1648–1655, 2020.

[49] B. G. G. Pinto, A. E. R. Oliveira, Y. Singh et al., "ACE2 expression is increased in the lungs of patients with comorbidities associated with severe COVID-19," *The Journal of Infectious Diseases*, vol. 222, no. 4, pp. 556–563, 2020.

[50] H. Cheng, Y. Wang, and G. Q. Wang, "Organ-protective effect of angiotensin-converting enzyme 2 and its effect on the prognosis of COVID-19," *Journal of Medical Virology*, vol. 92, no. 7, pp. 726–730, 2020.

[51] P. Rizzo, "COVID-19 in the heart and the lungs: could we "Notch" the inflammatory storm?," *Basic Research in Cardiology*, vol. 115, no. 3, p. 31, 2020.

[52] A. Cavezzi, E. Troiani, and S. Corrao, "COVID-19: hemoglobin, iron, and hypoxia beyond inflammation. A narrative review," *Clinics and Practice*, vol. 10, no. 2, 2020.

[53] X. Yang, J. Fu, H. Wan et al., "Protective roles and mechanisms of taurine on myocardial hypoxia/reoxygenation-induced apoptosis," *Acta Cardiologica Sinica*, vol. 35, no. 4, pp. 415–424, 2019.

[54] M. Zhao, M. Wang, J. Zhang et al., "Advances in the relationship between coronavirus infection and cardiovascular diseases," *Biomedicine & Pharmacotherapy*, vol. 127, article 110230, 2020.

[55] M. B. A. Oldstone and H. Rosen, "Sphingosine-1-phosphate signaling in immunology and infectious diseases," *Current Topics in Microbiology and Immunology*, vol. 378, pp. 1–19, 2014.

[56] P. Mehta, D. F. McAuley, M. Brown, E. Sanchez, R. S. Tattersall, and J. J. Manson, "COVID-19: consider cytokine storm syndromes and immunosuppression," *The Lancet*, vol. 395, no. 10229, pp. 1033-1034, 2020.

[57] C. Y. Cheung, L. L. M. Poon, I. H. Y. Ng et al., "Cytokine responses in severe acute respiratory syndrome coronavirus-infected macrophages in vitro: possible relevance to pathogenesis," *Journal of Virology*, vol. 79, no. 12, pp. 7819–7826, 2005.

[58] D. McGonagle, K. Sharif, A. O'Regan, and C. Bridgewood, "The role of cytokines including interleukin-6 in COVID-19 induced pneumonia and macrophage activation syndrome-like disease," *Autoimmunity Reviews*, vol. 19, no. 6, article 102537, 2020.

[59] B. Diao, C. Wang, Y. Tan et al., "Reduction and functional exhaustion of T cells in patients with coronavirus disease 2019 (COVID-19)," *Frontiers in Immunology*, vol. 11, pp. 1–7, 2020.

[60] L. A. Henderson, S. W. Canna, G. S. Schulert et al., "On the alert for cytokine storm: immunopathology in COVID-19," *Arthritis & Rhematology*, vol. 72, no. 7, pp. 1059–1063, 2020.

[61] C. Zhang, Z. Wu, J. W. Li, H. Zhao, and G. Q. Wang, "Cytokine release syndrome in severe COVID-19: interleukin-6 receptor antagonist tocilizumab may be the key to reduce mortality," *International Journal of Antimicrobial Agents*, vol. 55, no. 5, article 105954, 2020.

[62] Y. Yang, C. Shen, J. Li et al., "Exuberant elevation of IP-10, MCP-3 and IL-1ra during SARS-CoV-2 infection is associated with disease severity and fatal outcome," medRxiv, 2020.

[63] J. Zhang, B. Xie, and K. Hashimoto, "Current status of potential therapeutic candidates for the COVID-19 crisis," *Brain, Behavior, and Immunity*, vol. 87, pp. 59–73, 2020.

[64] G. E. Janka and K. Lehmberg, "Hemophagocytic syndromes - an update," *Blood Reviews*, vol. 28, no. 4, pp. 135–142, 2014.

[65] H. Zhu, J.-W. Rhee, P. Cheng et al., "Cardiovascular complications in patients with COVID-19: consequences of viral toxicities and host immune response," *Current Cardiology Reports*, vol. 22, no. 5, p. 32, 2020.

[66] N. Chen, M. Zhou, X. Dong et al., "Epidemiological and clinical characteristics of 99 cases of 2019 novel coronavirus pneumonia in Wuhan, China: a descriptive study," *The Lancet*, vol. 395, no. 10223, pp. 507–513, 2020.

[67] B. Siripanthong, S. Nazarian, D. Muser et al., "Recognizing COVID-19-related myocarditis: the possible pathophysiology and proposed guideline for diagnosis and management," *Heart Rhythm*, vol. 17, no. 9, pp. 1463–1471, 2020.

[68] R. M. Inciardi, L. Lupi, G. Zaccone et al., "Cardiac involvement in a patient with coronavirus disease 2019 (COVID-19)," *JAMA Cardiology*, vol. 5, no. 7, pp. 819–824, 2020.

[69] M. G. Friedrich, U. Sechtem, J. Schulz-Menger et al., "Cardiovascular magnetic resonance in myocarditis: a JACC White Paper," *Journal of the American College of Cardiology*, vol. 53, no. 17, pp. 1475–1487, 2009.

[70] E. Driggin, M. V. Madhavan, B. Bikdeli et al., "Cardiovascular considerations for patients, health care workers, and health systems during the COVID-19 pandemic," *Journal of the American College of Cardiology*, vol. 75, no. 18, pp. 2352–2371, 2020.

[71] S. Van Linthout and C. Tschöpe, "Viral myocarditis: a prime example for endomyocardial biopsy-guided diagnosis and therapy," *Current Opinion in Cardiology*, vol. 33, no. 3, pp. 325–333, 2018.

[72] N. S. Hendren, M. H. Drazner, B. Bozkurt, and L. T. Cooper, "Description and proposed management of the acute COVID-19 cardiovascular syndrome," *Circulation*, vol. 141, no. 23, pp. 1903–1914, 2020.

[73] Y. Kang, T. Chen, D. Mui et al., "Cardiovascular manifestations and treatment considerations in COVID-19," *Heart*, vol. 106, no. 15, pp. 1132–1141, 2020.

[74] I. H. Khan, S. A. Zahra, S. Zaim, and A. Harky, "At the heart of COVID-19," *Journal of Cardiac Surgery*, vol. 35, no. 6, pp. 1287–1294, 2020.

[75] N. Tang, H. Bai, X. Chen, J. Gong, D. Li, and Z. Sun, "Anticoagulant treatment is associated with decreased mortality in severe coronavirus disease 2019 patients with coagulopathy," *Journal of Thrombosis and Haemostasis*, vol. 18, no. 5, pp. 1094–1099, 2020.

[76] T. Iba, J. H. Levy, M. Levi, J. M. Connors, and J. Thachil, "Coagulopathy of coronavirus disease 2019," *Critical Care Medicine*, vol. 48, no. 9, pp. 1358–1364, 2020.

[77] W. Ullah, R. Saeed, U. Sarwar, R. Patel, and D. L. Fischman, "COVID-19 complicated by acute pulmonary embolism and right-sided heart failure," *JACC: Case Reports*, vol. 2, no. 9, pp. 1379–1382, 2020.

[78] D. Vivas, V. Roldán, M. A. Esteve-Pastor et al., "Recommendations on antithrombotic treatment during the COVID-19 pandemic. Position statement of the Working Group on Cardiovascular Thrombosis of the Spanish Society of Cardiology," *Revista Española de Cardiología*, vol. 73, no. 9, pp. 749–757, 2020.

[79] G. Burnstock, "Introduction to purinergic signaling," in *Purinergic Signaling. Methods in Molecular Biology*, P. Pelegrín, Ed., vol. - vol 2041, pp. 1–15, Humana, New York, NY, USA, 2020.

[80] B. N. Cronstein and M. Sitkovsky, "Adenosine and adenosine receptors in the pathogenesis and treatment of rheumatic diseases," *Nature Reviews Rheumatology*, vol. 13, no. 1, pp. 41–51, 2017.

[81] H. K. Eltzschig, M. V. Sitkovsky, and S. C. Robson, "Purinergic signaling during inflammation," *New England Journal of Medicine*, vol. 367, no. 24, pp. 2322–2333, 2012.

[82] M. V. Sitkovsky, "Use of the A 2A adenosine receptor as a physiological immunosuppressor and to engineer inflammation in vivo," *Biochemical Pharmacology*, vol. 65, no. 4, pp. 493–501, 2003.

[83] C. R. Hiley, F. E. Bottrill, J. Wamock, and P. J. Richardson, "Effects of pH on responses to adenosine, CGS 21680, carbachol and nitroprusside in the isolated perfused superior mesenteric arterial bed of the rat," *British Journal of Pharmacology*, vol. 116, no. 6, pp. 2641–2646, 1995.

[84] G. Burnstock and N. Dale, "Purinergic signalling during development and ageing," *Purinergic Signal*, vol. 11, no. 3, pp. 277–305, 2015.

[85] G. Burnstock, "The therapeutic potential of purinergic signalling," *Biochemical Pharmacology*, vol. 151, pp. 157–165, 2018.

[86] H. Li, L. Liu, D. Zhang et al., "SARS-CoV-2 and viral sepsis: observations and hypotheses," *The Lancet*, vol. 395, no. 10235, pp. 1517–1520, 2020.

[87] F. Di Virgilio, Y. Tang, A. C. Sarti, and M. Rossato, "A rationale for targeting the P2X7 receptor in coronavirus disease 19," *British Journal of Pharmacology*, vol. 177, no. 21, pp. 4990–4994, 2020.

[88] G. Burnstock and G. E. Knight, "The potential of P2X7 receptors as a therapeutic target, including inflammation and tumour progression," *Purinergic Signal*, vol. 14, no. 1, pp. 1–18, 2018.

[89] N. Mehta, M. Kaur, M. Singh et al., "Purinergic receptor P2X7: a novel target for anti-inflammatory therapy," *Bioorganic & Medicinal Chemistry*, vol. 22, no. 1, pp. 54–88, 2014.

[90] F. Di Virgilio, D. Dal Ben, A. C. Sarti, A. L. Giuliani, and S. Falzoni, "The P2X7 receptor in infection and inflammation," *Immunity*, vol. 47, no. 1, pp. 15–31, 2017.

[91] G. Burnstock, "P2X ion channel receptors and inflammation," *Purinergic Signal*, vol. 12, no. 1, pp. 59–67, 2016.

[92] V. M. Ruiz-Rodríguez, J. D. Cortes-García, B.-E. M. de Jesús et al., "P2X4 receptor as a modulator in the function of P2X receptor in CD4+ T cells from peripheral blood and adipose tissue," *Molecular Immunology*, vol. 112, pp. 369–377, 2019.

[93] J. Suurväli, P. Boudinot, J. Kanellopoulos, and S. R. Boudinot, "P2X4: a fast and sensitive purinergic receptor," *Biomedical Journal*, vol. 40, pp. 245–256, 2020.

[94] L. Antonioli, C. Blandizzi, M. Fornai, P. Pacher, H. T. Lee, and G. Haskó, "P2X4 receptors, immunity, and sepsis," *Current Opinion in Pharmacology*, vol. 47, pp. 65–74, 2019.

[95] V. Paalme, A. Rump, K. Mädo et al., "Human peripheral blood eosinophils express high levels of the purinergic receptor P2X4," *Frontiers in Immunology*, vol. 10, pp. 1–15, 2019.

[96] A. N. Guerra, P. L. Fisette, Z. A. Pfeiffer et al., "Purinergic receptor regulation of LPS-induced signaling and pathophysiology," *Journal of Endotoxin Research*, vol. 9, no. 4, pp. 256–263, 2003.

[97] E. R. Lazarowski and R. C. Boucher, "UTP as an extracellular signaling molecule," *News in Physiological Sciences*, vol. 16, no. 1, pp. 1–5, 2001.

[98] A. Cauwels, E. Rogge, B. Vandendriessche, S. Shiva, and P. Brouckaert, "Extracellular ATP drives systemic inflammation, tissue damage and mortality," *Cell Death & Disease*, vol. 5, no. 3, article e1102, 2014.

[99] M. Granado, S. Amor, J. J. Montoya, L. Monge, N. Fernández, and Á. L. García-Villalón, "Altered expression of P2Y2 and P2X7 purinergic receptors in the isolated rat heart mediates ischemia-reperfusion injury," *Vascular Pharmacology*, vol. 73, pp. 96–103, 2015.

[100] L. F. Thompson, H. K. Eltzschig, J. C. Ibla et al., "Crucial role for ecto-5′-nucleotidase (CD73) in vascular leakage during hypoxia," *The Journal of Experimental Medicine*, vol. 200, no. 11, pp. 1395–1405, 2004.

[101] A. Grenz, H. Zhang, T. Eckle et al., "Protective role of ecto-5′-nucleotidase (CD73) in renal ischemia," *Journal of the American Society of Nephrology*, vol. 18, no. 3, pp. 833–845, 2007.

[102] T. Eckle, L. Füllbier, M. Wehrmann et al., "Identification of ectonucleotidases CD39 and CD73 in innate protection during acute lung injury," *Journal of Immunology*, vol. 178, no. 12, pp. 8127–8137, 2007.

[103] M. L. Hart, A. Grenz, I. C. Gorzolla, J. Schittenhelm, J. H. Dalton, and H. K. Eltzschig, "Hypoxia-inducible factor-1α–dependent protection from intestinal ischemia/reperfusion Injury involves ecto-5′-nucleotidase (CD73) and the A2B adenosine receptor," *Journal of Immunology*, vol. 186, no. 7, pp. 4367–4374, 2011.

[104] F. Xiang, Y. S. Huang, D. X. Zhang, Z. G. Chu, J. P. Zhang, and Q. Zhang, "Adenosine A1 receptor activation reduces opening of mitochondrial permeability transition pores in hypoxic cardiomyocytes," *Clinical and Experimental Pharmacology & Physiology*, vol. 37, no. 3, pp. 343–349, 2010.

[105] G. Burnstock and A. Pelleg, "Cardiac purinergic signalling in health and disease," *Purinergic Signal*, vol. 11, no. 1, pp. 1–46, 2015.

[106] G. Burnstock and C. Kennedy, "A dual function for adenosine 5′-triphosphate in the regulation of vascular tone," *Circulation Research*, vol. 58, no. 3, pp. 319–330, 1986.

[107] V. Ralevic and G. Burnstock, "Roles of P2-purinoceptors in the cardiovascular system," *Circulation*, vol. 84, no. 1, pp. 1–14, 1991.

[108] C. A. Salvatore, S. L. Tilley, A. M. Latour, D. S. Fletcher, B. H. Koller, and M. A. Jacobson, "Disruption of the A3 adenosine receptor gene in mice and its effect on stimulated inflammatory cells," *The Journal of Biological Chemistry*, vol. 275, no. 6, pp. 4429–4434, 2000.

[109] D. T. Paez, M. Garces, V. Calabró et al., "Adenosine A1receptors and mitochondria: targets of remote ischemic preconditioning," *American Journal of Physiology-Heart and Circulatory Physiology*, vol. 316, no. 3, pp. H743–H750, 2019.

[110] C. Quast, C. Alter, Z. Ding, N. Borg, and J. Schrader, "Adenosine formed by CD73 on T cells inhibits cardiac inflammation and fibrosis and preserves contractile function in transverse aortic constriction-induced heart failure," *Circulation: Heart Failure*, vol. 10, no. 4, article e003346, 2017.

[111] M. Kitakaze, T. Minamino, K. Node et al., "Adenosine and cardioprotection in the diseased heart," *Circulation Journal*, vol. 63, no. 4, pp. 231–243, 1999.

[112] L. Jang Eun, B. Gary, and T. L. Bruce, "A novel cardioprotective role of RhoA: new signaling mechanism for adenosine," *The FASEB Journal*, vol. 15, no. 11, pp. 1886–1894, 2001.

[113] B. T. Liang and K. A. Jacobson, "A physiological role of the adenosine A3 receptor: sustained cardioprotection," *Proceedings of the National Academy of Sciences of the United States of America*, vol. 95, no. 12, pp. 6995–6999, 1998.

[114] C. Dougherty, J. Barucha, P. R. Schofield, K. A. Jacobson, and B. T. Liang, "Cardiac myocytes rendered ischemia resistant by expressing the human adenosine A 1 or A 3 receptor," *The FASEB Journal*, vol. 12, no. 15, pp. 1785–1792, 1998.

[115] T. Santhosh Kumar, S. Y. Zhou, B. V. Joshi et al., "Structure-activity relationship of (N)-methanocarba phosphonate analogues of 5′-AMP as cardioprotective agents acting through a cardiac P2X receptor," *Journal of Medicinal Chemistry*, vol. 53, no. 6, pp. 2562–2576, 2010.

[116] M. Asakura, H. Asanuma, J. Kim et al., "Impact of adenosine receptor signaling and metabolism on pathophysiology in patients with chronic heart failure," *Hypertension Research*, vol. 30, no. 9, pp. 781–787, 2007.

[117] R. D. Lopes, G. Heizer, R. Aronson et al., "Antithrombotic therapy after acute coronary syndrome or PCI in atrial fibrillation," *The New England Journal of Medicine*, vol. 380, no. 16, pp. 1509–1524, 2019.

[118] D. Wang, X. H. Yang, J. D. Zhang, R.-B. Li, M. Jia, and X. R. Cui, "Compared efficacy of clopidogrel and ticagrelor in treating acute coronary syndrome: a meta-analysis," *BMC Cardiovascular Disorders*, vol. 18, no. 1, pp. 1–7, 2018.

Hindawi
Journal of Immunology Research
Volume 2020, Article ID 8209737, 12 pages
https://doi.org/10.1155/2020/8209737

Research Article

Increased Frequencies of Switched Memory B Cells and Plasmablasts in Peripheral Blood from Patients with ANCA-Associated Vasculitis

Evelina Elmér,[1] **Sofia Smargianaki**,[1] **Åsa Pettersson**,[2] **Lillemor Skattum**,[3] **Sophie Ohlsson**,[2] **Thomas Hellmark**,[2] **and Åsa C. M. Johansson**[4]

[1]*Lund University, Skåne University Hospital, Department of Laboratory Medicine, Haematology and Transfusion Medicine, and Clinical Immunology and Transfusion Medicine, Region Skåne, Lund, Sweden*
[2]*Lund University, Skåne University Hospital, Department of Clinical Sciences Lund, Nephrology, Lund, Sweden*
[3]*Clinical Immunology and Transfusion Medicine, Region Skåne, and Department of Laboratory Medicine, Microbiology, Immunology and Glycobiology, Lund University, Lund, Sweden*
[4]*Lund University, Skåne University Hospital, Department of Laboratory Medicine, Haematology and Transfusion Medicine, and Clinical Genetics and Pathology, Region Skåne, Lund, Sweden*

Correspondence should be addressed to Evelina Elmér; evelina.elmer@med.lu.se

Received 24 July 2020; Revised 23 October 2020; Accepted 4 November 2020; Published 29 November 2020

Academic Editor: Margarete D. Bagatini

B cells are thought to play a central role in the pathogenesis of antineutrophil cytoplasmic antibody- (ANCA-) associated vasculitis (AAV). ANCAs have been proposed to cause vasculitis by activating primed neutrophils to damage small blood vessels. We studied a cohort of AAV patients of which a majority were in remission and diagnosed with granulomatosis with polyangiitis (GPA). Using flow cytometry, the frequencies of $CD19^+$ B cells and subsets in peripheral blood from 106 patients with AAV and 134 healthy controls were assessed. B cells were divided into naive, preswitch memory, switched memory, and exhausted memory cells. Naive and switched memory cells were further subdivided into transitional cells and plasmablasts, respectively. In addition, serum concentrations of immunoglobulin A, G, and M were measured and clinical data were retrieved. AAV patients displayed, in relation to healthy controls, a decreased frequency of B cells of lymphocytes (5.1% vs. 8.3%) and total B cell number. For the subsets, a decrease in percentage of transitional B cells (0.7% vs. 4.4%) and expansions of switched memory B cells (22.3% vs. 16.5%) and plasmablasts (0.9% vs. 0.3%) were seen. A higher proportion of B cells was activated ($CD95^+$) in patients (20.6% vs. 10.3%), and immunoglobulin levels were largely unaltered. No differences in B cell frequencies between patients in active disease and remission were observed. Patients in remission with a tendency to relapse had, compared to nonrelapsing patients, decreased frequencies of B cells (3.5% vs. 6.5%) and transitional B cells (0.1% vs. 1.1%) and an increased frequency of activated exhausted memory B cells (30.8% vs. 22.3%). AAV patients exhibit specific changes in frequencies of $CD19^+$ B cells and their subsets in peripheral blood. These alterations could contribute to the autoantibody-driven inflammatory process in AAV.

1. Introduction

Antineutrophil cytoplasmic antibody- (ANCA-) associated vasculitis (AAV) is a group of uncommon autoimmune disorders characterized by inflammation and destruction of predominantly small blood vessels and the presence of circulating ANCA [1]. Clinical disease phenotypes include eosinophilic granulomatosis with polyangiitis (EGPA), granulomatosis with polyangiitis (GPA), and microscopic polyangiitis (MPA) [2]. ANCAs are autoantibodies directed against cytoplasmic antigens, primarily proteinase 3 (PR3) and myeloperoxidase (MPO), found in the primary granules of neutrophils and in the lysosomes of monocytes. PR3-ANCA is associated with GPA (75%), whereas MPO-

ANCA is more commonly associated with MPA (60%). ANCAs are present in approximately 50% of patients with EGPA, typically MPO-ANCA [1, 3].

The majority of AAV patients have renal involvement in terms of rapidly progressing glomerulonephritis. There is no curative treatment, but current therapy has transformed AAV from a fatal disease to a chronic illness with relapsing course and limited morbidity. The pathogenesis is multifactorial and influenced by genetics, environmental factors, and responses of the innate and adaptive immune system [4]. ANCAs have been proposed to cause vasculitis by activating primed neutrophils to damage small blood vessels [5].

As precursors of antibody-secreting plasma cells, B cells have a central role in the pathogenesis of AAV [6]. In addition, B cells can act as antigen-presenting cells and hence initiate T cell responses by providing costimulatory signals and secrete cytokines and growth factors [7]. B cells regulate immunological functions by suppressing T cell proliferation and producing proinflammatory cytokines, such as interferon-γ, tumor necrosis factor-α, and interleukin-17 [8]. Further, the efficacy of B cell depletion therapy, e.g., rituximab, in AAV supports the importance of B cells in the pathogenesis. Rituximab has been shown to be as effective as cyclophosphamide treatment in inducing remission in severe AAV and possibly superior in relapsing disease [9, 10]. The return of B cells and ANCA positivity after rituximab treatment may predict relapse of AAV [11].

The B cell-activating factor (BAFF), also known as B Lymphocyte Stimulator (BLyS), is a positive regulator of B cell survival, differentiation, and proliferation and has been associated with autoimmunity. Sanders et al. found that plasma levels of BAFF were elevated in patients with AAV. The levels were not affected by disease activity or ANCA status [12]. Matsumoto et al. have shown that AAV patients display higher proportions of plasma cells and plasmablasts as compared to healthy controls. In addition, immune cell phenotyping was similar between patients with MPA, GPA, and EGPA [13]. Recently, von Borstel et al. demonstrated that an increased frequency of circulating plasmablasts and plasma cells ($CD27^+CD38^{++}$ B cells) in GPA patients during remission is related to a higher relapse risk [14]. Furthermore, the percentage of activated B cells in GPA has been shown to correlate with disease activity [15].

We hypothesized that AAV patients have altered frequencies of B cell subsets and that the alterations correlate with disease activity and/or tendency to relapse. Based on previously published observations, our primary objectives were to study transitional, naive, and memory B cell subsets and B cell count in peripheral blood. In addition, we explored if activated B cells/subsets and immunoglobulin levels correlated with disease activity and/or tendency to relapse.

2. Materials and Methods

2.1. Patients and Controls. 149 patients with AAV attending or referred to the outpatient clinics of Nephrology and Rheumatology, Skåne University Hospital, Lund, Sweden, were consecutively included from October 2011 to January 2019. The diagnosis was determined using the algorithm described by Watts et al. [16]. Patient blood samples were collected at diagnosis when possible and at follow-up visits.

Patients with known malignancy, ongoing infection, or coexisting autoimmune disorder were not included. Further, patients treated with rituximab ($n = 27$), in dialysis ($n = 6$), or less than 500 $CD19^+$ cells within the lymphocyte population ($n = 8$) were excluded. Two patients were excluded due to lack of B cell data because of technical problems. For the remaining 106, one sample was analyzed per patient, usually the last that did not meet any of the exclusion criteria. Patient characteristics and demographics are described in Table 1.

Blood samples were also acquired from 134 healthy blood donors (HBD) at the blood donor central in Lund. There was no age or gender matching between the patients and HBD. The study was approved by the regional ethical review board in Lund, Sweden (permit number 2008/110). Prior to inclusion, all subjects gave written informed consent.

2.2. Measurements and Clinical Parameters. Data on disease activity, date of diagnosis, white blood cell count (WBC), C-reactive protein (CRP), creatinine in plasma, ANCA serology, tendency to relapse, date of latest relapse, dialysis, and medication were obtained from medical records. Disease activity was estimated according to the Birmingham Vasculitis Activity Score version 3 (BVAS3) [17]. Active disease was defined as $BVAS3 \geq 2$ and remission as $BVAS3 \leq 1$. Tendency to relapse was defined as recurrence of disease after complete remission had been achieved, in patients who had at least one year of follow-up and had received standard of care. Recurrence of the disease was defined as $BVAS3 \geq 1$ in combination with increased immunosuppressive therapy. WBC, CRP, and creatinine in plasma were analyzed as routine clinical samples at Clinical Chemistry, Region Skåne, Lund. Serum levels of PR3-ANCA and MPO-ANCA were measured with ELISA including a capture technique at Wieslab (Svar Life Science AB, Malmö, Sweden) and at Clinical Immunology and Transfusion Medicine, Region Skåne, Lund. The estimated glomerular filtration rate (eGFR) was calculated for AAV patients using the CKD-EPI creatinine (2009) equation (http://www.mdrd.com). Immunoglobulins were analyzed as routine clinical samples at Clinical Immunology and Transfusion Medicine, Region Skåne, Lund.

2.3. Phenotypic Characterization of B Cells. Peripheral blood samples were collected from patients and HBD in heparin tubes (BD Vacutainer ref 369622) and stored at room temperature and protected from light until analyzed (within 24 h). The expression of selected surface markers on B cells was analyzed using flow cytometry. Briefly, peripheral blood was lysed using 0.84% NH_4Cl. An antibody cocktail of the following monoclonal fluorescent-labeled antibodies (BD Biosciences, San Jose, CA, USA) was added to the suspension of leukocytes: CD19 PerCP Cy5.5 (HIB19), IgD V450 (IA6-2), CD27 APC H7 (M-T271), CD38 PE Cy7 (HB-7), CD24 FITC (ML5), CD95 APC (DX2), and CD45 V500 (HI30).

Acquisition was performed on a FACSCanto II flow cytometer with the accompanying FACSDiva software (Becton Dickinson, Franklin Lakes, NJ, USA). Data were analyzed using Kaluza Analysis Software version 2.1 (Beckman

Table 1: Patient characteristics and demographics.

	GPA ($n = 64$)	MPA ($n = 35$)	EGPA ($n = 7$)
Age, years, median (IQR)	67.0 (55.0-73.8)	73.0 (63.0-82.0)	71.0 (56.0-76.0)
Female/male, *n* (%)	26 (41)/38 (59)	19 (54)/16 (46)	5 (71)/2 (29)
Age at diagnosis, years, median (IQR)	50.5 (37.3-66.0)	68.0 (60.0-75.0)	66.0 (38.0-71.0)
Disease duration, years, median (IQR)	6.74 (3.59-17.8)	2.21 (0.447-9.95)	7.91 (4.82-18.0)
ANCA specificity, *n* (%)			
PR3	45 (70)	2 (6)	0 (0)
MPO	17 (27)	30 (86)	3 (43)
PR3 and MPO	0 (0)	1 (3)	0 (0)
No ANCA	1 (1.5)	1 (3)	3 (43)
Data not available	1 (1.5)	1 (3)	1 (14)
Disease activity			
Active disease, *n* (%)	14 (22)	9 (26)	1 (14)
BVAS3, median (range)	6 (2-26)	14 (5-21)	4
Remission, *n* (%)	50 (78)	26 (74)	6 (86)
Tendency to relapse, *n* (%)			
Yes	29 (45)	8 (23)	1 (14)
Time since onset of the latest relapse, months, median (IQR)[a]	66.5 (24.5-178)	8.30 (4.73-26.8)	NA
No	18 (28)	13 (37)	5 (71)
Not applicable	17 (27)	14 (40)	1 (14)
WBC, 10^9/L, median (IQR)[b]	6.55 (5.10-8.45)	7.70 (5.65-9.40)	7.40 (5.48-10.1)
P-CRP, mg/L, median (IQR)[c]	2.25 (1.10-4.55)	6.70 (2.00-14.5)	0.00 (0.00-3.23)
P-creatinine, μmol/L, median (IQR)[d]	102 (80.0-136)	137 (101-193)	84.5 (62.8-108)
eGFR, mL/min/1.73 m^2, median (IOR)	58.0 (40.0-80.0)	39.0 (21.0-51.0)	69.0 (52.8-88.0)
Medication, *n* (%), dose, median (IQR)			
Prednisolone, mg/day	30 (47) 6.88 (5.00-13.1)	22 (63) 10.0 (8.75-31.3)	4 (57) 5.00 (2.13-16.9)
Azathioprine, mg/day	16 (25) 100 (75.0-144)	13 (37) 100 (75.0-100)	4 (57) 125 (100-188)
Methotrexate, mg/week	9 (14) 25.0 (17.5-25.0)	0 (0)	0 (0)
Mycophenolate mofetil, mg/day	6 (9) 2000 (1313-2125)	0 (0)	0 (0)
Cyclophosphamide	4 (6)	7 (20)	0 (0)
No medication	18 (28)	6 (17)	2 (29)

GPA: granulomatosis with polyangiitis; MPA: microscopic polyangiitis; EGPA: eosinophilic granulomatosis with polyangiitis; IQR: interquartile range; ANCA: antineutrophil cytoplasmic autoantibodies; PR3: proteinase 3; MPO: myeloperoxidase; BVAS3: Birmingham Vasculitis Activity Score version 3; NA: not applicable; WBC: white blood cell; CRP: C-reactive protein; eGFR: estimated glomerular filtration rate. [a]For those in remission at the time of sampling. $n = 19$ (GPA), $n = 6$ (MPA). [b]Reference range 3.5-8.8 10^9/L. [c]Reference range < 0.6 mg/L. [d]Reference range 60-105 μmol/L (male), 45-90 μmol/L (female). For BVAS3, WBC, P-CRP, P-creatinine, and eGFR, the cohort sizes were $n = 62$-64 (GPA), $n = 33$-35 (MPA), and $n = 6$-7 (EGPA).

Coulter, Brea, CA, USA). Doublet cells were excluded by plotting forward scatter height against forward scatter area, and single cells were divided into monocytes, lymphocytes, and granulocytes based on forward and side scatter properties. At least 50.000 lymphocytes were acquired. The phenotypes of immune cell subsets were defined based on the Human Immunology Project protocol [18]. Details of the gating strategy are shown in Figure S1. Analysis using this panel allowed identification of B cells ($CD19^+$ lymphocytes) and its subsets: naive B cells ($CD19^+CD27^-IgD^+$), preswitch memory B cells ($CD19^+CD27^+IgD^+$), switched memory B cells ($CD19^+CD27^+IgD^-$), exhausted memory B cells ($CD19^+CD27^-IgD^-$), transitional B cells ($CD19^+CD27^-IgD^+CD24^+CD38^{++}$), and plasmablasts ($CD19^+CD27^+IgD^-CD24^-CD38^{++}$). The percentages of activated ($CD95^+$) B cells, naive B cells, preswitch memory B cells, switched memory B cells, and exhausted memory B cells of the total number of $CD19^+$ lymphocytes were analyzed. Patients and controls were analyzed with flow cytometry in parallel. All values are given as a percentage of $CD19^+$ B cells if not otherwise specified. Absolute numbers of B cell subsets were based on the proportion (%) of B cells within the lymphocyte population combined with the absolute number of lymphocytes from the WBC count.

No absolute numbers of lymphocytes were available for HBD. However, a reference material of 50 healthy blood donors was collected at Clinical Immunology and Transfusion Medicine, Region Skåne, Lund in 2013 for B cells, giving a range of $CD19^+$ B cells (of lymphocytes) of 5.5-20% (70-460 10^6/L).

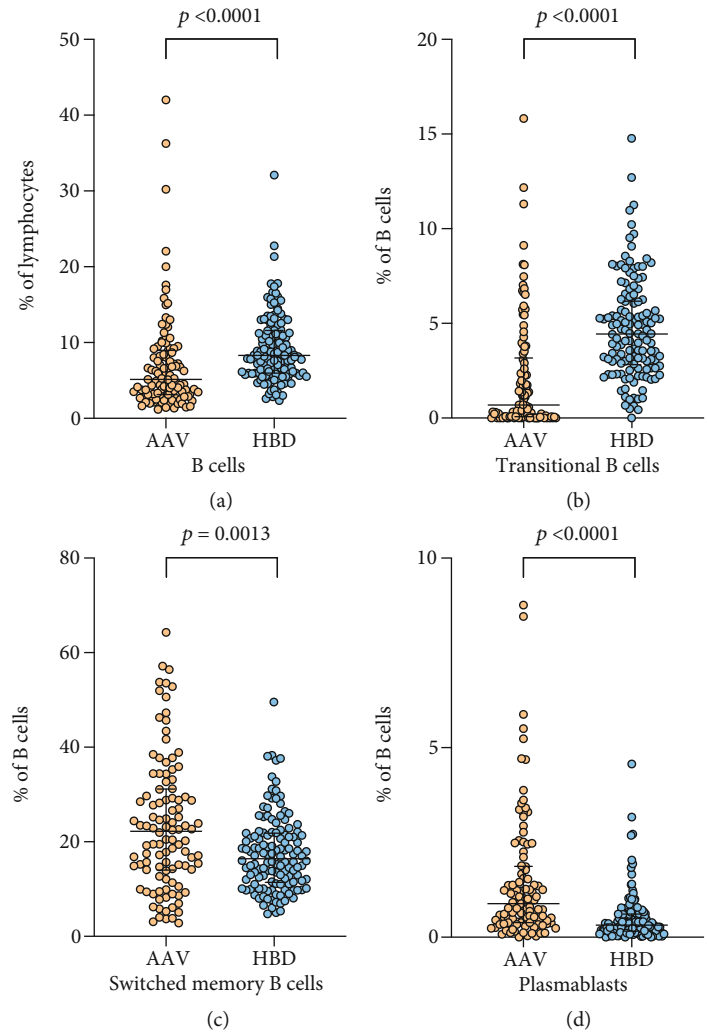

Figure 1: Comparisons of B cells and subsets between vasculitis patients and healthy blood donors. (a) Percentage of $CD19^+$ B cells of lymphocytes, (b) percentage of transitional B cells (of $CD19^+$ B cells), (c) percentage of switched memory B cells (of $CD19^+$ B cells), and (d) percentage of plasmablasts (of $CD19^+$ B cells), in peripheral blood from patients with antineutrophil cytoplasmic autoantibody-(ANCA-) associated vasculitis (AAV, $n = 106$) and healthy blood donors (HBD, $n = 134$). The Mann-Whitney test was used to calculate the level of significance. Data are presented with medians and interquartile ranges. In figure (d), one data point (20.56) in the AAV group is not shown for presentation purposes but included in statistical calculations.

2.4. Statistical Analysis. Statistical analyses were performed with GraphPad Prism 8.4.2 software (GraphPad Software, San Diego, CA, USA). The Mann-Whitney *U* test was used for two-group comparisons and Kruskal-Wallis with Dunn's multiple comparisons test for three or more groups. Correlations were determined by Spearman's correlation test and linear regression analysis. Statistical analysis was only performed for the parameters considered relevant for answering one or more of the hypotheses of the study. Samples with CRP concentrations below the lower limit of detection (<0.6 mg/L, $n = 13$) and IgA (< 0.07 g/L, $n = 2$) were set to 0. Subgroups of $n < 5$ patients were not included in the statistical analyses. Values are expressed as median with interquartile range (IQR) unless otherwise specified. Results were considered statistically significant at $p < 0.05$.

3. Results

3.1. Patient Characteristics. The clinical and demographic characteristics of the patients with AAV ($n = 106$) at the time of sampling are reported in Table 1. The median age was 70.0 years (57.5-75.3), and the female to male ratio was 1.12 to 1.0. The majority of patients were diagnosed with GPA (60%), whereas patients with MPA and EGPA represented 33% and 7% of the cohort, respectively. Most of the patients were in remission (77%), and 23% had disease activity with BVAS3 ≥ 2 (median score 6, range 2-26). A tendency to relapse was observed in 36% of the patients, and for those in remission at the time of sampling, the median time since the onset of the latest relapse was 43.3 months (12.6-144). Thirty-four percent of the patients had no tendency to relapse, and in 30%, it could not be decided according to

Table 2: Frequencies of B cells and subsets in patients with AAV and HBD.

Phenotype	Patients (AAV) ($n = 106$)	HBD ($n = 134$)	p value
B cells (% of lymphocytes)	5.13 (3.15-8.98)	8.33 (5.98-11.6)	<0.0001
B cells (10^6/L)[a]	26.5 (15.2-69.4)		
B cell subsets			
Naive (% of B cells)	47.8 (33.4-60.3)	56.7 (47.9-67.0)	0.0002
Naive (10^6/L)	12.1 (4.49-33.9)		
Preswitch memory (% of B cells)	6.32 (3.63-10.1)	7.00 (4.65-10.2)	ns
Preswitch memory (10^6/L)	1.86 (0.818-4.28)		
Switched memory (% of B cells)	22.3 (14.0-31.1)	16.5 (11.4-21.8)	0.0013
Switched memory (10^6/L)	5.78 (2.98-11.2)		
Exhausted memory (% of B cells)	21.2 (14.1-25.9)	17.4 (12.0-21.6)	0.0006
Exhausted memory (10^6/L)	5.30 (2.69-15.1)		
Transitional (% of B cells)	0.695 (0.0700-3.17)	4.44 (2.83-6.18)	<0.0001
Transitional (10^6/L)	0.278 (0.0107-1.29)		
Plasmablasts (% of B cells)	0.885 (0.390-1.87)	0.320 (0.160-0.613)	<0.0001
Plasmablasts (10^6/L)	0.293 (0.138-0.587)		
Activated B cells and subsets			
$CD95^+$ B cells (% of B cells)	20.6 (12.3-33.1)	10.3 (7.24-15.5)	<0.0001
$CD95^+$ B cells (10^6/L)	5.48 (3.24-11.2)		
$CD95^+$ naive (% of naive)	3.38 (1.49-7.24)	1.02 (0.575-1.71)	<0.0001
$CD95^+$ naive (10^6/L)	0.427 (0.194-0.833)		
$CD95^+$ preswitch memory (% of preswitch memory)	23.0 (16.4-38.7)	13.5 (9.07-19.8)	<0.0001
$CD95^+$ preswitch memory (10^6/L)	0.355 (0.190-0.892)		
$CD95^+$ switched memory (% of switched memory)	59.7 (51.2-73.0)	44.6 (36.0-51.9)	<0.0001
$CD95^+$ switched memory (10^6/L)	3.15 (1.70-6.66)		
$CD95^+$ exhausted memory (% of exhausted memory)	25.2 (15.0-35.0)	14.0 (8.38-18.2)	<0.0001
$CD95^+$ exhausted memory (10^6/L)	1.27 (0.667-2.78)		

Frequencies of B cells ($CD19^+$ lymphocytes) and subsets analyzed in patients and healthy controls using flow cytometry. The Mann-Whitney test was used to calculate the level of significance. Data are presented with medians and interquartile ranges. AAV: antineutrophil cytoplasmic autoantibody- (ANCA-) associated vasculitis; HBD: healthy blood donors; ns: not significant. [a]n equals 101 for absolute values.

the definition, e.g., too short follow-up period or onset of disease at the time of sampling.

At the time of sampling, 53% of the patients were treated with prednisolone (dose 10.0 mg/day, 5.00-15.0), 31% were treated with azathioprine (100 mg/day, 75.0-138), 8.5% were treated with methotrexate (25.0 mg/week, 17.5-25.0), 5.7% were treated with mycophenolate mofetil (2000 mg/day, 1313-2125), 10.4% were treated with cyclophosphamide infusion, and 24.5% had no medication.

Demographic data on age and gender were available for 102 of the 134 healthy controls, giving a median age of 49 years (range 19–74) and a female to male ratio of 1.1 to 1.0.

3.2. Decreased Frequencies of B Cells and Transitional B Cells in AAV Patients. To investigate differences in the distribution of B cells ($CD19^+$ lymphocytes) and its subsets between AAV patients and HBD, the percentages of activated ($CD95^+$) B cells, naive B cells ($CD19^+CD27^-IgD^+$), preswitch memory B cells ($CD19^+CD27^+IgD^+$), switched memory B cells ($CD19^+CD27^+IgD^-$), exhausted memory B cells ($CD19^{+-}CD27^-IgD^-$), transitional B cells ($CD19^+CD27^-IgD^+CD24^{+-}CD38^{++}$), and plasmablasts ($CD19^+CD27^+IgD^+CD24^-CD38^{++}$) of the total number of $CD19^+$ lymphocytes were analyzed. The AAV patients had a lower percentage of $CD19^+$ B cells of lymphocytes compared to HBD ($p < 0.0001$, Figure 1(a), Table 2) and a lower percentage of transitional B cells ($p < 0.0001$, Figure 1(b), Table 2). The absolute number of B cells was lower in AAV patients (26.5 10^6/L, 15.2-69.4) (Table 2) compared to a separate reference material of 50 healthy blood donors (70-460 10^6/L).

3.3. Increased Frequencies of Switched Memory B Cells and Plasmablasts in AAV Patients. Memory B cells can be defined by CD27, although some subsets, generally associated with exhausted B cells, do not express CD27. Switched memory B cells have undergone class-switching (do not express IgD) and are indicators of normal B cell activation and development in germinal centers in lymph nodes or other secondary lymphoid tissues.

The percentage of switched memory B cells was higher in patients compared to HBD ($p = 0.0013$, Figure 1(c), Table 2).

Plasmablast refers to a short-lived differentiation stage between a postgerminal center B cell and a mature plasma cell, the latter specialized to produce single isotype

Table 3: Concentrations of IgA, IgG, and IgM in patients with AAV.

Concentration (g/L)	IgA	IgG	IgM
AAV patients ($n = 92$-93)[a]	1.86 (1.32-2.75)	10.1 (8.46-12.9)	0.83 (0.60-1.33)
Diagnosis			
GPA ($n = 56$-57)[a]	1.80 (1.40-2.75)	9.99 (8.60-12.9)	0.83 (0.61-1.42)
MPA ($n = 33$)	1.86 (1.31-2.67)	10.1 (7.66-12.6)	0.73 (0.58-1.23)
EGPA ($n = 3$)	3.74 (0.73-5.12)	11.7 (10.4-15.6)	1.51 (0.33-2.81)
Disease activity			
Active disease ($n = 22$-23)[a]	1.99 (1.57-2.68)	9.79 (8.31-13.0)	0.72 (0.37-1.18)
Remission ($n = 70$)	1.86 (1.23-2.77)	10.4 (8.50-12.8)	0.83 (0.63-1.39)
Tendency to relapse			
Yes ($n = 32$-33)[a]	1.80 (1.43-2.41)	9.88 (7.76-12.0)*	0.98 (0.59-1.32)
No ($n = 33$)	2.02 (1.32-3.52)	11.4 (9.47-13.7)	0.75 (0.63-1.45)
Treatment			
AAV with ≥1 drugs ($n = 68$-69)[a]	1.79 (1.38-2.44)	9.32 (7.75-12.4)*	0.77 (0.54-1.30)
AAV no medication ($n = 24$)	2.82 (1.20-4.50)	12.0 (9.95-13.7)	0.96 (0.72-1.50)

Concentrations of IgA, IgG, and IgM in patients with AAV. Data are presented with medians and interquartile ranges. Ig: immunoglobulin; AAV: antineutrophil cytoplasmic autoantibody- (ANCA-) associated vasculitis; GPA: granulomatosis with polyangiitis; MPA: microscopic polyangiitis; EGPA: eosinophilic granulomatosis with polyangiitis. Reference range IgA 0.88-4.5 g/L, IgG 6.7-14.5 g/L, and IgM 0.27-2.1 g/L. [a]For one patient, only IgG and IgM were measured. The Mann-Whitney test was used to calculate the level of significance. Subgroups of $n < 5$ were not included in the statistical analyses. *Denotes statistical difference as compared to comparator patient subgroup (listed below in the table).

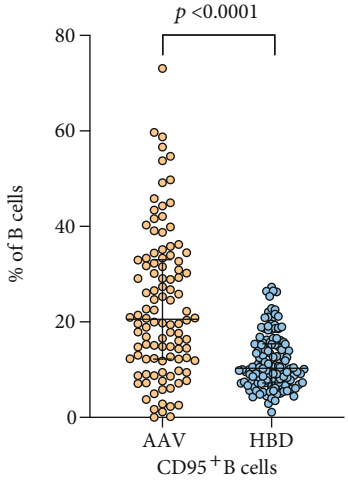

Figure 2: Comparison of $CD95^+$ B cells (of $CD19^+$ B cells) in peripheral blood from patients with antineutrophil cytoplasmic autoantibody- (ANCA-) associated vasculitis (AAV, $n = 106$) and healthy blood donors (HBD, $n = 134$). The Mann-Whitney test was used to calculate the level of significance. Data are presented with medians and interquartile ranges.

antibodies. The patients had a higher percentage of plasmablasts compared to HBD ($p < 0.0001$, Figure 1(d), Table 2).

3.4. Largely Unaltered Immunoglobulin Levels in AAV Patients. Since the percentage of plasmablasts, the precursors of antibody-producing plasma cells, was higher in AAV patients, we measured the levels of immunoglobulins in serum. The levels of immunoglobulins (IgA, IgG, and IgM) in AAV patients were within the reference range (Table 3), except for IgA in the EGPA group where the lower IQR was below the reference range. Two patients diagnosed with MPA had IgA deficiency. AAV patients with a tendency to relapse had lower IgG levels compared to AAV patients with no tendency to relapse ($p = 0.0446$). Patients with medication had lower IgG levels compared to patients without medication ($p = 0.0021$).

Overall, there were no correlations between immunoglobulin levels and plasmablasts in AAV patients, neither for percentage nor for absolute concentration of plasmablasts, except for a weak but significant correlation between IgG and the concentration of plasmablasts ($r^2 = 0.044$, $p = 0.0494$).

When analyzing only patients in remission, there was a correlation between IgG and the concentration of plasmablasts ($r^2 = 0.132$, $p = 0.0023$). Moreover, there were no correlations between immunoglobulin levels and the frequency or concentration of plasmablasts in patients in active disease, patients with or without a tendency to relapse, or patients with and without medication (data not shown).

3.5. Increased Frequencies of $CD95^+$ B Cells and Subsets in AAV Patients. The Fas receptor, CD95, has been suggested to be a marker of B cell activation. The percentage of $CD95^+$ B cells was increased in patients compared to HBD ($p < 0.0001$, Figure 2, Table 2). In all analyzed B cell subsets, the percentage of $CD95^+$ cells (of the respective subset) was higher compared to HBD (Table 2).

3.6. No Differences in B Cell Frequencies in Active and Inactive Disease. To characterize B cell subset distribution in relation to disease activity, patients were divided into two groups: active disease (BVAS3 ≥ 2) or remission (BVAS3 ≤ 1). Most of the AAV patients were in remission ($n = 82$). There were no differences in the frequencies of

Table 4: Frequencies of B cells and subsets in patients with AAV in active disease and remission.

Phenotype	Active disease ($n = 24$)	Remission ($n = 82$)	p value
BVAS3, median (range)	6 (2-26)	0 (0-1)	<0.0001
B cells (% of lymphocytes)	6.12 (2.97-9.70)	4.64 (3.15-8.98)	ns
B cells (10^6/L)[a]	32.3 (17.6-84.5)	25.9 (15.0-66.4)	ns
B cell subsets (% of B cells)			
Naive	51.7 (35.6-58.3)	47.5 (30.5-63.6)	ns
Preswitch memory	4.93 (2.89-9.76)	6.71 (3.69-10.3)	ns
Switched memory	21.0 (14.2-29.5)	22.3 (13.6-33.1)	ns
Exhausted memory	19.8 (16.4-25.9)	21.5 (12.7-25.9)	ns
Transitional	1.35 (0.103-5.67)	0.675 (0.0600-2.81)	ns
Plasmablasts	0.755 (0.398-3.12)	0.905 (0.390-1.70)	ns
Activated B cells and subsets			
$CD95^+$ B cells (% of B cells)	19.5 (9.50-33.8)	20.8 (12.3-32.8)	ns
$CD95^+$ naive (% of naive)	2.79 (0.920-6.53)	3.47 (1.60-7.80)	ns
$CD95^+$ preswitch memory (% of preswitch memory)	19.4 (11.3-39.5)	28.2 (16.8-38.7)	ns
$CD95^+$ switched memory (% of switched memory)	59.1 (51.5-76.5)	61.0 (50.8-72.7)	ns
$CD95^+$ exhausted memory (% of exhausted memory)	19.4 (11.2-33.0)	25.9 (16.3-35.6)	ns
Treatment, n (%)			
Prednisolone	17 (71)	39 (48)	
Azathioprine	6 (25)	27 (33)	
Methotrexate	1 (4)	8 (10)	
Mycophenolate mofetil	1 (4)	5 (6)	
Cyclophosphamide	5 (21)	6 (7)	
No medication	3 (13)	23 (28)	

Frequencies of B cells ($CD19^+$ lymphocytes) and subsets analyzed in patients using flow cytometry. Active disease: BVAS3 ≥ 2; remission: BVAS3 ≤ 1. The Mann-Whitney test was used to calculate the level of significance. Data are presented with medians and interquartile ranges. AAV: antineutrophil cytoplasmic autoantibody- (ANCA-) associated vasculitis; BVAS3: Birmingham Vasculitis Activity Score version 3; ns: not significant. [a]n equals 23 (active disease), 78 (remission) for absolute values.

$CD19^+$ B cells of lymphocytes, in its subsets, or in the absolute number of B cells between patients in active disease and patients in remission (Table 4).

3.7. Decreased Frequencies of B Cells and Transitional B Cells in Patients with a Tendency to Relapse. To characterize B cell subset distribution in relation to tendency to relapse (defined in Materials and Methods), patients were divided into two groups. Patients with a tendency to relapse ($n = 38$) had a lower frequency of B cells of lymphocytes (3.82%, 2.63-6.66) compared to patients with no tendency to relapse ($n = 36$) (6.53%, 3.68-9.21, $p = 0.0215$). Nine of the patients in the relapse group had an active disease, and the remaining were in remission ($n = 29$). In the group without a tendency to relapse, all patients were in remission.

When comparing only patients in remission, patients with a tendency to relapse had a lower frequency of B cells compared to patients with no tendency to relapse ($p = 0.0295$, Table 5). This was also reflected in the absolute number of B cells (Figure 3(a), Table 5). The frequency of transitional B cells was lower in patients with a tendency to relapse ($p = 0.0380$, Figure 3(b), Table 5). There was also a higher frequency of $CD95^+$ exhausted memory B cells (of exhausted memory B cells) in the patients in remission with a tendency to relapse ($p = 0.0032$, Figure 3(c), Table 5).

The immunomodulating medication for patients in remission is listed in Table 5. 42% of patients in remission with no tendency to relapse had no medication at the time of sampling; the corresponding figure for patients with tendency was 7%. There were no significant differences in doses of medications between the groups.

3.8. Decreased Frequency of B Cells in Patients with Immunomodulating Medication. To broadly report the immunomodulating medication, patients were divided into two groups. AAV patients with ≥1 of the following medications (75.5%, of which 74% were in remission): prednisolone, azathioprine, methotrexate, mycophenolate mofetil, cyclophosphamide, were compared to patients with none of the five medications (24.5%, 88% were in remission). BVAS3 did not differ between the groups (Table S1). Patients with pharmacological treatment had a lower percentage of B cells compared to patients without medications ($p < 0.0001$), which was reflected in the absolute B cell count ($p < 0.0001$) and in B cell subsets (Table S1).

4. Discussion

B cells are thought to have a central role in the pathogenesis of antineutrophil cytoplasmic antibody- (ANCA-) associated

Table 5: Frequencies of B cells and subsets in patients with AAV in remission with regard to tendency to relapse.

Phenotype	Tendency to relapse, remission ($n = 29$)	No tendency to relapse, remission ($n = 36$)	p value
B cells (% of lymphocytes)	3.51 (2.60-7.20)	6.53 (3.68-9.21)	0.0295
B cells (10^6/L)[a]	18.6 (11.0-43.7)	45.4 (25.0-82.1)	0.0037
B cell subsets (% of B cells)			
Naive	47.3 (29.5-60.9)	53.7 (32.6-65.9)	ns
Preswitch memory	7.25 (4.40-10.6)	5.68 (3.51-11.2)	ns
Switched memory	23.9 (14.1-32.8)	18.7 (13.0-29.0)	ns
Exhausted memory	21.4 (11.3-25.2)	19.4 (12.8-26.0)	ns
Transitional	0.0900 (0.00-2.34)	1.10 (0.205-3.86)	0.0380
Plasmablasts	0.990 (0.265-2.61)	0.710 (0.383-1.48)	ns
Activated B cells and subsets			
$CD95^+$ B cells (% of B cells)	25.3 (12.4-33.9)	16.7 (12.0-29.9)	ns
$CD95^+$ naive (% of naive)	3.43 (1.75-9.46)	2.60 (1.24-5.36)	ns
$CD95^+$ preswitch memory (% of preswitch memory)	29.9 (17.5-38.2)	21.4 (15.9-37.5)	ns
$CD95^+$ switched memory (% of switched memory)	62.1 (52.5-71.8)	59.2 (50.2-72.5)	ns
$CD95^+$ exhausted memory (% of exhausted memory)	30.8 (23.6-47.0)	22.3 (14.1-27.8)	0.0032
Treatment, n (%), dose			
Prednisolone, mg/day	19 (66) 7.50 (5.00-10.0)	13 (36) 5.00 (2.50-8.75)	ns
Azathioprine, mg/day	13 (45) 100 (75.0-100)	8 (22) 100 (62.5-150)	ns
Methotrexate, mg/week	5 (17) 25.0 (17.5-25.0)	2 (6) 18.8 (12.5-25.0)	
Mycophenolate mofetil, mg/day	2 (7) 2000 (2000-2000)	2 (6) 1125 (750-1500)	
Cyclophosphamide	2 (7)	2 (6)	
No medication	2 (7)	15 (42)	

Frequencies of B cells ($CD19^+$ lymphocytes) and subsets analyzed in patients using flow cytometry. The Mann-Whitney test was used to calculate the level of significance. Data are presented with medians and interquartile ranges. AAV: antineutrophil cytoplasmic autoantibody- (ANCA-) associated vasculitis; ns: not significant. [a]n equals 28 (tendency to relapse, remission), 33 (no tendency to relapse, remission) for absolute values.

vasculitis (AAV), a disease characterized by autoantibodies and effectively treated by B cell depletion using monoclonal antibodies directed against the B cell antigen CD20.

In this study, patients with AAV had a lower percentage and absolute number of $CD19^+$ B cells. This is in line with previous studies on GPA patients in remission, demonstrating that patients have lower absolute numbers of circulating $CD19^+$ B cells [19] and lower B cell frequency [14]. Lepse et al. on the other hand, found no difference in the percentage of $CD19^+$ B cells between AAV patients and healthy controls [20]. The discrepancy between the studies could possibly be related to differences in medication or disease activity between the cohorts.

Transitional B cells are immature B cells and are related to interleukin 10- (IL-10-) producing regulatory B cells (Bregs) in terms of phenotypical and functional similarities [6]. However, the overlap between transitional B cells and Bregs is debated. Transitional B cells can also produce IL-10 and regulate $CD4^+$ T cell proliferation and differentiation toward T helper effector cells [21].

We found that the patients had a lower proportion of transitional B cells. This is in contrast to von Borstel et al. that found no difference in transitional B cell frequencies between GPA patients with future relapse, nonrelapsing patients, and healthy controls [14]. Partly in agreement with our finding, Lepse et al. showed that AAV patients in active disease had a decreased percentage of transitional B cells compared to patients in remission and healthy controls [20]. In further support of our findings, a low frequency of transitional B cells has been noted in neuroimmunological diseases, including multiple sclerosis (MS) [22] and neuromyelitis optica (NMO) [23]. However, the frequency of $CD24^{hi}CD38^{hi}$ transitional B cells is elevated in patients with systemic lupus erythematosus (SLE) and Sjögren's syndrome (SS) [24].

Memory B cells are optimized to interact with T cells and to yield strong antibody responses. Autoreactive antibodies likely contribute to the chronic and progressive course typically observed in autoimmune disorders [25]. High frequencies of memory B cells are associated with poor clinical response to rituximab (anti-CD20) treatment [26]. We found an increased frequency of switched memory B cells in AAV patients, and patients with medication had a higher percentage of switched memory B cells compared to the nonmedication group and healthy controls.

Previously published observations have reported a decreased proportion of circulating $CD27^+$ memory B cells

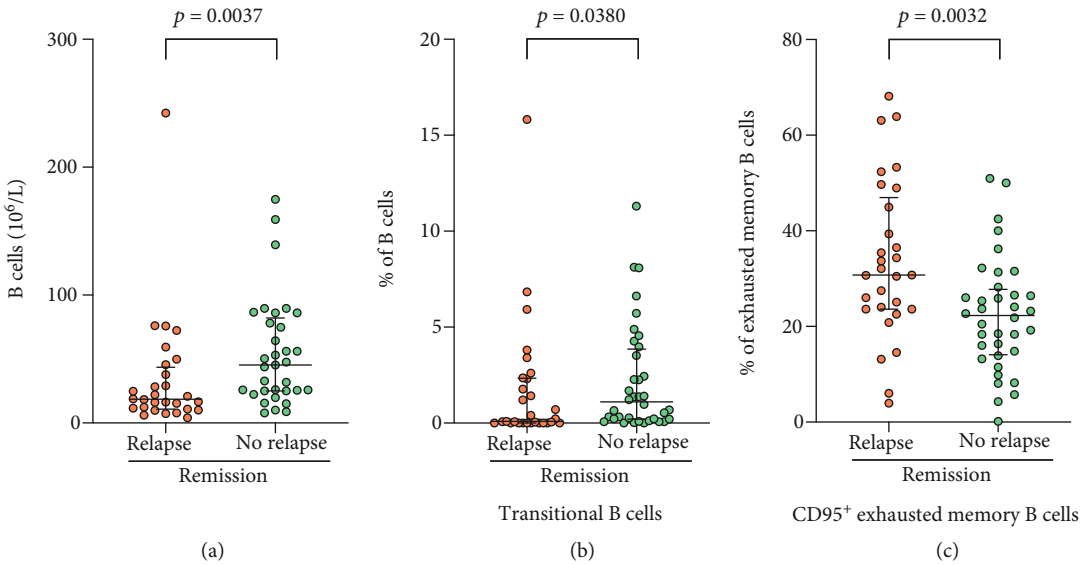

Figure 3: Comparisons of B cells and subsets between patients in remission with and without a tendency to relapse. (a) Concentration of $CD19^+$ B cells in peripheral blood from patients with antineutrophil cytoplasmic autoantibody- (ANCA-) associated vasculitis (AAV) in remission with ($n = 28$) and without ($n = 33$) tendency to relapse. (b) Percentage of transitional B cells (of $CD19^+$ B cells), (c) percentage of $CD95^+$ exhausted memory B cells (of exhausted memory B cells), in peripheral blood from patients with AAV in remission with ($n = 29$) and without ($n = 36$) tendency to relapse. The Mann-Whitney test was used to calculate the level of significance. Data are presented with medians and interquartile ranges.

in AAV patients [14, 19, 20, 27]. Two of the studies also showed that the AAV patients had an increased percentage of naive B cells [14, 20], whereas we found a decreased percentage of naive B cells in the patient cohort. The discrepancy could likely be attributed to differences in medication or disease severity as we found that AAV patients without medication do not display a decreased proportion of naive B cells. In support of our finding, patients with hepatitis C-related mixed cryoglobulinemia vasculitis had a decreased percentage of naive B cells and increased frequencies of memory B cells and plasmablasts compared to healthy and hepatitis C virus controls [28].

In the present study, none of the patients had received anti-B cell treatment and they all had immunoglobulin levels (total IgA, IgG, and IgM) within the reference range, except for IgA in the EGPA group where the lower IQR was below the reference range. We observed lower concentrations of IgG in patients with immunosuppressive medication and in those with a tendency to relapse. The difference in IgG levels between the relapse and nonrelapse groups could possibly be a result of differences in medication, since a higher proportion of patients in the relapse group had medication. It has been reported that 10-13% of patients with multisystem autoimmune disease have low IgG, IgM, and IgA and that the IgG levels are lower in patients who have received cyclophosphamide [29]. Another study on patients with autoimmune disease (the majority diagnosed with GPA) has shown that the total dose of cyclophosphamide is not associated with the IgG concentration [30].

Multiple biomarkers of disease activity in AAV have been proposed, including platelet count [31], lung involvement [32], and prognostic nutritional index [33]. A rise in or persistence of ANCAs during remission is only modestly predictive of future disease relapse [34]. A low percentage of circulating $CD5^+$ B cells, which partially overlaps with the immunophenotype of Bregs, has been shown to correlate with disease activity and a shorter time to relapse after rituximab treatment in AAV [35]. Further, temporal alterations in $CD14^{++}CD16^+$ intermediate monocyte counts have been associated with disease relapse in AAV patients [36].

The percentage of circulating plasmablasts and plasma cells ($CD27^+CD38^{++}$ B cells) has been shown to be increased in GPA patients with future relapse [14]. Increased frequency of circulating $CD27^+CD38^{++}$ B cells during remission could therefore be a potential marker to identify patients at risk of relapse. Also, in other autoimmune diseases such as SLE [37, 38] and IgG4-related disease [39], the plasmablast frequency has been reported to be related to disease activity. Here, we report that the AAV patients had a higher percentage of plasmablasts compared to healthy controls, but there was no difference between patients in active versus inactive disease, or between the relapse versus no-relapse group.

The Fas death receptor, CD95, is upregulated on B cells upon activation. We observed an increased frequency of activated ($CD95^+$) B cells in AAV patients, in B cells in total and in all analyzed B cell subsets, compared to healthy controls. In a previous study of GPA, B cell activation was related to active disease, whereas T cell activation persisted during remission [15]. In addition, the percentage of $CD38^{bright}$ B cells was higher in patients with generalized active disease compared to patients in less active disease groups and healthy controls. We observed no differences in the proportion of $CD95^+$ B cells between

patients in active and inactive disease. The percentage of $CD95^+$ B cells was higher in patients with medication compared to patients without medication and to healthy controls. This was reflected in all subsets of B cells except for $CD95^+$ switched memory B cells where both patients with and without medication displayed an increased frequency of similar magnitude.

While alterations of B cell subsets have been described in multiple autoimmune diseases, it remains unknown whether a specific B cell subset profile is associated with disease relapse. In our observations of patients in remission, the patients with a tendency to relapse had lower B cell frequency and lower B cell count compared to patients without relapsing disease. This may be a result of immunosuppressive treatment as a higher proportion of patients in the relapse group had medication. In line with this, we show that patients with immunosuppressants had lower percentage and lower B cell count compared to the nonmedication group, whereas there was no difference between patients without immunosuppressants and healthy controls. In agreement with our findings, Appelgren et al. found that the prednisolone dose correlated negatively with the absolute number of B cells and the number of naive and memory B cells (but not exhausted memory B cells) [27]. Treatment with cyclophosphamide has been shown to reduce B cell counts, albeit the rate and magnitude of the decrease are less than with rituximab [10].

Patients in the relapse group displayed no difference in the frequency of exhausted memory B cells as compared to the nonrelapse group; however, the relapse group had a higher percentage of $CD95^+$ exhausted memory B cells. In SLE, a specific population of exhausted memory B cells has been demonstrated to be highly enriched, which implicates these autoreactive cells in autoimmune disease [40].

Limitations of this study include heterogeneity of disease duration, type of vasculitis diagnosis, lack of timing of blood collection (samples were obtained from patients at routine clinical visits), that no absolute numbers of lymphocytes were available for the healthy blood donors, and that they were not age- or gender-matched. An additional important limitation is the possible influence of medications on disease severity and the hematopoietic system. To investigate whether the alterations in B cell subsets are specifically related to the immunosuppressive treatment or the autoimmune disease (or both), studies including age- and gender-matched therapy controls are required.

5. Conclusions

In the present study, we primarily investigated if patients with antineutrophil cytoplasmic antibody- (ANCA-) associated vasculitis have altered frequencies of B cells and subsets in peripheral blood. As the main findings, the patient cohort displayed both a decreased frequency of B cells (of lymphocytes) and total B cell number, as well as specific changes in frequencies of B cell subsets. There was an expansion of switched memory B cells as well as plasmablasts and a decrease in the percentage of transitional B cells. Patients with a tendency to relapse had decreased frequencies of B cells and transitional B cells, as well as a higher proportion of activated exhausted memory B cells, compared to patients without relapsing disease. B cells can exert both regulatory and effector functions. Alterations in B cell subsets could translate to changes in the balance of these functions and may contribute to the autoantibody-driven inflammatory process, influence disease activity, and risk of relapse. However, the relative influence of disease activity and effect of medication on the B cell phenotype is difficult to separate in a complex autoimmune disease such as vasculitis.

Data Availability

Raw data files from flow cytometry datasets used in the current study are available from the corresponding author on reasonable request.

Conflicts of Interest

The authors declare no conflict of interest regarding the publication of this paper.

Acknowledgments

This work was supported by Reumatikerförbundet, Anna-Greta Crafoord's Foundation for Rheumatological Research, King Gustaf V's 80th Birthday Foundation, the Swedish Kidney Foundation, Royal Physiographic Society of Lund, Alfred Österlunds Stiftelse, and Swedish Government Salary Funding for Clinically Oriented Medical Research (ALF-ST-grant to EE).

Supplementary Materials

Figure S1: gating strategy used to identify the B cell subpopulations. Table S1: frequencies of B cells and subsets in AAV patients with regard to medication. *(Supplementary Materials)*

References

[1] D. Geetha and J. A. Jefferson, "ANCA-associated vasculitis: core curriculum 2020," *American Journal of Kidney Diseases*, vol. 75, no. 1, pp. 124–137, 2020.

[2] J. C. Jennette, R. J. Falk, P. A. Bacon et al., "2012 revised international Chapel Hill consensus conference nomenclature of vasculitides," *Arthritis and Rheumatism*, vol. 65, no. 1, pp. 1–11, 2013.

[3] J. C. Jennette and P. H. Nachman, "ANCA glomerulonephritis and vasculitis," *Clinical Journal of the American Society of Nephrology*, vol. 12, no. 10, pp. 1680–1691, 2017.

[4] H. Xiao, P. Hu, R. J. Falk, and J. C. Jennette, "Overview of the pathogenesis of ANCA-associated vasculitis," *Kidney Diseases*, vol. 1, no. 4, pp. 205–215, 2016.

[5] J. C. Jennette and R. J. Falk, "Pathogenesis of antineutrophil cytoplasmic autoantibody-mediated disease," *Nature Reviews Rheumatology*, vol. 10, no. 8, pp. 463–473, 2014.

[6] K. Oleinika, C. Mauri, and A. D. Salama, "Effector and regulatory B cells in immune-mediated kidney disease," *Nature Reviews. Nephrology*, vol. 15, no. 1, pp. 11–26, 2019.

[7] N. Lepse, W. H. Abdulahad, C. G. M. Kallenberg, and P. Heeringa, "Immune regulatory mechanisms in ANCA-associated vasculitides," *Autoimmunity Reviews*, vol. 11, no. 2, pp. 77–83, 2011.

[8] H. Rincón-Arévalo, C. C. Sanchez-Parra, D. Castaño, L. Yassin, and G. Vásquez, "Regulatory B cells and mechanisms," *International Reviews of Immunology*, vol. 35, no. 2, pp. 156–176, 2016.

[9] R. B. Jones, J. W. C. Tervaert, T. Hauser et al., "Rituximab versus cyclophosphamide in ANCA-associated renal vasculitis," *The New England Journal of Medicine*, vol. 363, no. 3, pp. 211–220, 2010.

[10] J. H. Stone, P. A. Merkel, R. Spiera et al., "Rituximab versus cyclophosphamide for ANCA-associated vasculitis," *The New England Journal of Medicine*, vol. 363, no. 3, pp. 221–232, 2010.

[11] F. Alberici, R. M. Smith, R. B. Jones et al., "Long-term follow-up of patients who received repeat-dose rituximab as maintenance therapy for ANCA-associated vasculitis," *Rheumatology*, vol. 54, no. 7, pp. 1153–1160, 2015.

[12] J. S. Sanders, M. G. Huitma, C. G. Kallenberg, and C. A. Stegeman, "Plasma levels of soluble interleukin 2 receptor, soluble CD30, interleukin 10 and B cell activator of the tumour necrosis factor family during follow-up in vasculitis associated with proteinase 3-antineutrophil cytoplasmic antibodies: associations with disease activity and relapse," *Annals of the Rheumatic Diseases*, vol. 65, no. 11, pp. 1484–1489, 2006.

[13] K. Matsumoto, K. Suzuki, K. Yoshimoto et al., "Significant association between clinical characteristics and immunophenotypes in patients with ANCA-associated vasculitis," *Rheumatology*, vol. 59, no. 3, pp. 545–553, 2020.

[14] A. von Borstel, J. Land, W. H. Abdulahad et al., "$CD27^{+}CD38^{hi}$ B cell frequency during remission predicts relapsing disease in granulomatosis with polyangiitis patients," *Frontiers in Immunology*, vol. 10, p. 2221, 2019.

[15] E. R. Popa, C. A. Stegeman, N. A. Bos, C. G. M. Kallenberg, and J. W. C. Tervaert, "Differential B- and T-cell activation in Wegener's granulomatosis," *Journal of Allergy and Clinical Immunology*, vol. 103, no. 5, pp. 885–894, 1999.

[16] R. Watts, S. Lane, T. Hanslik et al., "Development and validation of a consensus methodology for the classification of the ANCA-associated vasculitides and polyarteritis nodosa for epidemiological studies," *Annals of the Rheumatic Diseases*, vol. 66, no. 2, pp. 222–227, 2007.

[17] C. Mukhtyar, R. Lee, D. Brown et al., "Modification and validation of the Birmingham vasculitis activity score (version 3)," *Annals of the Rheumatic Diseases*, vol. 68, no. 12, pp. 1827–1832, 2009.

[18] H. T. Maecker, J. P. McCoy, and R. Nussenblatt, "Standardizing immunophenotyping for the human immunology project," *Nature Reviews. Immunology*, vol. 12, no. 3, pp. 191–200, 2012.

[19] H. Tadema, W. H. Abdulahad, N. Lepse, C. A. Stegeman, C. G. M. Kallenberg, and P. Heeringa, "Bacterial DNA motifs trigger ANCA production in ANCA-associated vasculitis in remission," *Rheumatology*, vol. 50, no. 4, pp. 689–696, 2011.

[20] N. Lepse, W. H. Abdulahad, A. Rutgers, C. G. M. Kallenberg, C. A. Stegeman, and P. Heeringa, "Altered B cell balance, but unaffected B cell capacity to limit monocyte activation in anti-neutrophil cytoplasmic antibody-associated vasculitis in remission," *Rheumatology (Oxford)*, vol. 53, no. 9, pp. 1683–1692, 2014.

[21] Q. Simon, J. O. Pers, D. Cornec, L. le Pottier, R. A. Mageed, and S. Hillion, "In-depth characterization of $CD24^{high}CD38^{high}$ transitional human B cells reveals different regulatory profiles," *The Journal of Allergy and Clinical Immunology*, vol. 137, no. 5, pp. 1577–1584.e10, 2016.

[22] C. Lee-Chang, I. Top, H. Zéphir et al., "Primed status of transitional B cells associated with their presence in the cerebrospinal fluid in early phases of multiple sclerosis," *Clinical Immunology*, vol. 139, no. 1, pp. 12–20, 2011.

[23] C. Quan, H. Yu, J. Qiao et al., "Impaired regulatory function and enhanced intrathecal activation of B cells in neuromyelitis optica: distinct from multiple sclerosis," *Multiple Sclerosis*, vol. 19, no. 3, pp. 289–298, 2013.

[24] G. Carvajal Alegria, P. Gazeau, S. Hillion, C. I. Daïen, and D. Y. K. Cornec, "Could lymphocyte profiling be useful to diagnose systemic autoimmune diseases?," *Clinical Reviews in Allergy and Immunology*, vol. 53, no. 2, pp. 219–236, 2017.

[25] R. A. Manz, K. Moser, G. R. Burmester, A. Radbruch, and F. Hiepe, "Immunological memory stabilizing autoreactivity," *Current Topics in Microbiology and Immunology*, vol. 305, pp. 241–257, 2006.

[26] V. Reddy, C. Klein, D. A. Isenberg et al., "Obinutuzumab induces superior B-cell cytotoxicity to rituximab in rheumatoid arthritis and systemic lupus erythematosus patient samples," *Rheumatology*, vol. 56, no. 7, pp. 1227–1237, 2017.

[27] D. Appelgren, P. Eriksson, J. Ernerudh, and M. Segelmark, "Marginal-zone B-cells are main producers of IgM in humans, and are reduced in patients with autoimmune vasculitis," *Frontiers in Immunology*, vol. 9, p. 2242, 2018.

[28] D. Saadoun, M. Rosenzwajg, D. Landau, J. C. Piette, D. Klatzmann, and P. Cacoub, "Restoration of peripheral immune homeostasis after rituximab in mixed cryoglobulinemia vasculitis," *Blood*, vol. 111, no. 11, pp. 5334–5341, 2008.

[29] H. Marco, R. M. Smith, R. B. Jones et al., "The effect of rituximab therapy on immunoglobulin levels in patients with multisystem autoimmune disease," *BMC Musculoskeletal Disorders*, vol. 15, no. 1, 2014.

[30] D. M. Roberts, R. B. Jones, R. M. Smith et al., "Rituximab-associated hypogammaglobulinemia: incidence, predictors and outcomes in patients with multi-system autoimmune disease," *Journal of Autoimmunity*, vol. 57, pp. 60–65, 2015.

[31] P. Willeke, P. Kümpers, B. Schlüter, A. Limani, H. Becker, and H. Schotte, "Platelet counts as a biomarker in ANCA-associated vasculitis," *Scandinavian Journal of Rheumatology*, vol. 44, no. 4, pp. 302–308, 2015.

[32] T. M. Hassan, A. S. Hassan, A. Igoe et al., "Lung involvement at presentation predicts disease activity and permanent organ damage at 6, 12 and 24 months follow - up in ANCA - associated vasculitis," *BMC Immunology*, vol. 15, no. 1, 2014.

[33] S. S. Ahn, S. M. Jung, J. J. Song, Y. B. Park, and S. W. Lee, "Prognostic nutritional index is associated with disease severity and relapse in ANCA-associated vasculitis," *International Journal of Rheumatic Diseases*, vol. 22, no. 5, pp. 797–804, 2019.

[34] G. Tomasson, P. C. Grayson, A. D. Mahr, M. LaValley, and P. A. Merkel, "Value of ANCA measurements during remission to predict a relapse of ANCA-associated vasculitis–a meta-analysis," *Rheumatology*, vol. 51, no. 1, pp. 100–109, 2011.

[35] D. O'Dell Bunch, J. A. G. McGregor, N. B. Khandoobhai et al., "Decreased $CD5^{+}$ B cells in active ANCA vasculitis and relapse

after rituximab," *Clinical Journal of the American Society of Nephrology*, vol. 8, no. 3, pp. 382–391, 2013.

[36] K. Matsumoto, K. Suzuki, K. Yoshimoto et al., "Longitudinal immune cell monitoring identified $CD14^{++}$ $CD16^{+}$ intermediate monocyte as a marker of relapse in patients with ANCA-associated vasculitis," *Arthritis Research & Therapy*, vol. 22, no. 1, p. 145, 2020.

[37] A. M. Jacobi, H. Mei, B. F. Hoyer et al., "HLA-DR^{high}/$CD27^{high}$ plasmablasts indicate active disease in patients with systemic lupus erythematosus," *Annals of the Rheumatic Diseases*, vol. 69, no. 1, pp. 305–308, 2009.

[38] M. Odendahl, R. Keitzer, U. Wahn et al., "Perturbations of peripheral B lymphocyte homoeostasis in children with systemic lupus erythematosus," *Annals of the Rheumatic Diseases*, vol. 62, no. 9, pp. 851–858, 2003.

[39] W. Lin, P. Zhang, H. Chen et al., "Circulating plasmablasts/-plasma cells: a potential biomarker for IgG4-related disease," *Arthritis Research & Therapy*, vol. 19, no. 1, p. 25, 2017.

[40] S. A. Jenks, K. S. Cashman, E. Zumaquero et al., "Distinct effector B cells induced by unregulated toll-like receptor 7 contribute to pathogenic responses in systemic lupus erythematosus," *Immunity*, vol. 49, no. 4, pp. 725–739.e6, 2018.

Hindawi
Journal of Immunology Research
Volume 2020, Article ID 5825401, 13 pages
https://doi.org/10.1155/2020/5825401

Review Article

Cancer Vaccines: Toward the Next Breakthrough in Cancer Immunotherapy

Yuka Igarashi[1] **and Tetsuro Sasada**[1,2]

[1]*Kanagawa Cancer Center, Research Institute, Division of Cancer Immunotherapy, Japan*
[2]*Kanagawa Cancer Center, Cancer Vaccine and Immunotherapy Center, Japan*

Correspondence should be addressed to Yuka Igarashi; y-igarashi@gancen.asahi.yokohama.jp

Received 22 July 2020; Revised 26 September 2020; Accepted 30 September 2020; Published 17 November 2020

Academic Editor: Fabiano Carvalho

Until now, three types of well-recognized cancer treatments have been developed, i.e., surgery, chemotherapy, and radiotherapy; these either remove or directly attack the cancer cells. These treatments can cure cancer at earlier stages but are frequently ineffective for treating cancer in the advanced or recurrent stages. Basic and clinical research on the tumor microenvironment, which consists of cancerous, stromal, and immune cells, demonstrates the critical role of antitumor immunity in cancer development and progression. Cancer immunotherapies have been proposed as the fourth cancer treatment. In particular, clinical application of immune checkpoint inhibitors, such as anti-CTLA-4 and anti-PD-1/PD-L1 antibodies, in various cancer types represents a major breakthrough in cancer therapy. Nevertheless, accumulating data regarding immune checkpoint inhibitors demonstrate that these are not always effective but are instead only effective in limited cancer populations. Indeed, several issues remain to be solved to improve their clinical efficacy; these include low cancer cell antigenicity and poor infiltration and/or accumulation of immune cells in the cancer microenvironment. Therefore, to accelerate the further development of cancer immunotherapies, more studies are necessary. In this review, we will summarize the current status of cancer immunotherapies, especially cancer vaccines, and discuss the potential problems and solutions for the next breakthrough in cancer immunotherapy.

1. Introduction

When one hears the word "vaccine," many people think of vaccines against infectious agents, such as viruses and bacteria. For many years, such vaccines have protected humankind from catastrophic infections [1]. The mechanism through which vaccines provide protection against an infection involves the artificial induction of immune responses against infectious antigens by inoculating a healthy person with attenuated/detoxified bacteria, viruses, or extracted toxins [2]. The aim of a vaccine is to prevent or reduce the severity of life-threatening infectious diseases (prophylactic vaccines). Acquisition of immune memory from vaccines is often effective over long periods of time [3]. A global system of routine immunization against highly prevalent infections has been effectively established; this has resulted in multiple individuals developing immunity against various diseases. Additionally, the World Health Organization (WHO) recommends the administration of free mumps and varicella vaccines in developed countries, where vaccines are recognized as being among the most versatile and important preventive measures [4].

The immune system is directed at maintaining homeostasis in living organisms by monitoring the invasion of foreign pathogens (and associated factors), as well as the presence of abnormal or transformed cells, for their exclusion. This process is called immune surveillance [5]. In daily life, humans are exposed to external factors, such as bacteria, viruses, or harmful substances. Additionally, humans are exposed to various factors that lead to abnormalities and transformations in normal cells. However, it is rare that these exposures or transformations immediately lead to the development of disease, because humans are strongly protected by their immune systems. When there is an imbalance between

extraneous stimuli and biological defense and when components of the immune system are unable to eliminate the pathogen or malfunctioning cells, conditions, such as infections and cancers, develop [6].

2. History of Cancer Vaccines

Till now, chemotherapy, radiotherapy, and surgical excision are the three major cancer treatment methods that directly remove or target the cancer cells. In addition, immunotherapies for the treatment of cancer by leveraging the innate and/or adaptive immune function in humans have been extensively studied. The critical role of the tumor microenvironment (TME), which consists of cancer, stromal, and immune cells that interact with each other, is becoming increasingly apparent. Therefore, cancer immunotherapies have been reconsidered and recognized as the fourth treatment method (Figure 1) [7–9]. Preventive and therapeutic vaccines exist as representative strategies for cancer immunotherapy. The former is aimed at inducing immune memory by administering vaccines to healthy persons to prevent morbidity due to a particular cancer. The latter is administered to patients with cancer for disease management by reinforcing or reactivating the patient's own immune system.

Clinical application of cancer vaccines has faced extreme hurdles despite multiyear research and development efforts by many researchers. The administration of streptococcal organisms (Coley's toxin) as a therapeutic vaccine in patients with sarcoma in the 1890s by Dr. William B. Coley was the first report of cancer immunotherapy [10]. In this strategy, for both prophylactic and therapeutic purposes, specific immune responses were induced against certain sarcoma antigens. The development of this cancer vaccine was based on the clinical findings that the incidence of cancer was low in patients with certain infectious diseases. This phenomenon may reflect the fact that infection and inflammation induce the exposure of antigens abnormally expressed by cancer cells. It might also be a secondary effect, where the immunological memory acquired from past infection or inflammation affects the cancer cells. Similarly, antibodies against abnormal cell surface-associated mucin (MUC1) produced during mumps infection decreases the incidence of ovarian cancer [11]. Moreover, Bacillus Calmette-Guerin has been used as a tuberculosis vaccine for a long time [12, 13] and is now also widely employed as a therapeutic vaccine against bladder cancer.

As some types of cancers are caused by infectious viruses, prophylactic vaccines against viral infection can prevent cancer development [14, 15]. The Food and Drug Administration (FDA) has approved two types of prophylactic cancer vaccines for targeting the human papillomavirus (HPV) and hepatitis B virus (HBV) to prevent HPV-related cancers and HBV-related hepatocarcinoma. However, only a few types of cancer are caused by viral infections. In addition, the global vaccination rate for these prophylactic vaccines is not high. Thus, the number of patients in whom the antiviral vaccines have successfully prevented cancers is limited.

3. Immunological Characteristics of Cancers

Progress in the latter half of the 20th century in tumor immunology and molecular biology has been remarkable. Numerous studies have vigorously investigated the mechanism by which tumors evade the immune system. These efforts have identified a mechanism called "cancer immunoediting" as one of the immune evasion tactics utilized by the tumors [16]. Cancer immunoediting appears to be the consequence of antitumor immune responses mediated by antigen recognition in the tumor environment. The interaction between the immune system and cancer cells, which originally contained specific genetic mutations, may cause a selective and biased proliferation of the clones that have lost these mutations, leading to tumor escape from the immune system. For these cancers, the immune system might not discriminate cancer cells that have lost specific antigens from normal host cells, resulting in the possibility that cancer cells do not elicit a strong exclusionary immune response.

Additionally, the presentation of cancer cell antigens to the T cells differs from the presentation of antigens by mature antigen-presenting cells (APCs) in the context of the participation of costimulatory molecules. Antigen presentation by the APCs involves the presence of a simultaneous second signal from costimulatory molecules, such as CD28, for inducing T cell activation during antigen recognition. This second signal controls the subsequent T cell response [17]. When the antigen is presented to T cells without the second signal, antigen stimulation itself might be ignored; this is termed unresponsive anergy resulting in the loss of the antigen-specific T cell responses. Because cancer cells lack such critical second signals, they may not efficiently induce T cell responses, even if strong cancer-specific antigens derived from genetic mutations are presented to T cells.

Immunosuppressive cells (e.g., myeloid-derived suppressor cells (MDSCs) and regulatory T (Treg) cells) are recruited to the TME by chemotactic factors derived from tumor, stromal, or other immune cells and convey negative signals to the antitumor immune cells via the expression of inhibitory ligands (e.g., programmed death-ligand 1 (PD-L1)) and the secretion of immunosuppressive factors (e.g., interleukin 10 (IL-10), transforming growth factor-beta (TGF-b), and prostaglandin E2 (PGE 2)). In doing so, an environment favoring cancer cell growth is created [18].

4. Current Status of Cancer Vaccines

The identification of the mechanisms used by the cancer cells to evade the immune system has resulted in the development of several tools including antibodies, peptides, proteins, nucleic acids, and immunocompetent cells (dendritic cells, T cells, etc.) for cancer immunotherapy. With respect to cancer vaccines, these techniques fall into three major categories based on format and content, i.e., cell vaccines (tumor or immune cells), protein/peptide vaccines, and nucleic acid vaccines (DNA, RNA, or viral vector).

4.1. Cell Vaccines (Tumor Cell Vaccines or Dendritic Cell (DC) Vaccines). An autologous tumor cell vaccine using a patient's

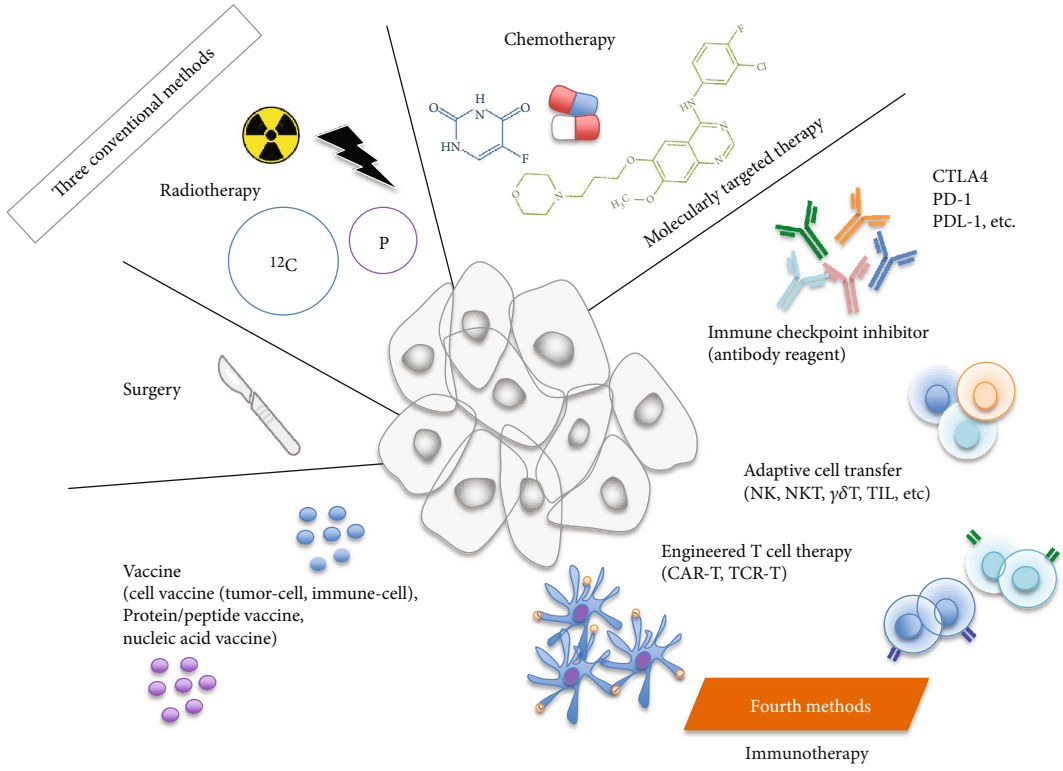

Figure 1: Cancer treatment methods. Conventional methods for cancer treatment include surgery, chemotherapy, and radiation therapy, which remove or directly attack the cancer cells. Recent advances in medical science have resulted in the addition of cancer immunotherapies as a fourth treatment method, which can indirectly attack cancers by regulating the patient's immunity.

own cancer cells is one of the vaccine strategies being evaluated. In this approach, irradiated tumor cells are administered along with an adjuvant. As this vaccine uses tumor cells, it might be possible to induce T cells specific to any antigen expressed by the used cells. However, the limitation of this strategy is that a sufficient number of cells is sometimes difficult to obtain [19–22]. This approach has been attempted in many tumors, including lung cancer [22–24], colorectal cancer [20, 25–27], melanoma [28–30], renal cell carcinoma [31–33], and prostate cancer [19, 34]. In many cases, tumor cells are genetically modified to add functions, such as cytokine production (e.g., IL-2 [35] and granulocyte-macrophage colony-stimulating factor (GM-CSF) [36–39]) and costimulation (e.g., B7-1) [32]. GVAX is a cancer vaccine based on tumor cells genetically modified to secrete GM-CSF. It is used after cancer irradiation to stop the uncontrollable growth of cancer cells. There are two types of GVAX vaccine approaches, one using autologous cells (patient-specific), and the other using allogeneic cells (non-patient-specific). GVAX phase 1/2 clinical trials in patients with non-small-cell lung carcinoma have shown good results, correlating GM-CSF secretion and patient prognosis [40]. However, no effects have been seen in phase 3 clinical trials for prostate cancer [41]. Currently, several phase 2 trials of GVAX therapy for advanced pancreatic cancer have been conducted in combination with body radiation or mesothelin-expressing *Listeria monocytogenes* vaccine or cyclophosphamide (CY), with promising results.

An allogeneic tumor cell vaccine that includes tumor cell lines, such as Canvaxin [42], may overcome the limitation associated with the individualization of autologous tumor vaccines. These vaccines have been studied in prostate [43, 44], breast [45], and pancreatic cancers [46]. Although homologous GVAX against metastatic castration-resistant prostate cancer (CRPC) did not achieve its phase 3 clinical trial goals, a combination strategy using allogeneic GVAX against CRPC and an immune checkpoint inhibitor is being studied [47, 48].

A new therapeutic approach focuses on DCs that present antigens to T cells and promote immune system activation. DC therapy has been intensively studied since the late 1990s [49], when Dr. Ralph M. Steinman, who discovered DCs, recognized their potential, and the possibility of using DCs as a vaccine [50]. A variety of antigens, including tumor cells, tumor-derived proteins or peptides, and DNA/RNA/-virus, could be potentially loaded on DCs. There are additional methods, such as the fusion of DCs with tumor cells. Several receptor types are expressed on the surface of DCs. For example, binding of an antigen to a lectin-like receptor known as scavenger receptor on DCs is reported to induce antigen-specific suppressive CD4(+) T cells. It is noteworthy that not all antigen presentation by DCs contributes to immune activation [51].

In 2010, Provenge (sipuleucel-T; Dendreon Corporation) was approved by the FDA as a prostate cancer vaccine and has drawn attention to the use of autologous immune cells for immunotherapy. It is a crude leukocyte fraction recovered from the peripheral blood of an individual patient, which is then cultured with a prostate carcinoma antigen (prostatic

acid phosphatase (PAP)) in the presence of GM-CSF. DCs are the main active components of Provenge (about 11.2% [52]) and display the PAP antigen to artificially stimulate and induce antigen-specific T cells in patients. Provenge is a good example of the complexity of personalized medicine, as personalized cancer vaccines can be effectively created using this approach. Nevertheless, all of the processes involved in the production of a personalized vaccine, from sample collection to transporting, processing, shipping, and administration of the cells, need to be customized for each patient, leading to increased labor and cost.

4.2. Protein/Peptide Vaccines. Protein/peptide vaccines can induce immunity against specific antigenic epitopes derived from the vaccinated protein/peptides that are expressed in cancer cells (and preferably not expressed in normal tissues). When an artificially synthesized antigen protein/peptide is administered, it is taken up by professional APCs and presented in complex with the HLA molecules on the cell surface. When T cells recognize the antigens, cancer-specific immune responses are induced. Antigenic epitopes derived from tumor-associated antigens (TAAs) capable of binding HLA have been extensively identified. In addition, antigens derived from cancer-specific gene mutations that are not present in normal tissues have recently attracted attention as neoantigens. To efficiently search for these neoantigens, algorithm-based computer searches are rapidly being developed [53–55].

As many early protein/peptide vaccine clinical trials have resulted in favorable results, phase 3 trials have been conducted to confirm the results. Unfortunately, most of these trials have failed, suggesting that single-protein/peptide vaccines do not exert sufficient antitumor effects [56]. Even if T cell responses were induced by protein-/peptide-derived epitopes, the antitumor effects can rarely be achieved with low response rate (less than 10%) [57, 58]. These unexpected results may be explained by several factors, including tumor immune escape mechanisms and immunosuppressive TMEs [59].

There may be problems with the vaccine formulations; most peptide vaccines developed thus far consist of short-chain peptides (SPs) restricted to MHC class I. Unlike long-chain peptides (LPs), SPs are able to bind to any cells without processing and might induce anergy if presented to CD8 T cells without the secondary costimulatory signal [60, 61]. In these situations, immune tolerance is induced, creating an environment favorable for cancer progression. Furthermore, MHC class I-restricted SPs cannot contribute to the activation of MHC class II-restricted helper T cells, which are important for efficient cytotoxic T lymphocyte (CTL) induction. However, LPs can be processed to both MHC class I- or class II-restricted antigens and presented by professional APCs, but not by other cell types. Professional APCs that present LP-derived antigens can activate CTL or helper T cells without inducing anergy by transmitting signals via both T cell receptors (TCRs) and costimulatory molecules [60, 62–64]. Currently, the development of LP vaccines that contain epitopes for both CTL and helper T cells is being actively pursued. In addition, a novel method with an immunostimulatory adjuvant has been developed to improve the responsiveness to peptide vaccines [65–68].

4.3. Nucleic Acid Vaccines (DNA, RNA, or Viral Vector). Nucleic acid (DNA/RNA) vaccines have advantages in that they can simultaneously activate immunity against multiple epitopes [69]. Further, these vaccines are inexpensive and can be synthesized stably. When an immunogenic viral vector is used, the adjuvants are not as important, unlike in peptide vaccines. However, when a viral vector is not used, developing an efficient delivery method becomes an important issue, especially as the efficiency of nucleic acid uptake into cells might be low [70].

DNA vaccines have shown promise in several preliminary studies [71, 72]. For example, VGX3100, a DNA vaccine for cervical cancer, is in phase 3 clinical trials (NCT03185013) [73]. RNA vaccines, unlike DNA vaccines, are not incorporated into the genome, thereby preventing carcinogenicity. Additionally, unlike DNA vaccines that need to enter the nucleus, RNA vaccines can function in the cytoplasm. Therefore, clearance is quick and the possibility of causing side effects might be low. RNA is more easily degraded than DNA, but stability can be enhanced by various modifications, such as formulations with liposomes or stabilizing adjuvants [74–77]. Techniques have also been developed to stabilize the RNA molecule itself ($5'$ cap structure, untranslated regions, and codon usage in translated regions) [78]. Phase 1/2 studies are ongoing for melanoma and kidney cancer [79–81]. A phase I study of liposome-encapsulated mRNA for patients with advanced melanoma is also underway [82]. Further development of nucleic acid delivery methods will serve as a breakthrough in nucleic acid vaccines.

Viral vectors are used to efficiently carry nucleic acids for vaccines. Adjuvants are not required for viral vectors, which can activate innate immunity and also induce immune responses to viruses. Commonly used viral vectors are derived from poxvirus, vaccinia virus, adenovirus, and alphavirus and are attenuated or replication-defective for safety. For example, some modified vaccinia virus Ankara (MVA) vector-based vaccines are used to target the renal cell carcinoma 5T4 and MUC1 antigens [83, 84]. Recombinant adenoviruses are commonly used in cancer gene therapy because they can transduce dividing and nondividing cells and are easy to produce ([85–87], NCT00583024, NCT00197522). Herpes simplex virus type 1 (HSV-1), an enveloped dsDNA virus, is used as an oncolytic virus. HSV-1 expressing GM-CSF (e.g., OncoVEXGM-CSF) is useful in melanoma [88, 89]. The disadvantage of viral vectors is that repeated administration might be difficult due to the induction of antiviral immune responses. For this reason, a heterologous prime-boost strategy is developing. For example, PROSTVAC, a vaccine consisting of two poxvirus vectors that express tumor-associated antigen prostate-specific antigen (PSA) combined with 3 immune-enhancing costimulatory molecules collectively designated as TRICOM (LFA-3, ICAM-1, and B7.1), is under development by Bavarian Nordic (Denmark) to stimulate an immune response in prostate cancer [90–92]. The results of the PROSTVAC-VF/TRICOM phase 3 trial were not as expected, but this vaccine shows promise when combined with immune checkpoint

inhibitors (NCT02933255, NCT02506114). In addition to viruses, bacteria and yeasts are also attracting attention as new vaccine carriers [93, 94].

4.4. Combination Therapy with Cancer Vaccines. Until recently, monotherapies using cancer vaccines often had minimal clinical effects except for certain specific cancer types. The relatively low efficacy of monotherapies was attributed to the multifaceted immune evasion mechanisms of cancer, which are difficult to control by either cancer vaccine alone. As described earlier, the immunosuppressive TME [95] may override any antitumor effects elicited by the cancer vaccine.

In accordance with the development of various immunotherapy types, more attention has focused on combination therapies. Several different approaches, including conventional chemotherapy/radiation therapy or the latest antibody therapies [96, 97], have been attempted in combination either simultaneously or in sequence with immunotherapies.

4.5. Issues in the Clinical Development of Cancer Vaccines. During the development of many conventional cancer vaccines for clinical use, the test designs may have been flawed. For example, clinical effects of cancer vaccines were often evaluated in patients with a terminal diagnosis whose immune conditions were already substantially compromised by exposure to several other treatments, such as surgery and chemotherapy/radiotherapy, or by progression of the disease.

In addition, it is essential to develop accompanying technologies such as adjuvants, manufacturing, and delivery methods to employ vaccines and to obtain expected results in clinical settings [98, 99]. The introduction of such state-of-the-art technology may create additional hurdles due to current drug regulations, which are controlled by regulatory authorities in individual countries, including the FDA, European Medicines Agency (EMA), and Ministry of Health, Welfare, and Labour in Japan [100, 101]. These hurdles are especially important in the development of drugs related to cancer immunotherapy, where it can be difficult to set up a primary endpoint to evaluate the effectiveness of a therapy. Thus far, some cytotoxic drugs under investigation have been known to generally prolong disease-free survival (DFS), but not overall survival (OS), but drugs that extend OS without improving DFS are not very common. Nevertheless, regarding immunotherapy approaches, a situation often arises where OS is extended even if tumor reduction is not observed [102]. In addition, as the immune status of individual patients may be affected by various factors such as age and past treatment history, it is difficult to adequately predict the antitumor effects in nonclinical studies.

5. The Current Status of Other Cancer Immunotherapies

In addition to cancer vaccines, other types of cancer immunotherapies are in development. These have been described below.

5.1. Tumor-Infiltrating Lymphocyte (TIL) Therapy. When tumor tissues are available, TIL therapy is a promising approach. For TIL therapy, T cells that recognize cancer-specific antigens are collected from tumor tissues in patients with cancer, artificially reactivated by using T cell-stimulating agents, such as a high IL-2 concentration, and are then returned to the patients. This approach is potentially simple because genetic modifications are not required, but the clinical effects might be dependent on the amount and quality of infiltrating lymphocytes collected from tumor tissues. Dudley et al. [103] have reported much information on TIL therapy in patients with cancer. Many researchers and doctors are fascinated by their reports on the potential of TIL therapy in melanoma [104–106]. In the latest method, IL-2 and TILs are simultaneously administered to patients to enhance clinical effects [107–109]. In addition, the same group has conducted similar TIL studies for advanced cervical cancer with potential success [110].

5.2. TCR/CAR-T Cell Therapy. The availability and performance of TIL therapy might be dependent on whether sufficient numbers of high-quality antigen-responsive T cells can be secured from tumor tissues in individual patients. To circumvent such limitations, peripheral blood mononuclear cell- (PBMC-) derived lymphocytes, which artificially express a desired TCR or chimeric antigen receptor (CAR), have been devised and clinically applied as a novel T cell therapy. TCR-T therapy is a therapeutic method using T cells transduced with antigen-specific TCRs [111]. CAR-T therapy is a method of administering T cells with a CAR gene, which is composed of a fragment derived from a cancer antigen-recognizing antibody gene, gene fragments from intracellular TCR domains, and other T cell costimulatory molecules.

CAR-T therapy is extremely effective in blood cancers [112]. In 2017, the FDA approved CD19 CAR-T therapy for B cell acute lymphoblastic leukemia (ALL) which has become refractory to first-line treatment or has recurred more than once [113, 114]. Although CAR-T therapy is highly effective, the issues surrounding the cost of care with CAR-T therapy (more than $500,000 for one administration) have yet to be resolved. Notably, CAR-T is effective when a tumor antigen is monolithic or tumor tissue heterogeneity is low (e.g., a genetically uniform tumor, which is often the case with blood tumors). However, the efficacy of CAR-T therapy to solid tumors remains limited, because these tumors generally show more heterogeneity [115].

Another problem with TCR/CAR-T cell therapy in solid tumors is the suppressive TME, which inhibits effective infiltration and/or accumulation of administered T cells inside the tumors. Therefore, a method for effectively driving infiltration of the genetically modified cells into the TME remains out of reach. Moreover, since target antigens are not uniformly expressed in solid tumors and are different depending on the cancer type, stage, and patient, current TCR/CAR-T cell therapy is not widely used in patients with cancer. Furthermore, commonly available target antigens similar to CD19 in blood cancers remain to be identified in solid cancers [116].

5.3. Immune Checkpoint Inhibitors. In the 1990s, immune checkpoint molecules, including cytotoxic T-lymphocyte-

Table 1: A list of currently approved cancer immunotherapies.

	FDA/EMA	MHLW (Japan)
Nivolumab (Anti-PD-1 Ab)	Melanoma non-small cell lung cancer renal cell carcinoma Hodgkin's lymphoma Head neck cancer MSI-H/dMMR colorectal cancer hepatocellular carcinoma small cell lung cancer	Melanoma non-small cell lung cancer renal cell carcinoma Hodgkin's lymphoma Head neck cancer gastric cancer diffuse malignant pleural mesothelioma Esophageal cancer MSI-high colorectal cancer
Pembrolizumab (Anti-PD-1 Ab)	Melanoma non-small cell lung cancer Head neck cancer Hodgkin's lymphoma Urothelial cancer MSI-high colorectal cancer MSI-high cancer gastric cancer cervical cancer hepatocellular carcinoma Merkel cell carcinoma renal cell carcinoma endometrial cancer	Melanoma non-small cell lung cancer Urothelial cancer MSI-high solid tumor renal cell carcinoma * (combination) Head neck cancer ** (mono/combination)
Avelmab (Anti-PD-L1 Ab)	Merkel cell carcinoma renal cell carcinoma Urothelial cancer	Merkel cell carcinoma renal cell carcinoma * (combination)
Atezolizumab (Anti-PD-L1 Ab)	Urothelial cancer non-small cell lung cancer breast cencer small cell lung cancer	non-small cell lung cancer extensive-disease small cell lung cancer. triple negative breast cancer
Durvalumab (Anti-PD-L1 Ab)	Urothelial cancer non-small cell lung cancer	non-small cell lung cancer (stage 3)
Ipilimumab (Anti-CTLA4 Ab)	Melanoma renal cell carcinoma MSI-H/dMMR colorectal cancer	Melanoma *** (mono/combination) renal cell carcinoma **** (combination)
Kymriah (CAR-T)	B-ALL (<25 yars-old) DLBCL (Hodgkin's lymphoma)	B-ALL (<25 yars-old)
Yescarta (CAR-T)	DLBCL (Hodgkin's lymphoma)	not approved
Sipuleucel-T (Provenge) (DC-vaccine)	Prostate cancer	not approved

*Combination with axitinib, **monotherapy or combination with chemotherapy, ***monotherapy or combination with nivolumab, ****combination with nivolumab. MSI-H/dMMR: microsatellite instability-high/deficient mismatch repair; B-ALL: B cell acute lymphoblastic leukemia; DLBCL: diffuse large B cell lymphoma; Ab: antibody; PD-1: programmed death-1; PD-L1: programmed death ligand-1; CAR: chimeric antigen receptor; DC: dendritic cell; FDA: Food and Drug Administration; EMA: European Medicines Agency; MHLW: Ministry of Health, Labour and Welfare.

associated protein 4 (CTLA-4) [117] and programmed death 1 (PD-1) [118], were discovered. Both molecules suppress T cell activation, which is important for exerting antitumor effects. The expression of these molecules increases in proportion to T cell activation, and they function as a defense system for organisms to inhibit excessive T cell activation and prevent autoimmune responses. The activity of T cells is suppressed by ligands binding to CTLA-4 and PD-1. For example, the costimulatory molecule CD80/CD86 expressed on APCs enhances T cell activation by simultaneously binding to CD28 on T cells during antigen presentation. In contrast, CTLA-4 is induced on activated T cells and inhibits

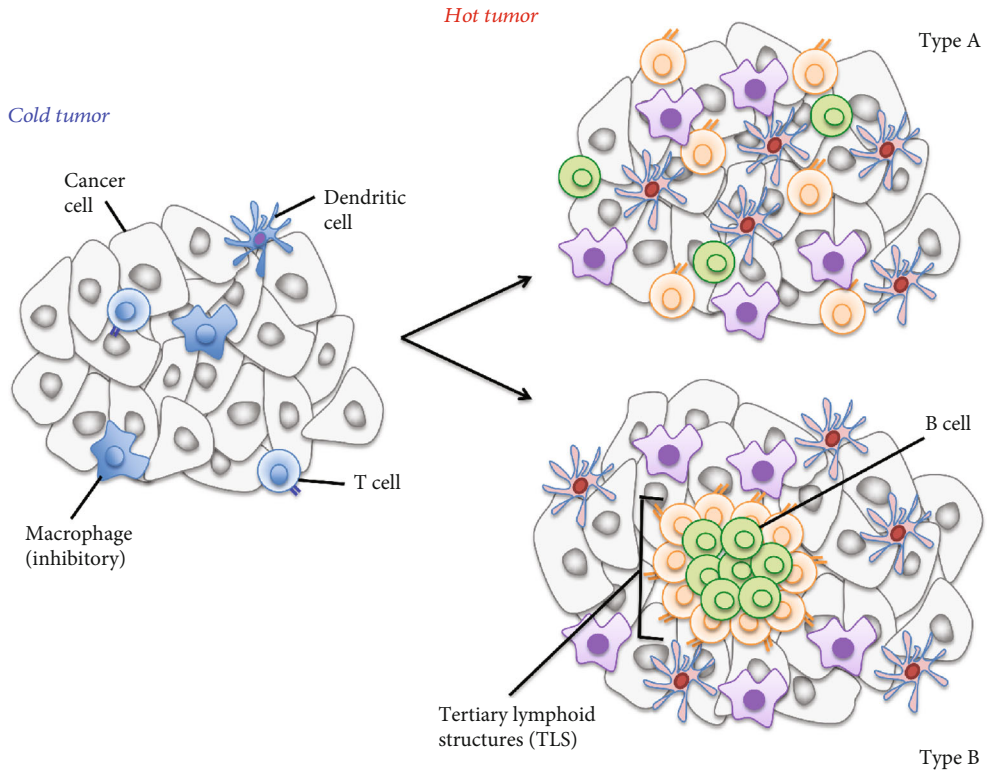

Figure 2: Classification of tumors by immune cell infiltration. Tumor types can be classified by the level of immune cell infiltration into tumors. "Cold tumor," characterized by the poor infiltration of immune cells, is reported to be one of the reasons why immune checkpoint inhibitors are ineffective. Contrastingly, a "hot tumor" is characterized by the abundant infiltration of immunocompetent cells, showing good responses to immune checkpoint inhibitors. Recently, aggregated infiltration of immune cells, known as the tertiary lymphoid structure (hot tumor, type B), has gained increasing attention compared to separated infiltration of immune cells (hot tumor, type A).

the costimulatory signal mediated by CD80/CD86 through competition with CD28. Additionally, antigen-stimulated T cells express PD-1, which suppresses excessive T cell activation by binding to its ligand, PD-L1 or programmed death-ligand 2 (PD-L2) [119]. Additional constituents of the cancer microenvironment, such as DCs [120], macrophages [121], and fibroblasts [122], can also express PD-L1 and/or PD-L2, forming an immunosuppressive environment where cancer is more prone to progress.

In addition to evading the immune system by deleting cell surface molecules required for antigen recognition, cancer cells can often directly use (e.g., hijack) the immunosuppression system, such as immune checkpoints. Some cancer cells strongly express ligands for immune checkpoint molecules, such as PD-L1 and PD-L2 [123, 124]. A remarkable antitumor effect can thus be observed in some patients by administering treatments that block inhibitory molecules in T cells [125, 126]. Once antitumor activity is induced and immune memory is established by immune checkpoint inhibitors in patients with cancer, their clinical effects should be long-lasting.

In 2011, both the FDA and EMA approved anti-CTLA-4 antibody treatment (ipilimumab) for patients with melanoma [127, 128]. Since then, several immune checkpoint inhibitors, anti-PD-1, and anti-PD-L1 antibodies have been approved every year. Table 1 shows several currently approved immune checkpoint inhibitors and their indications. These immune checkpoint inhibitors often show only limited and/or transient efficacy, reflecting the complexities of antitumor immunity [129, 130]. For example, immune checkpoint inhibitors are less effective in microsatellite stable tumors [131]. Such tumors often express only minor genetic abnormalities and thus possess little antigenic capacity. Therefore, these tumors fail to induce cancer antigen-specific T cells, resulting in unresponsiveness to immune checkpoint inhibitors. In addition, the immunosuppressive TME might also affect the clinical effects of immune checkpoint inhibitors.

6. Challenges for the Future Development of Cancer Immunotherapies: Requirement of Lymphocyte Infiltration/Accumulation within Tumors

Analysis of the interaction among tumor infiltrating immune cells (e.g., DCs, MDSCs, CD4/8T cells, and Tregs), stromal cells, and tumor cells is essential to understand the relationship between the TME and the clinical effects of cancer immunotherapies. Especially, many clinical trials using cancer immunotherapies indicate that TIL abundance in the tumor is an important prognostic factor [132]. For example,

the magnitude of lymphocyte infiltration to tumors significantly contributes to immune checkpoint inhibitor effectiveness [133, 134]. The effectiveness of immune checkpoint inhibitors is high against inflammatory-type tumors (hot tumors) [135, 136], where immunocompetent cells are sufficiently present. In contrast, in immune desert-type tumors (cold tumors) with less intratumoral lymphocyte infiltration [137], immune checkpoint inhibitors are less effective.

The difference between these tumor types might depend on whether the immune responses to tumors are maintained or not, suggesting that the recruitment/accumulation of tumor-specific T cells is the limiting factor for therapeutic effects. Treatment could thus be optimized by the development of techniques to increase lymphocyte infiltration into tumors either before or during immunotherapy treatment (Figure 2).

For the development of more effective CAR-T cell therapies, modification with cytokine/chemokine-related genes was recently reported to efficiently drive infiltration of administered CAR-T cells into tumors [138]. Nevertheless, few studies are available on the development of methods for changing cold tumors to hot tumors. Thus, more studies are needed to develop a method to efficiently recruit/accumulate lymphocytes within tumors in combination with immunotherapeutic approaches, including cancer vaccines to stimulate antigen-specific immunocompetent cells, antigen-specific cytotoxic T cell therapies using *ex vivo* genetic modification, or blockade of inhibitory signals from the tumor.

6.1. Induction of Tertiary Lymphoid Structures (TLS). As shown in "hot tumor (type B)" in Figure 2, the accumulation of various immune cell types, especially the formation of lymphoid follicles where immunocompetent cells can exchange information in the tumor, may be important [139, 140]. Indeed, lymphoid follicles in tumors, known as TLS, are associated with better prognosis in several cancers and have recently attracted attention. Several TLS-inducing factors have been reported, including CCL19, CCL21, CXCL12, CXCL13, LIGHT, and lymphotoxin [141–144]. While some basic studies for inducing lymphoid follicles have been conducted in mice, there are no promising methods that are clinically applicable for human therapy. Since efforts so far have been generally focused on a single factor, they might fail to reproduce an induction of TLS due to the complicated mechanisms within the TME. A novel method to efficiently induce TLS in humans, combined with other immunotherapies, such as cancer vaccines and immune checkpoint inhibitors, may be a promising approach for tumor control.

7. Conclusions

The clinical application of immune checkpoint inhibitors has greatly advanced cancer treatment. However, their effects are limited because tumor cells use various mechanisms to evade antitumor effects. To overcome these mechanisms and to improve the versatility of current cancer immunotherapies, it is necessary to understand the TME in more detail and develop novel approaches, including cancer vaccines. We hope that this review will facilitate the further development of cancer immunotherapies.

Conflicts of Interest

The authors declare that there is no conflict of interest regarding the publication of this paper.

Acknowledgments

This research was supported by JSPS KAKENHI Grant Number 19K09110 and AMED under Grant Number JP20ae0101076.

References

[1] WHO, *Assessment reports of the Global Vaccine Action Plan*, World Health Organization, Geneva, 2018, https://apps.who.int/iris/bitstream/handle/10665/276967/WHO-IVB-18.11-eng.pdf?ua=1.

[2] "Immunology and Vaccine-Preventable Diseases," in *Principles of Vaccination*Pink Bookhttps://www.cdc.gov/vaccines/Pubs/pinkbook/downloads/prinvac.pdf.

[3] F. Sallusto, A. Lanzavecchia, K. Araki, and R. Ahmed, "From vaccines to memory and back," *Immunity*, vol. 33, no. 4, pp. 451–463, 2010.

[4] WHO, *Vaccines and immunization*World Health Organizationhttps://www.who.int/health-topics/vaccines-and-immunization#tab=tab_1.

[5] R. R. Rich, "The human immune response," in *Clinical Immunology*, pp. 3–17, 2019.

[6] R. S. Goldszmid, A. Dzutsev, and G. Trinchieri, "Host immune response to infection and cancer: unexpected commonalities," *Cell Host & Microbe*, vol. 15, no. 3, pp. 295–305, 2014.

[7] A. D. Waldman, J. M. Fritz, and M. J. Lenardo, "A guide to cancer immunotherapy: from T cell basic science to clinical practice," *Nature Reviews Immunology*, pp. 1–18, 2020.

[8] K. Esfahani, L. Roudaia, N. Buhlaiga, S. del Rincon, N. Papneja, and W. H. Miller Jr, "A review of cancer immunotherapy: from the past, to the present, to the future," *Current Oncology*, vol. 27, Supplement 2, pp. S87–S97, 2020.

[9] P. S. Hegde and D. S. Chen, "Top 10 challenges in cancer immunotherapy," *Immunity*, vol. 52, no. 1, pp. 17–35, 2020.

[10] W. B. Coley, "II. Contribution to the knowledge of sarcoma," *Annals of Surgery*, vol. 14, no. 3, pp. 199–220, 1891.

[11] D. W. Cramer, A. F. Vitonis, S. P. Pinheiro et al., "Mumps and ovarian cancer: modern interpretation of an historic association," *Cancer Causes & Control*, vol. 21, no. 8, pp. 1193–1201, 2010.

[12] D. E. Morales, D. Eidinger, and A. W. Bruce, "Intracavitary Bacillus Calmette-Guerin in the treatment of superficial bladder tumors," *Journal of Urology*, vol. 116, no. 2, pp. 180–182, 1976.

[13] M. Kamat, J. Bellmunt, M. D. Galsky et al., "Society for immunotherapy of cancer consensus statement on immunotherapy for the treatment of bladder carcinoma," *Journal for ImmunoTherapy of Cancer*, vol. 5, no. 1, p. 68, 2017.

[14] A. R. Garbuglia, D. Lapa, C. Sias, M. R. Capobianchi, and P. del Porto, "The use of both therapeutic and prophylactic

vaccines in the therapy of papillomavirus disease," *Frontiers in Immunology*, vol. 11.

[15] M. H. Nguyen, G. Wong, E. Gane, J. H. Kao, and G. Dusheiko, "Hepatitis B virus: advances in prevention, diagnosis, and therapy," *Clinical Microbiology Reviews*, vol. 33, no. 2, 2020.

[16] G. P. Dunn, A. T. Bruce, H. Ikeda, L. J. Old, and R. D. Schreiber, "Cancer immunoediting: from immunosurveillance to tumor escape," *Nature Immunology*, vol. 3, no. 11, pp. 991–998, 2002.

[17] L. Chen and D. B. Flies, "Molecular mechanisms of T cell co-stimulation and co-inhibition," *Nature Reviews Immunology*, vol. 13, no. 4, pp. 227–242, 2013.

[18] D. Lindau, P. Gielen, M. Kroesen, P. Wesseling, and G. J. Adema, "The immunosuppressive tumour network: myeloid-derived suppressor cells, regulatory T cells and natural killer T cells," *Immunology*, vol. 138, no. 2, pp. 105–115, 2013.

[19] M. Berger, F. T. Kreutz, J. L. Horst, A. C. Baldi, and W. J. Koff, "Phase I study with an autologous tumor cell vaccine for locally advanced or metastatic prostate cancer," *Journal of Pharmacy & Pharmaceutical Sciences*, vol. 10, no. 2, pp. 144–152, 2007.

[20] J. E. Harris, L. Ryan, H. C. Hoover et al., "Adjuvant active specific immunotherapy for stage II and III colon cancer with an autologous tumor cell vaccine: Eastern Cooperative Oncology Group Study E5283," *Journal of Clinical Oncology*, vol. 18, no. 1, pp. 148–157, 2000.

[21] C. Maver and M. McKneally, "Preparation of autologous tumor cell vaccine from human lung cancer," *Cancer Research*, vol. 39, no. 8, 1979.

[22] R. S. Schulof, D. Mai, M. A. Nelson et al., "Active specific immunotherapy with an autologous tumor cell vaccine in patients with resected non-small cell lung cancer," *Molecular Biotherapy*, vol. 1, no. 1, pp. 30–36, 1988.

[23] J. Nemunaitis and J. Nemunaitis, "Granulocyte-macrophage colony-stimulating factor gene-transfected autologous tumor cell vaccine: focus on non-small-cell lung cancer," *Clinical Lung Cancer*, vol. 5, no. 3, pp. 148–157, 2003.

[24] D. Rüttinger, N. K. van den Engel, H. Winter et al., "Adjuvant therapeutic vaccination in patients with non-small cell lung cancer made lymphopenic and reconstituted with autologous PBMC: first clinical experience and evidence of an immune response," *Journal of Translational Medicine*, vol. 5, no. 1, p. 43, 2007.

[25] V. A. de Weger, A. W. Turksma, Q. J. M. Voorham et al., "Clinical effects of adjuvant active specific immunotherapy differ between patients with microsatellite-stable and microsatellite-instable colon cancer," *Clinical Cancer Research*, vol. 18, no. 3, pp. 882–889, 2012.

[26] M. G. Hanna, H. C. Hoover, J. B. Vermorken, J. E. Harris, and H. M. Pinedo, "Adjuvant active specific immunotherapy of stage II and stage III colon cancer with an autologous tumor cell vaccine: first randomized phase III trials show promise," *Vaccine*, vol. 19, no. 17–19, pp. 2576–2582, 2001.

[27] D. Ockert, V. Schirrmacher, N. Beck et al., "Newcastle disease virus-infected intact autologous tumor cell vaccine for adjuvant active specific immunotherapy of resected colorectal carcinoma," *Clinical Cancer Research*, vol. 2, no. 1, pp. 21–28, 1996.

[28] A. Baars, J. M. G. H. van Riel, M. A. Cuesta, E. H. Jaspars, H. M. Pinedo, and A. J. M. van den Eertwegh, "Metastasectomy and active specific immunotherapy for a large single melanoma metastasis," *Hepato-Gastroenterology*, vol. 49, no. 45, pp. 691–693, 2002.

[29] D. Berd, H. C. Maguire, P. McCue, and M. J. Mastrangelo, "Treatment of metastatic melanoma with an autologous tumor-cell vaccine: clinical and immunologic results in 64 patients," *Journal of Clinical Oncology*, vol. 8, no. 11, pp. 1858–1867, 1990.

[30] R. Méndez, F. Ruiz-Cabello, T. Rodríguez et al., "Identification of different tumor escape mechanisms in several metastases from a melanoma patient undergoing immunotherapy," *Cancer Immunology Immunotherapy*, vol. 56, no. 1, pp. 88–94, 2007.

[31] S. J. Antonia, J. Seigne, J. Diaz et al., "Phase I trial of a B7-1 (CD80) gene modified autologous tumor cell vaccine in combination with systemic interleukin-2 in patients with metastatic renal cell carcinoma," *Journal of Urology*, vol. 167, no. 5, pp. 1995–2000, 2002.

[32] M. Fishman, T. B. Hunter, H. Soliman et al., "Phase II trial of B7-1 (CD-86) transduced, cultured autologous tumor cell vaccine plus subcutaneous interleukin-2 for treatment of stage IV renal cell carcinoma," *Journal of Immunotherapy*, vol. 31, no. 1, pp. 72–80, 2008.

[33] Y. Kinoshita, T. Kono, R. Yasumoto et al., "Antitumor effect on murine renal cell carcinoma by autologous tumor vaccines genetically modified with granulocyte-macrophage colony-stimulating factor and interleukin-6 cells," *Journal of Immunotherapy*, vol. 24, no. 3, pp. 205–211, 2001.

[34] K. Tani, M. Azuma, Y. Nakazaki et al., "Phase I study of autologous tumor vaccines transduced with the GM-CSF gene in four patients with stage IV renal cell cancer in Japan: clinical and immunological findings," *Molecular Therapy*, vol. 10, no. 4, pp. 799–816, 2004.

[35] H. Asada, T. Kishida, H. Hirai et al., "Significant antitumor effects obtained by autologous tumor cell vaccine engineered to secrete interleukin (IL)-12 and IL-18 by means of the EBV/lipoplex," *Molecular Therapy*, vol. 5, no. 5, pp. 609–616, 2002.

[36] G. Dranoff, E. Jaffee, A. Lazenby et al., "Vaccination with irradiated tumor cells engineered to secrete murine granulocyte-macrophage colony-stimulating factor stimulates potent, specific, and long-lasting anti-tumor immunity," *Proceedings of the National Academy of Sciences of the United States of America*, vol. 90, no. 8, pp. 3539–3543, 1993.

[37] N. Mach, S. Gillessen, S. B. Wilson, C. Sheehan, M. Mihm, and G. Dranoff, "Differences in dendritic cells stimulated in vivo by tumors engineered to secrete granulocyte-macrophage colony-stimulating factor or Flt3-ligand," *Cancer Research*, vol. 60, no. 12, pp. 3239–3246, 2000.

[38] R. Salgia, T. Lynch, A. Skarin et al., "Vaccination with irradiated autologous tumor cells engineered to secrete granulocyte-macrophage colony-stimulating factor augments antitumor immunity in some patients with metastatic non-small-cell lung carcinoma," *Journal of Clinical Oncology*, vol. 21, no. 4, pp. 624–630, 2003.

[39] E. M. Jaffee, R. H. Hruban, B. Biedrzycki et al., "Novel allogeneic granulocyte-macrophage colony-stimulating factor-secreting tumor vaccine for pancreatic cancer: a phase I trial of safety and immune activation," *Journal of Clinical Oncology*, vol. 19, no. 1, pp. 145–156, 2001.

[40] J. Nemunaitis, T. Jahan, H. Ross et al., "Phase 1/2 trial of autologous tumor mixed with an allogeneic GVAX® vaccine in advanced-stage non-small-cell lung cancer," *Cancer Gene Therapy*, vol. 13, no. 6, pp. 555–562, 2006.

[41] P. M. Arlen, M. Mohebtash, R. A. Madan, and J. L. Gulley, "Promising novel immunotherapies and combinations for prostate cancer," *Future Oncology*, vol. 5, no. 2, pp. 187–196, 2009.

[42] D. L. Morton, L. J. Foshag, D. S. B. Hoon et al., "Prolongation of Survival in Metastatic Melanoma after Active Specific Immunotherapy With a New Polyvalent Melanoma Vaccine," *Annals of Surgery*, vol. 216, no. 4, pp. 463–482, 1992.

[43] J. W. Simons, "Phase I/II trial of an allogeneic cellular immunotherapy in Hormone-Naive prostate cancer," *Clinical Cancer Research*, vol. 12, no. 11, pp. 3394–3401, 2006.

[44] E. J. Small, N. Sacks, J. Nemunaitis et al., "Granulocyte macrophage colony-stimulating Factor-Secreting allogeneic cellular immunotherapy for hormone-refractory prostate cancer," *Clinical Cancer Research*, vol. 13, no. 13, pp. 3883–3891, 2007.

[45] L. A. Emens, J. M. Asquith, J. M. Leatherman et al., "Timed sequential treatment with cyclophosphamide, doxorubicin, and an allogeneic granulocyte-macrophage colony-stimulating factor-secreting breast tumor vaccine: a chemotherapy dose-ranging factorial study of safety and immune activation," *Journal of Clinical Oncology*, vol. 27, no. 35, pp. 5911–5918, 2009.

[46] E. Lutz, C. J. Yeo, K. D. Lillemoe et al., "A lethally irradiated allogeneic granulocyte-macrophage colony stimulating factor-secreting tumor vaccine for pancreatic adenocarcinoma. A phase II trial of safety, efficacy, and immune activation," *Annals of Surgery*, vol. 253, no. 2, pp. 328–335, 2011.

[47] A. J. M. van den Eertwegh, J. Versluis, H. P. van den Berg et al., "Combined immunotherapy with granulocyte-macrophage colony-stimulating factor-transduced allogeneic prostate cancer cells and ipilimumab in patients with metastatic castration-resistant prostate cancer: a phase 1 dose-escalation trial," *Lancet Oncology*, vol. 13, no. 5, pp. 509–517, 2012.

[48] X.-Y. Wang, D. Zuo, D. Sarkar, and P. B. Fisher, "Blockade of cytotoxic T-lymphocyte antigen-4 as a new therapeutic approach for advanced melanoma," *Expert Opinion on Pharmacotherapy*, vol. 12, no. 17, pp. 2695–2706, 2011.

[49] F. O. Nestle, S. Alijagic, M. Gilliet et al., "Vaccination of melanoma patients with peptide- or tumorlysate-pulsed dendritic cells," *Nature Medicine*, vol. 4, no. 3, pp. 328–332, 1998.

[50] R. M. Steinman and J. Banchereau, "Taking dendritic cells into medicine," *Nature*, vol. 449, no. 7161, pp. 419–426, 2007.

[51] D. Li, G. Romain, A.-L. Flamar et al., "Targeting self- and foreign antigens to dendritic cells via DC-ASGPR generates IL-10-producing suppressive CD4+ T cells," *Journal of Experimental Medicine*, vol. 209, no. 1, pp. 109–121, 2012.

[52] E. J. Small, P. Fratesi, D. M. Reese et al., "Immunotherapy of hormone-refractory prostate cancer with antigen-loaded dendritic cells," *Journal of Clinical Oncology*, vol. 18, no. 23, pp. 3894–3903, 2000.

[53] N. Meena, P. Mathur, K. M. Medicherla, and P. Suravajhala, "A bioinformatics pipeline for whole exome sequencing: overview of the processing and steps from raw data to downstream analysis," *bioRxiv*.

[54] L. C. Tsoi, B. Wolf, and Y. A. Chen, "The promise of genomic studies on human diseases: from basic science to clinical application," *International Journal of Genomics*, vol. 2017, Article ID 7983236, 2 pages, 2017.

[55] V. Roudko, B. Greenbaum, and N. Bhardwaj, "Computational prediction and validation of tumor-associated neoantigens," *Frontiers in Immunology*, vol. 11, p. 27, 2020.

[56] L. Buonaguro, A. Petrizzo, M. L. Tornesello, and F. M. Buonaguro, "Translating tumor antigens into cancer vaccines," *Clinical & Vaccine Immunology*, vol. 18, no. 1, pp. 23–34, 2011.

[57] I. Melero, G. Gaudernack, W. Gerritsen et al., "Therapeutic vaccines for cancer: an overview of clinical trials," *Nature Reviews Clinical Oncology*, vol. 11, no. 9, pp. 509–524, 2014.

[58] C. J. M. Melief and S. H. van der Burg, "Immunotherapy of established (pre)malignant disease by synthetic long peptide vaccines," *Nature Reviews Cancer*, vol. 8, no. 5, pp. 351–360, 2008.

[59] F. M. Marincola, E. M. Jaffee, D. J. Hicklin, and S. Ferrone, "Escape of human solid tumors from T-cell recognition: molecular mechanisms and functional significance," *Advances in Immunology*, vol. 74, pp. 181–273, 1999.

[60] M. S. Bijker, S. J. F. van den Eeden, K. L. Franken, C. J. M. Melief, S. H. van der Burg, and R. Offringa, "Superior induction of anti-tumor CTL immunity by extended peptide vaccines involves prolonged, DC-focused antigen presentation," *European Journal of Immunology*, vol. 38, no. 4, pp. 1033–1042, 2008.

[61] Y. Hailemichael, Z. Dai, N. Jaffarzad et al., "Persistent antigen at vaccination sites induces tumor-specific $CD8^+$ T cell sequestration, dysfunction and deletion," *Nature Medicine*, vol. 19, no. 4, pp. 465–472, 2013.

[62] M. S. Bijker, S. J. F. van den Eeden, K. L. Franken, C. J. M. Melief, R. Offringa, and S. H. van der Burg, "CD8+ CTL Priming by Exact Peptide Epitopes in Incomplete Freund's Adjuvant Induces a Vanishing CTL Response, whereas Long Peptides Induce Sustained CTL Reactivity," *The Journal of Immunology*, vol. 179, no. 8, pp. 5033–5040, 2007.

[63] E. M. Janssen, N. M. Droin, E. E. Lemmens et al., "CD4+ T-cell help controls CD8+ T-cell memory via TRAIL-mediated activation-induced cell death," *Nature*, vol. 434, no. 7029, pp. 88–93, 2005.

[64] R. A. Rosalia, E. D. Quakkelaar, A. Redeker et al., "Dendritic cells process synthetic long peptides better than whole protein, improving antigen presentation and T-cell activation," *European Journal of Immunology*, vol. 43, no. 10, pp. 2554–2565, 2013.

[65] C. G. Drake, E. J. Lipson, and J. R. Brahmer, "Breathing new life into immunotherapy: review of melanoma, lung and kidney cancer," *Nature Reviews Clinical Oncology*, vol. 11, no. 1, pp. 24–37, 2014.

[66] L. Liu, Q. Chen, C. Ruan et al., "Platinum-based nanovectors engineered with Immuno-modulating adjuvant for inhibiting tumor growth and promoting immunity," *Theranostics*, vol. 8, no. 11, pp. 2974–2987, 2018.

[67] B. J. Hos, E. Tondini, S. I. van Kasteren, and F. Ossendorp, "Approaches to improve chemically defined synthetic peptide vaccines," *Frontiers in Immunology*, vol. 9, pp. 884–891, 2018.

[68] E. M. Varypataki, N. Benne, J. Bouwstra, W. Jiskoot, and F. Ossendorp, "Efficient eradication of established tumors in

mice with cationic liposome-based synthetic long-peptide vaccines," *Cancer Immunology Research*, vol. 5, no. 3, pp. 222–233, 2017.

[69] L. Aurisicchio and G. Ciliberto, "Genetic cancer vaccines: current status and perspectives," *Expert Opinion on Biological Therapy*, vol. 12, no. 8, pp. 1043–1058, 2012.

[70] S. H. T. Jorritsma, E. J. Gowans, B. Grubor-Bauk, and D. K. Wijesundara, "Delivery methods to increase cellular uptake and immunogenicity of DNA vaccines," *Vaccine*, vol. 34, no. 46, pp. 5488–5494, 2016.

[71] B. Ferraro, M. P. Morrow, N. A. Hutnick, T. H. Shin, C. E. Lucke, and D. B. Weiner, "Clinical applications of DNA vaccines: current progress," *Clinical Infectious Diseases*, vol. 53, no. 3, pp. 296–302, 2011.

[72] N. Y. Sardesai and D. B. Weiner, "Electroporation delivery of DNA vaccines: prospects for success," *Current Opinion in Immunology*, vol. 23, no. 3, pp. 421–429, 2011.

[73] C. L. Trimble, M. P. Morrow, K. A. Kraynyak et al., "Safety, efficacy, and immunogenicity of VGX-3100, a therapeutic synthetic DNA vaccine targeting human papillomavirus 16 and 18 E6 and E7 proteins for cervical intraepithelial neoplasia 2/3: a randomised, double-blind, placebo-controlled phase 2b trial," *Lancet*, vol. 386, no. 10008, pp. 2078–2088, 2015.

[74] S. Espuelas, A. Roth, C. Thumann, B. Frisch, and F. Schuber, "Effect of synthetic lipopeptides formulated in liposomes on the maturation of human dendritic cells," *Molecular Immunology*, vol. 42, no. 6, pp. 721–729, 2005.

[75] M. Fotin-Mleczek, K. Zanzinger, R. Heidenreich et al., "Highly potent mRNA based cancer vaccines represent an attractive platform for combination therapies supporting an improved therapeutic effect," *Journal of Gene Medicine*, vol. 14, no. 6, pp. 428–439, 2012.

[76] P. Qiu, P. Ziegelhoffer, J. Sun, and N. S. Yang, "Gene gun delivery of mRNA in situ results in efficient transgene expression and genetic immunization," *Gene Therapy*, vol. 3, no. 3, pp. 262–268, 1996.

[77] B. Scheel, R. Teufel, J. Probst et al., "Toll-like receptor-dependent activation of several human blood cell types by protamine-condensed mRNA," *European Journal of Immunology*, vol. 35, no. 5, pp. 1557–1566, 2005.

[78] S. Pascolo, "Vaccination with messenger RNA (mRNA)," *Handbook of Experimental Pharmacology*, vol. 183, no. 183, pp. 221–235, 2008.

[79] B. Weide, J.-P. Carralot, A. Reese et al., "Results of the first phase I/II clinical vaccination trial with direct injection of mRNA," *Journal of Immunotherapy*, vol. 31, no. 2, pp. 180–188, 2008.

[80] B. Weide, S. Pascolo, B. Scheel et al., "Direct injection of protamine-protected mRNA: results of a phase 1/2 vaccination trial in metastatic melanoma patients," *Journal of Immunotherapy*, vol. 32, no. 5, pp. 498–507, 2009.

[81] H. Oshiumi, M. Matsumoto, K. Funami, T. Akazawa, and T. Seya, "TICAM-1, an adaptor molecule that participates in toll-like receptor 3-mediated interferon-beta induction," *Nature Immunology*, vol. 4, no. 2, pp. 161–167, 2003.

[82] L. M. Kranz, M. Diken, H. Haas et al., "Systemic RNA delivery to dendritic cells exploits antiviral defence for cancer immunotherapy," *Nature*, vol. 534, no. 7607, pp. 396–401, 2016.

[83] R. J. Amato, R. E. Hawkins, H. L. Kaufman et al., "Vaccination of metastatic renal cancer patients with MVA-5T4: a randomized, double-blind, placebo-controlled phase III study," *Clinical Cancer Research*, vol. 16, no. 22, pp. 5539–5547, 2010.

[84] S. Oudard, O. Rixe, B. Beuselinck et al., "A phase II study of the cancer vaccine TG4010 alone and in combination with cytokines in patients with metastatic renal clear-cell carcinoma: clinical and immunological findings," *Cancer Immunology, Immunotherapy*, vol. 60, no. 2, pp. 261–271, 2011.

[85] S. K. Das, S. Sarkar, R. Dash et al., "Cancer terminator viruses and approaches for enhancing therapeutic outcomes," *Advances in Cancer Research*, vol. 115, pp. 1–38, 2012.

[86] T.-C. Liu, T.-H. Hwang, J. C. Bell, and D. H. Kirn, "Translation of targeted oncolytic virotherapeutics from the lab into the clinic, and back again: a high-value iterative loop," *Molecular Therapy*, vol. 16, no. 6, pp. 1006–1008, 2008.

[87] J. Raty, J. Pikkarainen, T. Wirth, and S. Yla-Herttuala, "Gene therapy: the first approved gene-based medicines, molecular mechanisms and clinical indications," *Current Molecular Pharmacology*, vol. 1, no. 1, pp. 13–23, 2008.

[88] N. N. Senzer, H. L. Kaufman, T. Amatruda et al., "Phase II clinical trial of a granulocyte-macrophage colony-stimulating factor-encoding, second-generation oncolytic herpesvirus in patients with unresectable metastatic melanoma," *Journal of Clinical Oncology*, vol. 27, no. 34, pp. 5763–5771, 2009.

[89] H. L. Kaufman and S. D. Bines, "OPTIM trial: a phase III trial of an oncolytic herpes virus encoding GM-CSF for unresectable stage III or IV melanoma," *Future Oncology*, vol. 6, no. 6, pp. 941–949, 2010.

[90] J. W. Hodge, M. Chakraborty, C. Kudo-Saito, C. T. Garnett, and J. Schlom, "Multiple costimulatory modalities enhance CTL avidity," *Journal of Immunology*, vol. 174, no. 10, pp. 5994–6004, 2005.

[91] P. W. Kantoff, T. J. Schuetz, B. A. Blumenstein et al., "Overall survival analysis of a phase II randomized controlled trial of a poxviral-based PSA-targeted immunotherapy in metastatic castration-resistant prostate cancer," *Journal of Clinical Oncology*, vol. 28, no. 7, pp. 1099–1105, 2010.

[92] J. L. Gulley, P. M. Arlen, R. A. Madan et al., "Immunologic and prognostic factors associated with overall survival employing a poxviral-based PSA vaccine in metastatic castrate-resistant prostate cancer," *Cancer Immunology, Immunotherapy*, vol. 59, no. 5, pp. 663–674, 2010.

[93] C. Remondo, V. Cereda, S. Mostböck et al., "Human dendritic cell maturation and activation by a heat-killed recombinant yeast (Saccharomyces cerevisiae) vector encoding carcinoembryonic antigen," *Vaccine*, vol. 27, no. 7, pp. 987–994, 2009.

[94] E. K. Wansley, M. Chakraborty, K. W. Hance et al., "Vaccination with a recombinant Saccharomyces cerevisiae expressing a tumor antigen breaks immune tolerance and elicits therapeutic antitumor responses," *Clinical Cancer Research*, vol. 14, no. 13, pp. 4316–4325, 2008.

[95] W. Zou, "Immunosuppressive networks in the tumour environment and their therapeutic relevance," *Nature Reviews Cancer*, vol. 5, no. 4, pp. 263–274, 2005.

[96] Y. Yan, A. B. Kumar, H. Finnes et al., "Combining immune checkpoint inhibitors with conventional cancer therapy," *Frontiers in Immunology*, vol. 9, 2018.

[97] W. L. Hwang, L. R. G. Pike, T. J. Royce, B. A. Mahal, and J. S. Loeffler, "Safety of combining radiotherapy with immune-

checkpoint inhibition," *Nature Reviews Clinical Oncology*, vol. 15, no. 8, pp. 477–494, 2018.

[98] A. Bolhassani, S. Safaiyan, and S. Rafati, "Improvement of different vaccine delivery systems for cancer therapy," *Molecular Cancer*, vol. 10, no. 1, p. 3, 2011.

[99] R. S. Riley, C. H. June, R. Langer, and M. J. Mitchell, "Delivery technologies for cancer immunotherapy," *Nature Reviews Drug Discovery*, vol. 18, no. 3, pp. 175–196, 2019.

[100] European Medicines Agency, *Guideline on the evaluation of anticancer medicinal products in man: EMA/CHMP/205/95/Rev.4*, 2012, http://www.ema.europa.eu/docs/en_GB/document_library/Scientific_guideline/2013/01/WC500137128.pdf.

[101] FDA, *Guidance for industry: clinical considerations for therapeutic cancer vaccines*, 2011, http://www.fda.gov/downloads/BiologicsBloodVaccines/GuidanceComplianceRegulatoryInformation/Guidances/Vaccines/UCM278673.pdf.

[102] R. A. Madan, J. L. Gulley, T. Fojo, and W. L. Dahut, "Therapeutic cancer vaccines in prostate cancer: the paradox of improved survival without changes in time to progression," *The Oncologist*, vol. 15, no. 9, pp. 969–975, 2010.

[103] M. E. Dudley, J. R. Wunderlich, J. C. Yang et al., "Adoptive cell transfer therapy following non-myeloablative but lymphodepleting chemotherapy for the treatment of patients with refractory metastatic melanoma," *Journal of Clinical Oncology*, vol. 23, no. 10, pp. 2346–2357, 2005.

[104] S. Stevanović, L. M. Draper, M. M. Langhan et al., "Complete regression of metastatic cervical cancer after treatment with human papillomavirus-targeted tumor-infiltrating T cells," *Journal of Clinical Oncology*, vol. 33, no. 14, pp. 1543–1550, 2015.

[105] M. W. Rohaan, J. H. van den Berg, P. Kvistborg, and J. B. A. G. Haanen, "Adoptive transfer of tumor-infiltrating lymphocytes in melanoma: a viable treatment option," *Journal for ImmunoTherapy of Cancer*, vol. 6, no. 1, p. 102, 2018.

[106] G. U. Mehta, P. Malekzadeh, T. Shelton et al., "Outcomes of adoptive cell transfer with tumor-infiltrating lymphocytes for metastatic melanoma patients with and without brain metastases," *Journal of Immunotherapy*, vol. 41, no. 5, pp. 241–247, 2018.

[107] M. A. Forget, C. Haymaker, K. R. Hess et al., "Prospective analysis of adoptive TIL therapy in patients with metastatic melanoma: response, impact of anti-CTLA4, and biomarkers to predict clinical outcome," *Clinical Cancer Research*, vol. 24, no. 18, pp. 4416–4428, 2018.

[108] M. J. Besser, R. Shapira-Frommer, A. J. Treves et al., "Clinical responses in a phase II study using adoptive transfer of short-term cultured tumor infiltration lymphocytes in metastatic melanoma patients," *Clinical Cancer Research*, vol. 16, no. 9, pp. 2646–2655, 2010.

[109] M. E. Dudley, J. C. Yang, R. Sherry et al., "Adoptive cell therapy for patients with metastatic melanoma: evaluation of intensive myeloablative chemoradiation preparative regimens," *Journal of Clinical Oncology*, vol. 26, no. 32, pp. 5233–5239, 2008.

[110] L. G. Radvanyi, C. Bernatchez, M. Zhang et al., "Specific lymphocyte subsets predict response to adoptive cell therapy using expanded autologous tumor-infiltrating lymphocytes in metastatic melanoma patients," *Clinical Cancer Research*, vol. 18, no. 24, pp. 6758–6770, 2012.

[111] Z. Eshhar, T. Waks, G. Gross, and D. G. Schindler, "Specific activation and targeting of cytotoxic lymphocytes through chimeric single chains consisting of antibody-binding domains and the gamma or zeta subunits of the immunoglobulin and T-cell receptors," *Proceedings of the National Academy of Sciences of the United States of America*, vol. 90, no. 2, pp. 720–724, 1993.

[112] D. L. Porter, B. L. Levine, M. Kalos, A. Bagg, and C. H. June, "Chimeric antigen receptor-modified T cells in chronic lymphoid leukemia," *New England Journal of Medicine*, vol. 365, no. 8, pp. 725–733, 2011.

[113] *U.S. Food and Drug Administration FDA approves CAR-T cell therapy to treat adults with certain types of large B-cell lymphoma*, 2017, https://www.fda.gov/newsevents/newsroom/pressannouncements/ucm581216.htm.

[114] V. A. Chow, M. Shadman, and A. K. Gopal, "Translating anti-CD19 CAR T-cell therapy into clinical practice for relapsed/refractory diffuse large B-cell lymphoma," *Blood*, vol. 132, no. 8, pp. 777–781, 2018.

[115] M. Martinez and E. K. Moon, "CAR T cells for solid tumors: new strategies for finding, infiltrating, and surviving in the tumor microenvironment," *Frontiers in Immunology*, vol. 10, p. 128, 2019.

[116] A. Schmidts and M. V. Maus, "Making CAR T cells a solid option for solid tumors," *Frontiers in Immunology*, vol. 9, 2018.

[117] D. R. Leach, M. F. Lrimmel, and J. P. Allison, "Enhancement of antitumor immunity by CTLA-4 blockade," *Science*, vol. 271, no. 5256, pp. 1734–1736, 1996.

[118] Y. Ishida, Y. Agata, K. Shibahara, and T. Honjo, "Induced expression of PD-1, a novel member of the immunoglobulin gene superfamily, upon programmed cell death," *The EMBO Journal*, vol. 11, no. 11, pp. 3887–3895, 1992.

[119] S. C. Wei, C. R. Duffy, and J. P. Allison, "Fundamental mechanisms of immune checkpoint blockade therapy," *Cancer Discovery*, vol. 8, no. 9, pp. 1069–1086, 2018.

[120] T. J. Curiel, S. Wei, H. Dong et al., "Blockade of B7-H1 improves myeloid dendritic cell-mediated antitumor immunity," *Nature Medicine*, vol. 9, no. 5, pp. 562–567, 2003.

[121] K. Wu, I. Kryczek, L. Chen, W. Zou, and T. H. Welling, "Kupffer cell suppression of CD8+ T cells in human hepatocellular carcinoma is mediated by B7-H1/programmed death-1 interactions," *Cancer Research*, vol. 69, no. 20, pp. 8067–8075, 2009.

[122] M. R. Nazareth, L. Broderick, M. R. Simpson-Abelson, R. J. Kelleher Jr., S. J. Yokota, and R. B. Bankert, "Characterization of human lung tumor-associated fibroblasts and their ability to modulate the activation of tumor-associated T cells," *Journal of Immunology*, vol. 178, no. 9, pp. 5552–5562, 2007.

[123] M. E. Keir, M. J. Butte, G. J. Freeman, and A. H. Sharpe, "PD-1 and its ligands in tolerance and immunity," *Annual Review of Immunology*, vol. 26, no. 1, pp. 677–704, 2008.

[124] W. Zou and L. Chen, "Inhibitory B7-family molecules in the tumour microenvironment," *Nature Reviews. Immunology*, vol. 8, no. 6, pp. 467–477, 2008.

[125] J. R. Brahmer, C. G. Drake, I. Wollner et al., "Phase I study of single-agent anti-programmed death-1 (MDX-1106) in refractory solid tumors: safety, clinical activity, pharmacodynamics, and immunologic correlates," *Journal of Clinical Oncology*, vol. 28, no. 19, pp. 3167–3175, 2010.

[126] W. Zou, J. D. Wolchok, and L. Chen, "PD-L1 (B7-H1) and PD-1 pathway blockade for cancer therapy: mechanisms,

response biomarkers, and combinations," *Science Translational Medicine*, vol. 8, no. 328, p. 328rv4, 2016.

[127] F. S. Hodi, S. J. O'Day, D. F. McDermott et al., "Improved survival with ipilimumab in patients with metastatic melanoma," *New England Journal of Medicine*, vol. 363, no. 8, pp. 711–723, 2010.

[128] E. J. Lipson and C. G. Drake, "Ipilimumab: an anti-CTLA-4 antibody for metastatic melanoma," *Clinical Cancer Research*, vol. 17, no. 22, pp. 6958–6962, 2011.

[129] M. D. Vesely and R. D. Schreiber, "Cancer immunoediting: antigens, mechanisms, and implications to cancer immunotherapy," *Annals of the New York Academy of Sciences*, vol. 1284, no. 1, pp. 1–5, 2013.

[130] C. M. Koebel, W. Vermi, J. B. Swann et al., "Adaptive immunity maintains occult cancer in an equilibrium state," *Nature*, vol. 450, no. 7171, pp. 903–907, 2007.

[131] D. T. Le, J. N. Uram, H. Wang et al., "PD-1 blockade in tumors with mismatch-repair deficiency," *New England Journal of Medicine*, vol. 372, no. 26, pp. 2509–2520, 2015.

[132] P. S. Hegde, V. Karanikas, and S. Evers, "The where, the when, and the how of immune monitoring for cancer immunotherapies in the era of checkpoint inhibition," *Clinical Cancer Research*, vol. 22, no. 8, pp. 1865–1874, 2016.

[133] A. Ribas, R. Dummer, I. Puzanov et al., "Oncolytic virotherapy promotes intratumoral T cell infiltration and improves anti-PD-1 immunotherapy," *Cell*, vol. 170, no. 6, pp. 1109–1119.e10, 2017.

[134] S. Mariathasan, S. J. Turley, D. Nickles et al., "TGFβ attenuates tumour response to PD-L1 blockade by contributing to exclusion of T cells," *Nature*, vol. 554, no. 7693, pp. 544–548, 2018.

[135] J. E. Rosenberg, J. Hoffman-Censits, T. Powles et al., "Atezolizumab in patients with locally advanced and metastatic urothelial carcinoma who have progressed following treatment with platinum-based chemotherapy: a single-arm, multicentre, phase 2 trial," *Lancet*, vol. 387, no. 10031, pp. 1909–1920, 2016.

[136] E. B. Garon, N. A. Rizvi, R. Hui et al., "Pembrolizumab for the treatment of non-small-cell lung cancer," *New England Journal of Medicine*, vol. 372, no. 21, pp. 2018–2028, 2015.

[137] R. S. Herbst, J. C. Soria, M. Kowanetz et al., "Predictive correlates of response to the anti-PD-L1 antibody MPDL3280A in cancer patients," *Nature*, vol. 515, no. 7528, pp. 563–567, 2014.

[138] K. Adachi, Y. Kano, T. Nagai, N. Okuyama, Y. Sakoda, and K. Tamada, "IL-7 and CCL19 expression in CAR-T cells improves immune cell infiltration and CAR-T cell survival in the tumor," *Nature Biotechnology*, vol. 36, no. 4, pp. 346–351, 2018.

[139] N. Hiraoka, Y. Ino, and R. Yamazaki-Itoh, "Tertiary lymphoid organs in cancer tissues," *Frontiers in Immunology*, vol. 7, 2016.

[140] M.-C. Dieu-Nosjean, J. Goc, N. A. Giraldo, C. Sautès-Fridman, and W. H. Fridman, "Tertiary lymphoid structures in cancer and beyond," *Trends in Immunology*, vol. 35, no. 11, pp. 571–580, 2014.

[141] E. J. Colbeck, A. Ager, A. Gallimore, and G. W. Jones, "Tertiary lymphoid structures in cancer: drivers of antitumor immunity, immunosuppression, or bystander sentinels in disease?," *Frontiers in Immunology*, vol. 8, 2017.

[142] C. Sautès-Fridman, M. Lawand, N. A. Giraldo et al., "Tertiary lymphoid structures in cancers: prognostic value, regulation, and manipulation for therapeutic intervention," *Frontiers in Immunology*, vol. 7, 2016.

[143] H. Tang, M. Zhu, J. Qiao, and Y.-X. Fu, "Lymphotoxin signalling in tertiary lymphoid structures and immunotherapy," *Cellular & Molecular Immunology*, vol. 14, no. 10, pp. 809–818, 2017.

[144] F. Jing and E. Y. Choi, "Potential of cells and cytokines/chemokines to regulate tertiary lymphoid structures in human diseases," *Immune Network*, vol. 16, no. 5, pp. 271–280, 2016.

Hindawi
Journal of Immunology Research
Volume 2020, Article ID 5907591, 19 pages
https://doi.org/10.1155/2020/5907591

Research Article

Intranigral Administration of β-Sitosterol-β-D-Glucoside Elicits Neurotoxic A1 Astrocyte Reactivity and Chronic Neuroinflammation in the Rat Substantia Nigra

Claudia Luna-Herrera,[1] **Irma A. Martínez-Dávila**,[2] **Luis O. Soto-Rojas**,[3] **Yazmin M. Flores-Martinez**,[4] **Manuel A. Fernandez-Parrilla**,[2] **Jose Ayala-Davila**,[2] **Bertha A. León-Chavez**,[5] **Guadalupe Soto-Rodriguez**,[6] **Victor M. Blanco-Alvarez**,[6,7] **Francisco E. Lopez-Salas**,[2] **Maria E. Gutierrez-Castillo**,[8] **Bismark Gatica-Garcia**,[2] **America Padilla-Viveros**,[9] **Cecilia Bañuelos**,[9] **David Reyes-Corona**,[2] **Armando J. Espadas-Alvarez**,[8] **Linda Garcés-Ramírez**,[1] **Oriana Hidalgo-Alegria**,[1] **Fidel De La Cruz-lópez**,[1] **and Daniel Martinez-Fong**[2,10]

[1]*Departamento de Fisiología, Escuela Nacional de Ciencias Biológicas, Instituto Politécnico Nacional, Wilfrido Massieu y Cda. Manuel Stampa s/n, C.P. 07738 Ciudad de México, Mexico*
[2]*Departamento de Fisiología, Biofísica y Neurociencias, CINVESTAV, Av. Instituto Politécnico Nacional No. 2508, C.P. 07360 Ciudad de México, San Pedro Zacatenco, Mexico*
[3]*Facultad de Estudios Superiores Iztacala, Universidad Nacional Autónoma de México, Av. De los Barrios No. 1, Tlalnepantla, C.P. 54090 Edo. De México, Mexico*
[4]*Programa Institucional de Biomedicina Molecular, Escuela Nacional de Medicina y Homeopatía, Instituto Politécnico Nacional, Guillermo Massieu Helguera 239, C.P. 07320 Ciudad de México, Mexico*
[5]*Facultad de Ciencias Químicas, Benemérita Universidad Autónoma de Puebla, Av.14 Sur y Av. San Claudio, Cd. Universitaria, Puebla, C.P. 72570 Puebla, Mexico*
[6]*Facultad de Medicina, Benemérita Universidad Autónoma de Puebla, 13 Sur 2702, Puebla, C.P. 72420 Puebla, Mexico*
[7]*Facultad de Enfermería, Benemérita Universidad Autónoma de Puebla, Av. 25 Poniente 1304, Los Volcanes, Puebla, C.P. 72410 Puebla, Mexico*
[8]*Departamento de Biociencias e Ingeniería, Centro Interdisciplinario de Investigaciones y Estudios sobre Medio Ambiente y Desarrollo, Instituto Politécnico Nacional, 30 de Junio de 1520 s/n, C.P. 07340 Ciudad de México, Mexico*
[9]*Coordinación General de Programas Multidisciplinarios, Programa Transdisciplinario en Desarrollo Científico y Tecnológico para la Sociedad, Centro de Investigación y de Estudios Avanzados, Av. Instituto Politécnico Nacional No. 2508, C.P. 07360 Ciudad de México, Mexico*
[10]*Programa de Nanociencias y Nanotecnología, CINVESTAV, Av. Instituto Politécnico Nacional No. 2508, C.P. 07360 Ciudad de México, San Pedro Zacatenco, Mexico*

Correspondence should be addressed to Daniel Martinez-Fong; martinez.fong@gmail.com

Received 2 March 2020; Revised 1 June 2020; Accepted 9 June 2020; Published 16 November 2020

Guest Editor: Fabiano Carvalho

Chronic consumption of β-sitosterol-β-D-glucoside (BSSG), a neurotoxin contained in cycad seeds, leads to Parkinson's disease in humans and rodents. Here, we explored whether a single intranigral administration of BSSG triggers neuroinflammation and neurotoxic A1 reactive astrocytes besides dopaminergic neurodegeneration. We injected 6 μg BSSG/1 μL DMSO or vehicle into the left *substantia nigra* and immunostained with antibodies against tyrosine hydroxylase (TH) together with markers of microglia (OX42), astrocytes (GFAP, S100β, C3), and leukocytes (CD45). We also measured nitric oxide (NO), lipid

peroxidation (LPX), and proinflammatory cytokines (TNF-α, IL-1β, IL-6). The Evans blue assay was used to explore the blood-brain barrier (BBB) permeability. We found that BSSG activates NO production on days 15 and 30 and LPX on day 120. Throughout the study, high levels of TNF-α were present in BSSG-treated animals, whereas IL-1β was induced until day 60 and IL-6 until day 30. Immunoreactivity of activated microglia ($899.0 \pm 80.20\%$) and reactive astrocytes ($651.50 \pm 11.28\%$) progressively increased until day 30 and then decreased to remain $251.2 \pm 48.8\%$ (microglia) and 91.02 ± 39.8 (astrocytes) higher over controls on day 120. C3(+) cells were also GFAP and S100β immunoreactive, showing they were neurotoxic A1 reactive astrocytes. BBB remained permeable until day 15 when immune cell infiltration was maximum. TH immunoreactivity progressively declined, reaching $83.6 \pm 1.8\%$ reduction on day 120. Our data show that BSSG acute administration causes chronic neuroinflammation mediated by activated microglia, neurotoxic A1 reactive astrocytes, and infiltrated immune cells. The severe neuroinflammation might trigger Parkinson's disease in BSSG intoxication.

1. Introduction

Clinical studies indicate that neuroinflammation plays a pivotal role in Parkinson's disease (PD) [1], the second more common chronic neurodegenerative illness worldwide [2]. Postmortem studies have demonstrated the presence of activated microglia and reactive astrocytes, the professional immune cells of the central nervous system, in the brain of patients with PD. Activated microglia have been evidenced by the increased number of OX42 immunoreactive cells with a phagocytic phenotype [3]. Besides, inflammation mediators of microglial origin, such as nitric oxide (NO) and proinflammatory cytokines, have been found in mesencephalon slices, spinal cord fluid (SCF), and serum of PD patients [4–8]. Similarly, reactive astrocytes have been evidenced by the increased number of calcium-binding protein S100β immunoreactive cells in PD patients' brains and high levels of S100β in the SCF [9–11]. Different from the glial fibrillary acidic protein (GFAP), S100β is a more suitable neuroinflammation marker because this protein can act as a cytokine. It can be secreted and stimulates the expression of inducible nitric oxide synthase (iNOS), thus elevating NO production [12, 13]. NO is known to be involved in neuroinflammation and the subsequent degeneration of dopaminergic neurons [14] by promoting the generation of reactive oxygen species (ROS) and cyclooxygenase 2- (COX-2-) dependent synthesis of prostaglandin in microglial cells [15, 16]. A recent study has shown that the A1-classified reactive astrocytes are harmful, rapidly killing neurons and oligodendrocytes after acute central nervous system injury [10]. The A1 reactive astrocytes are induced by the classically activated neuroinflammatory microglia and identified by their immunoreactivity to complement component C3 [10].

The presence of neurotoxic A1 reactive astrocytes in PD patient brains suggests that these cells contribute to the death of dopaminergic neurons [10]. This is why the new antiparkinsonian therapy is aimed at inhibiting A1 reactive astrocytes [17, 18]. The mechanism by which neurotoxic A1 reactive astrocytes cause neuron death is still under research.

Pathological α-synuclein aggregates can elicit neuroinflammation in PD by activating microglia to produce ROS [19–22] and recruiting peripheral immune cells [23, 24]. T lymphocytes extravasate into the central nervous system (CNS) via a blood-brain barrier (BBB) leaky in PD patients [25]. Accordingly, large numbers of CD4(+) and CD8(+) T cells populate the ventral midbrain of patients and animal models of PD [26–28]. Recent studies indicate that the infiltrated T cells could generate an autoimmune response to α-synuclein [29], thus worsening and prolonging the primary neuroinflammation caused by the activated microglia. Regardless of the specific mechanism, activated microglia is the leading player in the α-synuclein-induced neuroinflammation. Therefore, microglia-activated A1 reactive astrocytes could also mediate the neurotoxic effect of pathological α-synuclein [17]. The study of this issue in other rat models of α-synucleinopathy is necessary to gain insight into PD pathology and validate new therapies.

Toxins present in the flour of washed seeds from the plant *Cycas micronesica* (cycad) have been linked to the amyotrophic lateral sclerosis/parkinsonism/dementia complex (ALS/PDC) in the Chamorro population of Guam island [30, 31] and have been used to generate PD-like disorders in rodents [32]. Sprague-Dawley rats fed with cycad flour for at least 16 weeks show a loss of dopaminergic neurons in the *substantia nigra pars compacta* (SNpc) and α-synuclein aggregates in the SNpc and striatum along with motor deficits [33].

Moreover, a faithful model for PD was developed in *Sprague-Dawley* rats chronically fed with pellets supplemented with β-sitosterol-D-glucoside (BSSG), a neurotoxin isolated from cycad [34, 35]. This model replicates the three cardinal features of PD, i.e., motor and cognitive dysfunctions, dopaminergic neurodegeneration, and insoluble α-synuclein aggregates that follow the Braak stages of PD [34]. Neuroinflammation also occurs in the chronic oral BSSG administration, as shown by a significant elevation in the number of activated microglia in the SNpc [34, 36]. However, whether BSSG administration could lead to reactive astrocyte induction, leukocyte infiltration, and production of chemical mediators of inflammation is still unknown. We recently showed that a single intranigral administration of BSSG reproduces, in less time, most of the features of oral administration, including dopaminergic neuron loss and pathological α-synuclein aggregation in the SNpc [37, 38].

Herein, we aim at demonstrating the induction of neurotoxic A1 reactive astrocytes as part of the inflammatory response and their link to nigral dopaminergic neurodegeneration after the stereotaxic administration of 6 μg BSSG/1 μL DMSO [37]. Our results confirm the activation of microglial cells and advance the knowledge showing the production of NO and proinflammatory cytokines, released by microglia, astrocytes, infiltrating leukocytes, neurons [39], and possibly by BBB-endothelial cells known to express IL-1β and IL-6 genes [40, 41]. We showed, for the first time, astrocyte

reactivity through increasing immunoreactivity to S100β and C3, two specific markers of neurotoxic A1 reactive astrocytes. The increase in these markers associated with the progressive loss of TH (+) cells suggests that the neurotoxic A1 reactive astrocytes mediate the death of nigral dopaminergic neurons in the stereotaxic BSSG model in the rat. This model can be used to analyze new antiparkinsonian therapies aimed at blocking the conversion of A1 astrocytes by microglia.

2. Materials and Methods

2.1. Ethics Statement. Adult male *Wistar* rats (210-230 g) were obtained from the Laboratory of Animal Production and Experimentation Unit of CINVESTAV-IPN (Protocol 162-15). Animals were kept under standard conditions of inverted light-dark 12 h cycles in a room with a temperature of 22 ± 2°C and relative humidity of 60 ± 5%, with access to water and Chow croquettes *ad libitum*.

2.2. Experimental Groups. Animals ($n = 147$ in total) were randomly assigned to the BSSG group ($n = 52$), with a stereotaxic infusion of 6 μg BSSG/1 μL of DMSO [42], the mock group (stereotaxic injection of 1 μL of DMSO; $n = 52$), and the untreated (Ut) group (without surgery and treatment; $n = 43$). Four rats of each experimental group were evaluated with nitrosative and oxidative stress assays ($n = 4$ rats per each procedure per group), three rats for ELISA ($n = 3$ rats per group), three rats for Evans blue staining (brain permeability; $n = 3$ rats per group), and three for immunostaining ($n = 3$ rats per group). These assays were performed at days 15, 30, 60, and 120 after the lesion. The total rats for the four times evaluated were 16 for nitrosative and oxidative stress assays, 12 for ELISA, and 12 for immunostaining assays. Brain permeability was evaluated at days 7, 15, 30, and 60 after the lesion ($n = 12$). For immunostaining assays, only 3 rats of the untreated group were evaluated on day 120 ($n = 3$). All the immunostaining measurements were performed in 4 anatomical levels (1 anterior, 2 medials, 1 posterior), from which mean value and SD were calculated. The total number of animals was 147, which was a minimum for statistical significance and by the experimental design in compliance with the Guide for the Care and Use of Laboratory Animals (The National Academies Collection: Reports funded by National Institutes of Health, 2011). No animal deaths occurred during the study (Supplementary Figure 1).

2.3. Stereotaxic Injection of BSSG. A mixture of xylazine/ketamine (10 mg/kg/100 mg/kg, i.p.) was used to anesthetize the rats and fix them with a stereotaxic apparatus. After trepanation, 1 μL of BSSG (6 μg/1 μL of DMSO; Sigma-Aldrich; St. Louis, MO, USA) was injected into the left *substantia nigra*. The stereotaxic coordinates were anterioposterior, +3.2 mm from the interaural midpoint; mediolateral, +2.0 mm from the intraparietal suture; and dorsoventral, -6.6 mm from the dura mater [43]. A microperfusion pump (Mod. 100; Stoelting; Wood Dale, IL, USA) maintained the flow rate at 0.16 μL/min. After injecting the total volume, the needle was allowed to remain in the brain for 5 min and then was withdrawn in 1 min steps to avoid reflux of the injected solution. The mock group was injected with 1 μL of DMSO. After surgery, the surgical wound was sutured, and rats were maintained in an individual cage until complete recovery.

2.4. Dissection of Cerebral Nuclei for Molecular and Biochemical Assays. Animals were euthanized with sodium pentobarbital (50 mg/kg; intraperitoneally). For biochemical measurements (nitrosative and oxidative stress) and ELISA assays, each brain was obtained after decapitation and dissected out free of meninges and immediately submerged in cold PBS. Using a cold metallic rat brain matrix (Stoelting; Wood Dale, IL, USA), we cut twelve 0.5 mm coronal slices of each brain between the occipitotemporal anterior border and the anterior border of the cerebellum [44]. The *substantia nigra* was quickly dissected out from each coronal slice in cold and sterile conditions using a stereomicroscope (Leica ZOOM 2000; Buffalo, NY, USA) equipped with a void metallic stage to contained dry ice [44]. Each sample was immediately stored in a respective Eppendorf tube at −70°C until used [45]. For immunostaining and brain permeability, the animals were intracardially perfused with 100 mL of PBS, followed by 100 mL 4% paraformaldehyde in PBS, as previously described by Flores-Martinez et al. [44]. The brain was dissected out and maintained in the fixative for 24 h at 4°C and then in 30% sucrose in PBS at 4°C. For immunostaining assay, the brain was frozen and then sectioned at 20 μm thickness using a sliding microtome (Leica SM1100; Heidelberg, Germany). The slices were consecutively collected in 6 wells, and only those in one well were used for immunostaining. For evaluation of brain permeability, the mesencephalon was cut into 100 μm thick coronal slices with the aid of a vibratome (Leica Microsystems Inc, VT1200S; Buffalo Grove, IL, USA).

2.5. NO Production Measurements. We followed the method of Flores-Martinez et al. [44] to measure nitrite (NO_2^-) accumulation in the supernatant of homogenized *substantia nigra* samples as an index of nitric oxide (NO) production. Briefly, the tissue samples were mechanically homogenized in phosphate-buffered saline pH 7.4 (PBS). Homogenates were centrifuged at 20,000 g for 30 min at 4°C, and 2.5 μL of supernatant was used to measure NO by adding 100 μL of the Griess reagent. The color in the samples was read at 540 nm with a Nanodrop (Thermo Fisher Scientific; Wilmington, USA), and the values were interpolated in a standard curve of sodium nitrite ($NaNO_2$; 1 to 10 μM) to calculate the experimental nitrite values. The protein content was measured in the pellet using the BCA method and bovine serum albumin (BSA) for the standard curve following the manufacturer's protocol (Thermo Fisher Scientific; Rockford, IL, USA). The nitrite content values were expressed as μmol/mg of protein.

2.6. Assessment of Lipid Peroxidation. We measured malondialdehyde (MDA) and 4-hydroxyalkenals (4-HAE) concentration in the supernatant of homogenized *substantia nigra* samples as an index of lipid peroxidation, following the

methodology reported by Flores-Martinez et al. [44]. Briefly, the samples were homogenized in PBS and centrifuged at 20,000 g at 4°C for 40 min. Then, 100 μL of the supernatant was supplemented with 325 μL of a mixture of acetonitrile to methanol (3 : 1 volume) containing 10.3 mM N-methyl-2-phenylindole. The colorimetric reaction was initiated by the addition of 75 μL of methanesulfonic acid. The reaction mixture was vigorously shaken and incubated at 45°C for 1 h and then centrifuged at 1000 g for 10 min. The absorbance was interpolated in a 1,1,3,3-tetramethoxypropane standard curve (0.5 to 5 μM) to calculate MDA and 4-HAE content in the samples. The protein content was measured in the pellet using the BCA method and bovine serum albumin (BSA) for the standard curve following the manufacturer's protocol (Thermo Fisher Scientific; Rockford, IL, USA). The values were expressed as μmol of MDA+ 4-HAE/mg of protein.

2.7. Immunostaining. The slices were permeabilized with PBS-0.1% Triton for 20 min and incubated with 1% BSA in PBS-0.1% Triton for 30 min to block unspecific binding sites. Then, they were incubated with the primary antibodies overnight at 4°C and with the secondary antibodies for 2 h at room temperature (RT). For immunofluorescence, the primary antibodies were a rabbit polyclonal anti-TH (1 : 1000; Merck Millipore, USA), a mouse monoclonal anti-CD11b/c (OX42; 1 : 200; Abcam, Cambridge, UK), a goat polyclonal anti-ionized calcium-binding adapter molecule 1 (Iba1) as a microglial marker (1 : 500 Abcam; Cambridge,UK), a mouse anti-CD45 (1 : 50; BD Bioscience, USA), a mouse monoclonal anti-GFAP Clone GA5 (1 : 500; Cell Signaling Technology; Danvers, Massachusetts, USA), a mouse monoclonal anti-S100β (1 : 200; Merck-Sigma-Aldrich, St. Louis, MO, USA), and a goat polyclonal anti-C3 (1 : 50; Invitrogen; Waltham, Massachusetts, USA). The secondary antibodies were an Alexa 488 chicken anti-rabbit H + L IgG (1 : 300; Invitrogen Molecular Probes; Eugene, OR, USA), an Alexa 488 chicken anti-goat H + L IgG (1 : 300; Invitrogen Molecular Probes; Eugene, OR, USA), and a Texas red horse anti-mouse H + L IgG (1 : 500; Vector Laboratories; Burlingame, CA, USA). After washing with PBS, the slices were mounted on glass slides using VECTASHIELD (Vector Laboratories; Burlingame, CA, USA). The fluorescence images were obtained with a Leica confocal microscope (TCS SP8; Heidelberg, Germany), using 20x, 40x, 63x, and 100x objectives. Serial 1 μm optical sections were also obtained in the *Z*-series (scanning rate of 600 Hz). The images were acquired and analyzed with the LAS AF software (Leica Application Suite; Leica Microsystems; Nussloch, Germany). The immunofluorescence area density (IFAD) for the double fluorescence assays was measured using the ImageJ software v.1.46r (National Institutes of Health; Bethesda, MD). The measurements were made on images taken with a 20x (TH-GFAP), 40x (TH-OX42, TH-S100β, and S100β-GFAP), and 63x (C3-GFAP, C3-S100β, and TH-CD45) of the central zone of the SNpc in four different anatomic levels (one rostral, two medials, and one caudal) per rat ($n = 3$ independent rats per group and time).

Immunohistochemistry staining of microglial cells was performed in permeabilized slices incubated with a chicken polyclonal Iba1 (1 : 1000; Abcam; Cambridge, UK) overnight at 4°C, followed by incubation with a biotinylated donkey anti-chicken IgG (1 : 500; Jackson ImmunoResearch; Palo Alto, CA, USA) for 2 h at RT. Endogenous peroxidase was eliminated by incubating the slices with 3% hydrogen peroxide in PBS/Triton and 10% methanol at RT for 10 min. The immunohistochemical staining was developed using the ABC kit (1,10; Vector Laboratories; Burlingame, CA, USA) and 3′3-diaminobenzidine (DAB; Sigma-Aldrich; St. Louis, MO, USA) as reported previously [38]. The brain slices were washed 3 times for 5 min in PBS, counterstained with β-Gal and mounted on slides using Entellan resin (Merck, KGaA; Darmstadt, Germany), and observed with a light Leica DMIRE2 microscope with 63x (oil immersion) objective (Leica Microsystems; Nussloch, Germany).

2.8. Enzyme-Linked Immunosorbent Assay (ELISA). We followed the methods of Flores-Martinez et al. [44] to measure TNF-α, IL-1β, and IL-6. Briefly, the left *substantia nigra* ($n = 3$ independent rats) was homogenized using extraction buffer containing 100 mM Tris HCl (pH 7.4), 750 mM NaCl (sodium chloride), 10 mM EDTA (ethylenediaminetetraacetic acid), 5 mM EGTA (ethylene glycol tetraacetic acid), and mix of protease inhibitors (Mini EDTA-free Protease Inhibitor Cocktail Tablets) used as indicated by the manufacturer (Roche, Basel, Switzerland) [46]. The *substantia nigra* samples were centrifuged at 1000 g for 10 minutes at 4°C. Then, the supernatant was centrifuged at 20000 g for 40 min at 4°C again to eliminate the remaining debris. The levels of inflammatory cytokines were detected by ELISA technique, using the Milliplex MAP Rat cytokine/chemokine magnetic bead panel kit (RECYTMAG_65K; Millipore; Temecula, CA, USA), and reading was done by the LUMINEX MAGPIX detection system with the xPONET software (Millipore Corporation; Billerica, MA, USA). The values in the supernatant were extrapolated in a curve of 2.4 to 10000 pg/mL for TNF-α and IL-1β and 73.2 to 300000 pg/mL for IL-6. The pellet was resuspended to measure protein content using the BCA method and bovine serum albumin (BSA) for the standard curve following the manufacturer's protocol (Thermo Fisher Scientific; Rockford, IL, USA). The values were expressed as pg of cytokine/mg of protein.

2.9. Evaluation of Brain Permeability. We injected a 2% Evans blue dye solution in PBS (4 mL/kg of body weight) into the caudal vein [47] of untreated, mock, and BSSG rats at days 7, 15, 30, and 60 after the BSSG injection. After 24 h, the rats were anesthetized and perfused as described in the immunostaining section. Upon completion perfusion of the fixative, the brain was dissected out, and the mesencephalon was cut into 100 μm thick coronal slices with the aid of a vibratome (Leica Microsystems Inc, VT1200S; Buffalo Grove, IL, USA). Immediately, images were captured using a Leica stereomicroscope MZ6 equipped with a digital camera (Heidelberg, Germany).

2.10. Statistical Analysis. All values were presented as the mean ± standard deviation (SD) from at least 3 independent experiments ($n = 3$). The differences among groups were

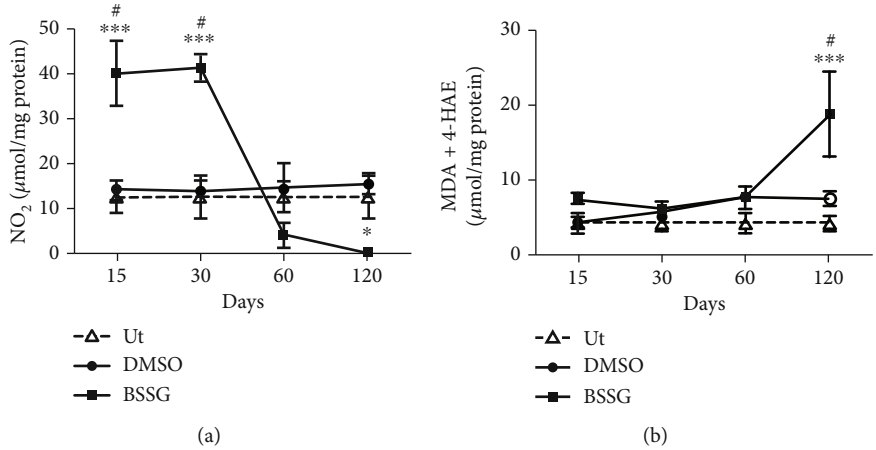

FIGURE 1: Nitrosative and lipid peroxidation after a BSSG injection in the SNpc. (a) Nitrosative stress was evaluated through the measurement of nitrite levels. (b) Lipid peroxidation was assessed as a proxy for oxidative stress by MDA and 4-HAE determinations. Ut: untreated control rats; Mock: rats injected with vehicle (DMSO); BSSG: rats injected with 6 μg of BSSG. The values represent the mean ± SD from 4 rats for each time point and each experimental condition. Two-way ANOVA and Bonferroni post hoc tests were applied. (***) indicates a $P < 0.001$ for statistical difference between the BSSG group compared with the Ut group or (#) for the respective mock group.

analyzed using repeated-measures two-way ANOVA and Bonferroni *post hoc* test. One-way ANOVA and Newman-Keuls *post hoc* test were used to analyze Iba1 data. The statistical analysis was made with Sigma Plot 12.0, and the graphs were built with GraphPad Prism 5.0 (GraphPad Software Inc; La Jolla, CA, USA). Statistical significance was considered at $P < 0.05$.

3. Results

3.1. Nitrosative and Oxidative Stress. Nitrite concentration was assessed as a marker of nitrosative stress ($n = 4$ rats for each time point), while MDA and 4-HAE levels were assessed as a lipid peroxidation marker of oxidative stress ($n = 4$). Importantly, these biomarkers remained constant in the Ut and mock control groups. BSSG administration in the SNpc provoked a 4-fold increase in NO levels on days 15 and 30 postadministration as compared with the untreated and mock groups (Figure 1(a)). Afterward, NO levels decreased and remained below the untreated and mock groups until the end of the study (Figure 1(a)).

A significant 1.5-fold increase in NO levels was observed after DMSO administration only at day 120 as compared with the untreated control group (Figure 1(a)). In contrast, lipid peroxidation was not different except at day 120 after BSSG injection as compared with the untreated and mock groups (Figure 1(b)).

3.2. Time Course of Microglia Activation. The double immunofluorescence assays showed that TH and OX42 immunoreactivities in the SNpc of the mock group were not statistically different from the respective untreated controls throughout the study (Figure 2 and Supplementary Figure 2). BSSG administration caused a progressive decrease of TH immunoreactivity in the SNpc, reaching an 83.6 ± 1.8% reduction on day 120 after the administration (Figures 2(a) and 2(b)). Conversely, OX42 immunoreactivity gradually increased up to 899.0 ± 80.20% over the control values on day 30 to decrease afterward and remain 251.2 ± 48.8% higher than the basal values at the end of the study (Figures 2(a) and 2(c)). Iba1 immunohistochemistry assays displayed the normal population and characteristics of microglia in the *substantia nigra* of the untreated healthy group (Supplementary Figure 3). A similar pattern in the population and morphology of Iba1(+) cells was observed in the DMSO group, confirming that this BSSG solvent did not activate microglia (Supplementary Figure 3 and Supplementary Figure 4). The opposite effect occurred in the BSSG group, where the increase in the Iba1(+) cell number over time was similar to that of OX42(+) cells (Figure 3 and Supplementary Figures 3 and 4), giving further support to microglial activation development.

Recent studies propose that changes in cell form reflect the activation state and function of microglia in acute lipopolysaccharide- (LPS-) induced neuroinflammation in the SNpc, as recently shown by Flores-Martinez et al. [44, 48]. Interestingly, BSSG-induced changes in the form of OX42-immunoreactive cells and Iba1(+) cells are similar to those induced by LPS, but they appear throughout the 120 days evaluated (Figure 3) than in the LPS model, where these changes in microglial shape occur only for 7 days [44]. OX42 and Iba1 immunoreactivity in untreated and mock conditions suggest the resting or quiescent condition of microglia (Figure 3). Robust branched cells, with long thick branches, and well-defined enlarged soma appeared on day 15 post-BSSG treatment (Figure 3). Irregular shaped OX42(+) and Iba1(+) cells with short, stout branches, and a larger soma and nucleus were seen on day 30. Round-shaped cells with scarce processes and enlarged body also referred to as the reactive-state or amoeboid form could be observed on day 60. Finally, OX42(+) and Iba1(+) small ovoid cells surrounded by 3 to 4 short and irregular nuclei appeared on day 120 post-BSSG administration suggesting cells in apoptosis (Figure 3). These changes suggest different activity states of microglia during chronic inflammation.

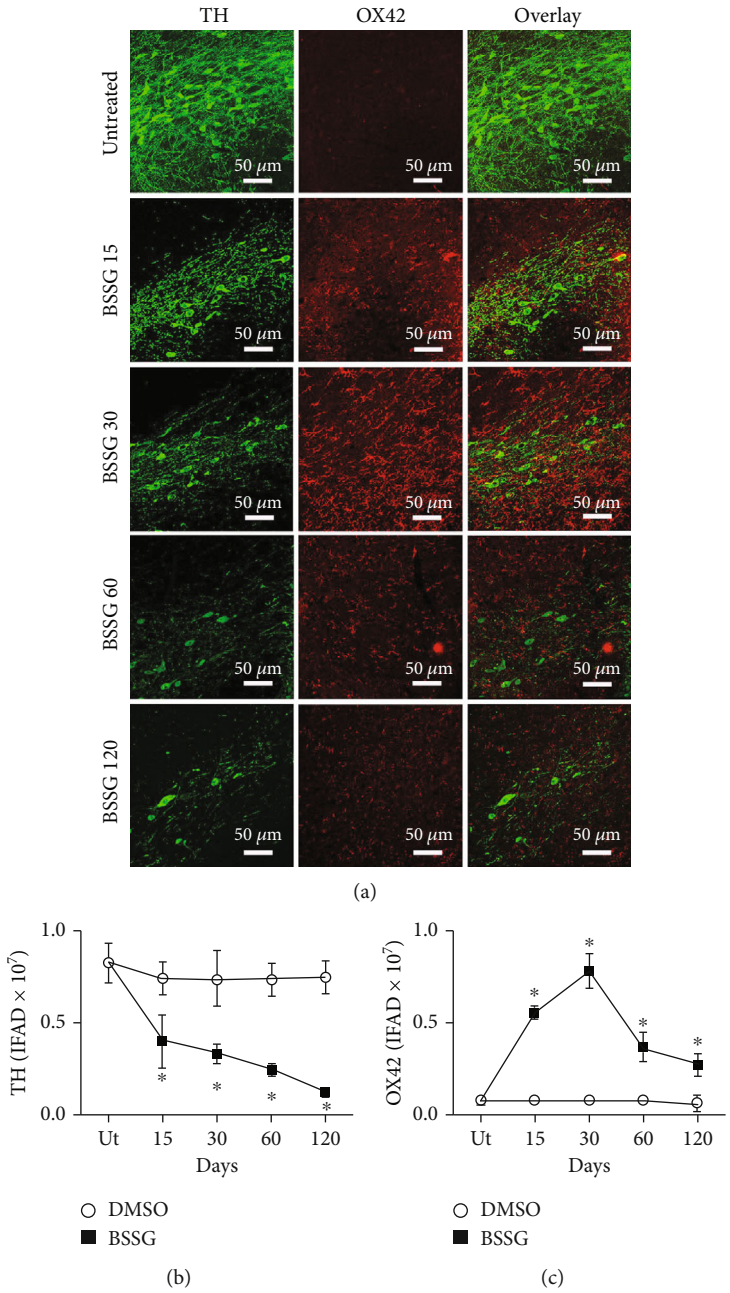

Figure 2: Time course of OX42 immunoreactivity after a BSSG injection in the SNpc. (a) Representative micrographs of the double immunofluorescence for TH and OX42 in untreated rats (Ut) and rats at different times (shown at the left side of micrographs) after BSSG injection. Immunofluorescence area density (IFAD) for TH (b) and OX42 (c) was determined using the ImageJ software v.1.46r (National Institutes of Health, Bethesda, MD). The TH and OX42 values for the mock rats correspond to the quantification in Supplementary Figure 2. The values are the mean ± SD from four anatomical levels. $n = 3$ independent rats in each time of each experimental condition. Two-way ANOVA and post hoc Bonferroni tests were applied for statistical analysis. (*) indicates a $P < 0.05$ compared with the DMSO mock and Ut groups of the respective immunostaining.

3.3. Time Course of Reactive Astrocyte Induction. The astrocytic response and its association with dopaminergic neurodegeneration were assessed with GFAP intermediate filament [49] and S100β calcium-binding protein [12] immunoreactivity following BSSG administration. GFAP (Figure 4) and S100β (Figure 5) immunoreactivity increased in response to BSSG following the time course of microglial activation. The two astroglial markers were observed together with TH (+) neurons, which declined in number as expected (Figures 4 and 5). The astroglial markers were also assessed in parallel showing substantial colocalization, best observed during the time points of maximal microglial activation, on days 15 and 30 (Figure 6).

3.4. Presence of Neurotoxic A1 Reactive Astrocytes. To identify the presence of neurotoxic A1 reactive astrocytes,

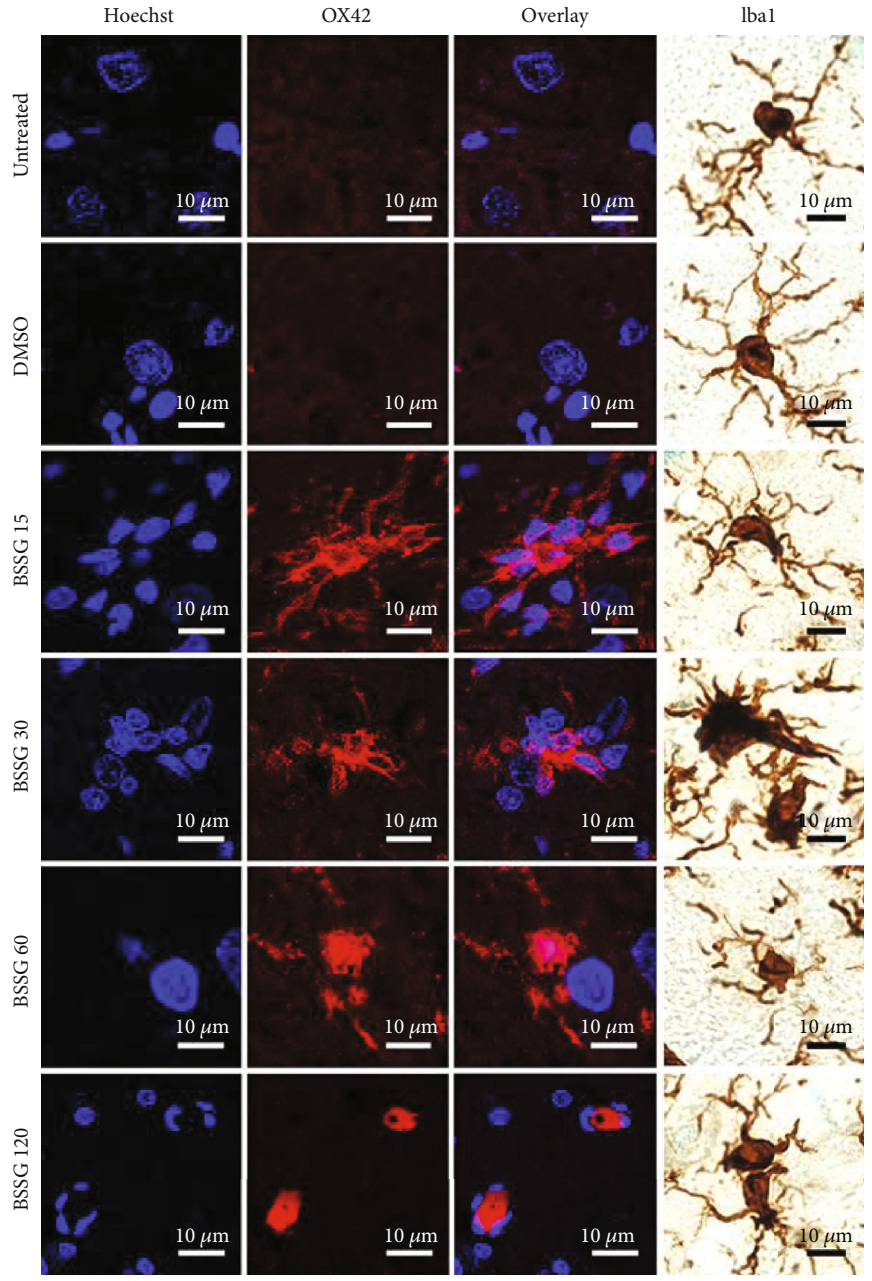

Figure 3: Changes in the cell form during activation of microglia in the SNpc after BSSG administration. Representative confocal micrographs of OX42(+) and Iba1(+) cells in the SNpc of untreated and DMSO mock control rats and of rats at different days post-BSSG injection (shown at the left side of the micrographs).

the specific marker C3, characteristic for these astrocytes [10], was monitored together with GFAP or S100β in double immunofluorescence assays. C3-immunoreactive cells were absent in the SNpc of untreated and mock groups (Figures 7 and 8). In contrast, a significant number of C3(+) cells appeared on day 15 after BSSG administration, and the cell amount significantly augmented on day 30 to decrease afterward. The pattern of appearance over time for GFAP(+) cells (Figures 7(a) and 7(c)) and S100β(+) cells (Figure 8) was consistent with reactive astrocytic induction on days 15 and 30 post-BSSG administration. C3(+) cells colocalized with GFAP(+) cells and S100β(+) cells on day 30 after BSSG administration, suggesting the presence of A1 cytotoxic astrocytes. Closer views of the colocalization between the three markers showed significant overlap but also an independent expression of these proteins in some cells (Figures 7(d) and 8(b)).

3.5. Leukocyte Infiltration. In neuroinflammation, activated microglia release proinflammatory cytokines, which promote the BBB opening, allowing leukocytes to pass from circulation to the brain parenchyma. Accordingly, CD45 immunoreactive leukocytes [50], which are absent in the

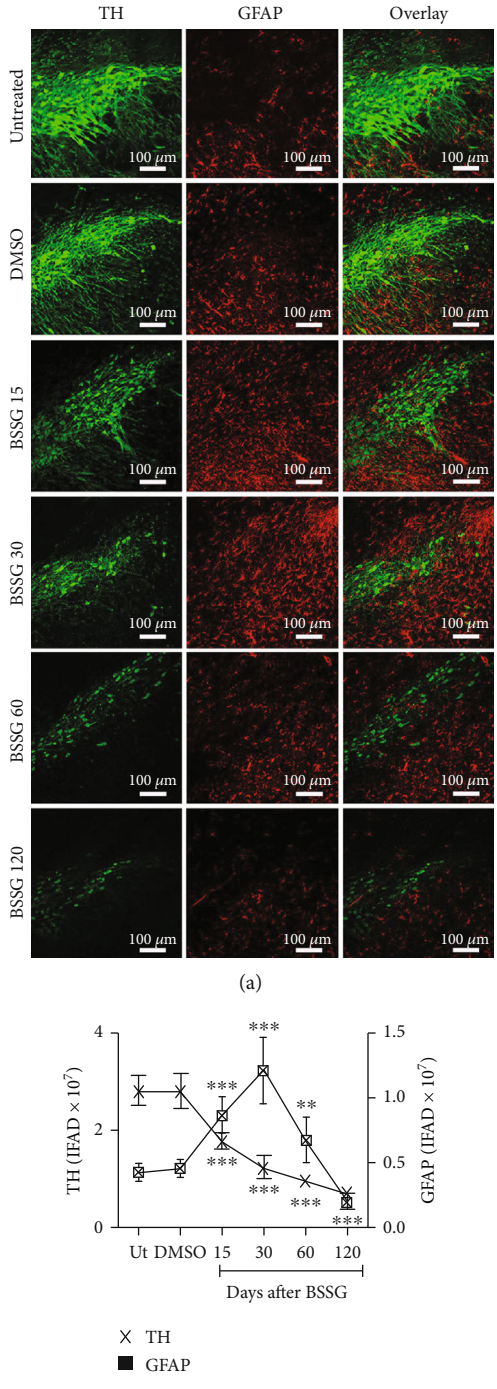

(a)

(b)

Figure 4: Time course of the astrocytic reactivity marker GFAP after a BSSG injection in the SNpc. (a) Representative micrographs of double immunofluorescence of TH and GFAP in untreated (Ut) control rats and rats at different times (shown at the left side of micrographs) after BSSG injection. (b) IFAD quantification for TH and GFAP during the experimental time course. The values are the mean ± SD from four anatomical levels. $n = 3$ independent rats in each time of each experimental condition. Two-way ANOVA and post hoc Bonferroni tests were applied for statistical analysis. The levels of significance were (*) $P < 0.05$, (**) $P < 0.01$, and (***) $P < 0.001$ compared with the DMSO mock and Ut groups of the respective immunostaining.

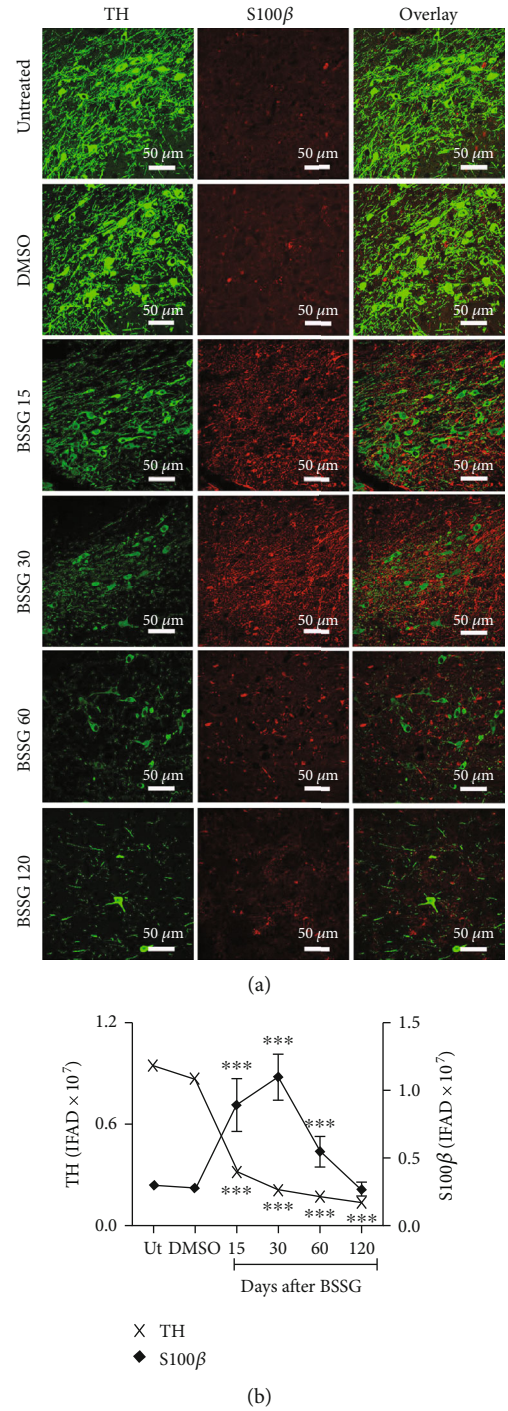

(a)

(b)

Figure 5: Time course of the reactive astrocyte induction marker S100β after a BSSG injection in the SNpc. (a) Representative micrographs of double immunofluorescence of TH and S100β in untreated (Ut) control rats and rats at different times (shown at the left side of micrographs) after BSSG injection. (b) IFAD quantification for TH and S100β during the experimental time course. The values are the mean ± SD from four anatomical levels. $n = 3$ independent rats in each time of each experimental condition. Two-way ANOVA and post hoc Bonferroni tests were applied for statistical analysis. (***) indicates a $P < 0.001$ compared with the DMSO mock and Ut groups of the respective immunostaining.

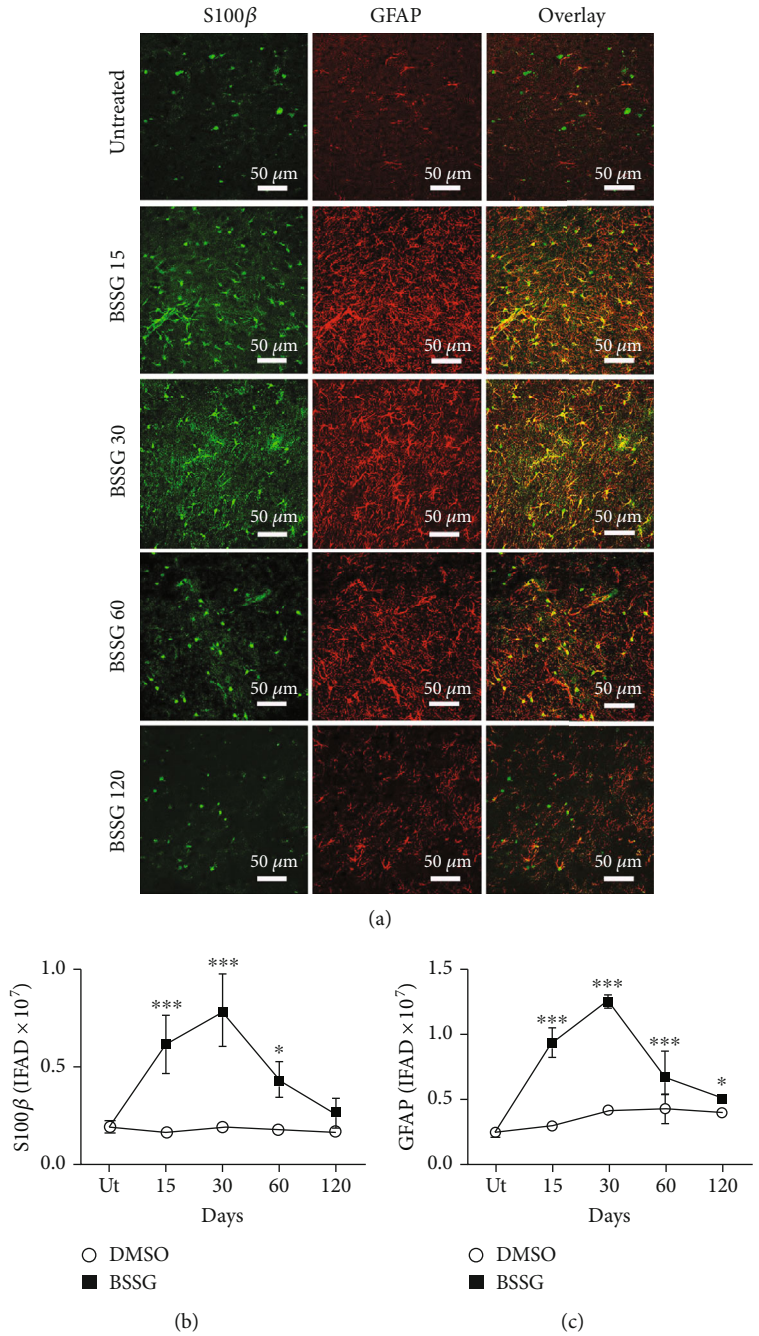

Figure 6: Colocalization of S100β and GFAP immunoreactivity after a BSSG injection in the SNpc. (a) Representative micrographs of the double immunofluorescence in untreated (Ut) control rats and rats at different times (shown at the left side of micrographs) after BSSG injection. IFAD quantification for S100β (b) and GFAP (c) during the experimental time course. The S100β and GFAP values for the mock rats correspond to the quantification in Supplementary Figure 5. The values are the mean ± SD from four anatomical levels. $n = 3$ independent rats in each time of each experimental condition. Two-way ANOVA and post hoc Bonferroni tests were applied for statistical analysis. The levels of significance were (***) $P < 0.001$ and (*) $P < 0.05$ compared with the DMSO mock and Ut groups of the respective immunostaining.

SNpc of untreated and DMSO mock groups (Figures 9(a) and 9(c)), appeared on day 15 after BSSG administration and then followed the time course of microglial activation. Once again, the TH (+) cells followed the pattern described in the previous assays (Figures 9(a) and 9(b)). The presence of Evans blue dye in the SNpc confirmed the loss of BBB integrity on days 7 and 15 following BSSG administration (Figure 9(d)). These results suggest that the BSSG treatment resulted in the infiltration of leukocytes across a leaky BBB, as a consequence of neuroinflammation.

3.6. Proinflammatory Cytokines. TNF-α, IL-1β, and IL-6 were evaluated in the *substantia nigra* through ELISA (Figure 10). The basal levels expressed in pg/mg of protein

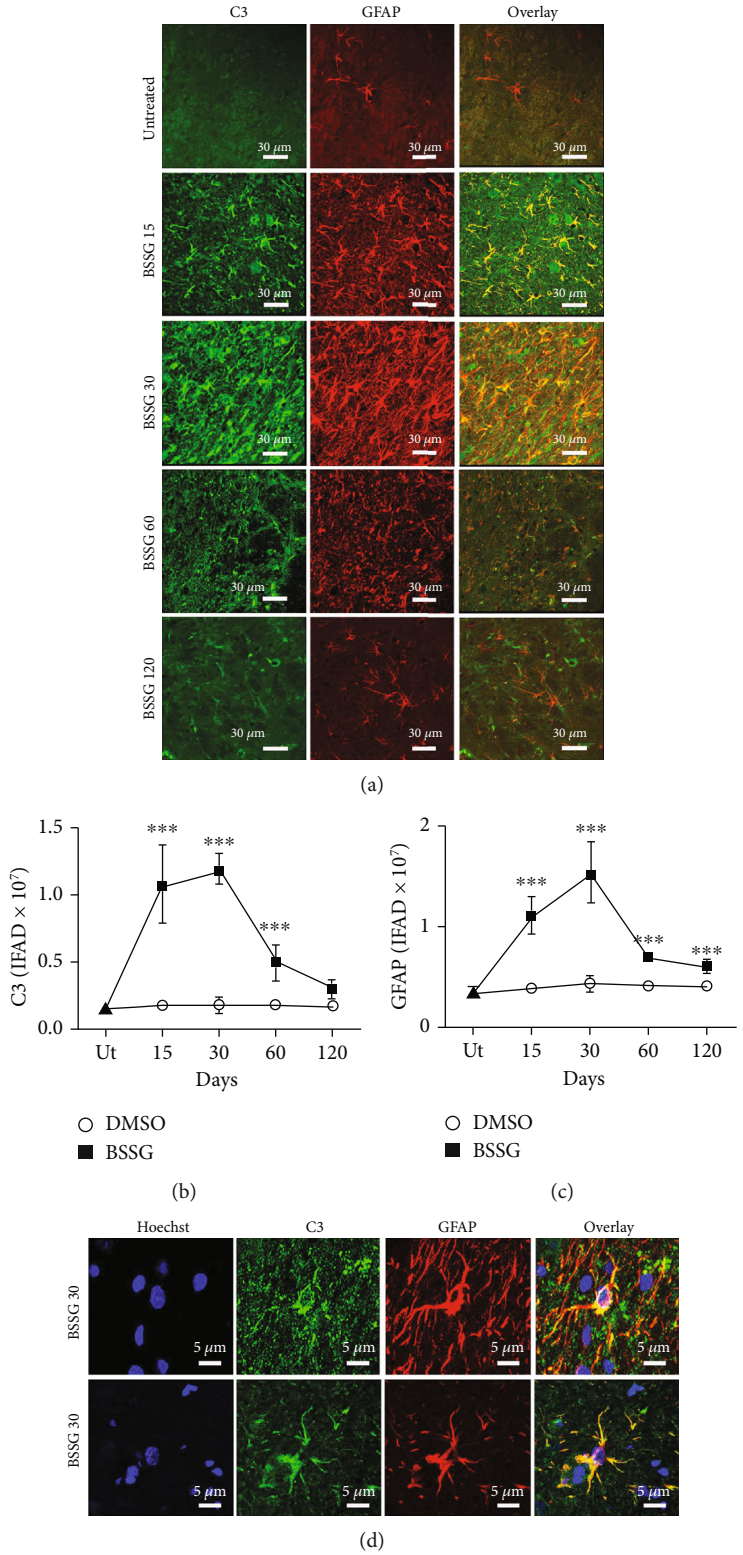

Figure 7: Colocalization of C3 and GFAP immunoreactivities after a BSSG injection in the SNpc. (a) Representative micrographs of the double in untreated (Ut) control rats and rats at different times (shown at the left side of micrographs) after BSSG injection. Immunofluorescence area density (IFAD) for C3 (b) and GFAP (c) was determined using the ImageJ software v.1.46r (National Institutes of Health, Bethesda, MD). The C3 and GFAP values for the mock rats correspond to the quantification in Supplementary Figure 6. (d) Details of cells coexpressing C3 and GFAP on day 30 after a BSSG injection in the SNpc. The values are the mean ± SD from four anatomical levels. $n = 3$ independent rats in each time of each experimental condition. Two-way ANOVA and post hoc Bonferroni tests were applied for statistical analysis. (***) indicates a $P < 0.001$ compared with the DMSO mock and Ut groups of the respective immunostaining.

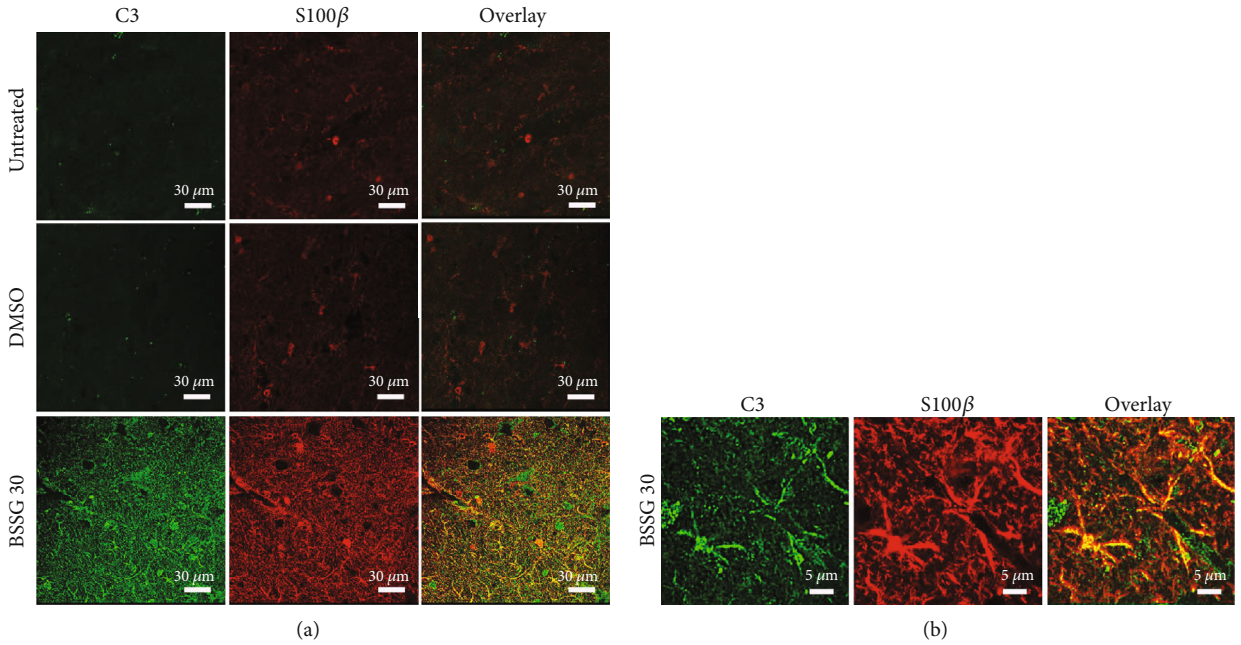

FIGURE 8: Cellular colocalization of C3 and S100β immunoreactivity on day 30 after a BSSG injection in the SNpc. (a) Representative micrographs of double immunofluorescence of C3 and S100β in untreated (Ut) control rats and rats injected with DMSO or BSSG. (b) Details of cells coexpressing C3 and S100β on day 30 after a BSSG injection in the SNpc.

were 41.5 ± 12.8 for TNF-α, 127.4 ± 31.7 for IL-1β, and 1619.9 ± 761.6 for IL-6.The DMSO vehicle injection did not significantly change the basal levels for the three proinflammatory cytokines (Figure 10). In contrast, the levels of those proinflammatory cytokines were significantly and differentially increased by the BSSG administration as compared with the Ut and DMSO groups. All proinflammatory cytokine levels were markedly higher from day 15 to day 30, corresponding to the period of BBB opening. TNF-α levels remained high throughout the time points included in this study, whereas IL-1β was induced until day 60, and IL-6 was not detected beyond day 30 (Figure 10). These results are consistent with the conclusion that BSSG injection caused chronic neuroinflammation.

4. Discussion

This report provides evidence that A1 neurotoxic reactive astrocytes contribute to chronic neuroinflammation elicited by a single intranigral administration of BSSG. Activated microglia may be involved in the induction of A1 astrocytes from GFAP(+) and S100β(+) cell populations through the release of proinflammatory cytokines [10, 18], which also could be released by infiltrating immune cells, neurons, and possibly by BBB-endothelial cells known to express IL-1β and IL-6 genes [40, 41]. *In vitro*, conditioned medium from LPS-activated microglia induces A1 reactive astrocytes, which rapidly kill neurons by secreting unidentified neurotoxins [10]. Based on this evidence, we propose that A1 reactive astrocytes could also participate in the death of dopaminergic neurons in the BSSG-treated animals, as shown here and also in the oral administration model [34]. This suggestion is further supported by the identification of A1 astrocytes in postmortem samples of PD brains [10].

Reactive oxygen and nitrogen species (RONS) are notable contributors to neuronal death in neuroinflammation through the irreversible oxidative or nitrosative injury to biomolecules [44, 51]. Here, we found that BSSG induced a fast NO production that remained increased during the first month after its intranigral administration. This fast increase in NO production might be due to the contribution of neuronal nitric oxide synthase (nNOS) in dopaminergic neurons that is stimulated by NMDA receptor-mediated excitotoxicity [52, 53]. This pathological process seems to mediate the BSSG-triggered dopaminergic loss [32] because these neurons express NMDA receptors [54, 55] and are sensitive to glutamate [56]. The increase in glutamate can be caused by pathological α-synuclein aggregates [57] known to occur in the acute [38] and chronic [35] BSSG administration. The sustained NO production that coincided with the periods of microglia activation, reactive astrocyte induction, and leukocyte infiltration can be due to the iNOS expression in those inflammatory cells [58, 59]. Nitrosative/oxidative stress affects particularly dopaminergic neurons because they lack an efficient antioxidant defense showing low levels of glutathione and moderate catalase, superoxide dismutase, and glutathione peroxidase activities [60, 61]. Besides, the SNpc is a nucleus with a high microglial population, which can detect a minimum imbalance of oxidative stress and mount a fast response [62, 63] that is potentiated by the infiltrating immune cells. We also found that BSSG-induced nitrosative stress coincided with the periods of reactive astrocyte induction and reduction of dopaminergic neuron viability. Since S100β can stimulate NO production [12, 13], then S100β released by reactive astrocytes after BSSG intranigral

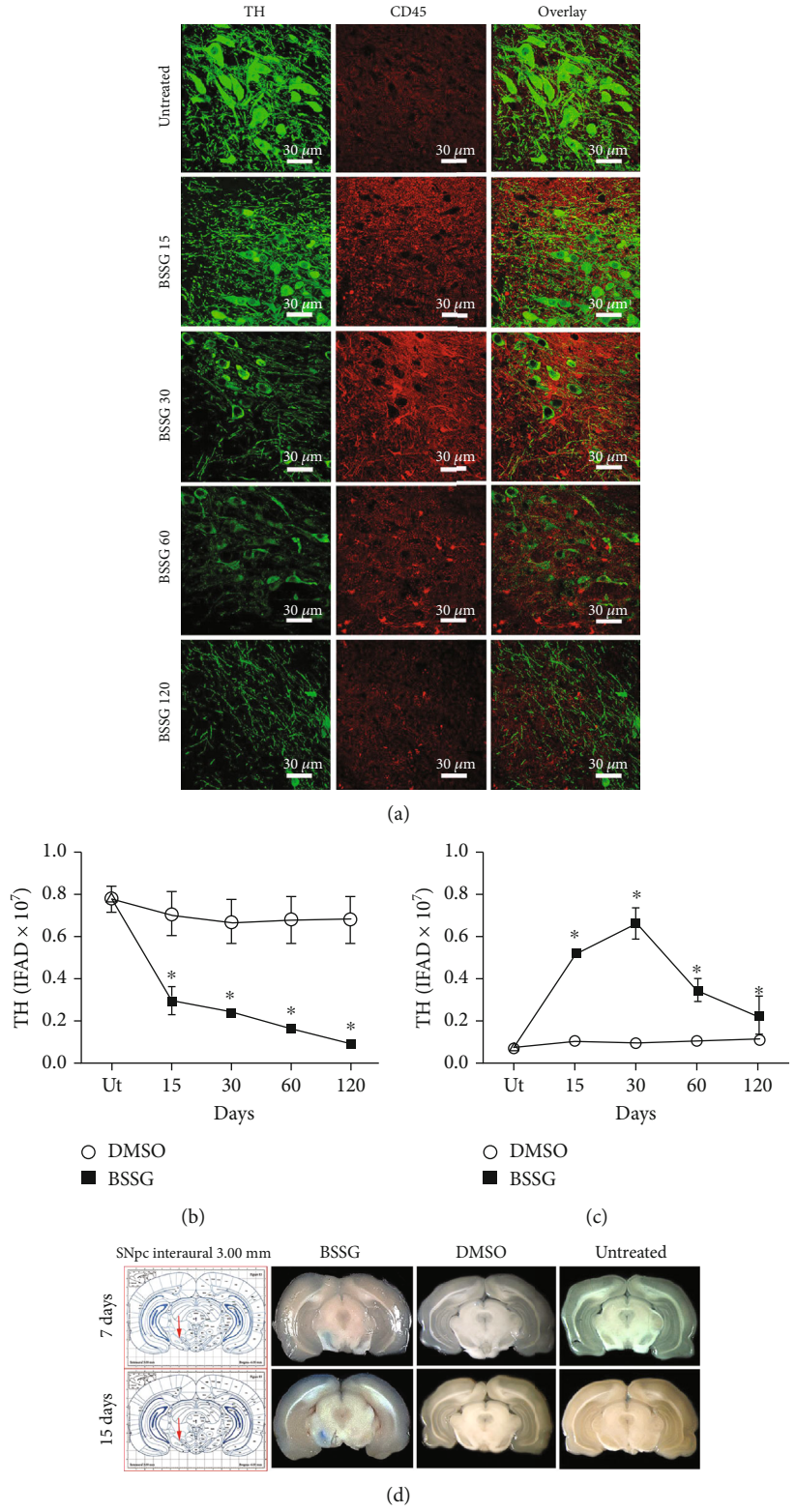

Figure 9: Time course of leukocyte infiltration after a BSSG injection in the SNpc. (a) Representative micrographs of double immunofluorescence of TH and CD45 in untreated (Ut) control rats and rats at different times (shown at the left side of micrographs) after BSSG injection. IFAD quantification for TH and CD45 during the experimental time course. The (b) TH and (c) CD45 values for the mock rats correspond to the quantification in Supplementary Figure 7. The values are the mean ± SD from four anatomical levels. $n = 3$ independent rats in each time of each experimental condition. Two-way ANOVA and post hoc Bonferroni tests were applied for statistical analysis. (*) indicates a $P < 0.05$ compared with the DMSO mock and Ut groups of the respective immunostaining. (d) Representative photographs of brain slices after intravenous injection of the Evans blue dye on the days shown at the left of each row.

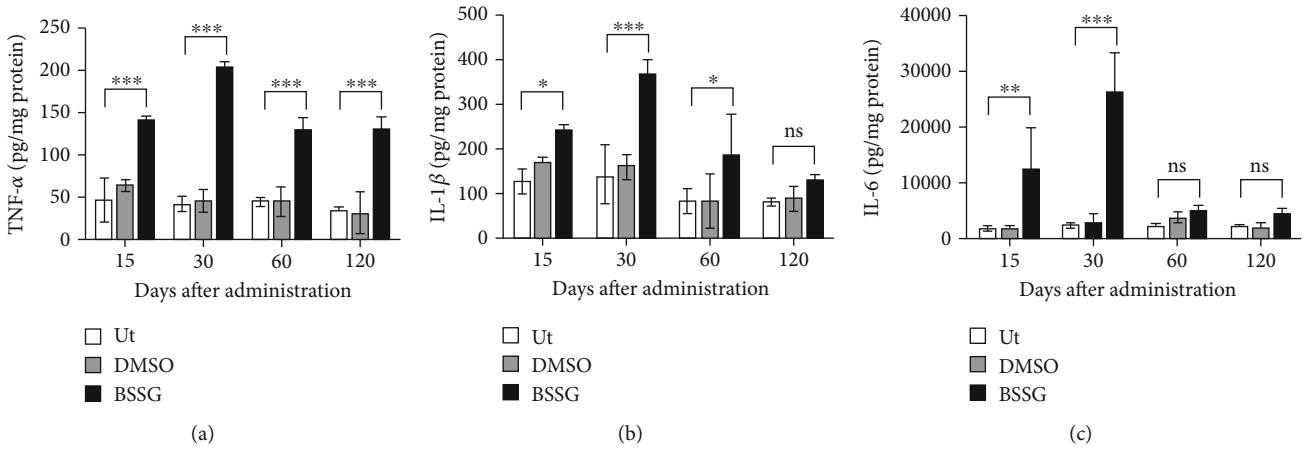

Figure 10: Levels of proinflammatory cytokines in the *substantia nigra* after BSSG intranigral injection. ELISA was used to measure protein levels of (a) TNF-α, (b) IL-1β, and (c) IL-6. All values represent the mean ± SD ($n = 3$ rats per time point per experimental condition). Two-way ANOVA and Bonferroni post hoc test were applied for statistical analysis. The levels of significance were $^{*}P < 0.05$, $^{**}P < 0.01$, and $^{***}P < 0.001$. ns: not significant.

administration may also contribute to nitrosative stress and consequently, to the death of dopaminergic neurons. Since S100β(+) cells colocalize with C3(+) cells, NO could be one of the unknown neurotoxins that mediate the harmful effect of A1 reactive astrocytes on dopaminergic neurons [14]. Interestingly, oxidative stress did not occur until day 120 after the BSSG administration, when the maximum decrease in dopaminergic neuron population was attained. This result suggests that apoptosis of dopaminergic neurons occurs during the NO production period and that other cells undergo lipid peroxidation in the late phase of neuroinflammation.

Microglia are parenchymal CNS macrophages that perform a surveillance function, scanning the entire brain tissue in the resting state [64]. Upon detecting a hazardous stimulus, they become rapidly activated, changing shape and acquiring immunological functions [44, 65]. In the BSSG injection model, microglia activation evidenced through OX42 and Iba1 markers and cell morphology [44, 48] developed progressively up to day 30 after the injection. In contrast, shape changes appeared for more prolonged times as compared with laser stimulation (up to 5.5 hours) [64], traumatic brain injury [66], neurotoxic lesions (24 hours after injury) [43], and LPS stimulation (up to 168 hours) [44] models. The relatively long duration of the response observed suggests that microglia was not activated by the direct hazardous stimulus of BSSG but by downstream effects. A possible activation stimulus could be the pathological α-synuclein aggregates that appear as a delayed outcome of stereotaxic [37] and oral [34] BSSG administration models. Accumulating evidence supports the notion that α-synuclein aggregates activate microglial cells by different mechanisms, including nitrosative/oxidative stress [19–22] and immune cell infiltration [23, 24, 44]. Here, these two events were associated with cell morphology and the increased OX42 and Iba1 markers over time, suggesting their participation in the development of microglia activation. This putative activation was also associated with the time course of proinflammatory cytokines (TNF-α, IL-1β, and IL-6), which were present throughout the study (120 days). Such interrelationship supports the microglia source of those cytokines, although they could also come from the infiltrating immune cells that showed a similar time course. Together, these findings show that the BSSG-induced neuroinflammation is chronic, similar to the one occurring in Parkinson's disease but in contrast to the acute response induced by LPS [44], traumatic brain injury [66], or transient ischemia [67]. In the acute neuroinflammation by LPS, TNF-α and IL-1β reached maximum levels at 5 h after the lesion and at 8 h for IL-6 [44]. The balance between pro- and anti-inflammatory cytokinesis is crucial for controlling the neuroinflammatory response, as recently shown in the acute LPS-induced neuroinflammation in the *substantia nigra* [44]. However, this issue was not explored in SNpc injected because the profound dopaminergic neurodegeneration suggests that the contribution of anti-inflammatory cytokines might be smaller than that of proinflammatory cytokines. Similar to A2 reactive astrocytes, it would be relevant to study the balance between pro- and anti-inflammatory cytokinesis to gain insight into the control of the immune response in those brain regions where neuroinflammation is emerging by the presence of pathological α-synuclein [37, 38].

Following traumatic brain injury, A1 neurotoxic astrocytes appeared before microglia, suggesting the existence of microglia-independent induction mechanisms *in vivo* [66]. In contrast, after BSSG injection, A1 neurotoxic astrocytes followed a similar time course with activated microglia and the increase in proinflammatory cytokine levels. These results do not identify the primary event for A1 reactive astrocyte induction because an earlier time after the BSSG administration was not explored. Nevertheless, it is possible that in chronic inflammation, a more complex interaction between astrocytes and microglia exists. For instance, A1 astrocytes induced in a microglia-independent manner might be themselves a cause of microglial activation [42, 68] and microglia migration by secreting S100β protein [69]. The colocalization of C3 and S100β immunoreactivities observed in our study would support such a notion. The

BSSG stereotaxic model can help clarify the mechanism of A1 astrocyte induction in chronic neuroinflammation. Contrary to neurotoxic A1 reactive astrocytes, A2 reactive astrocytes that are identified by the specific marker S100A10 have been postulated to be protective based on transcriptome analysis showing upregulation of many neurotrophic factors and thrombospondins, which promote synapse repair in animal models of acute injury [10, 70]. In the stereotaxic BSSG model, the severe and progressive dopaminergic neurodegeneration in the *substantia nigra* suggests that A2 reactive astrocytes do not play a significant protective role. The intranigral BSSG model is known to trigger pathological α-synuclein aggregates that spread from the neurotoxin application site to diverse brain regions, possibly producing neuroinflammation, as suggested by behavioral impairments [37, 38]. Then, it would be relevant to study the induction of A1 and A2 reactive astrocytes and determine the balance between cells with phenotype A1 and A2 in those brain regions where neuroinflammation is emerging.

A failure of BBB permeability in Parkinson's disease [25] permits the infiltration of lymphocytes [23, 24] that could generate an autoimmune response to α-synuclein aggregates [29]. In the stereotaxic model, BBB opening is of such magnitude as shown by the Evans blue assay that it enabled a great infiltration of bone marrow- (BM-) derived cells that can be detected by the antibody to CD45, which is a pan-leukocyte marker [71]. Therefore, it is plausible to assume that macrophages, lymphocytes, CD4, CD8, TReg, and NK infiltrate the *substantia nigra*. The immune response of such diverse immune cells does potentiate the response of resident defensive cells, thus contributing to the severity and irreversibility of BSSG-induced dopaminergic neurodegeneration, as shown here and by other works [34, 35, 37, 38]. Furthermore, the increased BBB permeability may also enable the invasion to the brain of microbiota metabolic products, peripheral α-synuclein aggregates, and mediators of the innate immune system resulting from gut dysbiosis and/or bacterial overgrowth, which are implicated in the brain-gut-microbiota axis in Parkinson's disease [72–74]. A contrary flow from the brain to blood circulation and peripheral organs of harmful cell decomposition products, proinflammatory cytokines, and pathological α-synuclein aggregates triggered by the BSSG-induced severe neuroinflammation might also occur [74, 75]. The BSSG stereotaxic model represents a valuable tool to clarify this hypothesis and advance the knowledge in the pathogenesis of Parkinson's disease.

In this work, DMSO was used to dissolve BSSG because pyridine used to solubilize BSSG [76] caused necrosis in the *substantia nigra* (data not shown). Although concentrated DMSO may be a methodological drawback, its single administration (1 μL) did not significantly change any variables studied as compared with the untreated healthy animals. These results agree with a recent report showing that DMSO does not trigger apoptosis or senescence in the *substantia nigra* cells, neither elicits changes in the cytoskeleton or density of dendritic spines [38] or behavioral alterations [37]. Other authors that used 100% DMSO also do not report damage or altered function *in vivo* [77–80]. In contrast, other studies have reported that DMSO is toxic in cell cultures. For instance, it affects cell proliferation and production of proinflammatory cytokines in cultures of peripheral blood lymphocytes [81] and impairs mitochondrial integrity and membrane potential in cultured astrocytes [81, 82]. However, our results with lipoperoxidation assay suggest that DMSO did not damage cell membranes at times here evaluated, neither augmented proinflammatory cytokines. A possible explanation is that the glymphatic system [83] diluted the DMSO concentration in the one μL injected, thus dampening its toxicity. On the contrary, cultured cells are directly exposed to DMSO because they lack the defensive physiological mechanisms present *in vivo*. It would be interesting to evaluate whether DMSO triggers neuroinflammation signaling in other cells, such as oligodendrocytes and ependymal cells in the stereotaxic BSSG model.

The chronic oral administration of BSSG to Sprague-Dawley rats faithfully models Parkinson's disease, reproducing the development of motor and nonmotor behavior impairments and insoluble α-synuclein appearance according to the Braak stages of PD [34]. Likewise, intranigral administration of BSSG replicates similar characteristics, such as the progression of behavioral alterations, dopaminergic neuron loss, and the presence of Lewy body-like synuclein aggregations in a shorter time [37]. The hallmark of the aggregates triggered by an acute BSSG intranigral injection is the ability to spread in a prion-like manner to anatomically interconnected and noninterconnected regions in the whole brain [38]. Furthermore, behavioral tests have shown that motor and nonmotor impairments could result from neurological damage in those diverse regions [37, 38]. These antecedents and the finding that pathological α-synuclein aggregates can induce neuroinflammation [84, 85] strongly suggest that the acute BSSG intranigral administration also leads to neuroinflammation in the whole brain. Thus, systematic or local BSSG administration models can be used to clarify the mechanisms of chronic neuroinflammation and validate the emerging therapeutic approaches for Parkinson's disease, such as anti-inflammatory gene therapy [45], anti-α-synuclein immunotherapy [86, 87], and A1 reactive astrocyte induction blocking therapy [17].

5. Conclusion

Our data show that a single intranigral BSSG injection triggers chronic neuroinflammation in the SNpc and degeneration of dopaminergic neurons. All markers of neuroinflammation, including those for neurotoxic A1 reactive astrocytes, showed similar changes over time with a maximum elevation in the first month, whereas the loss of dopaminergic neurons was progressive to reach a drastic decline on day 120 postadministration. These data suggest that neuroinflammation triggers dopaminergic neurodegeneration via neurotoxic A1 reactive astrocytes. However, infiltrating BM-derived cells in the SNpc due to BBB breakdown may also participate in the neuronal loss via an autoimmune response against α-synuclein aggregates present in the SNpc of both BSSG administration models [34, 37]. Besides, the sustained high levels of proinflammatory cytokines resulting from activated microglial cells, reactive astrocytes, infiltrating

BM-derived cells [10, 39, 65], and possibly BBB-endothelial cells [40, 41] could account for the severity of the BSSG-induced neuroinflammation in the SNpc. Further studies are needed to explore control mechanisms of neuroinflammation, such as the role of A2 reactive astrocytes and anti-inflammatory cytokines. The BSSG stereotaxic administration in the rat is an easy model of Parkinson's disease that will help to answer open questions on mechanisms of chronic neuroinflammation and neurodegeneration. Also, emerging therapies for Parkinson's disease can be validated in this rat model of chronic neuroinflammation.

Data Availability

The data that support the findings of this study are available from the corresponding author upon reasonable request.

Conflicts of Interest

The authors have no financial, personal, or other relationships with other people or organizations in the past three years of the beginning of the submitted work that could inappropriately influence, or be perceived to influence, their work. The authors declared that no competing interests exist.

Authors' Contributions

Irma A. Martínez-Dávila, Fidel De La Cruz-lópez, and Daniel Martinez-Fong contributed equally to this work.

Acknowledgments

The authors would like to thank the Unit for Production and Experimentation of Laboratory Animals (UPEAL) of the Center for Research and Advanced Studies (Cinvestav), BSc. Rafael Leyva, BSc Ricardo Gaxiola, and to Mr. René Pánfilo Morales for animal handling. YMFM, MAFP, DRC, LOSR, and CLH were recipients of doctoral fellowships from CONACYT. This work was supported by Consejo Nacional de Ciencia y Tecnología (CONACYT) (Grants #254686 (DMF) and FINNOVA 224222 (APV and CB)).

Supplementary Materials

Supplementary Figure 1: illustration of experimental design. (a) Timeline of the tests performed after the injection of BSSG or DMSO. Ut: untreated group. (b) Table with the number of animals used per assays every time point and group evaluated. Supplementary Figure 2: representative micrographs of TH and OX42 double immunofluorescence in untreated control and mock rats at different times (shown on the left side of micrographs) after DMSO injection. The immunofluorescence area (IFAD) density was measured in four anatomical levels per rat with the ImageJ software v.1.46r 40 (National Institutes of Health; Bethesda, MD). The mean ± SD values are shown in the graph of Figure 2(b) for TH and Figure 2(c) for OX42. $n = 3$ independent rats in each time of each experimental condition. Supplementary Figure 3: a single intranigral BSSG administration increases the Iba1(+) cell population over time. (a) Representative micrographs of Iba1 immunohistochemistry in the SNpc of a rat per condition (shown at the left side micrographs). (b) The graph shows the area density that was determined with the ImageJ software v.1.46r (National Institutes of Health; Bethesda, USA). The mean ± SD ($n = 3$ slices in each time of each experimental condition). One-way ANOVA and Newman-Keuls post hoc tests were applied for statistical analysis. (***) $P < 0.001$, (*) $P < 0.05$ as compared with the values of DMSO mock and untreated groups. Supplementary Figure 4: a single intranigral BSSG administration increases the Iba1(+) cell population over time. (a) Representative micrographs of Iba1 immunofluorescence in the SNpc of a rat per condition (shown at the left side micrographs). (b) The graph shows the immunofluorescence area density (IFAD) that was determined with the ImageJ software v.1.46r (National Institutes of Health; Bethesda, USA). The mean ± SD ($n = 3$ slices in each time of each experimental condition). One-way ANOVA and Newman-Keuls post hoc tests were applied for statistical analysis. (***) $P < 0.001$, (*) $P < 0.05$ as compared with the values of DMSO mock and untreated groups. Supplementary Figure 5: representative micrographs of S100β and GFAP double immunofluorescence in the SNpc of untreated control rats and mock rats at different times (shown at the left side of micrographs) after DMSO injection. The immunofluorescence area density (IFAD) was measured in four anatomical levels per rat with the ImageJ software v.1.46r 40 (National Institutes of Health; Bethesda, MD). The mean ± SD values are shown in the graph of Figure 6(b) for S100β and Figure 6(c) for GFAP. $n = 3$ independent rats in each time of each experimental condition. Supplementary Figure 6: representative micrographs of the double immunofluorescence for C3 and GFAP in the SNpc of untreated control rats and mock rats at different times (shown at the left side of micrographs) after DMSO injection. The immunofluorescence area density (IFAD) was measured in four anatomical levels per rat with the ImageJ software v.1.46r 40 (National Institutes of Health; Bethesda, MD). The mean ± SD values are shown in the graph of Figure 7(b) for C3 and Figure 7(c) for GFAP. $n = 3$ independent rats in each time of each experimental condition. Supplementary Figure 7: representative micrographs of the double immunofluorescence for TH and CD45 in untreated control rats and mock rats at different times (shown at the left side of micrographs) after DMSO injection. The immunofluorescence area density (IFAD) was measured in four anatomical levels per rat with the ImageJ software v.1.46r 40 (National Institutes of Health; Bethesda, MD). The mean ± SD values are shown in the graph of Figure 9(b) for TH and Figure 9(c) for CD45. $n = 3$ independent rats in each time of each experimental condition. Supplementary Figure 8: merged image sets below display double immunofluorescence assays in three independent rats per time point after DMSO or BSSG intranigral administration in comparison with untreated rats. Headings indicate the double immunostaining type. Left labels show the time and experimental condition. Legends indicate the main figure number where the quantification data appear. Set 1: DMSO effect on dopaminergic neurons (TH) and microglia (OX42) compared with untreated controls. Quantification data appear in the graph of Figure 2(b) for TH and

Figure 2(c) for OX42. Set 2: DMSO effect on dopaminergic neurons (TH) and astrocytes (GFAP) compared with untreated controls. Quantification data appear in the graph of Figure 4(b) for TH and Figure 4(c) for GFAP. Set 3: DMSO effect on dopaminergic neurons (TH) and astrocytes (S100β) compared with untreated controls. Quantification data appear in the graph of Figure 5(b) for TH and Figure 5(b) for S100β. Set 4: DMSO effect on astrocytes (S100β) and (GFAP) compared with untreated controls. Quantification data appear in the graph of Figure 6(b) for S100β and Figure 6(c) for GFAP. Set 5: DMSO effect on astrocytes (C3) and (GFAP) compared with untreated controls. Quantification data appear in the graph of Figure 7(b) for C3 and Figure 7(c) for GFAP. Set 6: DMSO effect on dopaminergic neurons (TH) and leukocytes (CD45) compared with untreated controls. Quantification data appear in the graph of Figure 9(b) for TH and Figure 9(c) for CD45. Set 7: BSSG effect on dopaminergic neurons (TH) and microglia (OX42) compared with untreated controls. Quantification data appear in the graph of Figure 2(b) for TH and Figure 2(c) for OX42. Set 8: BSSG effect on dopaminergic neurons (TH) and astrocytes (GFAP) compared with untreated controls. Quantification data appear in the graph of Figure 4(b) for TH and Figure 4(b) for GFAP. Set 9: BSSG effect on dopaminergic neurons (TH) and astrocytes (S100β) compared with untreated controls. Quantification data appear in the graph of Figure 5(b) for TH and Figure 5(b) for S100β. Set 10: BSSG effect on astrocytes (S100β) and (GFAP) compared with untreated controls. Quantification data appear in the graph of Figure 6(b) for S100β and Figure 6(c) for GFAP. Set 11: BSSG effect on astrocytes (C3) and (GFAP) compared with untreated controls. Quantification data appear in the graph of Figure 7(b) for C3 and Figure 7(c) for GFAP. Set 12: BSSG effect on dopaminergic neurons (TH) and leukocytes (CD45) compared with untreated controls. Quantification data appear in the graph of Figure 9(b) for TH and Figure 9(c) for CD45. *(Supplementary Materials)*

References

[1] Y. Lee, S. Lee, S. C. Chang, and J. Lee, "Significant roles of neuroinflammation in Parkinson's disease: therapeutic targets for PD prevention," *Archives of Pharmacal Research*, vol. 42, no. 5, pp. 416–425, 2019.

[2] B. L. Marino, L. R. Souza, K. P. Sousa et al., "Parkinson's disease: a review from the pathophysiology to diagnosis, new perspectives for pharmacological treatment," *Mini-Reviews in Medicinal Chemistry*, vol. 3, 2019.

[3] S. F. Yanuck, "Microglial phagocytosis of neurons: diminishing neuronal loss in traumatic, infectious, inflammatory, and autoimmune CNS disorders," *Frontiers in Psychiatry*, vol. 10, no. 712, 2019.

[4] D. Rathnayake, T. Chang, and P. Udagama, "Selected serum cytokines and nitric oxide as potential multi-marker biosignature panels for Parkinson disease of varying durations: a case-control study," *BMC neurology*, vol. 19, no. 1, 2019.

[5] K. N. Prasad, "Oxidative stress, pro-inflammatory cytokines, and antioxidants regulate expression levels of microRNAs in Parkinson's disease," *Current Aging Science*, vol. 10, no. 3, pp. 177–184, 2017.

[6] T. Nagatsu and M. Sawada, "Biochemistry of postmortem brains in Parkinson's disease: historical overview and future prospects," in *Neuropsychiatric Disorders An Integrative Approach*, pp. 113–120, Springer, Vienna, 2007.

[7] T. Nagatsu and M. Sawada, "Inflammatory process in Parkinson's disease: role for cytokines," *Current Pharmaceutical Design*, vol. 11, no. 8, pp. 999–1016, 2005.

[8] M. S. Moehle and A. B. West, "M1 and M2 immune activation in Parkinson's disease: foe and ally?," *Neuroscience*, vol. 302, no. 59-73, 2015.

[9] M. C. T. Dos Santos, D. Scheller, C. Schulte et al., "Evaluation of cerebrospinal fluid proteins as potential biomarkers for early stage Parkinson's disease diagnosis," *PLoS One*, vol. 13, no. 11, article e0206536, 2018.

[10] S. A. Liddelow, K. A. Guttenplan, L. E. Clarke et al., "Neurotoxic reactive astrocytes are induced by activated microglia," *Nature*, vol. 541, no. 7638, pp. 481–487, 2017.

[11] K. Sathe, W. Maetzler, J. D. Lang et al., "S100B is increased in Parkinson's disease and ablation protects against MPTP-induced toxicity through the RAGE and TNF-α pathway," *Brain*, vol. 135, no. 11, pp. 3336–3347, 2012.

[12] G. Esposito, D. de Filippis, C. Cirillo, G. Sarnelli, R. Cuomo, and T. Iuvone, "The astroglial-derived S100beta protein stimulates the expression of nitric oxide synthase in rodent macrophages through p38 MAP kinase activation," *Life Sciences*, vol. 78, no. 23, pp. 2707–2715, 2006.

[13] M. Bajor, M. Zaręba-Kozioł, L. Zhukova, K. Goryca, J. Poznański, and A. Wysłouch-Cieszyńska, "An interplay of S-nitrosylation and metal ion binding for astrocytic S100B protein," *PLoS One*, vol. 11, no. 5, article e0154822, 2016.

[14] J. D. Guo, X. Zhao, Y. Li, G. R. Li, and X. L. Liu, "Damage to dopaminergic neurons by oxidative stress in Parkinson's disease (review)," *International Journal of Molecular Medicine*, vol. 41, no. 4, pp. 1817–1825, 2018.

[15] J. Qiao, L. Ma, J. Roth, Y. Li, and Y. Liu, "Kinetic basis for the activation of human cyclooxygenase-2 rather than cyclooxygenase-1 by nitric oxide," *Organic & Biomolecular Chemistry*, vol. 16, no. 5, pp. 765–770, 2018.

[16] S. F. Kim, D. A. Huri, and S. H. Snyder, "Inducible nitric oxide synthase binds, S-nitrosylates, and activates cyclooxygenase-2," *Science*, vol. 310, no. 5756, pp. 1966–1970, 2005.

[17] S. P. Yun, T. I. Kam, N. Panicker et al., "Block of A1 astrocyte conversion by microglia is neuroprotective in models of Parkinson's disease," *Nature Medicine*, vol. 24, no. 7, pp. 931–938, 2018.

[18] J. T. Hinkle, V. L. Dawson, and T. M. Dawson, "The A1 astrocyte paradigm: new avenues for pharmacological intervention in neurodegeneration," *Movement Disorders*, vol. 34, no. 7, pp. 959–969, 2019.

[19] S. Wang, C. H. Chu, M. Guo et al., "Identification of a specific alpha-synuclein peptide (alpha-Syn 29-40) capable of eliciting microglial superoxide production to damage dopaminergic neurons," *Journal of neuroinflammation*, vol. 13, no. 1, p. 158, 2016.

[20] W. Zhang, T. Wang, Z. Pei et al., "Aggregated alpha-synuclein activates microglia: a process leading to disease progression in Parkinson's disease," *The FASEB Journal*, vol. 19, no. 6, pp. 533–542, 2005.

[21] C. Hoenen, A. Gustin, C. Birck et al., "Alpha-synuclein proteins promote pro-inflammatory cascades in microglia:

stronger effects of the A53T Mutant," *PLoS One*, vol. 11, no. 9, article e0162717, 2016.

[22] H. M. Gao, P. T. Kotzbauer, K. Uryu, S. Leight, J. Q. Trojanowski, and V. M. Y. Lee, "Neuroinflammation and oxidation/nitration of alpha-synuclein linked to dopaminergic neurodegeneration," *The Journal of Neuroscience*, vol. 28, no. 30, pp. 7687–7698, 2008.

[23] G. P. Williams, A. M. Schonhoff, A. Jurkuvenaite, A. D. Thome, D. G. Standaert, and A. S. Harms, "Targeting of the class II transactivator attenuates inflammation and neurodegeneration in an alpha-synuclein model of Parkinson's disease," *Journal of neuroinflammation*, vol. 15, no. 1, p. 244, 2018.

[24] A. S. Harms, V. Delic, A. D. Thome et al., "α-Synuclein fibrils recruit peripheral immune cells in the rat brain prior to neurodegeneration," *Acta neuropathologica communications*, vol. 5, no. 1, p. 85, 2017.

[25] M. T. Gray and J. M. Woulfe, "Striatal blood-brain barrier permeability in Parkinson's disease," *Journal of Cerebral Blood Flow and Metabolism*, vol. 35, no. 5, pp. 747–750, 2015.

[26] D. Sulzer, R. N. Alcalay, F. Garretti et al., "T cells from patients with Parkinson's disease recognize α-synuclein peptides," *Nature*, vol. 546, no. 7660, pp. 656–661, 2017.

[27] A. Roy, S. Mondal, J. H. Kordower, and K. Pahan, "Attenuation of microglial RANTES by NEMO-binding domain peptide inhibits the infiltration of CD8(+) T cells in the nigra of hemiparkinsonian monkey," *Neuroscience*, vol. 302, 2015.

[28] A. D. Reynolds, R. Banerjee, J. Liu, H. E. Gendelman, and R. Lee Mosley, "Neuroprotective activities of CD4+CD25+ regulatory T cells in an animal model of Parkinson's disease," *Journal of Leukocyte Biology*, vol. 82, no. 5, pp. 1083–1094, 2007.

[29] F. Garretti, D. Agalliu, C. S. Lindestam Arlehamn, A. Sette, and D. Sulzer, "Autoimmunity in Parkinson's disease: the role of alpha-synuclein-specific T cells," *Frontiers in immunology*, vol. 10, no. 303, 2019.

[30] L. T. Kurland, "Amyotrophic lateral sclerosis and Parkinson's disease complex on Guam linked to an environmental neurotoxin," *Trends in Neurosciences*, vol. 11, no. 2, pp. 51–54, 1988.

[31] P. A. Cox and O. W. Sacks, "Cycad neurotoxins, consumption of flying foxes, and ALS-PDC disease in Guam," *Neurology*, vol. 58, no. 6, pp. 956–959, 2002.

[32] J. M. Wilson, I. Khabazian, M. C. Wong et al., "Behavioral and neurological correlates of ALS-parkinsonism dementia complex in adult mice fed washed cycad flour," *Neuromolecular Medicine*, vol. 1, no. 3, pp. 207–221, 2002.

[33] W. B. Shen, K. A. McDowell, A. A. Siebert et al., "Environmental neurotoxin-induced progressive model of parkinsonism in rats," *Annals of Neurology*, vol. 68, no. 1, pp. 70–80, 2010.

[34] J. M. Van Kampen, D. C. Baranowski, H. A. Robertson, C. A. Shaw, and D. G. Kay, "The progressive BSSG rat model of Parkinson's: recapitulating multiple key features of the human disease," *PLoS One*, vol. 10, no. 10, article e0139694, 2015.

[35] J. M. Van Kampen and H. A. Robertson, "The BSSG rat model of Parkinson's disease: progressing towards a valid, predictive model of disease," *The EPMA Journal*, vol. 8, no. 3, pp. 261–271, 2017.

[36] J. M. Van Kampen, D. B. Baranowski, C. A. Shaw, and D. G. Kay, "Panax ginseng is neuroprotective in a novel progressive model of Parkinson's disease," *Experimental gerontology*, vol. 50, pp. 95–105, 2014.

[37] L. O. Soto-Rojas, L. Garces-Ramirez, C. Luna-Herrera et al., "A single intranigral administration of beta-sitosterol beta-d-glucoside elicits bilateral sensorimotor and non-motor alterations in the rat," *Behavioural Brain Research*, vol. 378, article 112279, 2019.

[38] L. O. Soto-Rojas, I. A. Martínez-Dávila, C. Luna-Herrera et al., "Unilateral intranigral administration of beta-sitosterol beta-D-glucoside triggers pathological alpha-synuclein spreading and bilateral nigrostriatal dopaminergic neurodegeneration in the rat," *Acta neuropathologica communications*, vol. 8, no. 1, 2020.

[39] H. Zhu, Z. Wang, J. Yu et al., "Role and mechanisms of cytokines in the secondary brain injury after intracerebral hemorrhage," *Progress in neurobiology*, vol. 178, article 101610, 2019.

[40] W. Y. Wang, M. S. Tan, J. T. Yu, and L. Tan, "Role of pro-inflammatory cytokines released from microglia in Alzheimer's disease," *Annals of translational medicine*, vol. 3, no. 10, 2015.

[41] V. Vukic, D. Callaghan, D. Walker et al., "Expression of inflammatory genes induced by beta-amyloid peptides in human brain endothelial cells and in Alzheimer's brain is mediated by the JNK-AP1 signaling pathway," *Neurobiology of Disease*, vol. 34, no. 1, pp. 95–106, 2009.

[42] J. Xu, H. Wang, S. J. Won, J. Basu, D. Kapfhamer, and R. A. Swanson, "Microglial activation induced by the alarmin S100B is regulated by poly(ADP-ribose) polymerase-1," *Glia*, vol. 64, no. 11, pp. 1869–1878, 2016.

[43] D. Hernandez-Baltazar, M. E. Mendoza-Garrido, and D. Martinez-Fong, "Activation of GSK-3β and caspase-3 occurs in nigral dopamine neurons during the development of apoptosis activated by a striatal injection of 6-hydroxydopamine," *PLoS One*, vol. 8, no. 8, article e70951, 2013.

[44] Y. M. Flores-Martinez, M. A. Fernandez-Parrilla, J. Ayala-Davila et al., "Acute neuroinflammatory response in the substantia nigra pars compacta of rats after a local injection of lipopolysaccharide," *Journal of Immunology Research*, vol. 2018, 19 pages, 2018.

[45] R. Nadella, M. H. Voutilainen, M. Saarma et al., "Transient transfection of human CDNF gene reduces the 6-hydroxydopamine-induced neuroinflammation in the rat substantia nigra," *Journal of Neuroinflammation*, vol. 11, 2014.

[46] M. E. Hernandez, J. D. Rembao, D. Hernandez-Baltazar et al., "Safety of the intravenous administration of neurotensin-polyplex nanoparticles in BALB/c mice," *Nanomedicine*, vol. 10, no. 4, pp. 745–754, 2014.

[47] A. Manaenko, H. Chen, J. Kammer, J. H. Zhang, and J. Tang, "Comparison Evans Blue injection routes: intravenous versus intraperitoneal, for measurement of blood-brain barrier in a mice hemorrhage model," *Journal of Neuroscience Methods*, vol. 195, no. 2, pp. 206–210, 2011.

[48] C. Kozlowski and R. M. Weimer, "An automated method to quantify microglia morphology and application to monitor activation state longitudinally in vivo," *PLoS One*, vol. 7, no. 2, article e31814, 2012.

[49] L. F. Eng, R. S. Ghirnikar, and Y. L. Lee, "Glial fibrillary acidic protein: GFAP-thirty-one years (1969-2000)," *Neurochemical Research*, vol. 25, no. 9/10, pp. 1439–1451, 2000.

[50] L. Woudstra, P. S. Biesbroek, R. W. Emmens et al., "CD45 is a more sensitive marker than CD3 to diagnose lymphocytic myocarditis in the endomyocardium," *Human Pathology*, vol. 62, pp. 83–90, 2017.

[51] S. Singh, S. Kumar, and M. Dikshit, "Involvement of the mitochondrial apoptotic pathway and nitric oxide synthase in dopaminergic neuronal death induced by 6-hydroxydopamine and lipopolysaccharide," *Redox Report*, vol. 15, no. 3, pp. 115–122, 2013.

[52] K. E. Hoque, R. P. Indorkar, S. Sammut, and A. R. West, "Impact of dopamine-glutamate interactions on striatal neuronal nitric oxide synthase activity," *Psychopharmacology*, vol. 207, no. 4, pp. 571–581, 2010.

[53] R. Kurosaki, Y. Muramatsu, M. Michimata et al., "Role of nitric oxide synthase against MPTP neurotoxicity in mice," *Neurological Research*, vol. 24, no. 7, pp. 655–662, 2013.

[54] M. G. Rosales, G. Flores, S. Hernández, D. Martínez-Fong, and J. Aceves, "Activation of subthalamic neurons produces NMDA receptor-mediated dendritic dopamine release in substantia nigra pars reticulata: a microdialysis study in the rat," *Brain Research*, vol. 645, no. 1-2, pp. 335–337, 1994.

[55] D. Martínez-Fong, M. G. Rosales, J. L. Góngora-Alfaro, S. Hernández, and G. Aceves, "NMDA receptor mediates dopamine release in the striatum of unanesthetized rats as measured by brain microdialysis," *Brain Research*, vol. 595, no. 2, pp. 309–315, 1992.

[56] F. Blandini, "An update on the potential role of excitotoxicity in the pathogenesis of Parkinson's disease," *Functional Neurology*, vol. 25, no. 2, pp. 65–71, 2010.

[57] M. dos Santos-Pereira, L. Acuña, S. Hamadat et al., "Microglial glutamate release evoked by α-synuclein aggregates is prevented by dopamine," *Glia*, vol. 66, no. 11, pp. 2353–2365, 2018.

[58] R. Cespuglio, D. Amrouni, E. F. Raymond, B. Bouteille, and A. Buguet, "Cerebral inducible nitric oxide synthase protein expression in microglia, astrocytes and neurons in Trypanosoma brucei brucei-infected rats," *PLoS One*, vol. 14, no. 4, article e0215070, 2019.

[59] W. D. Rajan, B. Wojtas, B. Gielniewski, A. Gieryng, M. Zawadzka, and B. Kaminska, "Dissecting functional phenotypes of microglia and macrophages in the rat brain after transient cerebral ischemia," *Glia*, vol. 67, no. 2, pp. 232–245, 2019.

[60] M. Smeyne and R. J. Smeyne, "Glutathione metabolism and Parkinson's disease," *Free Radical Biology and Medicine*, vol. 62, pp. 13–25, 2013.

[61] J. E. Yuste, E. Tarragon, C. M. Campuzano, and F. Ros-Bernal, "Implications of glial nitric oxide in neurodegenerative diseases," *Frontiers in cellular neuroscience*, vol. 9, 2015.

[62] L. J. Lawson, V. H. Perry, P. Dri, and S. Gordon, "Heterogeneity in the distribution and morphology of microglia in the normal adult mouse brain," *Neuroscience*, vol. 39, no. 1, pp. 151–170, 1990.

[63] W. G. Kim, R. P. Mohney, B. Wilson, G. H. Jeohn, B. Liu, and J. S. Hong, "Regional difference in susceptibility to lipopolysaccharide-induced neurotoxicity in the rat brain: role of microglia," *The Journal of Neuroscience*, vol. 20, no. 16, pp. 6309–6316, 2000.

[64] A. Nimmerjahn, F. Kirchhoff, and F. Helmchen, "Resting microglial cells are highly dynamic surveillants of brain parenchyma in vivo," *Science*, vol. 308, no. 5726, pp. 1314–1318, 2005.

[65] Q. Li and B. A. Barres, "Microglia and macrophages in brain homeostasis and disease," *Nature Reviews. Immunology*, vol. 18, no. 4, pp. 225–242, 2018.

[66] D. P. Q. Clark, V. M. Perreau, S. R. Shultz et al., "Inflammation in traumatic brain injury: roles for toxic A1 astrocytes and microglial-astrocytic crosstalk," *Neurochemical Research*, vol. 44, no. 6, pp. 1410–1424, 2019.

[67] Y. Wang, H. Jin, W. Wang, F. Wang, and H. Zhao, "Myosin1f-mediated neutrophil migration contributes to acute neuroinflammation and brain injury after stroke in mice," *Journal of neuroinflammation*, vol. 16, no. 1, 2019.

[68] P. Grotegut, S. Kuehn, W. Meißner, H. B. Dick, and S. C. Joachim, "Intravitreal S100B injection triggers a time-dependent microglia response in a pro-inflammatory manner in retina and optic nerve," *Molecular Neurobiology*, vol. 57, 2019.

[69] R. Bianchi, E. Kastrisianaki, I. Giambanco, and R. Donato, "S100B protein stimulates microglia migration via RAGE-dependent up-regulation of chemokine expression and release," *The Journal of Biological Chemistry*, vol. 286, no. 9, pp. 7214–7226, 2011.

[70] S. A. Liddelow and B. A. Barres, "Reactive astrocytes: production, function, and therapeutic potential," *Immunity*, vol. 46, no. 6, pp. 957–967, 2017.

[71] H. M. Shin, W. D. Cho, G. K. Lee et al., "Characterization of monoclonal antibodies against human leukocyte common antigen (CD45)," *Immune Network*, vol. 11, no. 2, pp. 114–122, 2011.

[72] D. Matheoud, T. Cannon, A. Voisin et al., "Intestinal infection triggers Parkinson's disease-like symptoms in Pink1(-/-) mice," *Nature*, vol. 571, no. 7766, pp. 565–569, 2019.

[73] A. Mulak and B. Bonaz, "Brain-gut-microbiota axis in Parkinson's disease," *World Journal of Gastroenterology*, vol. 21, no. 37, pp. 10609–10620, 2015.

[74] L. Leclair-Visonneau, M. Neunlist, P. Derkinderen, and T. Lebouvier, "The gut in Parkinson's disease: bottom-up, top-down, or neither?," *Neurogastroenterology & Motility*, vol. 32, no. 1, article e13777, 2020.

[75] S. M. O'Donovan, E. K. Crowley, J. R. Brown et al., "Nigral overexpression of α-synuclein in a rat Parkinson's disease model indicates alterations in the enteric nervous system and the gut microbiome," *Neurogastroenterology & Motility*, vol. 32, no. 1, article e13726, 2020.

[76] I. Khabazian, J. S. Bains, D. E. Williams et al., "Isolation of various forms of sterol beta-D-glucoside from the seed of Cycas circinalis: neurotoxicity and implications for ALS-parkinsonism dementia complex," *Journal of Neurochemistry*, vol. 82, no. 3, pp. 516–528, 2002.

[77] M. R. Karim, E. E. Liao, J. Kim et al., "alpha-Synucleinopathy associated c-Abl activation causes p53-dependent autophagy impairment," *Molecular neurodegeneration*, vol. 15, no. 1, 2020.

[78] Y. Shi, J. Yin, H. Hu et al., "Targeted regulation of sympathetic activity in paraventricular nucleus reduces inducible ventricular arrhythmias in rats after myocardial infarction," *Journal of Cardiology*, vol. 73, no. 1, pp. 81–88, 2019.

[79] P. Hayatdavoudi, H. R. Sadeghnia, N. Mohamadian-Roshan, and M. A. Hadjzadeh, "Beneficial effects of selective orexin-A receptor antagonist in 4-aminopyridine-induced seizures in male rats," *Advanced biomedical research*, vol. 6, 2017.

[80] M. W. Calik and D. W. Carley, "Intracerebroventricular injections of dronabinol, a cannabinoid receptor agonist, does not attenuate serotonin-induced apnea in Sprague-Dawley rats," *Journal of negative results in biomedicine*, vol. 15, no. 8, 2016.

[81] L. de Abreu Costa, M. Henrique Fernandes Ottoni, M. G. Dos Santos et al., "Dimethyl sulfoxide (DMSO) decreases cell proliferation and TNF-alpha, IFN-gamma, and IL-2 cytokines

production in cultures of peripheral blood lymphocytes," *Molecules*, vol. 22, no. 11, 2017.

[82] C. Yuan, J. Gao, J. Guo et al., "Dimethyl sulfoxide damages mitochondrial integrity and membrane potential in cultured astrocytes," *PLoS One*, vol. 9, no. 9, article e107447, 2014.

[83] H. Benveniste, X. Liu, S. Koundal, S. Sanggaard, H. Lee, and J. Wardlaw, "The glymphatic system and waste clearance with brain aging: a review," *Gerontology*, vol. 65, no. 2, pp. 106–119, 2019.

[84] M. F. Duffy, T. J. Collier, J. R. Patterson et al., "Lewy body-like alpha-synuclein inclusions trigger reactive microgliosis prior to nigral degeneration," *Journal of neuroinflammation*, vol. 15, no. 1, 2018.

[85] H. M. Gao, F. Zhang, H. Zhou, W. Kam, B. Wilson, and J. S. Hong, "Neuroinflammation and α-synuclein dysfunction potentiate each other, driving chronic progression of neurodegeneration in a mouse model of Parkinson's disease," *Environmental Health Perspectives*, vol. 119, no. 6, pp. 807–814, 2011.

[86] Z. Wang, G. Gao, C. Duan, and H. Yang, "Progress of immunotherapy of anti-alpha-synuclein in Parkinson's disease," *Biomedicine & Pharmacotherapy*, vol. 115, article 108843, 2019.

[87] S. M. A. Zella, J. Metzdorf, E. Ciftci et al., "Emerging immunotherapies for Parkinson disease," *Neurology and therapy*, vol. 8, no. 1, pp. 29–44, 2019.

Hindawi
Journal of Immunology Research
Volume 2020, Article ID 2180708, 10 pages
https://doi.org/10.1155/2020/2180708

Research Article

Anti-Tyro3 IgG Associates with Disease Activity and Reduces Efferocytosis of Macrophages in New-Onset Systemic Lupus Erythematosus

Zhuochao Zhou,[1] Aining Xu,[2] Jialin Teng,[1] Fan Wang,[1] Yun Tan,[2] Honglei Liu,[1] Xiaobing Cheng,[1] Yutong Su,[1] Hui Shi,[1] Qiongyi Hu,[1] Huihui Chi,[1] Jian Li,[3] Jiaqi Hou,[4] Yue Sun ,[1] Chengde Yang ,[1] and Junna Ye [1]

[1]*Department of Rheumatology and Immunology, Ruijin Hospital, Shanghai Jiao Tong University School of Medicine, Shanghai, China*
[2]*State Key Laboratory of Medical Genomics, Shanghai Institute of Hematology, Ruijin Hospital, Shanghai Jiao Tong University School of Medicine, Shanghai, China*
[3]*Clinical Research Center, Ruijin Hospital, Shanghai Jiao Tong University School of Medicine, Shanghai, China*
[4]*Department of Rheumatology and Immunology, Yueyang Hospital of Integrated Traditional Chinese and Western Medicine, Shanghai University of Traditional Chinese Medicine, Shanghai, China*

Correspondence should be addressed to Yue Sun; winniesun2015@163.com, Chengde Yang; yangchengde@sina.com, and Junna Ye; yjn0912@qq.com

Received 14 April 2020; Revised 11 September 2020; Accepted 20 October 2020; Published 11 November 2020

Academic Editor: Charles Elias Asmann

Background. Systemic lupus erythematosus (SLE) is a disease characterized by the production of a large number of autoantibodies. Defected phagocytosis of macrophage plays an important role in innate immunity in the pathogenesis of SLE. Tyro3 is a receptor responsible for the recognition of apoptotic cells during efferocytosis by macrophages. To investigate the role of Tyro3 receptor in macrophages' efferocytosis of apoptotic cells in SLE, we aimed to reveal the clinical relevance and impact of Tyro3 autoantibody on SLE. *Methods*. The serum levels of IgG-type autoantibody against Tyro3 receptor were detected in new-onset, treatment-naïve SLE patients ($n = 70$), rheumatoid arthritis (RA) ($n = 24$), primary Sjögren's Syndrome (pSS) ($n = 21$), and healthy controls (HCs) ($n = 70$) using enzyme-linked immunosorbent assay (ELISA). The effects of purified Tyro3 autoantibody from SLE patients on the efferocytosis of human monocyte-derived macrophages were measured by flow cytometry and immunofluorescence. *Results*. The serum levels of IgG-type autoantibody against Tyro3 receptor were significantly elevated in patients with SLE compared to RA, pSS, and HCs (all $p < 0.0001$). The levels of anti-Tyro3 IgG were positively associated with the SLE disease activity index (SLEDAI) score ($r = 0.254$, $p = 0.034$), erythrocyte sedimentation rate (ESR) ($r = 0.430$, $p < 0.001$), C-reactive protein (CRP) ($r = 0.246$, $p = 0.049$), and immunoglobulin G (IgG) ($r = 0.408$, $p = 0.001$) and negatively associated with haemoglobin (Hb) ($r = -0.294$, $p = 0.014$). ROC curves illustrated that the anti-Tyro3 antibody could differentiate patients with SLE from HCs. Furthermore, flow cytometry and immunofluorescence demonstrated that purified anti-Tyro3 IgG inhibited the efferocytosis of macrophages ($p = 0.004$ and 0.044, respectively) compared with unconjugated human IgG. *Conclusions*. These observations indicated that autoantibody against Tyro3 was associated with disease activity and could impair efferocytosis of macrophages. It might be a potential novel disease biomarker and might be involved in the pathogenesis of SLE.

1. Introduction

Systemic lupus erythematosus (SLE), which is characterized by the production of a large number of autoantigens and autoantibodies [1, 2], is a chronic autoimmune disease that affects almost all organs. A large number of studies have shown that functional defect of mononuclear macrophages, especially phagocytosis, plays an important role in innate

immunity in the pathogenesis of SLE [3]. Numerous lines of evidence have revealed that the overproduction of autoantibodies is attributed to the impaired efferocytosis of apoptotic cells and debris [1, 4, 5]. Our group previously reported that autoantibodies against type A scavenger receptors, which was a type of receptors related to the efferocytosis of macrophages, could reduce its ability to clear apoptotic cells in lupus patients [6]. However, the mechanism underlying the impairment of efferocytosis in SLE is not fully understood.

Macrophages belong to the largest subset of immune cells that are principally responsible for efferocytosis [2, 7]. Generally, efferocytosis in macrophages is initiated by the recognition of apoptotic cells via receptors on the cell surfaces of macrophages, which then trigger the phagocytic process [8, 9]. A 3-member transmembrane kinase receptor family named Tyro3/Axl/Mertk (TAM) is responsible for the recognition of apoptotic cells during efferocytosis by macrophages [10]. TAM family receptors include the Tyro3, Axl, and Mertk receptor tyrosine kinases and can be activated by interaction with the "eat-me" phosphatidylserine on the surfaces of apoptotic cells, which rely on the assistance of the ligands growth arrest-specific 6 (GAS6) and protein S [11, 12]. Emerging evidence has revealed that a deficiency in TAM receptors results in the accumulation of apoptotic cells [4, 13]. For instance, Mertk knockdown or knockout mice showed the delayed clearance of infused apoptotic cells [14]. Not only Mertk but also Axl and Tyro3 function in the phagocytosis of apoptotic cells. $Axl^{-/-}$ and $Tyro3^{-/-}$ macrophages had ~40–50% reduction in their abilities to phagocytose apoptotic thymocytes [15]. Furthermore, triple knockout Tyro3/Axl/Mertk mice developed SLE-like autoimmunity and overproduced autoantibodies, such as anti-double-stranded DNA (dsDNA) [16], indicating that the dysfunction of the TAM receptors on macrophages contributed to the development of SLE. Among TAM receptors, Tyro3 is the least characterized member. In the hematopoietic system, Tyro3 receptor is expressed on dendritic cells, natural killer cells, monocytes and macrophages, platelets and megakaryocytes, and osteoclasts [17]. It was reported that primary peritoneal macrophages isolated from $Tyro3^{-/-}$ mice had decreased ability to phagocytose apoptotic cells compared to macrophages from wild-type mice [17]. Clinical studies revealed that the levels of the soluble forms of Tyro3 (sTyro3) and Mertk receptors were increased in plasma from SLE patients [18]. Both levels of soluble forms of Mertk (sMertk) and sTyro3 were correlated with SLEDAI, and levels of sTyro3 were higher in patients with higher SLEDAI [19]. It might be responsible for the defective function of efferocytosis in the disease [20]. However, whether Tyro3 receptor could serve as an autoantigen to further affect the function of macrophages has remained unexplored. Here, we systematically investigated the profiles and clinical relevance of the Tyro3 autoantibody in new-onset and treatment-naïve SLE patients and further explored the implications of this about the efferocytosis by macrophages.

2. Methods

2.1. Patients and Healthy Controls. The study included consecutive 70 new-onset and treatment-naïve patients with SLE (including 60 females and 10 males) who met the 1997 American College of Rheumatology (ACR) classification criteria for the diagnosis of SLE confirmed by two qualified rheumatologists (Jialin Teng and Chengde Yang) [21]. Demographic data, clinical characteristics, and laboratory findings such as anti-dsDNA IgG levels, erythrocyte sedimentation rate (ESR), white blood cell counts in blood (WBC), haemoglobin (Hb), platelets (PLT), C-reactive protein (CRP), immunoglobulin G (IgG), complement 3 (C3), and complement 4 (C4) of SLE patients were collected. In addition, 24 rheumatoid arthritis (RA) and 21 primary Sjögren's Syndrome (pSS) were enrolled, and samples from 70 sex- and age-matched healthy donors with neither autoimmune nor infectious diseases were collected as healthy controls (HCs) (including 58 females and 12 males). All of the sera samples were stored at -80°C until use. Disease activity was measured using the SLEDAI score [22]. The study was performed in accordance with the Declaration of Helsinki and the Principles of Good Clinical Practice. Biological samples were obtained under a protocol approved by the Institutional Research Ethics Committee of Ruijin Hospital (ID: 2016-62), Shanghai, China. We have obtained the written consent from recruited patients and HCs.

2.2. Detection of Anti-Tyro3 Autoantibody. Recombinant human Tyro3 protein (Abnova, Taiwan) was prepared by a wheat germ expression system. The protein was fused with a GST-tag at N-terminal and purified by glutathione sepharose 4 fast flow. Antibody against human Tyro3 receptor in the sera of SLE patients and HCs was determined by an enzyme-linked immunosorbent assay (ELISA) at 450 nm. Ninety-six-well high-binding plates (Corning, New York, USA) were coated with recombinant human Tyro3 protein overnight at 4°C. The antigen-coated wells were washed three times with PBST buffer (PBS plus 0.05% Tween-20) and blocked with PBST buffer containing 5% bovine serum albumin (BSA) for 2 h at 37°C. The human Tyro3/Dtk antibody (R&D Systems, USA) was used as a positive control. The blocking buffer was removed, and the plates were washed as described above before the addition of 100 μl of serum sample (1 : 100 diluted in 1% BSA). The human sera were incubated for 2 h at room temperature followed by incubation with HRP-conjugated goat anti-human IgG (Abcam, Cambridge, UK) for another 1 h at room temperature. Then, the plates were washed, and 100 μl of tetramethylbenzidine substrate solution was added. It was then stopped by the addition of 50 μl of 0.5 M H_2SO_4. The absorbance was measured at a wavelength of 450 nm in a microplate reader (Bio-Rad Laboratories, Richmond, USA).

2.3. IgG Purification. Total IgG was isolated from the serum of new-onset SLE patients by a thiophilic adsorbent reagent (Pierce, Thermo Scientific, Rockford, USA) according to the manufacturer's instructions and concentrated in a centrifuge tube (Amicon, Millipore, Eschborn, Germany).

2.4. Purification of Anti-Tyro3 IgG. The purification of the specific antibody was performed using AminoLink Plus Coupling Resin according to the manufacturers' instructions

(MicroLink, Thermo Scientific, USA). We purchased recombinant human Tyro3 protein (Abnova, Taiwan) and coupled the protein to the resin. Then, we used the purified total IgG from SLE patients to form the resin-bound complex and incubated them with gentle end-over-end mixing. The eluted antibody was neutralized with 1 M Tris (pH = 9.0). After sterile filtration, the autoantibody was stored as small aliquots at -80°C.

2.5. Preparation of Macrophages. Peripheral blood mononuclear monocytes (PBMCs) were isolated from the blood of healthy volunteers using Ficoll density gradient centrifugation (GE Healthcare, Madison, USA). The CD14+ monocytes were isolated by positive selection using CD14 microbeads (Miltenyi Biotec, Auburn, USA) according to the manufacturer's instructions. The selected cells were cultured in RPMI 1640 medium containing 10% fetal calf serum (FCS; Gibco, NY, USA), 100 units/ml penicillin, and 100 μg/ml streptomycin that was supplemented with 100 ng/ml of macrophage colony-stimulating factor (M-CSF) (R&D Systems, Minneapolis, USA) in a humidified 5% CO_2 incubator. On day 4, the medium was replaced with RPMI 1640 medium containing M-CSF, and on day 7, the mature macrophages were harvested.

2.6. Preparation of Apoptotic Cells. To generate apoptotic cells, Jurkat cells (purchased from ATCC, Manassas, USA) were cultured in RPMI 1640 medium without FCS, and apoptosis was induced with 0.5 μg/ml staurosporine (BBI Life Science, Shanghai, China) for 3 h, as previously reported that the inhibitor of protein kinase staurosporine showed remarkable activity in inducing apoptosis in a wide variety of mammalian cells [23]. Afterwards, the cells were washed three times with PBS and resuspended in RPMI 1640 medium. Staurosporine treatment yielded a population of 90% apoptotic cells, which was verified by staining with annexin V and 7-amino-actinomycin D (7-AAD, Tianjin Sungene Biotech Co., China). Before being fed to the macrophages, the apoptotic cells were labeled with iFL Green dye (pHrodo, Invitrogen, Thermo Scientific, USA), which could be detected with FITC (fluorescein), protected from light at room temperature for 20 minutes.

2.7. Efferocytosis Assays. Human CD14-positive monocyte-derived macrophages were incubated with fresh medium containing 60 μg/ml purified human Tyro3 antibody from SLE patients or unconjugated human IgG (BBI Life Science, Shanghai) for 1 h at 37°C in an incubator.

Then, the macrophages were incubated with staurosporine-induced apoptotic Jurkat cells labeled with iFL Green dye (ratio of macrophages : apoptotic cells = 1 : 5) in RPMI 1640 medium without FCS in an incubator for 30 minutes. After being washed with PBS, the macrophages were collected using trypsin. Efferocytosis was determined according to the percentage of macrophages that phagocytosed apoptotic cells labeled with FITC using a FACS Canto II cytometer (BD Biosciences, San Jose, USA). The data were analyzed using FlowJo software (Tree Star Inc., Ashland, USA).

For immunofluorescence, the apoptotic cells were labeled with 5 μM 5-(and 6)-carboxyfluorescein diacetate succinimidyl ester (CFSE) (eBioscience, Invitrogen, Thermo Scientific, USA), protected from light at room temperature for 10 minutes, and washed with PBS. Then, the macrophages were incubated with induced apoptotic Jurkat cells for 30 minutes. After washing with PBS, macrophages were fixed with 4% formaldehyde for 20 minutes. After three rinses with PBS, the cells were permeabilized with Triton X-100 (Beyotime, Shanghai, China) for 5 minutes. The cytoskeleton was dyed with phalloidin (Servicebio, Shanghai, China) and incubated for 1 h protected from light. DNA was stained with 10 μg/ml 2-(4-amidinophenyl)-6-indolecarbamidine dihydrochloride (Hoechst 33324) (Thermo Scientific, USA) for 5 minutes protected from light. After rinsing 3 times with PBS, the cells were viewed by a confocal fluorescence microscope LSM 800 (ZEISS, Oberkochen, Germany).

2.8. Statistical Analysis. Continuous variables were tested for normality by the one-sample Kolmogorov-Smirnov test. Continuous variables were expressed as mean ± standard deviation (SD) or median (interquartile range) as per distribution type, and categorical data were expressed as frequency and percentages. The receiver operating characteristic (ROC) curve and the area under the curve (AUC) were used to assess the sensitivity and specificity of anti-Tyro3 IgG for the diagnosis of SLE. Statistical analysis was performed using the independent samples t-test for normal data and the Mann-Whitney U-test for nonnormal data. The analyses were carried out under the two-sided principle. Correlations between groups were evaluated by Spearman correlation. A p value less than 0.05 was considered statistically significant. Graphs were drawn using GraphPad Prism (version 7, GraphPad Software Inc., San Diego, USA), and data were analyzed using the SPSS software for Windows (version 23; SPSS Inc., Chicago, USA).

3. Results

3.1. Increased Serum Levels of Tyro3 Receptor Autoantibody in Patients with SLE. As TAM proteins are well-known kinase receptors that are crucial for macrophage efferocytosis for the clearance of apoptotic cells [10], to investigate the profile and clinical relevance of autoantibody against Tyro3 receptor in SLE, we detected the serum levels of anti-Tyro3 IgG in patients with SLE, RA, pSS, and HCs by ELISA. We recruited a total of 70 new-onset patients with SLE, and the clinical data are listed in Table 1. The results showed that the levels of anti-Tyro3 IgG were significantly higher in SLE patients than those in RA, pSS, and HCs (all $p < 0.0001$) (Figure 1). Then, we set a threshold using the mean control levels plus 2 SD for abnormal titers; the positive rate of anti-Tyro3 IgG in SLE, RA, and pSS was 24/70 (34.3%), 3/24 (12.5%), and 4/21 (19.0%), respectively, indicating that Tyro3 receptor antibody might be an important biomarker and play a role in the pathogenesis of SLE. Furthermore, the positivity of anti-Tyro3 in anti-Sm-negative patients was 16/53 (30.2%), while the positivity of which in anti-dsDNA-negative patients was 2/7 (28.6%). The results

Table 1: The clinical and laboratory characteristics of new-onset and treatment-naïve SLE patients.

Variable	SLE patients
Gender (female/male, *n*)	60/10
Age (mean ± SD, years)	39 ± 16
Disease duration (months, median, IQR)	3.5 (1, 24)
SLEDAI (mean ± SD)	12 ± 5
Fever (*n*, %)	32 (45.7)
Arthritis (*n*, %)	42 (60.0)
Rash (*n*, %)	36 (51.4)
Oral ulcer (*n*, %)	16 (22.9)
Alopecia (*n*, %)	16 (22.9)
Vasculitis (*n*, %)	5 (7.1)
Serositis (*n*, %)	16 (22.9)
Photosensitivity (*n*, %)	10 (14.3)
Raynaud's phenomenon (*n*, %)	13 (18.6)
Hematological (*n*, %)	54 (77.1)
Lupus nephritis (proteinuria ≥ 0.5 g/24 h) (*n*, %)	31 (44.3)
Neuropsychiatric manifestations (*n*, %)	1 (1.4)
Anti-dsDNA positive (*n*, %)	63 (90.0)
Anti-Sm positive (*n*, %)	17 (24.3)
Anti-SSA positive (*n*, %)	38 (54.3)
Anti-SSB positive (*n*, %)	8 (11.4)
Anti-U1RNP positive (*n*, %)	27 (38.6)
Anti-Rib-P positive (*n*, %)	29 (41.4)
Anti-nucleosome-A positive (*n*, %)	24 (34.3)

Note: SD: standard deviation; SLE: systemic lupus erythematosus; SLEDAI: SLE disease activity index; IQR: interquartile range; dsDNA: double-stranded DNA.

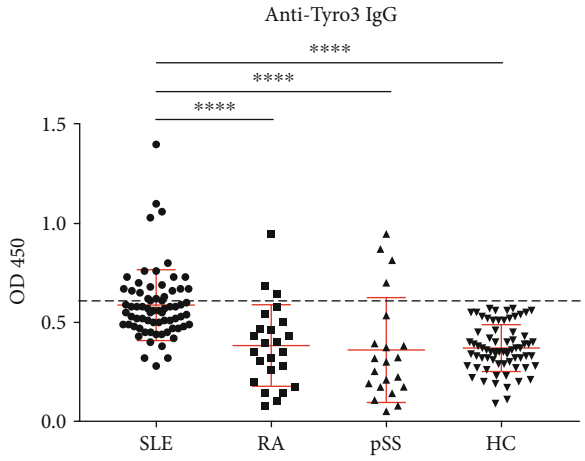

Figure 1: Detection of anti-Tyro3 IgG levels in SLE, RA, pSS, and HCs. SLE: systemic lupus erythematosus; RA: rheumatoid arthritis; pSS: primary Sjögren's Syndrome; HC: healthy control.

strengthen the significance of anti-Tyro3 antibody in the diagnosis of SLE. Besides, we detected serum from 11 patients before and after effective treatment by ELISA and there was no significant change of anti-Tyro3 antibody after effective treatment ($p > 0.05$, Supplementary Figure 1).

3.2. Association between Anti-Tyro3 IgG and the Clinical Manifestations in SLE Patients. Next, we analyzed the association of serum anti-Tyro3 IgG levels with the clinical data. The levels of anti-Tyro3 IgG were negatively associated with Hb ($r = -0.294$, $p = 0.014$) and positively correlated with the SLEDAI score ($r = 0.254$, $p = 0.034$), ESR ($r = 0.430$, $p < 0.001$), CRP ($r = 0.246$, $p = 0.049$), and IgG ($r = 0.408$, $p = 0.001$) (Figure 2). Furthermore, the differences of levels of anti-Tyro3 antibody in SLE patients with and without clinical characteristics were determined. As shown in Table 2, higher levels of anti-Tyro3 antibody were observed in patients with oral ulcers than patients without oral ulcers ($p = 0.035$).

We also detected autoantibodies against Axl and Mertk, which belong to TAM receptors, in the same cohort. The results showed that the levels of anti-Axl and anti-Mertk IgG were significantly higher in SLE patients than those in RA, pSS, and HCs (all $p < 0.05$, Supplementary Figures 2A and 2B). However, there was no correlation between anti-Axl IgG and SLEDAI score, neither did anti-Mertk IgG (all $p > 0.05$, Supplementary Figures 2C and 2D), indicating that the high levels of anti-Axl and anti-Mertk antibodies might not be associated with SLE disease activity.

3.3. Receiver Operating Characteristic Curves of Anti-Tyro3 IgG. To determine the efficacy of the measurement of autoantibody against Tyro3 receptor for diagnosing SLE, we calculated the ROC curves to determine the sensitivity and specificity of the autoantibody in distinguishing patients with SLE, RA, and pSS from HCs. As shown in Figure 3, the AUCs of anti-Tyro3 IgG in SLE, RA, and pSS were 0.8708 (95% CI: 0.8136-0.9281) ($p < 0.0001$), 0.5048 (95% CI: 0.3512-0.6583) ($p = 0.9447$), and 0.6146 (95% CI: 0.4468-0.7824) ($p = 0.1125$), respectively. ROC curves illustrated that the anti-Tyro3 antibody could differentiate patients with SLE from HCs.

3.4. SLE Patient-Derived Autoantibody against Tyro3 Receptor Inhibited the Efferocytosis of Macrophages. Since TAM receptors mainly functioned in macrophage-associated efferocytosis, we further determined the role of Tyro3 receptor autoantibody in the efferocytosis of macrophages. First, we purified specific IgG-type antibody against Tyro3 from the serum of new-onset SLE patients with high optical density (OD) values at 450 nm, which was further confirmed by silver staining compared to different quantity of unconjugated human IgG (Supplementary Figure 3). Furthermore, we explored the cross-reaction between purified anti-Tyro3 antibody and TAM receptors and CD14, a surface antigen preferentially expressed mainly on monocytes/macrophages, by ELISA assay following the standard procedure (Supplementary Table 1). Immunoprecipitation was also used to verify the binding of purified anti-Tyro3 IgG to recombinant human Tyro3 protein (Supplementary Figure 4). Then, primary human monocyte-derived macrophages and staurosporine-induced apoptotic Jurkat cells were incubated with purified anti-Tyro3 IgG or unconjugated human IgG, and macrophage efferocytosis was analyzed by flow cytometry and immunofluorescence. As shown in Figure 4,macrophage efferocytosis was significantly decreased after anti-Tyro3

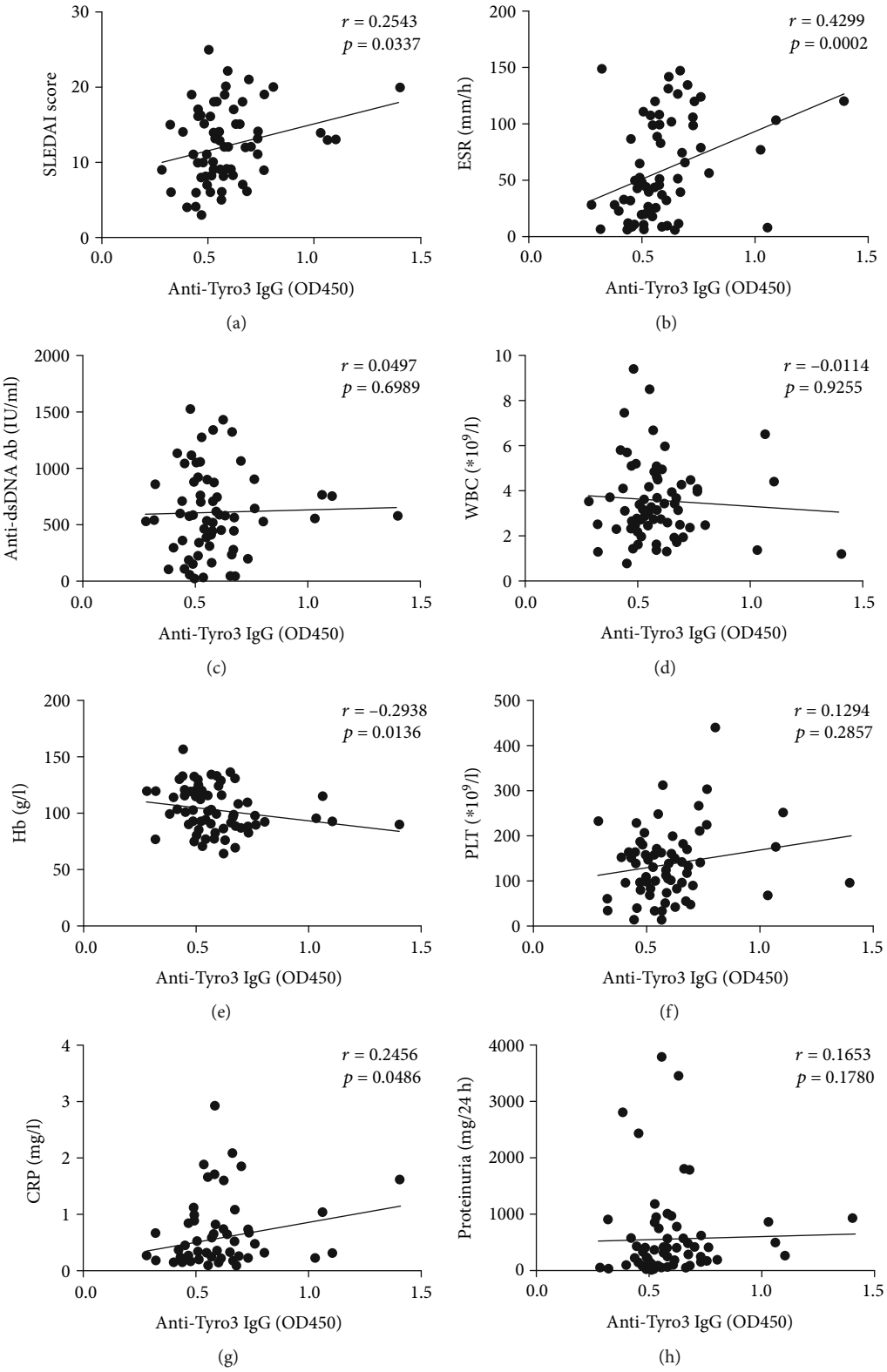

Figure 2: Continued.

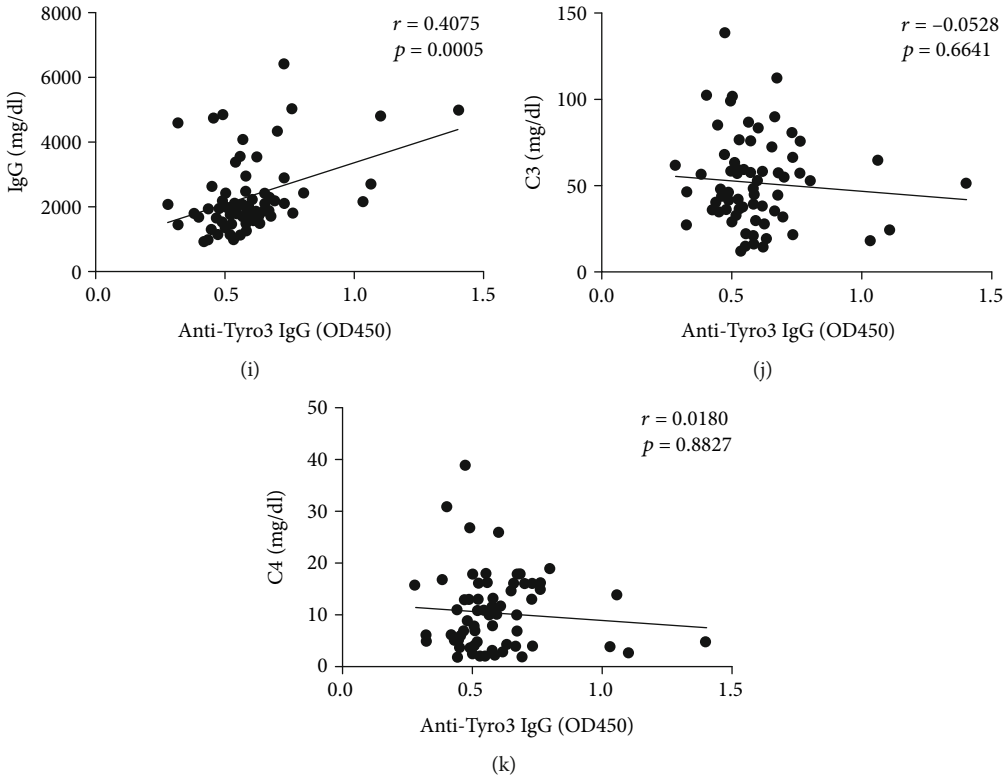

Figure 2: The correlation of anti-Tyro3 IgG levels and clinical manifestations in SLE patients. (a–k) The correlation between anti-Tyro3 IgG levels and SLEDAI score, ESR, Anti-dsDNA Ab, WBC, Hb, PLT, CRP, proteinuria, IgG, C3, and C4 in SLE patients. $p < 0.05$ represents a significant difference. SLE: systemic lupus erythematosus; HC: healthy control; ESR: erythrocyte sedimentation rate; SLEDAI: SLE disease activity index; anti-dsDNA Ab: anti-double-stranded DNA antibody; WBC: white blood cell; Hb: haemoglobin; PLT: platelet; CRP: C-reactive protein; IgG: immunoglobulin G; C3: complement 3; C4: complement 4.

IgG ($p = 0.004$) treatment compared with unconjugated human IgG treatment detected by flow cytometry. Furthermore, immunofluorescence assay showed a decreased engulfment of apoptotic cells in the macrophages incubated with purified anti-Tyro3 IgG ($p = 0.044$) compared with unconjugated human IgG. These data suggested that Tyro3 receptor autoantibody reduced the efferocytosis of macrophages by blocking Tyro3 receptor and might result in the accumulation of cell debris, thus might be involved in the pathogenesis of SLE.

4. Discussion

The overproduction of autoantibodies is a hallmark of the pathogenesis of SLE. The contribution of the dysregulation of macrophages to autoantibody overproduction in SLE has been widely studied, but the effect of autoantibodies on macrophages in SLE has rarely been reported. It was reported that these antibodies could affect many cells via direct binding to antigens on cells [24]. The functions of these autoantibodies included the activation or inhibition of downstream signaling and the blocking of interactions between targets and other proteins [25]. Recently, our team found that the overproduced antibodies in SLE included antibodies recognizing proteins specifically expressed in immune cells that were responsible for key immune responses, such as anti-PD-1 antibody [26]. These immune response-related antibodies might further disturb the balance of the immune system and contribute to the progression of SLE. Here, we demonstrated that patients with SLE produced high levels of autoantibody against Tyro3, which was one of the three key tyrosine kinases involved in the macrophage-mediated elimination of apoptotic cells. Besides, anti-Tyro3 antibody was associated with the SLEDAI score, ESR, and CRP, indicating that the antibody was related to SLE disease activity. Further functional studies revealed that anti-Tyro3 IgG inhibited the efferocytosis of macrophages, which might increase the accumulation of autoantigen and further promote the production of autoantibodies in SLE.

The major factor involved in the regulation of macrophage-mediated efferocytosis is TAM receptors [11, 13, 27]. Our study also detected the levels of anti-Axl and anti-Mertk IgG, which were significantly higher in SLE patients than those in RA, pSS, and HCs. However, there was no correlation between anti-Axl IgG and SLEDAI score, neither did anti-Mertk IgG. It indicated that only the levels of anti-Tyro3 IgG were associated with disease activity of SLE, supporting it as a potential novel disease biomarker.

It was interesting that the statistical analysis showed that patients with the presence of oral ulcers had higher levels of anti-Tyro3 IgG, and there was little known about the relationship between TAM autoantibodies and oral ulcers. It has been reported that CD68-positive macrophages are one of the main inflammatory cells relevant to the pathogenesis

Table 2: Comparison of anti-Tyro3 antibody according to disease manifestations in 70 new-onset and treatment-naïve SLE patients.

		Anti-Tyro3 IgG (OD 450)	p value
Photosensitivity	(+), $n = 10$	0.645 ± 0.185	0.185
	(-), $n = 60$	0.578 ± 0.177	
Raynaud's phenomenon	(+), $n = 13$	0.594 ± 0.187	0.898
	(-), $n = 57$	0.586 ± 0.178	
Fever	(+), $n = 32$	0.618 ± 0.228	0.402
	(-), $n = 38$	0.562 ± 0.121	
Serositis	(+), $n = 16$	0.606 ± 0.153	0.243
	(-), $n = 54$	0.582 ± 0.187	
Oral ulcer	(+), $n = 16$	0.698 ± 0.264	0.035*
	(-), $n = 54$	0.555 ± 0.131	
Rash	(+), $n = 36$	0.605 ± 0.214	0.953
	(-), $n = 34$	0.569 ± 0.132	
Alopecia	(+), $n = 16$	0.599 ± 0.157	0.796
	(-), $n = 54$	0.584 ± 0.186	
Arthritis	(+), $n = 42$	0.607 ± 0.178	0.148
	(-), $n = 28$	0.558 ± 0.179	
Vasculitis	(+), $n = 5$	0.634 ± 0.166	0.367
	(-), $n = 65$	0.584 ± 0.180	

Note: anti-Tyro3 IgG (OD 450) are shown as mean ± SD, and differences between two groups were analyzed using the independent samples t-test for normal data and the Mann-Whitney U test for nonnormal data. SLE: systemic lupus erythematosus. *$p < 0.05$.

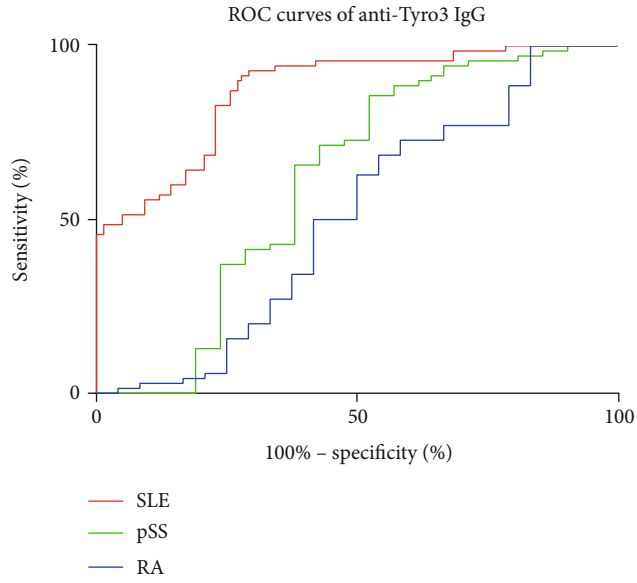

Figure 3: The receiver operating characteristic (ROC) curves of anti-Tyro3 IgG in SLE, RA, pSS, and HCs. The areas under the curve (AUC) of anti-Tyro3 IgG in SLE, RA, and pSS were 0.8708 (95% CI: 0.8136-0.9281) ($p < 0.0001$), 0.5048 (95% CI: 0.3512-0.6583) ($p = 0.9447$), and 0.6146 (95% CI: 0.4468-0.7824) ($p = 0.1125$), respectively. SLE: systemic lupus erythematosus; RA: rheumatoid arthritis; pSS: primary Sjögren's Syndrome.

of ulcers [28]. In oral ulcers, the apoptosis of epithelium remains in large quantity and poses a great pressure of scavenging cells such as macrophages. The rapidly apoptotic epithelial cell may exceed the ability of phagocytosis of macrophages, which lead to sloughing of the dead epithelial cells [29]. Furthermore, autoantibody-related defective phagocytosis of macrophages might in turn worsen the symptom of oral ulcers.

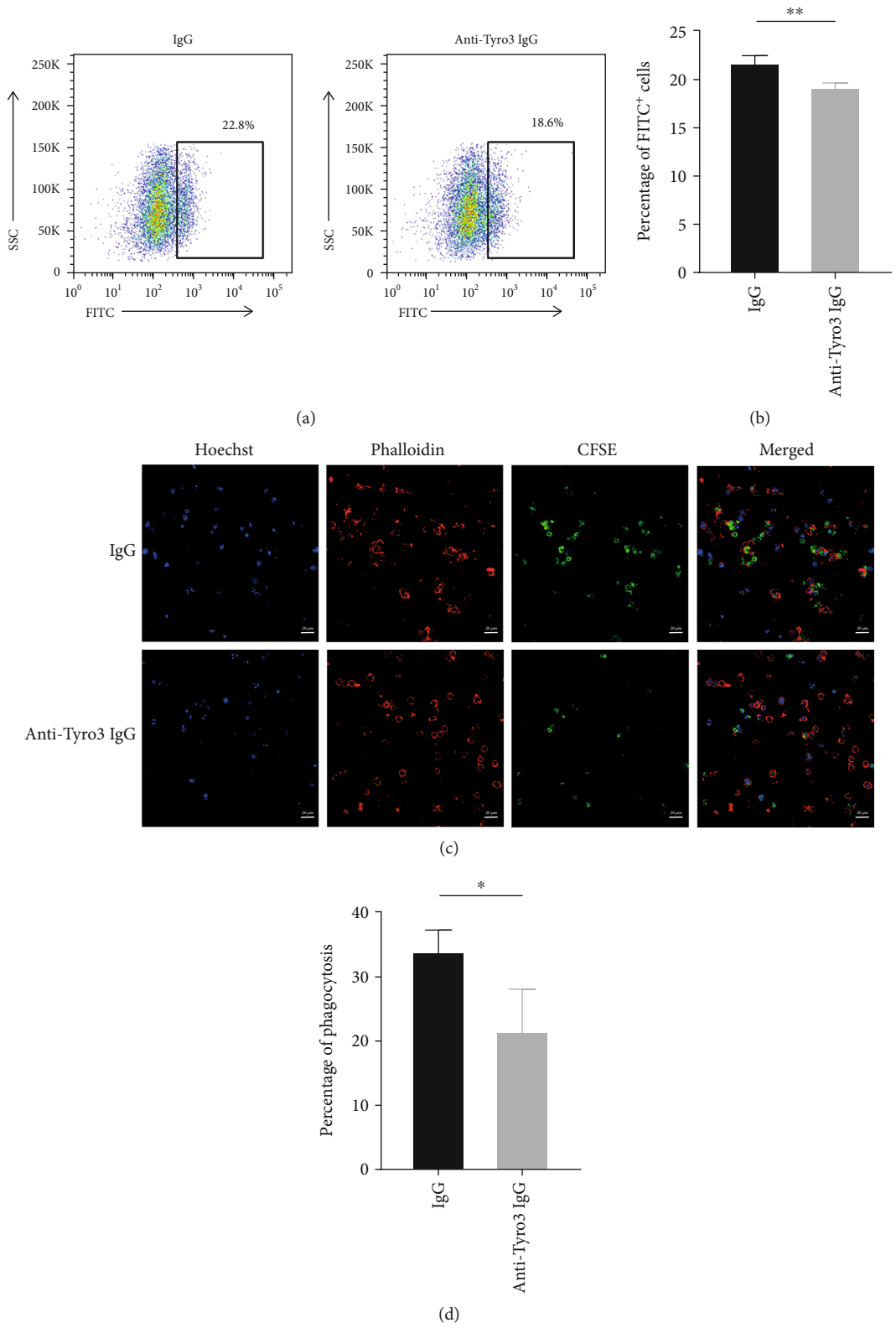

Figure 4: Autoantibody against Tyro3 receptor reduced macrophage efferocytosis by flow cytometry and immunofluorescence. (a) The efferocytosis of macrophages was analyzed by flow cytometry. (b) The statistical graph showing the flow cytometry data ($n = 4$). The values represent the mean ± SD. $^{**}p < 0.01$. (c) Representative photograph of the efferocytosis of macrophages monitored by immunofluorescence, presented as merged pictures of Hoechst (blue), phalloidin (red), and CFSE (green). Bar, 20 μm. (d) Statistical data of the percentage of efferocytosis in 100x views of the confocal microscope ($n = 3$). The values represent the mean ± SD. $^{*}p < 0.05$.

The identification of pathological antibodies is key to understand the abnormal events that occur in patients with SLE. Our study is the first to report the enrichment of pathological anti-Tyro3 antibody in SLE and its association with disease activity. We also indicated that autoantibody against Tyro3 might be responsible for the reduced efferocytosis of macrophages.

5. Conclusions

This study showed an elevated level of anti-Tyro3 IgG in patients with SLE compared to HCs and was associated with SLE disease activity, indicating anti-Tyro3 antibody a novel disease biomarker. In addition, our results demonstrated that autoantibody against Tyro3 impaired efferocytosis of macrophages, which might be involved in the pathogenesis of SLE.

Data Availability

The datasets generated and/or analyzed during the current study are available from the corresponding authors on reasonable request.

Conflicts of Interest

The authors declare that they have no conflicts of interest.

Authors' Contributions

Zhuochao Zhou, Aining Xu, and Jialin Teng contributed equally to this work.

Acknowledgments

The patients and healthy donors are gratefully acknowledged for their participation in this study. This work was supported by the National Natural Science Foundation of China (81801592), the Shanghai Sailing Program (18YF1414100), the Excellent Youth B Project (GCQN-2017-B05), and the National Innovative Research Team from High-Level Local Universities in Shanghai.

Supplementary Materials

Supplementary Table 1: cross-reaction between purified anti-Tyro3 antibody and TAM receptors and CD14 by ELISA. Supplementary Figure 1: the levels of anti-Tyro3 IgG in SLE before and after effective treatment. Supplementary Figure 2: the levels of anti-Axl and anti-Mertk IgG in patients with SLE, RA, pSS, and HCs and its association with the SLEDAI score. (A) The levels of anti-Axl IgG in patients with SLE, RA, pSS, and HCs detected by ELISA assay; (B) the levels of anti-Mertk IgG in patients with SLE, RA, pSS, and HCs detected by ELISA assay; (C) the correlation between anti-Axl IgG and SLEDAI score; (D) the correlation between anti-Mertk IgG and SLEDAI score. SLE: systemic lupus erythematosus; RA: rheumatoid arthritis; pSS: primary Sjögren's Syndrome; HC: healthy control; SLEDAI: SLE disease activity index. $^{*}p < 0.05$, $^{**}p < 0.01$, and $^{****}p < 0.0001$. Supplementary Figure 3: silver staining of purified anti-Tyro3 IgG from SLE patients. The heavy chain and light chain of IgG were 50 kD and 25 kD, respectively. The quantity of IgG-1, IgG-2, and IgG-3 was 1 μg, 0.3 μg, and 0.1 μg, respectively. The quantity of anti-Tyro3 IgG was 0.3 μg. IgG: unconjugated human IgG. Supplementary Figure 4: immunoprecipitation of recombinant human Tyro3 protein and purified anti-Tyro3 IgG vs. unconjugated human IgG using Protein A/G PLUS-Agarose. Tyro3: recombinant human Tyro3 protein; human IgG: unconjugated human IgG. *(Supplementary Materials)*

References

[1] G. C. Tsokos, M. S. Lo, P. C. Reis, and K. E. Sullivan, "New insights into the immunopathogenesis of systemic lupus erythematosus," *Nature Reviews Rheumatology*, vol. 12, no. 12, pp. 716–730, 2016.

[2] A. Kaul, C. Gordon, M. K. Crow et al., "Systemic lupus erythematosus," *Nature Reviews Disease Primers*, vol. 2, no. 1, p. 16039, 2016.

[3] Y. Li, P. Y. Lee, and W. H. Reeves, "Monocyte and macrophage abnormalities in systemic lupus erythematosus," *Archivum Immunologiae et Therapiae Experimentalis*, vol. 58, no. 5, pp. 355–364, 2010.

[4] L. E. Muñoz, K. Lauber, M. Schiller, A. A. Manfredi, and M. Herrmann, "The role of defective clearance of apoptotic cells in systemic autoimmunity," *Nature Reviews Rheumatology*, vol. 6, no. 5, pp. 280–289, 2010.

[5] I. K. H. Poon, C. D. Lucas, A. G. Rossi, and K. S. Ravichandran, "Apoptotic cell clearance: basic biology and therapeutic potential," *Nature Reviews Immunology*, vol. 14, no. 3, pp. 166–180, 2014.

[6] X. Chen, Y. Shen, C. Sun, F. X. Wu, Y. Chen, and C. D. Yang, "Anti-class a scavenger receptor autoantibodies from systemic lupus erythematosus patients impair phagocytic clearance of apoptotic cells by macrophages in vitro," *Arthritis research & therapy*, vol. 13, no. 1, p. R9, 2011.

[7] A. Barrera-Vargas, D. Gómez-Martín, C. Carmona-Rivera et al., "Differential ubiquitination in NETs regulates macrophage responses in systemic lupus erythematosus," *Annals of the Rheumatic Diseases*, vol. 77, no. 6, pp. 944–950, 2018.

[8] J. M. Blander, "The many ways tissue phagocytes respond to dying cells," *Immunological Reviews*, vol. 277, no. 1, pp. 158–173, 2017.

[9] B. Luo, W. Gan, Z. Liu et al., "Erythropoeitin signaling in macrophages promotes dying cell clearance and immune tolerance," *Immunity*, vol. 44, no. 2, pp. 287–302, 2016.

[10] D. K. Graham, D. DeRyckere, K. D. Davies, and H. S. Earp, "The TAM family: phosphatidylserine sensing receptor tyrosine kinases gone awry in cancer," *Nature Reviews Cancer*, vol. 14, no. 12, pp. 769–785, 2014.

[11] A. Zagórska, P. G. Través, E. D. Lew, I. Dransfield, and G. Lemke, "Diversification of TAM receptor tyrosine kinase function," *Nature Immunology*, vol. 15, no. 10, pp. 920–928, 2014.

[12] J. H. M. van der Meer, T. van der Poll, and C. van 't Veer, "TAM receptors, Gas6, and protein S: roles in inflammation and hemostasis," *Blood*, vol. 123, no. 16, pp. 2460–2469, 2014.

[13] C. V. Rothlin and G. Lemke, "TAM receptor signaling and autoimmune disease," *Current Opinion in Immunology*, vol. 22, no. 6, pp. 740–746, 2010.

[14] P. L. Cohen, R. Caricchio, V. Abraham et al., "Delayed apoptotic cell clearance and lupus-like autoimmunity in mice lacking the c-mer membrane tyrosine kinase," *Journal of Experimental Medicine*, vol. 196, no. 1, pp. 135–140, 2002.

[15] C. V. Rothlin, E. A. Carrera-Silva, L. Bosurgi, and S. Ghosh, "TAM receptor signaling in immune homeostasis," *Annual Review of Immunology*, vol. 33, no. 1, pp. 355–391, 2015.

[16] Q. Lu and G. Lemke, "Homeostatic regulation of the immune system by receptor tyrosine kinases of the tyro 3 family," *Science*, vol. 293, no. 5528, pp. 306–311, 2001.

[17] S. Smart, E. Vasileiadi, X. Wang, D. DeRyckere, and D. Graham, "The emerging role of TYRO3 as a therapeutic target in cancer," *Cancers*, vol. 10, no. 12, p. 474, 2018.

[18] J. Wu, C. Ekman, A. Jönsen et al., "Increased plasma levels of the soluble Mer tyrosine kinase receptor in systemic lupus erythematosus relate to disease activity and nephritis," *Arthritis Research & Therapy*, vol. 13, no. 2, p. R62, 2011.

[19] P. Recarte-Pelz, D. Tàssies, G. Espinosa et al., "Vitamin K-dependent proteins GAS6 and protein S and TAM receptors in patients of systemic lupus erythematosus: correlation with common genetic variants and disease activity," *Arthritis Research & Therapy*, vol. 15, no. 2, p. R41, 2013.

[20] L. Ballantine, A. Midgley, D. Harris, E. Richards, S. Burgess, and M. W. Beresford, "Increased soluble phagocytic receptors sMer, sTyro3 and sAxl and reduced phagocytosis in juvenile-onset systemic lupus erythematosus," *Pediatric Rheumatology*, vol. 13, no. 1, p. 10, 2015.

[21] M. C. Hochberg, "Updating the American College of Rheumatology revised criteria for the classification of systemic lupus erythematosus," *Arthritis & Rheumatology*, vol. 40, no. 9, p. 1725, 1997.

[22] D. D. Gladman, D. Ibañez, and M. B. Urowitz, "Systemic lupus erythematosus disease activity index 2000," *Journal of Rheumatology*, vol. 29, no. 2, pp. 288–291, 2002.

[23] F. Cusinato, I. Pighin, S. Luciani, and L. Trevisi, "Synergism between staurosporine and drugs inducing endoplasmic reticulum stress," *Biochemical Pharmacology*, vol. 71, no. 11, pp. 1562–1569, 2006.

[24] V. Racanelli, M. Prete, G. Musaraj, F. Dammacco, and F. Perosa, "Autoantibodies to intracellular antigens: generation and pathogenetic role," *Autoimmunity Reviews*, vol. 10, no. 8, pp. 503–508, 2011.

[25] F. Nimmerjahn and J. V. Ravetch, "Antibody-mediated modulation of immune responses," *Immunological Reviews*, vol. 236, no. 1, pp. 265–275, 2010.

[26] H. Shi, J. Ye, J. Teng et al., "Elevated serum autoantibodies against co-inhibitory PD-1 facilitate T cell proliferation and correlate with disease activity in new-onset systemic lupus erythematosus patients," *Arthritis Research & Therapy*, vol. 19, no. 1, p. 52, 2017.

[27] L. Fourgeaud, P. G. Través, Y. Tufail et al., "TAM receptors regulate multiple features of microglial physiology," *Nature*, vol. 532, no. 7598, pp. 240–244, 2016.

[28] W. A. Delgado, O. P. Almeida, P. A. Vargas, and J. E. León, "Oral ulcers in HIV-positive Peruvian patients: an immunohistochemical and in situ hybridization study," *Journal of Oral Pathology & Medicine*, vol. 38, no. 1, pp. 120–125, 2009.

[29] A. Al-Samadi, A. Drozd, A. Salem, J. Hietanen, R. Häyrinen-Immonen, and Y. T. Konttinen, "Epithelial cell apoptosis in recurrent aphthous ulcers," *Journal of Dental Research*, vol. 94, no. 7, pp. 928–935, 2015.

Hindawi
Journal of Immunology Research
Volume 2020, Article ID 8263598, 14 pages
https://doi.org/10.1155/2020/8263598

Research Article

Protective Effects of Thalidomide on High-Glucose-Induced Podocyte Injury through *In Vitro* Modulation of Macrophage M1/M2 Differentiation

Hui Liao, Yuanping Li, Xilan Zhang, Xiaoyun Zhao, Dan Zheng, Dayue Shen, and Rongshan Li

Department of Pharmacy, Shanxi Provincial People's Hospital of Shanxi Medical University, Taiyuan 030012, China

Correspondence should be addressed to Rongshan Li; rongshanli13@163.com

Received 21 April 2020; Revised 25 June 2020; Accepted 11 July 2020; Published 27 August 2020

Guest Editor: Charles Elias Assmann

Objective. It has been shown that podocyte injury represents an important pathological basis that contributes to proteinuria and eventually leads to kidney failure. High glucose (HG) activates macrophage polarization, further exacerbating HG-induced podocyte injury. Our previous study on diabetic nephropathy rats indicated that thalidomide (Tha) has renoprotective properties. The present study explored the effects of Tha on mRNA and protein expressions of inducible nitric oxide synthase (iNOS), tumor necrosis factor- (TNF-) α, mannose receptor (CD206), and arginase- (Arg-) 1 in HG-activated macrophages. iNOS and TNF-α are established as markers of classically activated macrophage (M1). CD206 and Arg-1 are regarded as markers of alternatively activated macrophages (M2). During the experiment, the supernatants of (HG)-treated and (Tha)-treated macrophages, designated as (HG) MS and (Tha) MS, were simultaneously collected and processed. TNF-α and interleukin- (IL-) 1β levels as well as protein expressions of nephrin and podocin in HG, (HG) MS, and (Tha) MS-cultured podocytes were evaluated. The results showed that compared to the 11.1 mM normal glucose (NG), the 33.3 mM HG-cultured RAW 264.7 cells exhibited upregulated iNOS and TNF-α mRNAs and protein expressions, and downregulated CD206 and Arg-1 expressions significantly ($p < 0.05$). Tha 200 μg/ml suppressed iNOS and TNF-α, and promoted CD206 and Arg-1 expressions significantly compared to the HG group ($p < 0.05$). Furthermore, (HG) MS-treated podocytes showed an increase in TNF-α and IL-1β levels and a downregulation in nephrin and podocin expression significantly compared to NG-treated and HG-treated podocytes ($p < 0.05$). The (Tha 200 μg/ml) MS group exhibited a decrease in TNF-α and IL-1β level, and an upregulation in nephrin and podocin expressions significantly compared to the (HG) MS group ($p < 0.05$). Our research confirmed that HG-activated macrophage differentiation aggravates HG-induced podocyte injury *in vitro* and the protective effects of Tha might be related to its actions on TNF-α and IL-1β levels via its modulation on M1/M2 differentiation.

1. Introduction

The 60-year history of thalidomide (Tha) is riddled with tragedy, resilience, and redemption [1]. It started in the late 1950s when Tha was given to pregnant women to relieve morning sickness. It was later (in 1991) confirmed that Tha selectively inhibited the production of human monocyte tumor necrosis factor- (TNF-) α in lipopolysaccharide- (LPS-) triggered cells [2].

From then on and for the next two decades, the redemption road was full of hardship until Tha became the first agent to gain approval by the FDA for the treatment of plasma cell myeloma in 2006 [3]. So far, its potential immunomodulatory, anti-inflammatory, and antiangiogenic properties make it a good candidate for the treatment of many diseases such as multiple myeloma, Behçet's syndrome, and inflammatory bowel disease [4–6].

Our preliminary work confirmed that pharmacologically and clinically, Tha had protective effects in diabetic renal injury [7–9]. Diabetic kidney disease (DKD) is considered an immune-mediated disease, with increasing emerging evidence suggesting greater immunological component in its

pathophysiology. Infiltration of immune cells, predominantly macrophages, into the diabetic kidney has been reported in a number of both experimental and clinical studies [10]. Macrophage polarization could induce podocyte injury, which is a typical characteristic of DKD [11]. Blocking activated macrophage subtype-derived TNF-α could be an important therapeutic approach for the treatment of DKD [12].

In the present study, we firstly explored the effects of Tha on high-glucose- (HG-) induced macrophage polarization. The classically activated macrophage (M1, damaged type) markers including inducible nitric oxide synthase (iNOS), TNF-α, and the markers of alternatively activated macrophage (M2, protective type) including mannose receptor (CD206) and arginase- (Arg-) 1 were compared. Secondly, we proceeded to assess the effects of Tha on podocyte injury via macrophage polarization. TNF-α and interleukin- (IL-) 1β levels and nephrin and podocin protein expressions were compared in podocytes treated with macrophage supernatant.

2. Methods

2.1. Cell Culture. The conditionally immortalized mouse MPC-5 podocyte cell line was purchased from Fuheng Biology Company (Shanghai, China) and cultured at 33°C in a 10% FBS (Gibco BRL, Gaithersburg, MD, USA) and recombinant interferon- (IFN-) γ (G1021, Achieve Perfection, Explore the Unknown, USA) supplemented RPMI-1640 (HyClone, GE Healthcare Life Sciences, Logan, UT, USA) medium. Podocytes were reseeded and cultured at 37°C in an RPMI-1640 medium with 10 mg/ml type-I collagen (BD Bioscience, Bedford, MA, USA) and without IFN-γ for 7–15 days to induce differentiation. Then, podocytes were cultured with serum starvation overnight before the stimulation.

The conditionally immortalized mouse RAW 264.7 macrophage cell line was purchased from the Absin Biotechnology Company (Shanghai, China) and cultured per the instructions. RAW 264.7 cells were briefly cultured in a 10% FBS supplemented with RPMI-1640 medium at 37°C in a 5% CO_2 incubator. The medium was then replaced with a new culture medium the next day. The serum-free RPMI-1640 medium was synchronized for 12 hours before the intervention.

2.2. Determination of the HG-Induced Phenotypic Transition of M1 Macrophage [13–15]. RAW 264.7 cells (99 μl, plated at 1×10^6 cells/ml) were stimulated with 25.0 mM, 33.3 mM, and 44.4 mM glucose after 12 hours, 24 hours, and 48 hours, before assessment of nitric oxide (NO) production. The 11.1 mM normal glucose (NG) group was considered as the normal group [13, 14]. LPS-stimulated cells (1 μl, 0.5 μg/ml, Wako Chemicals USA Inc., Richmond, VA, USA) were cultured in a normal medium and considered as the model control [15, 16]. Dimethyl sulfoxide (DMSO) was used as the solvent control of LPS. Nitrite, a stable end-product of NO metabolism, was measured using the Griess reaction.

2.3. Effects of Tha and HG on the Viability of Podocytes and Macrophages. Podocytes and macrophages were separately seeded into 96-well plates at a density of 5×10^4 cells/ml and cultured in a 10% FBS RPMI-1640 medium for 24 hours. Following another 24-hour treatment with 11.1 mM glucose, mannitol control, 33.3 mM glucose, and Tha (at 25 μg/ml (Tha25), 50 μg/ml (Tha50), 100 μg/ml (Tha100), and 200 μg/ml (Tha200)) in 33.3 mM glucose, the supernatants were removed, and each well was washed with PBS before the addition of 10% FBS RPMI-1640 medium and 10 μl CCK-8 reagent (Boster Biological Technology, Wuhan, China). Cell viability was determined by measuring the absorbance at 450 nm using a microporous plate reader (Model 550; Bio-Rad Laboratories, Inc., Hercules, CA, USA) after an incubation period of 2 hours at 37°C. The average optical density was determined by examining six wells per group.

2.4. Effects of Tha on iNOS, TNF-α, Arg-1, and CD206 Protein Expressions in HG-Induced Macrophages (Western Blot). The treated cells in the 11.1 mM glucose control, the 33.3 mM glucose model, the LPS model control [16], and the Tha50, Tha100, and Tha200 in the 33.3 mM glucose groups were removed from the culture medium after 24 hours and extracted using the RIPA lysis buffer (for 30 minutes) from Solarbio Science & Technology (Beijing, China). Protein concentrations were determined using a BCA Protein Assay Kit from Boster Biological Technology (Wuhan, China). Samples containing 50 μg of protein were run through 12% SDS-PAGE electrophoresis and transferred to the nitrocellulose membranes (Solarbio Science & Technology, Beijing, China). Nonspecific binding was blocked by immersing the membranes into 5% nonfat dried milk and 0.1% (v/v) Tween-20 in PBS for 3 hours at room temperature. After several consecutive rinses with a washing buffer (0.1% Tween-20 in PBS), the membranes were incubated with primary antibodies against iNOS at 1 : 500 dilution (Catalog No. BA0362, Boster), TNF-α (Catalog No. BA0131, Boster) at 1 : 500 dilution, CD206 (Catalog No. A02285-2, Boster) at 1 : 500 dilution, and antibody against Arg-1 (Catalog No. BM4000, Boster) at 1 : 500 dilution overnight at 4°C. The membranes were then washed several times and incubated with the corresponding anti-mouse secondary antibody (Proteintech, Wuhan, China) at room temperature for 3 hours. Subsequently, the analysis was performed on the Quantity One analysis system (Bio-Rad, Hercules, CA, USA). GAPDH was used as an internal loading control at a dilution of 1 : 1000 (Catalog No. A00227-1, Boster).

2.5. Effects of Tha on iNOS, TNF-α, Arg-1, and CD206 mRNA Expressions in HG-Induced Macrophages (Real-Time Quantitative PCR (qPCR)). Total RNAs were extracted from the 11.1 mM glucose, 33.3 mM glucose, LPS, and Tha-treated cells by TRIzol Reagent (Ambion, USA). An equal amount (1 μg) of RNAs was reverse transcribed using a high-capacity RNA-to-cDNA PCR kit (Takara, Beijing, China). Mouse gene PCR primer sets for TNF-α, Arg-1, and CD206 were obtained from SA Biosciences (Germantown, MD). The Power SYBR Green PCR Master Mix (Applied

Biosystems) was used with the step-one-plus real-time PCR system (Applied Biosystems). The protocol included denaturing for 15 min at 95°C, then 40 cycles of three-step PCR including denaturing for 15 sec at 95°C, annealing for 30 sec at 58°C, and extension for 30 sec at 72°C, with an additional 15-second detection step at 81°C, followed by a melting profile from 55°C to 95°C at a rate of 0.5°C per 10 sec. 25 ng samples of cDNA were analyzed in quadruplicates in parallel with RPLP1/3 controls. Standard curves (threshold 1 cycle vs. log 2 pg cDNA) were generated from a series of log dilutions of standard cDNAs (reverse transcribed from mRNAs of RAW 264.7 cells in growth medium) from 0.1 pg to 100 ng. Initial quantities of experimental mRNA were then calculated from the standard curves and averaged using the SA Bioscience software. The ratio of the experimental four marker genes to RPLP1/3 mRNA was calculated and normalized to the 11.1 mM glucose control.

2.6. Collection of Supernatants from HG- and Tha-Treated Macrophages [17]. RAW 264.7 cells were seeded into six-well plates and cultured in 33.3 mM glucose, Tha50, Tha100, and Tha200 in 33.3 mM glucose, respectively. The supernatants were collected 24 hours later and centrifuged at 1500 *g* for 15 minutes and then labeled as (33.3 mM glucose) MS, (Tha50) MS, (Tha100) MS, and (Tha200) MS. The collected supernatants were filtered with 0.22 μm sterile membranes and used immediately.

2.7. Determination of TNF-α, IL-1β, Nephrin, and Podocin Expressions in Podocytes. Podocytes were separately treated with 11.1 mM glucose, 33.3 mM glucose, (33.3 mM glucose) MS, (Tha50) MS, (Tha100) MS, and (Tha200) MS. Cell supernatants were then harvested after 24 hours and centrifuged at 1500 *g* for 10 minutes at 4°C. TNF-α and IL-1β levels were determined by an ELISA kit (Catalog No. EK0527 and EK0394, Boster). Absorbance was measured using a microplate reader (Model 550; Bio-Rad Laboratories, Inc.). Each sample was repeatedly tested six times.

The treated podocytes were extracted and collected. Then, protein expressions of nephrin and podocin were determined using the method described in Section 2.4. Antibodies against corresponding proteins, nephrin (Catalog No. A01991, Boster) and podocin (Catalog No. BA1688-2, Boster), were used at 1 : 500 dilution. The procedure was repeated in triplicate for each sample.

2.8. Statistical Analysis. The SPSS 19.0 software (IBM, Armonk, NY, USA) was used for statistical analysis. Data were expressed as the mean ± standard error of the mean. Comparisons among groups were conducted by one-way analysis of variance followed by Dunnett's multiple comparisons test for continuous variables. All reported p values were two-tailed, and a $p < 0.05$ was considered statistically significant.

3. Results

3.1. Determination of HG-Induced Phenotypic Transition of M1 Macrophage. The analysis results indicated that the 12-, 24-, and 48-hour LPS-induced NO productions were significantly higher than those of DMSO (the solvent control of LPS) ($p < 0.001$, Figure 1). Taking 0.5 μg/ml LPS as a model control [16], we proceeded to study the concentration of HG.

No significant difference was seen between the 12-, 24-, and 48-hour incubation period NO productions of macrophages in the 25.0 mM glucose group and the 11.1 mM glucose group (all: p = NS).

The results also showed that the 12-, 24-, 48-hour incubation period macrophages in the 33.3 mM and 44.4 mM glucose groups had significantly higher nitrite levels as compared to the 11.1 mM glucose group (all: $p < 0.01$). No statistically significant difference in LPS-induced NO production was seen between the 33.3 mM and 44.4 mM glucose groups 24 hours and 48 hours after the treatment (all: p = NS).

The comparison between the 11.1 mM glucose and the DMSO groups indicated that NO production was significantly higher in the 11.1 mM glucose 48 hours after the treatment ($p = 0.005$). Meanwhile, no significant difference in NO production was seen between the two groups at 12-hour and 24-hour time points (both: p = NS).

Based on above results, the 33.3 mM glucose group and the 24 hours after treatment time point were used as the HG model, while the 11.1 mM glucose group was used as control for both 33.3 mM glucose and LPS.

When compared to 11.1 mM glucose, the LPS-treated, and the 33.3 mM glucose-treated macrophages, the Tha at 25, 50, 100, and 200 μg/ml groups did not exhibit any effects on NO production in 11.1 mM glucose-cultured macrophage. Data did not show.

3.2. Effects of Tha and HG on Podocytes and Macrophage Viability. Figure 2 shows that the survival rate of podocytes in the 33.3 mM glucose group decreased significantly compared to the 11.1 mM glucose group and also the mannitol control group (both: $p < 0.001$). When compared to the 33.3 mM glucose-treated podocytes, the Tha at 25, 50, 100, and 200 μg/ml groups did not exhibit any protective effects on podocyte cell viability. However, all Tha groups did not show further exacerbation of podocyte death, a trend seen in the 33.3 mM glucose group (all: p = NS).

No significant difference in macrophage survival rate was observed between the 33.3 mM glucose, the 11.1 mM glucose, and the mannitol control groups. The results showed that the four tested Tha concentrations had no significant influence on the cell survival rate compared to the 33.3 mM glucose-treated macrophages (all: p = NS).

Figure 2 also shows that the survival rate of podocytes in the mannitol control and the 11.1 mM glucose groups did not differ significantly (p = NS), neither did the survival rate of macrophages (p = NS).

3.3. The Effects of Tha on iNOS, TNF-α, Arg-1, and CD206 Protein Expressions in 33.3 mM Glucose-Induced Macrophages. Western blot was used to determine the effects of Tha on iNOS, TNF-α, Arg-1, and CD206 protein expressions. Figure 3 shows that compared to the 11.1 mM glucose group, both the LPS and 33.3 mM glucose-cultured RAW 264.7 cell groups exhibited a significant increase in iNOS

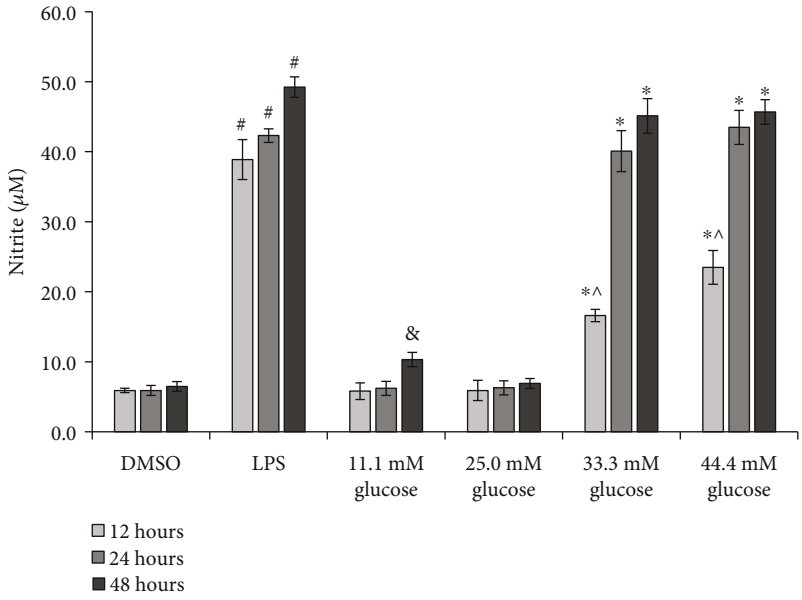

Figure 1: Effects of high glucose on nitric oxide production in RAW 264.7 cells. Values were expressed as the mean ± standard error of the mean ($n = 6$). $^{\#}p < 0.05$; LPS versus DMSO after 12, 24, and 48 hours' treatment separately. $^{*}p < 0.05$; 33.3 and 44.4 mM glucose versus 11.1 mM glucose after 12, 24, and 48 hours' treatment separately. $^{\wedge}p < 0.05$; 33.3 and 44.4 mM glucose versus LPS after 12 hours' treatment. $^{\&}p < 0.05$, 11.1 mM glucose versus DMSO after 48 hours' treatment. Abbreviations: LPS: lipopolysaccharide; DMSO: dimethyl sulfoxide, the solvent control of LPS.

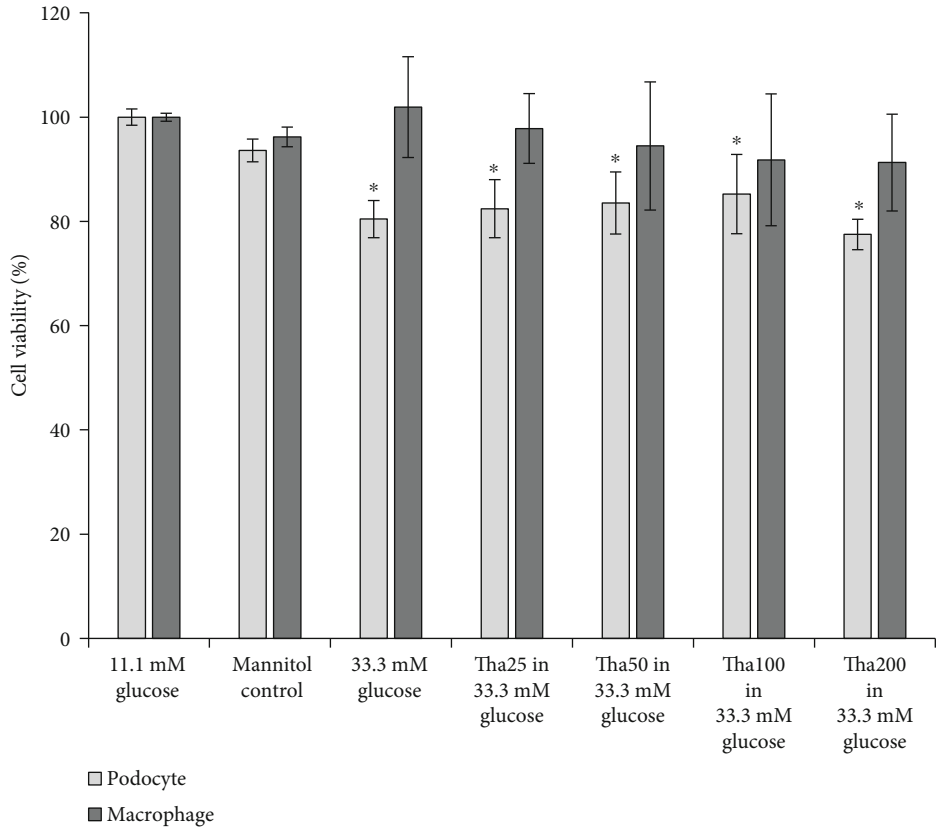

Figure 2: Effects of thalidomide on cell viability of podocyte and macrophage in 33.3 mM glucose. Values were expressed as the mean ± standard error ($n = 6$). $^{*}p < 0.05$; versus 11.1 mM glucose. Abbreviations: Tha25: 25 μg/ml thalidomide; Tha50: 50 μg/ml thalidomide; Tha100: 100 μg/ml thalidomide; Tha200: 200 μg/ml thalidomide.

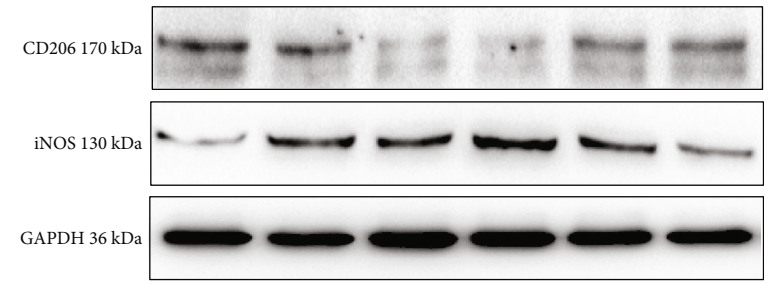

(a)

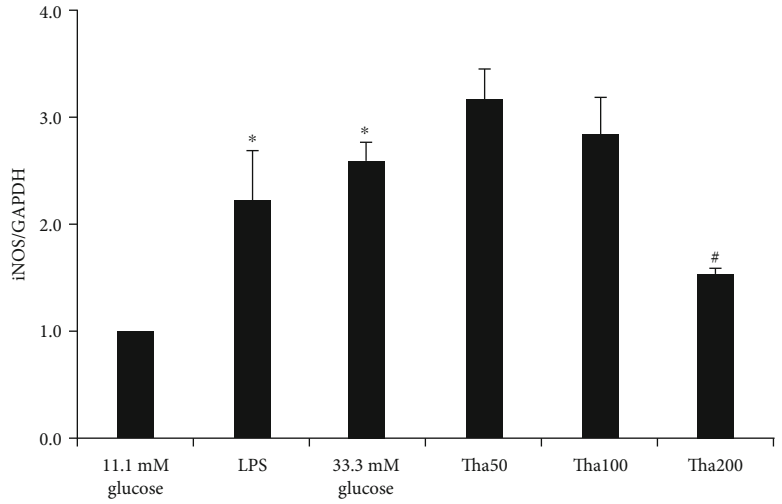

(b)

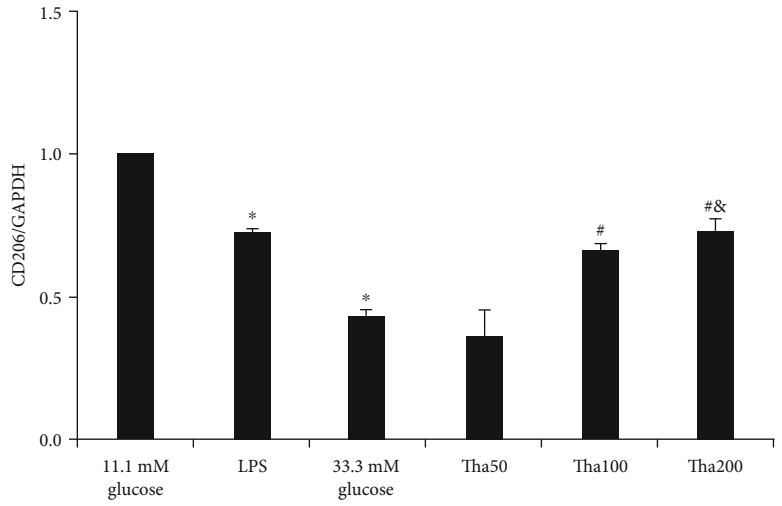

(c)

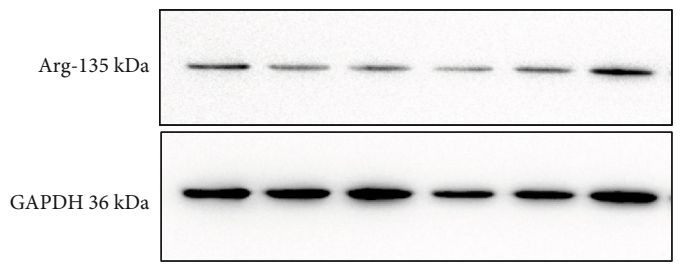

(d)

Figure 3: Continued.

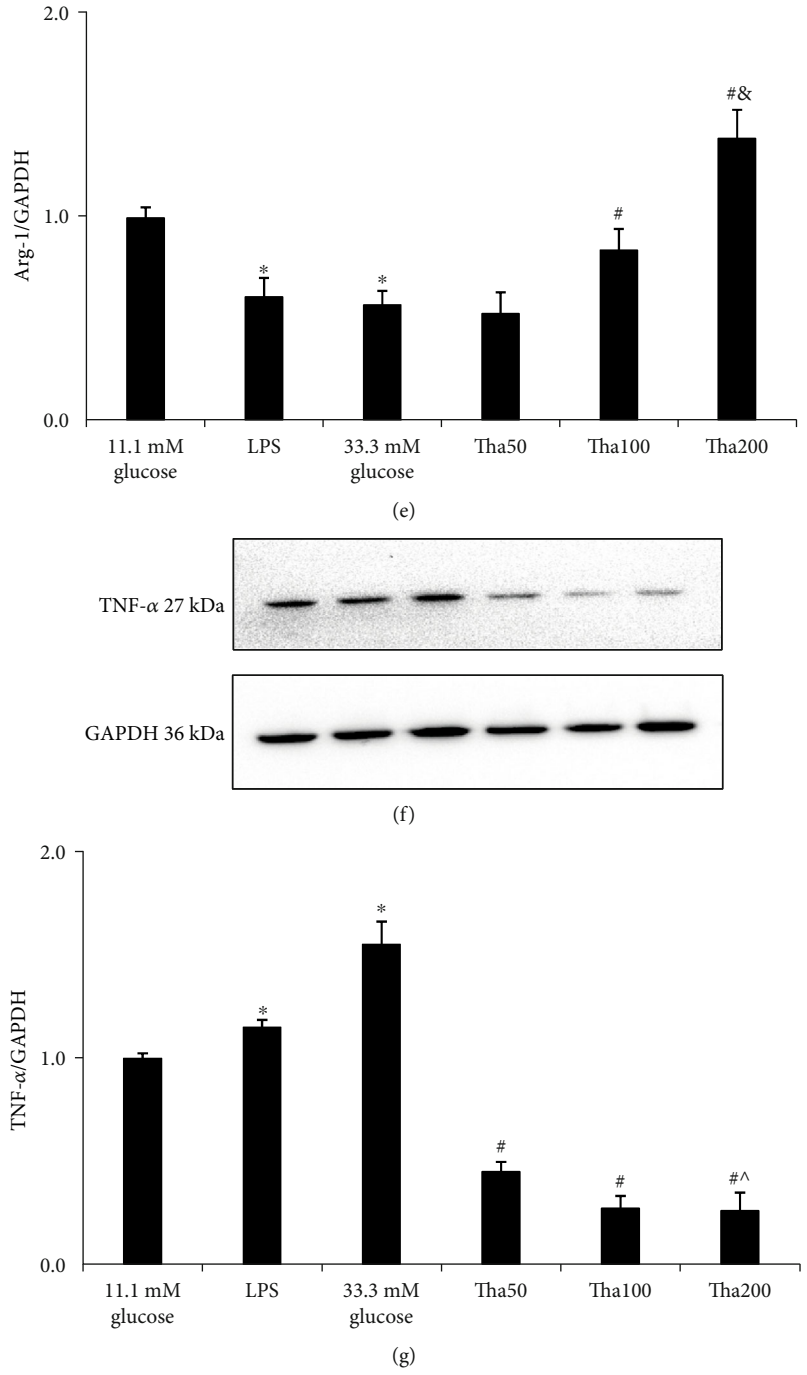

Figure 3: Effects of thalidomide on iNOS, CD206, Arg-1 and TNF-α protein expression in 33.3 mM glucose-induced macrophage. (a) iNOS and CD206 protein expressions. (d) Arg-1 protein expression. (f) TNF-α protein expression. The results of iNOS, CD206, Arg-1, and TNF-α were represented in (b), (c), (e), and (g), respectively. All results were expressed as a ration with respect to control and represented as the mean ± SD in triplicates. $^{*}p < 0.05$; versus 11.1 mM glucose. $^{\#}p < 0.05$; versus 33.3 mM glucose. $^{\&}p < 0.05$; versus Tha100. $^{\wedge}p < 0.05$; versus Tha50. Abbreviations: LPS: lipopolysaccharide; Tha50: 50 μg/ml thalidomide in 33.3 mM glucose; Tha100: 100 μg/ml thalidomide in 33.3 mM glucose; Tha200: 200 μg/ml thalidomide in 33.3 mM glucose; iNOS: inducible nitric oxide synthase; CD206: mannose receptor; TNF-α: tumor necrosis factor-α; Arg-1: arginase-1.

and TNF-α protein expressions and a significant decrease in Arg-1 and CD206 protein expressions ($p < 0.05$).

The above results further confirmed that the 0.5 μg/ml LPS, as a model control [16], induced M1 polarization but decreased M2 polarization. There were no significant differences in iNOS, TNF-α, CD206, and Arg-1 expressions between the LPS model and the 33.3 mM glucose model (all: p = NS).

The results of the four different Tha concentrations indicated that compared to the 33.3 mM glucose group, the 50 μg/ml Tha concentration significantly suppressed TNF-α expression ($p = 0.001$), while Tha with 100 μg/ml

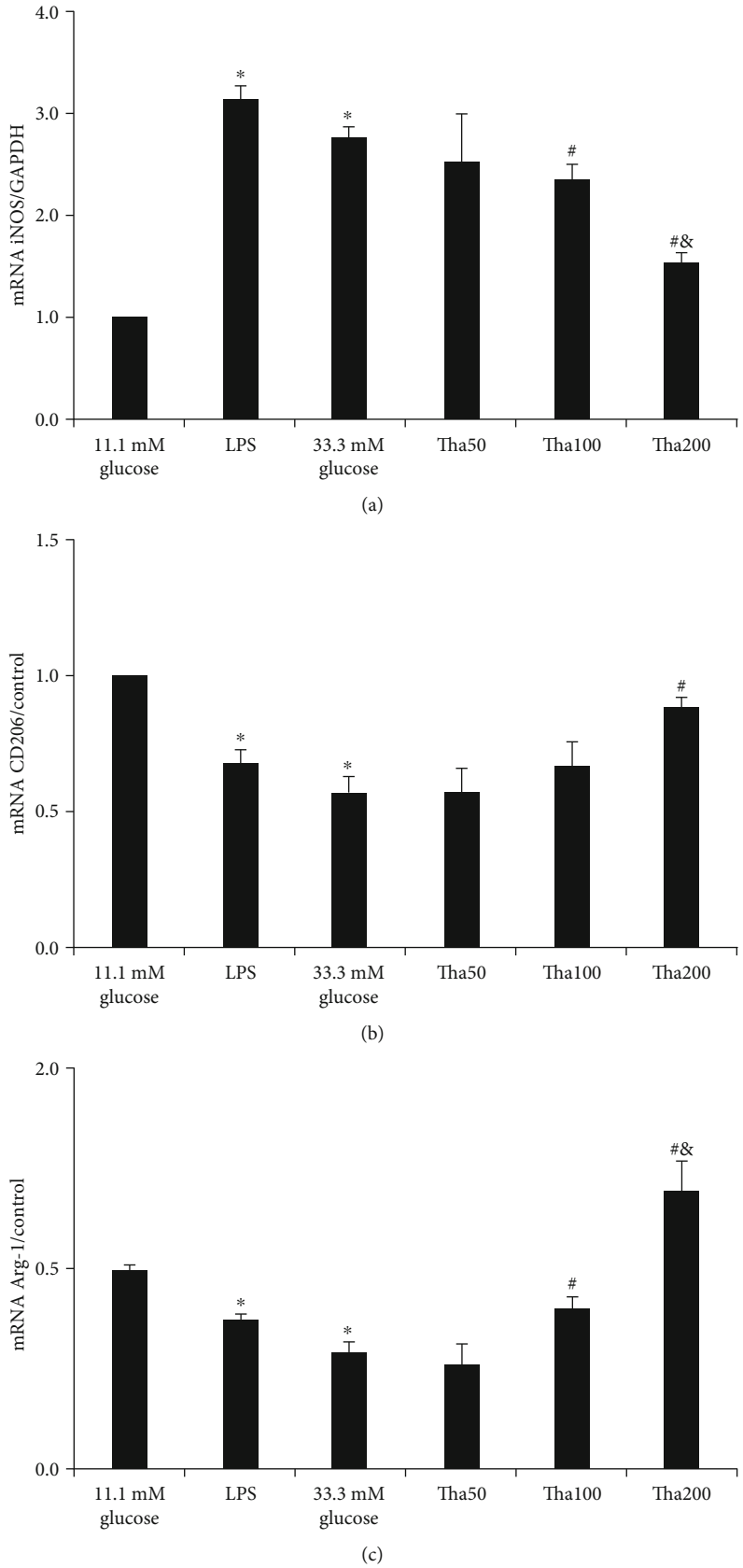

Figure 4: Continued.

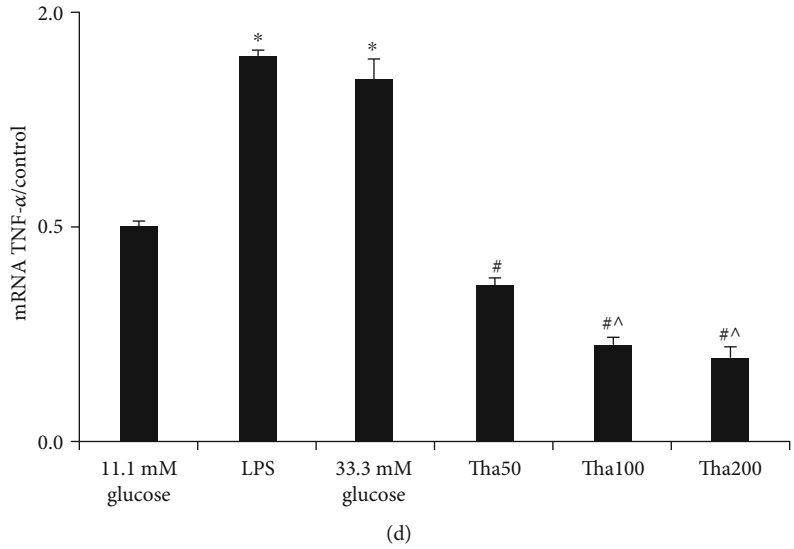

Figure 4: Effects of thalidomide on iNOS, CD206, Arg-1, and TNF-α mRNA expressions in 33.3 mM glucose-induced macrophage. (a) iNOS mRNA expression. (b) CD206 mRNA expression. (c) CD206 mRNA expression. (d) TNF-α mRNA expression.All the results were represented as the mean ± SD in triplicates $^{*}p < 0.05$; versus 11.1 mM glucose. $^{\#}p < 0.05$; versus 33.3 mM glucose. $^{\&}p < 0.05$; versus Tha100. $^{\wedge}p < 0.05$; versus Tha50. Abbreviations: LPS: lipopolysaccharide; Tha50: 50 μg/ml thalidomide in 33.3 mM glucose; Tha100: 100 μg/ml thalidomide in 33.3 mM glucose; Tha200: 200 μg/ml thalidomide in 33.3 mM glucose; iNOS: inducible nitric oxide synthase; CD206: mannose receptor; TNF-α: tumor necrosis factor-α; Arg-1: arginase-1.

concentration showed significant effects on TNF-α, CD206, and Arg-1 expressions (all: $p < 0.05$). Additionally, the 200 μg/ml Tha concentration also had significant effects on TNF-α, iNOS, CD206, and Arg-1 expressions (all: $p < 0.05$).

The between different Tha concentrations analysis indicated that the 200 μg/ml Tha concentration showed not only significant effects on CD206 and Arg-1 compared to the 100 μg/ml concentration ($p = 0.027$ and $p = 0.007$, respectively) but also showed significant effects on TNF-α compared to the 50 μg/ml concentration ($p = 0.047$).

3.4. Effects of Tha on iNOS, TNF-α, Arg-1, and CD206 mRNA Expressions in 33.3 mM HG-Induced Macrophages. qPCR was used to determine the effects of Tha on iNOS, TNF-α, Arg-1, and CD206 mRNA expressions. Compared to the 11.1 mM glucose group, both the LPS and the 33.3 mM glucose groups showed a significant increase in iNOS and TNF-α mRNA expressions and a significant decrease in Arg-1 as well as CD206 mRNA expressions (all: $p < 0.05$).

The 200 μg/ml Tha group exhibited significant effects on iNOS, TNF-α, CD206, and Arg-1 expressions compared to the 33.3 mM glucose group (all: $p < 0.05$). Additionally, the 100 μg/ml Tha group also showed significant effects on iNOS, TNF-α, and Arg-1 expressions compared to the 33.3 mM glucose group (all: $p < 0.05$). The analysis involving the 50 μg/ml Tha group indicated that 50 μg/ml Tha significantly decreased TNF-α expression ($p = 0.001$).

Tha 200 μg/ml concentration showed significant effects on iNOS and Arg-1 compared to Tha 100 μg/ml ($p = 0.003$ and $p = 0.011$). Tha at both 100 μg/ml and 200 μg/ml concentrations had significant effects on TNF-α compared to Tha 50 μg/ml concentration ($p = 0.002$ and $p = 0.001$). The above results are shown in Figure 4.

3.5. Determination of TNF-α and IL-1β Levels in Podocytes. We can see from Figure 5 that compared to the 11.1 mM glucose group, TNF-α levels increased significantly after 33.3 mM glucose stimulation ((76.9 ± 1.6) pg/ml *vs.* (27.0 ± 2.5) pg/ml, $p < 0.001$). Additionally, the (33.3 mM glucose) MS group showed significant promotion of TNF-α levels in podocytes ((107.5 ± 3.5) pg/ml) compared to the 33.3 mM glucose group ($p < 0.001$).

The (Tha50) MS, (Tha100) MS, and (Tha200) MS groups showed a significant decrease in TNF-α levels compared to that of the (33.3 mM glucose) MS group (all: $p < 0.001$). TNF-α levels of both the (Tha100) MS and (Tha200) MS groups were significantly lower than those of the 33.3 mM glucose group ((67.9 ± 3.1) pg/ml and (61.0 ± 2.5) pg/ml *vs.* (76.9 ± 1.6) pg/ml, both: $p < 0.01$).

The comparison in IL-1β levels between the 33.3 mM glucose group ((37.5 ± 2.1) pg/ml) and the 11.1 mM glucose group ((18.0 ± 1.2) pg/ml) indicated a significant difference between the two groups ($p < 0.001$). The results also showed that IL-1β was significantly promoted in the (33.3 mM glucose) MS group ((52.0 ± 2.2) pg/ml) compared to the 33.3 mM glucose group ($p < 0.001$).

Additionally, IL-1β levels were significantly lower in the (Tha100) MS and (Tha200) MS groups as compared to the (33.3 mM glucose) MS group (both: $p < 0.001$), with those levels being significantly decreased in the (Tha200) MS group compared to the 33.3 mM glucose group ($p = 0.003$).

3.6. Determination of Nephrin and Podocin Protein Expressions in Podocytes. Both nephrin and podocin expressions were significantly lower in the 33.3 mM glucose group than in the 11.1 mM glucose group (Figure 6, both: $p < 0.01$). The results also showed a further decrease in nephrin and podocin expressions in the (33.3 mM

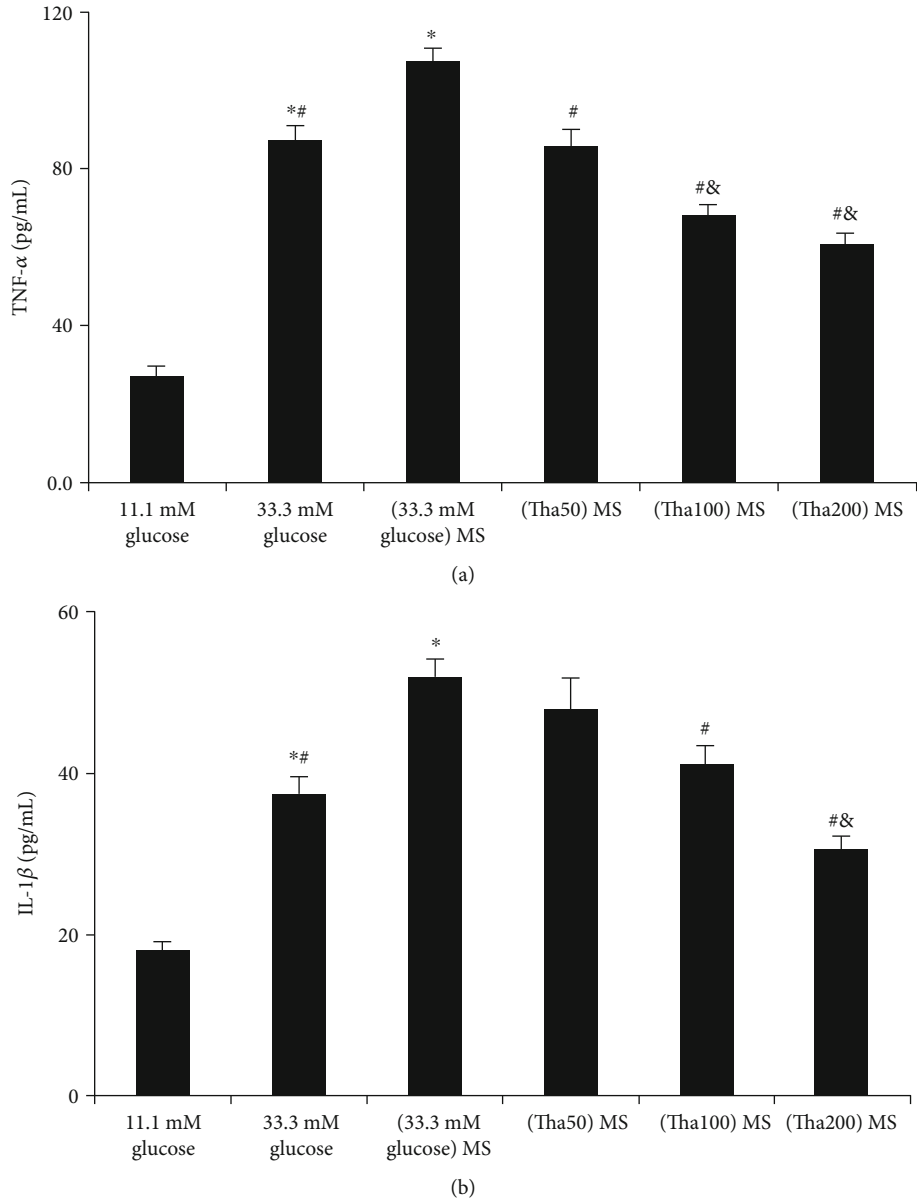

Figure 5: Effects of thalidomide on TNF-α and IL-1β level in podocyte. (a) TNF-α level. (b) IL-1β level. Values were expressed as the mean ± standard error of the mean ($n = 6$). $^{*}p < 0.05$; versus 11.1 mM glucose. $^{\#}p < 0.05$; versus (33.3 mM glucose) MS. $^{\&}p < 0.05$; versus 33.3 mM glucose. Abbreviations: (33.3 mM glucose) MS: the supernatant from 33.3 mM glucose-treated macrophage; (Tha50) MS: supernatant from 50 μg/ml thalidomide and 33.3 mM glucose-treated macrophage; (Tha100) MS: supernatant from 100 μg/ml thalidomide and 33.3 mM glucose-treated macrophage; (Tha200) MS: supernatant from 200 μg/ml thalidomide and 33.3 mM glucose-treated macrophage.

glucose) MS group as compared to the 33.3 mM glucose group (both: $p < 0.01$).

The Tha-related results indicated a significant increase in nephrin and podocin expressions in the (Tha200) MS group as compared to the (33.3 mM glucose) MS group (both: $p < 0.001$) and a significant increase in podocin expressions when compared to the 33.3 mM glucose group ($p = 0.006$).

4. Discussion

During the past 30 years, Tha and its analogs could be alternatively used in the treatment of neurological and renal diseases such as dyskinesia [18], Alzheimer's disease [19], lupus nephritis [20], and DKD [9] due to its immunomodulatory properties. It is reported that Alzheimer's disease is progressed by activated microglia, the resident brain macrophage, and release inflammatory mediators such as TNF-α [21]. A study demonstrates that human umbilical cord-derived mesenchymal stem cells ameliorated lupus nephritis by preventing podocyte injury possibly through reducing macrophage infiltration and polarizing macrophage into an anti-inflammatory phenotype [22].

Our preliminary work on streptozotocin-induced rats showed that Tha suppressed the inflammatory and fibrotic

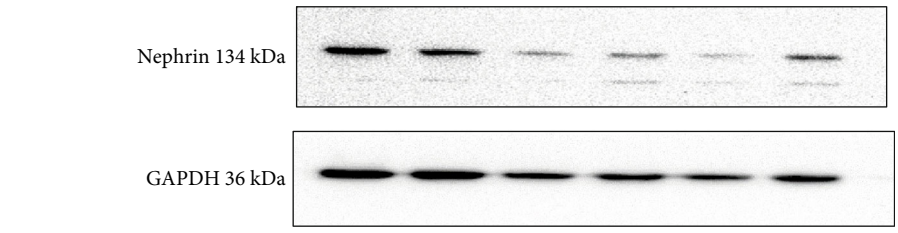

(a)

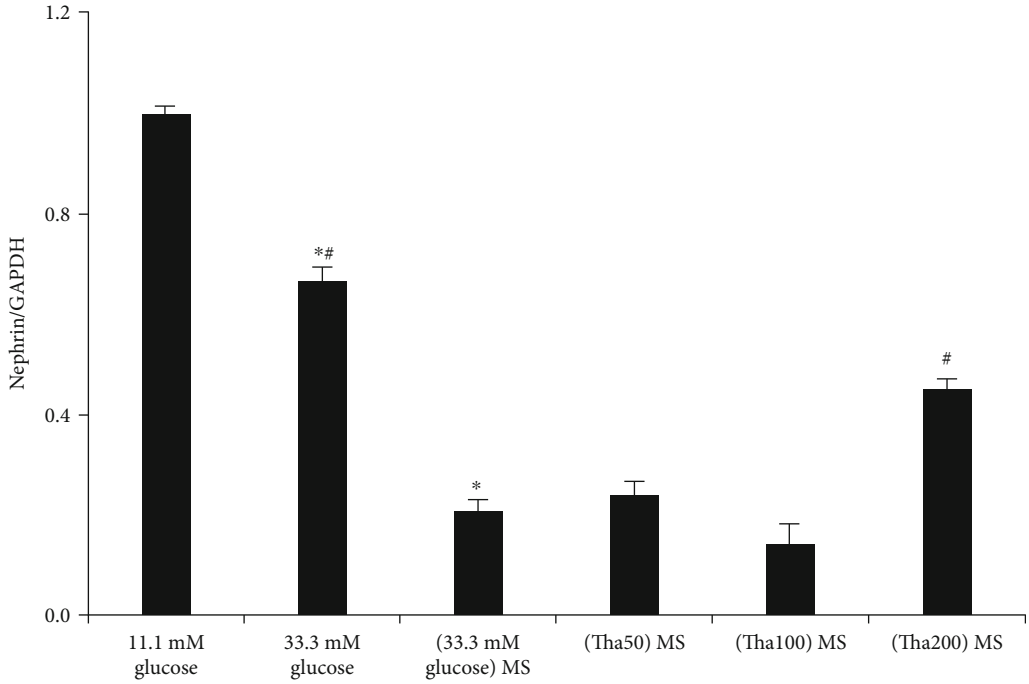

(b)

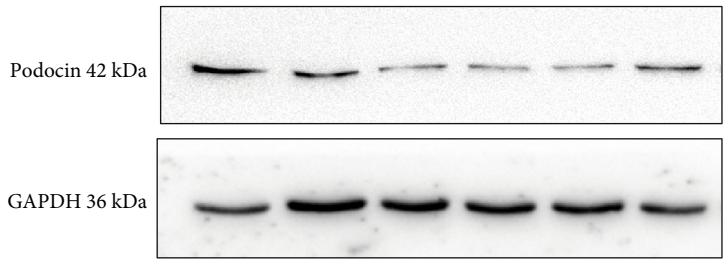

(c)

Figure 6: Continued.

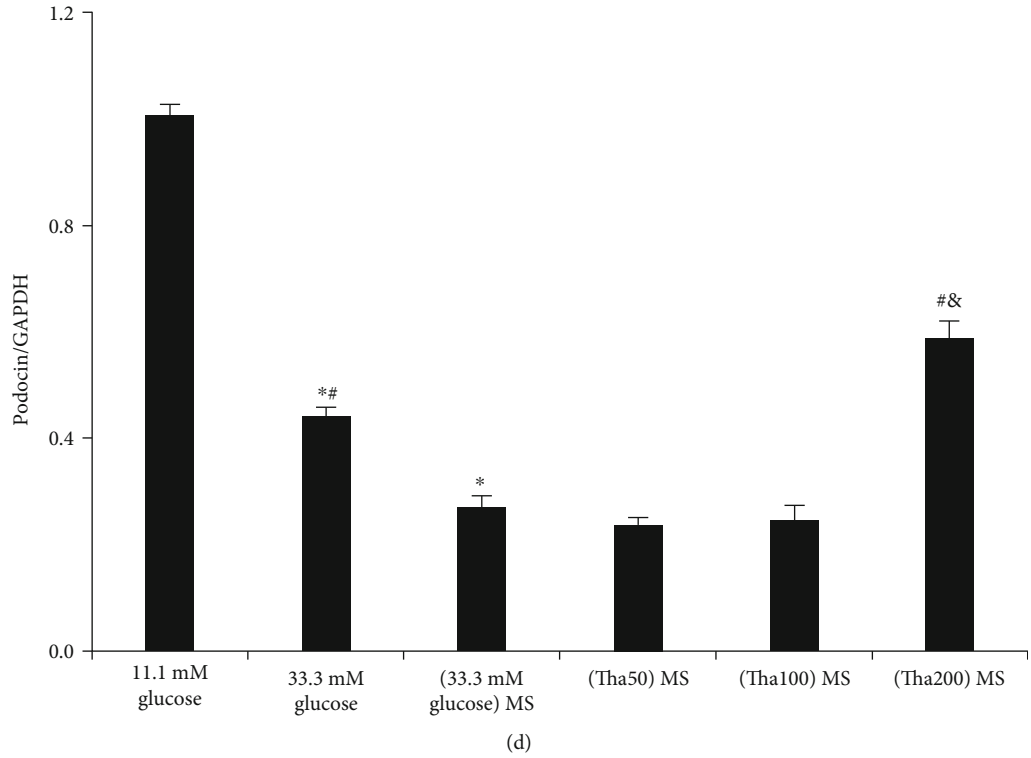

Figure 6: Effects of thalidomide on nephrin and podocin protein expressions in podocyte. (a) Nephrin expression. (c) Podocin expression. The results of nephrin and podocin were represented in (b) and (d). $^{*}p < 0.05$; versus 11.1 mM glucose. $^{\#}p < 0.05$; versus (33.3 mM glucose) MS. $^{\&}p < 0.05$; versus 33.3 mM glucose. Abbreviations: (33.3 mM glucose) MS: the supernatant from 33.3 mM glucose-treated macrophage. (Tha50) MS: supernatant from 50 μg/ml thalidomide and 33.3 mM glucose-treated macrophage; (Tha100) MS: supernatant from 100 μg/ml thalidomide and 33.3 mM glucose-treated macrophage; (Tha200) MS: supernatant from 200 μg/ml thalidomide and 33.3 mM glucose-treated macrophage.

processes in diabetic renal injury [8]. These effects were partly mediated by the activation of AMPKα and inhibition of the NF-κB/MCP-1 and TGF-β1/Smad signaling pathways [7]. The renoprotective effects of Tha were further confirmed clinically [9].

DKD is one of the major complications of diabetes mellitus and is currently the most common cause of end-stage renal disease in China [23]. Recent growing evidence hinted at the participation of immunologic and inflammatory mechanisms in the development and progression of DKD [24]. Macrophage polarization plays a pivotal role in the process of inflammation, a common occurrence in DKD. Therefore, interventions during the M1 and M2 macrophage polarization processes might be a novel therapeutic strategy for DKD [25].

Previous reports have shown that the M1 phenotype can be induced by LPS [16]. The inhibition of iNOS in LPS-induced macrophages may prove to be an important target for the anti-inflammatory effects of Tha [26]. LPS was used in our previous study to induce iNOS [15] and was considered as the model control in the present study.

As a TNF-α inhibitor [27], Tha had downregulatory effects on 33.3 mM glucose-induced iNOS and TNF-α mRNA and protein expressions in our present study. Both iNOS and TNF-α have been regarded as markers of the M1 subtype [28, 29]. Our results also showed that treatment with 33.3 mM glucose significantly downregulated Arg-1 and CD206 protein and mRNA expressions in macrophages, an effect that was reversed with Tha treatment. Interestingly, many studies have established that the upregulation of CD206 and Arg-1 is an important indicator of M2 polarization [30, 31]. This is to our knowledge the first study to explore the effects of Tha on markers of the M2 subtype.

A previous study revealed that activated macrophage played a crucial role in the injury of podocytes located in the outer layer of the filtration barrier. Such injury plays an important role in the inflammatory processes of DKD [11]. We could see that the survival rate of podocytes decreased significantly after treatment with 33.3 mM glucose. Tha neither alleviated nor aggravated the mortality rate of 33.3 mM glucose-cultured podocytes.

According to the present study, two kinds of cells are involved in the inflammatory process: the bone marrow-derived leukocytes, including neutrophils and macrophages, which are firstly activated, and the renal cells such as mesangial cells and podocytes [32]. We hypothesized that Tha has protective impacts on HG-induced podocyte injury via modulation of M1/M2 differentiation. To assess this hypothesis, we used supernatants from 33.3 mM glucose-treated and Tha-treated macrophages to treat podocytes (*in vitro*).

Podocin and nephrin are podocyte-specific markers, and a decrease in their expressions is indicative of podocyte damage [33]. Our results showed that podocin and nephrin protein expressions in the (33.3 mM glucose) MS-cultured

podocytes were significantly lower than those in the 33.3 mM glucose-cultured podocytes. This confirmed that HG-induced macrophage polarization aggravated HG-induced podocyte injury. On the other hand, the increase in podocin and nephrin expressions in the (Tha200) MS group proved that the protective effects of Tha might be related to the used supernatant.

Another study demonstrated that activated macrophages could induce podocyte injury via a TNF-α-JNK/p38-dependent mechanism [34]. Many inflammatory factors, such as TNF-α, IL-1β, IL-6, and IL-17, took part in the inflammation process and contributed to podocyte injury [35]. Our research demonstrated that the increase in TNF-α and IL-1β expressions played an important role in the podocyte injury process *in vitro*. The decreasing effect of Tha on TNF-α and IL-1β levels might explain the protective effects of Tha on podocyte injury via the macrophage supernatant.

It was previously revealed that vitamin D and calcineurin inhibitor prevented podocyte injury via regulation of macrophage M1/M2 phenotype in diabetic nephropathy rats [36, 37]. The connection between macrophage phenotype and its relationship with renal function and histological changes in human DKD has been extensively explored. It was demonstrated that there is a positive correlation between the M1/M2 differentiation state and the progress of DKD [38].

Metformin showed its podocyte-protective capacity in type 2 diabetic patients, and the underlying mechanisms might be partly attributable to its effects on the M1 polarization-related MIF-CD74 axis [39, 40]. Further exploratory studies on the protective effects of Tha on podocyte via modulation of the balance between the M1/M2 phenotype should be conducted in DKD animal models. The balance between M1/M2 on different progress of DKD models, such as early stages and late chronic tissue damage, will be further compared in our future researches.

Many studies suggested that DKD podocyte injury is induced by the association of multiple factors, including inflammatory reaction, oxidative stress, TGF-β1 induction, renin angiotensin aldosterone system activation, and AGEs accumulation [41]. At present study, we just focused only on NO, TNF-α, and IL-1β as proinflammatory cytokines produced by activated macrophage. The precise mechanism of macrophage-mediated podocyte injury induced by HG, and how podocytes themselves involve in the pathogenesis of DKD should be demonstrated in our future study.

From the perspective of drug toxicity, our research did not indicate significant Tha toxicity on used macrophages and podocytes in 33.3 mM glucose. However, we should still focus on daily dose-dependent toxicity and cumulative dose-dependent toxicity of Tha in animal researches [42–44]. A clinical phase II trial of Tha in patients with metastatic renal cell carcinoma was performed; the results showed that low doses of Tha resulted in manageable toxicity, better response rates, and progression-free survival [43]. However, high doses of Tha are not recommended [42], and reports have shown that a cumulative dose greater than 20 g represented a risk factor [44].

As a therapeutic alternative to traditional anti-TNF-α compounds, we should pay more attention to its dose-related side effects, with the most notable being peripheral neuropathy [45]. Many analogs of Tha, such as lenalidomide and pomalidomide, were clinically studied for the treatment of relapsed or refractory multiple myeloma [46, 47]. Simultaneously, the safety parameters of these analogs were closely monitored to achieve maximum clinical benefit [46, 47].

Summary of our results is as follows: (1) Macrophage M1/M2 polarization could be induced by 33.3 mM glucose, and Tha exhibited modulatory effects on the M1/M2 phenotype. (2) 33.3 mM glucose decreased nephrin and podocin expressions in podocytes *in vitro*. 33.3 mM glucose-induced macrophage M1/M2 polarization further exacerbated the decrease in nephrin and podocin expressions. (3) Tha displayed indirect protective effects on podocyte injury through modulation of macrophage M1/M2 differentiation-related activities. (4) Tha-related side effects should always be the center of attention during the experiment.

Data Availability

The data used to support the findings of this study are available from the corresponding author upon request.

Conflicts of Interest

The authors declare that they have no conflicts of interest.

Authors' Contributions

Hui Liao and Yuanping Li have contributed equally to this work.

Acknowledgments

This study was supported by the Basic Research Project of Shanxi Province (Key Fund Project) (No. 201701D111001), the Provincial Special Supporting Fund Scientific Research Project of Shanxi Provincial People's Hospital (No. SZ2019003 and No. SZ2019007), and the Key R&D Project of Shanxi Province (International Scientific and Technological Cooperation, Independent Topics, No. 201903D421061).

References

[1] A. K. Stewart, "How thalidomide works against cancer," *Science*, vol. 343, no. 6168, pp. 256-257, 2014.

[2] E. P. Sampaio, E. N. Sarno, R. Galilly, Z. A. Cohn, and G. Kaplan, "Thalidomide selectively inhibits tumor necrosis factor alpha production by stimulated human monocytes," *The Journal of Experimental Medicine*, vol. 173, no. 3, pp. 699–703, 1991.

[3] W. Rehman, L. M. Arfons, and H. M. Lazarus, "The rise, fall and subsequent triumph of thalidomide: lessons learned in drug development," *Therapeutic Advances in Hematology*, vol. 2, no. 5, pp. 291–308, 2011.

[4] C. H. Y. van Beurden-Tan, M. G. Franken, H. M. Blommestein, C. A. Uyl-de Groot, and P. Sonneveld, "Systematic literature review and network meta-analysis of treatment outcomes in relapsed and/or refractory multiple myeloma," *Journal of Clinical Oncology*, vol. 35, no. 12, pp. 1312–1319, 2017.

[5] Y. Ozguler, P. Leccese, R. Christensen et al., "Management of major organ involvement of Behçet's syndrome: a systematic review for update of the EULAR recommendations," *Rheumatology*, vol. 57, no. 12, pp. 2200–2212, 2018.

[6] M. Bramuzzo, A. Ventura, S. Martelossi, and M. Lazzerini, "Thalidomide for inflammatory bowel disease: systematic review," *Medicine*, vol. 95, no. 30, pp. 1–15, 2016.

[7] H. X. Zhang, J. Yuan, Y. F. Li, and R.-S. Li, "Thalidomide decreases high glucose-induced extracellular matrix protein synthesis in mesangial cells via the AMPK pathway," *Experimental and Therapeutic Medicine*, vol. 17, no. 1, pp. 927–934, 2019.

[8] H. Zhang, Y. Yang, Y. Wang, B. Wang, and R. Li, "Renal-protective effect of thalidomide in streptozotocin-induced diabetic rats through anti-inflammatory pathway," *Drug Design, Development and Therapy*, vol. Volume 12, pp. 89–98, 2018.

[9] Y. Gao, G. Wang, Y. Cheng, and R. Li, "Observation on the therapeutic effect of thalidomide on diabetic nephropathy," *Chinese Remedies & Clinics*, vol. 18, no. 8, pp. 1345-1346, 2018.

[10] F. B. Hickey and F. Martin, "Role of the immune system in diabetic kidney disease," *Current Diabetes Reports*, vol. 18, no. 4, article 20, 2018.

[11] J. Lu, Y. Yang, J. Peng et al., "Trichosanthes kirilowii lectin ameliorates streptozocin-induced kidney injury via modulation of the balance between M1/M2 phenotype macrophage," *Biomedicine & Pharmacotherapy*, vol. 109, pp. 93–102, 2019.

[12] A. S. Awad, H. You, T. Gao et al., "Macrophage-derived tumor necrosis factor-α mediates diabetic renal injury," *Kidney International*, vol. 88, no. 4, pp. 722–733, 2015.

[13] X. Zhang, M. Zhou, Y. Guo, Z. Song, and B. Liu, "1,25-Dihydroxyvitamin D3 promotes high glucose-induced M1 macrophage switching to M2 via the VDR-PPARγ signaling pathway," *BioMed Research International*, vol. 2015, Article ID 157834, 14 pages, 2015.

[14] Y. Zhao, Y. Guo, Y. Jiang, X. Zhu, Y. Liu, and X. Zhang, "Mitophagy regulates macrophage phenotype in diabetic nephropathy rats," *Biochemical and Biophysical Research Communications*, vol. 494, no. 1–2, pp. 42–50, 2017.

[15] H. Liao, "Effects of Shengjiang (Zingiberis Rhizoma Recens) and its processed products on nitric oxide production in macrophage RAW 264.7 cells," *Evidence-based Complementary and Alternative Medicine*, vol. 2015, Article ID 828156, 5 pages, 2015.

[16] C. Cunha, C. Gomes, A. R. Vaz, and D. Brites, "Exploring new inflammatory biomarkers and pathways during LPS-induced M1 polarization," *Mediators of Inflammation*, vol. 2016, Article ID 6986175, 17 pages, 2016.

[17] A. M. C. Martins, A. C. L. Nobre, A. C. Almeida et al., "Thalidomide and pentoxifylline block the renal effects of supernatants of macrophages activated with Crotalus durissus cascavella venom," *Brazilian Journal of Medical and Biological Research*, vol. 37, no. 10, pp. 1525–1530, 2004.

[18] L. Boi, A. Pisanu, N. H. Greig et al., "Immunomodulatory drugs alleviate l-dopa-induced dyskinesia in a rat model of Parkinson's disease," *Movement Disorders*, vol. 34, no. 12, pp. 1818–1830, 2019.

[19] B. Decourt, D. K. Lahiri, and M. N. Sabbagh, "Targeting tumor necrosis factor alpha for Alzheimer's disease," *Current Alzheimer Research*, vol. 14, no. 4, pp. 412–425, 2017.

[20] Y. Wang, M. H. Li, Y. Zhang, X. Y. Hu, and R. X. Ma, "Relationship between podocyte injury and macrophage infiltration in renal tissues of patients with lupus nephritis," *Journal of Peking University (Health Sciences)*, vol. 51, no. 4, pp. 723–727, 2019.

[21] D. Kempuraj, R. Thangavel, P. A. Natteru et al., "Neuroinflammation induces neurodegeneration," *Journal of Neurology, Neurosurgery and Spine*, vol. 1, no. 1, pp. 1–15, 2016.

[22] Z. Zhang, L. Niu, X. Tang et al., "Mesenchymal stem cells prevent podocyte injury in lupus-prone B6.MRL-Faslprmice via polarizing macrophage into an anti-inflammatory phenotype," *Nephrology, Dialysis, Transplantation*, vol. 34, no. 4, pp. 597–605, 2019.

[23] L. Zhang, J. Long, W. Jiang et al., "Trends in chronic kidney disease in China," *The New England Journal of Medicine*, vol. 375, no. 9, pp. 905-906, 2016.

[24] X. Yang and S. Mou, "Role of immune cells in diabetic kidney disease," *Current Gene Therapy*, vol. 17, no. 6, pp. 424–433, 2017.

[25] C. Li, X. Y. Ding, D. M. Xiang et al., "Enhanced M1 and impaired M2 macrophage polarization and reduced mitochondrial biogenesis via inhibition of AMP kinase in chronic kidney disease," *Cellular Physiology and Biochemistry*, vol. 36, no. 1, pp. 358–372, 2015.

[26] E. Park, W. R. Levis, N. Greig, E. Jung, and G. Schuller-Levis, "Effect of thalidomide on nitric oxide production in lipopolysaccharide-activated RAW 264.7 cells," *Journal of Drugs in Dermatology*, vol. 9, no. 4, pp. 330–333, 2010.

[27] T.-H. Li, P. C. Lee, K. C. Lee et al., "Down-regulation of common NFκB-iNOS pathway by chronic thalidomide treatment improves hepatopulmonary syndrome and muscle wasting in rats with biliary cirrhosis," *Scientific Reports*, vol. 6, no. 1, pp. 1–14, 2016.

[28] S. He, Q. Hu, X. Xu et al., "Advanced glycation end products enhance M1 macrophage polarization by activating the MAPK pathway," *Biochemical and Biophysical Research Communications*, vol. 525, no. 2, pp. 334–340, 2020.

[29] T. Maehara and K. Fujimori, "Contribution of FP receptors in M1 macrophage polarization via IL-10-regulated nuclear translocation of NF-κB p65," *Biochimica et Biophysica Acta (BBA) - Molecular and Cell Biology of Lipids*, vol. 1865, no. 5, pp. 158654–158658, 2020.

[30] A. Nawaz, A. Aminuddin, T. Kado et al., "$CD206^+$ M2-like macrophages regulate systemic glucose metabolism by inhibiting proliferation of adipocyte progenitors," *Nature Communications*, vol. 8, no. 1, article 286, 2017.

[31] Y. Jiang, J. Wang, H. Li, and L. Xia, "IL-35 promotes microglial M2 polarization in a rat model of diabetic neuropathic pain," *Archives of Biochemistry and Biophysics*, vol. 685, article 108330, 2020.

[32] X. M. Meng, "Inflammatory mediators and renal fibrosis," *Advances in Experimental Medicine and Biology*, vol. 1165, pp. 381–406, 2019.

[33] G. B. Singh, N. Kshirasagar, S. Patibandla, G. Puchchakayala, S. Koka, and K. M. Boini, "Nicotine instigates podocyte injury via NLRP3 inflammasomes activation," *Aging*, vol. 11, no. 24, pp. 12810–12821, 2019.

[34] Y. Ikezumi, T. Suzuki, T. Karasawa, H. Kawachi, D. J. Nikolic-Paterson, and M. Uchiyama, "Activated macrophages down-regulate podocyte nephrin and podocin expression via stress-activated protein kinases," *Biochemical and Biophysical Research Communications*, vol. 376, no. 4, pp. 706–711, 2008.

[35] F. Ren, M. Zhang, C. Zhang, and H. Sang, "Psoriasis-like inflammation induced renal dysfunction through the TLR/NF-κB signal pathway," *BioMed Research International*, vol. 2020, Article ID 3535264, 11 pages, 2020.

[36] X. L. Zhang, Y. F. Guo, Z. X. Song, and M. Zhou, "Vitamin D prevents podocyte injury via regulation of macrophage M1/M2 phenotype in diabetic nephropathy rats," *Endocrinology*, vol. 155, no. 12, pp. 4939–4950, 2014.

[37] X. M. Qi, J. Wang, X. X. Xu, Y. Y. Li, and Y. G. Wu, "FK506 reduces albuminuria through improving podocyte nephrin and podocin expression in diabetic rats," *Inflammation Research*, vol. 65, no. 2, pp. 103–114, 2016.

[38] X. Zhang, Y. Yang, and Y. Zhao, "Macrophage phenotype and its relationship with renal function in human diabetic nephropathy," *PLoS One*, vol. 14, no. 9, p. e0221991, 2019.

[39] Y. Xing, S. Ye, Y. Chen, A. Fan, Z. Xu, and W. Jiang, "MIF/CD74 axis is a target for metformin therapy in diabetic podocytopathy–real world evidence," *Endokrynologia Polska*, vol. 69, no. 3, pp. 264–268, 2018.

[40] Y. Zhou, W. Guo, Z. Zhu et al., "Macrophage migration inhibitory factor facilitates production of CCL5 in astrocytes following rat spinal cord injury," *Journal of Neuroinflammation*, vol. 15, no. 1, article 253, 2018.

[41] H. Dai, Q. Liu, and B. Liu, "Research progress on mechanism of podocyte depletion in diabetic nephropathy," *Journal of Diabetes Research*, vol. 2017, Article ID 2615286, 10 pages, 2017.

[42] B. Escudier, N. Lassau, D. Couanet et al., "Phase II trial of thalidomide in renal-cell carcinoma," *Annals of Oncology*, vol. 13, no. 7, pp. 1029–1035, 2002.

[43] M. A. Tunio, A. Hashmi, A. Qayyum, N. Naimatullah, and R. Masood, "Low-dose thalidomide in patients with metastatic renal cell carcinoma," *Journal of the Pakistan Medical Association*, vol. 62, no. 9, pp. 876–879, 2012.

[44] C. S. Yang, C. Kim, and R. J. Antaya, "Review of thalidomide use in the pediatric population," *Journal of the American Academy of Dermatology*, vol. 72, no. 4, pp. 703–711, 2015.

[45] S. Bastuji-Garin, S. Ochonisky, P. Bouche et al., "Incidence and risk factors for thalidomide neuropathy: a prospective study of 135 dermatologic patients," *Journal of Investigative Dermatology*, vol. 119, no. 5, pp. 1020–1026, 2002.

[46] M. A. Dimopoulos, J. San-Miguel, A. Belch et al., "Daratumumab plus lenalidomide and dexamethasoneversuslenalidomide and dexamethasone in relapsed or refractory multiple myeloma: updated analysis of POLLUX," *Haematologica*, vol. 103, no. 12, pp. 2088–2096, 2018.

[47] M. A. Dimopoulos, D. Dytfeld, S. Grosicki et al., "Elotuzumab plus pomalidomide and dexamethasone for multiple myeloma," *The New England Journal of Medicine*, vol. 379, no. 19, pp. 1811–1822, 2018.

Hindawi
Journal of Immunology Research
Volume 2020, Article ID 8986521, 12 pages
https://doi.org/10.1155/2020/8986521

Research Article

Igg-Dependent Hydrolysis of Myelin Basic Protein of Patients with Different Courses of Schizophrenia

Daria A. Parshukova,[1] Liudmila P. Smirnova,[1] Elena G. Kornetova,[1] Arkadiy V. Semke,[1] Valentina N. Buneva,[2] and Svetlana A. Ivanova[1]

[1]*Laboratory of Molecular Genetics and Biochemistry, Mental Health Research Institute, Tomsk National Research Medical Center of the Russian Academy of Sciences, Tomsk 634014, Russia*
[2]*Laboratory of Repair Enzymes, Institute of Chemical Biology and Fundamental Medicine, Siberian Branch of the Russian Academy of Sciences, Novosibirsk 630090, Russia*

Correspondence should be addressed to Liudmila P. Smirnova; lpsmirnova2016@gmail.com

Received 4 February 2020; Accepted 4 June 2020; Published 11 August 2020

Guest Editor: Cristina R. Reschke

The level hydrolysis of myelin basic protein (MBP) by IgG in patients with schizophrenia was studied depending on the clinical features and course of the disease. The patients were grouped according to type of schizophrenia and type of disease course. We found that IgGs isolated and purified from sera of schizophrenia patients' blood hydrolyses human MBP, and the level of this hydrolysis significantly exceeds that of healthy individuals. Detection of protease activity corresponding only to intact IgGs in polyacrylamide gel fragments, together with data of gel filtration of antibodies under conditions of "acid shock" (concordance of optical density profile of IgG with profile of MBP-hydrolyzing activity) and with the absence of any other proteins and bands in gradient SDS-PAGE and in PVDF membrane provides direct evidence that the IgGs from the schizophrenia patients have MBP-hydrolyzing activity. The antibodies-specific proteolytic activity of patients with acute schizophrenia (1.026 [0.205; 3.372] mg MBP/mg IgG/h) significantly exceeds the activity of IgG in patients in remission (0.656 [0.279; 0.873] mg MBP/mg IgG/h) and in healthy individuals (0.000 [0.00; 0.367] mg MBP/mg IgG/h). When comparing the specific activity in patients with different types of disease course, we have found that patients with a continuous course of paranoid schizophrenia (1.810 [0.746; 4.101 mg MBP/mg IgG/h]) had maximal activity values. It can be assumed that the increase in the activity of MBP-hydrolyzing antibodies is due to the activation of humoral immunity in acute schizophrenia.

1. Introduction

The interconnection between the nervous and immune systems has been recognised in recent years but many questions remain regarding their interactions in schizophrenia. The idea of an autoimmune component in the pathogenesis of schizophrenia was first proposed by Hermann Lehmann-Facius in 1937, and it was further developed by others [1–4].

In schizophrenia, the inhibition of regulatory T-lymphocytes was revealed, this leading to the activation of humoral immunity and resulting in the formation of antibodies to various components of the nervous tissue [5, 6]. It was shown in a BALB/c mouse model that autoantibodies (Abs) binding neuroantigens in the early stages of ontogeny promote the occurrence of various structural anomalies in the nervous system, and this subsequently leads to inhibitory effect on physical development, training processes, and memory [7, 8].

Postmortem studies in patients with schizophrenia have revealed deficits in myelination, abnormalities in myelin gene expression, and altered numbers of oligodendrocytes in the brain [9]. Studies in adult postmortem samples using electron microscopy and histochemistry suggest structural changes in oligodendroglia cells that produce the myelin sheath [10, 11], an atrophy of axons, abnormalities of the myelin sheath surrounding [12, 13], a reduction in myelin basic protein (MBP) in the anterior frontal cortex in cases of schizophrenia [14], and a decrease in MBP expression in

the gray matter of the frontal cortex of patients with schizophrenia [15]. MBP is one of the main protein components of the central nervous system myelin, and it reflects the myelin-forming activity of oligodendroglia through a positive correlation with the number of normal myelin fibres [16, 17].

Antibodies to MBP in the serum of patients with schizophrenia were found long ago [18]. An increase in the level of antibodies to neuroantigens, including MBP-antibodies, in schizophrenia correlates with the severity of clinical symptoms [19]. Increased antibody levels are often interpreted as a breakdown of immune tolerance, causing an autoimmune response [20]. But at the same time, this may reflect a hyperactivity of the immune system as part of the etiology of schizophrenia, in accordance with literature data about an increase in proinflammatory molecules with increased immune response in those undergoing both acute psychosis and chronic schizophrenia [21–23].

The existence of catalytic antibodies (so-called abzymes) has been known for over 30 years. The ability of immunoglobulins to catalyze many chemical reactions, e.g., hydrolysis of DNA, RNA, polysaccharides, and proteins has been described. Abzymes capable of hydrolyzing MBP were found and studied in detail in multiple sclerosis, systemic lupus erythematosus [24, 25], and in the serum of autistic children [26].

Recently, we reported an ELISA study showing that titers of autoantibodies against MBP in patients with schizophrenia are ~1.8 fold higher than in healthy individuals, but 5.0-fold lower than in patients with multiple sclerosis. More importantly, we also reported that such antibodies had abzyme (catalytic) activity, meaning that they were also capable of hydrolyzing MBP and its peptides [27]. In this report, we present data on the catalytic properties of the MBP-hydrolyzing abzymes in sera from patients having a more diverse diagnostic profile in comparison with the previous study.

In our previous study, it was shown that the greatest MBP-hydrolyzing activity is associated with negative symptoms and a long course of the disease, which allows us to suggest a connection between the severity of clinical symptoms and damage of myelin, causing an increase in the level of proteolytic activity of antibodies. Therefore, the purpose of this study was to investigate the characteristics of MBP proteolysis by serum polyclonal antibody (abzymes) of schizophrenia patients depending on the clinical features of the disease.

2. Materials and Methods

2.1. Characteristics of the Studied Subjects. In this work, 79 patients (61% males, 39% females) with schizophrenia were recruited to study the proteolytic activity of their antibodies. The age of patients varied from 21 to 61 years with a median 36.00 [31.00; 45.00] years. Inclusion criteria were the following: paranoid or simple schizophrenia according to the International Statistical Classification of Diseases and Related Health Problems, 10th Revision (ICD-10: F20.0 and F20.6), and the Structured Clinical Interview for DSM-IV Axis I Disorders (SCID). Exclusion criteria were the following: the presence of acute or chronic infectious, inflammatory, autoimmune or neurological diseases, other organic mental disorders, and mental retardation. The schizophrenia diagnosis was confirmed and verified in accordance with the international standard criterion, the psychometric PANSS scale.

The sample was formed from inpatients hospitalized due to clinical symptoms (hereinafter "acute schizophrenia") and outpatients in remission. Of these, 48 patients exhibited signs, according to ICD-10 criteria, for paranoid schizophrenia (continuous F20.00, episodic with progressive deficit F20.01, episodic with stable deficit F20.02) and simple schizophrenia F20.6. These patients received treatment at the Mental Health Research Institute TNMRC, Department of Endogenous Disorders (Tomsk, Russia). A total of 31 patients were assigned to a group with clinical remission (F20.05). Patients with clinical remission were invited to the study by their doctors of the Department of Endogenous Disorders. Data on the participants are presented in Tables 1 and 2.

The level of education of patients was as follows: higher—25 people (32%), incomplete higher—10 (12%), secondary special—27 (34%), secondary—17 (22%). Among the patients in the study sample, the majority were not married—55 people (70%), 16 (20%) married, 3 (4%) divorced, 2 (2%) in a civil marriage, and 3 people were widows (4%). Most patients received second-generation antipsychotics in maintenance dosages before admission to the hospital (olanzapine, 20 patients (25.32%), quetiapine, 24 (30.38%), risperidone, 30 (37.98%), or clozapine, 5 (6.3%)). They were often nonadherent, and thus were hospitalized due to exacerbation of symptoms of schizophrenia. Blood sampling was performed at hospitalization before the administration of antipsychotic therapy.

All individuals included in the study gave written informed consent. Ethical approval was granted (protocol N 78/1.2015) by the Local Bioethics Committee of the Mental Health Research Institute in accordance with Helsinki ethics committee guidelines. None of the participants were compromised in their capacity/ability to consent; thus, consent from the next-of-kin was not necessary, and it was not recommended by the local ethics committee.

The control group consisted of 24 subjects (38% males, 62% females). In this group, age varied from 23 to 53, with a median 39.00 [29.00; 46.00] years. These control subjects were mentally and somatically healthy individuals. The excluding criteria for the controls were the presence of acute and chronic infectious, inflammatory, autoimmune, or neurological diseases, and organic brain disorders.

2.2. Object of Study. Blood samples were obtained after an overnight fast from a vein into tubes with a clot activator (CAT, BD Vacutainer). To isolate the serum, the blood samples were centrifuged for 30 min at 2000 × g at 4°C. The sera were stored at −80°C until analysis.

2.3. Purification of IgGs. Affinity chromatography on a chromatographic matrix with immobilized protein G from group G streptococci is a widely used and effective method for the isolation of immunoglobulins. Protein G has a high affinity for the Fc regions of immunoglobulins G. This property allows selective elution of components of the immune complexes (proteins, polysaccharides, nucleic acids) under

Table 1: Demographic and clinical characteristics of schizophrenia patients and healthy control subjects.

	Healthy control subjects	Patients with acute schizophrenia	Patients with schizophrenia in remission	p value Mann–Whitney U test
Number	24	48	31	NS
Age median (IQR)	39.00 [29.00; 46.00]	38.00 [30.00; 46.00]	35.00 [31.00; 44.00]	NS
Male/female	9/15	12/28	16/15	NS
Duration of disease, years median (IQR)		12.50 [6.00; 17.00]	15.00 [10.00; 18.00]	NS
PANSS total score		89.00 [80.00; 105.00]	54.50 [52.00; 59.00]	0.0001

*NS: nonsignificant between the group of healthy control subjects and different groups of patients $p = 0.0001$ between the groups of patients with acute schizophrenia and patients in remission.

Table 2: Demographic and clinical characteristics of patients with different types of schizophrenia.

Subgroups of patients with schizophrenia	Continuous course of schizophrenia	Episodic course of schizophrenia with progressive deficit	Episodic course of schizophrenia with stable deficit	Simple schizophrenia	p value Kruskal–Wallis test
Number	12	12	12	12	NS
Age median (IQR)	34.00 [32.00; 54.00]	39.00 [38.00; 46.00]	39.00 [34.00; 41.00]	34.00 [26.00; 45.00]	NS
Male/female	4/7	3/8	2/7	3/6	NS
Duration of disease, years median (IQR)	14.00 [13.00; 20.00]	13.00 [6.00; 17.00]	11.00 [5.00; 12.00]	8.00 [5.00; 17.00]	NS
PANSS total score	100.00 [87.00; 116.00]	83.00 [74.00; 98.00]	76.00 [65.00; 81.00]	92.00 [84.00; 111.00]	0.0381

*NS: nonsignificant; p value for multiple comparisons with Kruskal–Wallis test including all groups of patients.

conditions with increased ionic strength or in the presence of nonionic detergents without destroying the Ig complexes with protein G [28]. Antibodies from the blood sera of schizophrenia patients and healthy controls were purified and analyzed by earlier developed procedures for purification of electrophoretically and immunologically homogenous IgG preparations from human blood serum [29, 30]. The procedure included affinity chromatography of serum proteins on Protein G-Sepharose, followed by high-performance gel filtration on a Superdex-200 HR 10/30 column. Quantitative elution of IgG was carried out using an acid buffer with a pH of 2.6, after which the resulting sample was immediately neutralized.

2.4. SDS-PAGE Analysis of Proteins. Electrophoretic separation of proteins according to the Laemmli method [31] was used to analyze the homogeneity of antibodies as well as to analyze the products of hydrolysis of MBP by Abs. The concentrating gel contained 4% acrylamide (AA: Bis-AA ratio = 30 : 1), 125 mM Tris-HCl, pH 6.8, and 0.5% SDS. The separating gel contained 5-20% AA, 375 mM Tris-HCl, pH 8.8, and 0.4% SDS. The protein preparations were incubated in buffer containing 50 mM Tris-HCl, pH 6.8, 2% SDS, 10% glycerol, 0.025%, and bromophenol blue at 100°C for 1 min and then applied to the gel. The electrophoresis was performed at the current 15-20 A. Homogeneity of the Abs was tested in 4–15% gradient gels (0.1% SDS). The polypeptides were visualized by silver or Coomassie R250 staining and by Western blotting on a nitrocellulose membrane [32]. The gels were imaged by scanning and quantified using the Image Quant 5.2 program.

2.5. FPLC Gel Filtration under "Acid Shock" Conditions. Acidic pH of the medium allows dissociation and subsequent separation of all components of immunocomplexes consisting of immunoglobulins and their associated antigens. Electrophoretically homogeneous preparations of IgG were preincubated in glycine buffer (pH 2.6) followed by gel filtration in the same buffer (acid shock). The IgG was separated by high-performance gel filtration on a Superdex 200 HR column equilibrated with 50 mM glycine-HCl (pH 2.6) containing 0.1 M NaCl (buffer B) using Akta Pure chromatography (GE). The IgG samples (150 μl, 20 mg/ml) were preincubated with 50 μl of buffer B; then, the high-performance gel filtration was performed at 22°C. The resulting fractions were immediately neutralized with 1 M Tris-HCl buffer (pH 8.8). The eluate was sequentially collected in individual tubes (Eppendorfs) at a volume of 1 ml. Each tube with 1 ml of antibody preparation is a separate fraction of the IgG preparation. The concentration of IgG preparations was determined at a wavelength of λ = 280 nm, in quartz cuvettes with 1 cm optical path length against a buffer in which IgG was dissolved on an Eppendorf BioPhotometer (Germany) single-beam spectrophotometer. After one week of storage at 4°C for refolding after the acid shock, the IgG was used in activity assays as described below.

This work was performed at the laboratory of Repair Enzymes of the Institute of Chemical Biology and Fundamental Medicine at the Siberian Branch of the Russian Academy of Sciences in Novosibirsk under the guidance of V. Buneva.

2.6. In Situ Proteolytic Activity Assay. This approach gives an indication of the enzymatic activity of a specific fragment of a

gel or a specific protein band. One of the options for this approach is to determine the activity of enzymes in the eluates of various fragments of the gel. After standard SDS-PAGE of IgGs, to restore the MBP-hydrolyzing activity of IgGs, SDS was removed by incubation of the gel for 1 h at 300 C with 4 M urea and washed 10 times (7-10 min) with H_2O. Then 2-4 mm cross-sections of longitudinal slices of the gel were cut up and incubated with 50 μl of 50 mM Tris-HCl, pH 7.5, containing 50 mM NaCl for 6-7 days at 40°C to allow protein refolding and eluting from the gel. The solutions were removed from the gels by centrifugation and used for assay of MBP hydrolysis as described below. Parallel control longitudinal lanes were used to detect the position of intact IgG as well as its light and heavy chains after Ab reduction on the gel by silver staining.

This work was performed at the laboratory of Repair Enzymes of the Institute of Chemical Biology and Fundamental Medicine at the Siberian Branch of the Russian Academy of Sciences in Novosibirsk under the guidance of V. Buneva.

2.7. Proteolytic Activity of Immunoglobulin G Fractions Purified from Serum. The purified IgG was tested for MBP-hydrolyzing activity with MBP isolated from human brain tissue. The MBP was obtained from the Department of Biotechnology, Research Center of Molecular Diagnostics and Therapy (Moscow). The reaction mixture (10-40 μl) for analysis of MBP-hydrolyzing activity of IgG contained IgG in concentration 0.2 mg/ml, 20 mM Tris-HCl (pH 7.5), and 0.2-0.7 mg/ml MBP. The products of MBP cleavage were analyzed in 4-15% or 12% SDS-PAGE as described earlier in Section 2.5. All quantitative measurements (initial rates) were taken under pseudo-first-order conditions of the reaction within the linear region of Abs concentrations, of the time courses (1-24 h), and the formation of products (15-40% of MBP hydrolysis). The catalytic activity of the IgG in the cleavage of MBP was estimated from the decrease in the intensity of the Coomassie-stained MBP band after electrophoresis. Differences in the hydrolysis levels of MBP incubated in the absence and in the presence of IgG were used to correct the values. Quantitative evaluation of proteins was estimated using the Image Quant 5.2 program. The activity of the Abs is expressed in units of specific enzyme activity as the quantity of substrate cleavage by 1 mg Abs per/h.

2.8. Statistical Analysis. Statistical analyses were performed with Statistica 10.0 software for Windows. The data were checked for normal distribution using the Shapiro–Wilk W test. Most of the sample sets did not meet the normal Gaussian distribution. For this reason, the differences between IgG samples of different groups were estimated using the Mann–Whitney test and the Kruskal–Wallis Test; a difference was considered statistically significant at $p < 0.05$. The median (M) and interquartile ranges (IQR) were estimated.

3. Results and Discussion

In this study, we analyzed Abs (IgGs), having MBP-hydrolyzing activity, purified from sera of patients with schizophrenia and healthy controls. The important tasks of our work with catalytic antibodies were to show that the studied activity belonged to the antibodies, but not to simultaneous-obtained competing proteases. It was proven that checking the three most stringent, indicative, and reliable criteria is sufficient to unambiguously conclude that the studied catalytic activity belongs to isolated antibodies. The efficiency of substrate hydrolysis by antibodies belonging to different subclasses may be different. Given this, we decided to study the content of IgG subclasses with proteolytic activity in the groups of schizophrenia patients.

3.1. Application of Strict Criteria for IgGs with Proteolytic Activity. Several strict criteria were tested to show that detected catalytic activity belonged to the antibodies: purification of Abs on sorbent with affinity to IgG, electrophoretic homogeneity of antibodies in SDS-PAGE, gel filtration chromatography of Abs under conditions of dissociation of immune complexes (pH shock analysis), and proteolytic activity in situ. It turned out that checking of these most stringent, indicative, and reliable criteria is sufficient to unambiguously conclude that the studied catalytic activity belongs to the Abs. These criteria for checking the presence of catalytic activity in antibodies are generally accepted and are used by various independent research teams [26, 28, 33–36].

Based on the specific binding of isolated IgG to Protein G-Sepharose sorbent, the catalytic activity of IgG is directly shown.

The isolated IgG preparations were electrophoretically and immunologically homogeneous in accordance with silver staining and immunoblotting after separation in gradient SDS-PAGE and transferred to the PVDF membrane.

The homogeneity of the 150 kDa IgG was confirmed by 4-18% SDS-PAGE, which showed a single protein band corresponding to the molecular mass of IgG (Figure 1(a)). The electrophoretic mobility of usually low molecular mass canonical proteases (24-25 kDa) cannot coincide with that of intact IgG (150 kDa). A major band 150 kDa corresponding to the whole IgG molecule consisting of two light and two heavy chains (H2L2) is visible (lane 1), also after incubation with 10 mM DTT (membrane stained with silver) bands corresponding to the light chain (25 kDa) and heavy chain of IgG (50 kDa) (lane 2).

Western blot analysis (Figure 1(b)) reveals additional bands—oligomeric forms of IgG of H2 composition. Partial decomposition of the Abs into their subunits L and H2 subunits in the presence of SDS is due to disulfide exchange [37]. Since the IgG molecule has two disulfide bonds between heavy chains and only one covalent bond is formed between the L and H chains, the probability of separation of the light chain from the IgG molecule in the presence of a denaturing agent is theoretically higher than the formation of HL dimers. Only in the IgG4 subclass, whose share is 3–4% of the total IgG pool, one S-S bond is formed between the heavy chains, and it is characterized by high lability [38].

Thus, in the SDS-PAGE analysis of the total IgG preparation, all oligomeric forms can be observed as minor components: H2L, HL, and H2, as well as the free L chain. The

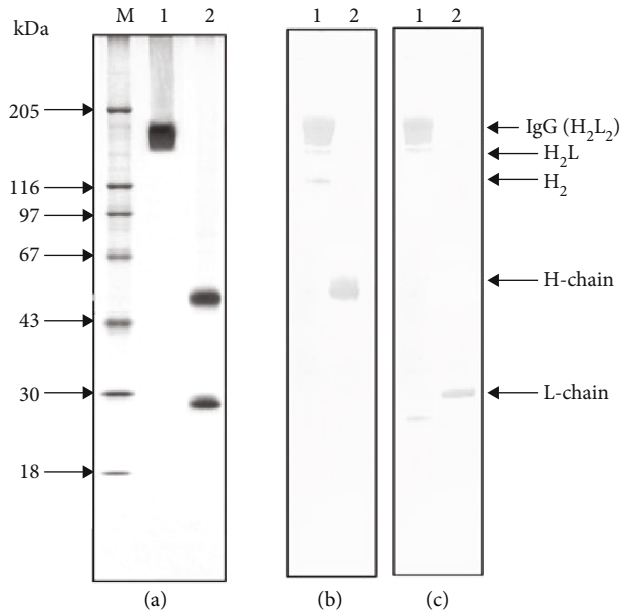

Figure 1: Analysis of homogeneity of IgG preparations using SDS-PAGE in 5–18% gradient gel and Western blot. (a) Silver staining: IgG preparation before (lane 1) and after (2) incubation with 10 mM DTT (membrane stained with silver). (b) Western blot analysis after incubation with horseradish peroxidase conjugates with rabbit anti-H IgG: 1 and 2, before and after incubation with 10 mM DTT, respectively. (c) Western blot analysis after incubation with a horseradish peroxidase conjugates with rabbit anti-L IgG: 1 and, 2 before and after incubation with 10 mM DTT, respectively. M—protein molecular mass markers.

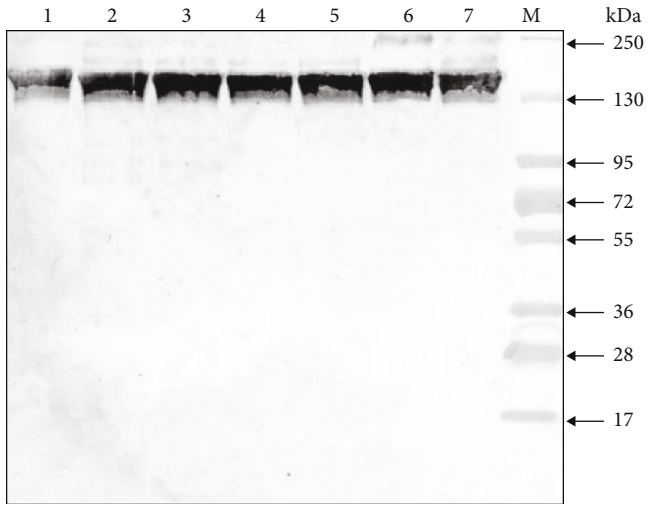

Figure 2: Analysis of homogeneity of IgG preparations after SDS-PAGE in a 5–18% gradient gel and silver staining. Lines 1-7—IgG of different schizophrenia patients; M—protein molecular mass markers.

mobility of the light chain decreases after the restoration of intra-chain S-S bonds, which is explained by the complete unfolding of the polypeptide chain and a decrease in its compactness. We also present an analysis of the electrophoretic homogeneity of IgG in several schizophrenic patients with silver stain (Figure 2).

One of the most important criteria for attributing the activity to Abs is gel filtration of the Abs under acidic conditions, where noncovalent complexes are dissociated. Electrophoretically homogeneous preparations of IgG were preincubated in glycine buffer (pH 2.6) followed by gel filtration in the same buffer (acid shock). After the gel filtration, we obtained 25 fractions of one IgG preparation with different antibody concentrations. To assess the level of antibody activity in MBP hydrolysis, we took the fraction corresponding to the peak of the chromatogram. Standard reaction conditions used with high-performance gel filtration of the IgGs under acid-shock conditions (pH 2.6) demonstrated the concordance of the optical density profile ($\lambda = 280$ nm) with the profiles of the MBP-hydrolyzing activity, which is another indication of the studied activity being due to the IgGs (Figure 3).

In addition, we present the results of the determination of proteolytic activity *in situ*. To exclude possible hypothetical traces of contaminating canonical proteases, the IgG preparations were separated by SDS-PAGE, and their MBP-hydrolyzing activity was detected after extraction of the proteins from the separated gel slices only in the IgG band, while the other gel fragments were catalytically inactive (Figure 4). The electrophoretic mobility of usually low molecular mass canonical proteases (24–25 kDa) cannot coincide with that of intact IgGs (150 kDa).

Therefore, the detection of protease activity in the gel fragments corresponding only to intact IgGs (Figure 4) together with data of gel filtration of the Abs under acid-shock conditions (Figure 3) and with the absence of any other proteins and bands (Figures 1 and 2) provides direct evidence that the IgGs have MBP-hydrolyzing activity.

3.2. Analysis Of the Product Profile of MBP Hydrolysis by Antibodies of Patients with Schizophrenia. Various molecular products are formed during the MBP hydrolysis by the catalytic IgG of schizophrenia patients. The MBP hydrolysis was accompanied by the appearance of new bands of MBP products that are not represented in the control in the molecular weight regions corresponding to 16.0 kDa, 14.3 kDa, 12.7 kDa, 11.5 kDa, 10.7 kDa, 9.7 kDa, and 7.4 kDa (Figure 5). A change in the color intensity of the bands represented in control was detected: in the area of molecular weight 18.5 kDa—a decrease in color intensity and band size; in the area of molecular weight 13.5 kDa and 12.8 kDa—an increase in color intensity and band size.

The spectrum of MBP hydrolysis products depended on the level of IgG activity. High activity IgGs were characterized by the formation of numerous low molecular weight products that were located in the 13.5-7.0 kDa region. MBP-products profile after hydrolysis by antibodies with medium or low activity was characterized by products with a molecular weight of 18.5-12.0 kDa. Thus, highly active antibodies almost completely hydrolyzed the band of intact MBP with an isoform of 18.5 kDa (the main isoform of this protein for humans). While in electrophoretic tracks corresponding to antibodies with medium or low activity, the band

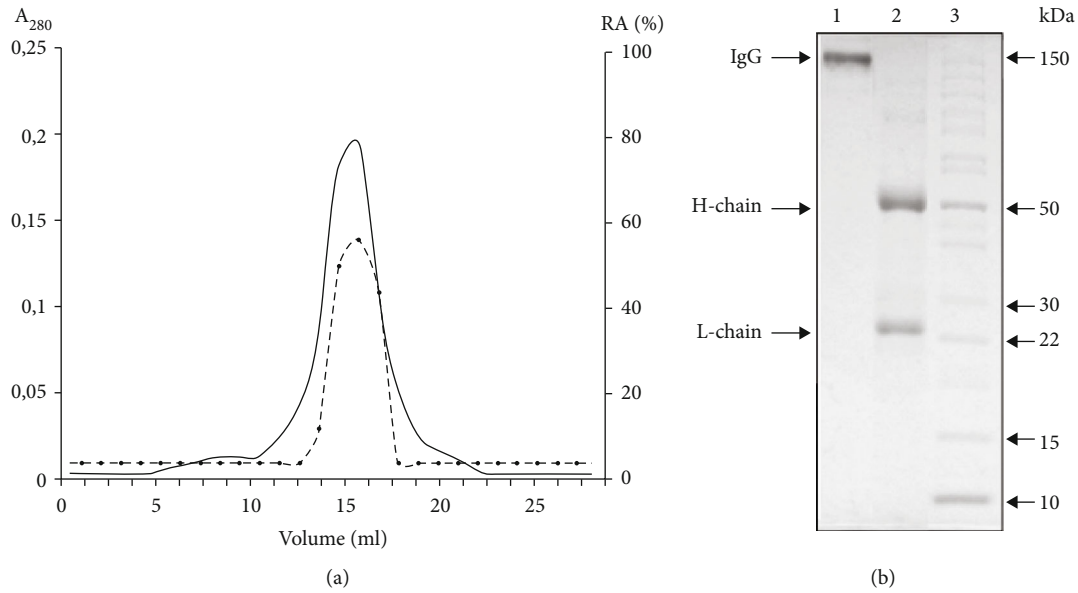

Figure 3: (a) Gel filtration of IgG on a Superdex 200 column in acidic buffer (pH 2.6) after preincubation of the Abs in the same buffer: (—). absorbance at 280 nm (A280) that reflects the content of IgG; (■). Relative activity (RA. %) of IgGs in the hydrolysis MBP. The complete hydrolysis of MBP for 5 h was taken for 100%. (b) Electrophoretic analysis in gradient PAGE (4.5–15%) of the fraction corresponding to the central part of the peak (Figure 2(a)) before (line 1) and after (line 2) incubation with a reducing agent (10 mM DTT). Line 3—protein molecular mass markers.

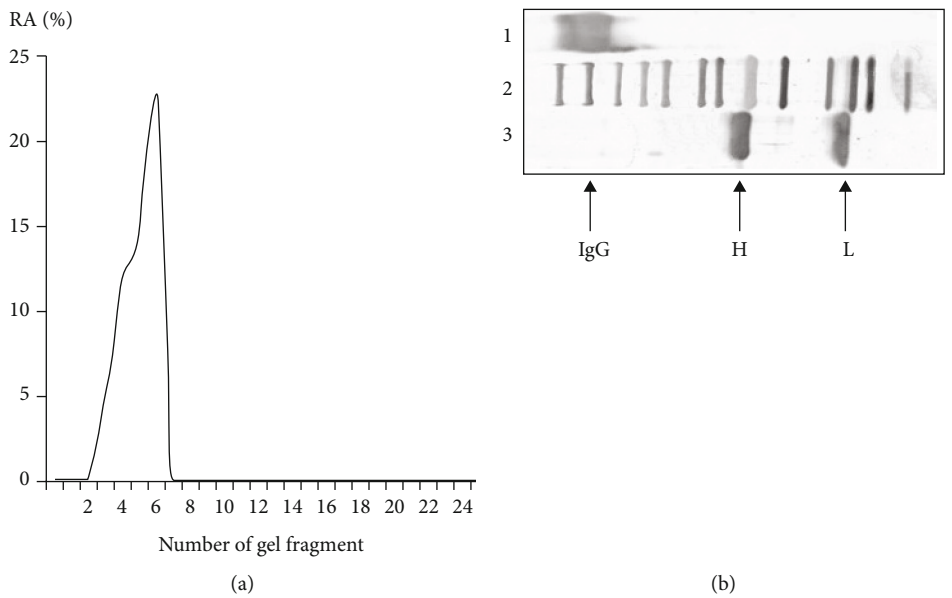

Figure 4: (a) Graph of MBP-hydrolyzing activity of extracts from various gel fragments after SDS-PAGE of an IgG preparation. (b) Electrophoretic analysis of IgG protein. Assay of MBP-hydrolyzing activity of purified IgG after SDS-PAGE in 4–15% gradient gel; the gel was incubated under special conditions for renaturation of the Abs. The relative proteolytic activity (RA. %) was revealed using extracts of many 2–3 mm fragments of one longitudinal slice of the gel. The RA of IgG corresponding to complete hydrolysis of 0.5 mg/mL MBP after incubation for 24 h with 10 μl of the extract was taken for 100%. The average error in the initial rate determination from three experiments did not exceed 10–15%. The second set of control longitudinal slices of the same gels corresponding to IgGs before (lane 1) and after (lane 3) incubation with DTT was stained with silver. Lane 2 shows the position of molecular mass markers. The IgG—band is in the region of 150 kDa, which corresponds to the native IgG; the H—band is in the region of 50 kDa, which corresponds to the heavy chains of IgG after incubation with DTT; the L—band in the region of 25 kDa, which corresponds to the light chains of IgG after incubation with DTT.

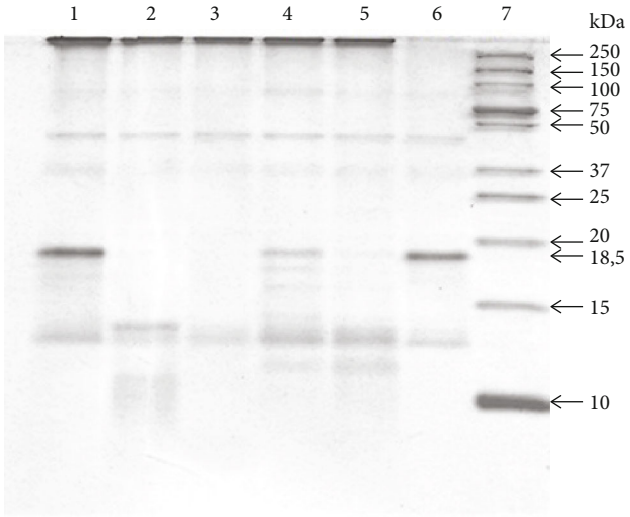

Figure 5: Electrophoretic analysis of MBP-hydrolyzing activity of IgG in SDS-PAGE 12.5% gel: 1-5 products profile of MBP-hydrolysis by individual IgG of patients with schizophrenia (line 1,4—low and medium rate of MBP-hydrolyzing activity; line 2,3,5—high rate of MBP-hydrolyzing activity); 6—control: MBP incubated without IgG; 7—protein molecular mass markers.

18.5 kDa remains clearly visible. For this reason, the activity level of catalytic IgG was assessed by the reduction of the color intensity of the bands in the region of 18.5 kDa.

Thus, the spectrum of products of the reaction of hydrolysis of MBP is extremely variable from person to person.

3.3. Proteolytic Activity of Autoantibodies to MBP in Sera of Schizophrenia Patients. We evaluated the proteolytic activities of polyclonal antibodies to MBP in the sera of schizophrenia patients. After incubation of MBP with IgG, the proteins were separated using gel electrophoresis and analyzed. The reaction conditions and the detection of the hydrolysis products are described in Section 2.

Analysis of our data showed that most patients had significant activity, while IgG from healthy controls had almost no such activity. Furthermore, the level of Abs activity was different depending on the type of the disease course.

Our results demonstrate that the specific anti-MBP IgGs from patients with schizophrenia catalyze the hydrolysis of MBP. The IgGs with the highest proteolytic activity are present in the analyzed serum samples of patients with acute schizophrenia, and the activity was twice higher than in patients in remission and significantly higher than in IgGs from healthy controls (Table 3). Thus, we conclude that the level of MBP hydrolysis by IgG of the schizophrenia patients decreased simultaneously with a decrease in the severity of their clinical symptoms. This was confirmed by their PANSS scores.

Comparison of MBP-hydrolyzing activity in IgGs using the Mann–Whitney U test showed the greatest difference between the groups of healthy controls and patients in acute schizophrenia ($p = 0.000009$); between healthy individuals and schizophrenia patients in remission ($p = 0.000037$); and between patients in the acute phase and patients in remission ($p = 0.000127$) (Figure 6).

Comparison of the level of MBP-hydrolyzing activity of Abs in groups with paranoid schizophrenia (median [Q1; Q2] 1.042 [0.123; 4.156] mg MBP/mg IgG/h) and simple schizophrenia (0.630 [0.309; 2.05] mg MBP/mg IgG/h) revealed no significant differences ($p = 0.334$).

A more detailed analysis of the MBP-hydrolyzing activity of patients with paranoid schizophrenia revealed that the activity differs significantly depending on the type of disease course (Table 4).

All groups of paranoid schizophrenia with different courses and simple schizophrenia also showed significant differences from the control group (Table 5).

Thus, the highest activity was found in patients with the continuous course of schizophrenia (median: 1.810 mg MBP/mg IgG/h), which differed significantly from that in patients in remission ($p = 0.000729$; Mann–Whitney U test) and in controls ($p = 0.000038$; Mann–Whitney U test). This result also coincided with the maximum PANSS score in patients with the continuous course of schizophrenia.

Multiple lines of evidence now suggest damage to oligodendroglia and myelin in schizophrenia patients. This is confirmed by genetic, morphological, immunohistochemical, and neuroimaging studies. Expression levels of a number of myelin-related genes were significantly downregulated in schizophrenic brains including myelin-associated glycoprotein (MAG), CNP, myelin and lymphocyte protein (MAL), gelsolin (CSN), ErbB3 (also called HER3), and transferrin [39–46]. It is known that MBP reflects the myelin-forming activity of oligodendroglia through a positive correlation with the number of normal myelin fibers [16, 17]. Postmortem studies show a decrease in the expression of MBP mRNA and protein levels in various regions of the brain [10, 11, 14]. Morphological studies also demonstrate ultrastructural anomalies of myelin fibers in schizophrenia patients according to studies on postmortem autopsy samples of the brain [12, 13]. These changes were most pronounced in the prefrontal cortex and reliably correlated with the degree of expression in the caudate nucleus and hippocampus. A decrease in the density of white matter oligodendrocytes in the postmortem frontal cortex was described for a small sample group of elderly schizophrenia patients, but myelin protein expression was not quantified for white matter [47]. Data of neuroimaging studies suggest that white matter abnormalities are present even before the onset of the illness but may be a stable characteristic of the disease. Changes in brain structure might be formed immediately after the first episode of schizophrenia and increase with the course of the disease [48–52].

Antibodies to MBP and an increase in the MBP level were detected in cerebrospinal fluid (CSF) and serum of patients with schizophrenia [53]. However, the total level of immunoglobulin G in both CSF and peripheral blood of patients with schizophrenia was not always found to be different from that in healthy individuals, and sometimes it was found to be lower than in healthy individuals [54, 55]. In studies with experimental animals, it was noted that autoantibodies binding neuroantigens in the early stages of ontogenesis contribute to the formation of various structural anomalies in the

Table 3: MBP-hydrolyzing activity levels in IgGs from schizophrenia patients and healthy control subjects.

Healthy control subjects, median [Q1-Q4] mg MBP/mg IgG/h	Patients with acute schizophrenia, median [Q1-Q4] mg MBP/mg IgG/h	Patients with schizophrenia in remission, median [Q1-Q4] mg MBP/mg IgG/h	p value Kruskal–Wallis test
$N = 24$	$N = 48$	$N = 31$	
0.00 [0.00; 0.24]	1.026 [0.205; 3.372]	0.656 [0.279; 0.873]	0.0001*

*p value from multiple comparisons with Kruskal–Wallis test including all groups of patients and healthy control group; p significant at <0.05.

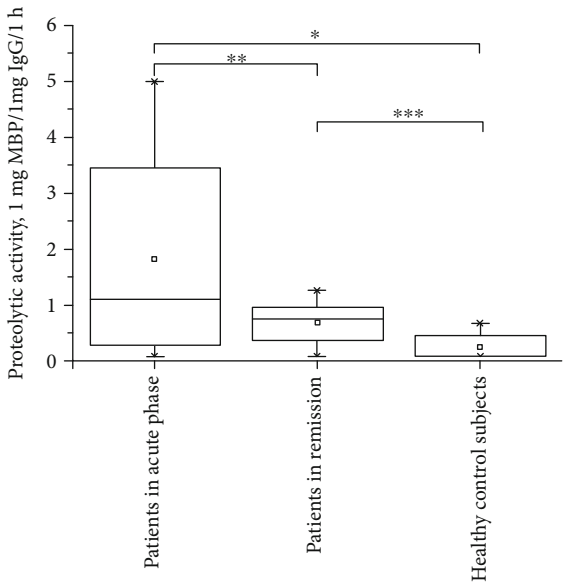

Figure 6: Levels of proteolytic activity in hydrolysis of MBP corresponding to IgG from sera of patients with acute schizophrenia, patients in remission, and healthy individuals; (—) median of catalytic activity; (between-group differences: $^{*}p = 0.000009$; $^{**}p = 0.000127$; $^{***}p = 0.000037$ (by the Mann–Whitney U test).

nervous system and subsequently lead to a violation of the behavior of young animals. Thus, a high level of antibodies to nerve growth factor in the blood of pregnant females has a pronounced inhibitory effect on the learning process and significantly increases the threshold of pain sensitivity in the offspring [8, 56, 57]. Considering the data on the penetration of immunoglobulins through the blood-brain barrier in autoimmune disorders [58, 59] and the detected BBB hyperpermeability in schizophrenia [60], this phenomenon can be explained by the fact that MBP stimulates the synthesis of antibodies to myelin components. Also, it is generally accepted that the detection of MBP in blood is indicative of impairment of myelination in the brain, but the reason for this is not established.

Our results demonstrate that IgGs from schizophrenia patients catalyze the hydrolysis of MBP, and this activity is significantly higher than in control subjects. We have found that the activity differs significantly depending on the type of the disease course, particularly patients with paranoid schizophrenia and continuous course of schizophrenia demonstrated the highest activity (1.810 mg MBP/mg IgG/h), which was significantly different from that in patients in remission and the control. Signs of continuous course are expressed in the regular development, complication, and deterioration of symptoms as the disease progresses, which affects the immunological reactivity of the organism on the whole. Our data suggest that in patients with a continuous course of schizophrenia, the violation of myelination is perhaps more pronounced.

According to the results of our colleagues from the Laboratory of Clinical Psychoneuroimmunology, specific features of dysregulation of the immune system in patients with schizophrenia were identified. Suppression of the T-cellular immune response (decrease CD2+, CD3+, CD4+, CD16+ subtypes of T-lymphocytes) and activation of humoral immunity (increase in levels of circulating immune complexes, IgM levels, and B-lymphocytes), a disturbance of cytokine production was revealed [61]. It should be noted that patients with a continuous course of schizophrenia have more pronounced changes in their immune system. In particular, they have simultaneous activation of Th1 and Th2 cytokines with the dominance profile of the Th1-cell-response pathway [62]. Thus, we assume that the proteolytic activity of Abs in MBP hydrolysis demonstrates the course of autoimmune reactions in patients with a continuous course of schizophrenia. According to recent studies, the immunological basis of schizophrenia is like that of chronic inflammation [63–66]. Proteolytic IgG in patients with schizophrenia can also play a positive role by hydrolyzing MBP as a potential immunogen in peripheral blood, since in some other diseases, catalytic antibodies can perform a protective function by hydrolyzing pathological proteins [67–70].

Since we cannot completely exclude the effect of antipsychotic drugs in our study, we must consider their potential impact on the immune response and catalytically activity. Clinical trials of risperidone have shown that the drug can reduce circulating levels of IL-1β in patients with schizophrenia, as well as increase the levels of neurotrophin BDNF [71]. Risperidone, clozapine, and haloperidol have a positive correlation with improved clinical symptoms of schizophrenia and decreased levels of circulating IL-2, IL-6, IL-18, IFN-γ, and TNF-α [72–74]. Haloperidol treatment inhibits the immune response by suppressing NF-κB signaling via the dopamine D2 receptor and inhibition of proinflammatory cytokine release [75, 76]. Moreover, according to the results of our study, proteolytic activity was maximal before the prescription of antipsychotic therapy and decreased after drug treatment in the remission group. Thereby, we suggest it is unlikely that the induction of catalytic activity is caused by the antipsychotics.

Table 4: Characteristics of IgG proteolytic activity levels in patients with different clinical forms of schizophrenia and in healthy control subjects.

Group	Healthy control subjects, mg MBP/mg IgG/h	Patients with remission, mg MBP/mg IgG/h	Continuous course of schizophrenia, mg MBP/mg IgG/h	Episodic course of schizophrenia with progressive deficit, mg MBP/mg IgG/h	Episodic course of schizophrenia with stable deficit, mg MBP/mg IgG/h	Simple schizophrenia, mg MBP/mg IgG/h	p value
N	24	31	12	12	12	12	
Median [Q1-Q4]	0.00[0.00; 0.24]	0.656[0.279; 0.873]	1.810[0.746; 4.101]	0.539[0.00; 4.460]	0.831[0.123; 1.859]	0.630[0309; 2.050]	0.0002*

*p value from multiple comparisons with Kruskal–Wallis test including all groups of patients and healthy control group; p significant at <0.05.

Table 5: Significance of differences in IgG proteolytic activity in patients with acute schizophrenia and patients with schizophrenia in remission and healthy control subjects, p value calculated using the Mann–Whitney U test.

Code for group of patients	Episodic course of schizophrenia with progressive deficit	Episodic course of schizophrenia with stable deficit	Simple schizophrenia	Patients with remission	Healthy control subjects
Continuous course of schizophrenia	0.187706	0.223449	0.183506	0.000729*	0.000038*
Episodic course of schizophrenia with progressive deficit		0.592055	0.731468	1.000000	0.011796*
Episodic course of schizophrenia with stable deficit			1.000000	0.398951	0.004769*
Simple schizophrenia				0.475707	0.001954*

*p value from pairwise comparison with Mann–Whitney U test between groups, which are named in the corresponding row and column headings for each cell; $p < 0.05$.

4. Conclusions

Our results demonstrate that IgGs from schizophrenia patients catalyze the hydrolysis of MBP, and this activity is significantly higher than IgGs from control subjects. We found that the activity level differs depending on the type of the disease course, particularly in patients with paranoid schizophrenia with continuous course demonstrating the highest activity level (1.810 mg MBP/mg IgG/h), which significantly exceeded the activity level in patients in remission and control. Thus, we suggest that patients with a continuous type of schizophrenia have a more pronounced violation of the myelination in brain structures. This reflects the peculiarity of the immunological reactivity of the organism as a whole of the continuous type of schizophrenia.

Data Availability

Data used to support the findings of this study are available from the corresponding author upon request.

Conflicts of Interest

The authors declare that there are no conflicts of interest regarding the publication of this paper.

Acknowledgments

We thank Richard H. Lozier for discussion and for language editing. The study was supported by the Russian Scientific Foundation (grant № 18-15-00053).

References

[1] R. D. Strous and Y. Shoenfeld, "Schizophrenia, autoimmunity and immune system dysregulation: a comprehensive model updated and revisited," *Journal of Autoimmunity*, vol. 27, no. 2, pp. 71–80, 2006.

[2] W. W. Eaton, M. Byrne, H. Ewald et al., "Association of schizophrenia and autoimmune diseases: linkage of Danish national registers," *American Journal of Psychiatry*, vol. 163, no. 3, pp. 521–528, 2006.

[3] S. Tiosano, A. Farhi, A. Watad et al., "Schizophrenia among patients with systemic lupus erythematosus: population-based cross-sectional study," *Epidemiology and Psychiatric Sciences*, vol. 26, no. 4, pp. 424–429, 2017.

[4] A. Mack, C. Pfeiffer, E. M. Schneider, and K. Bechter, "Schizophrenia or atypical lupus erythematosus with predominant psychiatric manifestations over 25 years: case analysis and review," *Frontiers in Psychiatry*, vol. 8, 2017.

[5] R. C. Drexhage, T. A. Hoogenboezem, D. Cohen et al., "An activated set point of T-cell and monocyte inflammatory networks in recent-onset schizophrenia patients involves

both pro- and anti-inflammatory forces," *International Journal of Neuropsychopharmacology*, vol. 14, no. 6, pp. 746–755, 2011.

[6] I. N. Otman, S. A. Zozulya, Z. V. Sarmanova, and T. P. Klushnik, "Inflammatory and autoimmune reactions in different forms of nervous system functioning disorders," *Patologicheskaia fiziologiia i eksperimental'naia terapiia*, vol. 45, no. 3, pp. 81–88, 2015.

[7] N. Muller and M. J. Schwarz, "Immune system and schizophrenia," *Current Immunology Reviews*, vol. 6, no. 3, pp. 213–220, 2010.

[8] S. G. Morozov, I. E. Gribova, T. P. Klushnik et al., "Influence of high level of antibodies to myelin basic protein in female mice on the postnatal development and behavioral reactions of the progeny," *Bulletin of Experimental Biology and Medicine*, vol. 144, no. 4, pp. 551–554, 2007.

[9] F. J. Raabe, S. Galinski, S. Papiol, P. G. Falkai, A. Schmitt, and M. J. Rossner, "Studying and modulating schizophrenia-associated dysfunctions of oligodendrocytes with patient-specific cell systems," *NPJ Schizophrenia*, vol. 4, no. 1, 2018.

[10] D. Martins-de-Souza, W. F. Gattaz, A. Schmitt et al., "Proteomic analysis of dorsolateral prefrontal cortex indicates the involvement of cytoskeleton, oligodendrocyte, energy metabolism and new potential markers in schizophrenia," *Journal of Psychiatric Research*, vol. 43, no. 11, pp. 978–986, 2009.

[11] D. Martins-de-Souza, "Proteome and transcriptome analysis suggests oligodendrocyte dysfunction in schizophrenia," *Journal of Psychiatric Research*, vol. 44, no. 3, pp. 149–156, 2010.

[12] N. S. Kolomeets and N. A. Uranova, "Pathology of oligodendroglia and myelinated fibers of the hippocampus in schizophrenia (an ultrastructural and morphometric study)," *Zhurnal Nevrologii i Psikhiatrii Imeni S.S. Korsakova*, vol. 108, no. 8, pp. 52–60, 2008.

[13] N. A. Uranova, V. M. Vostrikov, D. D. Orlovskaya, and V. I. Rachmanova, "Oligodendroglial density in the prefrontal cortex in schizophrenia and mood disorders: a study from the Stanley Neuropathology Consortium," *Schizophrenia Research*, vol. 67, no. 2-3, pp. 269–275, 2004.

[14] P. R. Matthews, S. L. Eastwood, and P. J. Harrison, "Reduced myelin basic protein and actin-related gene expression in visual cortex in schizophrenia," *PLoS ONE*, vol. 7, no. 6, article e38211, 2012.

[15] W. G. Honer, P. Falkai, C. Chen, V. Arango, J. J. Mann, and A. J. Dwork, "Synaptic and plasticity-associated proteins in anterior frontal cortex in severe mental illness," *Neuroscience*, vol. 91, no. 4, pp. 1247–1255, 1999.

[16] G. S. Burbaeva, I. S. Boksha, E. B. Tereshkina et al., "Systemic neurochemical alterations in schizophrenic brain: glutamate metabolism in focus," *Neurochemical Research*, vol. 32, no. 9, pp. 1434–1444, 2007.

[17] I. Boksha, *Specific Metabolism of Glutamate in Schizophrenia*, LAP Lambert Academic Publishing, Saarbrucken, Germany, 2012.

[18] R. Rimon, A. Ahokas, J. Ruutiainen, and P. Halonen, "Myelin basic protein antibodies in catatonic schizophrenia," *The Journal of Clinical Psychiatry*, vol. 47, no. 1, pp. 26–28, 1986.

[19] T. P. Klyushnik, T. M. Siriachenko, Z. V. Sarmanova, I. N. Otman, A. M. Dupin, and R. E. Sokolov, "Changes of the level of serum antibodies to neuroantigens in patients with schizophrenia during the treatment," *Zhurnal Nevrologii i Psikhiatrii Imeni S.S. Korsakova*, vol. 108, no. 8, pp. 61–64, 2008.

[20] C. A. Goldsmith and D. P. Rogers, "The case for autoimmunity in the etiology of schizophrenia," *Pharmacotherapy*, vol. 28, no. 6, pp. 730–741, 2008.

[21] G. M. Khandaker, L. Cousins, J. Deakin, B. R. Lennox, R. Yolken, and P. B. Jones, "Inflammation and immunity in schizophrenia: implications for pathophysiology and treatment," *The Lancet Psychiatry*, vol. 2, no. 3, pp. 258–270, 2015.

[22] G. F. van Rees, S. G. Lago, D. A. Cox et al., "Evidence of microglial activation following exposure to serum from first-onset drug-naïve schizophrenia patients," *Brain, Behavior, and Immunity*, vol. 67, pp. 364–373, 2018.

[23] V. Bergink, S. M. Gibney, and H. A. Drexhage, "Autoimmunity, inflammation, and psychosis: a search for peripheral markers," *Biological Psychiatry*, vol. 75, no. 4, pp. 324–331, 2014.

[24] D. I. Polosukhina, T. G. Kanyshkova, B. M. Doronin et al., "Hydrolysis of myelin basic protein by polyclonal catalytic IgGs from the sera of patients with multiple sclerosis," *Journal of Cellular and Molecular Medicine*, vol. 8, no. 3, pp. 359–368, 2004.

[25] A. M. Bezuglova, L. P. Konenkova, B. M. Doronin, V. N. Buneva, and G. A. Nevinsky, "Affinity and catalytic heterogeneity and metal-dependence of polyclonal myelin basic protein-hydrolyzing IgGs from sera of patients with systemic lupus erythematosus," *Journal of Molecular Recognition*, vol. 24, no. 6, pp. 960–974, 2011.

[26] M. Gonzalez-Gronow, M. Cuchacovich, R. Francos et al., "Catalytic autoantibodies against myelin basic protein (MBP) isolated from serum of autistic children impair *in vitro* models of synaptic plasticity in rat hippocampus," *Journal of Neuroimmunology*, vol. 287, pp. 1–8, 2015.

[27] D. Parshukova, L. P. Smirnova, E. A. Ermakov et al., "Autoimmunity and immune system dysregulation in schizophrenia: IgGs from sera of patients hydrolyze myelin basic protein," *Journal of Molecular Recognition*, vol. 32, no. 2, article e2759, 2019.

[28] A. C. Grodzki and E. Berenstein, "Antibody purification: affinity chromatography–protein A and protein G Sepharose," in *Immunocytochemical methods and protocols*, pp. 33–41, Humana press, 2010.

[29] E. A. Ermakov, L. P. Smirnova, T. A. Parkhomenko et al., "DNA-hydrolysing activity of IgG antibodies from the sera of patients with schizophrenia," *Open Biology*, vol. 5, no. 9, article 150064, 2015.

[30] E. A. Ermakov, L. P. Smirnova, N. A. Bokhan et al., "Catalase activity of IgG antibodies from the sera of healthy donors and patients with schizophrenia," *PLoS ONE*, vol. 12, no. 9, article e0183867, 2017.

[31] U. K. Laemmli, "Cleavage of structural proteins during the assembly of the head of bacteriophage T4," *Nature*, vol. 227, no. 5259, pp. 680–685, 1970.

[32] A. G. Baranovskii, N. A. Ershova, V. N. Buneva et al., "Catalytic heterogeneity of polyclonal DNA-hydrolyzing antibodies from the sera of patients with multiple sclerosis," *Immunology Letters*, vol. 76, no. 3, pp. 163–167, 2001.

[33] N. A. Ponomarenko, O. M. Durova, I. I. Vorobiev et al., "Autoantibodies to myelin basic protein catalyze site-specific degradation of their antigen," *Proceedings of the National Academy of Sciences*, vol. 103, no. 2, pp. 281–286, 2006.

[34] G. Sapparapu, S. A. Planque, Y. Nishiyama, S. K. Foung, and S. Paul, "Antigen-specific proteolysis by hybrid antibodies

containing promiscuous proteolytic light chains paired with an antigen-binding heavy chain," *Journal of Biological Chemistry*, vol. 284, no. 36, pp. 24622–24633, 2009.

[35] B. Wootla, O. D. Christophe, A. Mahendra et al., "Proteolytic antibodies activate factor IX in patients with acquired hemophilia," *Blood*, vol. 117, no. 7, pp. 2257–2264, 2011.

[36] A. S. Tolmacheva, E. A. Blinova, E. A. Ermakov, V. N. Buneva, N. L. Vasilenko, and G. A. Nevinsky, "IgG abzymes with peroxidase and oxidoreductase activities from the sera of healthy humans," *Journal of Molecular Recognition*, vol. 28, no. 9, pp. 565–580, 2015.

[37] E. S. Schauenstein, F. Dachs, M. Reiter, H. Gombotz, and W. List, "Labile Disulfide Bonds and Free Thiol Groups in Human IgG I," *International Archives of Allergy and Immunology*, vol. 80, pp. 180–184, 1986.

[38] J. Schurman, G. J. Perdok, A. D. Gorter, and R. C. Aalberse, "The inter-heavy chain disulfide bonds of IgG4 are in equilibrium with intra-chain disulfide bonds," *Molecular Immunology*, vol. 38, no. 1, pp. 1–8, 2001.

[39] K. L. Davis and V. Haroutunian, "Global expression-profiling studies and oligodendrocyte dysfunction in schizophrenia and bipolar disorder," *The Lancet*, vol. 362, no. 9386, p. 758, 2003.

[40] N. Takahashi, T. Sakurai, K. L. Davis, and J. D. Buxbaum, "Linking oligodendrocyte and myelin dysfunction to neurocircuitry abnormalities in schizophrenia," *Progress in Neurobiology*, vol. 93, no. 1, pp. 13–24, 2011.

[41] Y. Hakak, J. R. Walker, C. Li et al., "Genome-wide expression analysis reveals dysregulation of myelination-related genes in chronic schizophrenia," *Proceedings of the National Academy of Sciences*, vol. 98, no. 8, pp. 4746–4751, 2001.

[42] C. Aston, L. Jiang, and B. P. Sokolov, "Microarray analysis of postmortem temporal cortex from patients with schizophrenia," *Journal of Neuroscience Research*, vol. 77, no. 6, pp. 858–866, 2004.

[43] C. Aston, L. Jiang, and B. P. Sokolov, "Transcriptional profiling reveals evidence for signaling and oligodendroglial abnormalities in the temporal cortex from patients with major depressive disorder," *Molecular Psychiatry*, vol. 10, no. 3, pp. 309–322, 2005.

[44] S. Dracheva, K. L. Davis, B. Chin, D. A. Woo, J. Schmeidler, and V. Haroutunian, "Myelin-associated mRNA and protein expression deficits in the anterior cingulate cortex and hippocampus in elderly schizophrenia patients," *Neurobiology of Disease*, vol. 21, no. 3, pp. 531–540, 2006.

[45] P. Katsel, K. L. Davis, and V. Haroutunian, "Variations in myelin and oligodendrocyte-related gene expression across multiple brain regions in schizophrenia: a gene ontology study," *Schizophrenia Research*, vol. 77, no. 2-3, pp. 241–252, 2005.

[46] D. Tkachev, M. L. Mimmack, M. M. Ryan et al., "Oligodendrocyte dysfunction in schizophrenia and bipolar disorder," *The Lancet*, vol. 362, no. 9386, pp. 798–805, 2003.

[47] C. L. Beasley, A. J. Dwork, G. Rosoklija et al., "Metabolic abnormalities in fronto-striatal-thalamic white matter tracts in schizophrenia," *Schizophrenia Research*, vol. 109, no. 1-3, pp. 159–166, 2009.

[48] W. Cahn, H. E. H. Pol, E. B. Lems et al., "Brain Volume Changes in First-Episode Schizophrenia:A 1-Year Follow-up Study," *Archives of General Psychiatry*, vol. 59, no. 11, pp. 1002–1010, 2002.

[49] M. Y. Deng, G. M. McAlonan, C. Cheung et al., "A naturalistic study of grey matter volume increase after early treatment in anti-psychotic naïve, newly diagnosed schizophrenia," *Psychopharmacology*, vol. 206, no. 3, pp. 437–446, 2009.

[50] D. Moreno, M. Burdalo, S. Reig et al., "Structural neuroimaging in adolescents with a first psychotic episode," *Journal of the American Academy of Child & Adolescent Psychiatry*, vol. 44, no. 11, pp. 1151–1157, 2005.

[51] D. Sun, G. W. Stuart, M. Jenkinson et al., "Brain surface contraction mapped in first-episode schizophrenia: a longitudinal magnetic resonance imaging study," *Molecular Psychiatry*, vol. 14, no. 10, pp. 976–986, 2009.

[52] H. Witthaus, U. Mendes, M. Brüne et al., "Hippocampal subdivision and amygdalar volumes in patients in an at-risk mental state for schizophrenia," *Journal of Psychiatry and Neuroscience*, vol. 35, no. 1, pp. 33–40, 2010.

[53] S. Li, H. Wu, H. Guo, and Z. Zhao, "Neuron-specific Enolase and myelin basic protein in cerebrospinal fluid of patients with first episode schizophrenia," *Journal of Huazhong University of Science and Technology. Medical Sciences*, vol. 26, no. 2, pp. 228–230, 2006.

[54] K. Melkersson and S. Bensing, "Signs of impaired blood-brain barrier function and lower IgG synthesis within the central nervous system in patients with schizophrenia or related psychosis, compared to that in controls," *Neuro Endocrinology Letters*, vol. 39, no. 1, pp. 33–42, 2018.

[55] L. J. Glass, D. Sinclair, D. Boerrigter et al., "Brain antibodies in the cortex and blood of people with schizophrenia and controls," *Translational Psychiatry*, vol. 7, no. 8, article e1192, 2017.

[56] L. Zuckerman and I. Weiner, "Maternal immune activation leads to behavioral and pharmacological changes in the adult offspring," *Journal of Psychiatric Research*, vol. 39, no. 3, pp. 311–323, 2005.

[57] T. P. Klyushnik, S. A. Krasnolobova, Z. V. Sarmanova, I. V. Shcherbakova, S. G. Morozov, and I. E. Gribova, "Effect of antibodies to nerve growth factor and serum albumin on the development and behavior of mice," *Bulletin of Experimental Biology and Medicine*, vol. 138, no. 7, pp. 84–86, 2004.

[58] L. Brimberg, S. Mader, Y. Fujieda et al., "Antibodies as mediators of brain pathology," *Trends in Immunology*, vol. 36, no. 11, pp. 709–724, 2015.

[59] I. St-Amour, I. Paré, W. Alata et al., "Brain bioavailability of human intravenous immunoglobulin and its transport through the murine blood–brain barrier," *Journal of Cerebral Blood Flow & Metabolism*, vol. 33, no. 12, pp. 1983–1992, 2013.

[60] S. Najjar, S. Pahlajani, V. De Sanctis, J. N. Stern, A. Najjar, and D. Chong, "Neurovascular unit dysfunction and blood–brain barrier hyperpermeability contribute to schizophrenia neurobiology: a theoretical integration of clinical and experimental evidence," *Frontiers in Psychiatry*, vol. 8, 2017.

[61] T. P. Vetlugina, O. A. Lobacheva, A. V. Semke, V. B. Nikitina, and N. A. Bokhan, "An effect of quetiapine on the immune system of patients with schizophrenia," *Zhurnal nevrologii i psikhiatrii im. S.S. Korsakova*, vol. 116, no. 7, pp. 55–58, 2016.

[62] Y. S. Abrosimova, "Cytokine disbalance and Fas-dependent apoptosis in shift-like and continued schizophrenia," *Neurological bulletin named after Vladimir Bekhterev*, vol. 39, no. 3, pp. 23–27, 2007.

[63] E. F. Torrey and R. H. Yolken, "The schizophrenia–rheumatoid arthritis connection: infectious, immune, or both?," *Brain, Behavior, and Immunity*, vol. 15, no. 4, pp. 401–410, 2001.

[64] M. C. Hardoy, M. Cadeddu, A. Serra et al., "A pattern of cerebral perfusion anomalies between major depressive disorder and Hashimoto thyroiditis," *BMC Psychiatry*, vol. 11, no. 1, 2011.

[65] N. Müller, "Inflammation in schizophrenia: pathogenetic aspects and therapeutic considerations," *Schizophrenia Bulletin*, vol. 44, no. 5, pp. 973–982, 2018.

[66] M. E. Bauer and A. L. Teixeira, "Inflammation in psychiatric disorders: what comes first?," *Annals of the New York Academy of Sciences*, vol. 1437, no. 1, pp. 57–67, 2019.

[67] H. Taguchi, S. Planque, Y. Nishiyama et al., "Autoantibody-catalyzed hydrolysis of amyloid β peptide," *Journal of Biological Chemistry*, vol. 283, no. 8, pp. 4714–4722, 2008.

[68] E. S. Odintsova, S. V. Baranova, P. S. Dmitrenok et al., "Antibodies to HIV integrase catalyze site-specific degradation of their antigen," *International Immunology*, vol. 23, no. 10, pp. 601–612, 2011.

[69] G. A. Nevinsky, "Natural catalytic antibodies in norm and in HIV-infected patients," *Understanding HIV/AIDS management and care—pandemic approaches the 21st century*, pp. 151–192, 2011.

[70] G. A. Nevinsky and V. N. Buneva, "Natural catalytic antibodies in norm, autoimmune, viral, and bacterial diseases," *The Scientific World Journal*, vol. 10, Article ID 820417, 1233 pages, 2010.

[71] S.-J. Chen, Y.-L. Chao, C.-Y. Chen et al., "Prevalence of autoimmune diseases in in-patients with schizophrenia: nationwide population-based study," *The British Journal of Psychiatry*, vol. 200, no. 5, pp. 374–380, 2012.

[72] C. L. Cazzullo, E. Sacchetti, A. Galluzzo et al., "Cytokine profiles in schizophrenic patients treated with risperidone: a 3-month follow-up study," *Progress in Neuro-Psychopharmacology and Biological Psychiatry*, vol. 26, no. 1, pp. 33–39, 2002.

[73] X. Y. Zhang, D. F. Zhou, L. Y. Cao, P. Y. Zhang, G. Y. Wu, and Y. C. Shen, "Changes in serum interleukin-2, -6, and -8 levels before and during treatment with risperidone and haloperidol," *The Journal of Clinical Psychiatry*, vol. 65, no. 7, pp. 940–947, 2004.

[74] X. Y. Zhang, D. F. Zhou, L. Y. Cao, G. Y. Wu, and Y. C. Shen, "Cortisol and cytokines in chronic and treatment-resistant patients with schizophrenia: association with psychopathology and response to antipsychotics," *Neuropsychopharmacology*, vol. 30, no. 8, pp. 1532–1538, 2005.

[75] F. McKenna, P. J. McLaughlin, B. J. Lewis et al., "Dopamine receptor expression on human T-and B-lymphocytes, monocytes, neutrophils, eosinophils and NK cells: a flow cytometric study," *Journal of Neuroimmunology*, vol. 132, no. 1-2, pp. 34–40, 2002.

[76] S. Yamamoto, N. Ohta, A. Matsumoto, Y. Horiguchi, M. Koide, and Y. Fujino, "Haloperidol suppresses NF-kappaB to inhibit lipopolysaccharide-induced pro-inflammatory response in RAW 264 cells," *Medical Science Monitor*, vol. 22, pp. 367–372, 2016.

Hindawi
Journal of Immunology Research
Volume 2020, Article ID 4384696, 10 pages
https://doi.org/10.1155/2020/4384696

Research Article

ChIP-seq Profiling Identifies Histone Deacetylase 2 Targeting Genes Involved in Immune and Inflammatory Regulation Induced by Calcitonin Gene-Related Peptide in Microglial Cells

Xingjing Guo,[1,2] Dan Chen,[3] Shuhong An,[1] and Zhaojin Wang[1]

[1]*Department of Human Anatomy, Shandong First Medical University & Shandong Academy of Medical Sciences, Taian, China*
[2]*Department of Physiology, Shandong First Medical University & Shandong Academy of Medical Sciences, Taian, China*
[3]*Experimental Center, Shandong University of Traditional Chinese Medicine, Jinan, China*

Correspondence should be addressed to Shuhong An; shhan7766@126.com and Zhaojin Wang; zjwang@sdfmu.edu.cn

Received 16 April 2020; Accepted 7 July 2020; Published 4 August 2020

Guest Editor: Fabiano Carvalho

Calcitonin gene-related peptide (CGRP) is a mediator of microglial activation at the transcriptional level. The involvement of the epigenetic mechanism in this process is largely undefined. Histone deacetylase (HDAC)1/2 are considered important epigenetic regulators of gene expression in activated microglia. In this study, we examined the effect of CGRP on HDAC2-mediated gene transcription in microglial cells through the chromatin immunoprecipitation sequencing (ChIP-seq) method. Immunofluorescence analysis showed that mouse microglial cells (BV2) expressed CGRP receptor components. Treatment of microglia with CGRP increased HDAC2 protein expression. ChIP-seq data indicated that CGRP remarkably altered promoter enrichments of HDAC2 in microglial cells. We identified 1271 gene promoters, whose HDAC2 enrichments are significantly altered in microglia after CGRP treatment, including 1181 upregulating genes and 90 downregulating genes. Bioinformatics analyses showed that HDAC2-enriched genes were mainly associated with immune- and inflammation-related pathways, such as nitric oxide synthase (NOS) biosynthetic process, retinoic acid-inducible gene- (RIG-) like receptor signaling pathway, and nuclear factor kappa B (NF-κB) signaling pathway. The expression of these key pathways (NOS, RIG-I, and NF-κB) were further verified by Western blot. Taken together, our findings suggest that genes with differential HDAC2 enrichments induced by CGRP function in diverse cellular pathways and many are involved in immune and inflammatory responses.

1. Introduction

Microglia are innate immune cells of the central nervous system that are responsible for the excessive and chronic neuroinflammatory response following damage and disease [1, 2]. Calcitonin gene-related peptide (CGRP) as a mediator of glial cell activation plays a role as signaling molecule, mediating interactions between damaged neurons and surrounding glial cells [3]. Previous research has demonstrated that the presence of CGRP induced the activation of microglia at the transcriptional level through expression of the immediate-early genes in cultured microglia [4, 5].

CGRP operates via its receptor that, in many cell types, leads to a range of biological effects including those associated with neurons and microglia [6, 7]. A functional CGRP receptor consist of 3 components, the calcitonin receptor-like receptor (CRLR), receptor activity-modifying protein 1 (RAMP1), and CGRP receptor component protein (CRCP) that couple the receptor to the cellular signal pathway leading to increased intracellular cAMP and activated protein kinase A (PKA) [8]. Accumulating evidence suggested that microglia express functional CGRP receptors, as treatment with CGRP triggers microglial activation by induction of c-fos gene expression, cAMP accumulation, and release of proinflammatory mediators in microglia [4, 5, 9]. A previous study indicated that CGRP may act as a paracrine mediator to induce activation of glial activation [10, 11]. Administration of CGRP in rat models of temporomandibular joint disorder contributed to the increased microglial marker of OX-42 expression and microglial

activation in the spinal cord [12], suggesting a functional link between CGRP and microglial activation.

Histone deacetylase (HDAC)1/2 are essential for microglial survival and expansion during development [13]. Increased activity of HDAC2 is closely related to glial activation in a mouse model of retinal injury [14]. Selective inhibition of HDAC1 or 2 suppresses the expression of inflammatory cytokines in BV2 murine microglia activated with lipopolysaccharide (LPS) [15]. Previous data indicated that HDAC2 activates NF-κB and promotes NF-κB-dependent gene expression [16], which plays a crucial role in microglial activation [17].

The ability of CGRP to activate microglial cells at the level of transcription raises the question of whether the gene expression induced by CGRP associates with epigenetic regulation by HDAC2 in activated microglia. In the present study, we adopted chromatin immunoprecipitation followed by sequencing (ChIP-seq) to profile and compare the variation of HDAC2 enrichments in target genes at the genome-wide level in the microglial cell line (BV2) from treatment of CGRP and control to gain a better understanding of a potential role for this peptide in the responses of microglia. In addition, the expression of CGRP receptor components was also explored in BV2 cells and Western blot was used to determine whether the expression of HDAC2 in microglia was influenced by CGRP, hoping that these studies could further understand the underlying regulatory mechanism of microglial activation by CGRP at the molecular level.

2. Materials and Methods

2.1. Cell Culture and Drug Administration. The mouse microglial cell line (BV2) was obtained from the Cell Bank of the Chinese Academy of Sciences (Beijing, China). Microglial cells were cultured in Dulbecco's modified Eagle's medium (DMEM, Gibco) supplemented with 10% fetal bovine serum (FBS, Biological Industries) incubated at 37°C in an atmosphere of 5% CO_2. BV2 cells continuously stimulated with CGRP peptide (1 μmol/L, Tocris Bioscience, Cat. #1161) at 1, 2, 4, and 6 h, respectively. Cells without CGRP peptide were used as the control. To assess the possible impact of HDAC2 on the expression of iNOS, RIG-I, and NF-κB induced by CGRP, 0.5 mmol/L valproic acid (VPA, HDAC2 inhibitor, MedChemExpress, Cat. #1069-66-5) were preapplied for 60 min and coapplied together with CGRP for 2 h at 37°C.

2.2. Immunofluorescence of Cultured Cells. Immunofluorescence was performed essentially as described before [18]. BV2 cells were cultured on poly-L-lysine-coated coverslips in six-well plates. Following a single wash in phosphate-buffered saline (PBS), cultured microglial cells were fixed in 4% paraformaldehyde for 15 min at room temperature. Double-labeling immunofluorescence staining for primary antibodies against ionized calcium binding adaptor molecule 1 (Iba1, a marker for microglia; 1 : 200, Novus, Cat. #NB 100-1028) and CRLR (1 : 200, Abcam, Cat. #ab84467), RAMP1 (1 : 200, Sigma-Aldrich, Cat. #SAB250086), or CRCP (1 : 200, Proteintech, Cat. #14348-1-AP) on coverslip-cultured microglia was performed. Coverslips were incubated with a mixture of the two primary antibodies overnight. Following three washes with tris-buffered saline (TBS), coverslips were treated with a mixture of matching secondary antibodies (Jackson ImmunoResearch). The specificity of antibodies used was checked by Western blotting and/or omission of the primary antibodies. No specific immunoreactivity was detected in these controls.

2.3. Chromatin Immunoprecipitation. Chromatin was prepared from fixed mouse microglial cells (stimulated with 1 μmol/L CGRP, 2 h) and sonicated fragments ranged in size from 200 to 1500 bp. Approximately 2×10^7 cell equivalents were used for each immunoprecipitation. ChIP was performed as described previously [19], using anti-HDAC2 antibody (Abcam, Cat. #ab12169, ChIP Grade) or a control rabbit IgG.

2.4. Sequencing Library Preparation, Cluster Generation, and Sequencing. DNA samples were end-repaired, A-tailed, and adaptor-ligated using TruSeq Nano DNA Sample Prep Kit (Cat. #FC-121-4002, Illumina), following the manufacturer's instructions. ~200-1500 bp fragments were size-selected using AMPure XP beads. The final size of the library was confirmed by Agilent 2100 Bioanalyzer. Samples were diluted to a final concentration of 8 pmol/L, and cluster generation was performed on the Illumina cBot using HiSeq 3000/4000 PE Cluster Kit (Cat. #PE-410-1001, Illumina), following the manufacturer's instructions. Sequencing was performed on Illumina HiSeq 4000 using HiSeq 3000/4000 SBS Kit (300 cycles) (Cat. #FC-410-1003, Illumina), according to the manufacturer's instructions.

2.5. Data Collection and ChIP-seq Analysis. After sequencing platform-generated sequencing images, stages of image analysis and base calling were performed using Off-Line Basecaller software (OLB V1.8). Sequence quality was examined using the FastQC software. After passing Solexa CHASTITY quality filter, clean reads were aligned to mouse genome (UCSC MM10) using Bowtie software (V2.1.0) [20]. Aligned reads were used for peak calling of ChIP regions using MACS V1.4.2 [21]. Statistically significant ChIP-enriched regions (peaks) were identified by comparison of IP vs. input or comparison to a Poisson background model, using a P value threshold of 10^{-4}. Peaks in samples were annotated by the nearest gene using the newest UCSC RefSeq database [22]. The annotation of the peaks which were located within -2 kb to +2 kb around the corresponding gene TSS in samples can be found from the peaks-promoter-annotation.

2.6. Bioinformatics Analysis. The Gene Ontology (GO) functional and Kyoto Encyclopedia of Genes and Genomes (KEGG) pathway enrichment analyses were performed using the Database for Annotation, Visualization and Integrated Discovery (DAVID) and KEGG Orthology-Based Annotation System (KOBAS) online tools (http://www.geneontology.org and http://www.genome.jp/kegg) [23, 24].

2.7. Western Blotting. Western blot analysis was performed as described before [18]. Cultured microglial cells were lysed, and the protein was extracted. The protein lysate from each sample was separated electrophoretically on a 10% sodium dodecyl sulfate-polyacrylamide gel and then transferred to a polyvinylidene fluoride (PVDF) membrane. After blocking with 5% nonfat milk in TBS-T (containing 0.1% Tween-20) for 2 h, membranes were incubated with HDAC2 (Abcam, Cat. #ab32117), NF-κB (Abcam, Cat. #1559-1), RIG-I (Abcam, Cat. #ab45428), and iNOS (Abcam, Cat. #ab3523) in 5% nonfat milk in TBS-T overnight at 4°C. After washes with TBS-T, membranes were incubated with appropriate secondary antibodies for 2 h. Results were visualized using an ECL chemiluminescence system. GAPDH rabbit mAb antibody (Cell Signaling Technology, Cat. #2118) was also used as a probed control to ensure the loading of equivalent amounts of sample proteins. Band densities were compared in TotalLab software (version 2.01; Bio-Rad, Hercules, CA).

2.8. Statistical Analysis. Data are presented as the mean ± standard error of the mean (SEM). For the analyses of Western blot data, Mann-Whitney U tests were used for comparisons between two groups, and Kruskal-Wallis tests with Dunn's multiple comparisons post hoc tests were used for comparisons among multiple groups. The data from the Rotarod test were compared using Kruskal-Wallis tests with Dunn's multiple comparisons post hoc tests. Significance was defined by P values < 0.05.

3. Results

3.1. CGRP Increases HDAC2 Expression in Microglial Cells. To study the effect of CGRP on microglial cells, we first investigated the expression of CGRP receptor components on microglia. Figure 1(a) shows an example of colocalization of CRLR, RAMP1, and CRCP with the Iba1 (microglial marker) immunoreactivity on microglial cells in culture. Nearly all of the Iba1-positive cells expressed CGRP receptor components CRLR, RAMP1, and CRCP.

The expression of HDAC2 protein in microglia was assessed by Western blot following treatment with CGRP for 0, 1, 2, 4, and 6 h, respectively. As shown in Figure 1(b), CGRP treatment significantly increased the expression of the HDAC2 protein level in microglia ($P < 0.05$). CGRP was found to induce the expression of HDAC2 in a time-dependent manner with a maximal effect observed after 6 h.

3.2. Genome-Wide Profile of HDAC2 Targets in Microglia after CGRP Treatment. To investigate the role of HDAC2 on microglia after treatment with CGRP, the profile of HDAC2 targets in microglial cells was analyzed using an Illumina HiSeq 4000 sequencing technique after stimulation with CGRP for 2 h. Model-based Analysis of ChIP-seq (MACS, v1.4.2) software was used to detect the ChIP-enriched regions (peaks) from ChIP-seq data. Differentially enriched regions with statistical significance between the CGRP-treated group and the control were identified by Detecting Differential Chromatin Modification Sites from ChIP-seq Data with Biological Replicates (diffReps), cut-off: FC = 2.0, $P = 10^{-4}$).

The ChIP-seq for the CGRP-treated microglial cells generated 21827 enriched regions (peaks), including 17646 up peaks and 4181 down peaks, compared with the control group. The peak distribution of ChIP-seq reads of HDAC2 was showed in Figures 2(a) and 2(b). We identified 1271 gene promoters, whose HDAC2 enrichments are significantly altered in microglial cells treated with CGRP, including 1181 upregulated genes and 90 downregulated genes (Table S1). The distribution of HDAC2-enriched promoters was mapped to proximal regions of transcription start sites (TSSs) of RefSeq genes (from about -1800 bp to +1800 bp of TSSs, Figure 2(c)).

3.3. GO Analysis of Peaks Relative to Annotated Genes. To further understand functions of annotated genes related to peaks, they were functionally classified using GO terminology. According to the functional annotation in GO database, key upregulated HDAC2 target genes were mostly enriched for biological process (BP) terms associated with positive regulation of T cell cytokine production (e.g., tumor necrosis factor receptor associated factor 6 (TRAF6), mucosa-associated lymphoid tissue lymphoma translocation gene 1 (MALT1)), histone acetylation (e.g., lysine acetyltransferase 8 (KAT8), KAT8 regulatory NSL complex subunit 2 (KANSL2)), activation of NF-κB-inducing kinase activity (e.g., ZFP91 zinc finger protein (ZFP91), TRAF6, and MALT1), and NOS biosynthetic process (e.g., Fc fragment of IgE receptor II (FCER2A), nucleotide binding oligomerization domain containing 2 (NOD2), prostaglandin E receptor 4 (PTGER4), and toll-like receptor 2 (TLR2)). When focusing on cellular components (CC), the most represented categories were BLOC-1 complex, nuclear exosome (RNase complex), and NADPH oxidase complex. The most represented categories for molecular function (MF) were related to $3'$,$5'$-cGMP phosphodiesterase activity, histone acetyltransferase activity, nucleosomal DNA binding, and NADPH binding. Most genes are well-known immune and inflammatory responses (e.g., TRAF6, TLR2, and FCER2A). Association with immune- and inflammation-related genes seems therefore to be a feature of CGRP-mediated HDAC2 enrichments. GO enrichment terms of BP, CC, and MF for upregulated genes are shown in Figure 3(a).

Meanwhile, key dowregulated HDAC2 target genes were enriched in BP terms such as regulation of histone H3K9 acetylation, toll-like receptor 9 signaling pathway, astrocyte activation, and negative regulation of tumor necrosis factor signaling. The most represented categories for CC were related to SMN complex and nuclear lamina and MF terms such as cyclic nucleotide-gated ion channel activity and cGMP binding. GO enrichment terms of BP, CC, and MF for downregulated genes are shown in Figure 3(b).

3.4. KEGG Pathway Analysis of Peaks Relative to Annotated Genes. KEGG pathway enrichment analysis was performed using the software KOBAS. The $P < 0.05$ was set as the

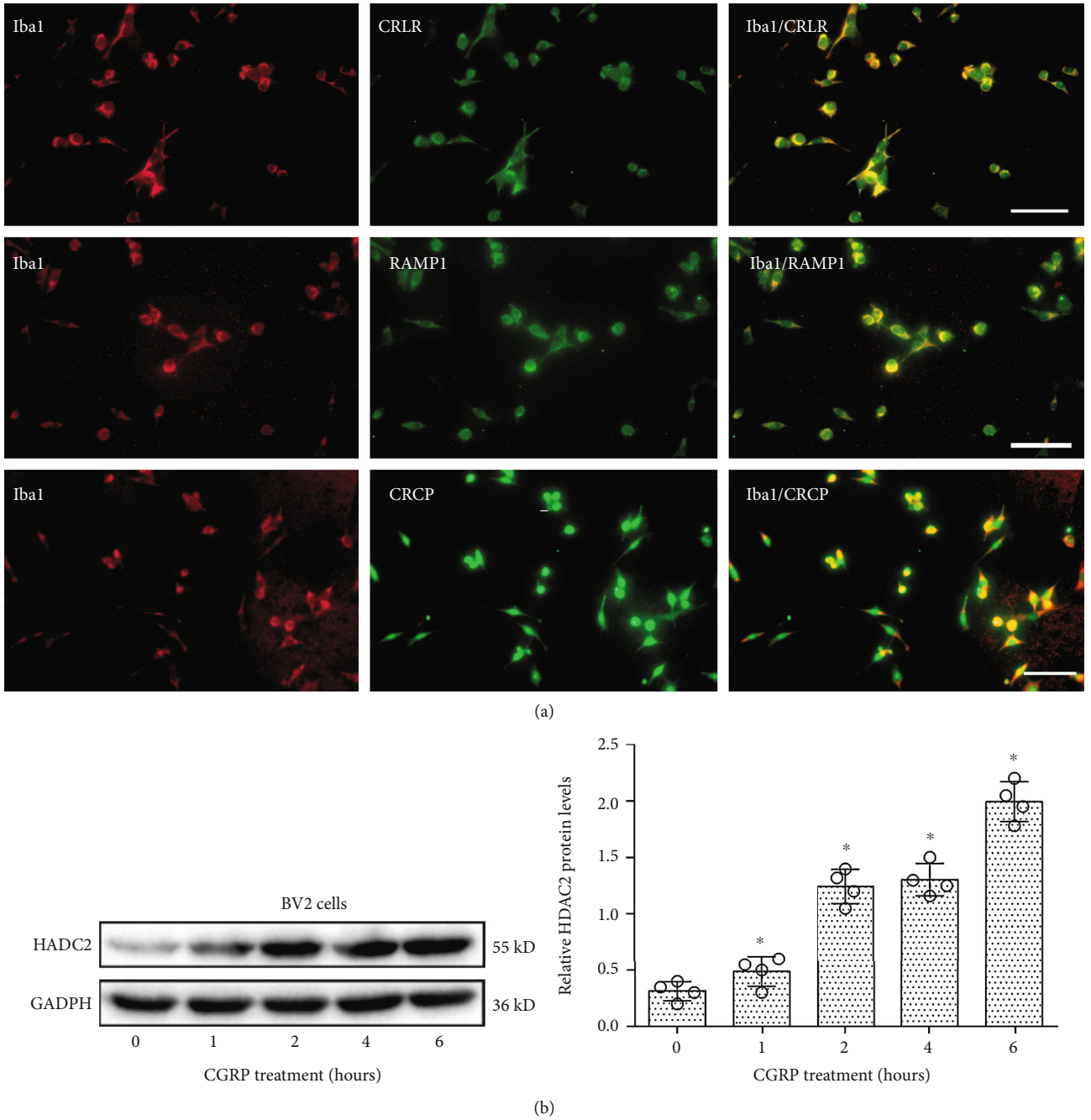

Figure 1: Cultured mouse microglial cells (BV2) expressed Iba1 and CGRP receptor components CRLR, RAMP1, or CRCP. (a) Expression of Iba1 (a marker of microglia, red) and its colocalization with CRLR, RAMP1, or CRCP staining (green) in cultured microglial cells. Scale bar 40 μm. (b) Western blot analysis of HDAC2 expression in microglia with treatment with CGRP at 0, 1, 2, 4, and 6 h, respectively. Relative amounts of proteins were calculated by normalizing to GAPDH. Data are presented as the mean ± SEM ($N = 4$ independent cell culture preparations, Mann-Whitney U tests or Kruskal-Wallis tests). $^*P < 0.05$.

threshold of significant enrichment. Based on the KEGG pathway enrichment analysis, key upregulated genes were significantly enriched in 10 signaling pathways, such as the Fc epsilon RI signaling pathway, RIG-like receptor signaling pathway, NF-κB signaling pathway, and T cell receptor signaling pathway, which were mostly related to immune and inflammatory responses (Figure 3(c)). From these data, KEGG enrichment analysis related to immune and inflammatory responses accounted for the enrichment score which also agree with the GO enrichment analysis above. However, none of downregulated genes was significantly enriched in any KEGG pathway.

3.5. Validation of Key Pathways from ChIP-seq by Western Blot. In order to explore whether or not CGRP involves the NOS biosynthetic process, RIG-like receptor signaling pathway, and NF-κB signaling pathway, the expression of iNOS, RIG-I, and NF-κB protein levels in microglial cells was

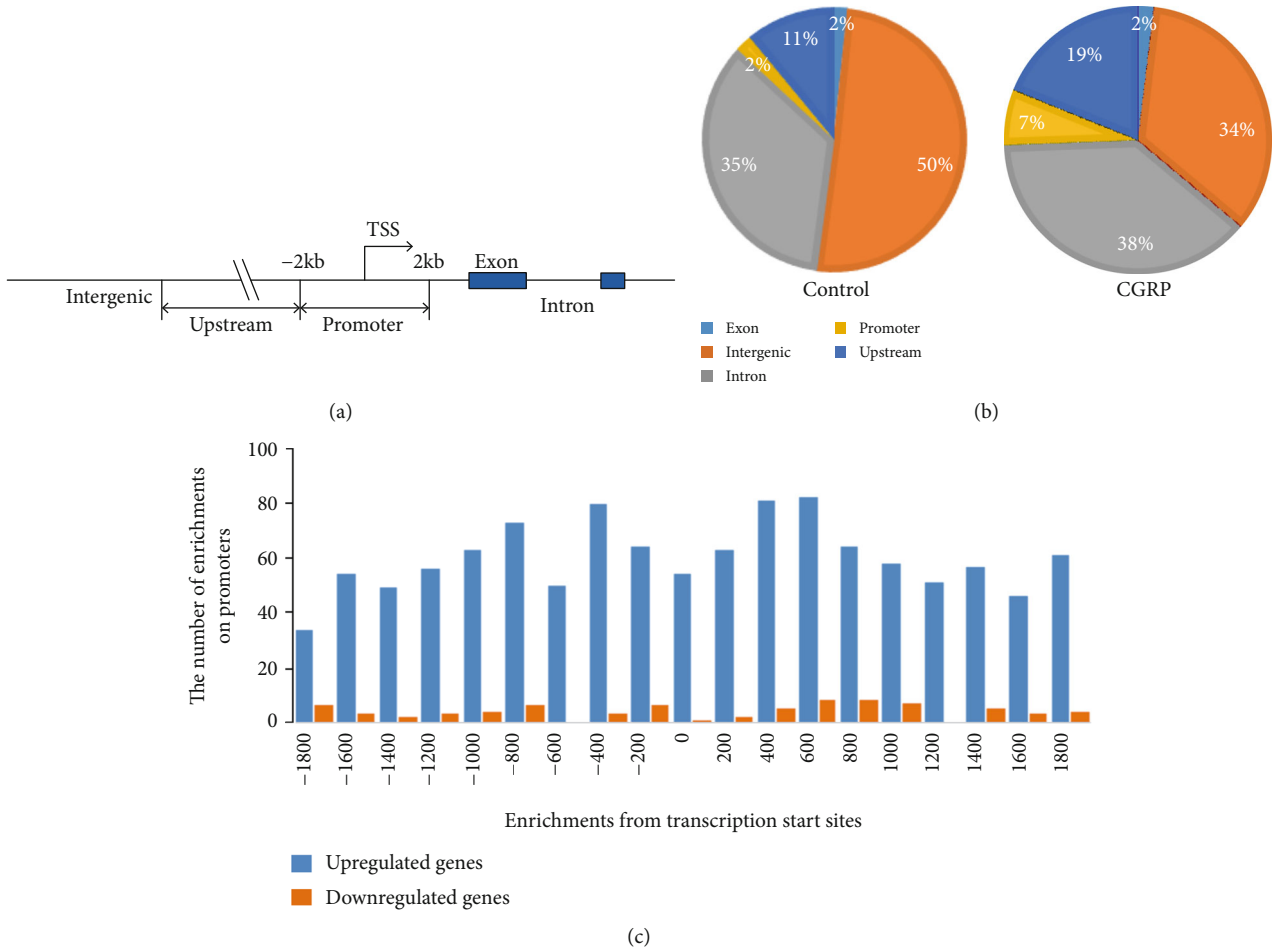

Figure 2: Effect of CGRP on the enriched region (peak) distribution of the ChIP-seq reads of HDAC2 in microglia treated with CGRP compared with the control. (a) Genome-wide distribution of enrichments relative to annotated genes. (b) The peak distribution of ChIP-seq reads of HDAC2 in control and microglial cells treated with CGRP. (c) The distribution of HDAC2 peaks on promoters relative to gene transcription start sites (TSSs). Shown are HDAC2 peak frequencies relative to the distance from the nearest annotated TSS in microglial cells treated with CGRP.

assessed by Western blot after treatment with CGRP for 0, 1, 2, 4, and 6 h, respectively. As shown in Figure 4(a), CGRP treatment significantly increased the expression of iNOS, RIG-I, and NF-κB protein levels in microglia ($P < 0.05$). CGRP was found to induce the expression of iNOS, RIG-I, and NF-κB in a time-dependent manner with a maximal effect observed after 6 h which was well in agreement with the HDAC2 enrichment analysis observed by bioinformatics analysis. The results of Western blot analyses provided evidence that the ChIP-seq method for large-scale gene expression quantification was reliable.

3.6. HDAC2 Inhibitor Suppresses the Increase of iNOS, RIG-I, and NF-κB Expression Induced by CGRP. A recent report showed that HDAC2 increased the expression of iNOS in macrophages following inflammatory stimulation [25]. To test whether HDAC2 was involved in CGRP-induced expression of iNOS, RIG-I, and NF-κB in this study, a HDAC2 inhibitor VPA was coapplied together with CGRP. As shown in Figure 4(b), CGRP increased the expression of iNOS, RIG-I, and NF-κB following treatment of microglia with CGRP, and the HDAC2 inhibitor VPA partially or completely blocked the CGRP-mediated upregulation of iNOS, RIG-I, and NF-κB ($P < 0.05$).

4. Discussion

Here, we mapped HDAC2 enrichment profiles induced by CGRP at these loci using ChIP-seq in mouse microglial cells and examined the influence of CGRP on HDAC2 enrichment profiles on promoter regions to test the hypothesis that the gene expression induced by CGRP was associated with HDAC2-mediated epigenetic regulation in microglia [15, 17]. ChIP-seq data showed that CGRP could substantially change HDAC2 enrichments on gene promoters, including 1181 upregulated genes and 90 downregulated genes, suggesting that CGRP could alter enrichment profiles of HDAC2 at promoters in a gene-specific manner.

HDAC2 is involved in regulating microglial activation and gene transcription [14, 15]. Our results showed that

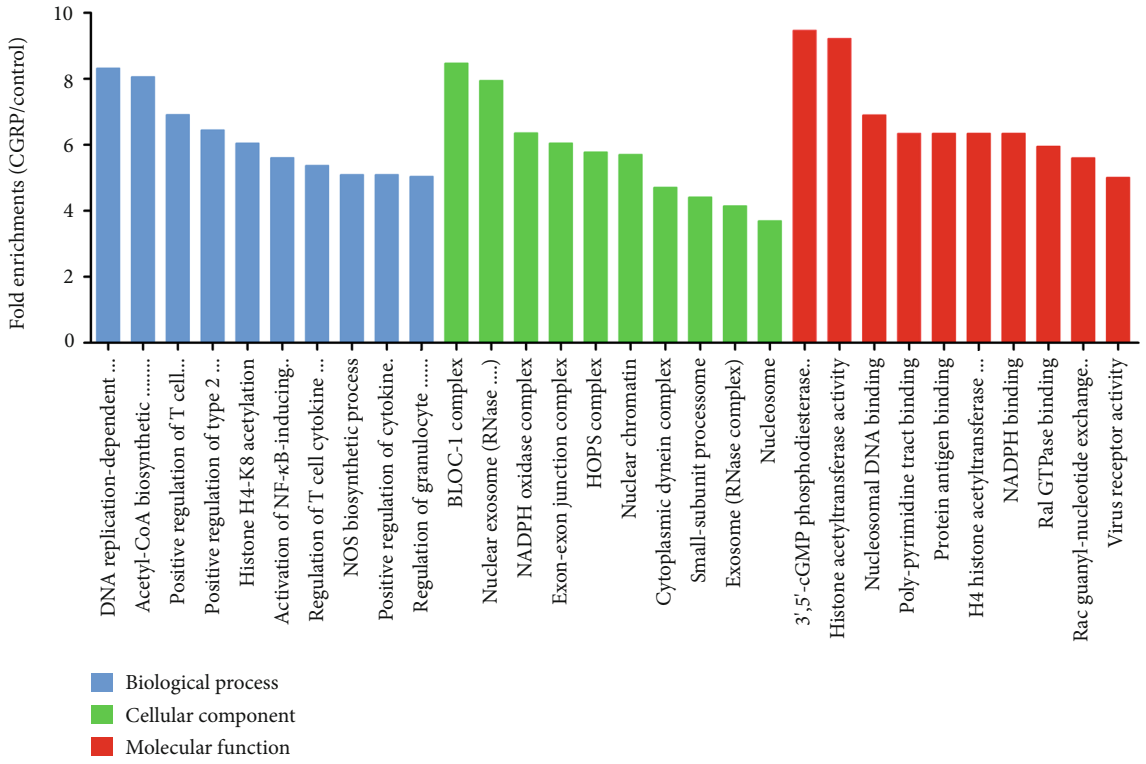

(a)

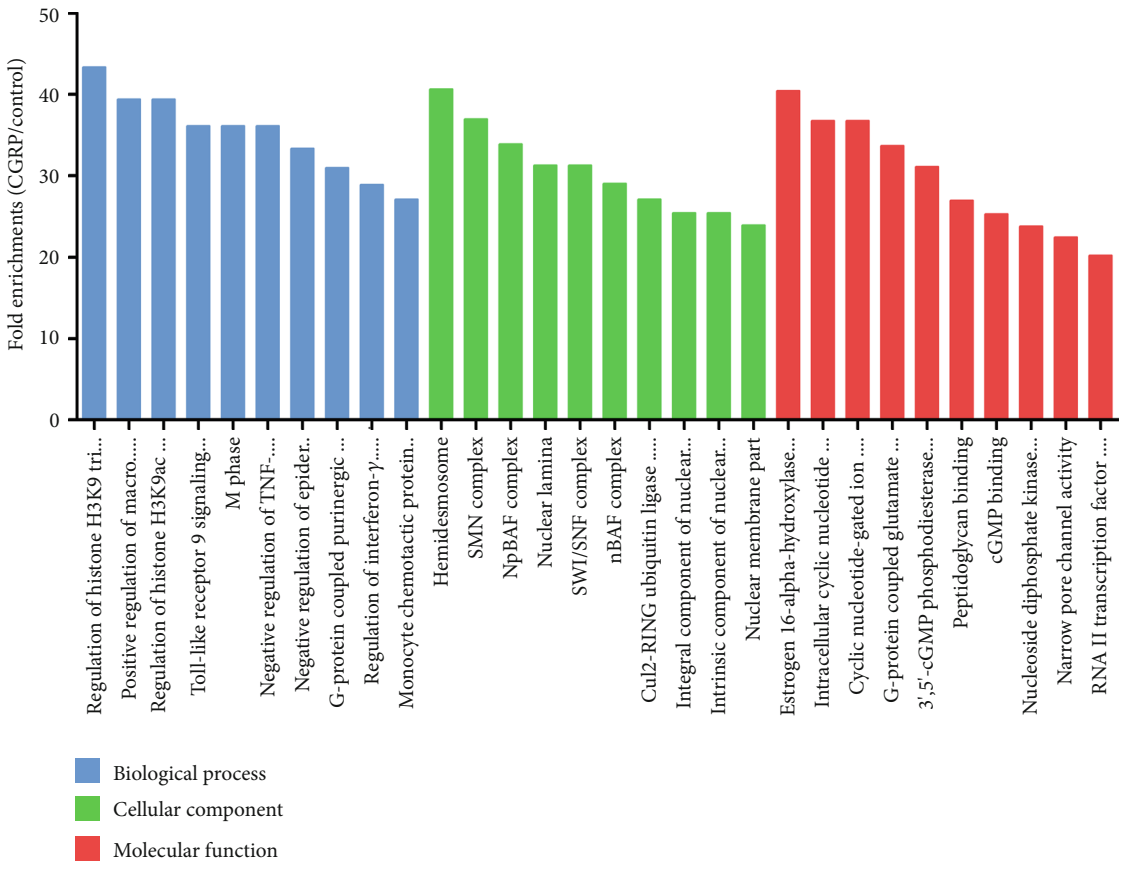

(b)

Figure 3: Continued.

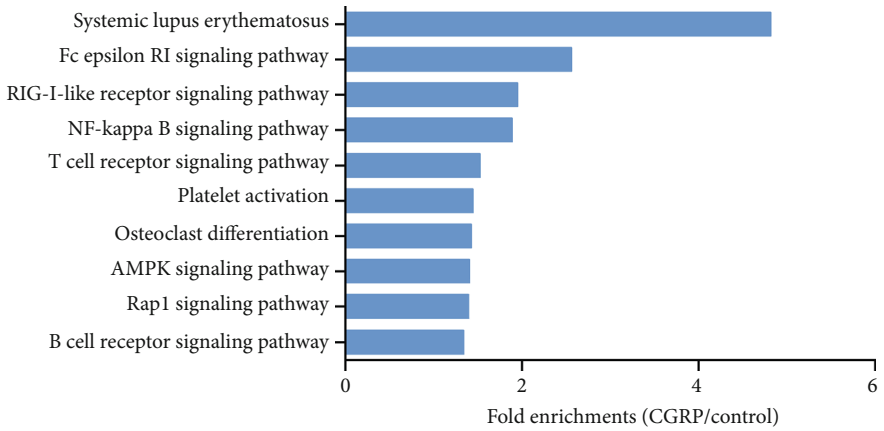

(c)

Figure 3: The Gene Ontology (GO) and Kyoto Encyclopedia of Genes and Genomes (KEGG) pathway analyses of genes with differentially enriched HDAC2 in microglial cells treated with CGRP. GO annotation of upregulated genes (a) or downregulated genes (b) with HDAC2 enrichments of the CGRP treatment group versus the control. Bar plots show the top ten fold enrichment values of the significant enrichment terms involving biological process (BP), cellular component (CC), and molecular function (MF). (c) KEGG pathway analysis of genes with differentially enriched HDAC2 in microglial cells treated with CGRP. The bar plot shows the top ten fold enrichment values of the significant enrichment pathway. Analysis by DAVID and KOBAS online tools (http://www.geneontology.org and http://www.genome.jp/kegg).

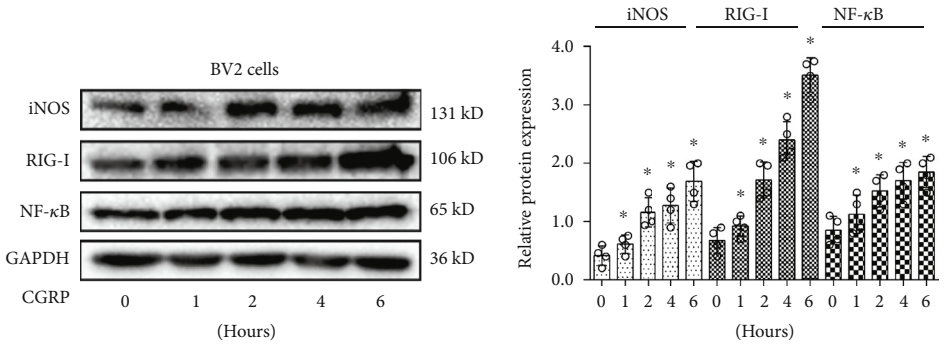

(a)

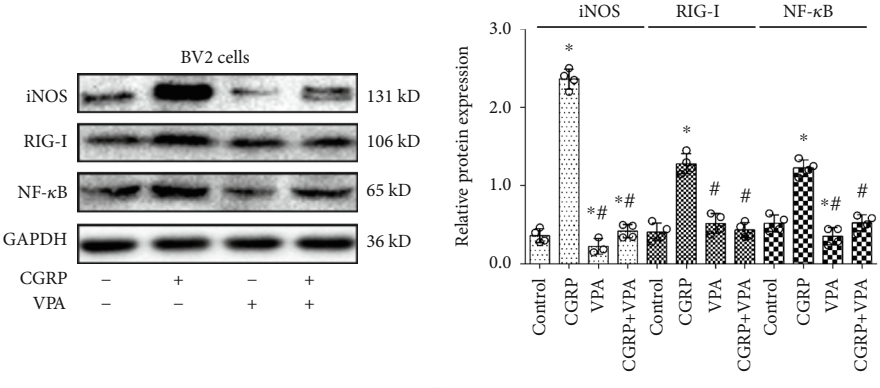

(b)

Figure 4: CGRP evokes increases in the expression of iNOS, RIG-I, and NF-κB in microglial cells in a time-dependent manner. (a) Western blot analysis of iNOS, RIG-I, and NF-κB expression in microglial cells with treatment of CGRP at 0, 1, 2, 4, and 6 h, respectively. (b) Western blotting analyses for the effect of HDAC2 inhibitor VPA on CGRP-evoked iNOS, RIG-I, and NF-κB protein expression in microglial cells with treatment of CGRP and pretreatment with VPA. Relative amounts of proteins were calculated by normalizing to GAPDH. All values are expressed as the means ± SEMs ($N = 4$ independent cell culture preparations, Mann-Whitney U tests or Kruskal-Wallis tests). $^{*}P < 0.05$ versus controls; $^{\#}P < 0.05$ versus CGRP only groups.

almost all cultured microglial cells expressed CGRP receptor components CRLR, RAMP1, and CRCP. Treatment of microglial cells with CGRP also increased the HDAC2 protein level. These results suggested that CGRP operated via its receptor that might contribute to modulation of gene transcription through HDAC2-medated epigenetic mechanism [26]. In order to obtain insights into HDAC2 target gene function, GO and KEGG analysis annotations were applied to the HDAC2 target gene pool. GO terms for BP process categories showed that key higher genes related with positive regulation of T cell cytokine production, NOS biosynthetic process, and activation of NF-κB-inducing kinase activity. KEGG pathways for upregulated genes were mainly related to the Fc epsilon RI signaling pathway, RIG-like receptor signaling pathway, and NF-κB signaling pathway. The expression of NOS, RIG-I, NF-κB was further verified by Western blot in microglia following CGRP treatment. Therefore, alterations of this histone deacetylase induced by CGRP could have severe consequences on microglial activation at the level of transcription [5].

HDAC2 has been shown to regulate microglial activation and induce cytokine expression through the NF-κB pathway [15, 17]. Previous data indicated that HDAC2 activates NF-κB and promotes NF-κB-dependent gene expression [16], which plays a crucial role in microglial activation [17]. NF-κB can interact with corepressors HDAC1 and HDAC2 to regulate gene transcription [27, 28]. Activation of NF-κB seems essential for the transcription of most of the proinflammatory molecules, such as cytokines and chemokines [29]. A previous report showed that activation of NF-κB regulates microglial conversion to a proinflammatory type [30]. In the present study, we found CGRP increased the expression of HDAC2 and NF-κB in microglia, suggesting that they might coordinately regulate the gene transcription for microglial activation induced by CGRP.

CGRP has been reported to activate microglia directly to produce proinflammatory mediators, including NOS and cytokines [31–33]. The specific recruitment of HDAC2 to NF-κB at target promoters and the consequent effects on acetylation status may play an important role in regulating iNOS as well as other NF-κB-dependent genes involved in inflammation [27, 34]. Activation of microglia displays NO production via iNOS activity which upregulates microglial phagocytosis and increases TRPV2 expression [35]. Our experiment showed that CGRP increased the expression of iNOS, NF-κB, and RIG-I protein levels in microglia after CGRP treatment. Nonetheless, these increases in iNOS, NF-κB, and RIG-I expression were inhibited by HDAC2 inhibitor, suggesting that increases of iNOS, NF-κB, and RIG-I expression in microglia by CGRP might be associated with HDAC2. Furthermore, activation of RIG-I may induce the expression of proinflammatory cytokines through the activation of NF-κB [36, 37]. A previous study demonstrated that HDAC2 inhibitor VPA reduced induction of RIG-I expression in different cancer cell lines by decitabine [38], suggesting that HDAC2 might be involved in regulation of RIG-I expression. Taken together with our results, these indicate that the upregulation of HDAC2 by CGRP may contribute to immune and inflammatory responses through the NO/iNOS, NF-κB, and RIG-I signal pathways in microglial activation [39].

5. Conclusions

In summary, we systematically evaluated CGRP-mediated HDAC2 enrichments in microglial cells and gained new insights into links between key pathways and HDAC2 induced by CGRP in the microglial activation. Genomic analyses suggested that genes with the differential HDAC2 enrichments induced by CGRP function in diverse cellular pathways and many are involved in immune and inflammatory responses. However, further studies are needed to confirm our results.

Data Availability

The data used to support the findings of this study are available from the corresponding authors upon request.

Conflicts of Interest

None of the authors has a conflict of interest to declare.

Authors' Contributions

Xingjing Guo and Dan Chen contributed equally to this work.

Acknowledgments

ChIP-seq experiments were performed by KangChen Biotech, Shanghai, China. The study was supported by the National Natural Science Foundation of China (Nos. 31871215 and 81371234) and Natural Science Foundation of Shandong Province of China (ZR2019MH027).

Supplementary Materials

Table S1: differentially enriched regions for up and down peak-promoter-annotation. *(Supplementary Materials)*

References

[1] K. Li, Y.-H. Tan, A. R. Light, and K.-Y. Fu, "Different peripheral tissue injury induces differential phenotypic changes of spinal activated microglia," *Clinical and Developmental Immunology*, vol. 2013, Article ID 901420, 8 pages, 2013.

[2] T. L. Tay, N. Hagemeyer, and M. Prinz, "The force awakens: insights into the origin and formation of microglia," *Current Opinion in Neurobiology*, vol. 39, no. 1, pp. 30–37, 2016.

[3] J. T. Malon, S. Maddula, H. Bell, and L. Cao, "Involvement of calcitonin gene-related peptide and CCL2 production in CD40-mediated behavioral hypersensitivity in a model of neuropathic pain," *Neuron Glia Biology*, vol. 7, no. 2-4, pp. 117–128, 2011.

[4] J. Priller, C. A. Haas, M. Reddington, and G. W. Kreutzberg, "Calcitonin gene-related peptide and ATP induce immediate early gene expression in cultured rat microglial cells," *Glia*, vol. 15, no. 4, pp. 447–457, 1995.

[5] M. Reddington, J. Priller, J. Treichel, C. Haas, and G. W. Kreutzberg, "Astrocytes and microglia as potential targets for

calcitonin gene related peptide in the central nervous system," *Canadian Journal of Physiology and Pharmacology*, vol. 73, no. 7, pp. 1047–1049, 1995.

[6] L. Yi-Zhen, M. Run-Pei, Y. Tian-Yuan et al., "Mild mechanic stimulate on acupoints regulation of CGRP-positive cells and microglia morphology in spinal cord of sciatic nerve injured rats," *Frontiers in Integrative Neuroscience*, vol. 13, 2019.

[7] L.-J. Zhou, J. Peng, Y.-N. Xu et al., "Microglia are indispensable for synaptic plasticity in the spinal dorsal horn and chronic pain," *Cell Reports*, vol. 27, no. 13, pp. 3844–3859.e6, 2019.

[8] S. Iyengar, M. H. Ossipov, and K. W. Johnson, "The role of calcitonin gene-related peptide in peripheral and central pain mechanisms including migraine," *Pain*, vol. 158, no. 4, pp. 543–559, 2017.

[9] C. Sardi, L. Zambusi, A. Finardi et al., "Involvement of calcitonin gene-related peptide and receptor component protein in experimental autoimmune encephalomyelitis," *Journal of Neuroimmunology*, vol. 271, no. 1-2, pp. 18–29, 2014.

[10] J. Li, C. V. Vause, and P. L. Durham, "Calcitonin gene-related peptide stimulation of nitric oxide synthesis and release from trigeminal ganglion glial cells," *Brain Research*, vol. 1196, no. 1, pp. 22–32, 2008.

[11] Y. Kawarai, S. Orita, J. Nakamura et al., "Changes in proinflammatory cytokines, neuropeptides, and microglia in an animal model of monosodium iodoacetate-induced hip osteoarthritis," *Journal of Orthopaedic Research*, vol. 36, no. 11, pp. 2978–2986, 2018.

[12] R. J. Cady, J. R. Glenn, K. M. Smith, and P. L. Durham, "Calcitonin gene-related peptide promotes cellular changes in trigeminal neurons and glia implicated in peripheral and central sensitization," *Molecular Pain*, vol. 7, pp. 1744–8069, 2011.

[13] M. Datta, O. Staszewski, E. Raschi et al., "Histone deacetylases 1 and 2 regulate microglia function during development, homeostasis, and neurodegeneration in a context-dependent manner," *Immunity*, vol. 48, no. 3, pp. 514–529.e6, 2018.

[14] M. S. Sung, H. Heo, G. H. Eom et al., "HDAC2 regulates glial cell activation in ischemic mouse retina," *International Journal of Molecular Science*, vol. 20, no. 20, p. 5159, 2019.

[15] B. S. Durham, R. Grigg, and I. C. Wood, "Inhibition of histone deacetylase 1 or 2 reduces induced cytokine expression in microglia through a protein synthesis independent mechanism," *Journal of Neurochemistry*, vol. 143, no. 2, pp. 214–224, 2017.

[16] T. Wagner, N. Kiweler, K. Wolff et al., "Sumoylation of HDAC2 promotes NF-κB-dependent gene expression," *Oncotarget*, vol. 6, no. 9, pp. 7123–7135, 2015.

[17] F. Z. Jiao, Y. Wang, H. Y. Zhang, W. B. Zhang, L. W. Wang, and Z. J. Gong, "Histone deacetylase 2 inhibitor CAY10683 alleviates lipopolysaccharide induced neuroinflammation through attenuating TLR4/NF-κB signaling pathway," *Neurochemical Research*, vol. 43, no. 6, pp. 1161–1170, 2018.

[18] S. An, G. Zong, Z. Wang, J. Shi, H. du, and J. Hu, "Expression of inducible nitric oxide synthase in mast cells contributes to the regulation of inflammatory cytokines in irritable bowel syndrome with diarrhea," *Neurogastroenterology and Motility*, vol. 28, no. 7, pp. 1083–1093, 2016.

[19] T. I. Lee, S. E. Johnstone, and R. A. Young, "Chromatin immunoprecipitation and microarray-based analysis of protein location," *Nature Protocols*, vol. 1, no. 2, pp. 729–748, 2006.

[20] B. Langmead and S. L. Salzberg, "Fast gapped-read alignment with Bowtie 2," *Nature Methods*, vol. 9, no. 4, pp. 357–359, 2012.

[21] J. Feng, T. Liu, and Y. Zhang, "Using MACS to identify peaks from ChIP-Seq data," *Current Protocols in Bioinformatics*, vol. 34, no. 1, pp. 2.14.1–2.14.14, 2011.

[22] M. Haeussler, A. S. Zweig, C. Tyner et al., "The UCSC Genome Browser database: 2019 update," *Nucleic Acids Research*, vol. 47, no. D1, pp. D853–D858, 2019.

[23] M. Ashburner, C. A. Ball, J. A. Blake et al., "Gene ontology: tool for the unification of biology. The Gene Ontology Consortium," *Nature Genetics*, vol. 25, no. 1, pp. 25–29, 2000.

[24] M. Kanehisa, Y. Sato, M. Kawashima, M. Furumichi, and M. Tanabe, "KEGG as a reference resource for gene and protein annotation," *Nucleic Acids Research*, vol. 44, no. D1, pp. D457–D462, 2016.

[25] C. Wu, A. Li, J. Hu, and J. Kang, "Histone deacetylase 2 is essential for LPS-induced inflammatory responses in macrophages," *Immunology & Cell Biology*, vol. 97, no. 1, pp. 72–84, 2019.

[26] C. A. Warwick, L. P. Shutov, A. J. Shepherd, D. P. Mohapatra, and Y. M. Usachev, "Mechanisms underlying mechanical sensitization induced by complement C5a: the roles of macrophages, TRPV1, and calcitonin gene-related peptide receptors," *Pain*, vol. 160, no. 3, pp. 702–711, 2019.

[27] B. P. Ashburner, S. D. Westerheide, and A. S. Baldwin, "The p65 (RelA) subunit of NF-kappaB interacts with the histone deacetylase (HDAC) corepressors HDAC1 and HDAC2 to negatively regulate gene expression," *Molecular and Cellular Biology*, vol. 21, no. 20, pp. 7065–7077, 2001.

[28] Y. Chen, H. Wang, S. O. Yoon et al., "HDAC-mediated deacetylation of NF-κB is critical for Schwann cell myelination," *Nature Neuroscience*, vol. 14, no. 4, pp. 437–441, 2011.

[29] O. T. Somade, B. O. Ajayi, O. A. Safiriyu, O. S. Oyabunmi, and A. J. Akamo, "Renal and testicular up-regulation of pro-inflammatory chemokines (RANTES and CCL2) and cytokines (TNF-α, IL-1β, IL-6) following acute edible camphor administration is through activation of NF-kB in rats," *Toxicology Reports*, vol. 6, no. 1, pp. 759–767, 2019.

[30] M. Galán-Ganga, Á. J. García-Yagüe, and I. Lastres-Becker, "Role of MSK1 in the induction of NF-κB by the chemokine CX3CL1 in microglial cells," *Cellular and Molecular Neurobiology*, vol. 39, no. 3, pp. 331–340, 2019.

[31] C. V. Vause and P. L. Durham, "CGRP stimulation of iNOS and NO release from trigeminal ganglion glial cells involves mitogen-activated protein kinase pathways," *Journal of Neurochemistry*, vol. 110, no. 3, pp. 811–821, 2009.

[32] F. R. Nieto, A. K. Clark, J. Grist, V. Chapman, and M. Malcangio, "Calcitonin gene-related peptide-expressing sensory neurons and spinal microglial reactivity contribute to pain states in collagen-induced arthritis," *Arthritis & Rheumatology*, vol. 67, no. 6, pp. 1668–1677, 2015.

[33] R. Q. Sun, Y. J. Tu, N. B. Lawand, J. Y. Yan, Q. Lin, and W. D. Willis, "Calcitonin gene-related peptide receptor activation produces PKA- and PKC-dependent mechanical hyperalgesia and central sensitization," *Journal of Neurophysiology*, vol. 92, no. 5, pp. 2859–2866, 2004.

[34] Z. Yu, "Histone deacetylases augment cytokine induction of the iNOS gene," *Journal of the American Society of Nephrology*, vol. 13, no. 8, pp. 2009–2017, 2002.

[35] M. J. E. Maksoud, V. Tellios, D. An, Y. Y. Xiang, and W. Y. Lu, "Nitric oxide upregulates microglia phagocytosis and increases transient receptor potential vanilloid type 2 channel expression on the plasma membrane," *Glia*, vol. 67, no. 12, pp. 2294–2311, 2019.

[36] P. Lagana, L. Soraci, M. E. Gambuzza, G. Mancuso, and S. A. Delia, "Innate Immune Surveillance In The Central Nervous System Following Legionella Pneumophila Infection," *CNS & Neurological Disorders-Drug Targets*, vol. 16, no. 10, pp. 1080–1089, 2018.

[37] M. Yu and S. J. Levine, "Toll-like receptor, RIG-I-like receptors and the NLRP3 inflammasome: key modulators of innate immune responses to double-stranded RNA viruses," *Cytokine and Growth Factor Reviews*, vol. 22, no. 2, pp. 63–72, 2011.

[38] D. Bensaid, T. Blondy, S. Deshayes et al., "Assessment of new HDAC inhibitors for immunotherapy of malignant pleural mesothelioma," *Clinical Epigenetics*, vol. 10, no. 1, 2018.

[39] L. Carniglia, D. Ramírez, D. Durand et al., "Neuropeptides and microglial activation in inflammation, pain, and neurodegenerative diseases," *Mediators Of Inflammation*, vol. 2017, Article ID 5048616, 23 pages, 2017.

Hindawi
Journal of Immunology Research
Volume 2020, Article ID 7927054, 8 pages
https://doi.org/10.1155/2020/7927054

Review Article

The Role of Gastric Mucosal Immunity in Gastric Diseases

Siru Nie[1,2,3] **and Yuan Yuan**[1,2,3]

[1]*Tumor Etiology and Screening Department of Cancer Institute and General Surgery, The First Hospital of China Medical University, Shenyang 110001, China*
[2]*Key Laboratory of Cancer Etiology and Prevention in Liaoning Education Department, The First Hospital of China Medical University, Shenyang 110001, China*
[3]*Key Laboratory of GI Cancer Etiology and Prevention in Liaoning Province, The First Hospital of China Medical University, Shenyang 110001, China*

Correspondence should be addressed to Yuan Yuan; yuanyuan@cmu.edu.cn

Received 26 February 2020; Accepted 30 March 2020; Published 24 July 2020

Guest Editor: Margarete D. Bagatini

Gastric mucosa plays its immune function through innate and adaptive immunity by recruiting immune cells and releasing corresponding cytokines, which have an inseparable relationship with gastric diseases. Whether infective gastric diseases caused by Helicobacter pylori, Epstein-Barr virus or other microbe, noninfective gastric diseases, or gastric cancer, gastric mucosal immunity plays an important role in the occurrence and development of the disease. Understanding the unique immune-related tissue structure of the gastric mucosa and its role in immune responses can help prevent gastric diseases or treat them through immunotherapy. In this review, we summarize the basic feature of gastric mucosal immunity and its relationship with gastric diseases to track the latest progress of gastric mucosal immunity, update relevant knowledge and provide theoretical reference for the prevention and treatment of gastric diseases based on the gastric mucosal immunity.

1. Introduction

The human body exerts immune responses through innate and adaptive immunity. After the invasion of pathogens, innate immunity acts as the first line of immune defense by recruiting innate immune cells, which belongs to natural nonspecific immunity. Adaptive immunity acts as a process of preventing infection by recruiting immune lymphocytes and producing immunoglobulins, which belongs to specific immunity. Gastrointestinal mucosal immune system is an important immune organ of the human body and exerts the same immune response as the human body [1]. However, some scholars reject the stomach as part of the gastrointestinal mucosal immune system, considering there is no mucosa-associated lymphoid tissue (MALT) in the gastric mucosa [2, 3]. With the deepening of research, it is now believed that the gastric mucosa can play its immune function in a layer-by-layer progressive mode through innate and adaptive immunity [4] and maintain the balance of microbe in an immune homeostasis mechanism [5]. On the one hand, when pathogens such as bacteria and viruses invade the gastric mucosa, both epithelial cells and innate immune cells begin to defend them through physical, chemical and biological processes. On the other hand, cytokines such as interleukin and chemokines secreted by immune cells help present antigens to lymphocytes such as T cells and B cells through antigen presentation, further triggering adaptive immunity. Understanding the unique immune-related tissue structure of the gastric mucosa and its role in immune responses can help prevent gastric diseases or treat them through immunotherapy. In this review, we will describe the basic feature of gastric mucosal immunity and its relationship with gastric diseases to track the latest progress of gastric mucosal immunity, update relevant knowledge

and provide theoretical reference for the prevention and treatment of gastric diseases based on the gastric mucosal immunity.

2. Basic Features of Gastric Mucosal Immune System (Composition and Function)

The gastric mucosa is the inner layer of the gastric wall, which can be divided into three layers in histology: epithelial layer, lamina propria, and mucosal muscle layer. The gastric mucosa exerts different physiological functions through substances secreted by cells in different layers. Under normal circumstances, the lamina propria of the gastric mucosa does not have the same diffuse lymphoid tissue as intestinal mucosa and it does not have immune cells that immune directly. When the gastric mucosa is infected, immune cells are recruited to the gastric mucosa through a complex process, in which chemokines play an important role [6]. When antigens contact with the human body, immune cells in the blood will interact with activated vascular endothelial cells, slow down the movement of cells in the blood, and induce them to roll along the vessel wall. During this rolling process, the combination of immune cells and chemokines induces immune cells to adhere to the cell adhesion factor of endothelial cells via integrins and then migrate across the endothelial cells to the stomach [7]. After the recruitment of immune cells, many immune-related cells gather in the lamina propria of the gastric mucosa and play an important role in the subsequent inflammation and immune response together with natural epithelial barrier of the gastric mucosa.

2.1. Gastric Mucosal Innate Immunity-Associated Cells. Gastric mucosal innate immunity-associated cells consist of gastric mucosal epithelial cells, macrophages, dendritic cells (DCs), etc. Gastric mucosal epithelial cells locate in the epithelium of the gastric mucosa as the first line of defensing in the gastric mucosal immunity. Since gastric mucosal epithelial cells can express the major class II histocompatibility complex (MHC-II), we can consider it as an antigen-presenting cell (APC) participating in the initiation of innate immune response, which plays an important role in immune alert [8–10]. Other immune cells (such as macrophages, (DCs and natural killer cells) recruited in the lamina propria of the gastric mucosa also play an important role in the gastric mucosal immunity [11]. Macrophage microaggregates are widely distributed in the gastric mucosa [12]. After activation, cytokines produced by macrophage stimulate the occurrence of immune response, play a role in immune regulation and also promote the occurrence of adaptive immune response [13, 14]. In 2010, Bimczok et al. first identified the presence of dendritic cells in human gastric mucosa and confirmed the role of DCs as key initiators of immune response [15]. Interestingly, only activated mature DCs can play the initial immune response to pathogens. In the process of activation and maturation, DCs are affected by pathogen-associated molecular patterns (such as lipopolysaccharide, flagellin and bacterial DNA [16, 17]) and gastric stroma [18]. After activation, mature DCs act as APCs to induce adaptive immune responses via Toll-like receptor (TLR) signaling by activating effector T and B cells [3, 7, 19–21]. Nature killer cells (NK cells) also play an important role in innate immunity [22, 23]. In addition, when the gastric mucosa is invaded by pathogens, lymphocytes can gather in the lamina propria of the gastric mucosa through the formation of gastric lymph follicles; neutrophils and eosinophils can perform the immune functions of phagocytosis of pathogens and inhibition of bacterial colonization by upregulating the expression of chemokines and chemokine receptors [19].

2.2. Gastric Mucosa Adaptive Immunity-Associated Cells. Gastric mucosa adaptive immunity-associated cells consist of T cells, B cells, and other immune lymphocytes and are closely related to the formation of immunoglobulin. In the cellular immunity of the gastric mucosa, $CD4^+$ T cells and Treg cells play an important role [2, 24]. Previous studies in mice have reported that Th1 and Th17 of $CD4^+$ T cells play a protective role under the intermediation of neutrophils to maintain the dynamic balance of the immune system [6, 24]. Activated $CD4^+$ T cells can also recruit neutrophils by secreting cytokines such as IL-17 and interferon-γ (IFN-γ) and upregulate the expression of β-protection and antimicrobial peptides [6]. The humoral immunity of the gastric mucosa mainly involves B cells and immunoglobulins. With the joint participation of macrophages, Th cells and chemokine (such as CCL28), B cells exert humoral immune functions [6]. As for immunoglobulins, as early as 40 years ago, S. Baur et al. [25] confirmed the existence of IgA and IgG containing cells in the glands of gastric lamina propria by immunofluorescence staining, which was further confirmed by A.J. Knox et al. [26]. They also confirmed the presence of IgG autoantibodies in inflammatory cells of the gastric mucosa. Nowadays, we believe that secretory IgA (sIgA) and IgM system play an important role in humoral immunity. After local immune cells produce immunoglobulins, dimer IgA and pentamer IgM act as secretory receptors to pass across the tight epithelium of the gastric mucosa through the way of selective transport [27]. The production of IgA is the first line of this immune defense. When the first line is breached, IgG was produced in the local gastric mucosa as the second line of defense and the number increased as the increase of inflammation in the gastric mucosa. Previous studies revealed that the ratio of IgA to IgG cells in normal gastric mucosa was 6 : 1. Although IgM is difficult to evaluate, a high proportion of IgM cells can also be seen in the gastric mucosa [27].

2.3. Basic Functions of Gastric Mucosal Immunity. In accordance with the immune response of the human body, the gastric mucosal immunity also exerts through innate immunity and adaptive immunity synergistically. The innate immunity of the gastric mucosa recognizes and phagocytizes pathogens through immune cells recruited in the lamina propria of the gastric mucosa and corresponding cytokines, playing a role of early immune alert as the first line of immune defense. In the gastric mucosal innate immunity, related cells (such as macrophages and dendritic cells) act as APCs to present antigens and then stimulate the adaptive immunity, as the second line of immune defense. As for the gastric mucosal

adaptive immunity infected by pathogens, on the one hand, mediums produced by immune cells play a protective role to the gastric mucosa. On the other hand, pathogens play a damaging role to the gastric mucosa by escaping immune responses. When the damage of the gastric mucosa cannot be repaired, the dynamic balance of gastric mucosa barrier will be broken, which further leads to gastric diseases.

3. Gastric Mucosal Immunity and Gastric Diseases

3.1. Gastric Mucosal Immunity and Helicobacter pylori (H. pylori) Infection-Associated Gastric Diseases

3.1.1. Gastric Mucosal Immunity and H. pylori-Infective Gastritis. *H. pylori*-infective gastritis is a very remarkable clinical outcome of *H. pylori* infection, which is closely related to the gastric mucosal immunity. After the infection of *H. pylori*, many innate immune cells play an important role. For example, the *H. pylori* $CagA^+$ chain can interact with DCs to help them secrete IL-23, therefore promoting the polarization of Th22 and the expression of IL-22 receptor 1 in gastric epithelial cells. Consequently, the increased release of IL-22 stimulates gastric epithelial cells to secrete CXCL2, which further suppresses the Th1 protective immune response and leads to the occurrence of gastritis [28]. Some studies suggest that pathogens phagocytized by macrophages can be released by *H. pylori* and the damage effect of *H. pylori* is gradually greater than the protection effect, which eventually causes the damage of the gastric mucosa [7]. Not only innate immune-related cells but also other cells and molecules are involved in the development of *H. pylori*-infective gastritis. Recent evidence reveals that $CCR6^+$ Treg cells in *H. pylori*-infected area of the gastric mucosa are positively correlated with the inflammation degree of *H. pylori*-related gastritis, which may be involved in the process of immunosuppression [29]. *H. pylori* infection can activate nucleotide-binding oligomerization domain 1(NOD1) and unable to regulate inflammatory body activation through mucin MUC1, which is also involved in the molecular mechanism of *H. pylori* infectious gastritis [30].

3.1.2. Gastric Mucosal Immunity and Gastric Ulcer. Gastric ulcer is another common clinical outcome of *H. pylori* infection. Different from the immune response in gastritis, gastric ulcer is closely related to the distribution of gastric T cell subpopulations, which mainly performs in the ratio difference of $CD4^+/CD8^+$ T cell in the gastric mucosa [31]. When gastric ulcer occurs, $CD3^+$ T cells transform into $CD4^+$ T cells and $CD19^+$ B cells [32]. The number of $CD3^+$ T cells in *H. pylori*-positive gastric ulcer patients is significantly higher than that in gastritis, while the number of $CD19^+$ B cells has no significant change [31]. According to the results of flow cytometry and immunohistochemistry, the number of $CD19^+$ B cells, $CD4^+$ Th cells, and $CD8^+$ Tc cells in the gastric mucosa of gastric ulcer patients was higher than that of non-gastric ulcer patients. In addition, gastric ulcer can promote the expression of upstream IL-8, IL-10, and IL-10 in chronic infection to inhibit the occurrence of adaptive immune responses and weaken the clearance effect on antigen [32].

3.1.3. Gastric Mucosal Immunity and Gastric MALT Lymphoma. Gastric MALT Lymphoma (GML) is an adaptive immune response to the immune inflammatory stimulation caused by *H. pylori*. It is a disease highly mediated by immune and inflammatory response. *H. pylori* infection initially leads to chronic infections, causing lymphoid hyperplasia. Then, under the chronic infection of *H. pylori*, *H. pylori* CagA is transferred from the human body to human B lymphocytes via type 4 secretion system encoded by cagPAI. After entering the cytoplasm, CagA binds to SHP-2 to form lymphoma by stimulating proliferation and inhibiting apoptosis of B lymphocytes through regulating intracellular pathway. CagA can also inhibit the proliferation of B lymphocytes by inhibiting the JAK-STAT signal pathway, helping bacteria escape from human body's specific immune response [33]. Moreover, data from several sources have identified the key role of directed mutation of immunoglobulin (Ig) heavy chain genes and the continuous activation of gene enhancer in the immune response of GML [34]. The involvement of Treg cells, BCR, and some cytokines (such as IL-22) was also confirmed in GML [35]. Recent evidence suggests that the chronic infection of *H. pylori* may cause GML, in which low-grade GML can possibly be cured by antibiotic therapy through eradicating *H. pylori* [36, 37].

3.1.4. The Pathophysiological Mechanism of Gastric Mucosal Immune-Related H. pylori Infection. The gastric mucosa is protected and damaged by innate and adaptive immune responses after *H. pylori* infection, but gastric diseases will not occur in the early stage of infection. Therefore, the immune mechanism of *H. pylori* infection in the gastric mucosa is worth exploring. The study of the gastric mucosal immunity in mice has shown the recruitment of eosinophils and $CD4^+$ T cells in the lamina propria of the gastric mucosa with increasing cell number as the increasing time of infection [6]. The large accumulation of immune cells and release of cytokines in the gastric mucosa offer a help to the activation of adaptive immune response [6, 38, 39]. In the gastric mucosal innate immunity associated with *H. pylori* infection, TIFA complex acting as the core regulatory factor and human β-defensin acting as the main component of the innate immune defense mechanism both stimulate the occurrence of adaptive immune response [40, 41]. In the gastric mucosal adaptive immunity associated with *H. pylori* infection, *H. pylori* initiates the immune response by recognizing pathogen-related molecular pattern through the pattern recognition receptor on gastric epithelial cells and innate immune cells [42] with the occurrence of Th1- and $CD4^+$ T cell-related response (Th17 and Tregs response), the infiltration of corresponding immune cells and the participation of TNF-α signal pathway [32, 38, 43]. *H. pylori* can lead to the formation of gastric lymph follicles and the aggregation of lymphocytes in the lamina propria and induce the adaptive immune response by promoting the

expression of T cells and B cells with the ability of adsorbing cell adhesion molecule-1 and attracting chemokines (CXCL10 and CCL28) [19].

At present, it is considered that *H. pylori* has both protective and damaging effects on mucosal immunity. Th1 and Th2 immune responses, along with cytokines and transcription regulators produced in the immune process, play an important role in the protective immune process of the gastric mucosa [32, 44, 45]. For example, the expression of chemokines CXCL1, CXCL2, and CXCL5 and their common receptor CXCR2 will increase to recruit neutrophils after *H. pylori* infection. The recruited neutrophils can kill *H. pylori* by directly phagocytosing bacteria or releasing active intermediates to resist *H. pylori* colonization and protect the gastric mucosa [6]; the expression of IFN-regulatory factor 8 and diversified immune-related gene characteristics of IL-11/STAT3 in the gastric mucosa are related to the inhibition of *H. pylori* colonization [45]. However, when the damage of the gastric mucosa cannot be completely repaired by the gastric mucosal immunity, *H. pylori* will smartly escape the immune response to cause further damage to the gastric mucosa, which is called immune escape. In this process, *H. pylori* escapes from immune response by activating inflammation and TLR cell signal pathways and changing surface molecules to avoid the recognition of innate immune receptors (such as TLRs and RIG-I of DCs) [38, 42]. In addition, the infiltration of immune cells (Th1, Treg cells, etc.) and the expression of corresponding cytokines (such as CCR6 ligand, chemokine CCL20, IFN-γ, and tumor necrosis factor-α) increase. Chemical gradients produced by cytokines can regulate the expression of cell adhesion receptor-ligand pairs and promote the recruitment of leukocytes to the site of injury, which is beneficial for *H. pylori* to escape from the host's immune defense, causing chronic inflammation and even gastric cancer [19, 42, 46–48].

3.2. Gastric Mucosal Immunity and Epstein-Barr Virus (EBV) Infection-Associated Gastric Diseases. EBV infection is closely related to gastritis and gastric cancer [49]. EBV can directly inhibit the proliferation of T cells and the toxicity of natural killer cells to maintain the activity of virus in host cells and cause continuously damage to the gastric mucosa [50]. The gastric mucosa infected by EBV can express high levels of ncRNA (EBV-encoded RNA and BART), and EBV miRNA can keep the virus at a very low expression level by targeting regulation of viral gene expression to avoid being attacked by human body's immune response [50, 51]. Increased expression of EBV-related genes also promotes the infiltration of immune cells and IFN-γ [52]. According to the infiltration of lymph immune cells in cellular immune responses, Epstein-Barr virus-associated gastric carcinoma (EBVaGC) can be divided into three histological subtypes: lymphoepithelial neoplasia (LELC), Crohn's disease-like lymphoid response (CLR), and conventional adenocarcinoma (CA) [52]. During the recruitment of immune lymphocytes to the gastric mucosa in EBVaGC, the expression of EBVaGC-related genes plays an important role. For example, IL-1β overexpression can recruit nonspecific lymphocytes to prevent direct contact between EBV-specific cytotoxic T cells and tumor cells [52]; IFN-γ overexpression can inhibit the proliferation and activation of CTL and NK cells [53]; PD-L1 expansion can inhibit the proliferation of T cells and the release of cytokines by interacting with PD-L1 receptors on T cells, and they can also induce CTL apoptosis and promote the differentiation from $CD4^+$ T cells into Treg cells [53]. If the above-mentioned reactive immune cells are recruited into the tumor site or the surrounding area of EBVaGC, it may play a role in prolonging the survival time of EBVaGC patients.

3.3. Gastric Mucosal Immunity and Other Microbial Infection-Associated Gastric Diseases. In recent years, it has been suggested that microbiota is closely related to the occurrence and development of gastric diseases, and the immunity status is an important determinant of gastric microbiota [54]. Under normal circumstances, gastric microbiota is mainly composed of Prevotella, Neisseria, Streptococcus, Fusobacteria, and other microorganisms [55]. However, under the influence of host factors (anatomical characteristics, physiological characteristics, gender, age, etc. [56, 57]), external factors (diet, drug treatment, etc. [58]), and environmental factors (race, geographical location, etc. [59]), the composition of microorganisms in the stomach will change. Interestingly, the normal or abnormal stomach function composed by various microorganisms is regulated by both innate and adaptive immune responses. For example, recent studies on Fusobacterium are very popular. According to the 16S rRNA gene sequencing result of gastric cancer tissue, the distribution of Fusobacterium in gastric cancer tissues is significantly different from the adjacent tissue [60, 61]. Some studies have shown that Fusobacterium can protect tumors from the kill of NK cells and tumor-infiltrating T cells; therefore, we have reason to believe that the change of microbiota also has a certain impact on the gastric mucosal immunity [62].

3.4. Gastric Mucosal Immunity and Noninfective Gastric Diseases. The noninfective gastric disease is mainly autoimmune gastritis. Autoimmune gastritis is a chronic gastritis characterized by gastric mucosa atrophy, which is closely related to the lack of intrinsic factors [63]. The main targets of autoimmune reaction are parietal cells and intrinsic factors, in which the parietal cell antibody (PCAs) can be found in the gastric mucosa of 90% patients with atrophic gastritis [64]. Treg cells also play an important role in autoimmune gastritis and maintain certain tolerance to gastric autoantibodies. Treg cells can control the response of Tfh cells (follicular helper T cells) and the production of autoantibodies caused by gastric H^+-K^+-ATP enzymes and internal factors. They can also produce immunosuppressive cytokines (IL-10, TGF-β, IL-35, etc.) to exert immunosuppressive effects [65]. Studies have shown that the occurrence of autoimmune gastritis in Treg-deficient mice is closely related to the Th2 immune response. The immune response allows eosinophils to penetrate from the submucosal layer to the deeper layer, accompanied by the decrease in parietal cells and the production of autoimmune antibodies, leading to serious CD^+ T cell dependent-autoimmune gastritis [66].

3.5. Gastric Mucosal Immunity and Gastric Cancer. Immunosuppression is an important factor in the development of gastric cancer. In recent years, immunotherapy for immune checkpoints represented by anti-PD-1/PD-L1 comes into the public eyes and plays an important role in tumor immunotherapy [67]. Immune checkpoint inhibitors enable immune cells such as T cells to recognize and kill tumor cells by lifting the restrictions of immune system and tumor cell defense system. Understanding the role and regulation of the gastric mucosal immunity in the development of gastric cancer may provide valuable reference for the diagnosis and treatment of gastric cancer. On the one hand, the activation of the gastric mucosal innate immunity and the increase of inflammatory cell infiltration lead to the increased risk of gastric cancer. On the other hand, the gastric mucosal adaptive immunity prevents the body from clearing pathogens, helping the pathogen escape the host's immune defense, leading to aggravated gastric mucosal damage and further developing gastric cancer.

In innate immune response, NK cells can play the role of innate immune response, and its mutation is closely related to the risk of gastric cancer. The activity of NK cells by killer cell immunoglobulin-like receptor (KIR), whose gene mutations can cause the mutation of NK cell activity to aggravate the inflammatory reaction of the gastric mucosa and the occurrence of gastric mucosa damage, eventually leads to gastric cancer [22, 23]. NOD1 is a sensor of intracellular innate immunity. Studies have shown that the expression level of NOD1 and TRAF3 in gastric cancer is lower than that in noncancer tissues. When the activation of the NOD1-TRAF3 signal pathway is impaired, it will appear intestinal metaplasia in the gastric mucosa [68]. Some other studies have reported that genetic mutations or gene polymorphisms are closely related to the gastric mucosal immunity in gastric cancer. For example, a Japanese study found that mutations of RIPK2 gene (receptor-interacting serine/threonine kinase 2) (rs16900627 minor allele genotype) increased the aggregation of inflammatory cells by changing the innate immune response of the gastric mucosa, leading to the atrophy of the gastric mucosa and increased risks of intestinal gastric cancer [69]. When pathogens pass APCs (such as DCs), aggregate through lymphocyte subsets and present antigens to corresponding immature T cells through TLRs, the adaptive immune response is activated [49]. In this way, under the specific conditions of foreign antigen presentation and cytokine aggregation, different types of T cells prevent the body from the elimination of pathogens through the corresponding inflammatory response and secretion of immunosuppressive cytokines, resulting in chronic infection and disease. Th17 can induce the production of specific matrix metalloproteinases by releasing IL-17 and IL-21, causing the damage of the gastric mucosa [46]. There are also studies showing that B cells are active in gastric cancer and can reflect the immune status of the gastric mucosa [70].

In addition to immune cells and cytokines in the above processes, genes that involved in the carcinogenesis of gastric cancer also play an important role in immune regulation. For example, when the gastric mucosa is infected with *H. pylori*, the expression of GATA-binding protein 3, a transcription factor regulating adaptive immune response, is increased, which inhibits the normal expression of Cx43 and causes the gastric mucosa to undergo a malignant transformation from inflammation to tumor [71]. Another transcription factor, Foxp3, promotes tumor growth by suppressing IL-10- and/or TGF-β-mediated tumor cell killing after increased infiltration of Treg cells [72]. SLFN5, as an IFN-α regulatory gene in immune cells, is also associated with the occurrence of gastric cancer [73]. When the gastric mucosa is infected with EBV, as mentioned above, PD-L1 and other immune checkpoints are closely related to the occurrence and prognosis of EBVaGC.

4. Conclusions and Prospect

In summary, the various immune cells, cytokines, and signal pathways effecting in the process of the gastric mucosal immunity have an inseparable relationship with gastric diseases. Whether *H. pylori*, EBV and other pathogen infective-associated gastric diseases, or noninfective-associated gastric diseases, the gastric mucosal immunity plays an important role in the occurrence and development of the disease. However, the gastric mucosal immunity induced by pathogen is a dynamic balance between protective immunity and damage immunity, by which this specific balance function mechanism needs further study. Among many pathogens, the study of microbial flora is in a hot spot and its mechanism of gastric mucosal immune regulation for gastric diseases still needs to be explored. Meanwhile, in view of the rapid development of immunotherapy, whether gastric diseases can be treated through more perfect and accurate immune targets according to the research progress of the gastric mucosal immunity and the corresponding mechanism is still worth further exploration. At present, some gastric cancer immune checkpoint inhibitors (such as PD1/PD-L1 inhibitors) have entered Phase 2 and Phase 3 clinical trials [74, 75] and immunotherapy combined with chemotherapy or radiotherapy has the opportunity to be used as first-line treatment for gastric cancer [76, 77]. In the future, based on the theory of the gastric mucosal immunity, searching for specific tumor microenvironment-related indicators as biomarkers for assessing treatment efficacy will play an important role in precision immunotherapy of gastric diseases.

Conflicts of Interest

All of the authors declare that there is no conflict of interest.

Authors' Contributions

Yuan Yuan conceived the study and revised the manuscript. Siru Nie collected the data and wrote the paper. All authors read and approved the final manuscript.

Acknowledgments

This study was supported partly by the National Key R&D Program of China (Grant #2018YFC1311600).

References

[1] B. Ahluwalia, M. K. Magnusson, and L. Ohman, "Mucosal immune system of the gastrointestinal tract: maintaining balance between the good and the bad," *Scandinavian Journal of Gastroenterology*, vol. 52, no. 11, pp. 1185–1193, 2017.

[2] M. Michetti, C. P. Kelly, J.–. P. Kraehenbuhl, H. Bouzourene, and P. Michetti, "Gastric mucosal $\alpha 4\beta 7$-integrin—positive CD4 T lymphocytes and immune protection against Helicobacter infection in mice," *Gastroenterology*, vol. 119, no. 1, pp. 109–118, 2000.

[3] J. Shiu and T. G. Blanchard, "Dendritic cell function in the host response to Helicobacter pylori infection of the gastric mucosa," *Pathogens and Disease*, vol. 67, no. 1, pp. 46–53, 2013.

[4] B. Zhang and J.-L. Ren, "Research progress of gastric mucosal immune mechanism," *World Chin J Digestol*, vol. 13, no. 21, pp. 2605–2609, 2005, (in Chinese).

[5] D. Bimczok, J. Y. Kao, M. Zhang et al., "Human gastric epithelial cells contribute to gastric immune regulation by providing retinoic acid to dendritic cells," *Mucosal Immunology*, vol. 8, no. 3, pp. 533–544, 2015.

[6] C. F. Flach, M. Mozer, M. Sundquist, J. Holmgren, and S. Raghavan, "Mucosal vaccination increases local chemokine production attracting immune cells to the stomach mucosa of Helicobacter pylori infected mice," *Vaccine*, vol. 30, no. 9, pp. 1636–1643, 2012.

[7] A. Ieni, V. Barresi, L. Rigoli, F. Fedele, G. Tuccari, and R. Caruso, "Morphological and cellular features of innate immune reaction in Helicobacter pylori gastritis: a brief review," *International Journal of Molecular Sciences*, vol. 17, no. 1, p. 109, 2016.

[8] C. Barrera, R. Espejo, and V. E. Reyes, "Differential glycosylation of MHC class II molecules on gastric epithelial cells: implications in local immune responses," *Human Immunology*, vol. 63, no. 5, pp. 384–393, 2002.

[9] S. Krauss-Etschmann, R. Gruber, K. Plikat et al., "Increase of antigen-presenting cells in the gastric mucosa of Helicobacter pylori-infected children," *Helicobacter*, vol. 10, no. 3, pp. 214–222, 2005.

[10] A. Gall, R. G. Gaudet, S. D. Gray-Owen, and N. R. Salama, "TIFA signaling in gastric epithelial cells initiates thecag-Type 4 secretion system-dependent innate immune response toHelicobacter pyloriInfection," *mBio*, vol. 8, no. 4, 2017.

[11] M. Moyat and D. Velin, "Immune responses to Helicobacter pylori infection," *World Journal of Gastroenterology*, vol. 20, no. 19, pp. 5583–5593, 2014.

[12] M. H. de Magalhães-Costa, B. R. dos Reis, V. L. A. Chagas, T. Nunes, H. S. P. de Souza, and C. Zaltman, "Focal enhanced gastritis and macrophage microaggregates in the gastric mucosa: potential role in the differential diagnosis between Crohn's disease and ulcerative colitis," *Arquivos de Gastroenterologia*, vol. 51, no. 4, pp. 276–282, 2014.

[13] M. Kaparakis, A. K. Walduck, J. D. Price et al., "Macrophages are mediators of gastritis in acute Helicobacter pylori infection in C57BL/6 mice," *Infection and Immunity*, vol. 76, no. 5, pp. 2235–2239, 2008.

[14] S. Gordon, "Alternative activation of macrophages," *Nature Reviews. Immunology*, vol. 3, no. 1, pp. 23–35, 2003.

[15] D. Bimczok, R. H. Clements, K. B. Waites et al., "Human primary gastric dendritic cells induce a Th1 response to H. pylori," *Mucosal Immunology*, vol. 3, no. 3, pp. 260–269, 2010.

[16] H. Tsujimura, T. Tamura, H. J. Kong et al., "Toll-like receptor 9 signaling activates NF-kappaB through IFN regulatory factor-8/IFN consensus sequence binding protein in dendritic cells," *Journal of Immunology*, vol. 172, no. 11, pp. 6820–6827, 2004.

[17] F. Re and J. L. Strominger, "Toll-like receptor 2 (TLR2) and TLR4 differentially activate human dendritic cells," *The Journal of Biological Chemistry*, vol. 276, no. 40, pp. 37692–37699, 2001.

[18] D. Bimczok, J. M. Grams, R. D. Stahl, K. B. Waites, L. E. Smythies, and P. D. Smith, "Stromal regulation of human gastric dendritic cells restricts the Th1 response to Helicobacter pylori," *Gastroenterology*, vol. 141, no. 3, pp. 929–938, 2011.

[19] M. Hansson, M. Sundquist, S. Hering, B. S. Lundin, M. Hermansson, and M. Quiding-Järbrink, "DC-LAMP+ dendritic cells are recruited to gastric lymphoid follicles in Helicobacter pylori-infected individuals," *Infection and Immunity*, vol. 81, no. 10, pp. 3684–3692, 2013.

[20] R. M. Steinman, "Decisions about dendritic cells: past, present, and future," *Annual Review of Immunology*, vol. 30, pp. 1–22, 2012.

[21] K. Kranzer, L. Söllner, M. Aigner et al., "Impact of Helicobacter pylori virulence factors and compounds on activation and maturation of human dendritic cells," *Infection and Immunity*, vol. 73, no. 7, pp. 4180–4189, 2005.

[22] N. Hafsi, P. Voland, S. Schwendy et al., "Human dendritic cells respond to Helicobacter pylori, promoting NK cell and Th1-effector responses in vitro," *Journal of Immunology*, vol. 173, no. 2, pp. 1249–1257, 2004.

[23] E. G. Hernandez, O. Partida-Rodriguez, M. Camorlinga-Ponce et al., "Genotype B of _Killer Cell Immunoglobulin-Like Receptor_ is Related with Gastric Cancer Lesions," *Scientific Reports*, vol. 8, no. 1, p. 6104, 2018.

[24] A. Carbo, J. Bassaganya-Riera, M. Pedragosa et al., "Predictive computational modeling of the mucosal immune responses during Helicobacter pylori infection," *PLoS One*, vol. 8, no. 9, p. e73365, 2013.

[25] S. Baur, N. Koo, and K. B. Taylor, "The immunoglobulin class of autoantibody-containing cells in the gastric mucosa," *Immunology*, vol. 19, no. 6, pp. 891–894, 1970.

[26] A. J. Knox, C. von Westarp, V. V. Row, and R. Volpe, "Thyroid antigen stimulates lymphocytes from patients with Graves' disease to produce thyroid-stimulating immunoglobulin (TSI)," *The Journal of Clinical Endocrinology and Metabolism*, vol. 43, no. 2, pp. 330–337, 1976.

[27] K. Valnes, P. Brandtzaeg, K. Elgjo, and R. Stave, "Quantitative distribution of immunoglobulin-producing cells in gastric mucosa: relation to chronic gastritis and glandular atrophy," *Gut*, vol. 27, no. 5, pp. 505–514, 1986.

[28] Y. Zhuang, P. Cheng, X. F. Liu et al., "A pro-inflammatory role for Th22 cells in Helicobacter pylori-associated gastritis," *Gut*, vol. 64, no. 9, pp. 1368–1378, 2015.

[29] Y. Y. Wu, C. T. Hsieh, G. J. Tsay et al., "Recruitment of CCR6(+) Foxp3(+) regulatory gastric infiltrating lymphocytes in Helicobacter pylori gastritis," *Helicobacter*, vol. 24, no. 1, p. e12550, 2019.

[30] G. Z. Ng, T. R. Menheniott, A. L. Every et al., "The MUC1 mucin protects against Helicobacter pylori pathogenesis in

mice by regulation of the NLRP3 inflammasome," *Gut*, vol. 65, no. 7, pp. 1087–1099, 2016.

[31] R. Goll, A. Husebekk, V. Isaksen, G. Kauric, T. Hansen, and J. Florholmen, "Increased frequency of antral CD4 T and CD19 B cells in patients with Helicobacter pylori-related peptic ulcer disease," *Scandinavian Journal of Immunology*, vol. 61, no. 1, pp. 92–97, 2005.

[32] R. Goll, F. Gruber, T. Olsen et al., "Helicobacter pylori stimulates a mixed adaptive immune response with a strong T-regulatory component in human gastric mucosa," *Helicobacter*, vol. 12, no. 3, pp. 185–192, 2007.

[33] P. Floch, F. Megraud, and P. Lehours, "Helicobacter pylori strains and gastric MALT lymphoma," *Toxins*, vol. 9, no. 4, p. 132, 2017.

[34] M. I. Pereira and J. A. Medeiros, "Role of Helicobacter pylori in gastric mucosa-associated lymphoid tissue lymphomas," *World Journal of Gastroenterology*, vol. 20, no. 3, pp. 684–698, 2014.

[35] A. M. Laur, P. Floch, L. Chambonnier et al., "Regulatory T cells may participate in Helicobacter pylori persistence in gastric MALT lymphoma: lessons from an animal model," *Oncotarget*, vol. 7, no. 3, pp. 3394–3402, 2016.

[36] A. Shirwaikar Thomas, M. Schwartz, and E. Quigley, "Gastrointestinal lymphoma: the new mimic," *BMJ Open Gastroenterol*, vol. 6, no. 1, p. e000320, 2019.

[37] J. B. Park and J. S. Koo, "Helicobacter pylori infection in gastric mucosa-associated lymphoid tissue lymphoma," *World Journal of Gastroenterology*, vol. 20, no. 11, pp. 2751–2759, 2014.

[38] B. Kronsteiner, J. Bassaganya-Riera, C. Philipson et al., "Systems-wide analyses of mucosal immune responses to Helicobacter pylori at the interface between pathogenicity and symbiosis," *Gut Microbes*, vol. 7, no. 1, pp. 3–21, 2016.

[39] S. Raghavan, A. K. Ostberg, C. F. Flach et al., "Sublingual immunization protects against Helicobacter pylori infection and induces T and B cell responses in the stomach," *Infection and Immunity*, vol. 78, no. 10, pp. 4251–4260, 2010.

[40] S. Zimmermann, L. Pfannkuch, M. A. Al-Zeer et al., "ALPK1- and TIFA-dependent innate immune response triggered by the Helicobacter pylori type IV secretion system," *Cell Reports*, vol. 20, no. 10, pp. 2384–2395, 2017.

[41] B. Bauer, T. Wex, D. Kuester, T. Meyer, and P. Malfertheiner, "Differential expression of human beta defensin 2 and 3 in gastric mucosa of Helicobacter pylori-infected individuals," *Helicobacter*, vol. 18, no. 1, pp. 6–12, 2013.

[42] A. Karkhah, S. Ebrahimpour, M. Rostamtabar et al., "Helicobacter pylori evasion strategies of the host innate and adaptive immune responses to survive and develop gastrointestinal diseases," *Microbiological Research*, vol. 218, pp. 49–57, 2019.

[43] U. Thalmaier, N. Lehn, K. Pfeffer, M. Stolte, M. Vieth, and W. Schneider-Brachert, "Role of tumor necrosis factor alpha in Helicobacter pylori gastritis in tumor necrosis factor receptor 1-deficient mice," *Infection and Immunity*, vol. 70, no. 6, pp. 3149–3155, 2002.

[44] K. Sakai, M. Kita, N. Sawai et al., "Levels of interleukin-18 are markedly increased in Helicobacter pylori-infected gastric mucosa among patients with specific IL18 genotypes," *The Journal of Infectious Diseases*, vol. 197, no. 12, pp. 1752–1761, 2008.

[45] T. R. Menheniott, L. M. Judd, and A. S. Giraud, "STAT3: a critical component in the response to Helicobacter pylori infection," *Cellular Microbiology*, vol. 17, no. 11, pp. 1570–1582, 2015.

[46] H. Maleki Kakelar, A. Barzegari, J. Dehghani et al., "Pathogenicity of Helicobacter pylori in cancer development and impacts of vaccination," *Gastric Cancer*, vol. 22, no. 1, pp. 23–36, 2019.

[47] H. F. Tsai and P. N. Hsu, "Interplay between Helicobacter pylori and immune cells in immune pathogenesis of gastric inflammation and mucosal pathology," *Cellular & Molecular Immunology*, vol. 7, no. 4, pp. 255–259, 2010.

[48] A. Razavi, N. Bagheri, F. Azadegan-Dehkordi et al., "Comparative immune response in children and adults with H. pylori infection," *Journal of Immunology Research*, vol. 2015, Article ID 315957, 6 pages, 2015.

[49] J. Martínez-López, J. Torres, M. Camorlinga-Ponce, A. Mantilla, Y. Leal, and E. Fuentes-Pananá, "Evidence of Epstein-Barr virus association with gastric cancer and non-atrophic gastritis," *Viruses*, vol. 6, no. 1, pp. 301–318, 2014.

[50] I. Polakovicova, S. Jerez, I. A. Wichmann, A. Sandoval-Bórquez, N. Carrasco-Véliz, and A. H. Corvalán, "Role of microRNAs and exosomes in Helicobacter pylori and Epstein-Barr virus associated gastric cancers," *Frontiers in Microbiology*, vol. 9, p. 636, 2018.

[51] M. Albanese, T. Tagawa, A. Buschle, and W. Hammerschmidt, "MicroRNAs of Epstein-Barr virus control innate and adaptive antiviral immunity," *Journal of Virology*, vol. 91, no. 16, 2017.

[52] J. Cho, M. S. Kang, and K. M. Kim, "Epstein-Barr virus-associated gastric carcinoma and specific features of the accompanying immune response," *Journal of Gastric Cancer*, vol. 16, no. 1, pp. 1–7, 2016.

[53] M. J. Strong, G. Xu, J. Coco et al., "Differences in gastric carcinoma microenvironment stratify according to EBV infection intensity: implications for possible immune adjuvant therapy," *PLoS Pathogens*, vol. 9, no. 5, p. e1003341, 2013.

[54] E. C. von Rosenvinge, Y. Song, J. R. White, C. Maddox, T. Blanchard, and W. F. Fricke, "Immune status, antibiotic medication and pH are associated with changes in the stomach fluid microbiota," *The ISME Journal*, vol. 7, no. 7, pp. 1354–1366, 2013.

[55] J. L. Espinoza, A. Matsumoto, H. Tanaka, and I. Matsumura, "Gastric microbiota: an emerging player in Helicobacter pylori-induced gastric malignancies," *Cancer Letters*, vol. 414, pp. 147–152, 2018.

[56] Human Microbiome Project, C, "Structure, function and diversity of the healthy human microbiome," *Nature*, vol. 486, no. 7402, pp. 207–214, 2012.

[57] E. Husebye, V. Skar, T. Hoverstad, and K. Melby, "Fasting hypochlorhydria with gram positive gastric flora is highly prevalent in healthy old people," *Gut*, vol. 33, no. 10, pp. 1331–1337, 1992.

[58] C. WILLIAMS and K. E. L. McCOLL, "Review article: proton pump inhibitors and bacterial overgrowth," *Alimentary Pharmacology & Therapeutics*, vol. 23, no. 1, pp. 3–10, 2006.

[59] G. Yu, N. Hu, L. Wang et al., "Gastric microbiota features associated with cancer risk factors and clinical outcomes: a pilot study in gastric cardia cancer patients from Shanxi, China," *International Journal of Cancer*, vol. 141, no. 1, pp. 45–51, 2017.

[60] X. H. Chen, A. Wang, A. N. Chu, Y. H. Gong, and Y. Yuan, "Mucosa-associated microbiota in gastric cancer tissues compared with non-cancer tissues," *Frontiers in Microbiology*, vol. 10, 2019.

[61] Y. Y. Hsieh, S. Y. Tung, H. Y. Pan et al., "Increased abundance of Clostridium and Fusobacterium in gastric microbiota of patients with gastric cancer in Taiwan," *Scientific Reports*, vol. 8, no. 1, p. 158, 2018.

[62] J. Abed, N. Maalouf, L. Parhi, S. Chaushu, O. Mandelboim, and G. Bachrach, "Tumor targeting by Fusobacterium nucleatum: a pilot study and future perspectives," *Frontiers in Cellular and Infection Microbiology*, vol. 7, p. 295, 2017.

[63] S. N. Hall and H. D. Appelman, "Autoimmune gastritis," *Archives of Pathology & Laboratory Medicine*, vol. 143, no. 11, pp. 1327–1331, 2019.

[64] R. Negrini, A. Savio, C. Poiesi et al., "Antigenic mimicry between Helicobacter pylori and gastric mucosa in the pathogenesis of body atrophic gastritis," *Gastroenterology*, vol. 111, no. 3, pp. 655–665, 1996.

[65] N. Bagheri, L. Salimzadeh, and H. Shirzad, "The role of T helper 1-cell response in Helicobacter pylori-infection," *Microbial Pathogenesis*, vol. 123, pp. 1–8, 2018.

[66] J. Harakal, C. Rival, H. Qiao, and K. S. Tung, "Regulatory T cells control Th2-dominant murine autoimmune gastritis," *Journal of Immunology*, vol. 197, no. 1, pp. 27–41, 2016.

[67] R. Park, S. Williamson, A. Kasi, and A. Saeed, "Immune therapeutics in the treatment of advanced gastric and esophageal cancer," *Anticancer Research*, vol. 38, no. 10, pp. 5569–5580, 2018.

[68] K. Minaga, T. Watanabe, K. Kamata, N. Asano, and M. Kudo, "Nucleotide-binding oligomerization domain 1 andHelicobacter pyloriinfection: a review," *World Journal of Gastroenterology*, vol. 24, no. 16, pp. 1725–1733, 2018.

[69] M. Ota, T. Tahara, T. Otsuka et al., "Association between receptor interacting serine/threonine kinase 2 polymorphisms and gastric cancer susceptibility," *Oncology Letters*, vol. 15, no. 3, pp. 3772–3778, 2018.

[70] T. Kunori, F. Shinya, T. Satomi et al., "Spontaneous antibody-secreting cells in the stomach of gastric cancer patients," *Journal of Gastroenterology*, vol. 31, no. 2, pp. 161–166, 1996.

[71] X. Liu, K. Cao, C. Xu et al., "GATA-3 augmentation down-regulates Connexin43 in Helicobacter pylori associated gastric carcinogenesis," *Cancer Biology & Therapy*, vol. 16, no. 6, pp. 987–996, 2015.

[72] B. Kindlund, Å. Sjöling, C. Yakkala et al., "CD4(+) regulatory T cells in gastric cancer mucosa are proliferating and express high levels of IL-10 but little TGF-β," *Gastric Cancer*, vol. 20, no. 1, pp. 116–125, 2017.

[73] O. C. Nápoles, A. C. Tsao, J. M. Sanz-Anquela et al., "SCHLAFEN 5 expression correlates with intestinal metaplasia that progresses to gastric cancer," *Journal of Gastroenterology*, vol. 52, no. 1, pp. 39–49, 2017.

[74] Y. K. Kang, N. Boku, T. Satoh et al., "Nivolumab in patients with advanced gastric or gastro-oesophageal junction cancer refractory to, or intolerant of, at least two previous chemotherapy regimens (ONO-4538-12, ATTRACTION-2): a randomised, double-blind, placebo-controlled, phase 3 trial," *Lancet*, vol. 390, no. 10111, pp. 2461–2471, 2017.

[75] K. Muro, H. C. Chung, V. Shankaran et al., "Pembrolizumab for patients with PD-L1-positive advanced gastric cancer (KEYNOTE-012): a multicentre, open-label, phase 1b trial," *The Lancet Oncology*, vol. 17, no. 6, pp. 717–726, 2016.

[76] Y. Kubota, A. Kawazoe, A. Sasaki et al., "The impact of molecular subtype on efficacy of chemotherapy and checkpoint inhibition in advanced gastric cancer," *Clinical Cancer Research*, p. clincanres.0075.2020, 2020.

[77] J. Taieb, M. Moehler, N. Boku et al., "Evolution of checkpoint inhibitors for the treatment of metastatic gastric cancers: current status and future perspectives," *Cancer Treatment Reviews*, vol. 66, pp. 104–113, 2018.

Hindawi
Journal of Immunology Research
Volume 2020, Article ID 1826587, 9 pages
https://doi.org/10.1155/2020/1826587

Review Article

Mechanism of Follicular Helper T Cell Differentiation Regulated by Transcription Factors

Long-Shan Ji,[1] Xue-Hua Sun,[2] Xin Zhang,[1] Zhen-Hua Zhou,[1] Zhuo Yu,[2] Xiao-Jun Zhu,[2] Ling-Ying Huang,[2] Miao Fang,[1] Ya-Ting Gao,[1] Man Li,[1] and Yue-Qiu Gao[1]

[1]*Laboratory of Cellular Immunity, Institute of Clinical Immunology, Shanghai Key Laboratory of Traditional Chinese Clinical Medicine, Shuguang Hospital, Affiliated to Shanghai University of Traditional Chinese Medicine, Shanghai 201203, China*
[2]*Department of Hepatopathy, Shuguang Hospital, Affiliated to Shanghai University of Traditional Chinese Medicine, Shanghai 201203, China*

Correspondence should be addressed to Man Li; liman121000@126.com and Yue-Qiu Gao; gaoyueqiu@hotmail.com

Long-Shan Ji and Xue-Hua Sun contributed equally to this work.

Received 22 April 2020; Accepted 15 June 2020; Published 20 July 2020

Guest Editor: Margarete D. Bagatini

Helping B cells and antibody responses is a major function of $CD4^+$T helper cells. Follicular helper T (Tfh) cells are identified as a subset of $CD4^+$T helper cells, which is specialized in helping B cells in the germinal center reaction. Tfh cells express high levels of CXCR5, PD-1, IL-21, and other characteristic markers. Accumulating evidence has demonstrated that the dysregulation of Tfh cells is involved in infectious, inflammatory, and autoimmune diseases, including lymphocytic choriomeningitis virus (LCMV) infection, inflammatory bowel disease (IBD), systemic lupus erythematosus (SLE), rheumatoid arthritis (RA), IgG4-related disease (IgG4-RD), Sjögren syndrome (SS), and type 1 diabetes (T1D). Activation of subset-specific transcription factors is the essential step for Tfh cell differentiation. The differentiation of Tfh cells is regulated by a complicated network of transcription factors, including positive factors (Bcl6, ATF-3, Batf, IRF4, c-Maf, and so on) and negative factors (Blimp-1, STAT5, IRF8, Bach2, and so on). The current knowledge underlying the molecular mechanisms of Tfh cell differentiation at the transcriptional level is summarized in this paper, which will provide many perspectives to explore the pathogenesis and treatment of the relevant immune diseases.

1. Introduction

$CD4^+$helper T cells play a critical role in forming and amplifying the abilities of the immune system. Follicular helper T (Tfh) cells are identified as a subset of $CD4^+$T helper cells, which provides help to B cells for the formation and maintenance of the germinal center (GC) , the production of high affinity class-switched antibodies, long-lived plasma cells, and memory B cells [1]. There were a great deal of researches about Tfh cells in the past 10 years; in particular, the differentiation and function of Tfh cells were involved in a range of diseases including infectious diseases, vaccines, autoimmune diseases, and allergies. Tfh cells are characterized by high expression of the chemokine receptor CXCR5, the transcription factor Bcl6, the costimulatory molecule ICOS, and the coinhibitory molecule PD-1. Once naïve $CD4^+$T cells are activated by antigen-presenting cells (APCs) together with IL-6 and IL-21, they will differentiate into Tfh cells.

A multiple-stage process is involved in the generation of Tfh cells from naïve $CD4^+$T cells, which consists of initiation, maintenance, and full polarization stages [1]. During the initiation phase of Tfh cell differentiation, multiple signals take part in the process, including transcription factors (Bcl6, Ascl2, Batf, IRF4, c-Maf, and so on), costimulatory molecule(ICOS), and cytokines(IL-6/IL-21); in particular, higher TCR affinity is necessary for initiation of Tfh cell

($Bcl6^+CXCR5^+$) differentiation at the phase of dendritic cell priming [2–7]. Then, $Bcl6^+CXCR5^+$ Tfh precursor cells move into the T-B border zone, where they accept other differentiation signals from activated B cells [8]. After this appointment, the toughened expression of Bcl6 regulates surface markers, which accelerates the migration of Tfh cells into GC, where they offer assistant signals for B cells [9, 10] (Figure 1).

Differentiation of naïve $CD4^+$T cells into Tfh cells is modulated by a multipart transcriptional network (Figure 2). Multiple transcription factors that either support or oppose the differentiation and function of Tfh cells have been identified (Table 1).

Now, the knowledge of the transcriptional mechanism underlying Tfh cell differentiation will be comprehensively described in this paper, which will highlight the possible future directions.

2. Bcl6 and Blimp-1

Bcl6 has been known as a key transcription factor for Tfh cell development by pathways essentially independent of Blimp-1 [3, 39]. Bcl6 consists of a zinc finger domain; a bric-a-brac, tramtrack, broad-complex (BTB) domain; and a middle domain [40]. The Bcl6 DNA binding zinc finger domain is essential for Bcl6 activity in $CD4^+$T cells [8]. The BTB domain of Bcl6 participates in the correct differentiation of Tfh cells most likely by interacting with Bcl6-interacting corepressor (BCOR) [41]. The middle domain of Bcl6 prevents the association with the corepressor metastasis-associated protein 3 (MTA3) and inhibits the differentiation and function of Tfh cells by distressing Prdm1 (encodes Blimp-1) and other crucial target genes [42].

Bcl6 expression is induced by IL-6-STAT1/STAT3 signaling [43], and it is driven very early after T cell activation in a CD28-dependent manner [44]. The E3 ubiquitin ligase Itch is essential for Bcl6 expression at the early stage of Tfh cell development [45]. The deficiency of the Wiskott-Aldrich syndrome protein suppresses Bcl6 transcription, which results in a deficient response of Tfh cells [46]. Research shows that Bcl6 inhibits the IL-7R/STAT5 axis during Tfh cell generation [47]. Bcl6 mediates the effect of activating transcription factor 3 (ATF-3) on Tfh cells in the gut [16]. ATF-3 is a stress-inducible transcription factor and plays a critical role in the prevention of colitis by regulating the development of Tfh cells in the gut. In addition, Bcl6 also suppresses the expression of specific microRNAs that are thought to control the differentiation of Tfh cells, such as miR-17-92 [9] and miR-31 [48]. The miR-17-92 inhibits CXCR5 expression, and miR-31 directly binds to Bcl6 promoter.

Blimp-1 has been found to be a critical transcriptional repressor for Tfh cell differentiation. Blimp-1 has the inhibitory effect on Bcl6 expression, indicating that Bcl6 and Blimp-1 are antagonistic regulators in the differentiation of Tfh cells. Blimp-1 is induced by IL-2/STAT5 signaling, and it suppresses the expression of Tfh-associated genes including Bcl6, c-Maf, Batf, CXCR5, and IL-21 [25, 26]. Blimp-1-deficient $CD4^+$T cells in mice show enhanced Tfh cell differentiation and GC formation [3, 49]. Taken together, these results indicate that Bcl6 is both necessary and sufficient for Tfh cell development and the proper differentiation of Tfh cells in vivo, and the differentiation of Tfh cells requires keeping the expression balance between Bcl6 and Blimp-1.

Bcl6 and Blimp-1 are associated with various infectious and autoimmune diseases by regulating Tfh cells. Bcl6 is highly expressed in sinus tissues, parotid gland tissues, and lacrimal gland tissues of IgG4-related disease (IgG4-RD) patients [14]. Blimp-1 in peripheral blood is upregulated in patients with IgG4-RD [14]. Compared with the healthy controls, higher expression of Bcl6 and lower Blimp-1 expression in the peripheral blood are observed in patients with rheumatoid arthritis (RA) [15].

3. c-Maf and Batf

c-Maf and Batf are the members of the activator protein 1 (AP-1) family. c-Maf is a bZIP transcriptional factor , and promotes the differentiation of Tfh cells. [6]. It is highly expressed in Th17 cells and mature Tfh cells. The selective loss of c-Maf expression in Tfh cells results in the downregulated expression of Bcl6, CXCR5, PD-1, and IL-21 [6]. In addition, one study reveals that Bcl6 and c-Maf synergistically orchestrate the expression of Tfh cell-associated genes (PD-1, ICOS, CXCR5, and so on) [4].

Batf is known to control switched antibody responses. Batf is highly expressed in Tfh cells and is essential for the differentiation of Tfh cells through regulating the expression of Bcl6 and c-Maf [50, 51]. Batf directly binds to and activates the conserved noncoding sequence 2 (CNS2) region in the IL-4 locus and then triggers the production of IL-4 in Tfh cells [52].

Both c-Maf and Batf are related with immune diseases. Compared with the healthy controls, c-Maf mRNA expression level and percentage of Tfh cells in peripheral blood mononuclear cells (PBMCs) are increased in patients with chronic immune thrombocytopenia (cITP), and they are decreased after the effective treatment [12]. Compared with the healthy controls, Batf in the submandibular glands and affected lymph nodes is markedly increased in patients with IgG4-RD [17].

4. IRF4 and IRF8

IRF4 and IRF8 belong to the evolutionarily conserved IRF family. IRF4 is expressed in hematopoietic cells and plays pivotal roles in the immune response. It has been acknowledged that the IRF4 locus "senses" the intensity of TCR signaling to determine the expression level of IRF4 [18]. IRF4 plays a critical role in regulating the generation of Tfh cells. In $IRF4^{-/-}$ mice, $CD4^+$T cells in lymph nodes and Peyer's patches fail to express Bcl6 and other Tfh-related molecules [53]. IL-21 is a key cytokine for the development of Tfh cells [54], and IRF4 regulates the production of IL-21 [55]. Therefore, IL-21 takes part in regulating the differentiation of Tfh cells by IRF4. In wild-type mice, IRF4 can interact with Batf-JUN family protein complexes to form a heterotrimer

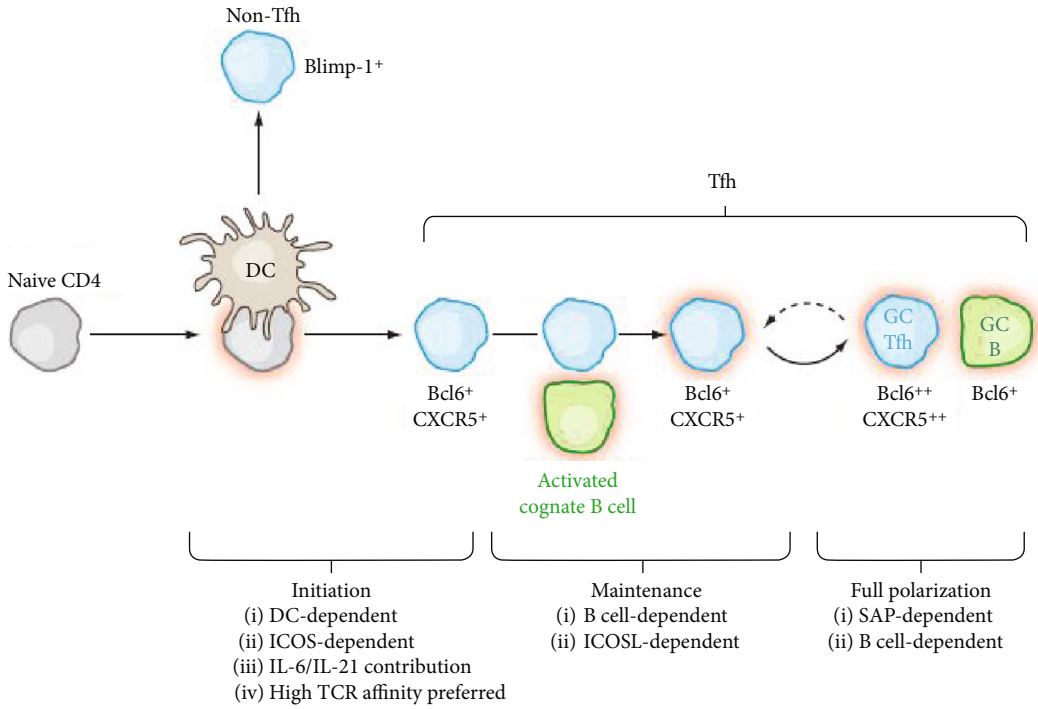

Figure 1: The differentiation of Tfh cells: multiple stages of Tfh cell differentiation, including initiation, maintenance, and full polarization stages (Annual Review of Immunology, 2011,29(1):621-663).

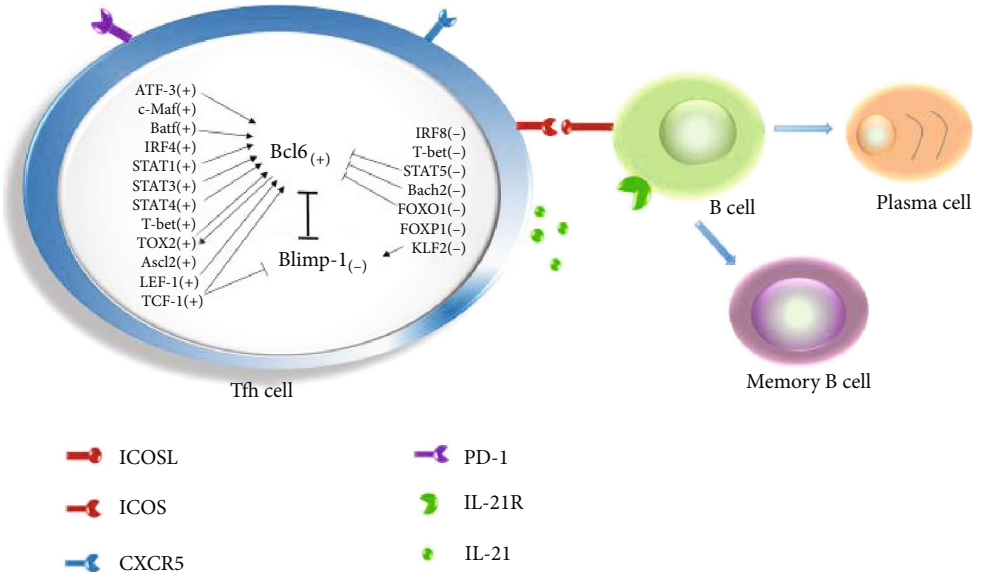

Figure 2: Network of transcription factors in the differentiation of Tfh cells. Tfh cells are regulated by a complex network of transcription factors, including Bcl6, Blimp-1, ATF-3, c-Maf, Batf, IRF4, IRF8, STATs, T-bet, TOX2, Ascl2, LEF-1, TCF-1, Bach2, FOXO1, FOXP1, and KLF2. "+" means positive factors and "–" means negative factors. "→" means the promoting effect and "⊣" means the inhibitory effect.

that can bind to AP1-IRF4 complexes and regulate Tfh cell differentiation [50, 51].

IRF8 plays various and important regulatory roles in the growth, differentiation, and function of immune cells in inflammatory bowel disease (IBD) patients [19]. IRF8 inhibits the differentiation of Tfh cells by directly binding to the promoter region of the IRF4 gene and inhibiting the transcription and activation of IRF4. In contrast, IRF8 deficiency significantly enhances IRF4 binding the promoter region of the IL-21 gene and results in the expansion of Tfh cell differentiation in vitro and in vivo [19].

5. STATs

Members of the STAT family including STAT1, STAT3, STAT4, and STAT5 are the important regulators for the

Table 1: Transcription factors in the differentiation of Tfh cells.

Transcription factors	Abbreviation of transcription factors	Function in Tfh cell differentiation	Signaling pathways	Related diseases
B-cell lymphoma 6 protein	Bcl6	Initiates the differentiation of Tfh cells at the early stage of Tfh cell generation	Be induced by IL-6-STAT1/STAT3 signaling, inhibits the IL-7R/STAT5 axis, suppresses microRNAs (miR-17-92 and miR-31), a direct target of ATF-3	Acute lymphocytic choriomeningitis virus (LCMV) infection [11] Chronic immune thrombocytopenia (cITP) [12] Systemic lupus erythematosus (SLE) [13] IgG4-related disease (IgG4-RD) [14] Rheumatoid arthritis (RA) [15]
B lymphocyte maturation protein 1	Blimp-1	Inhibits the differentiation of Tfh cells	Inhibits the expression of Bcl6	IgG4-RD [14]
Activating transcription factor 3	ATF-3	Initiates the differentiation of Tfh cells	Targets Bcl6 in $CD4^+$T cells	Colitis [16]
c-Musculoaponeurotic-fibrosarcoma	c-Maf	Promotes the differentiation of Tfh cells	c-Maf and Bcl6 synergistically orchestrate genes that define core characteristics of Tfh cell biology	cITP [12]
Basic leucine zipper transcription factor	Batf	Promotes the differentiation of Tfh cells	Regulates the expression of Bcl6 and c-Maf, cooperates with IRF4 during the development of Tfh cells, be regulated by IL-4-STAT6 and IL-6-STAT3 signaling	IgG4-RD [17]
Interferon regulatory factor 4	IRF4	Promotes the differentiation of Tfh cells	Regulates the generation of Tfh cells in a Bcl6-dependent manner, regulates the production of IL-21 and controls most IL-21-regulated genes by IL-21-STAT3 axis	LCMV infection [18]
Interferon regulatory factor 8	IRF8	Inhibits the differentiation of Tfh cells	Binds to the promoter region of IRF4 gene and inhibits transcription and transactivation of IRF4	Inflammatory bowel disease (IBD) [19]
Signal transducers and activators of transcription 1	STAT1	Promotes the differentiation of Tfh cells at the early stage of Tfh cell generation	Regulates the differentiation of Tfh cells by IL-6-STAT1-Bcl6 signaling	Viral infection [20] SLE [21, 22]
Signal transducers and activators of transcription 3	STAT3	Promotes the differentiation of Tfh cells	Regulates the expression of Bcl6	RA [23]
Signal transducers and activators of transcription 4	STAT4	Promotes the differentiation of Tfh cells	STAT4 and T-bet are coexpressed with Bcl6 to coordinate the production of IL-21 and IFN-γ by Tfh cells	Acute LCMV infection [24] SLE [22]
Signal transducers and activators of transcription 5	STAT5	Inhibits the differentiation of Tfh cells	Downregulates Bcl6 expression and upregulates Blimp-1 expression through IL-2/IL-7/IL-10-STAT5 signaling	LCMV infection [25, 26]

Table 1: Continued.

Transcription factors	Abbreviation of transcription factors	Function in Tfh cell differentiation	Signaling pathways	Related diseases
T-box expressed in T cells	T-bet	Mildly inhibits the early differentiation of Tfh cells, but promotes Tfh cell proliferation and apoptotic intervention at the late effector phase	T-bet and STAT4 are coexpressed with Bcl6 to coordinate the production of IL-21 and IFN-γ by Tfh cells	LCMV infection [2, 24, 27] SLE [22]
T cell-specific transcription factor 1	TCF-1	Promotes the differentiation of Tfh cells at the early stage of Tfh cell generation	Promotes the expression of Bcl6, but represses the expression of Blimp-1	LCMV infection [7, 28–30]
Lymphoid enhancer binding factor 1	LEF-1	Promotes the differentiation of Tfh cells at the early stage of Tfh cell generation	Works synergistically with TCF-1 to enhance the expression of ICOS and Bcl6	LCMV infection [30]
The high-mobility group- (HMG-) box 2	TOX2	Initiates the differentiation of Tfh cells	Be regulated by Bcl6 and STAT3 in the initial stage of Tfh cell generation, inhibits IL-2 and/or enhances IL-6 signaling to promote Bcl6 expression	Viral infection [31]
Achaete-scute homolog 2	Ascl2	Promotes the differentiation of Tfh cells	Upregulates CXCR5 but not Bcl6 and downregulates CCR7 expression as well as IL-2 signaling	Sjögren syndrome (SS) [32]
BTB and CNC homolog 2	Bach2	Inhibits the differentiation of Tfh cells	Suppresses the expression of Bcl6 by directly binding to the promoter, negatively regulates CXCR5 expression	Viral infection [33, 34]
Forkhead-box protein O1	FOXO1	Inhibits the differentiation of Tfh cells	Negatively regulates the differentiation of Tfh cells through an ICOS-mTORC2-FOXO1 signaling axis in the early stages of differentiation, negatively regulates the expression of Bcl6	Angioimmunoblastic T cell lymphoma induced [35]
Forkhead-box protein P1	FOXP1	Inhibits the differentiation of Tfh cells	Negatively regulates the expression of CTLA-4 and IL-21 in activated $CD4^+$T cells	LCMV infection [36]
Krüppel-like factor 2	KLF2	Inhibits the differentiation of Tfh cells	Downregulates S1PR1, induces the expression of Blimp-1, miRNA92a-mediated Tfh precursor induction is regulated by PTEN-PI3K-KLF2 signaling	Type 1 diabetes (T1D) [37] LCMV infection [38]

generation of Tfh cells [43, 54]. STAT1 is necessary for IL-6-mediated Bcl6 induction during the early differentiation of Tfh cells [43]. STAT3 has been found to be critical for Tfh cell development in a Bcl6-dependent manner [23]. The major STAT3-stimulating cytokines include IL-6, IL-21, IL-12, IL-10, and TGF-β [23, 56, 57]. Besides, STAT3 regulates Bcl6 expression by cooperating with the Ikaros zinc finger transcription factors Aiolos and Ikaros [58]. TRAF6 inhibits the activation of type I interferon-STAT3 signaling [59]. The latest research clearly shows that T-bet, although mildly inhibiting early Tfh cell differentiation, mainly plays a crucial and specific supporting role for Tfh cell response by promoting cell proliferation and apoptotic intervention at the end-stage effector phase of acute viral challenge [2]. T-bet and STAT4 are coexpressed with Bcl6 to coordinate the production of IL-21 and IFN-γ by Tfh cells and promote the GC response [24]. STAT5 is shown as an inhibitory factor for the differentiation of Tfh cells. Molecular analyses reveal that the activation of the IL-2/STAT5 signaling enhances the expression of Blimp-1 and prevents the binding of STAT3

to the Bcl6 locus [25], resulting in the decrease of GC and the long-lived antibody responses [26]. Similarly, IL-7-dependent activation of STAT5 contributes to Bcl6 repression [60]. The latest research shows that IL-10 suppresses the differentiation of Tfh cells in human and mice by promoting STAT5 phosphorylation [61]. He et al. [62] demonstrate that the secreted protein extracellular matrix protein 1 induced by IL-6 and IL-21 in Tfh cells promotes the differentiation of Tfh cells by downregulating the level of STAT5 phosphorylation and upregulating Bcl6 expression.

T-bet and STATs are the important regulators for Tfh cell development in infectious and autoimmune diseases. STAT1 serine-727 phosphorylation (designated STAT1-pS727) plays an important role in promoting Tfh cell responses, leading to systemic lupus erythematosus- (SLE-) associated autoantibody production [21]. Compared with the healthy controls, the expression levels of pSTAT1, pSTAT4, and T-bet in PBMCs are upregulated in patients with SLE [22]. The expression level of pSTAT3 in PBMCs in patients with RA is higher than that in healthy controls [23].

6. TCF-1 and LEF-1

TCF-1 is expressed in both developing and mature T cells and is essential for initiating and securing the differentiation of Tfh cells [7, 63]. TCF-1 directly binds to the Bcl6 transcription start site and Prdm1 $5'$ regulatory regions, which promotes the expression of Bcl6 and represses the expression of Blimp-1 during acute viral infection [7, 28, 29]. TCF-1 synergistically works with LEF-1 to promote the early differentiation of Tfh cells by the multipronged approach of maintaining the expression of IL-6Ra and gp130, enhancing the expression of ICOS, and promoting the expression of Bcl6 [30].

7. TOX2

The high-mobility group- (HMG-) box transcription factor TOX2 is selectively expressed in human Tfh cells and regulated by Bcl6 and STAT3 in the initial stage of Tfh cell generation [31]. There is a feed-forward loop centering on TOX2 and Bcl6, which drives Tfh cell development. TOX2 promotes Bcl6 expression by inhibiting IL-2 and/or enhancing IL-6 signaling during Tfh cell development. Furthermore, TOX2 is bound to the sites shared by Batf and IRF4, which suggests that TOX2, Batf, and IRF4 may functionally converge in developing Tfh cells.

8. Ascl2

Ascl2, a basic helix-loop-helix domain-containing transcription factor, is highly expressed in Tfh cells, and its expression may precede Bcl6 expression. The expression of Ascl2 in the spleen is upregulated in sjögren syndrome (SS) model mice compared with control mice [32]. Ascl2 initiates the differentiation of Tfh cells via upregulating CXCR5 and downregulating C-C chemokine receptor 7(CCR7) expression as well as the IL-2 level in T cells in vitro. The Ikappa BNS is highly expressed in Tfh cells and is essential for Ascl2-induced CXCR5 expression during the differentiation of Tfh cells [64]. After activation of the signals related to Tfh cells described above, Ascl2 accelerates T cell migration into the follicles in mice [5]. Acute deletion of Ascl2, as well as inhibition of its function with the Id3 protein, can result in impaired Tfh cell development and GC response [5]. In addition, epigenetic regulations, such as histone modifications, also coordinately control the differentiation and function of Tfh cells along with transcription factors. The Ascl2 locus is marked with the active chromatin marker trimethylated histone H3 lysine 4 (H3K4me3) in Tfh cells, and other transcription factors including Bcl6, Maf, Batf, and IRF4 are uniformly associated with H3K4me3 [65].

9. Bach2

Bach2 is a negative regulator of Tfh cell differentiation. Bach2 directly represses the expression of Bcl6 by inhibiting Bcl6 promoter activity [34] and negatively regulates CXCR5 expression [34]. Overexpression of Bach2 in Tfh cells inhibits the expression of Bcl6, IL-21, and the coinhibitory receptor TIGIT [34]. The deletion of Bach2 leads to the upregulation of CXCR5 expression and contributes to preferential Tfh cell differentiation [33].

10. FOXO1 and FOXP1

FOXO1 has been found to negatively regulate the differentiation of Tfh cells through the ICOS-mTORC2-FOXO1 signaling in the early stage of differentiation [66]. FOXO1 regulates the differentiation of Tfh cells by negatively regulating Bcl6. The E3 ubiquitin ligase Itch is essential for the differentiation of Tfh cells. Itch associates with FOXO1 and promotes its ubiquitination and degradation [45] and then positively regulates the differentiation of Tfh cells. FOXP1 negatively regulates the expression of CTLA-4 and IL-21 in activated $CD4^+$T cells [36]. Naïve $CD4^+$T cells deficient in the FOXP1 preferentially differentiate into Tfh cells, which results in substantially enhanced GC and antibody responses [67]. In addition, FOXP1-deficient Tfh cells restore the generation of high-affinity Abs when cocultured with high numbers of single clone B cells [36].

11. KLF2

The transcription factor KLF2 serves to inhibit Tfh cell generation by downregulating sphingosine-1-phosphate receptor (S1PR1). KLF2 deficiency in activated $CD4^+$T cells contributes to Tfh cell generation, whereas KLF2 overexpression prevents Tfh cell production. KLF2 also induces the expression of Blimp-1 and thereby inhibits the differentiation of Tfh cells [38]. ICOS maintains the phenotype of Tfh cells by downregulating KLF2. KLF2 is identified as a target of miRNA92a in inducting the expression of the human Tfh precursor, and the miRNA92a-mediated Tfh precursor induction is regulated by PTEN-PI3K-KLF2 signaling [37].

12. Conclusions

Multiple transcription factors have been found to regulate Tfh cell generation. In this paper, the regulatory mechanisms of transcription factors on Tfh cell differentiation are summarized. However, many questions remain to be further investigated. (i) Are there other Tfh-specific transcription factors beyond the abovementioned factors? (ii) How do Tfh-specific transcriptional factors impact epigenetic mechanisms during inducing Tfh cell generation? (iii) What are the factors' stage-specific requirements? (iv) What are the molecular mechanisms contributing to Tfh cell maintenance and memory formation?

As summarized in this review, Tfh cell-related transcription factors including Bcl6, IRF4, STAT1/STAT4/STAT5, T-bet, TCF-1, LEF-1, TOX2, Bach2, FOXP1, and KLF2 are all involved in the virus infection. Both Bcl6 and STAT3 play an important role in RA. ="The expression levels of Bcl6, STAT1, STAT4 and T-bet are upregulated in SLE patients. Bcl6, Blimp-1, and Batf are associated with IgG4-RD. Due to the association of Tfh cells with a broad spectrum of diseases, subsequent in-depth investigation of regulatory factors for the differentiation of Tfh cells may provide the potential therapeutic targets for various immune diseases, especially the virus infection, SLE, RA, and IgG4-RD.

Conflicts of Interest

The authors declare that they have no conflicts of interest.

Authors' Contributions

Long-shan Ji and Xue-hua Sun contributed equally to this work.

Acknowledgments

This work was supported by the National Natural Science Foundation of China (81673767, 81673938, 81673935, 81774240, 81874436, and 81973773); Training Plan for Excellent Academic Leaders of Shanghai Health System (2017BR007); Municipal Hospital Emerging Cutting Edge Technology Joint Research Project (SHDC12016121); Science Research Project of Thirteen Five-Year Plan (2018ZX10725-504); "Shuguang Program" supported by the Shanghai Education Development Foundation and Shanghai Municipal Education Commission (18SG39); Shanghai Sailing Program (20YF1450200); Training Plan of Outstanding Young Medical Talents, Shanghai Municipal Health Bureau (2018YQ43); Three-Year Action Plan of Development of TCM in Shanghai (ZY(2018-2020)-FWTX-4001, ZY(2018-2020)-FWTW-4004); Pilot Project of Clinical Cooperation between Chinese and Western Medicine for Major and Difficult Diseases (Hepatic Fibrosis); and Si Ming Foundation of Shuguang Hospital Affiliated to Shanghai University of Traditional Chinese Medicine (SGKJ-201912).

References

[1] S. Crotty, "Follicular helper CD4 T cells (T_{FH})," *Annual Review of Immunology*, vol. 29, no. 1, pp. 621–663, 2011.

[2] P. Wang, Y. Wang, L. Xie et al., "The transcription factor T-Bet is required for optimal type I follicular helper T cell maintenance during acute viral infection," *Frontiers in Immunology*, vol. 10, p. 606, 2019.

[3] R. J. Johnston, A. C. Poholek, D. DiToro et al., "Bcl6 and Blimp-1 are reciprocal and antagonistic regulators of T follicular helper cell differentiation," *Science*, vol. 325, no. 5943, pp. 1006–1010, 2009.

[4] M. A. Kroenke, D. Eto, M. Locci et al., "Bcl6 and Maf cooperate to instruct human follicular helper CD4 T cell differentiation," *The Journal of Immunology*, vol. 188, no. 8, pp. 3734–3744, 2012.

[5] X. Liu, X. Chen, B. Zhong et al., "Transcription factor achaete-scute homologue 2 initiates follicular T-helper-cell development," *Nature*, vol. 507, no. 7493, pp. 513–518, 2014.

[6] F. Andris, S. Denanglaire, M. Anciaux, M. Hercor, H. Hussein, and O. Leo, "The transcription factor c-Maf promotes the differentiation of follicular helper T cells," *Frontiers in Immunology*, vol. 8, p. 606, 2017.

[7] L. Xu, Y. Cao, Z. Xie et al., "The transcription factor TCF-1 initiates the differentiation of T_{FH} cells during acute viral infection," *Nature Immunology*, vol. 16, no. 9, pp. 991–999, 2015.

[8] R. I. Nurieva, Y. Chung, G. J. Martinez et al., "Bcl6 mediates the development of T follicular helper cells," *Science*, vol. 325, no. 5943, pp. 1001–1005, 2009.

[9] D. Yu, S. Rao, L. M. Tsai et al., "The transcriptional repressor Bcl-6 directs T follicular helper cell lineage commitment," *Immunity*, vol. 31, no. 3, pp. 457–468, 2009.

[10] D. Baumjohann, T. Okada, and K. M. Ansel, "Cutting edge: distinct waves of BCL6 expression during T follicular helper cell development," *The Journal of Immunology*, vol. 187, no. 5, pp. 2089–2092, 2011.

[11] Y. S. Choi, R. Kageyama, D. Eto et al., "ICOS receptor instructs T follicular helper cell versus effector cell differentiation via induction of the transcriptional repressor Bcl6," *Immunity*, vol. 34, no. 6, pp. 932–946, 2011.

[12] L. Dai, L. He, Z. Wang et al., "Altered circulating T follicular helper cells in patients with chronic immune thrombocytopenia," *Experimental and Therapeutic Medicine*, vol. 16, no. 3, pp. 2471–2477, 2018.

[13] Z. Wang, M. Zhao, J. Yin et al., "E4BP4-mediated inhibition of T follicular helper cell differentiation is compromised in autoimmune diseases," *Journal of Clinical Investigation*, vol. 130, no. article JCI129018, 2020.

[14] Y. Chen, W. Lin, H. Yang et al., "Aberrant expansion and function of follicular helper T cell subsets in IgG4-related disease," *Arthritis & Rheumatology*, vol. 70, no. 11, pp. 1853–1865, 2018.

[15] G. Cao, S. Chi, X. Wang, J. Sun, and Y. Zhang, "CD4+CXCR5 +PD-1+ T follicular helper cells play a pivotal role in the development of rheumatoid arthritis," *Medical Science Monitor*, vol. 25, pp. 3032–3040, 2019.

[16] Y. Cao, Q. Yang, H. Deng et al., "Transcriptional factor ATF3 protects against colitis by regulating follicular helper T cells in Peyer's patches," *Proceedings of the National Academy of Sciences*, vol. 116, no. 13, pp. 6286–6291, 2019.

[17] T. Maehara, H. Mattoo, V. S. Mahajan et al., "The expansion in lymphoid organs of IL-4 BATF T follicular helper cells is linked to IgG4 class switching in vivo," *Life Science Alliance*, vol. 1, no. 1, 2017.

[18] V. Krishnamoorthy, S. Kannanganat, M. Maienschein-Cline et al., "The IRF4 gene regulatory module functions as a read-write integrator to dynamically coordinate T helper cell fate," *Immunity*, vol. 47, no. 3, pp. 481–497.e7, 2017.

[19] R. Zhang, C. F. Qi, Y. Hu et al., "T follicular helper cells restricted by IRF8 contribute to T cell-mediated inflammation," *Journal of Autoimmunity*, vol. 96, pp. 113–122, 2019.

[20] X. Duan, P. Sun, Y. Lan et al., "1IFN-α modulates memory Tfh cells and memory B cells in mice, following recombinant FMDV adenoviral challenge," *Frontiers in Immunology*, vol. 11, p. 701, 2020.

[21] S. B. Chodisetti, A. J. Fike, P. P. Domeier et al., "Serine phosphorylation of the STAT1 transactivation domain promotes autoreactive B cell and systemic autoimmunity development," *The Journal of Immunology*, vol. 204, no. 10, pp. 2641–2650, 2020.

[22] X. Ma, S. Nakayamada, S. Kubo et al., "Expansion of T follicular helper-T helper 1 like cells through epigenetic regulation by signal transducer and activator of transcription factors," *Annals of the Rheumatic Diseases*, vol. 77, no. 9, pp. 1354–1361, 2018.

[23] J. Deng, C. Fan, X. Gao et al., "Signal transducer and activator of transcription 3 hyperactivation associates with follicular helper T cell differentiation and disease activity in rheumatoid arthritis," *Frontiers in Immunology*, vol. 9, p. 1226, 2018.

[24] J. S. Weinstein, B. J. Laidlaw, Y. Lu et al., "STAT4 and T-bet control follicular helper T cell development in viral infections," *Journal of Experimental Medicine*, vol. 215, no. 1, pp. 337–355, 2018.

[25] R. J. Johnston, Y. S. Choi, J. A. Diamond, J. A. Yang, and S. Crotty, "STAT5 is a potent negative regulator of T_{FH} cell differentiation," *Journal of Experimental Medicine*, vol. 209, no. 2, pp. 243–250, 2012.

[26] R. I. Nurieva, A. Podd, Y. Chen et al., "STAT5 protein negatively regulates T follicular helper (Tfh) cell generation and function," *Journal of Biological Chemistry*, vol. 287, no. 14, pp. 11234–11239, 2012.

[27] A. A. Sheikh, L. Cooper, M. Feng et al., "Context-dependent role for T-bet in T follicular helper differentiation and germinal center function following viral infection," *Cell Reports*, vol. 28, no. 7, pp. 1758–1772.e4, 2019.

[28] F. Li, Z. Zeng, S. Xing et al., "Ezh2 programs T_{FH} differentiation by integrating phosphorylation-dependent activation of Bcl6 and polycomb-dependent repression of p19Arf," *Nature Communications*, vol. 9, no. 1, p. 5452, 2018.

[29] P. Shao, F. Li, J. Wang, X. Chen, C. Liu, and H. H. Xue, "Cutting edge: Tcf1 instructs T follicular helper cell differentiation by repressing Blimp1 in response to acute viral infection," *The Journal of Immunology*, vol. 203, no. 4, pp. 801–806, 2019.

[30] Y. S. Choi, J. A. Gullicksrud, S. Xing et al., "LEF-1 and TCF-1 orchestrate T_{FH} differentiation by regulating differentiation circuits upstream of the transcriptional repressor Bcl6," *Nature Immunology*, vol. 16, no. 9, pp. 980–990, 2015.

[31] W. Xu, X. Zhao, X. Wang et al., "The transcription factor Tox2 drives T follicular helper cell development via regulating chromatin accessibility," *Immunity*, vol. 51, no. 5, pp. 826–839.e5, 2019.

[32] K. Otsuka, A. Yamada, M. Saito et al., "Achaete-Scute Homologue 2–Regulated Follicular Helper T Cells Promote Autoimmunity in a Murine Model for Sjögren Syndrome," *The American Journal of Pathology*, vol. 189, no. 12, pp. 2414–2427, 2019.

[33] J. Geng, H. Wei, B. Shi et al., "Bach2 negatively regulates T follicular helper cell differentiation and is critical for $CD4^+$T cell memory," *The Journal of Immunology*, vol. 202, no. 10, pp. 2991–2998, 2019.

[34] A. Lahmann, J. Kuhrau, F. Fuhrmann et al., "Bach2 controls T follicular helper cells by direct repression of Bcl-6," *The Journal of Immunology*, vol. 202, no. 8, pp. 2229–2239, 2019.

[35] M. Xu, F. Wang, H. Chen et al., "Inactivation of FOXO1 induces T follicular cell polarization and involves angioimmunoblastic T cell lymphoma," *Cancer Biology and Medicine*, vol. 16, no. 4, pp. 743–755, 2019.

[36] B. Shi, J. Geng, Y. H. Wang et al., "Foxp1 negatively regulates T follicular helper cell differentiation and germinal center responses by controlling cell migration and CTLA-4," *The Journal of Immunology*, vol. 200, no. 2, pp. 586–594, 2018.

[37] I. Serr, R. W. Fürst, V. B. Ott et al., "miRNA92a targets KLF2 and the phosphatase PTEN signaling to promote human T follicular helper precursors in T1D islet autoimmunity," *Proceedings of the National Academy of Sciences*, vol. 113, no. 43, pp. E6659–E6668, 2016.

[38] J.-Y. Lee, C. N. Skon, J. Y. Lee et al., "The Transcription Factor KLF2 Restrains $CD4^+$ T Follicular Helper Cell Differentiation," *Immunity*, vol. 42, no. 2, pp. 252–264, 2015.

[39] M. M. Xie, B. H. Koh, K. Hollister et al., "Bcl6 promotes follicular helper T-cell differentiation and PD-1 expression in a Blimp1-independent manner in mice," *European Journal of Immunology*, vol. 47, no. 7, pp. 1136–1141, 2017.

[40] S. Crotty, "T follicular helper cell differentiation, function, and roles in disease," *Immunity*, vol. 41, no. 4, pp. 529–542, 2014.

[41] J. A. Yang, N. J. Tubo, M. D. Gearhart, V. J. Bardwell, and M. K. Jenkins, "Cutting edge: Bcl6-interacting corepressor contributes to germinal center T follicular helper cell formation and B cell helper function," *The Journal of Immunology*, vol. 194, no. 12, pp. 5604–5608, 2015.

[42] J. P. Nance, S. Bélanger, R. J. Johnston, J. K. Hu, T. Takemori, and S. Crotty, "Bcl6 middle domain repressor function is required for T follicular helper cell differentiation and utilizes the corepressor MTA3," *Proceedings of the National Academy of Sciences*, vol. 112, no. 43, pp. 13324–13329, 2015.

[43] Y. S. Choi, D. Eto, J. A. Yang, C. Lao, and S. Crotty, "Cutting edge: STAT1 is required for IL-6-mediated Bcl6 induction for early follicular helper cell differentiation," *The Journal of Immunology*, vol. 190, no. 7, pp. 3049–3053, 2013.

[44] X. Long, L. Zhang, Y. Zhang et al., "Histone methyltransferase Nsd2 is required for follicular helper T cell differentiation," *Journal of Experimental Medicine*, vol. 217, no. 1, 2020.

[45] N. Xiao, D. Eto, C. Elly, G. Peng, S. Crotty, and Y. C. Liu, "The E3 ubiquitin ligase Itch is required for the differentiation of follicular helper T cells," *Nature Immunology*, vol. 15, no. 7, pp. 657–666, 2014.

[46] X. Zhang, R. Dai, W. Li et al., "Abnormalities of follicular helper T-cell number and function in Wiskott-Aldrich syndrome," *Blood*, vol. 127, no. 25, pp. 3180–3191, 2016.

[47] X. Liu, H. Lu, T. Chen et al., "Genome-wide analysis identifies Bcl6-controlled regulatory networks during T follicular helper

cell differentiation," *Cell Reports*, vol. 14, no. 7, pp. 1735–1747, 2016.

[48] A. Ripamonti, E. Provasi, M. Lorenzo et al., "Repression of miR-31 by BCL6 stabilizes the helper function of human follicular helper T cells," *Proceedings of the National Academy of Sciences*, vol. 114, no. 48, pp. 12797–12802, 2017.

[49] S. Crotty, R. J. Johnston, and S. P. Schoenberger, "Effectors and memories: Bcl-6 and Blimp-1 in T and B lymphocyte differentiation," *Nature Immunology*, vol. 11, no. 2, pp. 114–120, 2010.

[50] B. C. Betz, K. L. Jordan-Williams, C. Wang et al., "Batf coordinates multiple aspects of B and T cell function required for normal antibody responses," *Journal of Experimental Medicine*, vol. 207, no. 5, pp. 933–942, 2010.

[51] W. Ise, M. Kohyama, B. U. Schraml et al., "The transcription factor BATF controls the global regulators of class-switch recombination in both B cells and T cells," *Nature Immunology*, vol. 12, no. 6, pp. 536–543, 2011.

[52] A. Sahoo, A. Alekseev, K. Tanaka et al., "Batf is important for IL-4 expression in T follicular helper cells," *Nature Communications*, vol. 6, no. 1, article 7997, 2015.

[53] P. Li, R. Spolski, W. Liao et al., "BATF-JUN is critical for IRF4-mediated transcription in T cells," *Nature*, vol. 490, no. 7421, pp. 543–546, 2012.

[54] R. I. Nurieva, Y. Chung, D. Hwang et al., "Generation of T follicular helper cells is mediated by interleukin-21 but independent of T helper 1, 2, or 17 cell lineages," *Immunity*, vol. 29, no. 1, pp. 138–149, 2008.

[55] M. Huber, A. Brustle, K. Reinhard et al., "IRF4 is essential for IL-21-mediated induction, amplification, and stabilization of the Th17 phenotype," *Proceedings of the National Academy of Sciences*, vol. 105, no. 52, pp. 20846–20851, 2008.

[56] C. S. Ma, D. T. Avery, A. Chan et al., "Functional STAT3 deficiency compromises the generation of human T follicular helper cells," *Blood*, vol. 119, no. 17, pp. 3997–4008, 2012.

[57] N. Schmitt, Y. Liu, S. E. Bentebibel et al., "The cytokine TGF-β co-opts signaling via STAT3-STAT4 to promote the differentiation of human T_{FH} cells," *Nature Immunology*, vol. 15, no. 9, pp. 856–865, 2014.

[58] K. A. Read, M. D. Powell, C. E. Baker et al., "Integrated STAT3 and Ikaros zinc finger transcription factor activities regulate Bcl-6 expression in $CD4^{+}$Th cells," *The Journal of Immunology*, vol. 199, no. 7, pp. 2377–2387, 2017.

[59] J. Wei, Y. Yuan, C. Jin et al., "The ubiquitin ligase TRAF6 negatively regulates the JAK-STAT signaling pathway by binding to STAT3 and mediating its ubiquitination," *PLoS One*, vol. 7, no. 11, article e49567, 2012.

[60] P. W. McDonald, K. A. Read, C. E. Baker et al., "IL-7 signalling represses Bcl-6 and the T_{FH} gene program," *Nature Communications*, vol. 7, no. 1, article 10285, 2016.

[61] X. Lin, X. Wang, F. Xiao et al., "IL-10-producing regulatory B cells restrain the T follicular helper cell response in primary Sjogren's syndrome," *Cellular & Molecular Immunology*, vol. 16, no. 12, pp. 921–931, 2019.

[62] L. He, W. Gu, M. Wang et al., "Extracellular matrix protein 1 promotes follicular helper T cell differentiation and antibody production," *Proceedings of the National Academy of Sciences*, vol. 115, no. 34, pp. 8621–8626, 2018.

[63] J. Zhang, Z. He, S. Sen, F. Wang, Q. Zhang, and Z. Sun, "TCF-1 inhibits IL-17 gene expression to restrain Th17 immunity in a stage-specific manner," *The Journal of Immunology*, vol. 200, no. 10, pp. 3397–3406, 2018.

[64] J. Hosokawa, K. Suzuki, K. Meguro et al., "IκBNS enhances follicular helper T-cell differentiation and function downstream of ASCl2," *Journal of Allergy and Clinical Immunology*, vol. 140, no. 1, pp. 288–291.e8, 2017.

[65] H. Qiu, H. Wu, V. Chan, C. S. Lau, and Q. Lu, "Transcriptional and epigenetic regulation of follicular T-helper cells and their role in autoimmunity," *Autoimmunity*, vol. 50, no. 2, pp. 71–81, 2017.

[66] H. Zeng, S. Cohen, C. Guy et al., "mTORC1 and mTORC2 kinase signaling and glucose metabolism drive follicular helper T cell differentiation," *Immunity*, vol. 45, no. 3, pp. 540–554, 2016.

[67] H. Wang, J. Geng, X. Wen et al., "The transcription factor Foxp1 is a critical negative regulator of the differentiation of follicular helper T cells," *Nature Immunology*, vol. 15, no. 7, pp. 667–675, 2014.

Hindawi
Journal of Immunology Research
Volume 2020, Article ID 5692829, 9 pages
https://doi.org/10.1155/2020/5692829

Research Article

Effect of Interleukin-17 in the Activation of Monocyte Subsets in Patients with ST-Segment Elevation Myocardial Infarction

Montserrat Guadalupe Garza-Reyes,[1] Mónica Daniela Mora-Ruíz,[1] Luis Chávez-Sánchez,[1] Alejandra Madrid-Miller,[2] Alberto Jose Cabrera-Quintero,[3] José Luis Maravillas-Montero,[4] Alejandro Zentella-Dehesa,[3] Luis Moreno-Ruíz,[5] Selene Pastor-Salgado,[6] Erick Ramírez-Arias,[6] Nataly Pérez-Velázquez,[7] Adriana Karina Chávez-Rueda,[1] Francisco Blanco-Favela,[1] Wendy Guadalupe Vazquez-Gonzalez,[1] and Alicia Contreras-Rodríguez[8]

[1]*Unidad de Investigación Médica en Inmunología, UMAE, Hospital de Pediatría, Centro Médico Nacional Siglo XXI, Instituto Mexicano del Seguro Social, Ciudad de México, Mexico*
[2]*División de Programas Educativos de la Coordinación de Educación en Salud, Instituto Mexicano del Seguro Social, Ciudad de México, Mexico*
[3]*Unidad de Bioquímica, Instituto Nacional de Ciencias Médicas y Nutrición Salvador Zubirán and Instituto de Investigaciones Biomédicas, Universidad Nacional Autónoma de México, Programa Institucional de Cáncer de Mama, Depto. Medicina Genómica y Toxicología Ambiental, Instituto de Investigaciones Biomédicas, Universidad Nacional Autónoma de México, Ciudad de México, Mexico*
[4]*Red de Apoyo a la Investigación, Universidad Nacional Autónoma de México and Instituto Nacional de Ciencias Médicas y Nutrición, Salvador Zubirán, Ciudad de México, Mexico*
[5]*Servicio de Cardiología Adultos, División de Cardiología de la Unidad Médica de Alta Especialidad, Hospital de Cardiología, Centro Médico Nacional Siglo XXI, Instituto Mexicano del Seguro Social, Ciudad de México, Mexico*
[6]*Servicio de Urgencias de la Unidad Médica de Alta Especialidad, Hospital de Cardiología, Centro Médico Nacional Siglo XXI, Instituto Mexicano del Seguro Social, Ciudad de México, Mexico*
[7]*Servicio de Cardiología de la Unidad Médica de Alta Especialidad, Hospital de Especialidades, Dr. Ignacio García Téllez, Instituto Mexicano del Seguro Social, Mérida, Yucatán, Mexico*
[8]*Servicio de Gabinetes de la Unidad Médica de Alta Especialidad, Hospital de Cardiología, Centro Médico Nacional Siglo XXI, Instituto Mexicano del Seguro Social, Ciudad de México, Mexico*

Correspondence should be addressed to Luis Chávez-Sánchez; luischz@yahoo.com

Received 17 February 2020; Revised 12 May 2020; Accepted 21 May 2020; Published 27 June 2020

Guest Editor: Charles Elias Assmann

Interleukin- (IL-) 17 is increased in acute myocardial infarction (AMI) and plays a key role in inflammatory diseases through its involvement in the activation of leukocytes. Here, we describe for the first time the effect of IL-17 in the migration and activation of monocyte subsets in patients during ST-segment elevation myocardial infarction (STEMI) and post-STEMI. We analyzed the circulating levels of IL-17 in patient plasma. A gradual increase in IL-17 was found in STEMI and post-STEMI patients. Additionally, IL-17 had a powerful effect on the recruitment of $CD14^{++}CD16^{+}/CD14^{+}CD16^{++}$ monocytes derived from patients post-STEMI compared with the monocytes from patients with STEMI, suggesting that IL-17 recruits monocytes with inflammatory activity post-STEMI. Furthermore, IL-17 increased the expression of TLR4 on $CD14^{+}CD16^{-}$ and $CD14^{+}$ $^{+}CD16^{+}/CD14^{+}CD16^{++}$ monocytes post-STEMI and might enhance the response to danger-associated molecular patterns post-STEMI. Moreover, IL-17 induced secretion of IL-6 from $CD14^{++}CD16^{-}$ and $CD14^{++}CD16^{+}/CD14^{+}CD16^{++}$ monocytes both in STEMI and in post-STEMI, which indicates that IL-17 has an effect on the secretion of proinflammatory cytokines from

monocytes during STEMI and post-STEMI. Overall, we demonstrate that in STEMI and post-STEMI, IL-17 is increased and induces the migration and activation of monocyte subsets, possibly contributing to the inflammatory response through TLR4 and IL-6 secretion.

1. Introduction

Acute coronary syndromes comprise the acute manifestations of coronary artery disease, including ST-segment elevation myocardial infarction (STEMI), which in the majority of cases occurs from a complete thrombotic occlusion developing from an atherosclerotic plaque in an epicardial coronary vessel and is associated with great morbidity and mortality [1]. In the first days of STEMI, a strong inflammatory response is induced that involves an increased release of several cytokines and infiltration of leukocytes in the heart tissue [2], followed by a second phase starting on day 4 (post-STEMI) that is maintained for several days[3] .

After myocardial infarction, the monocyte subset ($CD14^{++}CD16^{-}$, $CD14^{++}CD16^{+}$, and $CD14^{+}CD16^{++}$) numbers in the circulation increase in patients with STEMI [4]. These cells release inflammatory mediators, such as tumor necrosis factor- (TNF-) α, interleukin- (IL-) 1, and IL-6, which contribute to myocardial injury [2]. Furthermore, previous studies have shown that $CD14^{++}CD16^{-}$ monocytes predict cardiovascular events [5] and that $CD14^{+}CD16^{-}$ monocytes predominate in the infarct border zone [6]. In addition, human monocytes express patterns of genes associated with inflammation after acute myocardial infarction (AMI) [7], suggesting that these populations of monocytes have a relevant role in AMI in humans.

Inflammatory cytokines in AMI potently activate endothelial cells, increase expression of adhesion molecules on endothelial cells, and promote the activation of leukocytes to enhance the inflammatory response. IL-17 is an inflammatory cytokine produced by a variety of cell types, including macrophages and T cells [8, 9]. IL-17 contributes to the expression of molecules such as IL-8 and CCL2 and increases that of intercellular adhesion molecule- (ICAM-) 1 on endothelial cells [8, 9]. It has also been proposed that IL-17 contributes to the recruitment of neutrophils and monocytes [10, 11] and even induces the activation of human macrophages, which secrete cytokines such as IL-1β and TNF-α [12]. IL-17 levels are increased in the plasma and tissues such as the aorta of apolipoprotein E-deficient ($Apoe^{-/-}$) mice, promoting monocyte recruitment into lesions, and blockade of the effect of IL-17A in $Apoe^{-/-}$ mice reduces atherosclerotic plaque burden. In humans, higher levels of IL-17 have been found in patients with AMI than in those with unstable angina or stable angina [13, 14].

The dynamics of monocyte subsets and levels of IL-17 post-STEMI have been reported. However, the role of IL-17 in the activation of monocyte subsets derived from patients with STEMI remains unclear. This prompted us to explore the circulating levels of IL-17 and its effect on the recruitment and activation of monocyte subsets derived from STEMI and post-STEMI patients.

2. Materials and Methods

2.1. Experimental Protocol. The study was approved by the Human Ethics and Medical Research Committee of the Instituto Mexicano del Seguro Social (IMSS) on April 30, 2013, and registered (R-2013-785-030). It was conducted according to the Helsinki Declaration guidelines, and all patients provided written informed consent.

2.2. Patient Population. This study included 65 patients evaluated during STEMI (patients who had an acute myocardial infarction with ST-segment elevation and successfully treated with primary angioplasty within the first 24 hours) and post-STEMI (patients who had an acute myocardial infarction with ST-segment elevation and successfully treated with primary angioplasty five days after the onset of STEMI) who were admitted to the Hospital de Cardiología, Centro Médico Nacional Siglo "XXI", IMSS. The plasma levels of cytokines in the 65 patients were determined, and 11 of these patients were included in the experimental assay. STEMI was diagnosed with the following criteria: (1) chest pain > 30 minutes, with or without shortness of breath, sweating, nausea, and/or vomiting; (2) ST-segment elevation and/or abnormal Q-wave on an electrocardiogram and/or the presence of an emerging left block bundle branch; and (3) an elevated troponin level, specifically 10% above the 99th percentile of the upper limit of the reference value, or an elevated creatinine kinase MB isoenzyme (CK MB) level, higher than the 99th percentile of the upper limit of the reference value. The exclusion criteria included the following: (1) hemodynamic instability or electrical shock; (2) mechanical complications of infarction; (3) presence of malignancies, hematological or immunological disorders, or any other inflammatory condition or infection likely to be associated with the acute phase response; (4) previous immunosuppressive or anti-inflammatory therapy; and (5) a serum creatinine level ≥ 1.5 mg/dl or known allergy to iodine contrast medium.

2.3. Plasma Cytokine Determinations. Plasma samples were obtained from the 65 STEMI and post-STEMI patients. The plasma levels of CX3CL1, CCL2, and IL-17A were analyzed using a ProcartaPlex multiplex assay according to the manufacturer's instructions (Merck Millipore, Darmstadt, Germany). The detection limit was >0.5 pg/ml for CX3CL1, 37.5 pg/ml for CCL2, and 2.4 pg/ml for IL-17A.

2.4. Human Umbilical Vein Endothelial Cells. Human umbilical vein endothelial cells (HUVECs) were obtained from human umbilical cords [15], and the cells were cultured at 37°C in a humidified atmosphere with 5% CO_2 using an Endothelial Cell Growth Medium (EGM-2) medium bullet kit (Lonza, Verviers, Belgium). Cells in their third or fourth passage were used for all the reported experiments.

Recuperated cells were stained with anti-CD31 FITC-conjugated, anti-CD309 (KDR/VEGFR2) APC-conjugated, and anti-CD146 PE-conjugated antibodies (BD Biosciences, San Jose, California, USA) and evaluated with a MACS Quant Analyzer 10 cytometer (Miltenyi Biotec, Bergisch Gladbach, Germany) flow cytometer; molecular analysis was performed with FlowJo software version 7.6.5 (TreeStar, Inc.).

2.5. Monocyte Isolation. Peripheral blood mononuclear cells (PBMCs) were obtained from patients on days 1 (STEMI) and 5 (post-STEMI) after the onset of STEMI by density centrifugation using Lymphoprep (Axis-Shield, Oslo, Norway). Blood samples were mixed with an equal volume of phosphate-buffered saline (PBS), pH 7.4, layered over 3 ml of Lymphoprep, and centrifuged at 700 × g for 30 minutes. The recovered PBMCs were washed three times with PBS (pH 7.4). Classical monocytes ($CD14^+CD16^-$) were then isolated from the PBMCs using Monocyte Isolation Kit II (Miltenyi Biotec, Bergisch Gladbach, Germany), and intermediate/nonclassical monocytes were isolated in two phases. In the first phase, all monocytes were enriched using human Pan Monocyte Isolation Kit (Miltenyi Biotec); in the second phase, intermediate/nonclassical monocytes were isolated using magnetic microbeads coupled to an anti-CD16 monoclonal antibody. The purified cells were stained for CD14; the purity of the classical monocytes was >93%, and that of the intermediate/nonclassical monocytes was >89%.

2.6. Transendothelial Migration Assay. HUVECs were grown overnight on 1% gelatin-coated porous membranes in a Transwell chamber (Corning Inc., Cambridge, USA) of 6.5 mm diameter, and 5 μm pore size until a monolayer was formed. The HUVECs were activated for 1 day with IL-17 (60 ng/ml), interferon- (IFN-) γ (25 ng/ml), which was used as an inhibitory control for monocyte migration, or IL-17/IFN-γ (R&D Systems, Minnesota, USA), and culture medium alone was used as a negative control. A total of 3×10^5 monocytes in 50 μl medium were added to the upper chamber. In the transendothelial migration assay, serum-free RPMI medium was used in both compartments, and culture medium alone was used as a negative control. CCL2 (10 ng/ml) and CX3CL1 (25 ng/ml) were used as positive controls for classical monocytes and intermediate/nonclassical monocytes, respectively. After 3 hours, the migrating monocytes were recovered and quantitated by flow cytometry. The concentrations of CCL2 and CX3CL1 used were obtained through curves (Additional files).

2.7. Expression of Receptors. A total of 3×10^5 $CD14^+CD16^-$ and $CD14^{++}CD16^+$/$CD14^+CD16^{++}$ monocytes were cultured for 1 day with IL-17 (60 ng/ml), IFN-γ (25 ng/ml), which was used as a positive control of monocyte activation, or IL-17/IFN-γ (R&D Systems); culture medium alone was used as a negative control. The monocyte subsets were then stained with anti-TLR (Toll-like receptor) 4 PE-conjugated, anti-CD86 PECy5-conjugated, and anti-HLA-DR FITC-conjugated antibodies (BioLegend, San Diego, CA, USA) or isotype control antibodies for 20 minutes in the dark at 4°C. The cells were washed twice with PBS containing 1% BSA and 1% sodium azide. The expression levels of different molecules were measured using a MACS Quant flow cytometer (Miltenyi Biotec), and the mean fluorescence intensity (MFI) of each sample was quantified using FlowJo software (TreeStar, Inc.). The concentrations of IL-17 and IFN-γ used were obtained through curves (Additional files).

2.8. TNF-α and IL-6 Assays. TNF-α and IL-6 levels in supernatant were measured using an enzyme-linked immunosorbent assay (ELISA) (eBioscience, San Diego, USA) according to the manufacturer's instructions. The measurements in each assay were performed in duplicate. The detection limit was 1.65 pg/ml for TNF-α and <2 pg/ml for IL-6.

2.9. Statistical Analysis. All statistical analyses were performed using GraphPad Prism version 7 (GraphPad Software, Inc., San Diego, CA, USA), and a level of $p < 0.05$ was considered statistically significant. Levels of CCL2, CX3CL1, and IL-17, which are presented as medians (interquartile ranges), were analyzed with the Wilcoxon test. Multiple comparisons of the groups were analyzed by the Mann-Whitney U and Kruskal-Wallis tests (data shown in the figures are expressed as the mean ± SEM). The experimental study included eleven independent experiments and measured circulating cytokine levels in sixty-five patients.

3. Results

3.1. Patient Characteristics. The characteristics of the study population are shown in Table 1. The STEMI patients included 51 men and 14 women, with a mean age of 63 ± 10 years (range, 37 to 83 years). Of these patients, 31 had diabetes, 32 had systemic arterial hypertension, 42 were smokers, 22 had obesity, and 30 had hyperlipidemia. The mean value of the maximum creatine kinase (CK) level was 2.216 ± 1.850 IU/l, the maximum CK-MB level was 196 ± 188.1, and the maximum creatine phosphokinase (CPK) level was 2.730 ± 1.827.

3.2. Cytokine Levels in Patients with STEMI and Post-STEMI. Cytokine secretion is particularly active after myocardial infarction and contributes to cellular recruitment and activation cellular [2, 16, 17]. To obtain a picture of the circulating levels of chemokines that contribute to the recruitment of monocytes and IL-17 in patients, we determined CCL2, CX3CL1, and IL-17 in the plasma of STEMI and post-STEMI patients. Plasma CCL2 levels were higher in patients with STEMI and decreased post-STEMI (Figure 1(a)) (CCL2: 497.2 ± 229.3 pg/ml vs. 346.3 ± 162.6 pg/ml, $p = 0.0001$). Conversely, circulating plasma CX3CL1 levels were lower in STEMI patients than in post-STEMI patients (CX3CL1: 271.0 ± 192.9 pg/ml vs. 334.8 ± 224.8 pg/ml, $p = 0.0094$), as shown in Figure 1(b). These findings suggest that CCL2 and CX3CL1 might facilitate the mobilization of circulating $CD14^{++}CD16^-$ and $CD14^{++}CD16^+$/$CD14^+CD16^{++}$ monocytes, respectively. Interestingly, IL-17 levels were higher in post-STEMI patients than in STEMI patients, as shown in Figure 1(c) (IL-17: 12.25 ± 11.69 vs. 19.09 ± 17.86, $p = 0.0001$). This result suggests that IL-17 may favor proinflammatory responses to induce cell activation after AMI.

Table 1: Characteristics of the population on day 1.

Patient characteristics Characteristic	STEMI ($n = 65$)
Age (years)	70 (63-80)
Sex, male/female	51/14
Diabetes mellitus, *n* (%)	31 (47)
Hypertension, *n* (%)	32 (49)
Hyperlipidemia, *n* (%)	30 (46)
Smoking, *n* (%)	42 (64)
Obesity, *n* (%)	22 (33)
Statin, *n* (%)	63 (96)
Beta-blocker, *n* (%)	31 (47)
ACE/ARB, *n* (%)	34 (52)
Aspirin, *n* (%)	63 (96)
Serum creatinine (mg/dl)	1.0 (0.9-1.3)
Max CK (IU/l)	2216 (1361-3438)
Max CK-MB (IU/l)	196 (117-340)
Glucose (mg/dl)	130 (130-218)
Total cholesterol (mg/dl)	138 (125-176)
Triglyceride (mg/dl)	140 (106-175)
Body mass index (kg/m^2)	26.7 (24.2-29.4)

3.3. Effect of IL-17 on the Transendothelial Migration of Monocyte Subsets. The recruitment of monocyte subsets toward damaged tissue requires migration of monocytes through the endothelium [16–18]. First, we examined the transmigration of monocyte subsets from STEMI and post-STEMI patients in response to CCL2 and CX3CL1 and found that $CD14^+CD16^-$ monocytes from the former patients migrated more than those derived from the latter patients in response to CCL2 (Figure 2(a)). Moreover, CX3CL1 induced, in a similar way, the transmigration of $CD14^{++}CD16^+/CD14^+CD16^{++}$ monocytes in patients during STEMI and post-STEMI (Figure 2(d)). IL-17 has the ability to promote inflammation through the induction of cytokines and chemokines, which contribute to the migration of monocytes [8, 19, 20]. To characterize the role of IL-17 in the migration of monocyte subsets through the endothelium in patients with STEMI, we assessed whether treatment of HUVECs with IL-17 results in an increased migration of monocyte subsets across the endothelial monolayer. Indeed, treatment of HUVECs with IL-17 induced the transmigration of $CD14^{++}CD16^-$ monocytes from patients during STEMI and post-STEMI (Figures 2(b) and 2(c)). However, treatment of HUVECs with IFN-γ (inhibition of migration control for monocytes) and the combination of IL-17/IFN-γ resulted in lower migration of $CD14^{++}CD16^-$ monocytes than with IL-17 alone. Nonetheless, IL-17 induced the migration of $CD14^{++}CD16^+/CD14^+CD16^{++}$ monocytes from STEMI patients via HUVECs, and IL-17 increased the migration of $CD14^{++}CD16^+/CD14^+CD16^{++}$ monocytes from post-STEMI patients (Figures 2(e) and 2(f)) in relation to IFN-γ or IL-17/IFN-γ. These results suggest that IL-17 similarly contributes to the transmigration of $CD14^+CD16^-$ monocytes in STEMI and post-STEMI and considerately enhances the migration of $CD14^{++}CD16^+/CD14^+CD16^{++}$ monocytes in post-STEMI versus STEMI.

3.4. Effect of IL-17 on Markers in Monocyte Subsets. IL-17 is an inflammatory cytokine that induces the activation of myeloid lineage cells [12]. In this context, we treated the two patient monocyte subsets (obtained during STEMI or post-STEMI) with IL-17 and evaluated the markers TLR4, CD86, and HLA-DR. Stimulation of $CD14^+CD16^-$ or $CD14^{++}CD16^+/CD14^+CD16^{++}$ monocytes from patients with STEMI with IL-17 did not affect expression of TLR4 (Figures 3(a) and 3(c)). However, IL-17 treatment of $CD14^+CD16^-$ and $CD14^{++}CD16^+/CD14^+CD16^{++}$ monocytes from patients post-STEMI resulted in a 2.6-fold and 1.3-fold increase in the expression of TLR4, respectively, compared to unstimulated cells (Figures 3(b) and 3(d)). In contrast, IL-17 did not affect expression of CD86 (Figures 3(e)–3(h)) or HLA-DR (Figures 3(i)–3(l)) on $CD14^+CD16^-$ and $CD14^{++}CD16^+/CD14^+CD16^{++}$ from STEMI and post-STEMI patients. Additionally, IFN-γ (positive control) and IL-17/IFN-γ treatment significantly increased the levels of TLR4, CD86, and HLA-DR in STEMI and post-STEMI monocyte subsets; $CD14^{++}CD16^+/CD14^+CD16^{++}$ monocytes treated with IL-17/IFN-γ exhibited a 1.6-fold increase in expression of TLR4 compared with monocytes treated with IFN-γ. These results suggest that IL-17 slightly affects expression of molecules related to pattern recognition receptors such as TLR4 in both monocyte subsets in post-STEMI patients, which may contribute to the inflammatory response.

3.5. Effect of IL-17 on the Secretion of Proinflammatory Cytokines in Monocyte Subsets. Next, we determined the effect of IL-17 on $CD14^+CD16^-$ and $CD14^{++}CD16^+/CD14^+CD16^{++}$ monocytes with regard to the secretion of cytokines. Monocytes are essential cells in the inflammatory response during infarction [2, 7, 4]. $CD14^+CD16^-$ monocytes from STEMI and post-STEMI patients treated with IL-17 exhibited increased the levels of TNF-α (Figures 4(a) and 4(b)). However, $CD14^{++}CD16^+/CD14^+CD16^{++}$ monocytes from post-STEMI patients cultured with IL-17 displayed 2.6-fold increased production of TNF-α compared with cells cultured with medium alone (Figures 4(e) and 4(f)). IL-17 induced a 3.4-fold increase in IL-6 levels in $CD14^+CD16^-$ monocytes from STEMI patients and a 1.9-fold increase in post-STEMI patients compared with monocytes cultured in medium alone (Figures 4(c) and 4(d)). In addition, IL-17 treatment of $CD14^{++}CD16^+/CD14^+CD16^{++}$ monocytes from STEMI and post-STEMI patients caused 3.7-fold and 7.4-fold increases in IL-6, respectively, in relation to monocytes cultured only with medium alone (Figures 4(g) and 4(h)). We also found that IFN-γ and the combination of IL-17/IFN-γ increased TNF-α and IL-6 levels in $CD14^+CD16^-$ and $CD14^{++}CD16^+/CD14^+CD16^{++}$ monocytes from patients with STEMI and post-STEMI. These results suggest that IL-17 induces the activation of $CD14^+CD16^-$ and $CD14^{++}CD16^+/CD14^+CD16^{++}$ monocytes to produce inflammatory cytokines, which might contribute to the inflammatory response in STEMI and post-STEMI.

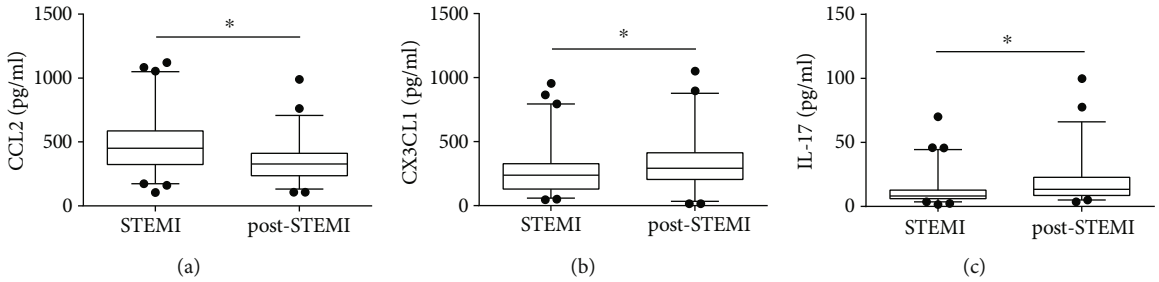

Figure 1: Circulating cytokines during STEMI and post-STEMI. Patient plasma was obtained during STEMI and post-STEMI, and the circulating levels of (a) CCL2, (b) CX3CL1, and (c) IL-17 were assessed. The concentrations of the cytokines in the plasma were determined by a multiplex assay. $n = 65$.

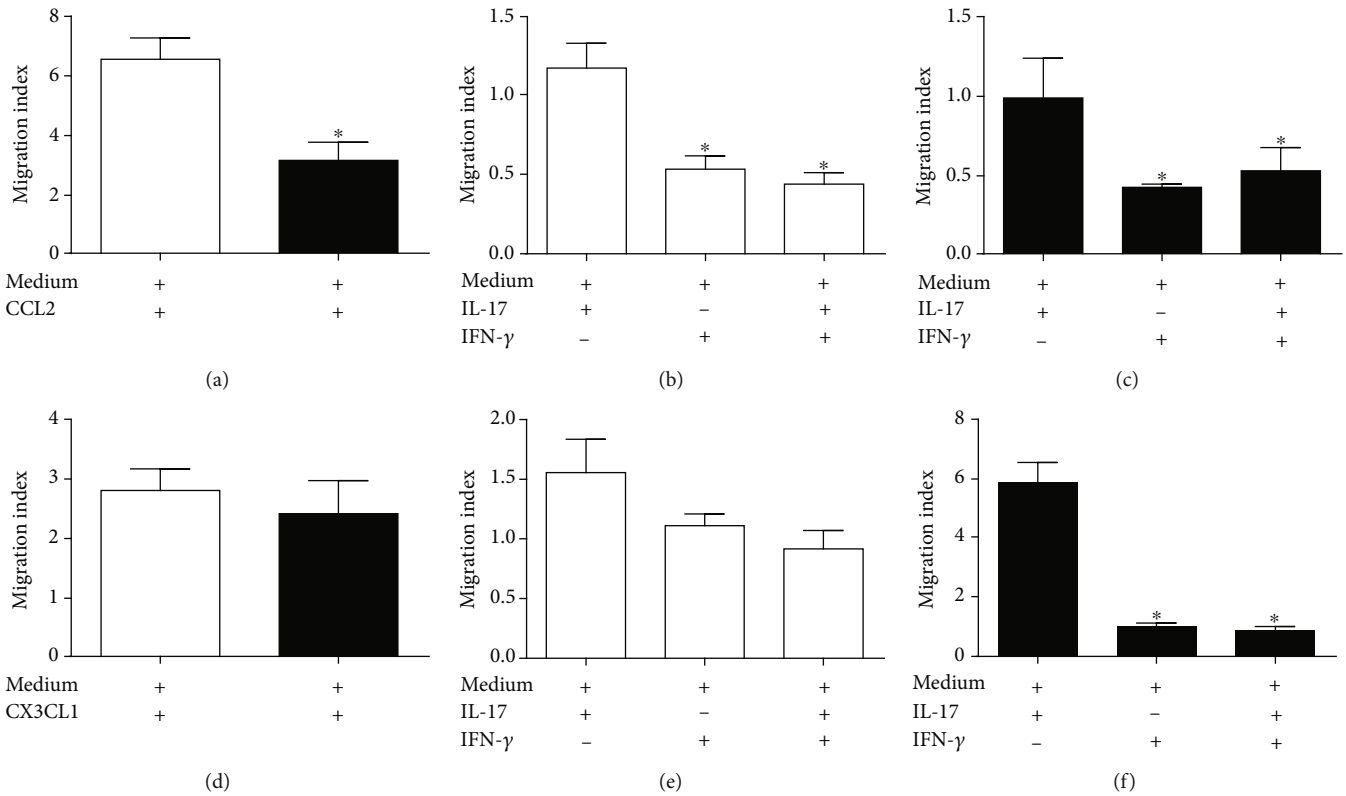

Figure 2: Monocytes transmigrate across a human umbilical vein endothelial cell monolayer in response to IL-17. A sample of 3×10^5 (a–c) $CD14^{++}CD16^{-}$ or (d–f) $CD14^{++}CD16^{+}/CD14^{+}CD16^{++}$ monocytes was added to the upper surface of monolayers of human umbilical vein endothelial cells (HUVECs) previously treated with IL-17, IFN-γ, or IL-17/IFN-γ; culture medium alone was used as a negative control. The monocytes were allowed to transmigrate across the HUVEC monolayers in the presence of CCL2, CX3CL1, or culture medium for 3 hours. All data are presented as the migration index, which relates the number of cells that migrated in response to the indicated stimulus to the number of cells that migrated in response to the negative control. White column: STEMI: black column: post-STEMI; $n = 11$. $^{*}p < 0.05$.

4. Discussion

This study demonstrates for the first time higher circulating levels of IL-17 post-STEMI than during STEMI. Additionally, IL-17 differentially induces the migration and activation of $CD14^{+}CD16^{-}$ and $CD14^{++}CD16^{+}/CD14^{+}CD16^{++}$ monocytes during STEMI and post-STEMI.

During AMI, cytokines in the circulation play essential roles in the recruitment of cells to damaged tissue and in the activation of cells of the innate immune system [2]. We found that patients with STEMI had high levels of CCL2 and that these levels decreased post-STEMI [21–24], which is crucial for $CD14^{++}CD16^{-}$ monocyte recruitment [16, 17] and monocyte infiltration into the infarcted area [25]. On the other hand, we found higher levels of CX3CL1 in post-STEMI patients than in STEMI patients. Previous reports have shown increased circulating levels of CX3CL1 in patients with STEMI [26]. Additionally, *in vivo* studies in mouse models of AMI found an increase in the expression of CX3CL1 during phase 2 of infarction, which suggested

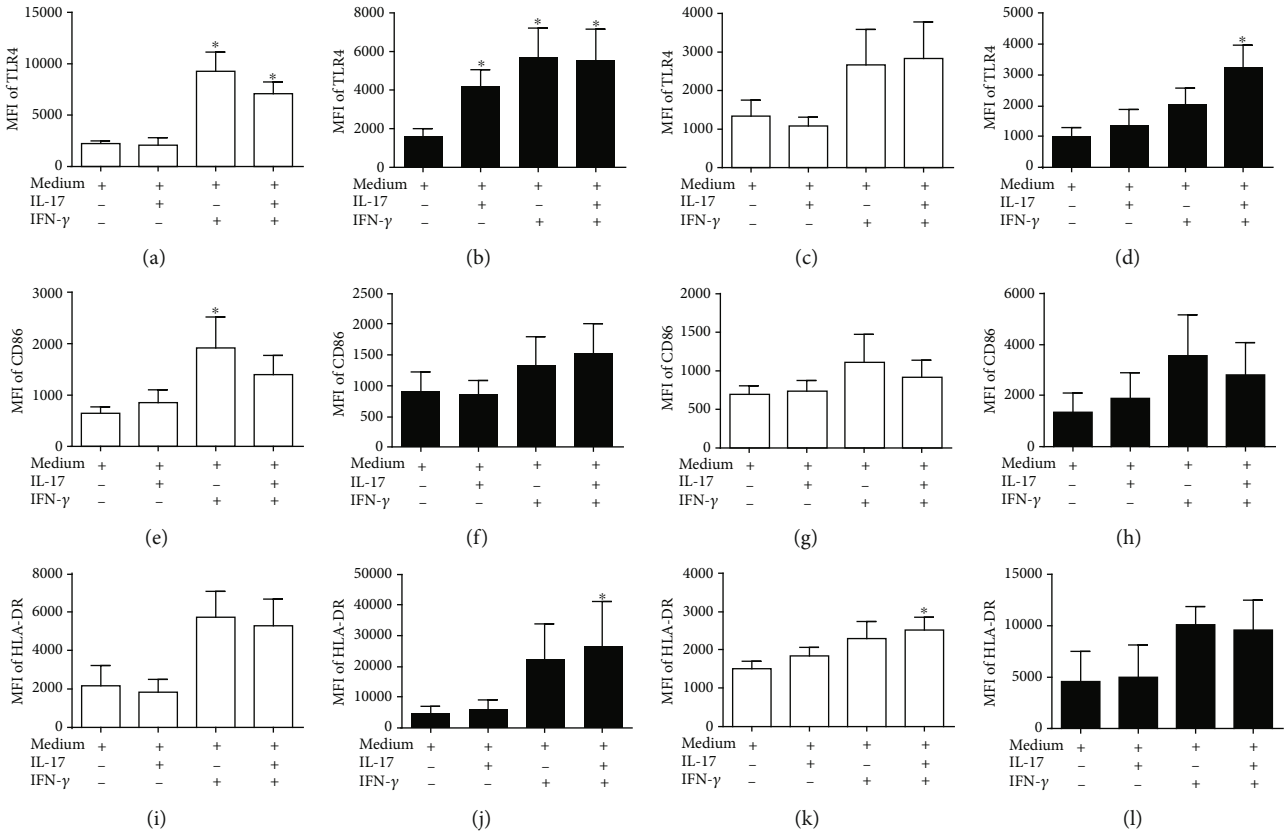

Figure 3: Expression of surface markers on monocytes stimulated with IL-17. Human $CD14^{++}CD16^{-}$ and $CD14^{++}CD16^{+}/CD14^{+}CD16^{++}$ monocytes were treated with IL-17, IFN-γ, which was used as a positive control, IL-17/IFN-γ, or culture medium alone, which was used as a negative control, for 24 hours. Human $CD14^{++}CD16^{-}$ in STEMI: (a) TLR4, (e) CD86, and (i) HLA-DR. Human $CD14^{++}CD16^{-}$in post-STEMI: (b) TLR4, (f) CD86, and (j) HLA-DR. Human $CD14^{++}CD16^{+}/CD14^{+}CD16^{++}$ monocytes in STEMI: (c) TLR4, (g) CD86, and (k) HLA-DR. $CD14^{++}CD16^{+}/CD14^{+}CD16^{++}$ monocytes post-STEMI: (d) TLR4, (h) CD86, and (l) HLA-DR. Expression levels of TLR4, CD86, and HLA-DR are expressed as MFI. White column: STEMI; black column: post-STEMI; $n = 11$. $^{*}p < 0.05$.

the mobilization of Ly-$6C^{low}$ monocytes (mouse counterparts of human $CD14^{++}CD16^{+}/CD14^{+}CD16^{++}$ monocytes) [4, 6]. Our results also demonstrate that patients had higher levels of IL-17 in the circulation post-STEMI than during STEMI. Several reports have shown elevated levels of IL-17 in infarction and even a significant increase in IL-17 expression have been observed during the first hours of STEMI [13, 27]. These results suggest that IL-17 might have proinflammatory activity in STEMI and post-STEMI.

In this context, we hypothesize that circulating IL-17 in STEMI and post-STEMI patients might be essential for endothelial activation and the subsequent recruitment and activation of $CD14^{++}CD16^{-}$ and $CD14^{++}CD16^{+}/CD14^{+}CD16^{++}$ monocytes, which may induce the secretion of proinflammatory cytokines. IL-17 is a cytokine whose level increases after AMI [28]. These findings suggest that IL-17 may be involved in the pathophysiology of infarction. We demonstrate that IL-17 contributes to similar transmigration of $CD14^{+}CD16^{-}$ monocytes from STEMI and post-STEMI patients through a HUVEC monolayer; we also found that IL-17 preferentially contributes to the transmigration of $CD14^{+}CD16^{+}/CD14^{+}CD16^{++}$ monocytes from post-STEMI patients. In accordance with our results, *in vitro* studies have shown that IL-17 contributes to the recruitment of mononuclear cells, such as monocytes, through its ability to induce expression of CCL2 and increase that of adhesion molecules, such as selectin E, ICAM-1, and VCAM-1, in HUVECs [11, 13, 29]. Moreover, direct inhibition of IL-17 in $Apoe^{-/-}$ mice causes a considerable reduction in the accumulation of macrophages in atherosclerotic plaques [30]. Additionally, IFN-γ and IL-17/IFN-γ reduced the migration of $CD14^{+}CD16^{-}$and $CD14^{+}CD16^{+}/CD14^{+}CD16^{++}$ monocytes through a HUVEC monolayer, which is consistent with previous reports [31, 32]. On the other hand, we found only slight increases in TLR4, CD86, and HLA-DR expression on $CD14^{+}CD16^{-}$ and $CD14^{+}CD16^{+}/CD14^{+}CD16^{++}$ monocytes in response to IL-17, and this effect was most evident for TLR4, suggesting an increase in the response to danger-associated molecular patterns post-STEMI. Previous reports have indicated that IL-17 in human macrophages induces the expression of TLR4, which is essential in the inflammatory response [2, 33]. Additionally, we show that IFN-γ or the combination of IL-17 and IFN-γ markedly increased the expression levels of TLR4, CD86, and HLA-DR on monocytes from STEMI and post-STEMI patients. IFN-γ plays an essential role in the inflammatory response through activation of monocytes [34] and shows a synergistic effect with IL-17 [35].

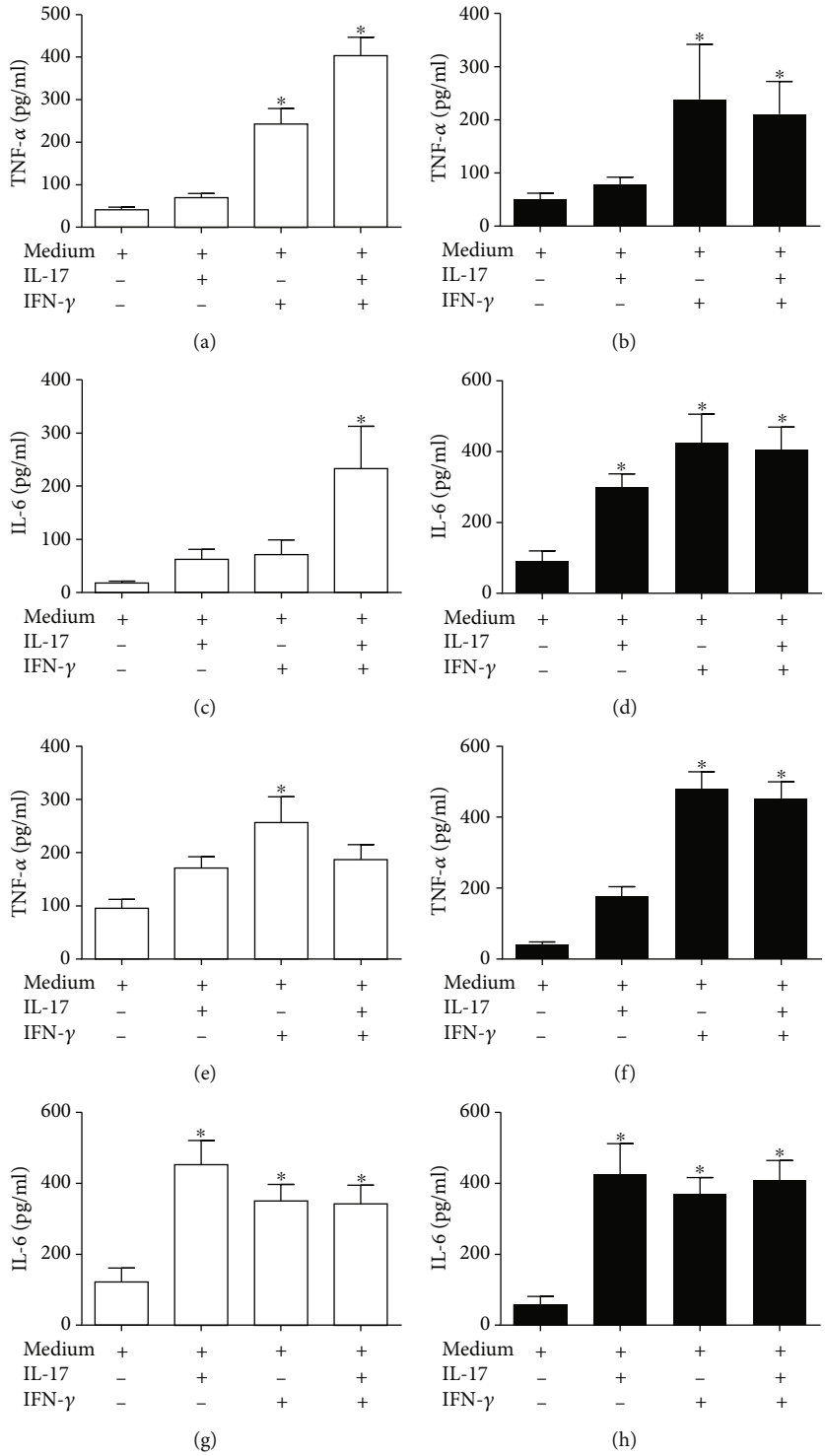

Figure 4: IL-17 induces the secretion of proinflammatory cytokines in monocyte subsets. Human $CD14^{++}CD16^{-}$ or $CD14^{+}CD16^{+}$/$CD14^{+}CD16^{++}$ monocytes were treated with IL-17, IFN-γ, which was used as a positive control, IL-17/IFN-γ, or culture medium alone, which was used as a negative control, for 24 hours. Human $CD14^{++}CD16^{-}$ in STEMI: (a) TNF-α and (c) IL-6. Human $CD14^{+}CD16^{-}$ in post-STEMI: (b) TNF-α and (d) IL-6. Human $CD14^{++}CD16^{+}$/$CD14^{+}CD16^{++}$ monocytes in STEMI: (e) TNF-α and (g) IL-6. $CD14^{++}CD16^{+}$/$CD14^{+}CD16^{++}$ monocytes post-STEMI: (f) TNF-α and (h) IL-6. Concentrations of TNF-α and IL-6 in the culture supernatants were determined by ELISA. White column: STEMI; black column: post-STEMI; $n = 11$. $^{*}p < 0.05$.

Monocytes that infiltrate into ischemic cardiac tissue can be activated by inflammatory mediators such as IL-17 [2, 20]. According to our results, $CD14^{++}CD16^{-}$ and $CD14^{+}CD16^{+}$/$CD14^{+}CD16^{++}$ monocytes produce low levels of TNF-α in response to IL-17, both during STEMI and post-STEMI. However, post-STEMI $CD14^{++}CD16^{+}$/$CD14^{+}CD16^{++}$

monocytes exhibited increased secretion of TNF-α after stimulation with IL-17. Additionally, we showed that IL-17 induced a slight increase in IL-6 production in $CD14^{+}CD16$ monocytes derived from patients during STEMI, and this level of IL-6 was markedly increased in monocytes from patients post-STEMI. IL-17 was also able to enhance secretion of IL-6 by $CD14^{++}CD16^{+}/CD14^{+}CD16^{++}$ monocytes from STEMI patients and lower secretion by the corresponding post-STEMI monocytes. Previous reports have found that IL-17 induces secretion of TNF-α and IL-6 by human monocytes and macrophages [12, 36]. Similarly, blocking IL-17 decreases TNF-α and, to a larger magnitude, IL-6 production in atherosclerotic lesions in mouse models [29]. Our results suggest that IL-17 acts on $CD14^{++}CD16^{-}$ monocytes in the post-STEMI environment and on $CD14^{++}CD16^{+}/CD14^{+}CD16^{++}$ monocytes in both the STEMI and post-STEMI environments, indicating that IL-17 induces a proinflammatory effect on both monocyte subsets. This likely occurs through IL-6 production, which may contribute to inflammation in cardiac tissue during both stages of infarction. Additionally, our results demonstrate that IFN-γ or the combination of IL-17/IFN-γ induced a proinflammatory effect on both monocyte subsets during STEMI and post-STEMI, though we did not find an additive or synergistic effect with the combination of IFN- γ and IL-17.

5. Conclusions

In conclusion, we show a gradual increase in IL-17 in STEMI and post-STEMI patients. IL-17 increases the expression of TLR4 on $CD14^{+}CD16^{-}$ and $CD14^{++}CD16^{+}/CD14^{+}CD16^{++}$ cells post-STEMI. Moreover, IL-17 has a potential role in the recruitment of $CD14^{++}CD16^{+}/CD14^{+}CD16^{++}$ monocytes post-STEMI. In addition, IL-17 contributes to secretion of IL-6 by $CD14^{++}CD16^{-}$ and $CD14^{++}CD16^{+}/CD14^{+}CD16^{+}$ monocytes in STEMI and post-STEMI. These findings for an *in vitro* model suggest that in STEMI and post-STEMI patients, IL-17 induces the recruitment and activation of monocyte subsets through an increase in TLR4 and IL-6 secretion, which might cause damage to myocardial tissue in STEMI and post-STEMI.

Abbreviations

STEMI: ST-segment elevation myocardial infarction
TNF: Tumor necrosis factor
IL: Interleukin
AMI: Acute myocardial infarction
ICAM: Intercellular adhesion molecules
Apoe: Apolipoprotein E
CK MB: Creatine kinase MB isoenzyme
HUVECs: Human umbilical vein endothelial cells
PBMCs: Peripheral blood mononuclear cells
PBS: Phosphate-buffered saline
IFN: Interferon
TLR: Toll-like receptor
MFI: Mean fluorescence intensity
CK: Creatine kinase
CPK: Creatine phosphokinase
ELISA: Enzyme-linked immunosorbent assay.

Data Availability

Data are available upon request and may be obtained by contacting the corresponding author.

Conflicts of Interest

The authors declare that no competing interests exist.

Acknowledgments

This work was supported in part by the Instituto Mexicano del Seguro Social projects of the Found Health Research (Grant numbers FIS/IMSS/PROT/G13/1221 and FIS/IMSS/PROT/G16/1588).

Supplementary Materials

Figure S1: effect of CCL2, CX3L1, and IFN-γ on migration of monocytes. Figure S2: assay of IL-17 and IFN-γ on monocytes. *(Supplementary Materials)*

References

[1] J. L. Anderson and D. A. Morrow, "Acute myocardial infarction," *New England Journal of Medicine*, vol. 376, no. 21, pp. 2053–2064, 2017.

[2] N. G. Frangogiannis, "The inflammatory response in myocardial injury, repair, and remodelling," *Nature Reviews Cardiology*, vol. 11, no. 5, pp. 255–265, 2014.

[3] S. D. Prabhu and N. G. Frangogiannis, "The biological basis for cardiac repair after myocardial infarction," *Nature Reviews Cardiology*, vol. 119, no. 1, pp. 91–112, 2016.

[4] H. Tsujioka, T. Imanishi, H. Ikejima et al., "Impact of heterogeneity of human peripheral blood monocyte subsets on myocardial salvage in patients with primary acute myocardial infarction," *Journal of the American College of Cardiology*, vol. 54, no. 2, pp. 130–138, 2009.

[5] K. E. Berg, I. Ljungcrantz, L. Andersson et al., "Elevated CD14 CD16 monocytes predict cardiovascular events," *Circulation: Cardiovascular Genetics*, vol. 5, no. 1, pp. 122–131, 2012.

[6] U. Hofmann and S. Frantz, "Immunity strikes: heart failure as a systemic disease," *European Heart Journal*, vol. 35, no. 6, pp. 341–343, 2014.

[7] N. Ruparelia, J. Godec, R. Lee et al., "Acute myocardial infarction activates distinct inflammation and proliferation pathways in circulating monocytes, prior to recruitment, and identified through conserved transcriptional responses in mice and humans," *European Heart Journal*, vol. 36, no. 29, pp. 1923–1934, 2015.

[8] S. Shahrara, S. R. Pickens, A. M. Mandelin II et al., "IL-17–mediated monocyte migration occurs partially through CC chemokine ligand 2/monocyte chemoattractant protein-1 induction," *The Journal of Immunology*, vol. 184, no. 8, pp. 4479–4487, 2010.

[9] J. Mai, G. Nanayakkara, J. Lopez-Pastrana et al., "Interleukin-17A promotes aortic endothelial cell activation via transcriptionally and post-translationally activating p38 mitogen-activated protein kinase (MAPK) pathway," *Journal of Biological Chemistry*, vol. 291, no. 10, pp. 4939–4954, 2016.

[10] M. Laan, *Neutrophil recruitment by human IL-17 via C-X-C chemokine release in the airways*, 1999, http://www.jimmunol.org/content/162/4/http://www.jimmunol.org/content/162/4/2347.full#ref-list-1.

[11] C. Erbel, M. Akhavanpoor, D. Okuyucu et al., "IL-17A influences essential functions of the monocyte/macrophage lineage and is involved in advanced murine and human atherosclerosis," *The Journal of Immunology*, vol. 193, no. 9, pp. 4344–4355, 2014.

[12] D. V. Jovanovic, J. A. di Battista, J. Martel-Pelletier et al., "IL-17 stimulates the production and expression of proinflammatory cytokines, IL-beta and TNF-alpha, by human macrophages," *The Journal of Immunology*, vol. 160, no. 7, pp. 3513–3521, 1998.

[13] X. Cheng, X. Yu, Y. J. Ding et al., "The Th17/Treg imbalance in patients with acute coronary syndrome," *Clinical Immunology*, vol. 127, no. 1, pp. 89–97, 2008.

[14] L. Zhang, T. Wang, X. Q. Wang et al., "Elevated frequencies of circulating Th22 cell in addition to Th17 cell and Th17/Th1 cell in patients with acute coronary syndrome," *PLoS ONE*, vol. 8, no. 12, p. e71466, 2013.

[15] L. N. López-Bojórquez, F. Arechavaleta-Velasco, F. Vadillo-Ortega, D. Móntes-Sánchez, J. L. Ventura-Gallegos, and A. Zentella-Dehesa, "NF-?B translocation and endothelial cell activation is potentiated by macrophage-released signals co-secreted with TNF-α and IL-1β," *Inflammation Research*, vol. 53, no. 10, pp. 567–575, 2004.

[16] R. M. Kratofil, P. Kubes, and J. F. Deniset, "Monocyte conversion during inflammation and injury," *Arteriosclerosis, Thrombosis, and Vascular Biology*, vol. 37, no. 1, pp. 35–42, 2017.

[17] L. Chávez-Sánchez, J. E. Espinosa-Luna, K. Chávez-Rueda, M. V. Legorreta-Haquet, E. Montoya-Díaz, and F. Blanco-Favela, "Innate immune system cells in atherosclerosis," *Archives of Medical Research*, vol. 45, no. 1, pp. 1–14, 2014.

[18] E. A. Liehn, O. Postea, A. Curaj, and N. Marx, "Repair after myocardial infarction, between fantasy and reality," *Journal of the American College of Cardiology*, vol. 58, no. 23, pp. 2357–2362, 2011.

[19] S. K. Lundy, S. Sarkar, L. A. Tesmer, and D. A. Fox, "Cells of the synovium in rheumatoid arthritis. T lymphocytes," *Arthritis Research and Therapy*, vol. 9, no. 1, p. 202, 2007.

[20] M. D. Mora-Ruíz, F. Blanco-Favela, A. K. Chávez Rueda, M. V. Legorreta-Haquet, and L. Chávez-Sánchez, "Role of interleukin-17 in acute myocardial infarction," *Molecular Immunology*, vol. 107, pp. 71–78, 2019.

[21] A. Arakelyan, J. Petrkova, Z. Hermanova, A. Boyajyan, J. Lukl, and M. Petrek, "Serum levels of the MCP-1 chemokine in patients with ischemic stroke and myocardial infarction," *Mediators of Inflammation*, vol. 2005, no. 3, pp. 175–179, 2005.

[22] Y. Murakami, K. Kurosaki, K. Matsui, K. Shimada, and U. Ikeda, "Serum MCP-1 and VEGF levels are not affected by inhibition of the renin-angiotensin system in patients with acute myocardial infarction," *Cardiovascular Drugs and Therapy*, vol. 17, no. 3, pp. 249–255, 2003.

[23] J. T. Parissis, S. Adamopoulos, K. F. Venetsanou, D. G. Mentzikof, S. M. Karas, and D. T. Kremastinos, "Serum profiles of C-C chemokines in acute myocardial infarction: possible implication in postinfarction left ventricular remodeling," *Journal of Interferon & Cytokine Research*, vol. 22, no. 2, pp. 223–229, 2002.

[24] A. Ngkelo, A. Richart, J. A. Kirk et al., "Mast cells regulate myofilament calcium sensitization and heart function after myocardial infarction," *Journal of Experimental Medicine*, vol. 213, no. 7, pp. 1353–1374, 2016.

[25] K. Kaikita, T. Hayasaki, T. Okuma, W. A. Kuziel, H. Ogawa, and M. Takeya, "Targeted deletion of CC chemokine receptor 2 attenuates left ventricular remodeling after experimental myocardial infarction," *American Journal of Pathology*, vol. 165, no. 2, pp. 439–447, 2004.

[26] S. E. Boag, R. Das, E. V. Shmeleva et al., "T lymphocytes and fractalkine contribute to myocardial ischemia/reperfusion injury in patients," *Journal of Clinical Investigation*, vol. 125, no. 8, pp. 3063–3076, 2015.

[27] T. Bochaton, N. Mewton, N. D. Thiam et al., "Early kinetics of serum interleukine-17A and infarct size in patients with reperfused acute ST-elevated myocardial infarction," *PLoS ONE*, vol. 12, no. 11, p. e0188202, 2017.

[28] U. Hofmann and S. Frantz, "Role of lymphocytes in myocardial injury, healing, and remodeling after myocardial infarction," *Circulation Research*, vol. 116, no. 2, pp. 354–367, 2015.

[29] E. Smith, K. M. R. Prasad, M. Butcher et al., "Blockade of interleukin-17A results in reduced atherosclerosis in apolipoprotein E-deficient mice," *Circulation*, vol. 121, no. 15, pp. 1746–1755, 2010.

[30] C. Erbel, L. Chen, F. Bea et al., "Inhibition of IL-17A attenuates atherosclerotic lesion development in apoe-deficient mice," *The Journal of Immunology*, vol. 183, no. 12, pp. 8167–8175, 2009.

[31] J. Melrose, N. Tsurushita, G. Liu, and E. L. Berg, "*IFN-gamma* inhibits activation-induced expression of E- and P-selectin on endothelial cells," *The Journal of Immunology*, vol. 161, no. 5, pp. 2457–2464, 1998.

[32] Y. Hu, X. Hu, L. Boumsell, and L. B. Ivashkiv, "IFN-γ and STAT1 arrest monocyte migration and modulate RAC/CDC42 pathways," *The Journal of Immunology*, vol. 180, no. 12, pp. 8057–8065, 2008.

[33] M. de La Paz Sánchez-Martínez, F. Blanco-Favela, M. D. Mora-Ruiz, A. K. Chávez-Rueda, M. Bernabe-García, and L. Chávez-Sánchez, "IL-17-differentiated macrophages secrete pro-inflammatory cytokines in response to oxidized low-density lipoprotein," *Lipids in Health and Disease*, vol. 16, no. 1, p. 196, 2017.

[34] R. P. Donnelly, M. J. Fenton, D. S. Finbloom, and T. L. Gerrard, "Differential regulation of IL-1 production in human monocytes by IFN-gamma and IL-4," *The Journal of Immunology*, vol. 145, no. 2, pp. 569–575, 1990.

[35] Q. Li, J. Li, J. Tian et al., "IL-17 and IFN-γ production in peripheral blood following BCG vaccination and Mycobacterium tuberculosis infection in human," *European Review for Medical and Pharmacological Sciences*, vol. 16, no. 14, pp. 2029–2036, 2012.

[36] Q. Zhao, X. Xiao, Y. Wu et al., "Interleukin-17-educated monocytes suppress cytotoxic T-cell function through B7-H1 in hepatocellular carcinoma patients," *European Journal of Immunology*, vol. 41, no. 8, pp. 2314–2322, 2011.

Hindawi
Journal of Immunology Research
Volume 2020, Article ID 7084268, 10 pages
https://doi.org/10.1155/2020/7084268

Research Article

High CXCR3 on Leukemic Cells Distinguishes *IgHV*^{mut} from *IgHV*^{unmut} in Chronic Lymphocytic Leukemia: Evidence from CD5^{high} and CD5^{low} Clones

Gayane Manukyan,[1,2] **Tomas Papajik**,[3] **Zuzana Mikulkova**,[1] **Renata Urbanova**,[3] **Veronika Smotkova Kraiczova**,[1] **Jakub Savara**,[4] **Milos Kudelka**,[4] **Peter Turcsanyi**,[3] **and Eva Kriegova**[1]

[1]*Department of Immunology, Faculty of Medicine and Dentistry, Palacký University Olomouc and University Hospital, Olomouc, Czech Republic*
[2]*Laboratory of Molecular and Cellular Immunology, Institute of Molecular Biology NAS RA, Yerevan, Armenia*
[3]*Department of Hemato-Oncology, Faculty of Medicine and Dentistry, Palacký University and University Hospital, Olomouc, Czech Republic*
[4]*Department of Computer Science, Faculty of Electrical Engineering and Computer Science, VSB-Technical University of Ostrava, Czech Republic*

Correspondence should be addressed to Eva Kriegova; eva.kriegova@email.cz

Received 20 April 2020; Accepted 21 May 2020; Published 20 June 2020

Guest Editor: Margarete D. Bagatini

Despite the shared pattern of surface antigens, neoplastic cells in chronic lymphocytic leukemia (CLL) are highly heterogeneous in CD5 expression, a marker linked to a proliferative pool of neoplastic cells. To further characterize CD5^{high} and CD5^{low} neoplastic cells, we assessed the chemokine receptors (CCR5, CCR7, CCR10, CXCR3, CXCR4, CXCR5) and adhesion molecules (CD54, CD62L, CD49d) on the CD5^{high} and CD5^{low} subpopulations, defined by CD5/CD19 coexpression, in peripheral blood of CLL patients ($n = 60$) subgrouped according to the *IgHV* mutational status (*IgHV*^{mut}, $n = 24$; *IgHV*^{unmut}, $n = 36$). CD5^{high} subpopulation showed a high percentage of CXCR3 ($P < 0.001$), CCR10 ($P = 0.001$), and CD62L ($P = 0.031$) and high levels of CXCR5 ($P = 0.005$), CCR7 ($P = 0.013$) compared to CD5^{low} cells expressing high CXCR4 ($P < 0.001$). Comparing *IgHV*^{mut} and *IgHV*^{unmut} patients, high levels of CXCR3 on CD5^{high} and CD5^{low} subpopulations were detected in the *IgHV*^{mut} patients, with better discrimination in CD5^{low} subpopulation. Levels of CXCR3 on CD5^{low} subpopulation were associated with time to the next treatment, thus further confirming its prognostic value. Taken together, our analysis revealed higher CXCR3 expression on both CD5^{high} and CD5^{low} neoplastic cells in *IgHV*^{mut} with a better prognosis compared to *IgHV*^{unmut} patients. Contribution of CXCR3 to CLL pathophysiology and its suitability for prognostication and therapeutic exploitation deserves future investigations.

1. Introduction

Chronic lymphocytic leukemia (CLL) is a lymphoproliferative malignancy of clonally expanded heterogeneous pool of neoplastic B cells with aberrant expression of CD5 [1, 2], which are highly variably distributed between bone marrow, lymphoid organs, and peripheral blood. There is a growing body of evidence that proliferation of neoplastic cells plays a critical role in CLL pathogenesis [3–5], with the highest degree of proliferation being observed in the lymph nodes [6].

CD5, a marker normally present on T cells, acts as a repressor of B-cell receptor (BCR) signalling in CLL [7]. Proliferating, migrating CLL cells have been shown to preferentially express high levels of CD5, while the low levels of CD5 are associated with resting, circulating cells [8]. The overlapping BCR repertoires between CD5^{high} and CD5^{low} cells suggest a dynamic relationship of these two B-CLL cell

subpopulations [2]. The inversed expression of CD5 and CXCR4 was used for the identification of fractions enriched in recently born/divided and older/quiescent CLL cells [8, 9]. It has been shown that $CXCR4^{dim}CD5^{bright}$ "proliferative" cells overexpress more "cell division" genes, while $CXCR4^{bright}CD5^{dim}$ "resting" cells express higher levels of "antiproliferative" genes, suggesting that the last subset could be a distinct self-renewing one from which all clonal members derive [8, 9].

Given the dynamic variability and heterogeneity of CD5 expression and its link to the proliferative pool of neoplastic cells, we aimed to further characterize the chemokine and adhesion molecule profile of $CD5^{high}$ and $CD5^{low}$ neoplastic clones using the novel CD5/CD19 model in peripheral blood of CLL patients. Being important for lymphocyte migration, we evaluated the expression of molecules linked to adhesion and extravasation (CD54, CD62L, CD49d), migration into lymph nodes (CCR7, CXCR3, CXCR5), homing lymphocytes to the bone marrow (CXCR4), and lymphocyte trafficking (CCR5, CCR10) in $CD5^{high}$ and $CD5^{low}$ neoplastic clones. Moreover, the differential expression pattern of chemokines and adhesion molecules on $CD5^{high}$ and $CD5^{low}$ clones was for the first time studied in two biologically and clinically distinct CLL subtypes defined by the abundance of somatic hypermutations affecting the Ig variable heavy-chain locus (*IgHV*), which markedly differ in their prognosis and response to the chemoimmunotherapy [10–12].

2. Materials and Methods

2.1. Patients. The patient cohort consisted of 60 patients with CLL, all diagnosed according to the IWCLL guidelines [13]. Patient subgroups were formed based on *IgHV* mutational status ($IgHV^{mut}$, $n = 24$; $IgHV^{unmut}$, $n = 36$). Clinical characteristics of CLL patients are shown in Table 1. All patients provided written informed consent for the use of peripheral blood for research purposes in accordance with the Declaration of Helsinki. The study was approved by the ethics committee of University Hospital and Palacký University Olomouc.

2.2. Flow Cytometry Analysis of Chemokine Receptors and Adhesion Molecules. Cells in whole blood were stained with optimal concentrations of monoclonal antibody combinations directed against the following surface antigens: CD45-PerCP/Cy5.5, CD5-PE, CD19-APC/Cy7, CD54-FITC, CD62L-APC, CD49d-PE/Cy7, CD183-FITC (CXCR3), CD184-APC (CXCR4), CD185-FITC (CXCR5), CD197-PE/Cy7 (CCR7), CD195-PE/Cy7 (CCR5), CCR10-APC (all BioLegend), as reported previously [14, 15]. Isotype-matched antibodies were used as negative controls. The analysis was performed on BD FACSCanto II (Becton Dickinson). Data acquisition was performed using BD FACSDiva software (Becton Dickinson). Flow cytometry data were analysed using the FlowJo vX0.7 software (Tree Star, Inc, San Carlos, CA). In all experiments, a minimum of 10,000 events was counted. Results are expressed as the percentage and median fluorescence intensity (MFI).

2.3. Identification of $CD5^{high}$ and $CD5^{low}$ Subpopulations. Coexpression of CD5 and CD19, surface molecules essential for phenotypic characteristic of CLL cells, was used to discriminate between $CD5^{high}$ and $CD5^{low}$ subsets of CLL cells. Gating strategy for detection of $CD5^{high}$ and $CD5^{low}$ subpopulations and representative examples of CXCR3 and CXCR4 expression in $IgHV^{mut}$ and $IgHV^{unmut}$ patients are shown in Figure 1.

2.4. Chemotaxis Assay. Peripheral blood mononuclear cells (PBMC) were isolated using a Ficoll density gradient centrifugation; only samples containing more than 70% CLL cells in PBMC were chosen for the assay. Transmigration of CLL cells was assessed using polycarbonate Transwell inserts with 5-μm pore size (Corning Costar). Briefly, the cells at 1×10 exp 6/mL were applied to the upper chamber in RPMI-1640 containing 1% bovine serum albumin (BSA) in the presence or absence of CXCL11 (BioLegend). Filters were transferred into the lower wells containing RPMI-1640 with 1% BSA in the presence or absence of CXCL12 (BioLegend). After 3 hours at 37°C in 5% CO_2, cells that migrated into the lower chambers were counted and analysed for CXCR3 and CXCR4 expression on BD FACSCanto II.

2.5. Statistical and Data Mining Analyses. Statistical analyses (Mann-Whitney ***U***-test, paired Wilcoxon nonparametric test, Kruskal-Wallis test, 95% confidence intervals (CI), receiver operating characteristic (ROC) curves, the Kaplan-Meier curve, Spearman correlation analysis) were performed using the ***R*** statistical software package (http://www.r-project.org/). The multivariate patient similarity networks (PSNs) based on the nearest neighbour analysis [16, 17] were applied for the visualization of patient similarities of chemokine profiles. Correlation networks using LRNet algorithm [16] and Spearman's rank correlation coefficient were constructed and visualized to investigate the relationships between expression of individual molecules on CLL cells [18]. ***P*** values <0.05 were considered significant.

3. Results

3.1. CD5/CD19 Markers as Identifiers of $CD5^{high}$ and $CD5^{low}$ Cells. First, we identified $CD5^{high}$ and $CD5^{low}$ cells based on the CD5/CD19 model and compared it with the reported $CD5^{low}/CXCR4^{high}$ model [8, 9]. The $CD5^{high}$ cells in the CD5/CD19 model corresponded to those in the $CD5^{high}/CXCR4^{low}$ model, and similarly $CD5^{low}$ cells corresponded to those in the $CD5^{low}/CXCR4^{high}$ one (Figure S1A). High interindividual variability in the proportion of both closely related subpopulations of $CD5^{high}$ and $CD5^{low}$ cells was observed, irrespective of *IgHV* mutational status and other clinical characteristics (Figure S1B).

3.2. Differential Expression of Chemokine Receptors and Adhesion Molecules on $CD5^{high}$ and $CD5^{low}$ CLL Cells. The expression of CD54, CD62L, CD49d, CCR5, CCR7, CCR10, CXCR3, CXCR4, and CXCR5 was evaluated on $CD5^{high}$ and $CD5^{low}$ subpopulations (Table S1).

When analysing levels of studied markers (MFI) in $CD5^{high}$ and $CD5^{low}$ subpopulations, the $CD5^{high}$ cells

Table 1: Patient demographic and clinical characteristics.

Parameter	CLL ($n = 60$)
Age, years, median (min-max)	67 (50-86)
Gender (male/female)	35/25
Binet stage (A/B/C)	26/23/11
IgHV gene mutational status∗ (mutated/unmutated)	24/36
Genetics	
11q-/17p-	13/6
N/O	6/46
Not determined	2
Follow-up time months (mean, min–max)	53 (0-160)
Treatment history (yes/no)	29/31
Time of last treatment in treated patients (in respect to the sampling time) months (mean, min–max)	23 (1-61)
Time to the next treatment (in respect to the sampling time) months (mean, min–max)	29 (0-49)
CLL cells in peripheral blood	
Percentage, mean (95% CI)	69.3 (62.3-76.3)
Absolute number ($\times 10^9$/L), mean (95% CI)	49.1 (32.3-65.9)

∗ *IgHV* mutational status was defined as follows: $IgHV^{unmut}$ with a cut-off of 2% deviation or >98% sequence identity to germline in the *IgHV* sequence (13). 11q- and 17p-: any FISH or karyotypic abnormality involving 11q or 17p; N: no detectable cytogenetic aberration by FISH; O: other cytogenetic abnormality (excluding 11q- or 17p-).

expressed higher levels of CXCR5 ($P = 0.005$) and CCR7 ($P = 0.013$) and lower levels of CXCR4 receptor ($P < 0.001$) than the population of $CD5^{low}$ cells. Besides, more $CD5^{high}$ cells were positive for CXCR3 ($P < 0.001$), CCR5 ($P = 0.012$), CCR10 ($P = 0.007$), and CD62L ($P = 0.047$) than $CD5^{low}$ cells (Figure 2, Table S1).

3.3. Characterization of $CD5^{high}$ and $CD5^{low}$ CLL Cells in Patient Subgroups according to the IgHV Mutational Status. To characterize the CLL cells and their subpopulations in patient subgroups according to the *IgHV* mutational status, we compared the expression of studied markers on CLL cells as a whole and separately on $CD5^{high}$ and $CD5^{low}$ cells in CLL patients with $IgHV^{mut}$ and $IgHV^{unmut}$ status (Figure 3, Table S2, Table S3).

Of the studied markers, patients with $IgHV^{mut}$ had a higher percentage of cells expressing CXCR3 ($P = 0.003$, Figure 3(a)) and CD62L ($P = 0.003$) in the whole population of CLL cells compared to those with $IgHV^{unmut}$ status. When $IgHV^{mut}$ and $IgHV^{unmut}$ patients were evaluated separately, in both groups, a higher proportion of CLL cells positive on CXCR3 (in both $P < 0.001$) and lower expression of CXCR4 (in both $P < 0.001$) was observed on $CD5^{high}$ subpopulation in comparison with $CD5^{low}$ cells (Figure 3(b)). Similarly, when $CD5^{high}$ and $CD5^{low}$ cell populations were evaluated separately, the $IgHV^{mut}$ group exhibited higher percentages of CXCR3 (in both $P < 0.001$), CD62L (in both $P = 0.003$) positive cells, as well as higher expression of CXCR5 ($P < 0.001$ and $P = 0.011$, respectively) in comparison with $IgHV^{unmut}$ (Table S2, Table S3).

To exclude possible influence of the treatment on the studied parameters, we performed subanalysis on a cohort of untreated patients subdivided according to the *IgHV* mutational status, and we confirmed the differences for studied markers observed in the whole patient cohort (Figure S2A). Moreover, we did not observe significant differences in studied markers between $IgHV^{unmut}$ patients untreated and those with treatment history (Figure S2B).

3.4. Correlation of CXCR3, CXCR4, and CXCR5 with CD5 Expression on CLL Cells. On CLL cells, CD5 expression (MFI) positively correlated with the percentages and MFI of CXCR3 ($rs = 0.54$, $P < 0.001$ and $rs = 0.54$, $P < 0.001$) and MFI of CXCR5 ($rs = 0.34$, $P = 0.010$). There was a trend towards inverse correlation between CD5 and CXCR4 expression on the whole CLL subpopulation ($rs = -0.23$, P=0.086) (Figure 4(a)). Further information about correlations of CXCR3, CXCR4, and CXCR5 expression on $CD5^{high}$ and $CD5^{low}$ subpopulations is provided in the Supplementary file.

Regarding the relationship between CXCR3 and CXCR4, correlation analysis revealed a negative correlation between percentages as well as expression (MFI) of CXCR3 with CXCR4 on CLL cells ($rs = -0.35$, $P = 0.009$ and $rs = -0.38$, $P = 0.006$, respectively) (Figure S3). Network correlation analysis among studied chemokines and CD5 further confirmed a relationship and importance of CD5-CXCR3-CXCR5 axis on CLL cells (Figure 4(b)).

3.5. Migration Rate of CLL Cells in the Presence of CXCL11. To analyse the cooperative interplay between CXCR3 and CXCR4, we analysed the migratory ability of CXCL11-treated and untreated CLL cells towards chemokine CXCL12. The highest migration rates were observed for the CXCL11-untreated cells that migrated towards CXCL12 ($P = 0.010$) (Figure 5). When CLL cells were treated with CXCL11, their spontaneous migration as well as migration rate toward CXCL12 decreased (Figure 5).

3.6. CXCR3 On CLL Cells as a Prognostic Marker. To study the prognostic value of studied markers, we constructed ROC curves for CLL patients with favourable ($IgHV^{mut}$) and unfavourable ($IgHV^{unmut}$) prognostic groups. Among the studied markers, CXCR3 had the highest sensitivity and specificity on both $CD5^{high}$ and $CD5^{low}$ populations. Cut-off values for CXCR3 were 65.2%, 24.0%, and 54.8% for $CD5^{high}$, $CD5^{low}$, and CLL cells as a whole, respectively. Correspondingly, AUC reached values of 0.810, 0.859, and 0.763 on $CD5^{high}$, $CD5^{low}$, and CLL cells as a whole (Figure 6(a)). Kaplan-Meier curves using CXCR3 cut-off values showed the prognostic value of CXCR3 on $CD5^{low}$ ($P = 0.030$) on time to the next treatment, calculated from the sampling time (Figure 6(b)). For the analysis, only patients with sufficient follow-up time were included.

3.7. Multivariate Patient Similarity Networks. To gain more insights into $CD5^{high}$ and $CD5^{low}$ subpopulations in $IgHV^{mut}$

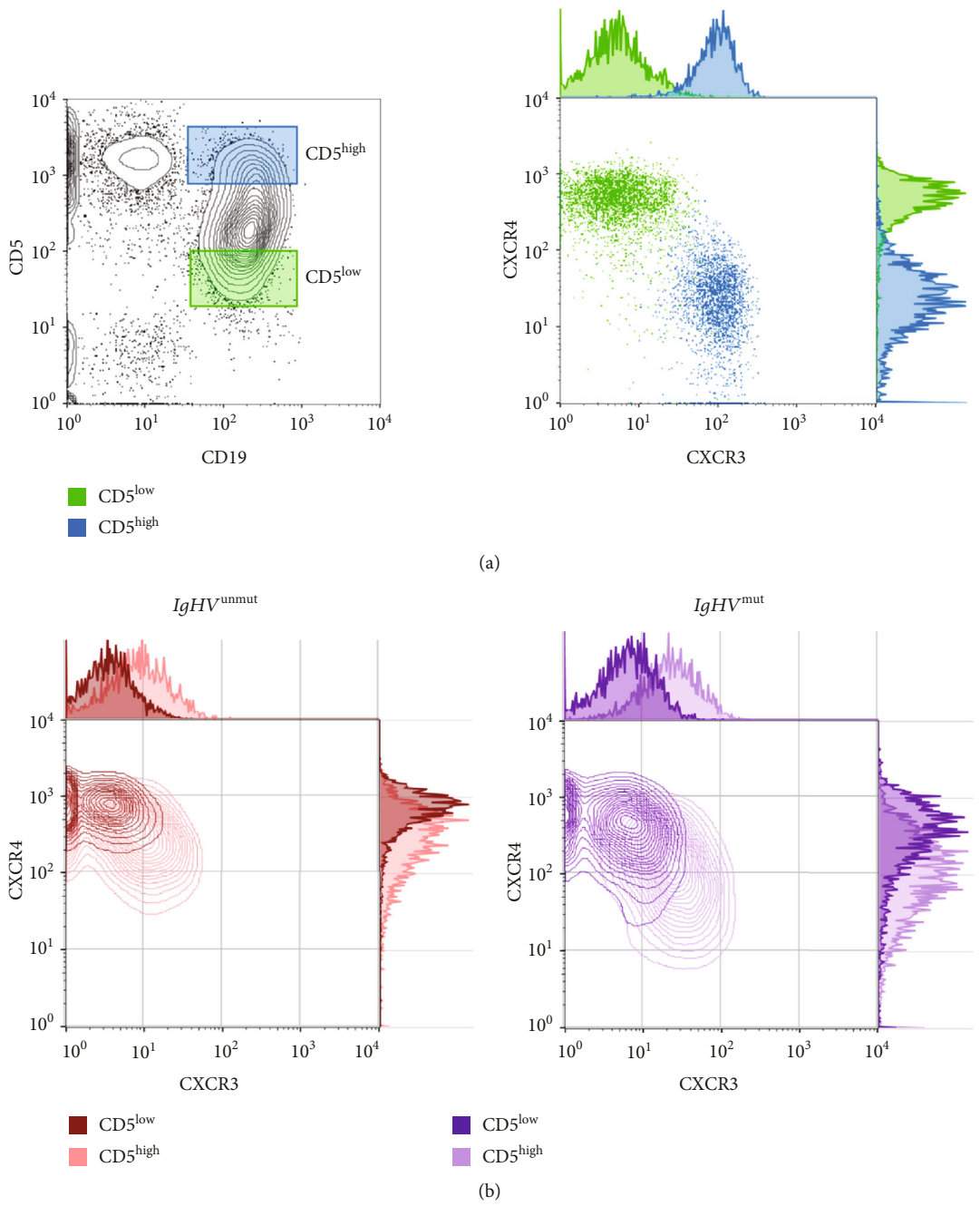

Figure 1: (a) Gating strategy for detection of $CD5^{high}$ and $CD5^{low}$ subpopulations within CD5+CD19+neoplastic cells and visualization of their CXCR3 and CXCR4 expression. (b) CXCR3 and CXCR4 expression on $CD5^{high}$ and $CD5^{low}$ subpopulations in $IgHV^{unmut}$ and $IgHV^{mut}$ patient—representative example.

and $IgHV^{unmut}$ patients, we constructed the multivariate PSNs and performed their clustering based on the CXCR3, CXCR4, CXCR5, and CCR7 expression in enrolled CLL patients. Clusters with high CXCR3 include predominantly patients with $IgHV^{mut}$ status, and vice versa clusters with low CXCR3 include predominantly patients with $IgHV^{unmut}$ status. CXCR3 and other selected markers on $CD5^{low}$ subpopulations better discriminate between patients with $IgHV^{mut}$ and $IgHV^{unmut}$ subgroups than markers on $CD5^{high}$ (Figure 7). For clustering and distribution of chemokine expression in particular clusters and corresponding expression patterns, see the Supplementary file (Figure S4).

4. Discussion

There is a growing body of evidence that CLL neoplastic cells are composed of subpopulations of cells that differ in their biological function [1, 2, 8, 19, 20]. Our study revealed differences in the expression of molecules linked to adhesion, extravasation, migration, and homing, on $CD5^{high}$

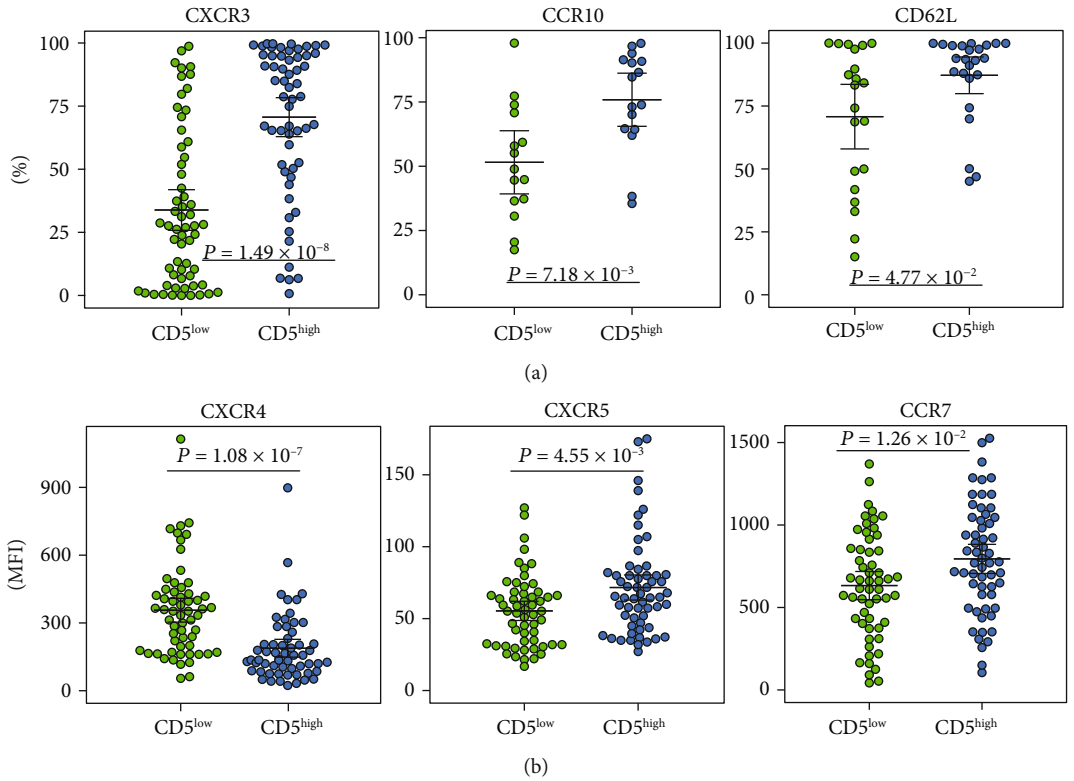

Figure 2: Distribution of (a) percentages of positive cells for CXCR3, CCR10, and CD62L and (b) expression (MFI) of CXCR4, CXCR5, and CCR7 on $CD5^{high}$ and $CD5^{low}$ subpopulations in patients with CLL. Group means are indicated by horizontal bars, error bars indicate 95% CI.

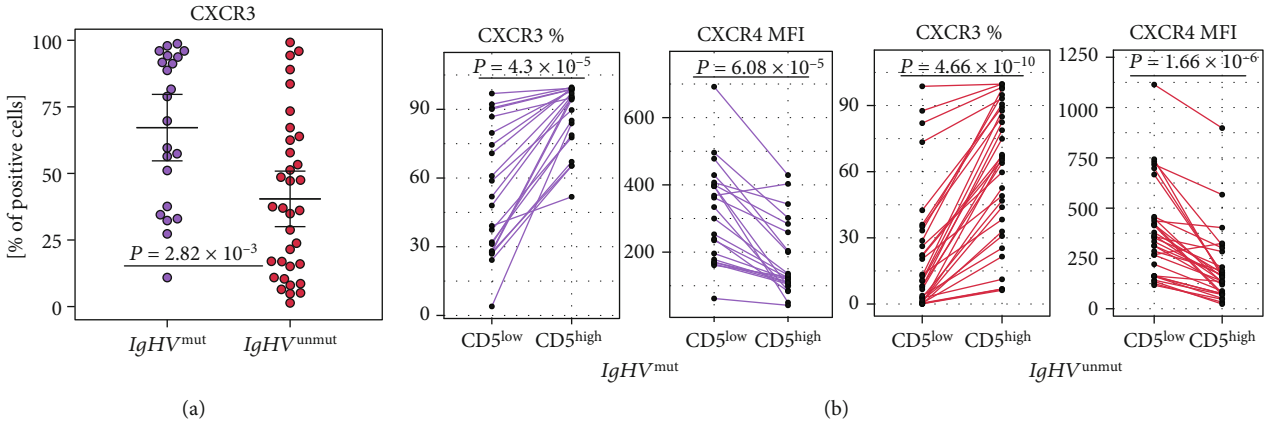

Figure 3: Distribution of CXCR3 and CXCR4 chemokines in $IgHV^{mut}$ (violet) and $IgHV^{unmut}$ (red) patients in (a) CLL cells as a whole, (b) $CD5^{high}$, and $CD5^{low}$ subpopulations in a paired analysis. The lines connect the values on $CD5^{high}$ and $CD5^{low}$ subpopulations in the same patient.

and $CD5^{low}$ CLL populations, defined using the CD5/CD19 coexpression model, in the patient subgroups according to the *IgHV* mutational status.

In our CLL cohort, we observed high expression levels of CXCR3, CXCR5, CCR10, and CD62L on $CD5^{high}$ cells and high CXCR4 on $CD5^{low}$ cells, which is in line with a previous study [8]. Interestingly, our data showed that CXCR3 better discriminates both $CD5^{high}$ and $CD5^{low}$ cell populations than CXCR4, a key chemokine receptor involved in migration of CLL cells to the supportive lymphoid tissues [1, 21, 22]. Moreover, our study revealed differences in expression pattern between patient subgroups according to the *IgHV* mutational status, a key prognostic predictor of overall survival and treatment-response duration [10–12]. The most prominent were the differences between the percentages of CXCR3 on $CD5^{low}$ cell subpopulation between $IgHV^{mut}$ and $IgHV^{unmut}$ statuses. Moreover, our results revealed that CXCR3 on $CD5^{low}$ cells has the best prognostic utility in discriminating

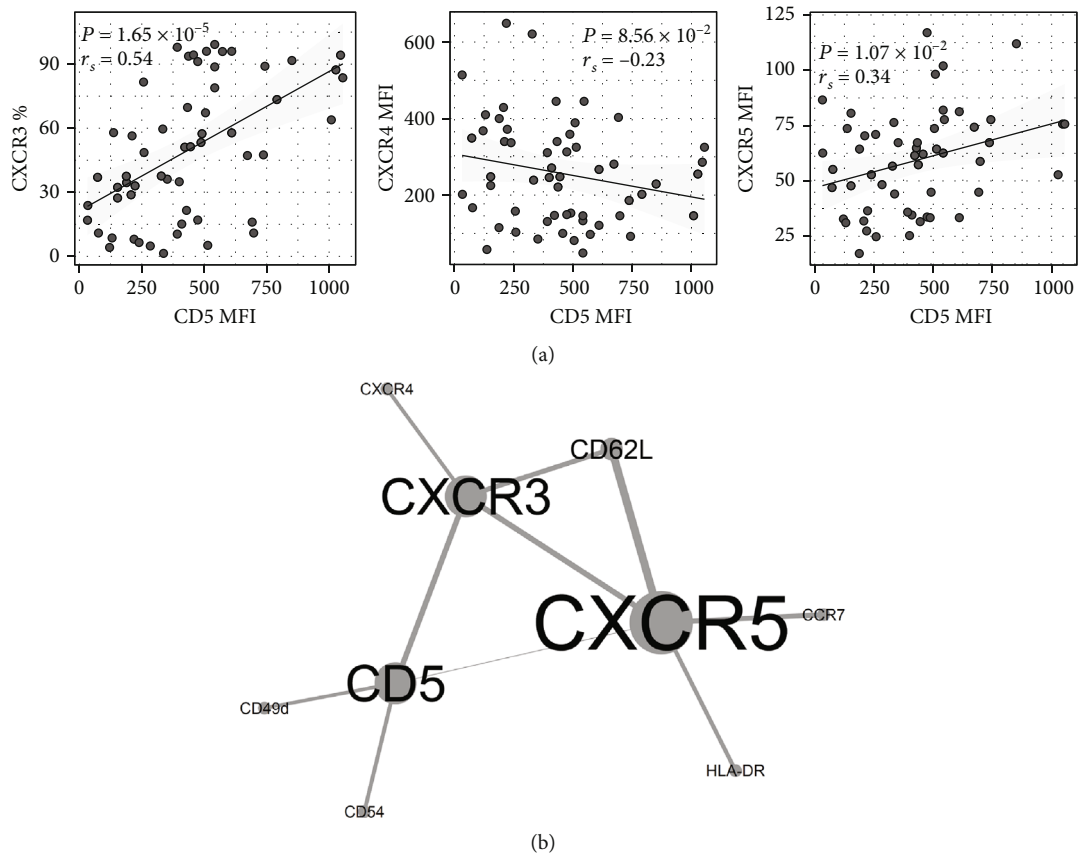

Figure 4: Correlation of CD5 expression with (a) percentages of CXCR3, levels (MFI) of CXCR4 and CXCR5 on CLL cells, and (b) studied chemokines on CLL cells assessed by the correlation network analysis.

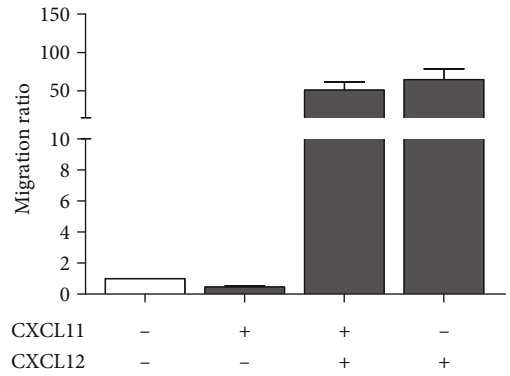

Figure 5: Cooperative effect of CXCL11 and CXCL12 on the migratory ability of CLL cells. CLL cells ($n = 6$), with/without pretreatment with 200 ng/mL CXCL11, were added to the upper chamber of Transwell inserts. 200 ng/mL CXCL12 was added to the medium in the bottom chamber, and migrated cells were counted after 3 hours by flow cytometry. Migration index was calculated as the ratio of cells that transmigrated through the insert in the chemokine-treated cells vs untreated ones (CXCR11-/CXCR12-).

patients with $IgHV^{mut}$ and $IgHV^{unmut}$ status, and correspondingly the patients with favourable or poor prognosis. This observation contributes to further characterization of $IgHV^{mut}$ and $IgHV^{unmut}$ mutation statuses, known to differ in gene expression [23], methylation status [24], and the mutational landscape [25].

Recently, CXCR3 has been found as a marker of independent prognostic significance in CLL [26]. High CXCR3 expression and CXCR3/CXCR4 ratio delineated patients with a significantly better clinical course, as opposed to patients with low CXCR3 and high CXCR4 expression [26, 27]. To date, there is no clear understanding of how CXCR3 influences the pathogenesis of CLL. A formation of CXCR3-CXCR4 heteromers and a negative binding cooperativity between CXCR3 and CXCR4 at the cell surface was reported on CLL [26] and HEK293T [28] cells. Importantly, the CXCR3-CXCR4 heteromerization has been shown to alter the ligand-binding kinetics: CXCR3 and CXCR4 agonists have been proved to inhibit each other's equilibrium binding on membranes and specifically accelerate dissociation of CXCL12 from CXCR4 [28]. The negative impact of CXCR3 stimulation by its ligands CXCL9, CXCL10, and CXCL11 was shown to be highly specific for CXCR4-induced migration and resulted in reduced CXCR4-CXCL12 chemotaxis [26], as we also confirmed by the migration experiment in our patients. Given the critical role of CXCR4-CXCL12 axis in migration of CLL cells between blood and supportive lymphoid tissues in CLL, the formation of CXCR3-CXCR4 heterodimers on CLL cells and its consequences may

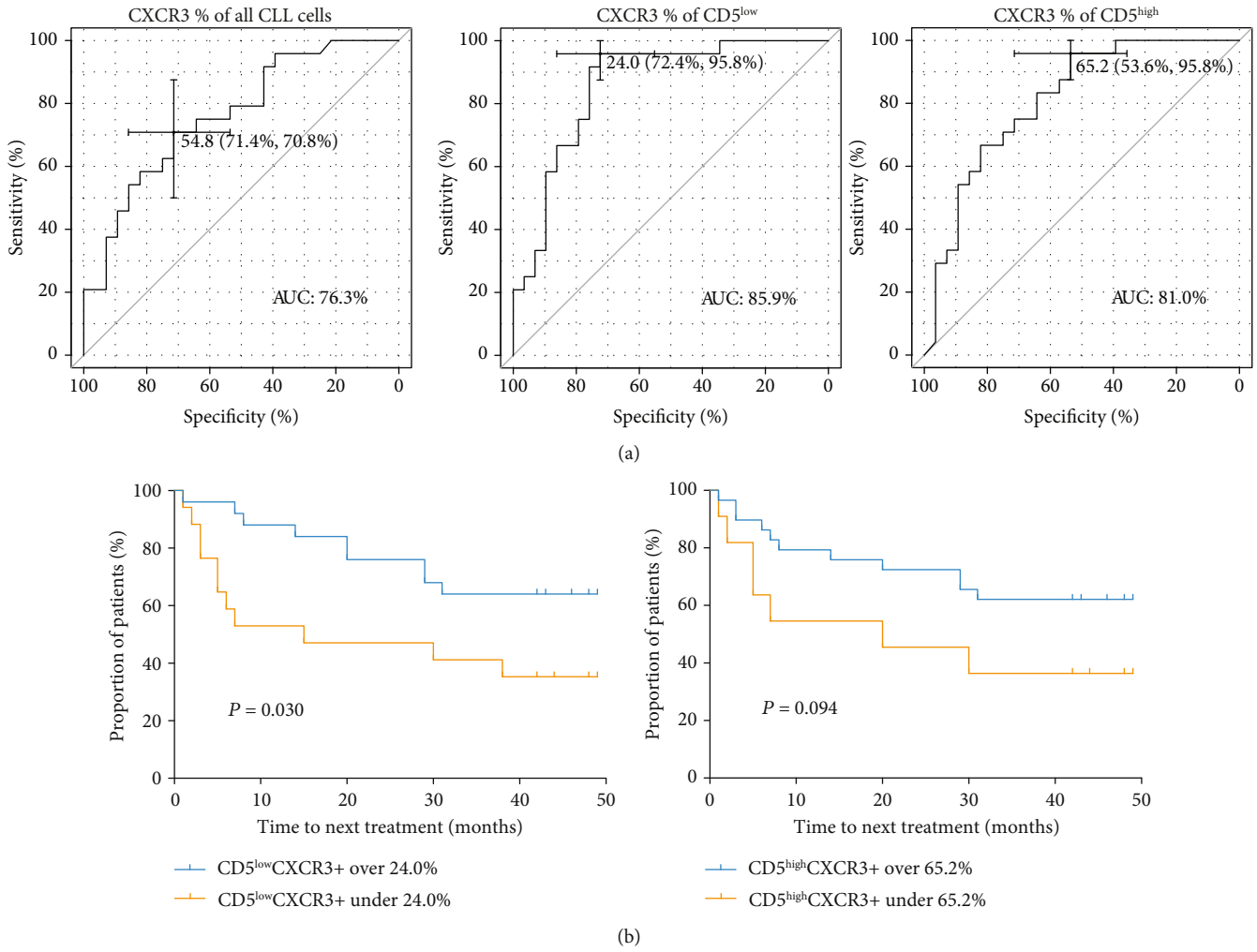

FIGURE 6: (a) Receiver operating characteristic (ROC) curves created for the percentage of CXCR3 positive all CLL cells, $CD5^{low}$ and $CD5^{high}$ cells, respectively, in patients with $IgHV^{mut}$ and $IgHV^{unmut}$ status. AUC: area under ROC curve. (b) Kaplan-Meier curves of time to next treatment in CLL patients according to the cut-off values of the percentage of CXCR3 on $CD5^{low}$ and $CD5^{high}$ cells.

significantly reduce the migration of CLL cells [1, 21, 22]. Since the proportion of CXCR3-CXCR4 heteromers is relative to homomers of both receptors [28], low levels of CXCR3 on CLL cells, observed in our patients with mutated *IgHV* status, might not be sufficient to abrogate migration of CLL cells driven by CXCR4. Contribution of CXCR3 to better prognosis and attenuation of CLL cell migration deserves future investigations.

Our study introduced a simple model based on CD5/CD19 coexpression for studying the CLL subpopulations. Given comparable data to a study using markers CD5/CXCR4 [8], CD5/CD19 coexpression might represent a combination of markers capable of reflecting biological differences between CLL clones, an assumption that needs to be verified in future studies. Moreover, the fact that the subpopulation of CLL cells in the CD5/CD19 model correspond to those in the CD5/CXCR4 model suggests that CD5 may play a more important pathogenic role in CLL than previously recognized. The precise function of CD5 in the interactions of immune cells remains unclear, especially on CLL cells. It was shown that this molecule negatively regulates B1 cell activation and activation-induced cell death [29, 30]. There is growing evidence of several pools of leukemia cells present in CLL, including circulating cell cycle arrested CLL cells expressing preferably low levels of CD5, and migrated activated cells that express high levels of CD5 and that are driven to proliferate via signals from the lymphoid tissue microenvironment [2, 8, 31, 32]. Despite this, CD5 positive cells were shown to have a longer lifespan than CD5 negative cells [29]. Whether CD5 contributes also to the recirculating capacity of CLL cells and their differential proliferative potential deserves further investigations. A deeper understanding of the CD5 role in CLL clones' biology may permit potentiation of current immunotherapeutic strategies.

The study has several limitations. First, we analysed a diagnostic real-world CLL cohort of patients sampled at different time points and treatment regimes. Second, our exploratory study should be followed by functional investigations on

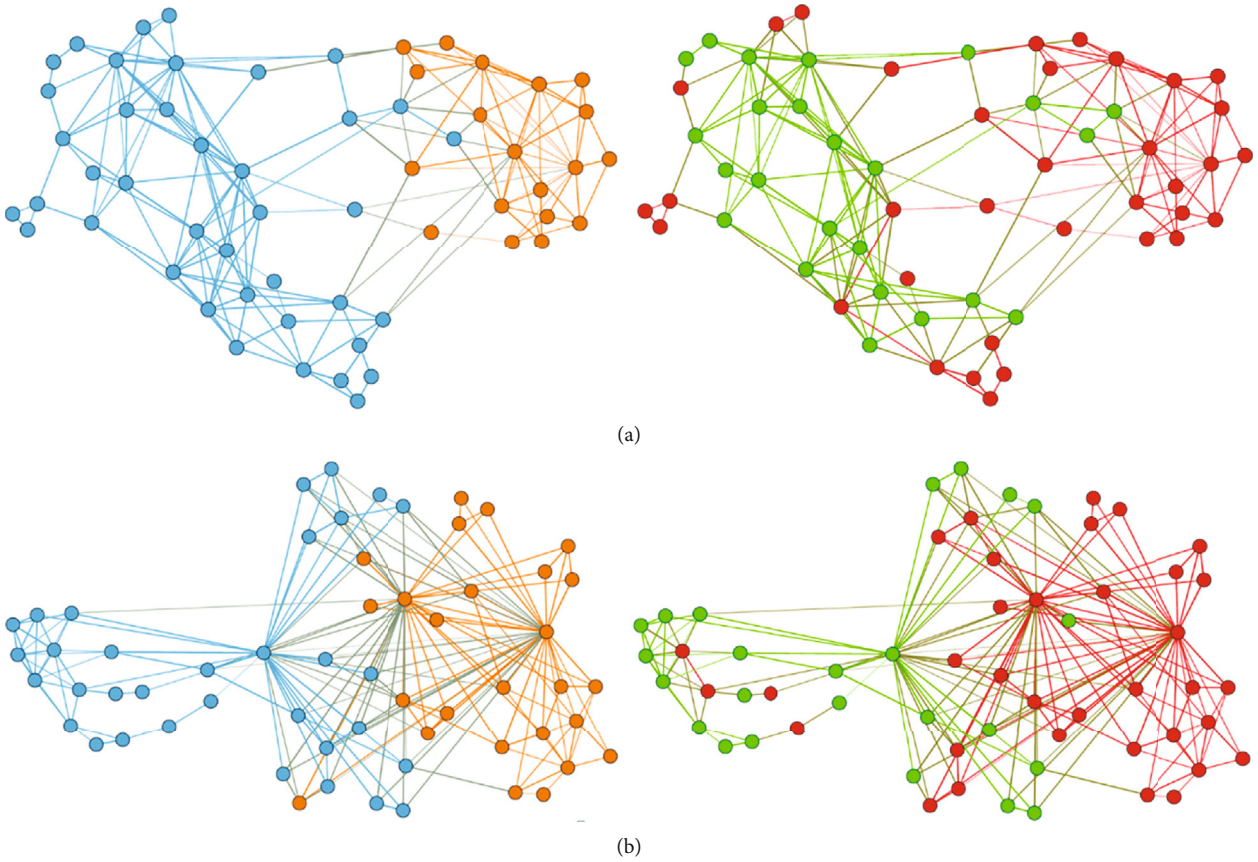

FIGURE 7: Patient similarity networks for the combination of chemokine expression (% of CXCR3, and MFI of CXCR4, CXCR5, CCR7) on (a) $CD5^{high}$ and (b) $CD5^{low}$ subpopulations in CLL patients. The nodes represent individual CLL patients, the lines connect the patients with high similarity in chemokine profiles. $IgHV^{mut}$ patients are presented in green, $IgHV^{unmut}$ patients in red. CXCR3 positive cells with cut-off <65% for $CD5^{high}$ and <24% for $CD5^{low}$, respectively, are orange, and CXCR3 positive cells with cut-off >65% for $CD5^{high}$ and >24% for $CD5^{low}$ are blue.

the role of CXCR3 on $CD5^{high}$ and $CD5^{low}$ cell populations in future studies. Despite these limitations, we believe that our novel model for distinguishing between proliferative and resting fractions of neoplastic cells and first study on characteristics of CLL subpopulations in CLL patients with different *IgHV* mutational statuses highlights the critical contribution of chemokine receptors to the disease outcome in CLL.

In summary, we present for the first time the marked differences in expression of chemokine receptor CXCR3 on $CD5^{high}$ and $CD5^{low}$ cell populations in patients with different *IgHV* mutational statuses. The wide presence of CXCR3 marker on CLL cells appears to portend a favourable prognosis, thus further supporting its potential as a prognostic marker. Understanding the pathological relevance of $CD5^{high}$ and $CD5^{low}$ cell subsets, their characteristics and phenotypes may likely broaden our understanding of CLL pathology as well as reveal novel therapeutic avenues.

Data Availability

The data used to support the findings of this study are available from the corresponding author upon request.

Conflicts of Interest

The authors declare that the research was conducted in the absence of any commercial or financial relationships that could be construed as a potential conflict of interest.

Authors' Contributions

GM and EK conceived the study, planned the experiments, interpreted the data, and wrote the manuscript. GM, ZM, and VSM performed the analysis. RU, PT, and TP collected the patient samples and clinical data. JS and MK performed the statistical and data mining analysis. ZM, TP, and MK revised the manuscript. All authors read the final version of the manuscript.

Acknowledgments

We would like to thank Martina Divoka for routine laboratory assessment of *IgHV* mutational status, Lenka Kruzova for routine cytogenetic assessment and FISH analysis, and Martin Dihel and Sarka Zehnalova for their help with data analysis and figure preparation. This work was supported

by a grant of the Ministry of Health of the Czech Republic (MZ ČR VES16-32339A), in part by MH CZ–DRO (FNOL, 00098892) and IGA_LF UP_2020_16.

Supplementary Materials

Table S1: percentage of cells positive for studied chemokine receptors and adhesion molecules and their surface expression (MFI) on $CD5^{low}$ and $CD5^{high}$ subpopulations in enrolled patients. Table S2: percentage of cells positive for studied chemokine receptors and adhesion molecules on $CD5^{low}$ and $CD5^{high}$ subpopulations in CLL patients subdivided according to the $IgHV^{unmut}$ and $IgHV^{mut}$ status. Table S3: expression (MFI) of studied chemokine receptors and adhesion molecules on $CD5^{low}$ and $CD5^{high}$ subpopulations in $IgHV^{unmut}$ and $IgHV^{mut}$ patients. Figure S1: analysis of CLL cell subpopulations. Figure S2: distribution of cells positive for CXCR3, CXCR4, and CXCR5 on $CD5^{high}$ and $CD5^{low}$ subpopulations between untreated $IgHV^{mut}$ and $IgHV^{unmut}$ CLL patients and CLL patients with $IgHV^{unmut}$ with/without treatment history. Figure S3: correlation analysis between percentages and MFI of CXCR3 and CXCR4 on CLL cells. Figure S4: patient similarity network based on levels of CXCR3, CXCR4, CRCR5, and CCR7, and distribution of chemokine expression in individual clusters. *(Supplementary materials)*

References

[1] C. Calissano, R. N. Damle, G. Hayes et al., "In vivo intraclonal and interclonal kinetic heterogeneity in B-cell chronic lymphocytic leukemia," *Blood*, vol. 114, no. 23, pp. 4832–4842, 2009.

[2] R. J. M. Bashford-Rogers, A. L. Palser, C. Hodkinson et al., "Dynamic variation of CD5 surface expression levels within individual chronic lymphocytic leukemia clones," *Experimental Hematology*, vol. 46, pp. 31–37.e10, 2017.

[3] R. N. Damle, S. Temburni, C. Calissano et al., "CD38 expression labels an activated subset within chronic lymphocytic leukemia clones enriched in proliferating B cells," *Blood*, vol. 110, no. 9, pp. 3352–3359, 2007.

[4] B. T. Messmer, D. Messmer, S. L. Allen et al., "In vivo measurements document the dynamic cellular kinetics of chronic lymphocytic leukemia B cells," *The Journal of Clinical Investigation*, vol. 115, no. 3, pp. 755–764, 2005.

[5] A. Os, S. Bürgler, A. P. Ribes et al., "Chronic lymphocytic leukemia cells are activated and proliferate in response to specific T helper cells," *Cell Reports*, vol. 4, no. 3, pp. 566–577, 2013.

[6] Y. Herishanu, P. Pérez-Galán, D. Liu et al., "The lymph node microenvironment promotes B-cell receptor signaling, NF-kappaB activation, and tumor proliferation in chronic lymphocytic leukemia," *Blood*, vol. 117, no. 2, pp. 563–574, 2011.

[7] D. R. Friedman, E. Guadeloupe, A. Volkheimer, and J. B. Weinberg, "Surface CD5 protein risk stratifies chronic lymphocytic leukemia," *Blood*, vol. 128, no. 22, p. 3212, 2016.

[8] C. Calissano, R. N. Damle, S. Marsilio et al., "Intraclonal complexity in chronic lymphocytic leukemia: fractions enriched in recently born/divided and older/quiescent cells," *Molecular Medicine*, vol. 17, no. 11-12, pp. 1374–1382, 2011.

[9] M. Pasikowska, E. Walsby, B. Apollonio et al., "Phenotype and immune function of lymph node and peripheral blood CLL cells are linked to transendothelial migration," *Blood*, vol. 128, no. 4, pp. 563–573, 2016.

[10] T. J. Hamblin, Z. Davis, A. Gardiner, D. G. Oscier, and F. K. Stevenson, "Unmutated Ig V(H) genes are associated with a more aggressive form of chronic lymphocytic leukemia," *Blood*, vol. 94, no. 6, pp. 1848–1854, 1999.

[11] J.-L. Binet, "Perspectives on the use of new diagnostic tools in the treatment of chronic lymphocytic leukemia," *Blood*, vol. 107, no. 3, pp. 859–861, 2005.

[12] K. Stamatopoulos, C. Belessi, A. Hadzidimitriou et al., "Immunoglobulin light chain repertoire in chronic lymphocytic leukemia," *Blood*, vol. 106, no. 10, pp. 3575–3583, 2005.

[13] M. Hallek, B. D. Cheson, D. Catovsky et al., "Guidelines for the diagnosis and treatment of chronic lymphocytic leukemia: a report from the International Workshop on Chronic Lymphocytic Leukemia updating the National Cancer Institute-Working Group 1996 guidelines," *Blood*, vol. 111, no. 12, pp. 5446–5456, 2008.

[14] G. Manukyan, P. Turcsanyi, Z. Mikulkova et al., "Dynamic changes in HLA-DR expression during short-term and long-term ibrutinib treatment in patients with chronic lymphocytic leukemia," *Leukemia Research*, vol. 72, pp. 113–119, 2018.

[15] E. Kriegova, G. Manukyan, Z. Mikulkova et al., "Gender-related differences observed among immune cells in synovial fluid in knee osteoarthritis," *Osteoarthritis and Cartilage*, vol. 26, no. 9, pp. 1247–1256, 2018.

[16] E. Ochodkova, S. Zehnalova, and M. Kudelka, "Graph Construction Based on Local Representativeness," in *Computing and Combinatorics. COCOON 2017*, Lecture Notes in Computer Science, Y. Cao and J. Chen, Eds., Springer, Cham, 2017.

[17] P. Turcsanyi, E. Kriegova, M. Kudelka et al., "Improving risk-stratification of patients with chronic lymphocytic leukemia using multivariate patient similarity networks," *Leukemia Research*, vol. 79, pp. 60–68, 2019.

[18] A. Petrackova, P. Horak, M. Radvansky et al., "Cross-disease innate gene signature: emerging diversity and abundance in RA comparing to SLE and SSc," *Journal of Immunology Research*, vol. 2019, 10 pages, 2019.

[19] G. Pavlasova, M. Borsky, V. Seda et al., "Ibrutinib inhibits CD20 upregulation on CLL B cells mediated by the CXCR4/SDF-1 axis," *Blood*, vol. 128, no. 12, pp. 1609–1613, 2016.

[20] G. Pavlasova, M. Borsky, V. Svobodova et al., "Rituximab primarily targets an intra-clonal BCR signaling proficient CLL subpopulation characterized by high CD20 levels," *Leukemia*, vol. 32, no. 9, pp. 2028–2031, 2018.

[21] J. A. Burger, "Chemokines and chemokine receptors in chronic lymphocytic leukemia (CLL): from understanding the basics towards therapeutic targeting," *Seminars in Cancer Biology*, vol. 20, no. 6, pp. 424–430, 2010.

[22] A. Majid, T. T. Lin, G. Best et al., "CD49d is an independent prognostic marker that is associated with CXCR4 expression in CLL," *Leukemia Research*, vol. 35, no. 6, pp. 750–756, 2011.

[23] A. Rosenwald, A. A. Alizadeh, G. Widhopf et al., "Relation of gene expression phenotype to immunoglobulin mutation genotype in B cell chronic lymphocytic leukemia," *The Journal of Experimental Medicine*, vol. 194, no. 11, pp. 1639–1648, 2001.

[24] C. C. Oakes, M. Seifert, Y. Assenov et al., "DNA methylation dynamics during B cell maturation underlie a continuum of disease phenotypes in chronic lymphocytic leukemia," *Nature Genetics*, vol. 48, no. 3, pp. 253–264, 2016.

[25] A. Burns, R. Alsolami, J. Becq et al., "Whole-genome sequencing of chronic lymphocytic leukaemia reveals distinct differences in the mutational landscape between IgHVmut and IgHVunmut subgroups," *Leukemia*, vol. 32, no. 2, pp. 332–342, 2018.

[26] S. Ganghammer, J. Gutjahr, E. Hutterer et al., "Combined CXCR3/CXCR4 measurements are of high prognostic value in chronic lymphocytic leukemia due to negative cooperativity of the receptors," *Haematologica*, vol. 101, no. 3, pp. e99–102, 2016.

[27] E. Ocana, L. Delgado-Perez, A. Campos-Caro et al., "The prognostic role of CXCR3 expression by chronic lymphocytic leukemia B cells," *Haematologica*, vol. 92, no. 3, pp. 349–356, 2007.

[28] A. O. Watts, M. M. van Lipzig, W. C. Jaeger et al., "Identification and profiling of CXCR3-CXCR4 chemokine receptor heteromer complexes," *British Journal of Pharmacology*, vol. 168, no. 7, pp. 1662–1674, 2013.

[29] H. Gary-Gouy, J. Harriague, G. Bismuth, C. Platzer, C. Schmitt, and A. H. Dalloul, "Human CD5 promotes B-cell survival through stimulation of autocrine IL-10 production," *Blood*, vol. 100, no. 13, pp. 4537–4543, 2002.

[30] K. L. Hippen, L. E. Tze, and T. W. Behrens, "CD5 maintains tolerance in anergic B cells," *The Journal of Experimental Medicine*, vol. 191, no. 5, pp. 883–890, 2000.

[31] A. F. Muggen et al., "Targeting signaling pathways in chronic lymphocytic leukemia," *Current Cancer Drug Targets*, vol. 16, no. 8, pp. 669–688, 2016.

[32] J. A. Burger and E. Montserrat, "Coming full circle: 70 years of chronic lymphocytic leukemia cell redistribution, from glucocorticoids to inhibitors of B-cell receptor signaling," *Blood*, vol. 121, no. 9, pp. 1501–1509, 2013.

Hindawi
Journal of Immunology Research
Volume 2020, Article ID 2038746, 12 pages
https://doi.org/10.1155/2020/2038746

Research Article

Th2-Immune Polarizing and Anti-Inflammatory Properties of Insulin Are Not Effective in Type 2 Diabetic Pregnancy

Adnette Fagninou,[1] **Magloire Pandoua Nekoua**,[1] **Darius Sossou**,[2] **Kabirou Moutairou**,[1] **Nadine Fievet**,[2] **and Akadiri Yessoufou**[1]

[1]*Faculty of Sciences and Technology (FAST), University of Abomey-Calavi, Institute of Applied Biomedical Sciences (ISBA), Laboratory of Cell Biology and Physiology, 01 BP 526 Cotonou, Benin*
[2]*Center for Study and Research on Malaria Associated with Pregnancy and Childhood (CERPAGE) and IRD-UMR261, Cotonou, Benin*

Correspondence should be addressed to Akadiri Yessoufou; akadiri.yessoufou@gmail.com

Received 15 March 2020; Accepted 21 May 2020; Published 15 June 2020

Guest Editor: Margarete D. Bagatini

Background. The implication of the immune system in the physiopathology of pregnancy complicated by diabetes has been reported. Here, we investigated the effects of insulin treatment on the frequencies of immune cell subpopulations as well as T cell-derived cytokines in type 2 diabetic (T2D) pregnancy compared to gestational diabetes mellitus (GDM). *Methods*. Fifteen (15) women with GDM, twenty (20) insulin-treated T2D pregnant women, and twenty-five (25) pregnant controls were selected. Immune cell subpopulation frequencies were determined in blood using flow cytometry. The proliferative capacity of T cells was performed, and serum and cell culture supernatant cytokine levels were also quantified. *Results*. The frequencies of total CD3+ and CD4+ T cells and nonclassical monocytes significantly increased in insulin-treated T2D pregnant women compared to pregnant controls. The proportions of CD4+ T cells as well as B cells were significantly higher in women with GDM than in pregnant controls. GDM was associated with high frequencies of total CD3+ and CD4+ T cells and B cell expansion, suggesting a concomitant activation of cellular and humoral immunity. Concomitantly, Th1/Th2 ratio, determined as IFN-γ/IL-4, was shifted towards Th1 phenotype in women with GDM and insulin-treated T2D pregnant women. Besides, isolated T cells elicited similar proliferative capacity in the three groups of women. Insulin-treated T2D pregnant women and women with GDM exhibited a low serum IL-10 level, without any change in the number of Treg cells. *Conclusion*. Our study showed that, despite insulin treatment, pregnant women with T2D displayed a proinflammatory status consistent with high proportions of CD3+ and CD4+ T cells, upregulation of Th1 cytokines, and low IL-10 production, suggesting a reduced immune-suppressive activity of regulatory T cells. However, GDM, although associated with proinflammatory status, has shown increased humoral immunity consistent with high proportion of CD19+ B cells. Thus, the lack of response to insulin in diabetes during pregnancy and clinical implications of these immunological parameters deserves further investigations.

1. Introduction

Several studies have gained interest into the immunopathology and physiopathology of gestational diabetes mellitus (GDM), type 1 or type 2 diabetic pregnancy [1–4]. However, few is known about the implication of immune cells in pregnancy complicated by diabetes. In a recent study, we have investigated the modulation of immunological parameters in insulin-treated type 2 diabetic patients, without pregnancy [5]. However, not much is known how insulin treatment can modulate immune status in GDM and T2D during pregnancy. Gestational diabetes mellitus (GDM) is defined as glucose intolerance and increased insulin resistance which occurs most often during the second or third trimester of pregnancy while type 2 diabetes (T2D) is characterized by defects in insulin secretion and by impaired insulin sensitivity [6, 7]. The physiopathology of GDM and T2D appears to be similar, so that GDM may reflect an early stage of T2D

occurring in the context of pregnancy [8]. GDM and T2D are known as a state of chronic systemic inflammation mediated by proinflammatory cytokines which are involved in the development of insulin resistance and in the increase of miscarriage rate during pregnancy [1, 9–12]. Thus, patients with GDM have an increased risk of developing T2D after their pregnancy [13, 14]. Moreover, T2D is currently regarded as a chronic inflammatory disease associated with proinflammatory cytokine production and immune cell activities, including B and T cell subsets as pathogenic mediators [15–17]. But so far, not much literature exists about circulating immune cell distribution in pregnant women with T2D and GDM. Nonetheless, some studies showed that GDM is not only due to metabolic disturbances during pregnancy but also by a state of low-grade systemic inflammation [18]. This dysregulation of the immune system is characterized by an altered profile of monocytes and regulatory T cells in peripheral blood and an imbalance between T helper 1 (Th1) and 2 (Th2) cells favoring proinflammatory responses [12, 19–21]. As the hyperglycemia and disrupted immunological adaptations during pregnancy are responsible for increased maternal-fetal morbidity, as well as the short- and long-term complications in mothers and offspring [1, 22, 23], improving glycemic control by insulin therapy may substantially reduce the risks of these maternal and neonatal outcomes of diabetes in pregnancy [24–26]. In fact, insulin not only prevents the deleterious effects of hyperglycemia by improving the anabolism of glucose, proteins, and lipids but also promotes a systemic anti-inflammatory response through the reduction of proinflammatory cytokines. Conversely, the increase of anti-inflammatory cytokines supports a successful pregnancy due to their immunosuppressive effects [27–30]. Moreover, many studies have shown that insulin can modulate *in vitro* the proliferation, differentiation, metabolism, and immune functions of neutrophils, monocytes, macrophages, effector, and regulatory T cells [31–33]. In a recent previous study, we have showed, in type 2 diabetes without pregnancy, that insulin treatment can modulate immunological parameters, through immune cell subpopulation and cytokines, and confer to these patients a protective Th2 phenotype [5]. However, despite some progress in understanding the immunophysiopathology of GDM and T2D during pregnancy, there still exists some controversies about the profile of immune parameters in diabetes during pregnancy. Moreover, it remains unclear whether insulin treatment can modulate the immune status of pregnant women with GDM and T2D through the pattern of immune cell subtypes and cytokines. Therefore, the present study was undertaken to investigate the effect of insulin treatment on the frequencies of leucocyte subpopulations along with the profile of T cell-derived cytokines in pregnant women with T2D in comparison with women with GDM and healthy pregnant women.

2. Material and Methods

2.1. Subjects and Diabetes Diagnosis in Pregnant Women. For first general selection of participants in this cross-sectional study, a total of one hundred and seventy-five (175) pregnant women were enrolled by specialist clinicians of the Department of Obstetrics and Gynecology of three national hospital centers in southern Benin. Based on the exclusion criteria (please see below), one hundred and fifty-three (153) pregnant women, aged from 19 to 43 years, were selected and then screened for GDM (please see below the detailed protocol). Consequently, fifteen (15) pregnant women were found as positive for GDM which represent 9.80% of total. Among women negative for GDM, twenty-five (25) age-matched and body mass index-matched pregnant women were selected and considered as the control group. Pregnant women with preexisting insulin-treated T2D were separately selected in the population of women already monitored by the clinicians at the department of obstetrics and gynecology of these hospital centers. The number of twenty (20) insulin-treated T2D pregnant women corresponds to the mean of the number of women with GDM (15) and the number of control pregnant (25) women. The size of each group, fifteen (15) women with GDM, twenty (20) pregnant women with insulin-treated T2D, and twenty-five (25) pregnant controls, was appropriate for statistics. All selected participants were then submitted to blood collection for biochemical and immunological assays.

GDM was diagnosed in pregnant women by an oral glucose tolerance test (OGTT), according to the criteria of the International Association of Diabetes and Pregnancy Study Group (IADPSG). Briefly, women between 24 and 28 weeks of gestation, after overnight fasting, were given 75 g of glucose. Subjects were declared as positive for GDM when overnight fasting plasma glucose was $\geq$92 mg/dL (5.1 mmol/L), or 1 h OGTT plasma glucose level was $\geq$180 mg/dL (10.0 mmol/L), or 2 h OGTT plasma glucose level was $\geq$153 mg/dL (8.5 mmol/L) [34–36]. Pregnant women with T2D were long-established diabetic patients (disease duration = 3.4 ± 2.1 years) diagnosed according to the criteria of the American Diabetes Association [37] and were on insulin treatment.

Exclusion criteria included clinical coronary artery disease, renal and hepatic diseases, and clinical signs of infectious disease, hepatitis B, hepatitis C, HIV, and malaria infection after blood sample tests. Subjects were included after informed and written consent. The study was conducted in accordance with the Declaration of Helsinki (1964) (as revised in Edinburgh 2000) and was approved by the Ethics Committee on Research of the Institute of Applied Biomedical Sciences of Cotonou, Benin, under the number Dec.n°100/CER/ISBA-2016.

2.2. Blood Samples. In women with GDM, blood samples were collected immediately after diagnostic of GDM, between 24 and 28 weeks of gestation, and before any treatment. In pregnant control women as well as in insulin-treated pregnant women with T2D, blood samples were collected between 24 and 28 weeks of gestation. A fasting whole blood sample was collected by venipuncture from each woman into sterile vacuum blood collection tubes (Vacutainer System, Becton Dickinson, CA, USA) containing either ethylenediaminetetraacetic acid (EDTA) or fluoride oxalate or nothing. EDTA tube was used for immune cell subtypes

phenotyping within 2 h after sampling. Glycosylated hemoglobin (HbA1c) levels were determined in the whole blood. HbA1c concentration was calculated using a percentage of total hemoglobin, according to the manufacturer's instructions (Ref. 41190, Labkit Chemelex SA, Barcelona, Spain). Plasma from blood collected in fluoride oxalate tubes was immediately used for glucose determinations by a glucose oxidase method using a glucose analyzer (Beckman Instruments). Serum was obtained by low-speed centrifugation (1000 g/20 min), distributed in aliquots and frozen at −80°C for the measurement of cytokine concentrations.

2.3. Immune Cell Phenotyping. The following monoclonal antibody combinations (mAbs) purchased from BD Pharmingen (France) were used to evaluate the frequencies of innate and adaptive immunity cells in whole blood: anti-CD3-FITC/anti-CD4-PerCP/anti-CD8-PE/anti-CD25-PE/anti-CD127-FITC/anti-FoxP3-APC for T cell staining, anti-CD19-FITC for B lymphocytes, anti-CD3-FITC/anti-CD56-APC for NK and NKT cells, anti CD45-APC/anti-CD14-FITC/CD16-PE for monocytes, and anti-CD45-APC/anti-CD16-PE for polynuclear cells, according to the manufacturer's instructions. Briefly, whole blood was stained with appropriate combination of specific mAbs for 45 min at 4°C in the dark. After erythrocyte lysing with FACS lysing solution (BD Pharmingen), cells were washed twice with FACS buffer. Regulatory T (Treg) cells were labelled by double staining. Anti-CD4-PerCP, anti-CD25-PE, and anti-CD127-FITC were used for Treg cell membrane labelling. Anti-FoxP3-APC was used for intracellular staining of FoxP3 in Treg cells after permeabilization and fixation with BD Cytoperm/Cytofix for 20 min at 4°C. Cells were then washed with Cytoperm/Wash and resuspended in 200 μL of PBS 1x. The stained cells were acquired using a FACSCanto II flow cytometer (BD Pharmingen, France) and analyzed using FlowJo version V 10.6.1. gating strategies shown in Figure 1.

2.4. PBMC Isolation and T Cell Proliferation Assay. Peripheral blood mononuclear cells (PBMCs) were isolated from peripheral blood collected in tubes containing EDTA by Ficoll-Paque™PLUS (GE Healthcare, Vélizy-Villacoublay, France) gradient centrifugation (30 min at 500×g, 20°C). Cells were then suspended in RPMI-1640 culture medium (Gibco BRL, Thermo Fischer Scientific, Villebon sur Yvette, France) supplemented with 10% of complement-inactivated fetal calf serum (Invitrogen, France), 1% of nonessential amino acids (Invitrogen, France), 50 μg/mL of penicillin and streptomycin (Invitrogen, France), and 2 mM of L-glutamine (Invitrogen, France). The concentration of viable cells was assessed by trypan blue staining. Cells were distributed in quadruplicate at a concentration of 10^5 per well in a Falcon polystyrene 96-well plate (Thermo Fisher Scientific, Illkirch-Graffenstaden, France) and were cultured either in the absence or in the presence of 5 μg/mL of PHA (Sigma Chemical Company, MO, USA) or of anti-CD3/anti-CD28 (BD Pharmingen, France) at a respective dose of 1 μg/mL and 2 μg/mL. After 6 days of culture at 37°C in a humid environment with 5% CO_2, the supernatants were collected and stored at -80°C for cytokine measurement (IFN-γ, IL-2, IL-4, and IL-10) and T cell proliferation was evaluated through cell count using the trypan blue exclusion test on microscopy [38].

2.5. In Vivo and In Vitro Cytokine Level Determinations. Cytokines were quantified in serum samples and in PBMC culture supernatants using enzyme-linked immunosorbent assay kits (BioLegend human Th1/Th2 ELISA MAX™ Deluxe, San Diego, CA, USA), according to the manufacturer's instructions. The minimum detectable concentrations were 4 pg/mL (standard ranges = 7.8 – 500 pg/mL) for IL-2 and IFN-γ and 2 pg/mL (standard ranges = 3.9 – 250 pg/mL) for IL-4 and IL-10.

2.6. Statistical Analysis. Data analyses were performed using GraphPad Prism 6.0 (GraphPad Inc., CA, USA). Values are means ± SD or medians ± IQR. The Kruskal-Wallis test, followed by Dunn's multiple comparison test, was used to analyze differences between the three groups (women with GDM, pregnant women with T2D, and healthy pregnant women). The Mann–Whitney U test was also used when appropriate. p values < 0.05 were considered to indicate statistically significant differences.

3. Results

3.1. Anthropometric and Biochemical Data of Subjects. Anthropometric and biochemical data of the participants appear in Table 1. There was no significant difference in age and gestational age between the three groups of participants. HbA1c values did not differ between the three groups of pregnant women. As compared to control pregnant women, insulin-treated T2D pregnant women showed a normal level of fasting glycemia. However, fasting glycemia was significantly higher in women with GDM than in either insulin-treated T2D pregnant women (1.23 ± 0.05 g/L *vs.* 0.89 ± 0.02 g/L, $p = 0.001$) or pregnant controls (1.23 ± 0.05 g/L *vs.* 0.80 ± 0.03 g/L, $p = 0.001$) (Table 1). The duration of disease was 3.4 ± 2.1 years in insulin-treated T2D pregnant women (Table 1).

3.2. Immune Cell Frequencies in GDM and Insulin-Treated T2D. The frequencies of total CD3+ and CD4+ T lymphocytes were significantly higher in insulin-treated pregnant women with T2D compared to pregnant controls ($p = 0.0008$ and $p = 0.019$, respectively) (Figures 2(a) and 2(b)). The proportions of CD4+ T cells as well as B cells were significantly higher in women with GDM than in pregnant controls ($p = 0.043$ and $p = 0.017$, respectively) (Figures 2(b) and 2(f)). The frequencies of CD8+ T cells, effector T cells, and regulatory T cells did not significantly change between the three groups (Figures 2(c)–2(e)). Besides, the frequencies of NK cells, NKT cells, intermediate monocytes, and polynuclear neutrophils did not differ between the three groups (Figures 3(a)–3(c) and 3(e)). In contrast, the frequency of classical monocytes was significantly lower in women with GDM than in pregnant controls ($p = 0.022$) (Figure 3(d)) and nonclassical monocytes were increased in insulin-treated pregnant women with T2D compared to those in pregnant controls ($p = 0.011$) (Figure 3(f)).

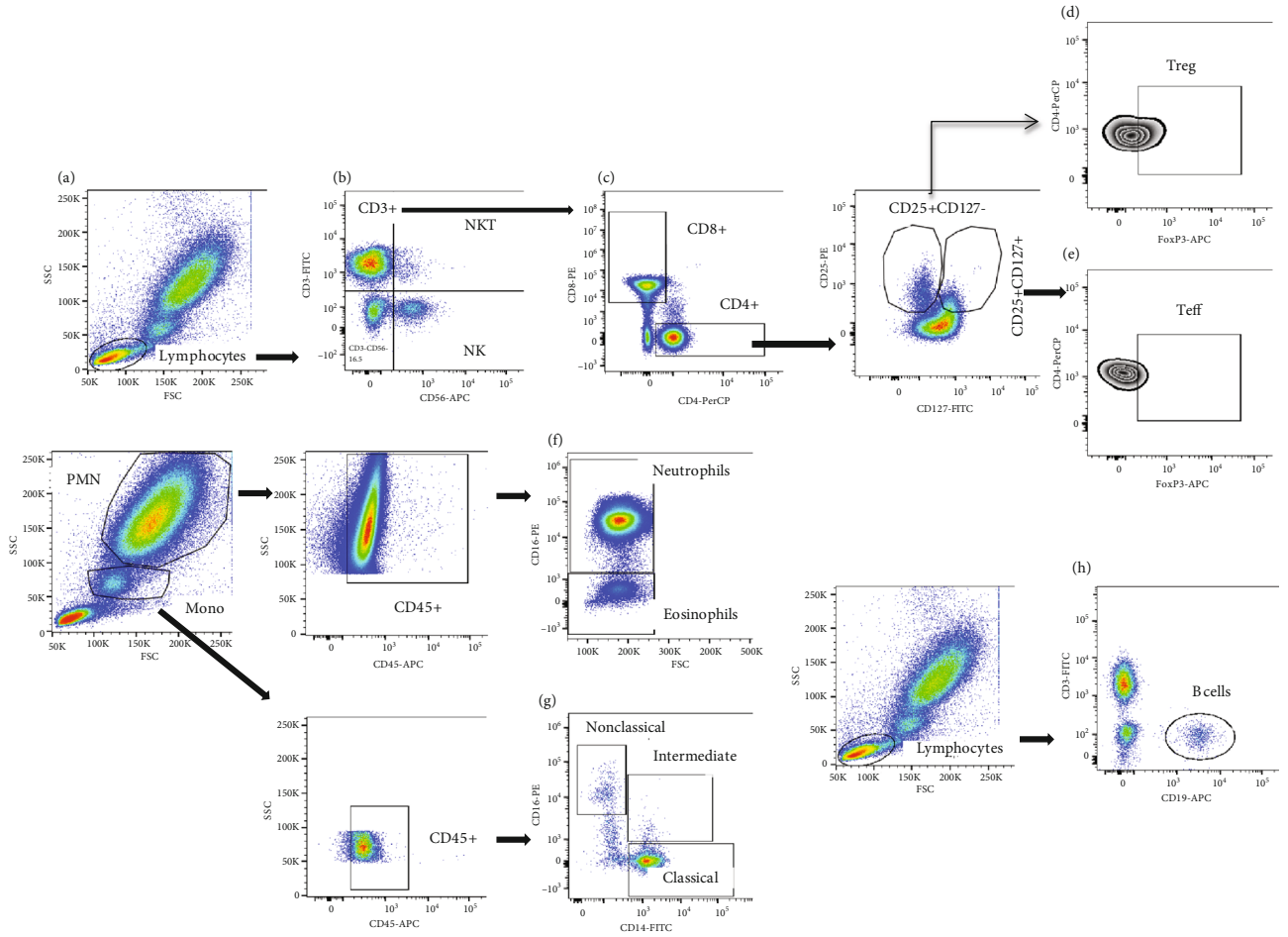

Figure 1: Cytometry-based gating strategies. Total lymphocytes (a) were gated to identify NK cells (CD3-CD56+) and NKT cells (CD3 +CD56+) (b). CD4+ and CD8+ cells were gated from CD3 T cells (c). Regulatory T cells (d) and effector T cells (e) were, respectively, gated from CD4+CD25+CD127- and CD4+CD25+CD127+ cells. Neutrophil and eosinophil cells were identified based on CD16 from CD45+ cells in polymorphonuclear (PMN) cells (f). The nonclassical (CD16++CD14+), intermediate (CD14++CD16+), and classical (CD14++CD16-) monocytes were gated from CD45+ in total monocyte region (g). Total B cells were gated from lymphocytes (h).

Table 1: Anthropometric and biochemical data of subjects.

	Pregnant controls $n = 25$	Women with GDM $n = 15$	Insulin-treated T2D pregnant women $n = 20$
Age of subjects			
Mean	29.19 ± 3.94	30.6 ± 3.04	33 ± 3.38
Minimum-maximum	25-39	26-37	29-38
Gestational age (weeks)	28-32	28-35	28-36
Fasting glucose (g/L)	0.80 ± 0.03	$1.23 \pm 0.05^{\alpha\beta}$	0.89 ± 0.02
HbA1c (%)	5.62 ± 0.27	6.58 ± 0.53	5.90 ± 0.1
Duration of disease (years)	—	—	3.4 ± 2.1

HbA1c: glycosylated hemoglobin. Values are means ± SEM. $n = 15$ women with GDM, $n = 20$ insulin-treated T2D pregnant women, and $n = 25$ pregnant controls. $^{\alpha}p < 0.001$ indicates significant difference between pregnant controls and women with GDM. $^{\beta}p < 0.001$ indicates significant difference between women with GDM and insulin-treated T2D pregnant women.

3.3. Proliferative Capacity of T Cells in GDM and Insulin-Treated T2D. Under anti-CD3/anti-CD28 and PHA stimulation, the proliferative abilities of T cells were similar between the three groups, women with GDM ($p = 0.035$ and $p = 0.04$), insulin-treated T2D pregnant women ($p = 0.028$ and $p = 0.012$), and pregnant control women ($p = 0.001$ and $p = 0.001$), as compared to unstimulated cells (Figure 4). However, it is interesting to note that the mitogens (antiCD3/CD28

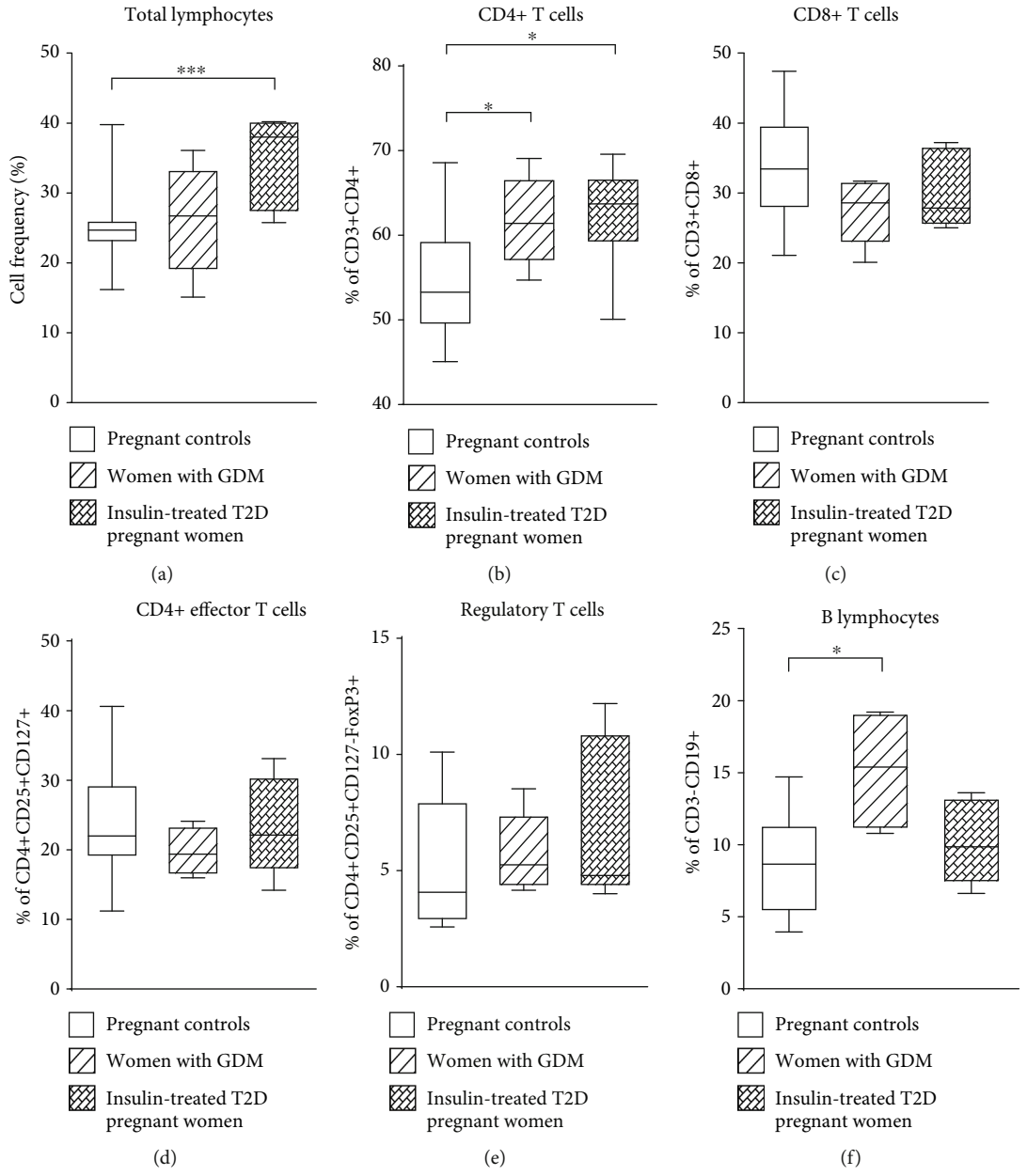

Figure 2: Frequencies of peripheral blood adaptative immunity cells in women with gestational diabetes mellitus (GDM), insulin-treated T2D pregnant women, and pregnant controls. Data shown as box plots representing medians (with 25th and 75th percentiles) and whiskers (10th and 90th percentiles) of immune cell subset frequencies: (a) total lymphocytes, (b) CD4+ T cells, (c) CD8+ T cells, (d) effector T cells (CD4 +CD25+CD127+), (e) regulatory T cells (CD4+CD25+CD127-FoxP3+), (f) CD19+ B lymphocytes from $n = 15$ women with GDM, $n = 20$ insulin-treated T2D pregnant women, and $n = 25$ pregnant controls. The statistical differences were determined using the nonparametric Kruskal-Wallis test. $^{*}p < 0.05$; $^{**}p < 0.01$; $^{***}p < 0.001$.

and PHA) have shown the same power of stimulation on T cells from three groups of pregnant women (Figure 4).

3.4. Cytokine Profiles in Serum and in T Cell Culture Supernatants. As compared to control pregnant women, serum IL-2 and IFN-γ increased ($p = 0.002$ and $p = 0.029$) while IL-10 diminished ($p = 0.017$ and $p = 0.002$) in women with GDM and insulin-treated T2D pregnant woman (Figure 5). However, IL-4 concentrations did not differ between the three groups of pregnant women. Th1/Th2 ratios determined as IL-2/IL-4 and IFN-γ/IL-4 were shifted towards Th1 phenotype in women with GDM and insulin-treated T2D pregnant women (Table 2).

Besides, in PBMC culture supernatants, IL-2 and IFN-γ concentrations were significantly increased after PHA stimulation in the three groups compared to unstimulated cells (Figure 6). The IL-4 secretion level in culture supernatant did not differ in all pregnant women before and after stimulation with PHA (Figure 6). In contrast, IL-10 production in the supernatant after PHA-stimulation significantly increased in pregnant controls ($p = 0.002$) and in insulin-treated T2D pregnant women ($p = 0.027$) but not in women

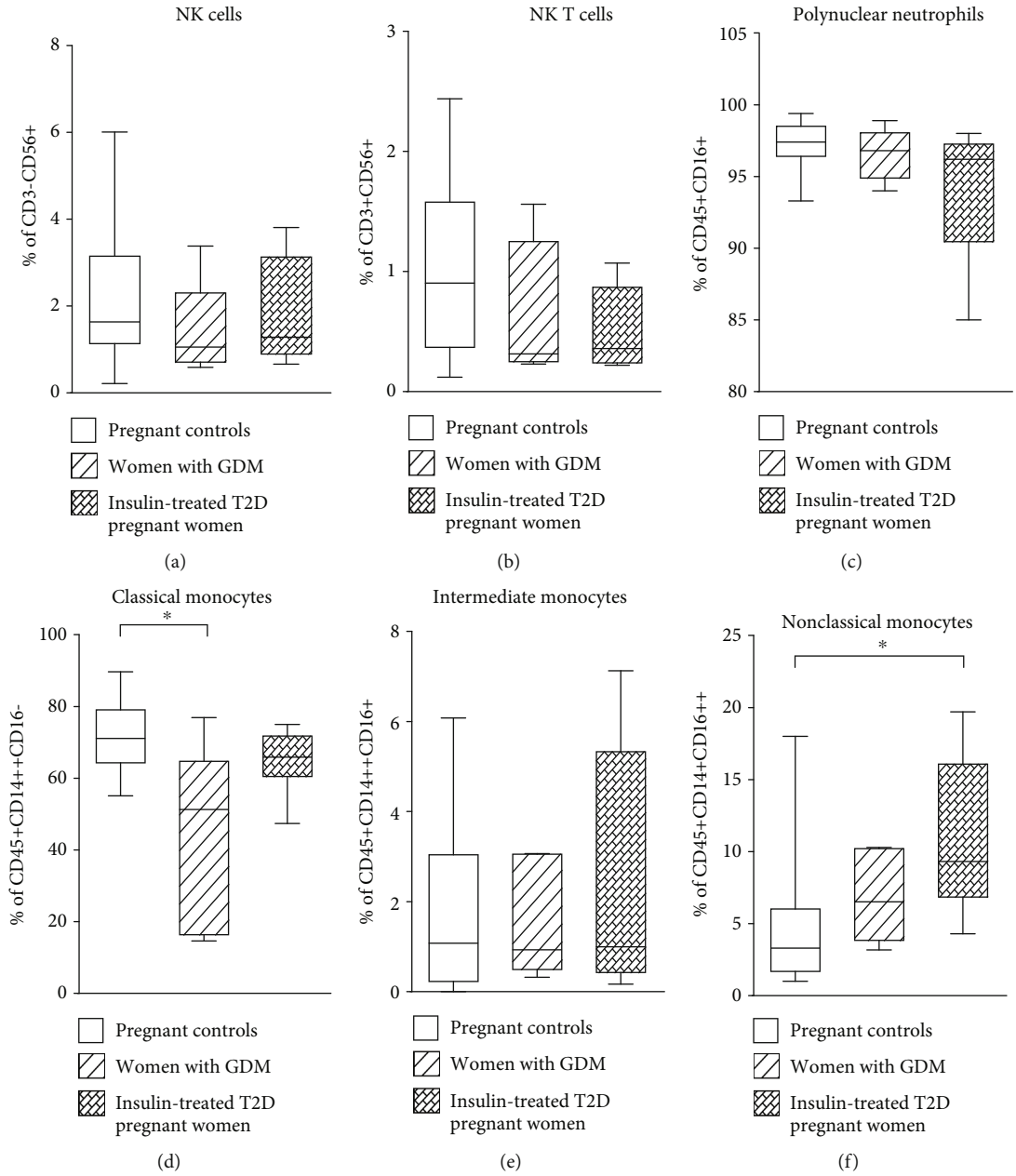

Figure 3: Frequencies of peripheral blood innate immunity cells in women with gestationnel diabetes mellitus (GDM), insulin-treated T2D pregnant women and pregnant controls. Data shown as box plots representing medians (with 25th and 75th percentiles) and whiskers (with 10th and 90th percentiles) of immune cell subset frequencies: (a) NK cells (CD3-CD56+), (b) NKT cells (CD3+CD56+), (c) polynuclear neutrophils (CD45+CD16+), (d) classical monocytes (CD45+CD14++CD16-), (e) intermediate monocytes (CD45+CD14++CD16+), (f) nonclassical monocytes (CD45+CD14+CD16++) from $n = 15$ women with GDM, $n = 20$ insulin-treated T2D pregnant women, and $n = 25$ pregnant controls. The statistical differences were determined using the nonparametric Kruskal-Wallis test. $^{*}p < 0.05$; $^{**}p < 0.01$; $^{***}p < 0.001$.

with GDM (Figure 6). It is worthy to note that, IL-2, IFN-γ, and IL-4 increased at a similar level after PHA stimulation (Figure 6).

4. Discussion

More and more evidence is accumulating and showing that the immune system, through immune cells and their products (cytokines and antibodies), plays a crucial role in modulating the severity of preexisting diabetes or diabetes occurring during pregnancy called gestational diabetes mellitus [39, 40]. In this context, any therapeutic intervention that could minimize the severity of diabetes during pregnancy could have an impact on the immune status of women with GDM and T2D pregnancy. Here, we investigated the effect of insulin treatment on the profile of immune cell subpopulations and their cytokines in pregnant women with T2D in comparison to women with GDM and healthy pregnant

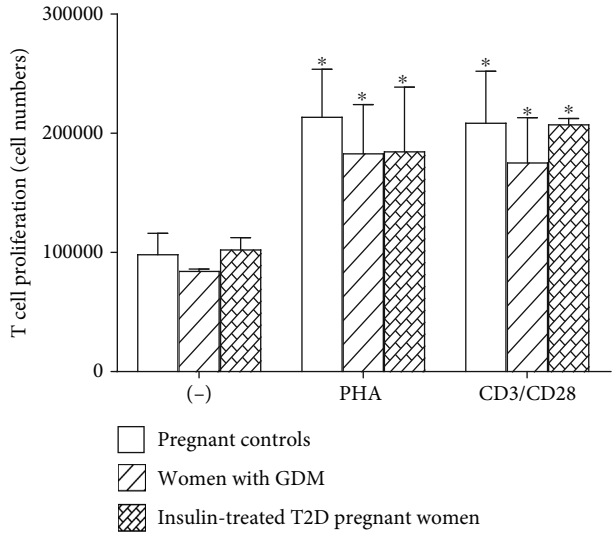

Figure 4: Lymphocyte proliferation of women with gestational diabetes mellitus (GDM), insulin-treated T2D pregnant women, and pregnant controls. PBMCs were cultured 6 days either in the absence or in the presence of 5 μg/mL of PHA or combination of 1 μg/mL of anti-CD3 and 2 μg/mL of anti-CD28. Values are means ± SEM of four determinations.

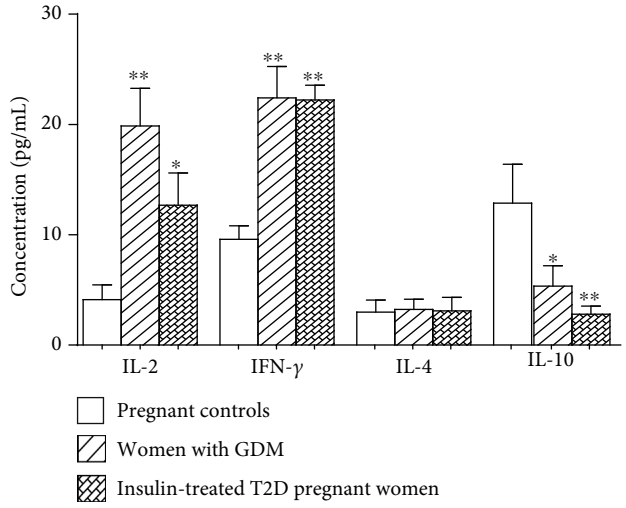

Figure 5: Serum concentrations of cytokines Th1 (IL-2, INF-γ), Th2 (IL-4), and IL-10 in women with gestational diabetes mellitus (GDM), insulin-treated T2D pregnant women, and pregnant controls. Values are means ± SD. $n = 15$ women with GDM, $n = 20$ insulin-treated T2D pregnant women, and $n = 25$ pregnant controls. $^*p$ values indicate significant difference between pregnant controls and pregnant diabetic patients (GDM and T2D).

women. As far as the model of diabetes is concerned, several points are worth noting. The GDM offers the opportunity to study the early pathogenesis of T2D due to their similar pathophysiology and their interrelationship [7]. Thus, women with newly diagnosed GDM represent an ideal population model to study the immune status of pregnant women with T2D before insulin treatment. By the same way, prepregnancy care is also needed to prepare women with preexisting

Table 2: Ratios of serum Th1 and Th2 cytokine concentrations of subjects.

	IL2/IL4	IFN-γ/IL4
Pregnant controls	1.38	3.21
Women with GDM	6.13*	6.92*
Insulin-treated T2D pregnant women	4.08*	7.15*

diabetes for pregnancy, such as improving glycemic control by insulin therapy [23].

As far as metabolic aspect is concerned, all the three groups of pregnant women, in the present study, exhibited normal levels of HbA1c, suggesting adequate glycemic control, although women with GDM elicited high fasting glycemia as compared to other groups. It has been proven that insulin therapy may improve glycemic control and reduce the risk of long-term complications in persons with diabetes [41, 42]. The high glycemia was observed in women with GDM although their normal level of glycosylated hemoglobin might be explained by the fact that these pregnant women are newly diagnosed for GDM and they have not yet been submitted to any treatment [41, 42]. However, pregnant women with type 2 diabetes who showed normal glycemia and HbA1c were still on insulin treatment during almost 3.4 ± 2.1 years of duration of disease [43, 44].

It has been proven that insulin therapy through the regulation of metabolic mechanisms and immune responses may improve glycemic control and reduce the risk of long-term complications in persons with diabetes [45, 46]. However, it remains unclear whether the control of glycemia may modulate the immune status in persons with diabetic pregnancy on insulin treatment. Very recently, we investigated the effect of glycemic control on a wide array of immune parameters in insulin-treated persons with type 1 diabetes [47]. We found that the insulin-treated persons with type 1 diabetes displayed a Th2-biased immune phenotype with a high proportion of effector CD4+ T cells and CD19+ B cells, and a downregulation of Th1 serum cytokines, irrespective of their capacity for glycemic control [47]. Moreover, we have recently conducted another study on nonpregnant person with type 2 diabetes on insulin treatment. We have observed in these patients, compared to control subjects, a shift of Th1/Th2 balance towards an anti-inflammatory Th2 phenotype [33]. This phenotype was consistent with a decrease of the percentages of total lymphocytes (CD3+) and CD8+ T-cells without any change in CD4+ T cells. However, the frequencies of effector CD4+ T cells, regulatory T cells, and B cells increased, suggesting a decrease of proinflammatory cellular immunity in nonpregnant type 2 diabetic patients treated with insulin, as compared to control subjects [33]. The present study evaluates the effects of insulin in combined context of type 2 diabetes and pregnancy, and we observed an inverse situation: increased frequencies of total CD3+ lymphocytes and CD4+ T cells, without any change in the frequencies of effector CD4+ T cells, and regulatory T (Treg) cells and B cells in insulin-treated pregnant women with T2D. Based on these observations, we may state that pregnancy did not permit insulin treatment to shift the Th1/Th2

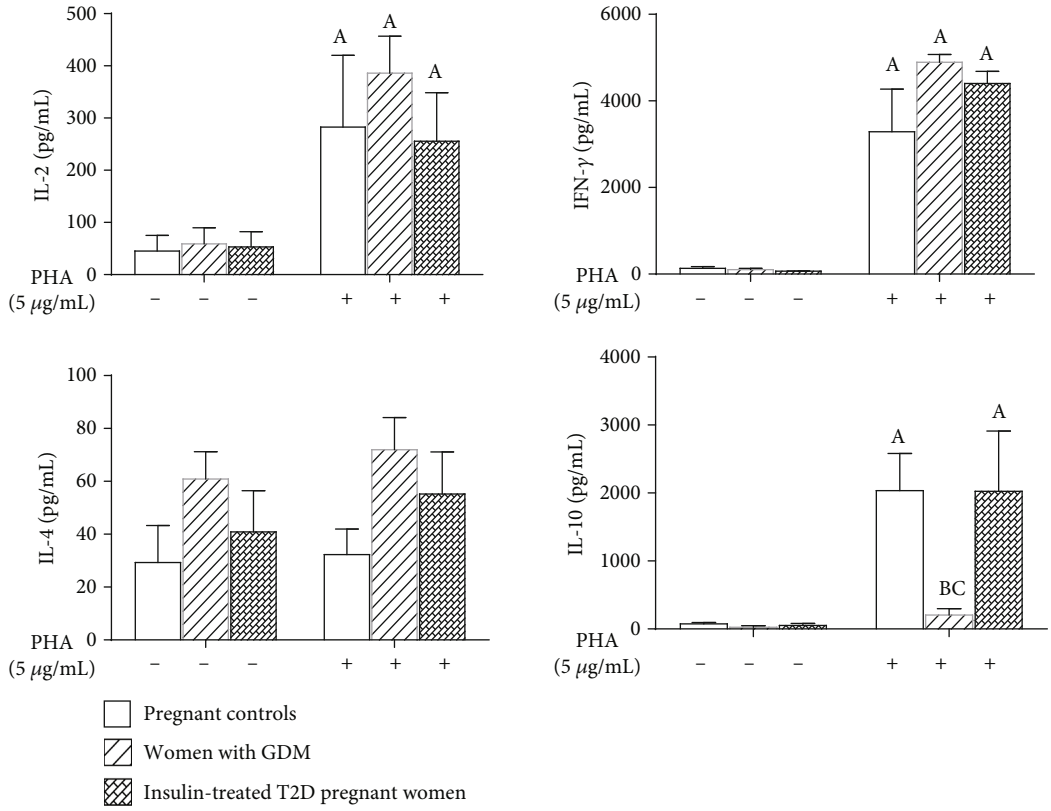

Figure 6: Cytokine level in the supernatants of PBMC culture under PHA stimulation. $n = 15$ women with gestational diabetes mellitus (GDM), $n = 20$ insulin-treated T2D pregnant women, and $n = 25$ pregnant controls. (A) ($p < 0.05$) indicates significant difference between cytokine levels in culture supernatant of PHA-stimulated cells and unstimulated cells of each group, (B) ($p < 0.05$) indicates significant difference between cytokine concentrations in culture supernatant after PHA stimulation between the pregnant controls and pregnant diabetic patients groups (GDM and DT2), and (C) ($p < 0.05$) indicates significant difference between cytokine concentrations in culture supernatant after PHA stimulation between women with GDM and pregnant controls and insulin-treated T2D pregnant women. Values are means ± SEM.

balance to an anti-inflammatory phenotype in pregnant women with T2D [26–29, 31]. The same observations had been made in women with GDM in whom the profiles of CD3+, CD4+, and CD8+ T and Treg cells were similar to those observed in insulin-treated pregnant women with T2D, with the exception of B cells which increased in GDM compared to pregnant women with T2D and control pregnant women. In fact, our results were supported by those of Angelo et al. [20] and Mahmoud et al. [48] who have also observed high percentages of CD4+CD25+ and CD4+Th17 cells in insulin-treated women with GDM, suggesting that insulin treatment did not influence the proportion of these cells in pregnant women with in type 2 diabetes as well as in women with GDM [49].

In addition, the decrease of cellular immunity observed in nonpregnant women with T2D treated with insulin was concomitant with the increase of the humoral immunity, consistent with a high number of B cells in these patients [33]. This is not the case in pregnant women with T2D treated with insulin as in the present study. However, the proportion of B cells increased in women with GDM, suggesting an increased humoral immunity during GDM, although the cellular immunity increased. This finding was in accordance with previous results which reported that GDM was associated with an increased maternal humoral immune response against paternal HLA antigens expressed by the fetus [50]. Besides, other researchers have very recently confirmed that the percentage of B lymphocytes was positively associated with insulin resistance in GDM [51].

Interestingly in the present study, high frequencies of total CD3+ and CD4+ T cells were concomitant with high serum IL-2 and IFN-γ concentrations observed in insulin-treated pregnant women with T2D and women with GDM compared to pregnant controls. In fact, being a T cell growth factor, IL-2 could induce the increase of T cells by its autocrine action [52]. High production of IFN-γ and low level of IL-4 confirmed the proinflammatory Th1 phenotype in insulin-treated T2D pregnant women as well as in women with GDM in this study. Our results are in agreement with those of Seck et al. [4] who reported the proinflammatory status in pregnant diabetic women, which could be responsible of recurrent miscarriage and spontaneous abortion [3].

The anti-inflammatory effect of insulin has been also revealed in our previous study through the increase of serum IL-10 level in T2D patients without pregnancy treated with insulin [33]. In the present study, the serum IL-10 level was

lower in insulin-treated T2D pregnant women and women with GDM compared to pregnant controls. In fact, the present results showed that, despite its anti-inflammatory and immunoregulatory properties [26–29, 31], insulin did not induce an anti-inflammatory effect on T2D pregnancy or GDM. Similar results have been obtained by Seck et al. [4] who have observed, at a transcriptional level, a decrease of IL-10 mRNA expression in obese gestational diabetic mothers without insulin treatment, suggesting that insulin had no effect on this cytokine in diabetic mothers [4]. Such observations could be explained by a strong correlation between low systemic IL-10 levels and hyperinsulinemia and insulin resistance or by impaired suppressive activity of regulatory T cells in insulin-treated T2D pregnant women and in women with GDM [53, 54]. Again, low IL-10 levels, confirming decreased suppressive activity of Treg cells, were consistent with Th1 proinflammatory phenotype and increased cellular immunity in these patients. However, it is important to recognize that other studies have reported a downregulation of Th1 cytokines in GDM [1]. Be that it may, our current findings showed that insulin could not induce the shift of Th1/Th2 balance to an anti-inflammatory Th2 phenotype in T2D pregnant patients, as we had previously observed in nonpregnant T2D patients [4]. However, the proinflammatory phenotype associated with GDM was offset by the increased humoral immunity in women with GDM [50, 51].

The T cell functional test performed by in vitro stimulation assay of T cells showed similar proliferative capacity of T lymphocytes and similar secretion of IL-2 and IFN-γ in pregnant women, regardless of GDM and T2D, suggesting that lymphocyte reactivity was not affected neither by GDM nor by insulin-treated T2D. Moreover, the mitogen did not increase IL-10 secretion in the supernatants of T cell culture in women with GDM, although it increased its secretion in insulin-treated T2D pregnant women and pregnant controls, despite the no difference in the proportion of regulatory T cells between the three groups. These data were supported by previous studies which showed that the percentage of total CD4+CD127low+/−CD25+FoxP3+ Treg cells was not affected in women with GDM although immune-suppressive activity of these cells reduced as observed in these patients compared to pregnant controls [53]. This may also explain the low IL-10 secretion by PBMCs in women with GDM. In fact, it has been reported that high IL-10 production capacity could confer protection against insulin resistance and T2D [55].

As well as innate immunity cells are concerned, human blood monocytes can be classified into three subsets: classical monocytes (CD14++CD16-), intermediate monocytes (CD14++CD16+), and nonclassical monocytes (CD14+CD16++) [56]. Since monocytes which express CD16 represent a sensitive marker of inflammation or cellular activation, the role of these cells in various diseases has considerable interest in recent years [57–60]. In the present study, the frequencies of classical monocytes decreased while those of nonclassical monocytes increased without any change in intermediate monocytes in women with GDM and insulin-treated T2D pregnant women, compared to control pregnant women. In fact, contradictory results have been obtained by other researchers who have observed an increased percentage of total and classical monocytes in women with GDM compared to the controls [19]. This discrepancy may be explained by the proinflammatory status of GDM women [4], since nonclassical monocytes are involved in the production of inflammatory cytokines [61]. Similar results have been reported in type 2 diabetic patients without pregnancy [60–62], suggesting that pregnancy did not affect the number of these cells.

In summary, our study showed that, although treated with insulin, T2D pregnant women displayed a proinflammatory status consistent with high proportions of CD3+ and CD4+ T cells, upregulation of Th1 cytokines, and low IL-10 production, suggesting a reduced immune-suppressive activity of regulatory T cells. However, GDM, showing proinflammatory status, was associated with activation and maintenance of humoral immunity consistent with high proportion of CD19+ B cells. Further investigations are needed to better understand the lack of response to insulin in T2D pregnancy and the clinical implications of theses immunological parameters in the monitoring of complications associated with diabetes during pregnancy.

Data Availability

The data used to support the findings of this study are available from the corresponding author upon request.

Disclosure

We confirm that neither the manuscript submitted nor any part of it has been published or is being considered for publication elsewhere.

Conflicts of Interest

The authors declare that there is no conflict of interest regarding the publication of this paper.

Authors' Contributions

AF was in charge of the major parts of technical aspects of work and participated in the manuscript writing. DS and MPN participated in the technical work and participated in the interpretation of data. NF contributed to the development of protocol. AY designed the study, supervised the work, wrote the manuscript, and established the collaborative aspects. KM read and approved the final manuscript.

Acknowledgments

The authors thank the Ministry of Higher Education and Scientific Research of Benin through the University of Abomey-Calavi (UAC) and the Institute of Applied Biomedical Sciences (ISBA) which sanctioned the contingent grants to Professor Akadiri Yessoufou for this work. We also express our sincere thanks to the Centre d'Etude et de Recherche sur le Paludisme associé à la Grossesse et à l'Enfance and the Institute of Research for Development (CERPAGE/UMR216-IRD) who provided with cytometry platform. We also thank

Professor Anatole Laleye, Dr. Marius Adjagba, Tatiana Hountohotegbe, and Odilon Nouatin for their valuable technical advices. This work was supported by the University of Abomey-Calavi (UAC) and the Institute of Applied Biomedical Sciences (ISBA) under the Ministry of Higher Education and Scientific Research of Benin.

References

[1] J.-M. Atègbo, O. Grissa, A. Yessoufou et al., "Modulation of adipokines and cytokines in gestational diabetes and macrosomia," *The Journal of Clinical Endocrinology and Metabolism*, vol. 91, no. 10, pp. 4137–4143, 2006.

[2] N. Khan, A. Yessoufou, M. Kim, and A. Hichami, "N-3 fatty acids modulate Th1 and Th2 dichotomy in diabetic pregnancy and macrosomia," *Journal of Autoimmunity*, vol. 26, no. 4, pp. 268–277, 2006.

[3] A. Yessoufou, A. Hichami, P. Besnard, K. Moutairou, and N. A. Khan, "Peroxisome proliferator-activated receptor α deficiency increases the risk of maternal abortion and neonatal mortality in murine pregnancy with or without diabetes mellitus: modulation of T cell differentiation," *Endocrinology*, vol. 147, no. 9, pp. 4410–4418, 2006.

[4] A. Seck, A. Hichami, S. Doucouré et al., "Th1/Th2 dichotomy in obese women with gestational diabetes and their macrosomic babies," *Journal Diabetes Research*, vol. 2018, pp. 1–7, 2018.

[5] M. P. Nekoua, R. Fachinan, A. K. Atchamou et al., "Modulation of immune cells and Th1/Th2 cytokines in insulin-treated type 2 diabetes mellitus," *African Health Sciences*, vol. 16, no. 3, pp. 712–724, 2016.

[6] S. G. Gabbe, "Gestational diabetes mellitus," *New England Journal of Medecine*, vol. 315, no. 16, pp. 1025-1026, 1986.

[7] H. W. Baynest, "Classification, pathophysiology, diagnosis and management of diabetes mellitus," *Journal of Diabetes & Metabolism*, vol. 6, no. 5, 2015.

[8] T. A. Buchanan and A. H. Xiang, "Gestational diabetes mellitus," *The Journal of Clinical Investigation*, vol. 115, no. 3, pp. 485–491, 2005.

[9] D. A. Clark and K. Croitoru, "TH1/TH2,3 imbalance due to cytokine-producing NK, gammadelta T and NK-gammadelta T cells in murine pregnancy decidua in success or failure of pregnancy," *American Journal of Reproductive Immunology*, vol. 45, no. 5, pp. 257–265, 2001.

[10] K. Ito, M. Karasawa, T. Kawano et al., "Involvement of decidual Valpha 14 NKT cells in abortion," *PNAS*, vol. 97, no. 2, pp. 740–744, 2000.

[11] J. T. Greenberg, P. Monach, J. H. Chou, P. D. Josephy, and B. Demple, "Positive control of a global antioxidant defense regulon activated by superoxide-generating agents in Escherichia coli," *Proceedings of the National Academy of Sciences of the United States of America*, vol. 87, no. 16, pp. 6181–6185, 1990.

[12] A. C. Richardson and M. W. Carpenter, "Inflammatory mediators in gestational diabetes mellitus," *Obstetrics and Gynecology Clinics of North America*, vol. 34, no. 2, pp. 213–224, 2007.

[13] R. K. Peters, A. Xiang, S. L. Kjos, and T. A. Buchanan, "Long-term diabetogenic effect of single pregnancy in women with previous gestational diabetes mellitus," *The Lancet*, vol. 347, no. 8996, pp. 227–230, 1996.

[14] A. Horsch, J. Gross, F. R. Jornayvaz, S. Lanzi, and J. J. Puder, "Diabète gestationnel–quelles sont les approches non médicales [Gestational diabetes–what are the non-medical approaches?]," *Revue medicale suisse*, vol. 521, no. 12, pp. 1089–1091, 2016.

[15] B. S. Nikolajczyk, M. Jagannathan-Bogdan, H. Shin, and R. Gyurko, "State of the union between metabolism and the immune system in type 2 diabetes," *Genes and Immunity*, vol. 12, no. 4, pp. 239–250, 2011.

[16] M. Y. Donath and S. E. Shoelson, "Type 2 diabetes as an inflammatory disease," *Nature Reviews Immunology*, vol. 11, no. 2, pp. 98–107, 2011.

[17] J. E. Snyder-Cappione and B. S. Nikolajczyk, "When diet and exercise are not enough, think immunomodulation," *Molecular Aspects of Medicine*, vol. 34, no. 1, pp. 30–38, 2013.

[18] E. Sifnaios, G. Mastorakos, K. Psarra et al., "Gestational diabetes and T-cell (Th1/Th2/Th17/Treg) immune profile," *In Vivo*, vol. 33, no. 1, pp. 31–40, 2018.

[19] T. Lekva, E. R. Norwitz, P. Aukrust, and T. Ueland, "Impact of systemic inflammation on the progression of gestational diabetes mellitus," *Current Diabetes Reports*, vol. 16, no. 4, 2016.

[20] A. G. S. Angelo, C. T. C. Neves, T. F. Lobo et al., "Monocyte profile in peripheral blood of gestational diabetes mellitus patients," *Cytokine*, vol. 107, pp. 79–84, 2018.

[21] A. Sheu, Y. Chan, A. Ferguson et al., "A proinflammatory CD4 + T cell phenotype in gestational diabetes mellitus," *Diabetologia*, vol. 61, no. 7, pp. 1633–1643, 2018.

[22] A. Yessoufou and K. Moutairou, "Maternal Diabetes in Pregnancy: Early and Long-Term Outcomes on the Offspring and the Concept of "Metabolic Memory"," *Experimental Diabetes Research*, vol. 2011, 12 pages, 2011.

[23] A. Vambergue, A. S. Valat, P. Dufour, M. Cazaubiel, P. Fontaine, and F. Puech, "Physiopathologie du diabète gestationnel: Le diabète gestationnel," *Journal de gynécologie obstétrique et biologie de la reproduction*, vol. 31, no. 2, pp. 4S3–4S10, 2002.

[24] D. R. McCance, "Diabetes in pregnancy," *Best Practice & Researc Clinical Obstetrics & Gynaecology*, vol. 29, no. 5, pp. 685–699, 2015.

[25] M. Balsells, A. Garcia-Patterson, I. Sola, M. Roque, I. Gich, and R. Corcoy, "Glibenclamide, metformin, and insulin for the treatment of gestational diabetes: a systematic review and meta-analysis," *BMJ*, vol. 350, no. jan21 14, p. h102, 2015.

[26] J. Brown, L. Grzeskowiak, K. Williamson, M. R. Downie, and C. A. Crowther, "Insulin for the treatment of women with gestational diabetes," *The Cochrane Database of Systematic Reviews*, vol. 2017, 2017.

[27] T. G. Wegmann, H. Lin, and T. R. Mosmann, "Bidirectional cytokine interactions in the maternal-fetal relationship: is successful pregnancy a T_H2 phenomenon?," *Immunology Today*, vol. 14, no. 7, pp. 353–356, 1993.

[28] P. Dandona, A. Aljada, P. Mohanty et al., "Insulin inhibits intranuclear nuclear factor κB and stimulates IκB in mononuclear cells in obese subjects: evidence for an anti-inflammatory effect?," *The Journal of Clinical Endocrinology and Metabolism*, vol. 86, no. 7, pp. 3257–3265, 2001.

[29] M. G. Jeschke, D. Klein, U. Bolder, and R. Einspanier, "Insulin attenuates the systemic inflammatory response in endotoxemic rats," *Endocrinology*, vol. 145, no. 9, pp. 4084–4093, 2004.

[30] M. G. Jeschke, D. Klein, and D. N. Herndon, "Insulin treatment improves the systemic inflammatory reaction to severe trauma," *Annals of Surgery*, vol. 239, no. 4, pp. 553–560, 2004.

[31] M. C. Foss-Freitas, N. T. Foss, E. A. Donadi, and M. C. Foss, "Effect of metabolic control on the in vitro proliferation of peripheral blood mononuclear cells in type 1 and type 2 diabetic patients," *São Paulo Medical Journal*, vol. 124, no. 4, pp. 219–222, 2006.

[32] H. Deng and J. Chai, "The effects and mechanisms of insulin on systemic inflammatory response and immune cells in severe trauma, burn injury, and sepsis," *International Immunopharmacology*, vol. 9, no. 11, pp. 1251–1259, 2009.

[33] F. Xiu, M. Stanojcic, L. Diao, and M. G. Jeschke, "Stress hyperglycemia, insulin treatment, and innate immune cells," *International Journal of Endocrinology*, vol. 2014, 9 pages, 2014.

[34] E. M. Wendland, M. R. Torloni, M. Falavigna et al., "Gestational diabetes and pregnancy outcomes - a systematic review of the World Health Organization (WHO) and the International Association of Diabetes in Pregnancy Study Groups (IADPSG) diagnostic criteria," *BMC Pregnancy Childbirth*, vol. 12, no. 1, 2012.

[35] K. Benhalima, M. Hanssens, R. Devlieger, J. Verhaeghe, and C. Mathieu, "Analysis of pregnancy outcomes using the new IADPSG recommendation compared with the Carpenter and Coustan criteria in an area with a low prevalence of gestational diabetes," *International Journal of Endocrinology*, vol. 2013, 6 pages, 2013.

[36] E.-T. Wu, F.-J. Nien, C.-H. Kuo et al., "Diagnosis of more gestational diabetes lead to better pregnancy outcomes: comparing the International Association of the Diabetes and Pregnancy Study Group criteria, and the Carpenter and Coustan criteria," *Journal of Diabetes Investigation*, vol. 7, no. 1, pp. 121–126, 2016.

[37] American Diabetes Association, "Standards of Medical Care in Diabetes—2018 abridged for primary care providers," *Clinical Diabetes*, vol. 36, no. 1, pp. 14–37, 2018.

[38] R. Fachinan, A. Fagninou, M. P. Nekoua et al., "Evidence of immunosuppressive and Th2 immune polarizing effects of antidiabetic Momordica charantia fruit juice," *BioMed Research International*, vol. 2017, Article ID 9478048, 13 pages, 2017.

[39] B. Groen, A. E. van der Wijk, P. P. van den Berg et al., "Immunological adaptations to pregnancy in women with type 1 diabetes," *Science Reports*, vol. 5, no. 1, 2015.

[40] B. Groen, T. P. Links, P. P. van den Berg, P. de Vos, and M. M. Faas, "The role of autoimmunity in women with type 1 diabetes and adverse pregnancy outcome: a missing link," *Immunobiology*, vol. 224, no. 2, pp. 334–338, 2019.

[41] B. Fullerton, K. Jeitler, M. Seitz, K. Horvath, A. Berghold, and A. Siebenhofer, "Intensive glucose control versus conventional glucose control for type 1 diabetes mellitus," *Cochrane Database of Systematic Reviews*, vol. 2, 2014.

[42] J. Rosenbauer, A. Dost, B. Karges et al., "Improved metabolic control in children and adolescents with type 1 diabetes: a trend analysis using prospective multicenter data from Germany and Austria," *Diabetes Care*, vol. 35, no. 1, pp. 80–86, 2011.

[43] American Diabetes Association, "Standards of Medical care in Diabetes—2018Abridged for primary care providers," *Clinical Diabetes*, vol. 36, no. 1, pp. 14–37, 2018.

[44] M. Lind, A. M. Svensson, and A. Rosengren, "Glycemic control and excess mortality in type 1 diabetes," *The New England Journal of Medicine*, vol. 372, no. 9, pp. 879–881, 2015.

[45] P. Home, M. Riddle, W. T. Cefalu et al., "Insulin therapy in people with type 2 diabetes: opportunities and challenges?," *Diabetes Care*, vol. 37, no. 6, pp. 1499–1508, 2014.

[46] M. C. Petersen and G. I. Shulman, "Mechanisms of insulin action and insulin resistance," *Physiological Reviews*, vol. 98, no. 4, pp. 2133–2223, 2018.

[47] M. P. Nekoua, R. Fachinan, A. Fagninou et al., "Does control of glycemia regulate immunological parameters in insulin-treated persons with type 1 diabetes?," *Diabetes Research and Clinical Practice*, vol. 157, p. 107868, 2019.

[48] F. Mahmoud, H. Abul, A. Omu, and D. Haines, "Lymphocyte sub-populations in gestational diabetes," *American Journal of Reproductive Immunology*, vol. 53, no. 1, pp. 21–29, 2005.

[49] A. Viardot, S. T. Grey, F. Mackay, and D. Chisholm, "Potential antiinflammatory role of insulin via the preferential polarization of effector T cells toward a T helper 2 phenotype," *Endocrinology*, vol. 148, no. 1, pp. 346–353, 2007.

[50] A. Steinborn, G. Saran, A. Schneider, N. Fersis, C. Sohn, and E. Schmitt, "The presence of gestational diabetes is associated with increased detection of anti-HLA-class II antibodies in the maternal circulation," *American Journal of Reproductive Immunology*, vol. 56, no. 2, pp. 124–134, 2006.

[51] Y. Zhuang, J. Zhang, Y. Li et al., "B lymphocytes are predictors of insulin resistance in women with gestational diabetes mellitus," *Endocrine, Metabolic & Immune Disorders - Drug Targets*, vol. 19, no. 3, pp. 358–366, 2019.

[52] Y. Jacques and E. Mortier, "Le renouveau de l'interleukine 2," *médecine/sciences*, vol. 32, no. 6-7, pp. 612–618, 2016.

[53] L. Schober, D. Radnai, J. Spratte et al., "The role of regulatory T cell $_{(Treg)}$ subsets in gestational diabetes mellitus," *Clinical and Experimental Immunology*, vol. 177, no. 1, pp. 76–85, 2014.

[54] S. Leon-Cabrera, Y. Arana-Lechuga, E. Esqueda-León et al., "Reduced systemic levels of IL-10 are associated with the severity of obstructive sleep apnea and insulin resistance in morbidly obese humans," *Mediators of Inflammation*, vol. 2015, 9 pages, 2015.

[55] E. van Exel, J. Gussekloo, A. J. M. de Craen, and M. Frolich, "Low production capacity of interleukin-10 associates with the metabolic syndrome and type 2 diabetes : the Leiden 85-plus study," *Diabetes*, vol. 51, no. 4, pp. 1088–1092, 2002.

[56] K. L. Wong, W. H. Yeap, J. J. Y. Tai, S. M. Ong, T. M. Dang, and S. C. Wong, "The three human monocyte subsets: implications for health and disease," *Immunologic Research*, vol. 53, no. 1-3, pp. 41–57, 2012.

[57] C. Ulrich, G. H. Heine, M. K. Gerhart, H. Köhler, and M. Girndt, "Proinflammatory CD14+CD16+ monocytes are associated with subclinical atherosclerosis in renal transplant patients," *American Journal of Transplantation*, vol. 8, 2007.

[58] C. Barisione, S. Garibaldi, G. Ghigliotti et al., "CD14CD16 monocyte subset levels in heart failure patients," *Disease Markers*, vol. 28, no. 2, pp. 115–124, 2010.

[59] A. Pettersson, A. Sabirsh, J. Bristulf et al., "Pro- and anti-inflammatory substances modulate expression of the leukotriene B $_4$ receptor, BLT1, in human monocytes," *Journal of Leukocyte Biology*, vol. 77, no. 6, pp. 1018–1025, 2005.

[60] K. S. Rogacev, S. Seiler, A. M. Zawada et al., "CD14++CD16+ monocytes and cardiovascular outcome in patients with chronic kidney disease," *European Heart Journal*, vol. 32, no. 1, pp. 84–92, 2011.

[61] S. Y. Bae, S. Y. Yoon, and Y. K. Kim, "CD14/CD16 subpopulations of circulating monocytes in type 2 diabetes mellitus patients with/without coronary artery disease," *Korean Journal of Clinical Pathology*, vol. 21, pp. 520–526, 2001.

[62] M. Yang, H. Gan, Q. Shen, W. Tang, X. Du, and D. Chen, "Proinflammatory CD14+CD16+ monocytes are associated with microinflammation in patients with type 2 diabetes mellitus and diabetic nephropathy uremia," *Inflammation*, vol. 35, no. 1, pp. 388–396, 2012.